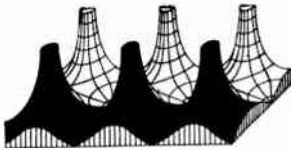# Proceedings of the IRE

Poles and Zeros

Have Electronics—Will Tackle! On this page last month we stated our personal philosophy that a professional publication must do more than report the present—it should also prepare its members for their professional and technical futures. As an example of the problems ahead for which technical preparation is necessary, we cited a few confronting us as we moved into space. Space, however, is only one segment of the future for which we must be prepared, as a group, in this burgeoning and broadening field called electronics.

While there is certainly considerable doubt as to what the field of electronics does not contain, yet some of its directions of movement are indicated by certain of the topics mentioned in "Scanning the Transactions" in any issue of the PROCEEDINGS. Among the topics abstracted in this issue we find a preparatory paper on the problems of electric power transmission for the day of hydrogen fusion power generation, the new problems of system design which will be introduced by almost noiseless parametric or maser amplification, electronic studies in biophysics, the heart, physiology, the effect of high intensity sound on pigs (measured *in situ*), the automatic abstraction of literature, and the virtues of gambling. Last month there was mention of sound, light, heat, and nuclear radiation as communication media, a paper dealing with improvement of reading speed, and another pointing out the inefficiency of speech as a form of communication. (Would silent commercials be an improvement?).

Assuming that you are not yet convinced of the many directions in which we are going, let us mention a few topics of discussion gleaned from the Los Angeles IRE Section Bulletin. During January that Section or its Subsections listened to formal papers on navigating the Nautilus, four dimensional antenna systems, deep ocean research, statistical characterization of control system nonlinearities, maze structure and information retrieval, application of statistical theory to inflight reduction of telemetry data, environmental testing of the explorers, survey of space experiments, among others.

And if all the above is still not enough, we call attention to the session on "Psychology and Electronics in the Teaching-Learning System," which is planned for the National Convention by the Professional Group on Education.

Of course you personally may not be interested in statistics, biology, antennas, space travel, or gambling (no?), but other members of our profession are. What you are not interested in today may be your bread and butter ten years from now—just how interested were you in transistors in 1948? The pages of PROCEEDINGS or TRANSACTIONS are much like a cafeteria with a good deep freeze. Each member may select to suit his current appetite and diet, or he may feel sure that a midnight snack can be found in the roast beef or turkey stored in earlier issues.

To us the above seems to confirm our philosophy of the duty of a professional publication. It also illustrates the breadth of the electronics field of the future, and points out the willingness and ability of electronics-oriented engineers to move into new fields and to take up new problems. These new problems may involve particle-wave interaction, systems analysis, solid-state materials, information, biology, psychology, medicine, or power transmission, but they all seem to be met by capable minds, ample curiosity, and a lack of fear in exploring the new world. The evidence for the existence of this curiosity and the willingness to tackle the new need include no more than solid-state phenomena and the transistor, which could well have put most of us into apple sales or on the park benches.

And once upon a time there was radio. . . .

Gonnabethere? Once more we aid New York City in greeting the arrival of spring with the IRE National Convention. Even though our systems planning is not always of the best, and the greetings to Maia must be transmitted at low power level through a narrow-band channel of high noise figure, The Convention still remains a technical event of vast importance and size. It brings together world-renowned figures in all our branches, passes on the latest word in research, shows the most recent advances in hardware, and allows you to meet ole Joe Gloop, whom you haven't seen since you both graduated from Almost Normal College way back in '31. Poor old Joe, he had such bushy hair.

Electronics Is Youth. As a sequel to the above comment, and having been impressed with the small number of graying heads at IRE functions, although we sometimes doubt the general availability of Happy Halo Hair Tonic which we use, the Editor asked for data—were we as young as we looked or was it true that high frequency power affects the glands? Our dependable headquarters research staff supplied the data, based on a random sample as is always appropriate to such sociologic surveys.

We are now happy to be able to report to the waiting world that gray hair or the absence of any is not yet standard equipment or even a JAN-spec for an electronics man. Seventy per cent of our members are below the age of forty, ninety per cent below the age of fifty, and ninety-nine and one-half per cent are below the age of sixty. To save you the trouble—that one-half per cent represents 359.7 members.

Statistics are wonderful.—J.D.R.

E. Leon Chaffee

Winner of the
1959 Medal of Honor

E. Leon Chaffee was born in Somerville, Mass. on April 15, 1885. He received the B.S. degree in electrical engineering in 1907 from the Massachusetts Institute of Technology. He then attended the Graduate School of Arts and Sciences at Harvard University where he received the M.S. degree in physics in 1908 and the Ph.D. degree in physics in 1911.

In 1910, during his doctoral research. Dr. Chaffee discovered a method of producing the first coherent continuous electrical oscillations from 1 to 100 or more megacycles and applied them to radiotelephony. For this work he was awarded the Bowdoin Prize at Harvard and the Longstretch Medal of Merit of the Franklin Institute.

He remained on the faculty of Harvard University until his retirement in 1953. Appointed instructor in electrical engineering in 1911, he progressed to Assistant Professor of Physics in 1917, Associate Professor of Physics in 1923, and Professor of Physics in 1926. He was appointed as Rumford Professor of Physics in 1940, and Gordon McKay Professor of Applied Physics in 1946. These last two appointments were continued as emeritus professorships after retirement.

During his forty-two years of active teaching and research, Dr. Chaffee served as Director of Cruft Laboratory from 1940, Co-director of the Lyman Laboratory of Physics from 1947, Chairman of the Department of Engineering Sciences and Applied Physics 1949–52, and head of wartime Pre-Radar Training Course for Officers of the three services.

He was awarded the honorary degrees of Doctor of Science from Harvard in 1944, and Doctor of Engineering from Case Institute of Technology in 1955.

An early researcher in the theory of vacuum tubes, he published many papers in electronics, physics, and biophysics. He was author of two books and co-author of another.

Dr. Chaffee served as Vice-President of the IRE in 1922 He is Fellow of the American Academy of Arts and Sciences the American Physical Society, and the IRE, and member of Tau Beta Pi and Sigma Xi.

Scanning the Issue

Transoceanic Communication by Means of Satellites (Pierce and Kompfner, p. 372)—On an historic summer day 101 years ago, President Buchanan exchanged greetings with Queen Victoria by submarine cable, opening the first direct communication link across an ocean. In a single stroke the transmit time for messages between continents had been cut by a factor of 10^7. At the turn of the century Marconi dramatically added another major communication route by spanning the Atlantic by radio. More than half a century has now passed and we are still using basically the same two narrow-band types of systems for transoceanic communication. They have served us well, but the day will inevitably come when present facilities must be greatly expanded. The use of earth satellites to relay radio signals across the ocean is an extremely attractive, indeed a revolutionary, proposal. It would open up a whole new region of the radio spectrum—microwaves—for global communication. Even more important, it would make available, possibly at less cost, new transoceanic channels which would have far greater bandwidths than any we can now provide. Not only could more traffic flow across the ocean, but also new kinds, such as television, or possibly "radio mail" to augment air mail. Due to recent advances in rocketry and in low-noise amplifiers, it is time to consider seriously the feasibility of a satellite radio link. The broad results of such a study are presented in this unusually interesting paper. It should be noted that after this paper was written the U.S. used an Atlas satellite for relaying messages. Moreover, the National Aeronautics and Space Agency has announced that during 1959 they plan to place in orbit one or more 100-foot metallized balloons of the type discussed in this paper. The authors show that if 24 such balloon-type reflectors were randomly placed in a polar orbit at an altitude of 3000 miles, 99 per cent of the time at least one would be in a position to relay a 5-mc-wide signal from a 9.5-kw 6000-mc transmitter in Nova Scotia to a receiving station in Scotland, using radio equipment that is feasible within the present microwave art. This finding is a clear call to our profession to give this important proposal further, earnest consideration.

The Band Between Microwave and Infrared Regions (Kaufman, p. 381)—An excellent review is presented of a subject which promises to be of great importance in the near future. Microwave techniques have now been pushed well into the millimeter range (300 kmc). At the same time there has recently been extensive development in the infrared region (above 3000 kmc). However, the "ultramicrowave" range between 300 and 3000 kmc is as yet virtually unexploited. To the communications engineer this region offers enormous bandwidths. It also makes possible extremely narrow-beam radiation and high energy concentration with antennas of reasonable size, an attribute that may find important application in space technology. Ultramicrowaves would also provide a new research tool in the field of spectroscopy and conceivably could find important application in monitoring and controlling nuclear fusion reactors of the future. This discussion of the problems and possibilities of generation, transmission and detection of ultramicrowaves is required (and enjoyable) reading for every PROCEEDINGS reader.

The Physical Principles of a Negative-Mass Amplifier (Krömer, p. 397)—This paper deals with one of the most exciting possibilities yet suggested for obtaining amplification in solids. It is shown that a semiconductor having the right combination of physical properties can be made to exhibit negative resistance, and hence could amplify, over an extremely wide frequency range. Still unanswered is the vital question of whether such a combination of properties can be found. If it can, this new solid-state device will probably be as important as masers and parametric amplifiers. It would 1) operate from low frequencies up to exceedingly high fre-

quencies—about 1000 kmc, 2) operate also as a bistable switching element, 3) provide a low noise figure, and 4) unlike the maser, it would have a very wide bandwidth and be tunable. It is also interesting to note that items 3 and 1 may relate this device to the first and second papers in this issue.

Simple General Analysis of Amplifier Devices with Emitter, Control, and Collector Functions (Johnson and Rose, p. 407)—Many types of semiconductor and vacuum tube devices have in common the fact that they consist of emitter, control, and collector electrodes and that their operation depends on charge control, charge storage, and charge motion. This approach provides a very simple and convenient basis for comparing the general amplifying properties of one device against another without getting involved in extensive calculations on the detailed behavior of each. The author has worked out some simple rule-of-thumb relations for comparing unipolar and bipolar transistors, spacistors, and pentode, tetrode and beam-deflection tubes with respect to transconductance, amplification, amplification-bandwidth product, and upper frequency limit. These relations will be very useful to a wide audience of device users, regardless of whether they are device experts.

Traveling-Wave Couplers for Longitudinal Beam-Type Amplifiers (Gould, p. 419)—One of the outstanding advances reported during 1958 was the development of a parametric type of traveling-wave amplifier with a greatly reduced noise figure. Amplification occurs by means of the fast space-charge wave instead of the slow wave used in conventional beam-type devices. The distinction is important because noise can be completely removed from the fast wave, but not from the slow wave. This paper describes the properties of a new class of couplers which make it possible to couple to the fast space-charge wave only. Due to the current importance of parametric amplifiers, this paper is extremely timely and may well become a standard reference work.

IRE Standards on Static Magnetic Storage: Definitions of Terms, 1959 (p. 427)—The IRE Committee on Electronic Computers has standardized the meanings of some three score terms used in connection with magnetic storage systems.

The Effects of Automatic Gain Control Performance on the Tracking Accuracy of Monopulse Radar Systems (Dunn and Howard, p. 430)—A target with a complex structure, such as an aircraft, will present several reflecting surfaces to a radar. Thus, any change in aspect of the target will produce changes in the apparent angle of arrival and amplitude of the echo. The radar sees these variations as noise. This paper investigates how the automatic gain control characteristics of the receiver affect these and other noise components, and specifies the AGC design that gives the best tracking accuracy for an automatic tracking radar.

High-Frequency Breakdown in Air at High Altitudes (MacDonald, p. 436)—This paper presents an excellent engineering report on a subject of current and future interest to many groups of engineers working in the antenna, radar, and missile fields. As the title implies, the author calculates the electric field intensities at which air will break down and become conducting at altitudes up to 500,000 feet and at frequencies between 100 mc and 35 kmc. The study shows that considerably more power per unit area of antenna aperture can be transmitted at the higher frequencies. The results, which are presented in readily understood graphical form, clearly spell out the limitations that air breakdown imposes on high-flying radars.

IRE National Convention Program (p. 456)—This feature includes abstracts of the 275 papers to be presented in New York on March 23–26. The 950 exhibitors are listed in the advertising section.

Scanning the Transactions appears on page 490.

Transoceanic Communication by Means of Satellites*

J. R. PIERCE†, FELLOW, IRE AND R. KOMPFNER†, FELLOW, IRE

Summary—The existence of artificial earth satellites and of very low-noise maser amplifiers makes microwave links using spherical satellites as passive reflectors seem an interesting alternative to cable or tropospheric scatter for broad-band transatlantic communication.

A satellite in a polar orbit at a height of 3000 miles would be mutually visible from Newfoundland and the Hebrides for 22.0 per cent of the time and would be over 7.25° above the horizon at each point for 17.7 per cent of the time. Out of 24 such satellites, some would be mutually visible over 7.25° above the horizon 99 per cent of the time. With 100-foot diameter spheres, 150-foot diameter antennas, and a noise temperature of 20°K, 85 kw at 2000 mc or 9.5 kw at 6000 mc, could provide a 5-mc base band with a 40-db signal-to-noise ratio.

The same system of satellites could be used to provide further communication at other frequencies or over other paths

I. INTRODUCTION

THE time will certainly come when we shall need a great increase in transoceanic electronic communications. For example, the United States and Western Europe have a wide community of interests and are bound to demand more and more communication facilities across the Atlantic. If we are to be ready to fill these growing needs, we shall have to investigate all promising possibilities.

In doing so, we shall certainly want to keep in mind a rule founded on experience. This rule is that telephone circuits become cheaper the more of them we can handle in one bundle. Then, too, there is the possibility of requirements for television. In either case, there is a premium on availability of wide bands of frequency.

The submarine cable art is presently distinctly limited in bandwidth. No doubt its capability in this respect will improve as the years go by, but we may well run into economic or technical restrictions not suffered by other techniques.

A chain of UHF scatter links over a northern route might provide channels across the Atlantic Ocean but the quality is dubious, the available bandwidth is limited, and the cost is great. Indeed, we cannot now imagine how one might improve quality of bandwidth while at the same time reducing the costs of such a system. Moreover, such links would not serve for some transoceanic routes.

An undersea millimeter wave system using a round waveguide excited in the TE_{01} mode is a possibility for the remote future, but such a system is far beyond present technology.

A microwave system using satellite repeaters may have many advantages over the foregoing alternatives.

Present rocket technology is at least close to the point of putting in orbit some structure which could act as a reflector or passive repeater. The maser amplifier, which introduces only around a hundredth the noise of earlier amplifiers, cuts down the transmitting power required to a hundredth of that arrived at in an earlier study.[1] This means that a satellite link with attractive properties could be attained within existing microwave art. The cost of a pair of microwave installations at the terminals would probably be less than the cost of a cable of far less bandwidth.

When highly reliable long-life microwave components and power supplies suited to a space environment are available, active repeaters may provide useful communication. When, in addition, accurate enough guidance is available, together with long-life means for adjusting attitude and position in orbit, a "fixed" repeater in a 24-hour orbit could be used.

Obviously, the present state of knowledge is insufficient for the design of a transatlantic satellite communication system of assured performance and cost. Much remains to be learned. For this very reason, and because they appear to be serious contenders for the future, it is important that research on satellite systems be given serious attention.

II. ALTERNATIVE SATELLITE REPEATER SCHEMES

A number of alternative types of orbital radio relays was discussed by Pierce.[1] These can be divided into classes in two essentially different ways: 1) active and passive repeaters, and 2) fast-revolving (relatively near) repeaters and repeaters in 24-hour orbits (stationary with respect to earth). The most important characteristics of these four possible types of repeater systems are summarized in Table I.

It should be noted that in the case of the passive repeater the bandwidth available is almost unlimited. The passive repeater is a truly linear device, and it can be used simultaneously in many ways, at many frequencies, and with many power levels, without crosstalk. Thus, the only cost in adding new channels is that of adding terminals, and these may be of many sorts.

In contrast, active repeaters have a limited dynamic range, as well as a limited bandwidth and, hence, can be used for a limited number of separate simultaneous signals only, and the levels and natures of several signals passing simultaneously through an active repeater must be carefully controlled if they are not to jam one another.

[1] J. R. Pierce, "Orbital radio relays," *Jet Propulsion*, vol. 25, pp. 153–157; April, 1955.

TABLE I

Orbit	Repeater	
	Passive	Active
Near (1- to 3-hour period)	Simplest embodiment. Metallized plastic sphere, 100-foot diameter. (On the ground: large-size steerable antenna.)	Carries lightweight microwave repeater and power supplies. Low-directivity antennas (On the ground: medium-size steerable antennas.)
Far (24-hour period)	Plane reflector. Attitude stabilized. (On the ground: extra-large fixed antennas.)	Carries heavy microwave repeaters and power supplies. High-directivity antennas. Attitude stabilized. (On the ground: fixed medium-size and small antennas.)

On the other hand, smaller ground antennas and transmitter powers can be used with active repeaters, although for broad-band use large antennas and large transmitter powers have certain advantages.

Certain other considerations concerning these various possible systems will be brought out in the following sections.

III. Orbits, Mutual Visibility, and Distances

A. The 24-hour Orbit

The 24-hour orbit has received considerable attention and does not need extensive discussion here. If fixed antennas, perhaps of very large size, are to be used, a satellite will have to revolve in the equatorial plane at a distance of roughly 26,000 miles from the earth's center. It is hoped that perturbations from its mean position due to the attraction of the moon and sun will be small enough so that only relatively small motions of the antenna feeds and corrections of orbital position would be required. One repeater would suffice to span the Atlantic Ocean, and one to span the Pacific. Areas of mutual visibility could be controlled by means of the size and orientation of the reflecting surfaces, or antennas, on the satellite. With the advanced technology required for an active 24-hour repeater, it should be easy and desirable to provide switching or readjustment of antennas to provide communication over various paths, and so, to some degree, to overcome the limitations imposed by the fact that active repeaters can handle only a limited number of signals lying in a limited range of power levels.

Many variations on this theme are possible and will be realized in due course. The transmission provided by such a system would of course be uninterrupted.

B. Near Orbits

The near orbits, that is, orbits between 1000 and 3000 miles above the earth, can be classified into equatorial, polar, and inclined orbits. It is intuitively clear that the utility of a satellite orbit depends on the distances from the satellite to the terminal points for the portion of the orbit for which the satellite is visible from both terminal points. It is also obvious that this distance should be as small as possible, consistent with the requirement that a substantial portion of the whole orbit should be simultaneously visible from the terminal points.

Transatlantic communications appear to be of the greatest immediate importance, for the North Atlantic routes are already carrying the heaviest traffic in every available medium. Thus, we shall choose a transatlantic route as an example. Equatorial orbits, which are not suited to this route, will not be examined here. In order to determine whether inclined or polar orbits are more advantageous for transatlantic use, computations of mutual visibility have been made for two comparable cases; the result is that polar orbits are more efficient for terminations which might be chosen for a transatlantic link. Therefore, all the subsequent calculations have been made on the basis of polar orbits only.

C. Visibility Considerations

A computation has been made of the durations of simultaneous visibility of a satellite at various heights from points in North America and Europe, selected, somewhat arbitrarily, in the following locations:

Terminal A—Newfoundland	48° north 55° west
Terminal B—Island of Lewis in the Hebrides, Scotland	58° north 7° west

They are about as close to each other as can be found on a map, keeping in mind that there will have to be microwave links between the terminals and the respective continental communication networks.

Assuming the radius of the earth to be 3950 miles, we find that the distance between terminals A and B is 2060 miles. For the sake of simplicity we have assumed that the satellite becomes visible as soon as it crosses the horizon and that it moves in perfectly circular orbits.

A map showing the regions of mutual visibility of satellites at heights of 500, 1000, 1500, 2000, 2500, and 3000 miles will be found in Fig. 1. These regions are projected onto the earth's surface, with the earth's center as the center of projection, and this in turn is shown in orthogonal projection, with the North Pole at the center. At the higher altitudes these regions extend close to the equator and are very much foreshortened, and another projection (not shown) has been used in computing visibility involving these regions. So far these visibility regions do not depend on the type of orbit. However, it is a simple matter to compute visibility durations for polar orbits, and this is what has been done.

The constructions of Fig. 1 have been used in calculating the length of time a satellite is visible from terminals

A and B simultaneously, as a function of height h above the earth's surface and as a function of longitude of the orbit. Since, in general, the period of rotation of the earth will not be an integral multiple of the period of the satellite, the orbit will in due course occupy all possible orientations with equal probability. Therefore, an *average* percentage visibility could be calculated, an average which has been determined by summing over 72 equally spaced orbits, *i.e.*, every 5° of longitude. The longest and shortest visibility durations have also been calculated. It will be appreciated that above a certain height (which turns out to be 1350 miles for the terminations chosen) the satellite will be mutually visible

from A and B for some time during every revolution, although such time may only be of short duration.

Table II gives the results. Note, for instance, that at a height of 2500 miles the satellite is visible every time it goes around, the shortest visibility lasting 24 minutes, and the longest, 46 minutes. With a period of revolution of about 3 hours, an average visibility is about 20 per cent.

A look at Fig. 2, showing the regions in which the satellite is visible both from A and B, now with quasi-equatorial orbits (in which the various sputniks move), shows that these orbits are not as favorable as the polar ones just discussed.
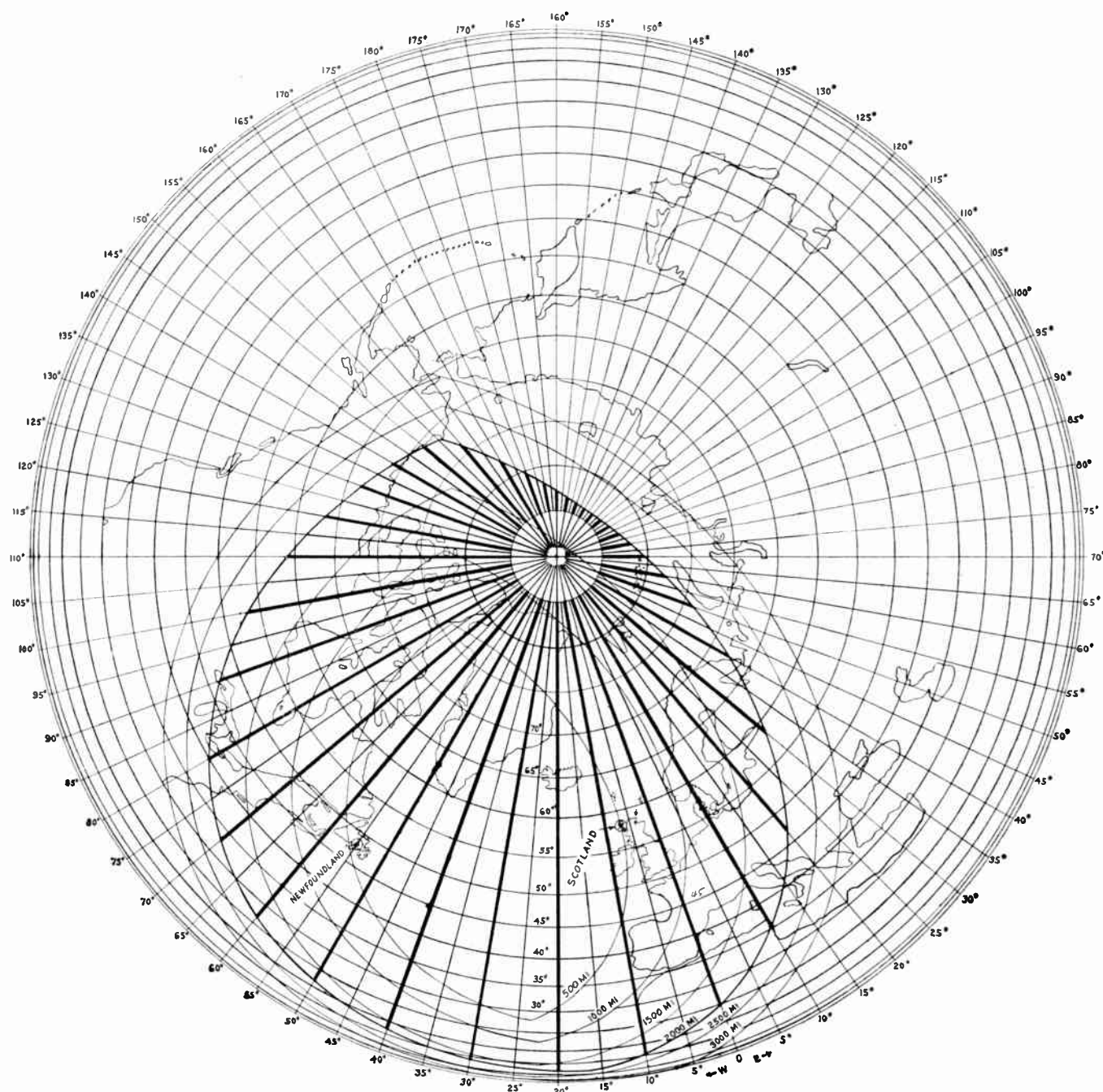

Fig. 1—Regions of mutual visibility of satellites in circular orbits at various heights. *Note:* For the sake of comparison with Fig. 2, polar orbits at the 2000-mile height have been darkened.

TABLE II

	Height above surface of earth (miles)					
	500	1000	1500	2000	2500	3000
Time of one revolution (minutes)	100.4	118.0	136.0	155.0	175.2	195.2
Shortest visibility (minutes)	0	0	8.0	12.5	23.8	31.4
Longest visibility (minutes)	14.7	20.0	29.6	36.6	46.2	55.4
Average visibility (per cent)	3.5	6.9	12.9	17.7	19.6	22.0
Longest distance from A or B to satellite (miles)	2050	2980	3755	4450	5099	5718
Shortest distance from A or B to satellite (miles)	1180	1540	2100	2670	2820	3300

Assumptions: Terminals in Newfoundland and Hebrides.
Polar orbits.
Refraction effects ignored.
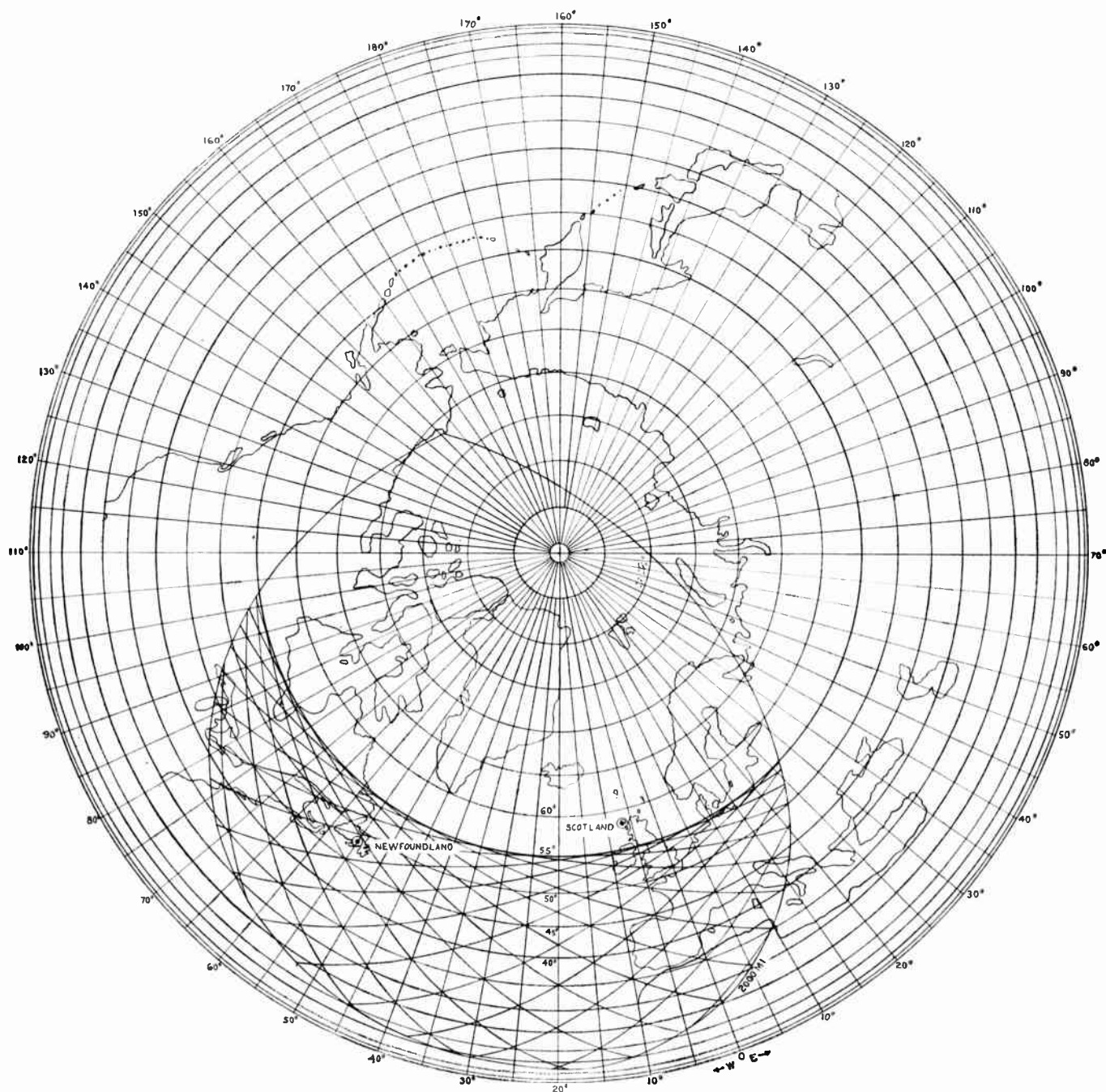Visibility from horizon to horizon.

Fig. 2—Region of mutual visibility of satellites in orbits inclined 55° at a height of 2000 miles.

It is assumed here that the satellites are launched at an inclination so that the farthest excursions are 55° north or south. In computing the average visibility, the rotation of the earth has been neglected, as it was when computing the polar orbits. For a satellite height of 2000 miles, it turns out that the average visibility is 10.2 per cent for inclined orbits, whereas it is 17.7 per cent for polar orbits. For equatorial orbits to yield visibility durations comparable to polar ones, terminals would have to be much nearer the equator than the ones chosen. Such locations would be farther apart from each other; moreover, they would be rather remote from the more densely populated areas of the world which possess microwave networks. Therefore, a polar orbit should be chosen.

So far it has been assumed that satellites are visible and fully utilizable right down to the horizon. There may be systems for which this is so; however, in many cases it must be assumed that satellites have to rise to a certain minimum elevation before they can be properly acquired. In particular, this will be so with systems which use maser amplifiers of high effective sensitivity (of low effective noise temperature). Propagation anomalies due to the earth's atmosphere can also be expected to be of importance very near the horizon, which is another reason for avoiding working near the horizon.

Hogg[2] has calculated the thermal noise due to the oxygen in the atmosphere. The "tail" of the well-known absorption in the 5-mm band extends far into the longer wavelengths, and thermal noise radiation is accordingly generated and will be received by any antenna in amounts depending on the frequency and on the angle at which its beam traverses the atmosphere. Fig. 3 (based on Hogg's calculation) shows the effective temperature of an ideal antenna as function of frequency and angle of elevation. Also shown are curves indicating the approximate limits of effective noise temperature due to cosmic noise sources.

The optimum frequency for satellite radio systems of high sensitivity will lie somewhere between 2000 mc and 6000 mc. We further note there is no point in making the receiver noise temperature lower than 10°K if the antenna elevation is less than 10° above the horizon. Lowering the antenna right down to the horizon increases its temperature nearly tenfold; this would hardly be noticeable with old-fashioned receivers, but would seriously degrade the performance of a receiver using a maser amplifier as the input stage.

Rather than calculate visibility regions, times, and distances afresh for various satellite heights and minimum elevations, we have taken the 3000-mile high orbit and calculated the minimum elevations which give

[2] D. C. Hogg, "Effective temperatures of high gain antennas due to oxygen and water vapor in the atmosphere," paper submitted for publication.

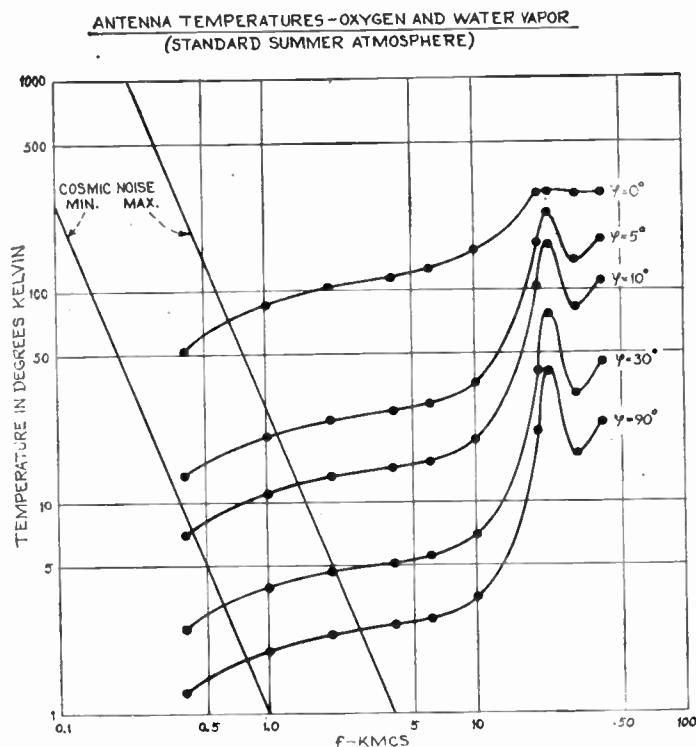ANTENNA TEMPERATURES—OXYGEN AND WATER VAPOR (STANDARD SUMMER ATMOSPHERE)

Fig. 3—Temperature due to oxygen absorption seen by an ideal antenna as a function of elevation angle ϕ and frequency.

the same visibility regions and periods as satellites followed right down to the horizon in orbits at the following heights: 2500, 2000, and 1500 miles. The results are given in Table III.

TABLE III

	Minimum elevation angle (degrees)			
	0	3.25	7.25	12.60
Average visibility (per cent)	22	19.6	17.7	12.9
Shortest visibility (minutes)	31.4	26.5	15.5	11.5
Longest visibility (minutes)	55.4	51.5	45.5	42.5
Longest distance (miles)	5718	5520	5240	4960

Assumptions: Terminals in Newfoundland and Hebrides.
Satellite height: 3000 miles.
Orbital period: 195.2 minutes.

Comparing Tables II and III, note that the price paid for using the sky only down to, say, $7\frac{1}{4}°$ above the horizon is a drop in average visibility from 22.0 to 17.7 per cent.

IV. NUMBER OF SATELLITES

One could get a great deal of useful communication with one satellite, but to provide nearly uninterrupted transmission requires many. While it is, in principle, possible to imagine satellites placed in perfectly circular

orbits at regular intervals, so that they provide un-interrupted service, it is at present more realistic to assume that they will tend to appear with complete randomness. Thus sometimes there will be several visible at the same time, and sometimes there will be none. The question arises: what fraction of the time, on the average, will there be none visible?

Let f be the average fraction of the satellite period when it is visible from both terminals. This is also the probability of mutual visibility, and $(1-f)$ is then the probability of the satellite *not* being seen. Hence, the probability of not seeing any of n satellites:

$$(1 - f)^n.$$

If this is set equal to i, the average fraction of service interrupted, the required number of satellites is obtained:

$$n = \frac{\log i}{\log (1 - f)}.$$

Table IV shows the minimum numbers of satellites required to give service interrupted, on the average, by the amounts indicated. This has been done for various satellite heights, assuming visibility right down to the horizon. In Table V there is a similar set of numbers of satellites calculated for various minimum elevations, assuming all satellites to travel at a height of 3000 miles. Note that doubling the number of satellites reduces the amount of interruption by one tenth.

TABLE IV

NUMBER OF RANDOMLY SPACED SATELLITES TO PROVIDE SERVICE
INTERRUPTED BY NO MORE THAN 100i PER CENT

Satellite Height	Number of satellites for indicated percentage of service interruption			
miles	10 per cent	1 per cent	0.1 per cent	0.01 per cent
500	62.5	125.0	187.5	2500.0
1000	32.3	64.6	96.9	129.2
1500	16.7	33.3	50.0	66.6
2000	11.8	23.6	35.4	47.2
2500	10.5	21.0	31.5	42.0
3000	9.3	18.5	27.8	37.0

Assumptions: Terminals in Newfoundland and Hebrides.
Polar orbits.
Visibility from horizon to horizon.

TABLE V

NUMBER OF RANDOMLY SPACED SATELLITES REQUIRED TO GIVE
SERVICE INTERRUPTED NO MORE THAN 100i PER CENT, AS A
FUNCTION OF MINIMUM ELEVATION FOR ORBITS AT
3000-MILE HEIGHT

Minimum elevation angle	Number of satellites for indicated percentage of service interruption		
degrees	10 per cent	5 per cent	1 per cent
0	9	12	19
3.25	11	14	21
7.25	12	15	24
12.60	17	22	33

Assumptions: Terminals in Newfoundland and Hebrides Polar orbits.

It should be noted at this point that the interruptions, though happening at irregular intervals, should be predictable well in advance, and the communication services can be organized accordingly.

V. PATH-LOSS CALCULATIONS

Many factors enter into a calculation of transmission performance of a system involving satellite repeaters between terminals on earth. Rather than carry out calculations on a variety of schemes, we shall concentrate on one in particular, namely frequency modulation with feedback,[3] which is particularly applicable to satellite communications, as has been pointed out by Ruthroff and Goodall.[4] The proposed system compares favorably with other known systems, such as PPM, PCM, or SSB. The results will be obtained in a fashion so that extrapolations to other systems can be easily performed.

Starting with the case of the passive repeater in the form of a reflecting sphere with a diameter D, the path loss can be written, as for the well-known radar case:

$$L = \frac{P_T}{P_R} = \frac{16\lambda^2 p^4}{A^2 \eta^2 D^2},$$

where

P_T = transmitter power,

P_R = receiver power,

λ = wavelength,

p = geometric mean of the distances between the satellite and the terminals,

A = antenna area (assumed to be the same for both transmitter and receiver),

η = antenna efficiency.

The noise power at the receiver input can be written

$$N = kTB,$$

where

k = Boltzmann's constant (1.38×10^{-23} watt per degree per cycle per second, or -228.9 dbw for $1°$K and 1 cps),

T = effective noise temperature of receiver (including sky noise, antenna loss, tube noise, etc.) in degrees Kelvin,

B = the RF bandwidth in cycles per second,

b = base-band modulation bandwidth.

In an FM receiver, noise problems are minimized if feedback is applied to reduce the deviation in the IF stages and the limiter. The operation of such a receiver is described by Chaffee[3] and Carson[5] and has been digested by Goodall and Ruthroff.[4] More recently, a

[3] J. G. Chaffee, "Application of negative feedback to frequency modulation systems," *Bell Sys. Tech. J.*, vol. 18, pp. 404–437; July, 1939.

[4] C. L. Ruthroff and W. M. Goodall, private communication.

[5] J. R. Carson, "Frequency-modulation: theory of the receiving feedback circuit," *Bell Sys. Tech. J.*, vol. 18, pp. 395–403; July, 1939.

closely related system has been described by Jaffe and Rechtin.[6]

An optimized receiver of this kind will use sufficient feedback to reduce the deviation in the IF circuits to near zero. Under these conditions

$$(S/N) \cong 3\left(\frac{C}{N}\right) M^2$$

and

$$B \cong 2(1 + M)b,$$

where

M = modulation index,
(S/N) = signal-to-noise ratio at the receiver output,
(C/N) = signal-to-noise ratio at the IF frequency.

To give reliable operation

$$\left(\frac{C}{N}\right) \geqq 16,$$

which is the usual 12-db threshold. Now, since the IF bandwidth required is twice the modulation bandwidth

$$N_{1F} = 2kTb,$$

and since

$$C = \frac{P_T}{L},$$

then

$$\frac{P_T}{L} \geqq 32\ kTb, \text{ or } 15.1 \text{ db above a power } kTb.$$

It follows from the above that if

$$\left(\frac{S}{N}\right) = 10^4\ (40 \text{ db}),$$

then $M = 14.5$, and a 5-mc signal bandwidth requires a 155-mc RF bandwidth. To accomplish this exactly requires infinite feedback, but for practical purposes a feedback factor of 145 (43 db), reducing the modulation index in the IF to 0.1, should suffice.

The transmitter power can be kept constant and the output signal-to-noise ratio increased (up to the limit given by information theory) by further increasing in equal amounts the transmitter index, receiver feedback, and bandwidth in the medium.

Consider what this implies in terms of an actual system.

A. FM Feedback—Passive Repeater

Assuming a maser amplifier is in use, the receiver

[6] R. Jaffe and E. Rechtin, "Design and performance of phase-lock circuits capable of near-optimum performance over a wide range of input signal and noise levels," IRE TRANS. ON INFORMATION THEORY, vol. IT-1, pp. 66-76; March, 1955.

noise becomes negligible. The sky temperature is then the dominant factor and, referring to Fig. 3, choose 2000 mc for the operating frequency; assuming that the antennas point at elevations no lower than 7.25°, the effective receiver noise temperature is 20°K, so that the noise is 13 db above that at 1°K. With no more than one per cent interruption of service, this requires 24 satellites at orbits 3000 miles high. The maximum distance (RMS) is 5240 miles (Table III). The shortest distance, that is, when the satellite is half-way between the terminals, is 3300 miles (Table II).

Suppose the antenna diameters are 150 feet, and efficiencies 60 per cent. Further, assume that the passive repeater is a metallic sphere of 100-foot diameter. Thus, the maximum path loss:

$$L = \frac{16 \times (\frac{1}{2})^2 \times (5240)^4 \times (5280)^4}{(\pi \times 75^2)^2 \times (0.60)^2 \times (100)^2}$$

$$L = 2.04 \times 10^{18} \text{ or } 183.1 \text{ db}.$$

The minimum loss turns out to be 8 db less.

For one-cps base-band bandwidth and 1°K, the received power must be 15.1 db above the thermal level of -228.9 dbw. A temperature of 20°K increases the required power by 13.0 db, and a bandwidth b of 5 mc increases the power by 67.0 db.

In db-watt

$$P_T = +183.1 + 15.1 - 228.9 + 13 + 67 \text{ dbw}$$

$$P_T = 49.3 \text{ dbw or } 85 \text{ kw}.$$

This amount of CW power can, in principle, be supplied with existing tubes (Varian Associates VA-800, 1.7 to 2.4 kmc, 10-kw klystrons), eight of them driven in parallel.

Suppose a higher frequency is chosen, for example, 8000 mc. This reduces the power requirement by a factor

$$\left(\frac{8000}{2000}\right)^2 = 16.$$

On the other hand, the antenna noise temperature will be increased by a few degrees, e.g., from 20 to 25°K, giving a factor 1.25. We assume that antenna size and efficiency are unchanged, which actually implies a considerable increase in the cost of the antennas, and arrive at a transmitter power of:

$$P_T = \frac{85 \times 1.25}{16} = 6.65 \text{ kw}.$$

This amount of power can be supplied by four klystrons in parallel, such as the Varian Associates VA-806. Further, it appears that single tubes could be developed for either of the cases discussed above.

B. FM Feedback—Active Repeater

In the active repeater it is assumed that there is a wide-band low-noise RF amplifier with a power output limited to P_a by weight, life, and bulk considerations.

It is connected to the earth terminals by means of non-directional antennas, namely dipoles with effective areas $3\lambda^2/8\pi$.

It can be shown that the crucial factors are the size and noise temperature of the antenna at the receiving terminal and the satellite output power. The transmitter power on the ground and the noise figure of the satellite amplifier are of minor importance.

The path loss of importance now is given by

$$\frac{P_R}{P_a} = \frac{A_{sat} A_R \cdot \eta}{\lambda^2 p^2} = \frac{1}{L}.$$

where

$A_{sat} = 3\lambda^2/8\pi$,
$A_R = \pi a^2/4$, a being the antenna diameter.
η = antenna efficiency.
p = path length.

Hence

$$L = \frac{32}{3}\left(\frac{p^2}{a^2\eta}\right).$$

Employing FM with feedback as before, use the formula

$$\frac{P_a}{L} = 32 \, kTb.$$

Thus, the necessary RF power at the satellite

$$P_a = 326 \frac{p^2}{a^2\eta} \, kTb.$$

Take the same antenna, frequency, noise temperature, bandwidth, and distance as used before in the passive repeater case, namely:

$p = 5240$ miles,
$a = 150$ foot,
$\eta = 0.6$,
$T = 20°$K at 2000 mc,
$b = 5$ mc.

This requires a satellite transmitter power of $P_a = 25.4$ mw.

This does not seem to be much in the way of RF power; an increase of one order of magnitude is perhaps not out of the question. Over-all efficiencies of something like a few per cent may perhaps be achieved, leading to a continuous power requirement of a few watts. This can be satisfied by a combination of solar and storage batteries, but owing to the limited life of existing storage batteries, the life of such a repeater would at present be restricted.

An active repeater in a 24-hour orbit with the ground installations much as described above will have to put out approximately $(25,000/5000)^2 = 25$ times the transmitter power calculated above, that is, about 625 mw. This is more than enough, since a 24-hour satellite will, in all probability, be attitude stabilized and therefore could carry a high-gain antenna to great advantage.

The power available on this kind of repeater has to include provision for the maintenance of accurate position, velocity, and attitude; how much, it is difficult to estimate at this time. Life will again be a serious problem.

VI. MODULATION SYSTEMS

Microwave tubes such as klystrons, traveling-wave tubes, and backward-wave oscillators lend themselves very conveniently to frequency modulation. Magnetrons and amplitrons are operated advantageously under pulse conditions.

Ruthroff and Goodall have shown[3] that FM with feedback and PPM give practically the same performance when the same mean transmitter power is employed. It would not be surprising if other modulation schemes were to be found to give similar performance when all requisite conditions are optimized.

All modulation systems will have to operate in the presence of large and continuously varying Doppler-frequency shifts. With approximately spherical reflectors at an elevation higher than a few degrees above the horizon, no fading, scintillating, or glinting is expected to occur; thus, no fading margin was deemed to be necessary in the path-loss calculations. The noise temperature, antenna size, power, etc, are the most reasonable estimate that can be made at present of what is necessary to provide the performance specified. In an actual system, a greater power might be used in order to provide a margin of safety.

VII. UNKNOWNS IN SATELLITE COMMUNICATIONS

The authors have a great deal of confidence in the over-all feasibility of satellite communications. Nevertheless, quite a few unknowns exist. Experiments, development, and experience are needed before all problems can be considered solved. Some problems are of a fundamental nature, such as the influence of the earth's atmosphere on the propagation of radiation; others are instrumental, such as the limits on receiver noise temperature due to losses and mismatches.

A. Satellite Construction

The passive repeater envisioned in Section V-A is a metallized plastic sphere of 100-foot diameter. A considerable amount of work is being done by the National Aeronautics and Space Agency (NASA), who have announced that they will place one or more balloons of this type into orbit sometime in 1959. The major unknown at present is the life of such balloons. Also in question is the ultimate shape.

Other satellite constructions, such as metallic wire-mesh spheres, the mesh being small compared with a wavelength, have been suggested, and methods of placing them in orbits deserve to be studied.

A spherical satellite scatters the radiation which it intercepts isotropically. Satellites of shapes other than

spherical could be used to reflect a greater fraction of the radiation striking them from the transmitter to the receiver.

A great deal of work needs to be done on active repeaters, particularly on components such as microwave tubes, storage batteries, capacitors, etc., before a sufficiently long life can be assured. Many components may have to be constructed on an entirely new basis, taking into account that the environment will be radically different from any encountered so far, namely ultra-high vacuum, intense ultraviolet, X-ray and cosmic ray bombardment and micrometeorites.

B. Propagation Effects

The whole of the earth's atmosphere will have to be traversed twice in every satellite radio link; it is therefore important to know the effect it will have on the beams of microwave radiation. It is fairly certain that nothing harmful will happen to beams pointing at more than 10° above the horizon, except perhaps when traversing auroral regions. Nevertheless, propagation measurements are required.

It would be desirable to know the actual instantaneous angle of arrival of beams of radiation coming from all possible directions over a wide frequency range and covering a wide range of climatic conditions. Data concerning rotation of the plane of polarization are also important. The effective sky temperature as a function of frequency and elevation must be ascertained.

C. Antenna Considerations

Some of the research results of the preceding section will determine the largest size of antenna which can be used with advantage.

Another problem to be solved is that of an antenna with low effective noise temperature; that is, one in which the losses and the side and back lobes have been reduced below a certain tolerable limit.

Problems of very large steerable antennas call for solution; these may be divided into electrical and mechanical problems. It may be that both will be solved eventually by adopting the principles of multielement steerable arrays.

D. Over-all System Noise Figure

This is largely an RF input problem, once the antenna itself has been "cleaned up." With very large antennas it will be necessary, for economical and mechanical reasons, to combine into one unit both transmitter and receiver feed horns and also perhaps the output and input of a tracking radar. The frequencies employed for all these functions may be spaced widely apart so that efficient filtering should not be too difficult.

Nevertheless, to achieve an effective low-noise temperature will require much competent and painstaking experimentation. Considerable development work is already in progress on masers and parametric amplifiers. Not so much has been done on tying them in with a particular communication system.

E. Tracking of Satellites

Satellites move in smooth, regular orbits, predictable with high precision. This makes it attractive to think of using computers, analog or digital, for the purpose of steering antennas on them.

The alternative method employs a tracking radar. For relatively small antennas, or in case only a feed system has to move, the tracking radar may have a separate antenna, and the communication antenna be "slaved" to the radar.

With large antennas, which may distort, sag, or twist as they are slewed about or in the presence of high winds, it might be necessary to make the radar output and input integral with the communication feed system in order to point the antenna accurately despite distortions with respect to the mounting and drive.

Similar considerations also apply to the Doppler-shift of the reflected radiation, which can be computed beforehand, or which can be derived instantaneously from the radar data.

The results of the research on propagation effects will affect solutions to the tracking problems. Any satellite communication system involving very large antennas at microwave frequencies will depend entirely on an accurate and dependable tracking system such as probably has never been built before.

VIII. Acknowledgment

The Band Between Microwave and Infrared Regions*

I. KAUFMAN†, MEMBER, IRE

The following paper is one of a planned series of invited papers, in which men of recognized standing will review recent developments in, and the present status of, various fields in which noteworthy progress has been made.—*The Editor*

Summary—Microwave techniques have been stretched well into the millimeter range. The infrared range has recently found extensive practical application. The portion of the spectrum that lies between the two, stretching from about 300 to 3000 kmc (1.0 to 0.1 mm), is, to date, almost unexplored and virtually unexploited. The chief reason for this sparseness of activity is the lack of 300–3000-kmc generators. This paper mentions some factors that have prevented microwave generation techniques from entering this region. A number of ideas and schemes, some extrapolations of microwave techniques, others of a more revolutionary nature, may result in satisfactory generators. Some of these are discussed herein.

In addition to generation, there are the associated problems of detection, control, transmission, and measurement. These are discussed briefly, along with some advances in the art that approach solutions.

I. INTRODUCTION

THE need for more channels for transmitting information has led the radio engineer to develop means of generating and utilizing electromagnetic waves of higher and higher frequencies. Techniques and properties peculiar to these shorter wavelength bands, such as the higher directivity obtained at higher frequencies, have led to extensive development of microwaves and, more recently, of the millimeter wave range.

The techniques for much higher frequencies, *i.e.*, for the visible region of the spectrum, preceded radio engineering by a number of years. There has also been extensive development in the infrared region. However, the frequency range between 300 and 3000 kmc, which stretches between infrared and microwaves, is as yet virtually unexploited.

Several names for this range have been suggested. Motz[1] has suggested the names "interwaves" and "Zwischenwellen"; others have used the terms "submillimeter waves" and "ultramicrowaves." The ultimate choice for a name will probably depend on whether microwave or infrared techniques will become predominant in this range. In this paper we shall use the term "ultramicrowaves," (umw).

The success of high-power, dependable sources in the microwave and millimeter wave regions has made it very tempting to hope for an extrapolation to umw. Until now, however, neither CW nor pulsed sources of

essentially single frequencies of any reasonable power have yet been built, even at the milliwatt level.

Accompanying the need for sources is a need for dependable detectors and for schemes of control, amplification, and transmission of this energy, should it be produced.

The applications of successful umw sources and receivers will surely be manifold. The relatively enormous bandwidths that will become available can make umw an ideal portion of the spectrum. Space technology will soon need to communicate over enormous distances, requiring the concentration of high-power electromagnetic energy into extremely narrow beams. UMW will be well suited for this job, for here very narrow beams will be achieved with antennas of reasonable size.

Besides applications to radio engineering, there are a number of scientific studies in which immediate use could be made of narrow band umw sources of reasonable power. Among these are the detailed analyses of energy gaps in superconductors,[2] which can lie in the umw range, and the umw spectroscopic analyses of materials. Relatively few of the latter have been performed to date because of lack of suitable narrow band sources of reasonable power.

Finally, a very important immediate application is in nuclear fusion research where umw energy is needed to study highly ionized, high-density gas plasma. It is conceivable that the nuclear fusion reactors of the future could be monitored and controlled by umw radiation.

II. IDEAS RELATED TO ULTRAMICROWAVE GENERATION

By far the most difficult aspect of the umw problem is the creation of single frequency sources of appreciable power. Essentially single frequency can be approached by very narrow band filtering of black body radiation. Appreciable power, say milliwatts of CW or watts of pulsed power, cannot be achieved so easily and has, indeed, not yet been attained.

In the search for appreciable power at essentially a single frequency, we look for schemes in which large numbers of elementary sources (electrons, atoms, etc.) radiate energy at that frequency coherently, *i.e.*, with definite phase relations that cause constructive addition

[1] H. Motz, "Cerenkov and undulator radiation," IRE TRANS. ON ANTENNAS AND PROPAGATION, vol. AP-4, pp. 374–384; July, 1956.

[2] M. A. Biondi, A. T. Forrester, M. P. Garfunkel, and C. B. Satterthwaite, "Experimental evidence for an energy gap in superconductors," *Rev. Mod. Phys.*, vol. 30, pp. 1109–1136; October, 1958.

of fields. Particular requirements for achieving such co-herent radiation are discussed with reference to some of the schemes of generation described below. The follow-ing sections list some ideas related to umw genera-tion.

A. Conventional Microwave Tube Techniques

As the useful radio spectrum was raised to increas-ingly higher frequencies, radical changes in schemes for generation and amplification were required. Such basic limitations as transit time of electrons and the dis-tributed circuit effects were not only overcome, but were put to use in klystrons and magnetrons, where transit time is used to "bunch" electrons; and the inter-action between electrons and fields now takes place in-side or in the immediate vicinity of distributed circuit resonators.

However, as the frequency approaches 300 kmc, even klystrons and magnetrons become increasingly difficult to build and operate. For the usual (fundamental) mode of operation the dimensions of the resonant elements are somewhat smaller than the wavelength to be gener-ated. Dimensions of a reflex klystron cavity that oscil-lated at 5.5 mm when coupled by 1600-v electron beam are shown in Fig. 1.[3] It is easily seen that to reduce these dimensions by a factor of ten and hold any reasonable degree of tolerances is practically out of the question.
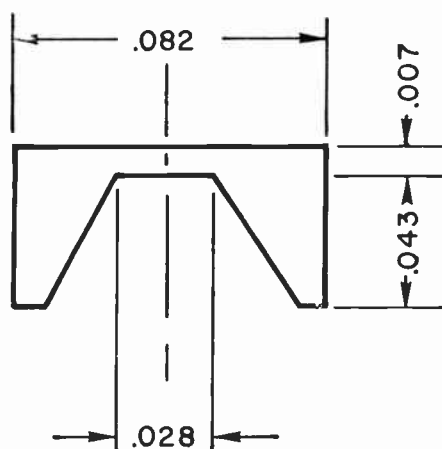

Fig. 1—Dimensions of klystron cavity of $\lambda_0 = 5.5$ mm (after Lafferty). Note: all dimensions in inches.

An equally serious problem is met from current den-sity considerations. An oscillator tube requires a mini-mum, or "starting" current before it can maintain oscil-lations; an amplifier tube has gain only under sufficient current flow. Since the area allowed for electron beam passage decreases with increase in frequency, the cur-rent density must be raised. This is limited, however, by the cathode emission density that can be achieved and by the ability to contain the beam. The limitations are summarized:

[3] J. M. Lafferty, "A millimeter-wave reflex oscillator," *J. Appl. Phys.*, vol. 17, pp. 1061–1066; December, 1946.

1) Mechanical construction [linear dimension $\sim (1/f)$].
2) Losses (by skin effect, $\sim f^{1/2}$).
3) Current density ($\sim f^{5/2}$).
4) Heat dissipation per unit volume ($\sim f^{7/2}$).

Despite these limitations, reflex klystrons are now commercially available to 69.5–77.5 kmc ($\lambda \approx 4$ mm).[4]

More spectacular even are the results of magnetron research. An example of the achievements in that field is given by the following characteristics of a magnetron developed at the Columbia Radiation Laboratory:[5]

Tube no. = RPB 3-27A.
Wavelength = 3.32 mm.
Maximum power output = 8.9 kw.
Efficiency = 8.1 per cent.
Pulse length = 0.30 μsec.
Duty cycle = 0.00015.

Columbia magnetrons have also operated at 2.6 mm,[6] though it is reported that the difficulties of in-creasing the frequency become extremely severe. There has been some success recently in designing centimeter-wave magnetrons for optimizing harmonic output.[7] Per-haps this technique can be extrapolated to the low millimeter range.

Klystrons and magnetrons use cavities in which the region of interaction between electron stream and an electromagnetic wave is confined to a small, closed volume. In the traveling-wave tube this situation is somewhat alleviated. By stretching the interaction over many cycles, only two dimensions need to be minute. Tolerances in the periodicity of the structure, however, now become a critical factor.

The highest frequency traveling-wave tube reported in the literature to date is Karp's 200-kmc backward wave oscillator.[8] Its basic structure is illustrated in Fig. 2. It uses a beam voltage of 2500 volts and produces a power output of somewhat less than 1 mw. As in other traveling-wave tubes, it uses a structure that reduces the phase velocity of the electromagnetic wave to nearly the electron beam velocity, so that coherent energy ex-change between electron beam and waves exists through-out the length of the tube. It is a characteristic of such a "slow wave structure" that the fields are strong only in the immediate vicinity of the walls. For a 200-kmc slow wave structure satisfactory for a 2500-v beam the situation is so drastic that the only electrons that inter-

[4] For example, the Amperex Type DX-151, developed by Philips Res. Labs., Eindhoven, The Netherlands.
[5] "Research Investigation Directed Toward Extending the Useful Range of the Electromagnetic Spectrum," Columbia Rad. Lab., Columbia Univ., New York, N. Y., Signal Corps Contract DA-36-039 SC-64630; December 15, 1956.
[6] M. J. Bernstein and N. M. Kroll, "Magnetron research at Columbia Radiation Laboratory," IRE TRANS. ON MICROWAVE THEORY AND TECHNIQUES, vol. MTT-2, pp. 33–35; September, 1954.
[7] "Research Investigation Directed Toward Extending the Useful Range of the Electromagnetic Spectrum," Columbia Rad. Lab., Columbia Univ., New York, N. Y., Signal Corps Contract DA-36-039 SC-64630; September 15, 1957.
[8] A. Karp, "Backward-wave oscillator experiments at 100 to 200 kilomegacycles," PROC. IRE, vol. 45, pp. 496–503; April, 1957.

act appreciably with the field lie within $\lambda_0/100$ of the structure, where λ_0 is the free-space wavelength of the field. Because of limits in cathode emission and space charge repulsion, this means only few electrons are useful, even in a strong axial magnetic field with perfect mechanical alignment. Karp, accordingly, comments that the possibility of reaching frequencies higher than 200 kmc is limited chiefly by the beam density.
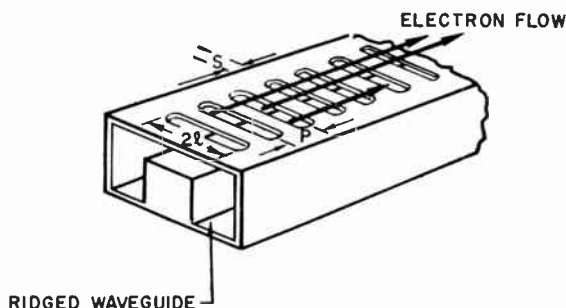

Fig. 2—Basic circuit structure of 200-kmc backward-wave oscillator (after Karp). For 200 kmc, $P=0.005$ inch, $2l=0.024$ inch, and $S=0.002$ inch.

Some of the limitations of present microwave tubes might be overcome by the following techniques:

1) Beams of electrons of megavolt energies: For such beams the radial space charge repulsion problem is less severe than for low-voltage beams. More important, they have velocities close to the velocity of light and can therefore interact with the transversely extended fields of fast wave structures and of higher order mode resonators,[9] which are physically larger and therefore easier to fabricate than fundamental-mode resonators.

2) Monotrons using higher order mode resonators: A recent analysis[10] indicates the possibility of a 300-kmc monotron, provided a rather severe requirement of electron beam density can be met in practice.

3) Traveling-wave interaction of the field of an unloaded structure with the space harmonic type of space charge wave: In contrast with a slow wave structure, the fields of a fast wave, or unloaded structure, can extend far from the structure. These fields can interact with a fast space charge wave of a low-voltage electron beam to produce gain or oscillations. A simple example is shown in Fig. 3(a), where an electron beam interacts only intermittently, but synchronously with a field that moves against the beam. Here, if an electron is to interact only with the peak of each wave it encounters, the requirement for synchronism is

$$v_p = u_0 \left(n \frac{\lambda_q}{p} - 1 \right) \qquad (1)$$

where

$v_p =$ phase velocity of wave,
$u_0 =$ electron beam axial velocity,
$\lambda_q =$ guide wavelength,
$p =$ axial period of beam,
$n =$ an integer.

By making n arbitrarily large, synchronism for arbitrarily large phase velocities can be achieved.

Traveling-wave tube interaction without slow wave structures has been treated by several authors.[11] Construction of a working model of a Helical Beam Oscillator at S band that operates in this manner, shown in Fig. 3(b), has recently been achieved by Pantell[12] at Stanford University.

4) High pulsed magnetic fields for beam containment: This method, however, is accompanied by the very difficult problem of operating conductors in pulsed magnetic fields.
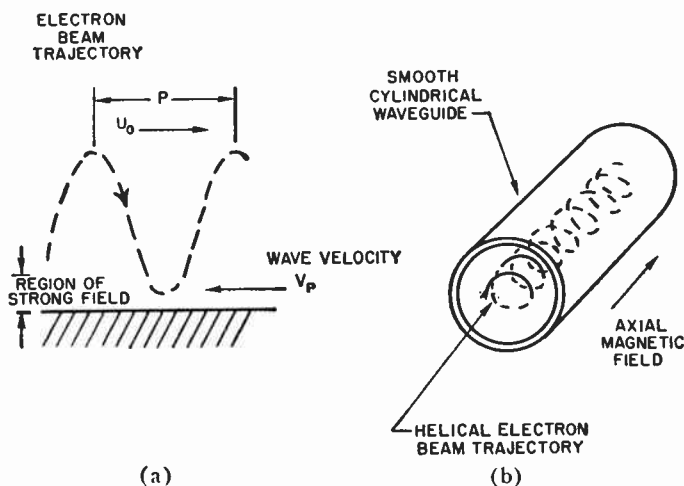
5) New methods of beam focusing.

Fig. 3—Traveling-wave tube oscillator operating on principle of intermittent interaction. (a) A general scheme. (b) Helical beam oscillator (after Pantell).

It can be concluded from the preceding discussion that the extension of existing microwave tube techniques into the umw range must be accompanied by rather revolutionary methods, if it is possible to accomplish at all.

B. Black Body Radiation

Among the sources of umw power, the most obvious is black body radiation. It is of interest to compute the amount of power available here. For the 300–3000-kmc range the Rayleigh-Jeans approximation to Planck's

[9] M. D. Sirkis and P. D. Coleman, "The harmodotron—a megavolt electronics millimeter wave generator," *J. Appl. Phys.*, vol. 28, pp. 944–950; September, 1957.

[10] H. D. Arnett and A. J. Ruhlig, "A Starting-Current Analysis of Monotrons with a Cylindrical TM_{01n} Resonator," Naval Res. Lab., Washington, D. C., Rep. 4819; September 5, 1956.

[11] For a discussion and bibliography, see R. Müller, "Teilwellen in Elektronenströmung," *Arch. elek. Übertragung*, vol. 10, pp. 505–511; December, 1956.

[12] R. H. Pantell. Private communication.

law is applicable. It has been shown[13] that the available power from an antenna that points at a surface of temperature T and delivers power through a single mode transmission line can be computed through application of the Rayleigh-Jeans law or its equivalent, the formula for Johnson noise,

$$P_f = kT. \quad (2)$$

Here

P_f = available power per unit frequency increment,
k = Boltzmann's constant,
T = absolute temperature.

For a receiver capable of absorbing all the energy received between 300 and 400 kmc, and for a radiating surface at 10,000°K, the power received is

$$P = kT\Delta_f = 1.38 \times 10^{-8} \text{ watts.} \quad (3)$$

We see that even for such a wide-band receiver of bandwidth that is 29 per cent of the center frequency, the amount of power involved is only minute. Because of the much lower number of "frequencies," this power is much lower than that received for the same relative bandwidth in the infrared range. Therefore, although black body radiation can be detected by radiometric means,[14] it is not the answer to the problem of generating appreciable power (watts) in the 300–3000-kmc range.

In the search for umw generators black body radiation would, at best, be only a stopgap measure. We ultimately desire single frequency sources which could be controlled and modulated in the manner of lower frequency engineering. At present, however, the generation of appreciable amounts of umw power of any quality would be an achievement.

C. Spark Oscillators and Mass Radiators

The earliest laboratory sources of radio waves were spark oscillators that excited Hertzian dipoles. These were used by a number of workers prior to 1900 to produce centimeter and millimeter wave radiation.[15] Nichols and Tear[16] used this type of oscillator to bridge the gap between infrared and radio waves by producing 0.22 mm radiation in 1923. In the operation of such oscillators there occurs a charging and discharging of small conductors, whose dimensions determine the frequencies of radiation.

If by either conduction or induction a nonequilibrium charge distribution is placed on a conductor, this conductor radiates at frequencies close to its natural frequencies. The situation is analogous to an LC tank circuit which has been impulse excited and then "rings" at the resonant frequency of the tank.

An example of radiation by such oscillations is given by Stratton,[17] who treats the problem of the natural modes of a sphere. For a perfectly conducting excited sphere in free space the fields in the lowest (and least damped) mode vary as

$$\epsilon^{-i\omega t} = \epsilon^{\frac{0.5ct}{a} \mp i\frac{0.86ct}{a}} = \epsilon^{\alpha t \mp i\omega_0 t} \quad (4)$$

where

a = radius of sphere,
c = velocity of light.

From this equation the following is obtained:

$$\omega_{0_{rad}} = \frac{0.86c}{a}; \qquad \lambda_{rad} = \frac{2\pi c}{\omega_0} = 7.3a \quad (5)$$

$$Q_{sphere} = \frac{\omega_0}{2\alpha} = 0.86. \quad (6)$$

The wavelength of the radiation is therefore of the order of magnitude of the diameter of the sphere. The Q of the system, however, is only about 1, so that the resulting spectrum from a shock-excited sphere will be quite broad. It is of interest to note that the damping here is due entirely to radiation.

For other configurations, such as a thin dipole, the Q is considerably above 1, so that the resulting radiation will be of narrower band.

There has been considerable work on such oscillators, or mass radiators (Massensender, as they are sometimes called). An example is the work of Cooley and Rohrbaugh,[18] who generated 0.2–2.2-mm radiation from small aluminum particles suspended in a rapidly flowing stream of oil in a gap pulsed with high voltages, then used this radiation with gratings for the identification of HI absorption lines. Another recent mass radiator, the Clarendon generator,[19] emitted about 30 mw with a spectrum spread from 3 to 9 mm.

Thus the mass radiator is indeed a umw generator and has been used as a source for scientific investigations. However, the models built have been characterized by broad spectra with only small power output in any very narrow frequency increment and with considerable fluctuations in output level.

D. Harmonic Generators

Manley and Rowe[20] have shown that, ideally, by use

[13] R. H. Dicke, "The measurement of thermal radiation at microwave frequencies," *Rev. Sci. Instr.*, vol. 17, pp. 268–275; July, 1946.
[14] H. H. Theissing and P. J. Caplan, "Atmospheric attenuation of solar mm wave radiation," *J. Appl. Phys.*, vol. 27, pp. 538–543; May, 1956.
[15] For an interesting account of these early techniques, see J. F. Ramsay, "Microwave antenna and waveguide techniques before 1900," PROC. IRE, vol. 46, pp. 405–415; February, 1958.
[16] E. F. Nichols and J. D. Tear, "Joining the infrared and electric wave spectra," *Proc. Natl. Acad. Science*, vol. 9, pp. 211–214; 1923.

[17] J. A. Stratton, "Electromagnetic Theory," McGraw-Hill Book Co., Inc., New York, N. Y., pp. 558–560; 1900.
[18] J. P. Cooley and J. H. Rohrbaugh, "The production of extremely short electromagnetic waves," *Phys. Rev.*, vol. 67, pp. 296–297; May, 1945.
[19] R. Q. Twiss, "On the generation of millimeter radiation," *Services Electronics Res. Lab. Tech. J.*, vol. 2, p. 10; 1952.
[20] J. M. Manley and H. E. Rowe, "Some general properties of nonlinear elements," PROC. IRE, vol. 44, pp. 904–913; July, 1956.

of a nonlinear reactance all the power from a source can be converted to power at any or all harmonics of the source frequency. This principle makes harmonic generation very attractive for the production of umw power. Although the ultimate goal in the search for umw sources is a compact primary source, the production of considerable umw power by harmonic generation techniques will be a distinct achievement.

Although practical limitations have until now prevented the efficient conversion of lower frequency power into a harmonic located in the umw range, it is harmonic generation that has yielded the only essentially single frequency sources of umw power (in minute amounts) to date.

There are a number of schemes of generating harmonics. Some of those investigated or considered follow.

1) Harmonics from Electron Beam

a) Direct harmonic output of microwave tubes: The equations of electron motion in microwave tubes contain nonlinear terms. Although these terms are normally small, they do predict harmonic components. Following are results of the harmonic content measurements of type 3J31 magnetrons,[21] whose fundamental wavelength is 1.25 cm:

Fundamental power = 2.0×10^4 watts.
3rd harmonic power = 2.4×10^{-1} watts.
8th harmonic power = 1.8×10^{-4} watts.
10th harmonic power ($\lambda = 1.25$ mm)
    (peak of several tubes) = 1.2×10^{-4} watts.

It is seen that the harmonic content of such a tube is surprisingly small.

b) Microwave tubes designed for high harmonic content: There have been a number of attempts at designing microwave tubes for the specific purpose of harmonic generation. A Columbia Radiation Laboratory magnetron,[7] for example, has recently produced 12 kw at the fundamental wavelength of 3.39 cm, but up to 34 kw at the second harmonic. Similar tubes have produced up to 1.2 kw at the third harmonic.

Klystrons have also been designed for high harmonic generation. With a klystron cavity resonant at a fundamental frequency as well as at a harmonic, Bernier and Leboutet[22] were able to produce power simultaneously at 4.08 cm and 1.7 mm, the 24th harmonic.

c) Tightly bunched relativistic electron beams: In the rebatron,[23,24] a compact, pulsed 1-mev linear accelerator, the electrons of a beam are bunched into tight, high density bunches by high intensity RF electric fields. The resultant output current has a very high harmonic content. This electron current has been used to shock-excite a higher order mode harmodotron[25] cavity to generate power at a high harmonic of the linear accelerator driving frequency. (See Fig. 4.) Generation up to the 34th harmonic ($\lambda = 3.18$ mm) of the *S*-band driving frequency has been reported.
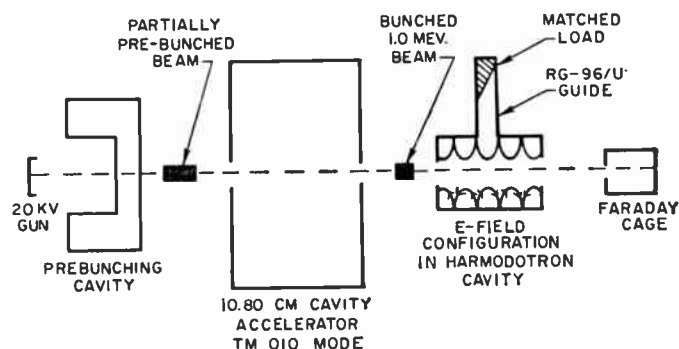

Fig. 4—Rebatron-harmodotron assembly (after Sirkis and Coleman). Fundamental frequency = 2.77 kmc, harmonic frequency (here) = 36.1 kmc.

Advantages claimed for the rebatron over other electron bunching schemes are:

1) Extremely tight bunching, corresponding to the production of harmonics up to the 1000th harmonic, has been predicted.
2) The high velocity permits a high density bunch to be maintained for a long distance.
3) The use of million-volt electrons eliminates the need for slow wave coupling structures, permitting higher order mode harmonic output coupling cavities of reasonable size and electron beams of relatively large cross-sectional area.

A disadvantage is the high-power requirement, which makes the rebatron inherently a pulsed device.

d) Field emission: The approximate current-voltage relationship for field emission[26] is

$$I = C\epsilon^{-B/v}. \tag{7}$$

This highly nonlinear behavior immediately suggests the use of field emission for frequency multiplication. The extensive development in field emission in the last few years[27] has made it feasible to use fine wire field emitter cathodes in some types of electron tubes. A particular scheme that has been considered[28] uses a cavity that is resonant at the driving frequency as well as at

[21] J. A. Klein, N. Lobser, A. H. Nethercott, Jr., and C. H. Townes, "Magnetron harmonics at millimeter wavelengths," *Rev. Sci. Instr.*, vol. 23, pp. 78–82; February 23, 1952.

[22] J. Bernier and H. Leboutet, "Sur la possibilité d'obtenir des ondes entretenues très courtés en utilisant un klystron reflex donnant de l'energie sur des frequences harmonique d'ordre élevé de l'ocillation fondomentale," *Acad. Sci., Compt. Rend. (Paris)*, vol. 239, pp. 796–798; October 4, 1954.

[23] P. D. Coleman, "Theory of the rebatron—a relativistic electron bunching accelerator for use in megavolt electronics," *J. Appl. Phys.*, vol. 28, pp. 927–935; September, 1957.

[24] I. Kaufman and P. D. Coleman, "Design and evaluation of an S-band rebatron," *J. Appl. Phys.*, vol. 28, pp. 936–944; September, 1957.

[25] M. D. Sirkis and P. D. Coleman, "The harmodotron—a megavolt electronics millimeter wave generator," *J. Appl. Phys.*, vol. 28, pp. 944–950; September, 1957.

[26] P. A. Milliken and C. C. Lauritsen, *Proc. Natl. Acad. Science*, vol. 14, pp. 45–49; January 15, 1928.

[27] W. P. Dyke and W. W. Dolan, "Field emission," *Advances in Electronics and Electron Phys.*, vol. 8, pp. 89–185; 1956.

[28] Elec. Eng. Res. Lab., Univ. of Illinois, Urbana, Ill., Contract AF 18 (603)-62, Rep. No. 7; December 1, 1957.
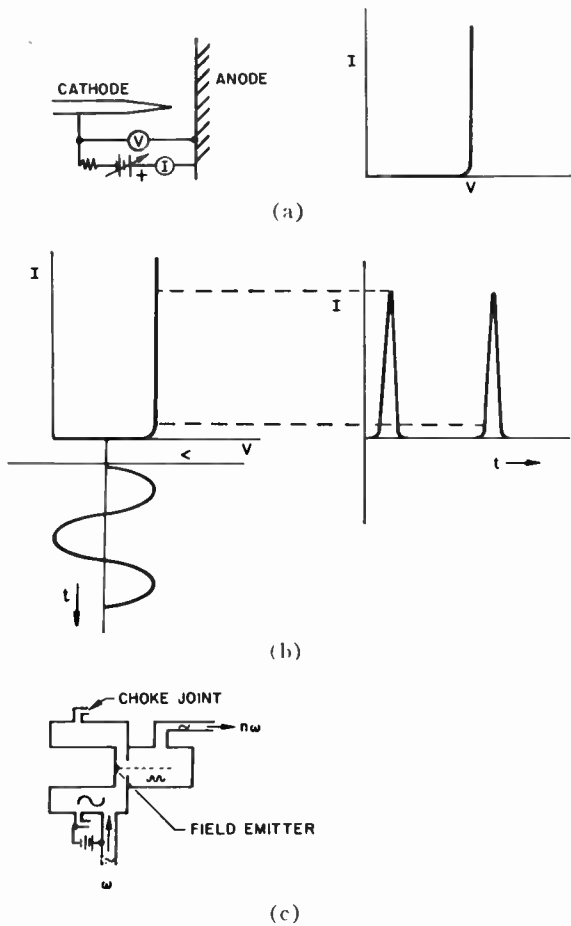
Fig. 5—Field emitter. (a) Current-voltage characteristic. (b) Use of characteristic to achieve nonsinusoidal currents. (c) Conceptual harmonic multiplier.

its fourth harmonic. The fields are such as to cause short pulses of electrons, which then give up some of their energy to the fourth harmonic fields. (See Fig. 5.)

Since field emission cathodes are of microscopic size, their use in very short wave (umw) generation is additionally attractive. Their practical application to this field, however, is still a challenging problem.

2) Harmonics from Other Nonlinear Effects

a) Metal semiconductor junctions: The current-voltage characteristic of a metal semiconductor junction is given by[29]

$$I = A(\epsilon^{aV} - 1). \tag{8}$$

As in the field emitter, the exponential dependence of current on voltage causes the junction to act as a highly nonlinear resistance and therefore makes it useful for frequency conversion. This was recognized early and resulted in the development of the microwave point contact crystal diode.

To date, the only sources of essentially single frequency umw power are harmonic generators using such
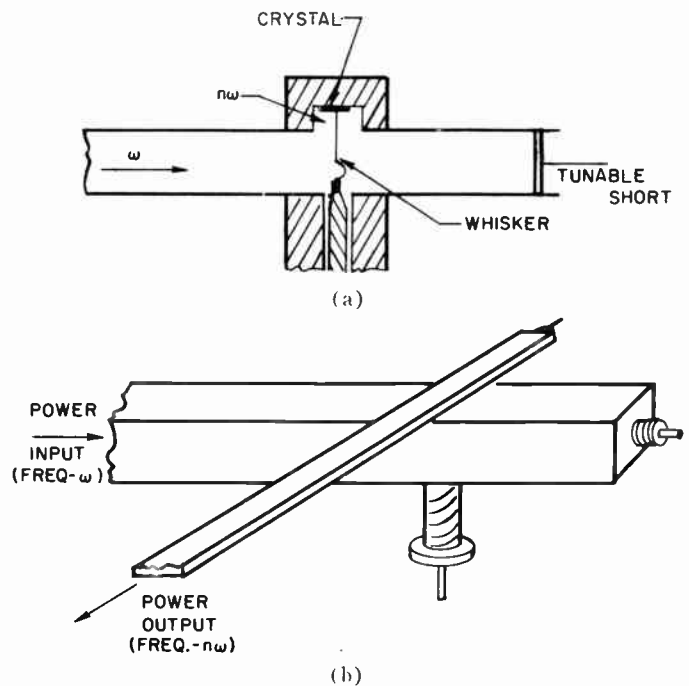
[29] H. C. Torrey and C. A. Whitmer, "Crystal Rectifiers," McGraw-Hill Book Co., Inc., New York, N. Y. 1948.

Fig. 6—Crossed waveguide harmonic multiplication using point contact rectifier.

microwave diodes.[30] With K-band klystrons feeding point contact crystal rectifiers, energy up to 511 kmc has been extracted.[31] Fig. 6 shows a typical arrangement.

Here energy at the fundamental frequency enters the large waveguide and encounters the whisker antenna placed across it. A voltage is induced across the barrier layer of the point contact junction. Because of the nonlinear V-I characteristic the resulting antenna current contains harmonics, which radiate harmonic energy into the small waveguide.

Power generated by this technique has been quite low. A typical efficiency reported[32] for conversion from 24 kmc to the fifth harmonic at 120 kmc is −60 db. For a typical input power of 3.5×10^{-2} watts, this means a fifth harmonic power output of 3.5×10^{-8} watts.

The point contact rectifier acts as a nonlinear resistance and is therefore inefficient. Harmonic generation by the nonlinear Q-V curve of an element, *i.e.*, by a nonlinear capacitance, can have efficiencies up to 100 per cent.[20] There has been considerable recent emphasis on the development of such nonlinear capacitances for microwave parametric amplification, utilizing the voltage-sensitive depletion layer capacitance of a p-n junction. For a linearly graded junction this is given by[33]

[30] See for example, W. C. King and W. Gordy, "One-to-two millimeter wave spectroscopy. IV. Experimental methods and results for OCS, CH_3F, and H_2O," *Phys. Rev.*, vol. 93, pp. 407–412; February 1, 1954.

[31] M. Cowan and W. Gordy, "Further extension of microwave spectroscopy in the submillimeter wave region," *Phys. Rev.*, vol. 104, pp. 551–552; October 15, 1956.

[32] C. M. Johnson, D. M. Slager, and D. D. King, "Millimeter waves from harmonic generators," *Rev. Sci. Instr.*, vol. 25, pp. 213–217; March, 1954.

[33] W. Shockley, "The theory of p-n junctions in semiconductors and p-n junction transistors," *Bell Sys. Tech. J.*, vol. 28, pp. 435–489; July, 1949.

$$C \approx \frac{C_0}{\sqrt[3]{1 - V/\Phi}} \qquad (9)$$

where

V = applied voltage,
C_0 and Φ are constants.

To date, however, such variable capacitance diodes are still limited to UHF and the lower microwave frequencies.

Frequency limitations of the point contact rectifier are illustrated in the simplified equivalent circuit in Fig. 7,[29] which shows an undesirable barrier shunting capacitance, C, and a series resistance, r, the so-called "spreading resistance" of the rectifier contact. At high frequencies these two elements reduce the voltage across the nonlinear resistance R and thereby reduce the efficiency of the crystal as a nonlinear element and harmonic generator. In a recent paper Messenger[34] has indicated methods for reducing the RC product to lead the way, among other things, to more dependable crystal harmonic generators that are effective well into the umw range.

Harmonic multiplication by *p-n* junctions, even if it can be made more efficient, is at low power levels (<1 watt) since the nonlinearity used resides in a minute volume. To produce high power by harmonic generation it is necessary to employ other means.

b) Volume nonlinearities: To produce a high level harmonic generator it is necessary to use materials that exhibit nonlinearities throughout a relatively large volume. Examples are nonlinear dielectrics, plasmas, and ferrimagnetic materials. To date no dielectrics suitable for harmonic generation (high nonlinearity, low losses) to umw have been reported.

i. Plasmas: Margenau and Hartman,[35] discussing the theory of high-frequency gas discharges, show that the current density in an ac gas discharge can be expressed as:

$$I_x = \frac{4}{3} \pi e \int_0^\infty \Big\{ f_0'$$

$$+ \sum_m (f_m' \cos m\omega t + g_m' \sin m\omega t) \Big\} v^3 dv. \quad (10)$$

Here

I_x = current density,
x = direction of applied ac field,
ω = applied field frequency,
v = electron speed,
f_0', f_m', and g_m' are functions related to the velocity distribution, computed by use of the Boltzmann transfer equation.

[34] G. C. Messenger, "New concepts in microwave mixer diodes," PROC. IRE, vol. 46, pp. 1116–1121; June, 1958.
[35] H. Margenau and L. M. Hartman, "Theory of high frequency gas discharges. II. Harmonic components of the distribution function," *Phys. Rev.*, vol. 73, pp. 309–315; February 15, 1948.
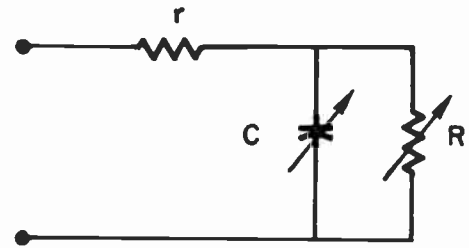

Fig. 7—Equivalent circuit of a crystal rectifier. r = spreading resistance, caused by constriction of current lines in semiconductor in vicinity of junction; may be reduced by increasing conductivity. C = barrier shunting capacitance [see (9)]. R = barrier nonlinear resistance [see (8)].

This presence of harmonic content in the current density has been demonstrated by Uenohara, *et al.*,[36] using a microwave discharge between two posts in a waveguide at S band. They report the following conversion:

Fundamental power input = 12.4 watts.
Second harmonic output = 60 mw.
Third harmonic output = 21 mw.
Fourth harmonic output = 0.6 mw.

By essentially the same scheme, approximately 10 mw of seventh harmonic power from a discharge fed by a 10-kw X-band source have recently been obtained.[37]

Second harmonic generation has also been accomplished by cyclotron resonance in a plasma.[38] Here a plasma is placed in a magnetic field and excited to cyclotron resonance by an RF field. Because of the influence of both electric and magnetic RF field components, the oscillating electron motion has harmonic components, so that harmonic currents flow in the plasma. These are coupled to an output system to generate harmonic power.

The magnetic field required for cyclotron resonance is

$$B = \frac{\omega m}{e}, \qquad (11)$$

where

B = flux density (webers/sq. m).
ω = angular frequency,
m = electronic mass,
e = electronic charge.

For cyclotron resonance of free electrons at 300 kmc ($\lambda = 1$ mm), $B = 10.7$ webers/sq. m. Such a high magnetic field is beyond the realm of easily attainable flux densities. Lower magnetic fields should be possible,

[36] M. Uenohara, M. Uenohara, T. Masutani, and K. Inada, "A new high-power frequency multiplier," PROC. IRE, vol. 45, pp. 1419–1420; October, 1957.
[37] Private communication with Prof. P. D. Coleman, Univ. of Illinois, Urbana, Ill.
[38] Hughes Aircraft Co., Culver City, Calif., Signal Corps Contract DA 36-039 SC-73063, Final Progress Rep.; July 1, 1956–June 30, 1957.

however, if particles of higher charge-to-mass ratio, such as the effective mass electrons and holes of semiconductors, are used. It should therefore be possible to use a semiconductor as the plasma in cyclotron resonance at low millimeter waves with reasonable magnetic fields[38] so that umw harmonic power results.

ii. *Ferrites:* The frequency doubling capabilities of ferrites have been demonstrated, both from X band and from the 70-kmc range.[39],[40] A conversion efficiency of 25 per cent has been obtained from a pulsed 32-kw X-band source. For the 70-kmc experiments a peak pulse power output of 9 watts at 2 mm was reported.

The nonlinear effect utilized here occurs because the magnetization of a ferrimagnetic material obeys the well-known Bloch equation

$$\frac{d\overline{M}}{dt} = \gamma(\overline{M} \times \overline{H}). \tag{12}$$

Here, for simplicity, the damping term has been omitted. An example of the frequency multiplication behavior is shown by (13) for a ferrite saturated in the Z direction by a dc field, with an RF field h_x applied,

$$\dot{m}_x = \gamma m_y H_0$$
$$\dot{m}_y = \gamma(M_0 h_x - m_x H_0)$$
$$\dot{m}_z = -\gamma m_y h_x. \tag{13}$$

Here capital letters designate steady-state terms, small letters ac terms. The quantity γ is the gyromagnetic ratio, 1.76×10^7 radians/second oersted. A sinusoidal field h_x of frequency ω causes an RF m_x and m_y, also of frequency ω. Since $\dot{m}_z$ is the product of two sinusoids, its frequency is 2ω, so that frequency doubling exists.

The presence of higher harmonics has also been detected. The writer has detected the third, fourth, and fifth harmonic in a microwave circuit similar to that of Melchor, Ayres, and Vartanian.

E. Plasma Oscillations

The electrons in the plasma of an ionized gas can oscillate about their mean locations. Associated with synchronous oscillations of electrons in a plasma is a resonant "plasma frequency."[41] It is hoped that a plasma can be excited to act as a distributed resonator, thus eliminating the consideration of impossibly small dimensions normally associated with umw.

There are three facets to the problem of generating umw power by plasma oscillations:

1) Creation of the necessary plasma densities.
2) Excitation of plasma oscillations.

3) Conversion of the kinetic energy of plasma oscillations into electromagnetic energy.

The density of ionized electrons is related to the plasma frequency by[41]

$$N = 1.3 \times 10^{-8}f^2, \tag{14}$$

where

N = number of electrons per cm^3,
f = plasma resonant frequency.

Thus, plasma resonance at 300 kmc requires 1.1×10^{15} electrons/cm^3. An electron density of 10^{13} electrons/cm^3 has usually been considered high for gas discharge devices. Recently, however, a hollow glow discharge has been described, which is capable of stable operation at high densities.[42] In this discharge, shown in Fig. 8, the main glow is confined to the inside of a spherical cavity, so that material sputtered away from the cathode is redeposited on it instantly. Measurements of the properties of this discharge have shown that plasma densities in excess of 10^{15} electrons/cm^3 may be obtained.[43]
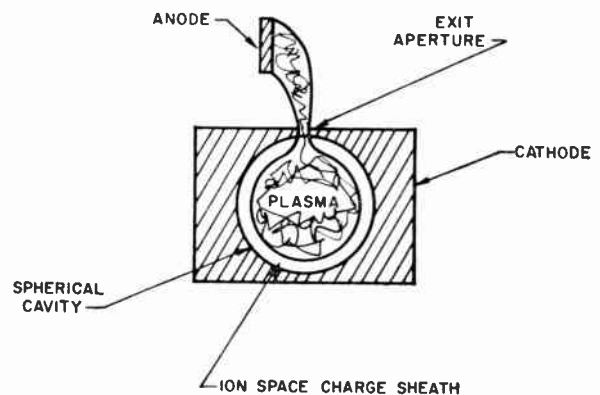

Fig. 8—Cross section of basic structure for hollow cathode glow discharge (after Hernquist).

The other two facets of the volume plasma oscillation problem, *i.e.*, excitation and coupling at umw frequencies, have apparently not yet been solved. A method that has been considered for producing plasma oscillations is excitation by an electron beam which would originate in the main discharge or be externally injected.

A successful centimeter range oscillator utilizing a plasma was described by Wehner.[44] This tube, shown in Fig. 9, was similar to a two-cavity klystron, in that two regions of RF fields were separated by a neutral region. Oscillations existed therefore in sheaths, instead of in the main plasma. Such sheath oscillations have also been reported by Gabor[45] and others. We know of no success-

[39] J. L. Melchor, W. P. Ayres, and P. H. Vartanian, "Microwave frequency doubling from 9 to 18 kmc in ferrites," Proc. IRE, vol. 45, pp. 643–646; May, 1957.
[40] W. P. Ayres, "Millimeter wave generation utilizing ferrites," presented at 1958 PGMTT Natl. Symp., Stanford Univ., Stanford, Calif.; May 5–7, 1958.
[41] L. Tonks and I. Langmuir, "Oscillations in ionized gases," Phys. Rev., vol. 33, pp. 195–210; February, 1929.

[42] A. D. White, "A novel form of hollow cathode and its discharge characteristics," presented at Ninth Ann. Conf. on Gaseous Electronics, Pittsburgh, Pa.; November, 1956.
[43] K. G. Hernqvist, "Hollow cathode glow discharge in mercury vapor," RCA Rev., vol. 19, pp. 35–48; March, 1958.
[44] G. Wehner, "Electron plasma oscillations," J. Appl. Phys., vol. 22, pp. 761–765; June, 1951.
[45] D. Gabor, "Plasma oscillations," IRE Trans. on Antennas and Propagation, vol. AP-4, pp. 526–530; July, 1956.
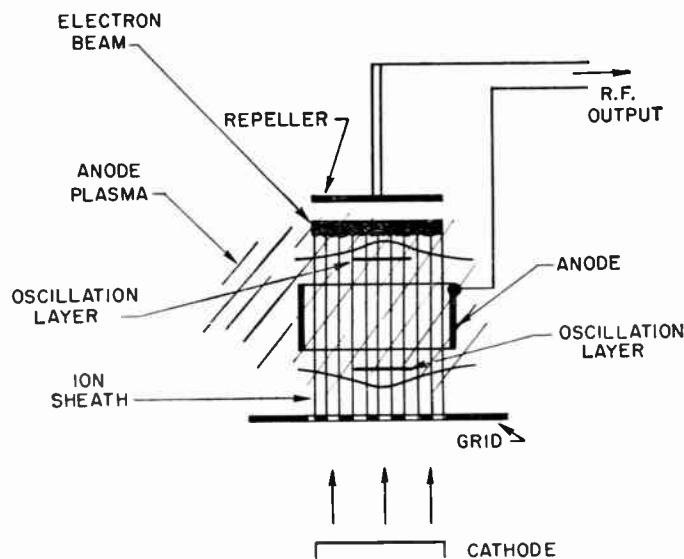
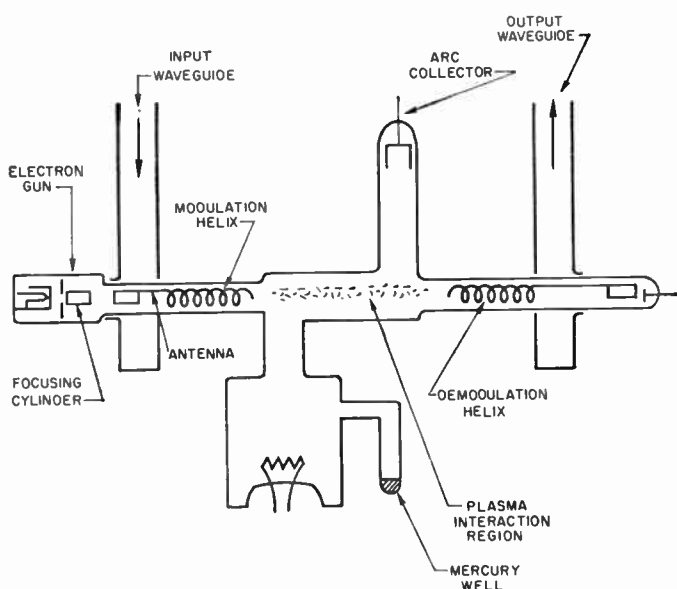Fig. 9—Electron plasma oscillator (after Wehner).

Fig. 10—Plasma amplifier (after Boyd, *et al.*).

ful attempts to carry Wehner's work to the millimeter or umw range.

The distributed interaction of an electron beam with a gaseous plasma at centimeter wavelengths was recently demonstrated by Boyd, *et al.*[46] In this scheme, shown in Fig. 10, an electron beam is velocity modulated by a helix, sent through a mercury discharge, then passed through an output coupling helix. The interaction of beams and plasma waves, very similar to that in the double stream amplifier,[47] produces traveling-wave tube gain, *i.e.*, electron bunching that increases exponentially with distance.

To adapt this scheme to a successful umw oscillator would require:

1) The high plasma and beam densities previously discussed.
2) Successful interaction of beam with a backward wave plasma mode, so that a feedback mechanism without external circuitry exists.
3) A method of converting electron kinetic energy into umw electromagnetic energy.

Several other schemes of exciting plasma oscillations have been proposed. One of these involves the use of 5-mev alpha particles for generating transient high-frequency plasma oscillations.[48] In another,[49] excitation of the plasma of a doped semiconductor with its built-in high electron densities has been considered. Here collision damping appears too high to permit build-up of oscillations except, perhaps, at very low temperatures.

F. Doppler-Shifted Radiation

The frequency of a wave seen by an observer is Doppler-shifted by relative motion between observer and source of the radiation. This source may either be the primary radiator or a moving mirror reflecting incident radiation.

1) Moving Radiator: An electron that oscillates about a fixed point in space radiates electromagnetic energy, primarily at the frequency of the oscillations. If this electron simultaneously undergoes translational motion at a speed close to the velocity of light, the radiation is Doppler shifted to a band of much higher frequencies. To a first-order approximation, a "mechanical wavelength" λ_e (Fig. 11) is compressed into an electromagnetic wavelength λ_p, according to

$$\lambda_p = \frac{\lambda_e}{\beta} (1 - \beta \cos \theta), \qquad (15)$$

where $\beta = v/c$, *i.e.*, the ratio of electron velocity to the speed of light.

A typical value of electron speed required to produce a reasonable amount of wavelength compression is $v = 0.989c$, for $\lambda_e = 5$ cm, a desired $\lambda_p = 0.5$ mm, and $\theta = 0$. The energy of an electron of $\beta = 0.989$ is 3 mev, a number that can easily be achieved with a small linear accelerator.

Such a scheme of generating umw has been considered by a number of workers.[50-52] A particular embodiment of the idea is given in Fig. 12. The radiation is

[46] G. D. Boyd, L. M. Field, and R.W. Gould, "Excitation of plasma oscillations in growing plasma waves," *Phys. Rev.*, vol. 109, pp. 1393–1394; February 15, 1958.
[47] A. V. Haeff, "The electron-wave tube," Proc. IRE, vol. 37, pp. 4–10; January, 1949.

[48] L. Goldstein, "Electromagnetic wave generation," U. S. Patent No. 2,712,069.
[49] M. A. Lampert, "Plasma oscillations at extremely high frequencies," *J. Appl. Phys.*, vol. 27, pp. 5–11; January, 1956.
[50] V. L. Ginsburg, *Bull. Acad. Sci. U.S.S.R. Ser. Phys.*, vol. 11, pp. 165–182; 1947.
[51] P. D. Coleman, "Theory of Generation of Submillimeter Waves by Accelerated Electrons, 1. Doppler Effect," Univ. of Illinois, Urbana, Ill., AF 18(600)-23 Eng. Rep. No. 1-1; 1952.
[52] H. Motz, "Cerenkov and undulator radiation," IRE Trans. on Antennas and Propagation, vol. AP-4, pp. 374–384; July, 1956.
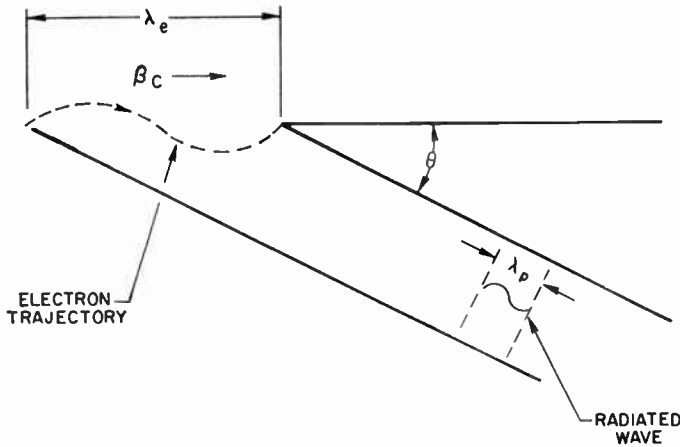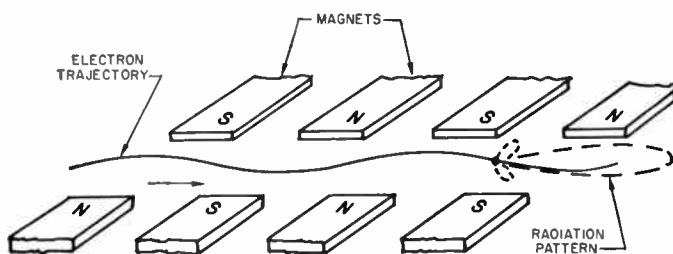
Fig. 11—Doppler-type wavelength compression.

Fig. 12—Doppler-shifted radiation from fast electrons.

not monochromatic. Its frequency is not only angular dependent, as shown by (15), but is a continuous spectrum of limits[51] (on the axis)

$$\left(\frac{1-\beta}{\beta}\right)\lambda_e \leq \lambda_p \leq \left(\frac{1+\beta}{\beta}\right)\lambda_e. \qquad (16)$$

The major portion of this energy lies at the higher frequencies. The power radiated by a single electron per cycle of motion,[51] P_{AV},

$$P_{AV} = (9)(10^{-14})\left(\frac{a}{\lambda_e^2(1-\beta)}\right)^2 \text{ watts}, \qquad (17)$$

where

a = amplitude of oscillations (cm),
λ_e = mechanical wavelength (cm),
$a \ll \lambda_e$.

We see that the amount of power radiated varies as

$$\left(\frac{1}{1-\beta}\right)^2,$$

so that, from the viewpoint of maximizing power, it is desirable to have β as large as possible. For the typical values of $a/\lambda_e = 0.10$, $\lambda_e = 2$ cm, and $\beta = 0.99$, we find $P_{AV} = 2.25 \times 10^{-12}$ watts with a minimum wavelength of 0.2 mm.

Motz,[52] who has performed experiments with a structure of the type of Fig. 12, which he has called an undulator, estimates that pulsed millimeter and umw power

of about 1-watt total was generated in his initial experiments.

A very important consideration in the production of large amounts of power is the structure of the electron beam. Consider the power radiated per λ_e from a 1-ampere beam of 3-mev electrons, as in the previous example. For the 2-cm length, the number of electrons is

$$N_{\lambda_e} = \left(\frac{I}{e\beta c}\right)\lambda_e = 4.2 \times 10^8. \qquad (18)$$

If these electrons were part of a continuous beam of equal linear density, the power radiated would be extremely small since radiation would occur only because of the fluctuations in beam structure. A perfectly smooth beam in an infinite length undulator could not radiate since radiation from any one segment in the beam would be cancelled by that from another segment.

If, however, we were able to pack the 4.2×10^8 electrons into a bunch of length small compared to

$$\left[(\lambda_e)\frac{(1-\beta)}{\beta}\right]$$

so as to create a supercharge, then the radiated power would be

$$P_{N_{\lambda_e}} = (P_{AV})(N_{\lambda_e}^2) = (2.25)(10^{-12})\left[(4.2)(10^8)^2\right]$$
$$= 4 \times 10^5 \text{ watts}, \qquad (19)$$

since the power radiated by a charge is proportional to the square of the charge.

The chief technical problem to be solved here is, therefore, the one mentioned in connection with harmonics from electron beams. The electrons must be so bunched that the electron current contains strong Fourier components of the frequencies to be radiated.

In practice it is very difficult to produce high density electron bunches of submillimeter dimensions. However, some progress along this line has recently been reported.[23,24]

An interesting variation of the scheme of producing radiation from accelerated charges was demonstrated by Smith and Purcell,[53] who obtained visible light by shooting a 300-kev electron beam across a metal diffraction grating, perpendicular to the rulings. The wavelengths generated obeyed (15). This radiation has been ascribed to be principally due to the effective oscillations of the induced surface charges which follow the hills and valleys of the grating.

2) Moving Mirror: We saw above that the generation of appreciable amounts of umw power by Doppler radiation from accelerated charges requires tightly bunched megavolt electron beams. Is this also true if a moving mirror for Dopper-shifting power to higher frequencies were used? In free space the frequencies of the incident

[53] S. J. Smith and E. M. Purcell, "Visible light from localized surfaces moving across a grating," *Phys. Rev.*, vol. 93, pp. 1069; November 15, 1953.

waves (f_i) and reflected waves (f_r), as in Fig. 13(a), are related by

$$f_r = f_i \frac{(1 + \beta)}{(1 - \beta)}, \qquad (20)$$

where β is the v/c ratio of the moving mirror. Thus, to convert 75 kmc (presently about the highest commercially available frequency of high power) to 300 kmc ($\lambda = 1$ mm) requires $\beta = 0.60$. Such a high velocity is easily attainable only by a "moving mirror" composed of a cloud of electrons; $\beta = 0.60$ corresponds to an electron energy of 128 kev.

An electron cloud will indeed reflect electromagnetic energy. To a first approximation it has a dielectric constant ϵ_r given by

$$\epsilon_r = 1 - \left(\frac{f_p}{f}\right)^2, \qquad (21)$$

where

$f =$ applied frequency,
$f_p =$ plasma frequency, according to (14).

An embodiment of the idea of Doppler-shifting reflection is shown in Fig. 13(b), where a moving electron cloud acts as a moving reflector in a transmission line. Workers of the RCA Research Laboratories have computed the Doppler-shifted power reflected from electron bunches and semi-infinite electron clouds in such a system.[54] Typical values of efficiency computed for conversion from 30 to 300 kmc, for electron densities of 1.5×10^8 electrons/cm³, are -74 db to -90 db. Calculations have also been made of Doppler reflection by an electron gas in the vicinity of a slow wave structure.[55]

The conversion efficiencies computed are rather poor. However, they might be improved by increasing electron densities by operating at electron cyclotron resonance,[54] or by choosing a different ratio of frequencies. The chief limitation, however, is the same practical one that limits radiation from the moving radiator, *i.e.*, that of electron bunching. If an electron cloud is to be an efficient reflector, the reflecting edge must be sharp in terms of the wavelength to be reflected, for otherwise it acts only as a very weak discontinuity. But a sharp reflecting edge is so similar to a tight electron bunch that the problem is the same.

Accordingly, the generation of umw power by reflection of millimeter wave power is also entirely dependent on the ability to produce tight high density electron bunches.

G. Cerenkov Radiation

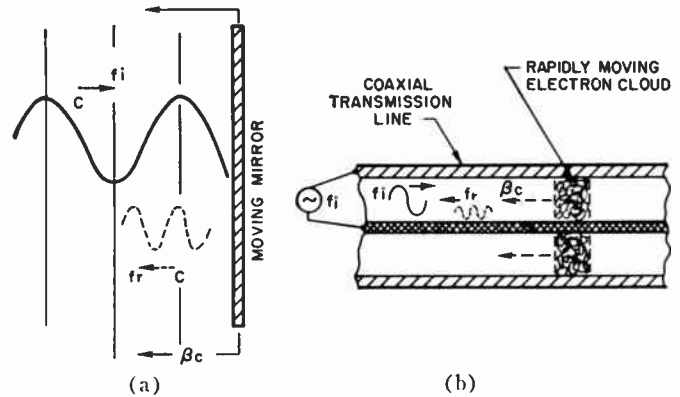In 1934, Cerenkov observed a visible radiation ema-

Fig. 13—Doppler reflection from moving mirror. (a) General scheme. (b) Reflection from electron cloud in transmission line.

nating from certain dielectric liquids in the proximity of a radium source.[56] Frank and Tamm[57] explained the phenomenon by showing that electromagnetic radiation will emanate from a dielectric if an electron moves in this dielectric at a speed higher than the phase velocity of light in it. The phenomenon has been considered as a mechanism for generating umw.[52,58]

The power radiated by a charge moving in an infinite dielectric is given by[52]

$$W = \frac{e^2}{c^2} \int_{v(\epsilon)^{1/2} > c} \left(1 - \frac{c^2}{\epsilon_r{}^2}\right) \omega d\omega, \qquad (22)$$

where ϵ is the dielectric constant and the integral extends over all frequencies for which $(v)(\epsilon)^{1/2} > c$. Again the radiated power varies as the square of the charge; again the generation of appreciable amounts of power can be accomplished only by tight, high density electron bunches. Ginsburg[50] has estimated a peak possible radiated power of 30 kw from a 10-kv, 10^{-2}-ampere beam, which has been bunched so that 10^9 electrons per bunch (a very optimistic number) radiate coherently for an interaction distance of 20 cm while passing through a dielectric of refraction index $n = 7$.

Obviously, the electrons would be scattered long before they could pass through 20 cm of dielectric. However, Cerenkov radiation may also be obtained by passing the electron beam through a small channel in the dielectric, or in the immediate vicinity of it.

An experimental arrangement that has been used for generating K-band ($\lambda_0 = 1.25$ cm) Cerenkov radiation is shown in Fig. 14. It has produced[59] about 10^{-7} watts with a 400-μa, 10-kv beam and an interaction distance of 1.7 cm.

[54] "Research and Development on Microwave Generators, Mixing Devices, and Amplifiers. Phase II—Millimeter Wave Generation," RCA Res. Lab. Div., Princeton, N. J., Contract No. DA 36-039 sc-5548; December 23, 1954.

[55] M. A. Lampert, "Incidence of an electromagnetic wave on a Cerenkov electron gas," *Phys. Rev.*, vol. 102; pp. 299–304; April 15, 1956.

[56] P. A. Cerenkov, *C. R. Acad. Sci., U.S.S.R.*, vol. 2, p. 451; 1934. For further bibliography see J. V. Jelly, "Cerenkov radiation," *Prog. Nuc. Phys.*, vol. 3, pp. 84–103; 1953.

[57] I. Frank and I. Tamm, *C. R. Acad. Sci., U.S.S.R.*, vol. 14, pp. 109–114; January 25, 1937.

[58] M. Danos, S. Geschwind, H. Lashinsky, and A. Van Trier, "Cerenkov effect at microwave frequencies," *Phys. Rev.*, vol. 92, pp. 828–829; November 1, 1953.

[59] M. Danos and H. Lashinsky, "Millimeter wave generation by Cerenkov radiation," IRE TRANS. ON MICROWAVE THEORY AND TECHNIQUES, vol. MTT-2, pp. 21–22; September, 1954.
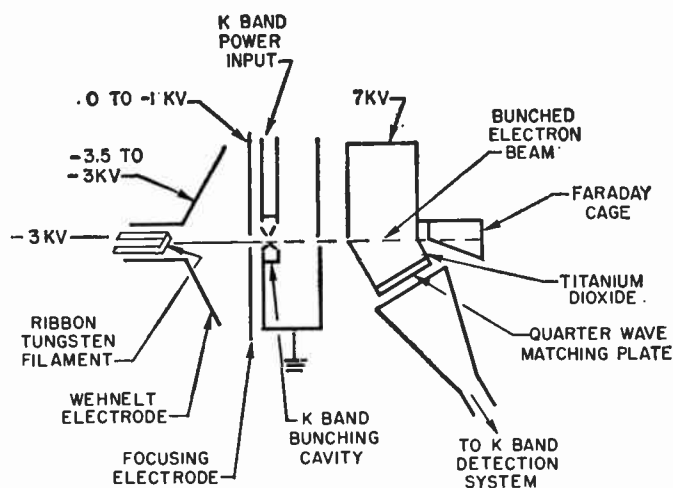
Fig. 14—K-band Cerenkov radiator (after Danos, et al.).

It has been suggested that the scheme of Smith and Purcell,[53] in which an electron beam was shot past a metal grating, produces a type of Cerenkov radiation. The grating is a slow wave structure, so that it acts as an artificial dielectric.

In this sense there is a strong link between the traveling-wave tube and the Cerenkov radiator. The chief difference in the manner by which these two subjects have been treated in the literature lies in their application. Papers dealing with Cerenkov radiation have been concerned chiefly with the mechanism of the radiation, neglecting the influence of the fields on the beam ballistics. In traveling-wave tube analyses the beam ballistics are of interest, for it is the interaction of a beam with a field to produce bunching that is of utmost importance in TWT behavior.

The Cerenkov radiator is subject to the same severe limitations in generating umw as the traveling-wave tube. The fields that can interact favorably with electron beams of conventional voltages (≤ 10 kv) hug the dielectric, so that very high density beams must be passed within a distance of $\lambda/100$ of the surface to produce any appreciable radiation.

The production of more than just minute amounts of umw power by Cerenkov radiation will therefore require means of longitudinally bunching the beam, along with one of the following techniques:

1) New types of high current cathodes.
2) New methods of beam concentration.
3) The use of high energy electrons ($\sim$1 mev), so that dielectrics (real or artificial) with phase velocities only slightly less than c are possible.

II. Quantum Transition Approaches

Since the announcement of the molecular amplifier-oscillator in 1954,[60] a considerable amount of attention

has been focused on the use of quantum transitions between energy states of molecules, atoms, or ions as means of producing or amplifying microwave energy. A comprehensive summary of the field has been given by Wittke.[61]

The ammonia beam maser is by now well known for its use as an extremely stable frequency source. From the viewpoint of its use as an oscillator, however, it is even more remarkable, for it is a device that converts thermal energy directly into essentially single frequency microwave energy without the need for the intermediate dc energy that is found in the vacuum tube oscillator. Perhaps a scheme equally as revolutionary in principle will eventually result in a practical umw generator.

A number of oscillators and amplifiers employing coherent transitions between quantum states have recently been built for the microwave and UHF regions. Besides the necessary experimental techniques that must be developed for successful umw generators, the requirements are:

1) A set of energy levels with at least one gap in the range from 0.001 to 0.01 ev, the $h\nu$ energies corresponding to the umw range.
2) Control of lifetimes of the states.
3) Means of producing the proper population differences required for maser action.
4) The probability of spontaneous emission must be much less than the probability of stimulated emission.

Although we know of no maser that operates at infrared frequencies at the time of this writing, there has been work along this line in the semiconductor field. Here the proper placement of donor, acceptor, or trap levels can produce a large number of energy gaps, and therefore practically any frequency

$$\left(f = \frac{E_{\text{gap}}}{h} \right)$$

desired by recombination between electrons and holes (See Fig. 15.)

Such recombination radiation has been produced by at least two schemes. Moss and Hawkins[62] have detected recombination radiation of wavelength $\lambda = 8$ microns by irradiation of indium antimonide with visible and ultraviolet light. Haynes and Westphal[63] demonstrated infrared recombination radiation from p-n junctions pulsed with unidirectional current. This process is very attractive since radiation of a narrow frequency band is produced by mere current injection without the requirement of higher frequency excitation.

[60] J. P. Gordon, H. J. Zeiger, and C. H. Townes, "Molecular microwave oscillator and new hyperfine structure in the microwave spectrum of NH₃," Phys. Rev., vol. 95, pp. 282–284; July 1, 1954.

[61] J. P. Wittke, "Molecular amplification and generation of microwaves," Proc. IRE, vol. 45, pp. 291–316; March, 1957.
[62] T. S. Moss and T. H. Hawkins, "Recombination radiation from InSb," Phys. Rev., vol. 101, pp. 1609–1610; March 1, 1956.
[63] J. R. Haynes and J. C. Westphal, "Radiation from recombination of holes and electrons in silicon," Phys. Rev., vol. 101, pp. 1676–1678; March 15, 1956.
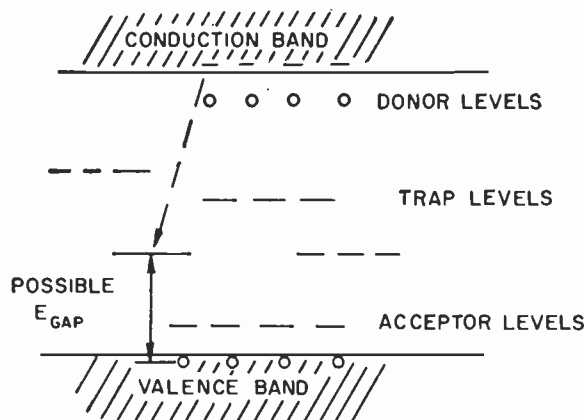
Fig. 15—Levels in a semiconductor.

Similar experiments have been performed by Aigrain[64] and Benoit à La Guillaume, who shaped their samples in a Weierstrass sphere to prevent loss of radiation by internal reflection. (See Fig. 16.) They detected infrared radiation thought to be due to two causes:

1) Electron hole recombination.
2) Interband transitions between accelerated holes.

Considerable work on recombination radiation has also been reported elsewhere.[54]

I. *Miscellaneous Ideas*

This section contains a few of the miscellaneous ideas suggested for umw generation that have not been included under the preceding general topics.

1) Bremsstrahlung: A scheme recently proposed[65] utilizes bremsstrahlung from 30-kv electrons shot into a solid where the radiation higher in frequency than umw is rejected by appropriate filters. As in other schemes utilizing electron beams, tight bunching is required for reasonable power output.

2) Radiation from Rapidly Swirling Electron Beam: A novel method of utilizing the radiation from electrons moving in a circular orbit has recently been proposed by Weibel.[66] In this method a Brillouin-focused electron beam is injected into a chamber where it is repelled back toward the cathode. By time-programmed changing of the electrode potentials, a number of electrons are trapped as a rotating column. This column is then caused to orbit by application of a microwave field. Finally, by application of a longitudinal pulsed magnetic field of 10 to 100 webers/sq. m. the electron column is betatron-accelerated to rotate at a umw frequency and radiate umw power. Up to 16 kw of umw power have been predicted.
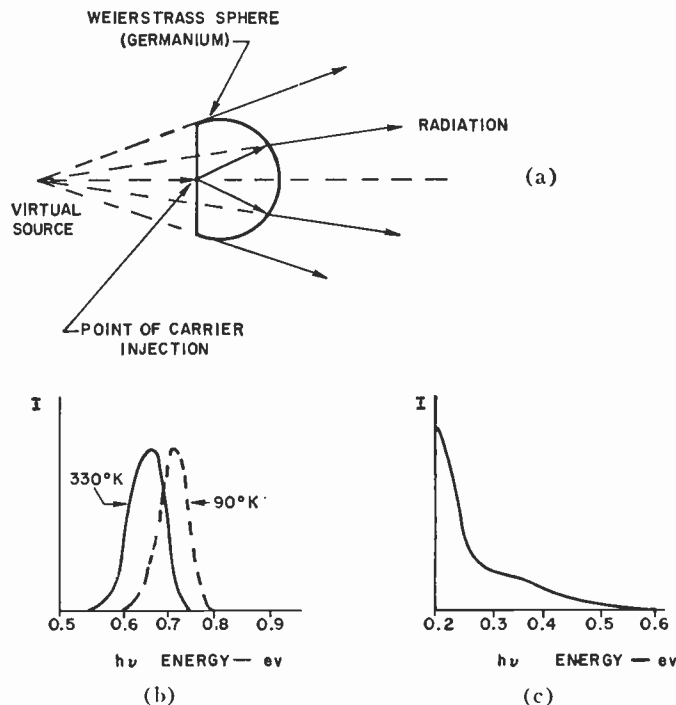

Fig. 16—Infrared radiation from germanium injected with carriers (after Aigrain, *et al.*). (a) The Weierstrass sphere method of liberating the radiation. (b) Spectrum of electron-hole recombination. (c) Long-wave spectrum thought due to radiation from high-velocity holes.

3) Conversion of Acoustic to Electromagnetic Energy: The bombardment of a solid by a small particle sets up acoustic waves. The possibility of generation of electromagnetic energy through these acoustic waves, because they may be oscillations of charged lattice points, has recently been considered.[67] Although the initial experiments were not reported as successful, the idea of coupling acoustic to electromagnetic energy may be well worthy of consideration.

4) Miscellaneous Semiconductor Effects: There have been recent efforts to exploit the possibility of a negative conductivity in some semiconductors for electromagnetic wave generation.[67]

Another entirely different phenomenon is the recently observed generation of low-power 9-kmc radiation by the rapid breakdown of a point in a diffused *p-n* junction diode.[68] The amplitudes of the radiation correlated well with the assumption of breakdown time of the order of 10^{-11} seconds or less.

III. Transmission, Control, and Measurement of UMW

Because of the lack of ultramicrowave sources, relatively little in the way of detection and transmission

[64] P. Aigrain and C. Benoit à La Guillaume, "L'emission infrarouge du germanium," *J. Phys. Rad.*, vol. 17, pp. 709–711; August/September, 1956.

[65] G. A. Askar'ian, "Pulsed coherent generation of millimeter radiowaves by nonrelativistic electron bunches," *Soviet Phys. JETP*, vol. 3, pp. 613–614; November, 1956.

[66] G. E. Weibel, "High magnetic field submillimeter wave generators with parametric excitation," presented at Symp. on Electronic Waveguides, New York, N. Y.; April 8–10, 1958.

[67] W. R. Beam, H. Kromer, E. Langberg, and R. W. Peter, "Generation of Millimeter Wave in Solids," RCA Labs., Princeton, N. J., Contract No. DA 36–039-sc-73054; October 15, 1956.

[68] J. L. Moll, A. Uhlir, Jr., and B. Sentizky, "Microwave transients from avalanching silicon diodes," Proc. IRE, vol. 46, pp. 1306–1307; June, 1958.

equipment for this range of the spectrum has been developed.

Waveguide test equipment is now commercially available from several U. S. manufacturers for the 60–90-kmc range; there is also some present development of 150-kmc equipment. Crystal harmonic multipliers[30] that are rated to produce power up to 170 kmc are also available, but their power output is minute and somewhat uncertain.

Microwave test equipment is manufactured in various sizes. The size of the waveguide is usually so chosen that only one mode is propagated in the frequency band for which it is designed. The field configuration is then known, so that such components as attenuators, detectors, etc., can be built and so that standard techniques of testing (standing wave measurements, etc.) can be applied. For uniform waveguide the "cutoff" wavelength, *i.e.*, the lower frequency limit of propagation, is determined by the dimensions and the mode of propagation. Examples of cutoff wavelengths (free space) for rectangular guide, with reference to Fig. 17, are as follows.

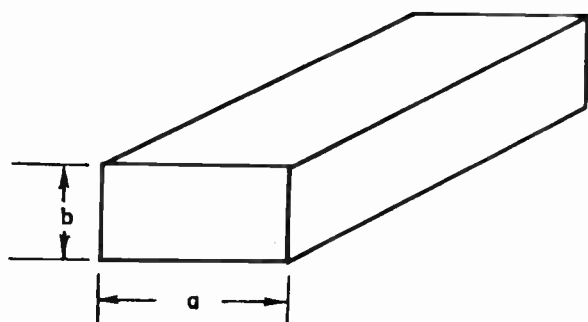| Mode	λ Cutoff
TE$_{10}$ (lowest)	$2a$
TE$_{11}$, TM$_{11}$	$\dfrac{2ab}{\sqrt{a^2+b^2}}$

Fig. 17—Rectangular waveguide.

The useful bandwidth of a guide is approximately the difference between the two frequencies corresponding to the above two cutoff wavelengths. If $a = 2b$ (a compromise between bandwidth and power handling capability), rectangular waveguide suitable for 600-kmc ($\lambda = 0.5$ mm) work would have the dimensions: $a = 0.014$ inch and $b = 0.007$ inch.

Since the height of this guide is only 2–3 human hairs, it is easy to see that standard microwave measurement techniques will be very difficult to apply in the umw range. In addition to the size limitation there is a problem of attenuation, which increases with frequency. RG-139/U, for example,[69] made of silver and listed as

operative from 220 to 325 kmc, has a theoretical attenuation of 3.48 to 5.12 db per foot. Accordingly, there is need not only for research in techniques of generation, but also in transmission and measurement. Successful schemes will probably combine microwave with optical techniques.

Several laboratories have done work to produce better transmission lines and measuring systems for the millimeter and, eventually, the umw range. Some waveguides have been found to possess modes whose attenuation decreases with frequency. Among these are the cylindrical guide operating in the TE$_{01}$ mode, which has been investigated extensively[70] as a transmission medium at 50–60 kmc, and the *H* guide,[71] consisting of two parallel conducting strips separated by a dielectric slab. Other guiding systems use nonradiating surface waves on dielectrics placed on metal slabs or other metal-dielectric combinations. Some of these have been tested at millimeter wavelengths,[72] though no application to the umw range is as yet known to the writer.

The application of optical techniques to umw has been achieved at several laboratories. Motz,[52] for example, measured wavelengths of his undulator radiation with an echelette spectrometer. Rohrbaugh[73] has reported on a spectrometer intended to operate from millimeter wavelengths to the far infrared. Work of a similar nature has also been described elsewhere.[74]

A great deal of effort has been expended in recent years on ferrite devices, used to control microwave power. There will eventually be need for similar control devices at umw. Some very recent work exploring the physics of antiferromagnetic materials and other substances with high, effectively built-in magnetic fields indicates that here is a new field of research that could result in engineering applications for umw components.[75]

Power measurement is accomplished by calorimetric means throughout most of the electromagnetic spectrum. Steady power levels may be measured to higher sensitivity by integration techniques. Dicke's microwave radiometer[13] with an input bandwidth of 16 mc and an output time constant of 2.5 seconds had a minimum detectable power of 10^{-16} watts. This instrument contained electronic amplifiers which at present are not available in the umw range.

[69] "Armed Services Index of R.F. Transmission Lines and Fittings," Armed Services Electro Standards Agency ASESA 49-2B, (Navships 900-102B), May 31, 1956.

[70] S. E. Miller, "Waveguide as a communication medium," *Bell Sys. Tech. J.*, vol. 33, pp. 1209–1265; November, 1954. (There are many other references on this subject.)

[71] F. J. Tischer, "H-guide—a new microwave concept," *Electronic Ind. and Tele-Tech.*, vol. 15, pp. 50–51, 130, 134, 136; November, 1956.

[72] J. C. Wiltse, "Some characteristics of dielectric image lines at millimeter wavelengths," presented at PGMTT Natl. Symp., Stanford University, Stanford, Calif.; May 5–7, 1958.

[73] J. H. Rohrbaugh, "A Study of the Generation and Detection of Electromagnetic Waves in the Millimeter Wave Region," New York Univ., New York, N. Y., Final Rep., Contract AF 19(604)-1115; August 31, 1957.

[74] For example, L. Genzel and W. Eckhardt, "Spektraluntersuchungen im Gebiet um 1 mm Wellenlänge," *Z. Phys.*, vol. 139, pp. 578–598; December, 1954.

[75] S. Foner, "High Field Antiferro-, Ferri- and Paramagnetic Resonance," Lincoln Lab., Mass. Inst. Tech., Lexington, Mass., Rep. No. M37-26; April 7, 1958.

An instrument that is capable of sensitive power measurement from infrared well into the millimeter range is the Golay cell detector[76] which functions by detecting minute changes in a small volume of gas that is heated by impinging radiation. This apparatus can detect signals above 5×10^{-11} watts when its response time is 0.1 second. It could therefore be used to detect such very small quantities of umw power.

When compared to detection at other frequencies, however, 0.1 second is a long time. Visible light can be detected in times much less than a microsecond by photoemission. Semiconducting infrared detectors are capable of response times of a few microseconds. The frequency limitation of photoconductors is that photon energies of the far infrared range and lower frequencies are too low to produce photoconduction in present semiconductors. Development of semiconductors for umw detection requires energy gaps of 0.001 to 0.01 electronvolt and operation at very low temperatures.

Approaching umw from the microwave region, we find that there has been a considerable amount of work on bolometers in waveguides. A bolometer is a circuit element whose resistance changes as it is heated by the energy that it is to detect. A sensitive bolometer, therefore, has as high a resistance change per joule of received energy as possible. To achieve sensitivity, it is necessary to:

1) Isolate the bolometer element from heat sinks. A bolometer in vacuum is more sensitive than one in air.
2) Use as low a thermal mass as possible. Fine wire bolometers are more sensitive than thick ones.
3) Use a material with a high temperature coefficient of resistance.

Rohrbaugh[73] has reported on fine-wire bolometers that can be used not only to measure power down to as low as 7×10^{-10} watts at $\lambda_0 = 1.4$ mm, but also have a response time as low as 100 μsec. These bolometers are Wollaston wires with cores that, when deplated, are as small as 6 micro-inches. It appears that this is a successful extrapolation of microwave power measurement techniques to the low-frequency fringe of the umw range.

Of great utility and very rapid response in microwave work is the crystal receiver, either as a straight video detector or in its more sensitive use in a superheterodyne receiver. It is of interest to review its status as applied to umw work. Point contact rectifier crystals are used by microwave spectroscopists, not only as the nonlinear elements that produce up to 511 kmc of essentially single frequency power,[31] but also as detectors. Successful video detectors for the 200–300-kmc range are described by King and Gordy.[30]

Superheterodyne receivers for the umw range require a local umw oscillator, not presently available. However, the problem can be solved by harmonic mixing. Johnson,[77] for example, describes a superheterodyne receiver that operated between 100 and 150 kmc, using a 25-kmc local oscillator with the following characteristics:

Sensitivity = -86 dbm ($= 2.5 \times 10^{-12}$ watts).
IF bandwidth = 4 mc.
Over-all noise figure = 35–40 db.

His sensitivity for straight video detection was only -57 dbm.

These techniques of the microwave spectroscopists have sometimes required the ultimate in patience. In the laboratory adjustment times of up to several weeks have been reported.

Not only do the mechanical problems become severe, but there are limitations in the physics and structure of the semiconductor junctions. In the equivalent circuit representation of Fig. 7, a high RC product means high conversion loss, and therefore a lowering of crystal sensitivity as the frequency increases. Recently, techniques have been suggested for reducing this RC product with promise of extending satisfactory crystal operation into the umw range. The details of the design and application of crystal detectors are discussed in recent review articles by McCoy,[78] Uhlir,[79] and Messenger[34] and will not be repeated here. Messenger has outlined that microwave diodes can be improved by a basic modification of contact geometry, application of new semiconductor materials of higher majority carrier mobility and cooling. He suggests that these improvements can extend the upper frequency limit of good crystal detectors from 100,000 to 1,000,000 mc, or well into the umw range.

In addition to sources and components for transmission and measurement there exists the desirability of constructing umw amplifiers. A number of the techniques discussed in connection with the problem of generation of ultramicrowaves also applies to amplification. These include such topics as plasma oscillations, masers, and others. The parametric amplifier, which has become so popular of late, will probably invade the umw region. Although the early parametric amplifiers used a pump of a frequency that was higher than the frequency to be amplified, this is no universal requirement. Chang and Bloom[80] describe a parametric amplifier, operating at much longer wavelengths, that used a

[76] M. J. E. Golay, "The theoretical and practical sensitivity of the pneumatic infrared detector," *Rev. Sci. Instr.*, vol. 20, p. 816; November, 1949.

[77] C. M. Johnson, "Superheterodyne receiver for the 100 to 150 kmc region," IRE TRANS. ON MICROWAVE THEORY AND TECHNIQUES, vol. MTT-2, pp. 27–32; September 1954.
[78] C. T. McCoy, "Present and future capabilities of microwave crystal receivers," PROC. IRE, vol. 46, pp. 61–66; January, 1958.
[79] A. Uhlir, Jr., "The potential of semiconductor diodes in high-frequency communications," PROC. IRE, vol. 46, pp. 1099–1115; June, 1958.
[80] K. K. N. Chang and S. Bloom, "A parametric amplifier using lower-frequency pumping," PROC. IRE, vol. 46, pp. 1383–1386; July, 1958.

pump frequency lower than that of the amplified signal. The ratio of signal-to-pump frequency that can be achieved is limited by the degree of nonlinearity of the variable parameter element. This is also essentially the picture in a harmonic generator, where the order of the harmonic that can be generated efficiently also depends on the degree of nonlinearity of an element. Accordingly, if a nonlinear reactive element that generates umw signals efficiently when fed from a millimeter wave source can be found, the answer to a umw parametric amplifier will also be found.

IV. CONCLUSION

This paper has outlined some of the current thoughts related to ultramicrowave generation and, briefly, the methods likely to be used for transmission, control, and measurement. Since a variety of ideas are involved, it has been possible in this paper to cite only a few representative references. Many other workers have engaged in research directly or indirectly related to umw work. Similarly, because of the wide scope of this field, there are, no doubt, many other ideas besides those presented.

In terms of today's thinking, the solution to the problem of producing appreciable amounts of essentially single frequency umw power will probably be attained by further developments of the following approaches:

1) Concentration (into small volumes) of large amounts of energy for coherent conversion into ultramicrowave form.

2) Schemes of providing coherent interactions over distributed regions much larger than one wavelength.

3) Coherent radiation from large numbers of radiators.

On the other hand, it is quite possible that the problem will be solved more desirably by schemes not yet conceived. The field presents a challenge full of opportunities for invention and successful developments.

[81] P. D. Coleman, "Final Report on Research and Investigation Leading to Methods of Generating and Detecting Radiation in the 100 to 1000 Micron Range of the Spectrum," Elec. Eng. Res. Lab., Univ. of Illinois, Urbana, Ill., Contract No. AF 33(616)2448; May 30, 1956.

The Physical Principles of a Negative-Mass Amplifier*

HERBERT KRÖMER,† MEMBER, IRE

Summary—By providing in a crystal, carriers of such an energy and such a momentum that at least one of their three main effective masses is negative, it should be possible to obtain wave amplification in such a crystal. The amplifier should work up to about 1000 kmc (0.3 mm wavelength), with a large bandwidth. To obtain carriers of sufficient energy and proper momentum, acceleration by a high field seems most feasible at present. Negative effective masses for relatively low energies may be obtained if the energy contours are re-entrant near the band edge, as is the case for the heavy holes in germanium and, as may be the case for other semiconductors with degenerate band edges. The optical-phonon collision cross-section should also be high in order to obtain sufficient concentration in *k*-space. If the latter is the case for germanium a verifiable microwave amplifier using the principle would consist of a wafer of *p*-type germanium with a strong bias field applied in a crystallographic (100) direction, and inserted into a waveguide or a cavity such that the electric vector of the microwave field is perpendicular to the bias field. Such a bulk amplifier has no critical dimensions, receives its power from a dc battery, and has essentially no frequency dependence over the entire radio spectrum.

The principle is not restricted to germanium, but should also work with certain other semiconductors. Low-frequency amplifiers and bistable devices are also possible. Some design problems are discussed.

LIST OF SYMBOLS

a	width of waveguide
A, B, C	parameters describing the band structure
α	attenuation constant
δ	phase angle
e	electronic charge
$E, \mathbf{E}, E_0, \mathbf{E}_0, \mathbf{E}_\omega$	electric field
ϵ	carrier energy
ϵ_{opt}	optical phonon energy
h	index for "heavy"
$\hbar$	Planck's constant, divided by 2π
j	current density
k (in kT)	Boltzmann's constant
$k, \mathbf{k}$	electron wave vector
$k, k_z, k_3, k_i, k_j, k_x, k_y, k_z$	components of electron wave vector
l	index for "light"
L	index for "longitudinal"
m	effective mass
$\bar{m}, m^*, m_1, m_2, m_3$	special effective masses
m_0	mass of free electron
μ	mobility
n	carrier density
ω	circular frequency
π	conversion probability
R	sheet resistance
s	integration variable
σ	conductivity
t	time
T (in kT)	absolute temperature
T	index for "transverse"
τ	collision time
$v, \mathbf{v}, v_0, v_{opt}, v_{sat}$	carrier velocities
$w, w_0, w_1, w_2, \overline{w_2}, \overline{w}_{2,ac}, w_{2,dc}$	energy exchange rates

I. INTRODUCTION

THIS paper describes the physical principles of a recently proposed [1] new class of solid-state devices for the broadband amplification and generation of electrical waves from low frequencies up to very high frequencies in the microwave range. This class of devices utilizes the fact that at sufficiently high kinetic energies the effective masses of the charge carriers in semiconductors become negative. Under the influence of a force, a negative-mass particle is accelerated opposite to that force. Electrically, this means that, in a crystal containing negative-mass carriers, the electrical current flows against the electric field. In other words, the carriers have a negative mobility, and the crystal has a negative resistance.

The energy source for the process is the high kinetic energy of the carriers, which energy of course has first to be supplied to these carriers from the outside. This can be done in several ways, *i.e.*, by irradiation, illumination or, most conveniently, by acceleration with an electric field until the carriers reach the negative-mass region. Whatever the supply mechanism is, the whole class will be lumped together here under the name Negative-Effective Mass Amplifiers and Generators, which may be abbreviated NEMAG. Since negative effective masses are an exclusive solid-state property, the NEMAG is a device that has no analogy physically in vacuum electronics. Circuit-wise, of course, it is simply a negative impedance medium, but one that should operate up to very high microwave frequencies.

In the following sections, we will attempt to give a detailed theory of the NEMAG. As to the generation of the high-energy carriers, it will be assumed that this is done by an electric field. This is presently considered to be the most promising method. The signal field then will ride on top of a bias field.

Sec. II deals with the motion in a crystal of an electron with a varying effective mass under the influence of a dc bias field plus an ac signal field.

Different general types of band structures are discussed, and the difference is studied between the cases of parallel bias and signal fields, and of crossed fields. Sec. III is devoted to a special case which is perhaps the

most promising of all possibilities: crossed fields in bands with re-entrant energy contours. This situation should apply for the holes in germanium. Finally, in sec. IV the basic principles of a rough design theory are given for a crossed-field NEMAG using *p*-germanium.

Except in sec. IV, the theory will be stated in terms of electrons. But, unless otherwise stated, everything holds for holes as well, provided one makes the usual and well-known changes of the sign of the charge, etc.

For simplicity and because the presently most interesting semiconductors, germanium and silicon, have a cubic structure, it will always be assumed that the crystal structure is cubic. This represents no basic limitation of the general conclusions.

II. GENERAL PRINCIPLES

A. Dynamics of a Single Electron

A crystal electron with a wave vector k and an energy $\epsilon = \epsilon(k)$ with respect to the bottom of the conduction band, has a velocity,

$$v = \frac{1}{h} \nabla_k \epsilon(k) \tag{1}$$

where ∇_k means the gradient in k-space.[1] Under the influence of an electric field E, the electron is accelerated according to

$$\dot{k} = -\frac{e}{h} E \tag{2}$$

and, therefore

$$\dot{v} = -e \left\|\frac{1}{m}\right\| E \tag{3}$$

where $\|1/m\|$ is a symmetrical tensor, the so-called effective mass tensor,

$$\left\|\frac{1}{m}\right\| = \frac{1}{h^2} \left\|\frac{\partial^2 \epsilon}{\partial k_i \partial k_j}\right\|. \tag{4}$$

By a suitable rotation of the coordinate axes this tensor can always be diagonalized:

$$\left\|\frac{1}{m}\right\| = \left\|\begin{array}{ccc} \frac{1}{m_1} & 0 & 0 \\ 0 & \frac{1}{m_2} & 0 \\ 0 & 0 & \frac{1}{m_3} \end{array}\right\| = \frac{1}{h^2} \left\|\begin{array}{ccc} \partial^2\epsilon/\partial k_1^2 & 0 & 0 \\ 0 & \partial^2\epsilon/\partial k_2^2 & 0 \\ 0 & 0 & \partial^2\epsilon/\partial k_3^2 \end{array}\right\|. \tag{5}$$

The three values m_1, m_2, and m_3 will be referred to as the main masses.

[1] Equality between a vector in *x*-space and one in *k*-space means that the components of the *x*-space vector with respect to the three crystallographic axes are equal to the corresponding components of the *k*-space vector with respect to the main axes of the *k*-space.

The work done per unit time on the electron by the electric field is

$$w = -e(Ev). \tag{6}$$

If, at $t = t_0$, the electron had undergone a collision after which it had the velocity $v = v_0$,

$$w(t) = -e(Ev_0) + e^2 \left(E \int_{t_0}^{t} \left\|\frac{1}{m}\right\| Eds \right). \tag{7}$$

Assume that the electric field consists of a dc field and a purely sinusoidal ac field[2]

$$E = E_0 + E_\omega \sin \omega t. \tag{8}$$

Then, $w(t)$ can be split up into three parts

$$w(t) = w_0 + w_1 + w_2, \tag{9}$$

where

$$w_0 = -e(E_0 v_0) + e^2 \left(E_0 \int_{t_0}^{t} \left\|\frac{1}{m}\right\| E_0 ds \right) \tag{10a}$$

$$\begin{aligned} w_1 = &-e(E_\omega v_0) \sin \omega t \\ &+ e^2 \left(E_\omega \int_{t_0}^{t} \left\|\frac{1}{m}\right\| E_0 ds \right) \sin \omega t \\ &+ e^2 \left(E_0 \int_{t_0}^{t} \left\|\frac{1}{m}\right\| E_\omega \sin \omega s\, ds \right) \end{aligned} \tag{10b}$$

$$w_2 = +e^2 \left(E_\omega \int_{t_0}^{t} \left\|\frac{1}{m}\right\| E_\omega \sin \omega s\, ds \right) \sin \omega t. \tag{10c}$$

B. The Constant-Mass Approximation

To illustrate the principle of the NEMAG, let us assume that the time between two collisions is so short that with the existing field strength the electron is being accelerated only through such a small portion of the k-space that the effective-mass tensor remains practically constant along the path of the electron. From (10) then

$$w_0 = -e(E_0 v_0) + e^2 \left(E_0 \left\|\frac{1}{m}\right\| E_0 \right) \cdot (t - t_0), \tag{11a}$$

$$\begin{aligned} w_1 = &\, e(E_0 v_0) \sin \omega t + e^2 \left(E_0 \left\|\frac{1}{m}\right\| E_\omega \right) \\ &\cdot \left[(t - t_0) \sin \omega t + \frac{1}{\omega} (\cos \omega t_0 - \cos \omega t) \right], \end{aligned} \tag{11b}$$

$$w_2 = +e^2 \left(E_\omega \left\|\frac{1}{m}\right\| E_\omega \right) \frac{(\cos \omega t_0 - \cos \omega t) \cdot \sin \omega t}{\omega}. \tag{11c}$$

The three terms have the following meaning. w_0 is the energy taken up from the dc field. w_1 is due to the fact that an electron is accelerated at a slightly different rate depending upon whether, at the instance of the last collision, the ac field aided the bias field or opposed it. At any rate, the w_1-term does not contribute to the net

[2] The two fields need not have the same direction but may be at any angle.

amplification or attenuation since its time-average is zero if one first averages the term of all the electrons with different t_0's.

The actual amplification term is w_2. If the ac part $w_{2,ac}$ of this term is negative, the electron delivers ac energy to the field rather than taking energy away from it. A crystal where the average value of the ac part of w_2 is negative therefore presents a wave-amplifying medium or, in a different terminology, a medium of negative impedance. Inserted into a resonant circuit, be it a lumped-constant circuit or a resonant cavity, it can support stable continuous oscillations of the circuit and, therefore, may be used as a wave generator. Inserted into a properly matched circuit or in combination with nonreciprocal elements, it can act as an amplifier.

In order to split off any dc part in w_2 and to establish the sign of $w_{2,ac}$, the value of the trigonometrical factor in (11c) must be determined. For $\omega(t-t_0) \ll 1$, it is positive. For its exact determination it must be averaged over the t_0-values of all electrons.

To this end we make the assumption that every electron collides exactly a time interval τ after the previous collision, *i.e.*,

$$\overline{w_2} = \frac{1}{\tau} \int_0^\tau w_2 d(t - t_0). \qquad (12)$$

The reason for this assumption is not only that it simplifies the calculations, but even more that it does actually correspond closely to the case of optical-phonon scattering which will be shown below to be of great importance.

From (11c) and (12) then

$$\overline{w_2} = + e^2 \left(E_\omega \left\| \frac{1}{m} \right\| E_\omega \right)$$

$$\frac{1}{\omega^2 \tau} \sqrt{\omega^2 \tau^2 + 2 - 2\omega\tau \sin \omega\tau - 2 \cos \omega\tau}$$

$$\cdot \left[\sin^2 (\omega t - \delta) - \sin^2 \delta \right] \qquad (13)$$

where δ is given by

$$\tan 2\delta = \frac{\omega\tau - \sin \omega\tau}{1 - \cos \omega\tau}. \qquad (14)$$

The last factor in (13) shows that we actually have a time-dependent component, $\overline{w_{2,ac}}$, and a time-independent component, $\overline{w_{2,dc}}$, with the opposite sign. The ac component is the amplification component. If the $\omega\tau$-dependent factor in (13) is expanded into a power series, one can write down the ac component of $\bar{w}_2$ simply as

$$\overline{w_{2,ac}} = e^2 \left(E_\omega \left\| \frac{1}{m} \right\| E_\omega \right)$$

$$\cdot \frac{\tau}{2} \left[1 - \left(\frac{\omega\tau}{6} \right)^2 \right] \sin^2 (\omega t - \delta) \qquad (15)$$

with

$$\delta = \frac{\omega\tau}{6}. \qquad (16)$$

In Fig. 1 the frequency dependence of $|\overline{w_{2,ac}}|$ and of δ is shown.

Eq. (15) then has two consequences.

1) The sign of the ac component of $\overline{w_2}$ is equal to that of the "net effective mass" in the direction of the ac field

$$\bar{m} = E_\omega^2 \bigg/ \left(E_\omega \left\| \frac{1}{m} \right\| E_\omega \right), \qquad (17)$$

and amplification can occur if $\bar{m} < 0$.

In order for $\bar{m}$ to be negative, it is necessary that at least one of the main masses be negative and that the direction of the signal field be sufficiently close to the direction corresponding to that main mass so that any positive contributions from the other masses are overridden. The restriction on the direction of E_ω is less severe for two negative main masses, and it disappears altogether if all three m's are negative. It is the main purpose of the bias field to accelerate the electron into such regions in k-space where negative $\bar{m}$'s are available.

2) If $\bar{m} < 0$, the ac energy transfer from the electron to the ac field is practically constant from zero frequency up to the collision frequency, τ; this gives an upper frequency limit of the order of 1000 kmc.
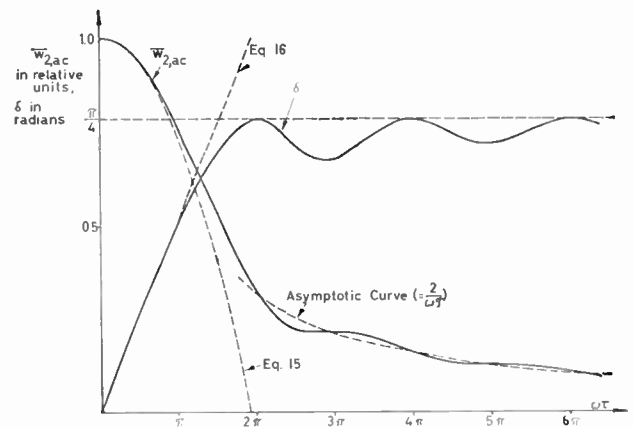
Fig. 1—Relative amplitude and phase shift of the energy exchange between field and electron, as a function of frequency and collision time.

Being essentially a negative resistor and not a resonance type device, a NEMAG is automatically broad banded and tunable. In this respect, it is different from MASER-type devices which utilize a built-in atomic resonance frequency.

We had assumed above that the effective mass tensor is constant along the path in k-space of the electron. In general, this will not be the case. This has the consequence that not only the mathematical evaluation of the several integrals in (10), (11), and (13) changes, but

that, in addition, w_0 and w_1 also now contribute to the ac energy exchange between the electrons and the ac field, since they contribute terms quadratic in E_ω.

The details of these changes will depend very much upon many details, such as the band structure, the angle between the bias field and ac field, and the orientation of both with respect to the crystal axes. To attempt a general theory covering all the possibilities would be beyond the scope of this paper. Instead, these things should be included in discussions of special NEMAG types. We, therefore, will not discuss the effects of mass variations here.

C. Energy Range Restrictions

In order for the negative masses in a semiconductor to be useful for NEMAG purposes it is necessary that they occur at sufficiently low energies. This is because at elevated energies two effects set in which limit the practically obtainable electron energies: avalanche multiplication [2] and optical phonon scattering.[3].

Avalanche multiplication sets in as soon as the electron reaches a kinetic energy higher than the forbidden band ϵ_G of the semiconductor. With a very high probability, the electron then falls back down to the bottom of the band, transferring its energy to another electron from the valence band by lifting this electron up into the conduction band, leaving a hole behind. This process not only makes energy regions above $\epsilon = \epsilon_G$ inaccessible to the electrons, it is also harmful if negative masses occur already below ϵ_G, because the secondary electrons and holes created by those electrons that reach $\epsilon = \epsilon_G$ produce a positive contribution, dn/dE, to the differential conductance,

$$\sigma = \frac{dj}{dE} = en \frac{dv}{dE} + ev \frac{dn}{dE} \qquad (18)$$

where n is the carrier density. This positive contribution may override an actually present negative dv/dE contribution.

Optical phonon scattering can occur only in crystals with more than one atom per unit cell. All semiconductors belong in this class. Like avalanche multiplication, it is a threshold process. As soon as the electron reaches a kinetic energy higher than the optical phonon energy ϵ_{opt}, it has a chance to dissipate all or most of its energy by exciting an optical phonon. The threshold energy, however, is generally much lower than the band gap energy. The obtainable electron energies are therefore limited to values even lower than the band gap if the optical phonon collision cross section is large enough.

From high-field mobility measurements [4]–[6] one must conclude [3] that the optical phonon scattering does limit the electron energy already fairly efficiently in germanium and silicon, at least at intermediate fields of the order of 5000 volt per cm [5]. But germanium is elemental and, therefore, nonpolar. Semiconductor compounds are always partially polar, and their optical phonon cross section should be much larger.

From these considerations it follows that for NEMAG purposes such semiconductors are promising where negative masses occur low enough, preferably lower than the optical phonon energy. This is a stringent requirement.

D. Direction Dependence, Parallel and Crossed Fields

Wherever the last requirement is fulfilled, that is, wherever negative masses occur at all at sufficiently low energies, one can expect quite generally that

1) they will occur only within certain limited negative portions of k-space, and that
2) not all three main masses will become negative within one of those regions.

This will be illustrated below and in Figs. 2–4. These facts have the consequence that the direction of both the bias field and the signal field are highly restricted.

1) The bias field direction has to be such that the charge carriers are driven away from the band edge into one of those regions of negative mass, that is, it should be parallel to that k-vector that connects the band edge with one of those regions.[3]
2) The signal field direction should be close to the direction of that axis of the mass tensor along which the negative mass occurs. If two masses are negative, it should lie in the plane given by the two corresponding axes.
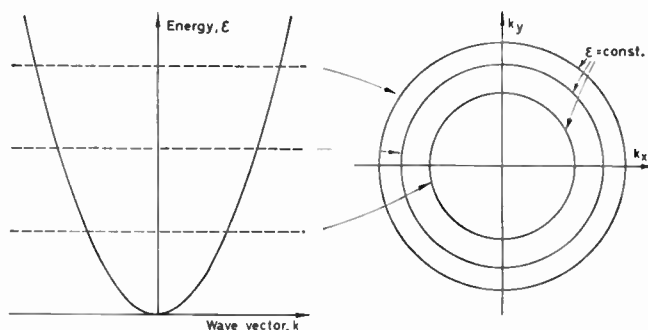
Fig. 2—For free electrons the energy is parabolic in the wave-number (left), independent of the direction of the wave vector. The energy contours are spheres (right).

These considerations may lead to the same direction or to entirely different directions for the two fields. The two extreme cases are what might be called a parallel-field NEMAG and a crossed-field NEMAG.

In most cases, particularly in single-valley semiconductors, the negative-mass-region will be centered about one of the symmetry axes of k-space. If this is so, this axis will also be one of the main axes of the mass-tensor, the two other axes being perpendicular to it. In this case, we automatically obtain a pure parallel-field NEMAG or crossed-field NEMAG depending upon

[3] In multivalley semiconductors this may lead to conflicting requirements for the different valleys even though negative mass regions exist.

whether the longitudinal mass, m_L, in direction of the axis becomes negative or whether one of the two transverse masses, m_T, does. If the latter is the case and if the symmetry axis is of higher than two-fold symmetry, the two transverse masses are identical and one obtains a crossed-field NEMAG where the signal field may have any direction perpendicular to the bias field unless secondary considerations dictate a special direction.

It is possible to draw rather far-reaching conclusions from a simple consideration of the difference between the direction of the two fields in a NEMAG. To show this, we want to restrict ourselves to the two extreme cases of a parallel-field and a crossed-field NEMAG, the intermediate cases being a matter of simple interpolation. For the following see Figs. 2–4.
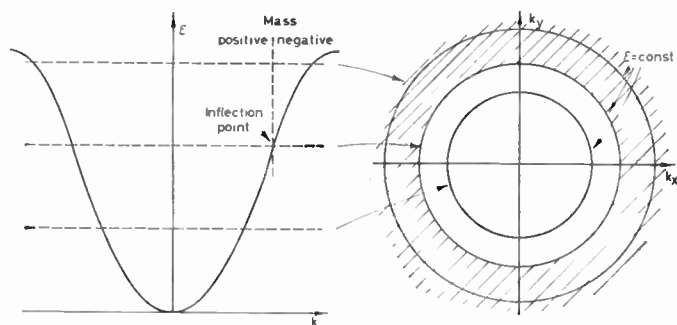
Fig. 3—Schematic band structure for a case where the energy remains isotropic as for free electrons, but is nonparabolic. Above the inflection point the longitudinal mass (*i.e.*, taken in the direction of k) becomes negative (shaded region).

Fig. 4—Schematic band structure for a case where the energy remains parabolic as for free electrons, but where the parabola depends on the direction. If the energy contours become re-entrant the transverse mass (*i.e.*, taken perpendicular to k) becomes negative within the re-entrant sections (shaded regions). See also Figs. 5 and 6.

In comparing the band structure requirements for a parallel-field and a crossed-field NEMAG, one realizes that they are entirely different. Bo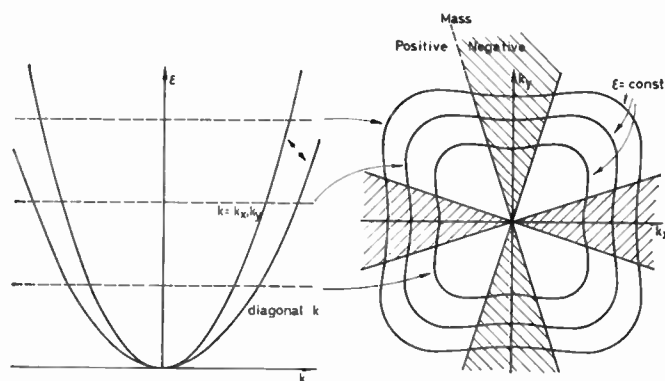th require deviations from the isotropic-parabolic $\epsilon(k)$ behavior of free electrons. For the parallel-field effect, strong deviations from the parabolic behavior are required, whether isotropic or not. For the crossed-field effect, deviations from the parabolic behavior alone are not sufficient. If the energy surfaces are spherical (or ellipsoidal) up to

the highest energies, but nonparabolic, no negative transverse masses could occur even though m_L would at some energy turn negative. Negative m_T's are therefore not an effect of nonparabolic behavior but of strong anisotropies. The condition for their occurrence is that the energy contours are partially re-entrant towards the energy minimum (Fig. 4). This is true even if the bands remain parabolic in any fixed direction. If the bands are nondegenerate near the band edge, (for example, the conduction bands in Ge and Si), neither negative longitudinal masses nor re-entrant energy contours are likely to occur at energies close to the band edge. With increasing energy no general statements can be made as to which of the two situations may occur first.

Assume now that the bands are degenerate at the band edge. Except for accidental degeneracies, this will occur only if the band edge lies at a point of high symmetry in k-space, for example, at $k = 0$ (*e.g.*, the valence bands in Ge and Si). Going away from that point of symmetry, the different bands will then split up. This splitting-up will not in general introduce negative longitudinal masses near the band edge. Instead, the different bands will all remain parabolic near the band edge, although with different curvatures. But the splitting will often be highly directional, and it may be so highly directional that re-entrant energy contours are created. The energy contours then will not be re-entrant only above a certain energy, but down directly to the band edge (Fig. 4). This happens in the valence bands of Ge and Si. It should happen in many other cases.

Somewhat in between the case of degenerate and of clearly nondegenerate bands lies the case of bands that are " almost degenerate," where the band edge does not lie at a point of symmetry and of degeneracy but very close to it, accidentally or due to an originally existing degeneracy that has been lifted by some perturbation effects. The latter is the case, for example, in the valence bands of III–V compounds where the lack of a center of symmetry shifts the band edge slightly away from $k = 0$ [6]. If in such cases the bands are still "almost degenerate," one can expect that re-entrant contours will still occur, not down to the band edge but only slightly above it. For practical purposes, such a semiconductor would also be useful.

The conclusion one might draw from all these considerations is that the crossed-field NEMAG utilizing degenerate or almost degenerate bands appears as the most promising type of a NEMAG. In the following sections we will therefore concentrate exclusively on the theory of this special structure.

III. Degenerate Bands

A. *The Negative Transverse Mass of the Heavy Holes in Germanium and Silicon*

In this section we want to study the re-entrant energy contours that may occur if the band edge lies at a point of symmetry in k-space. We shall not attempt to discuss the band splitting near such a point for the most general

case. Without loosing any of the essential features of even the most general case, we may restrict the mathematical treatment to that case that is simplest of all and of most immediate importance: a doubly degenerate band edge, located at $k=0$, in a cubic crystal. This is the case of the valence band of Ge and Si.

The theory then [8] predicts that the two bands split according to

$$\epsilon(k) = \frac{\hbar^2}{2m_0} \left[A k^2 \pm \sqrt{B^2 k^4 + C^2(k_x^2 k_y^2 + k_y^2 k_z^2 + k_z^2 k_x^2)} \right] \quad (19)$$

where m_0 is the mass of a free electron, k_x, k_y, and k_z are the components of k with respect to the three (100) axes of k-space, and A, B, and C are numbers characteristic of the semiconductor in question. It is apparent from (19) that $\epsilon(k)$ increases parabolically, i.e., with constant m_L, in every direction through $k=0$ but that the steepness of the increase depends on the direction. The band with the plus sign in (19) obviously has a lower longitudinal mass than the band with the minus sign, so the two are called "light" and "heavy" band.

We will show next that the heavy band can actually have re-entrant energy contours such as sketched in Fig. 4. Note first that m_T should be most negative along the three main axes of k-space. We find along the k_x-axis

$$\frac{1}{m_T} = \frac{1}{\hbar^2} \frac{\partial^2 E}{\partial k_y^2} = \frac{1}{\hbar^2} \frac{\partial^2 E}{\partial k_z^2} = \frac{1}{m_0} \frac{2B(A-B)-C^2}{2B} \quad (20)$$

independent of k_x and independent of the direction in the k_y/k_z-plane.[4] The condition for a negative transverse mass is

$$C^2 > 2B(A-B). \quad (21)$$

For the holes in Germanium and Silicon the numbers A, B and C are known experimentally [9]:

Ge: $A = 13.1 \pm 0.4$ $B = 8.3 \pm 0.6$ $C = 12.5 \pm 0.5$

Si: $A = 4.0 \pm 0.1$ $B = 1.1 \pm 0.4$ $C = 4.1 + 0.4$.

These numbers satisfy (21), leading to the values

$$m_{T,Ge} = -0.22 m_0 \qquad m_{T,Si} = -0.43 m_0.$$

These numbers are not only negative but also reasonably low in absolute value. This is desirable since it leads to a high negative transverse mobility.

If one moves away from the k_x-axis, the transverse mass becomes gradually less negative and it begins to depend on the direction of the signal field in the k_y/k_z-plane. One can show that one obtains a conical region of negative mass. The boundary of this cone is given by radial beams away from $k=0$, as shown in Fig. 4. The width of the cone, measured in the direction of the ac field, is smallest for an ac field in the (100 direction, largest for a (110) field. This is illustrated in Figs. 5 and 6.
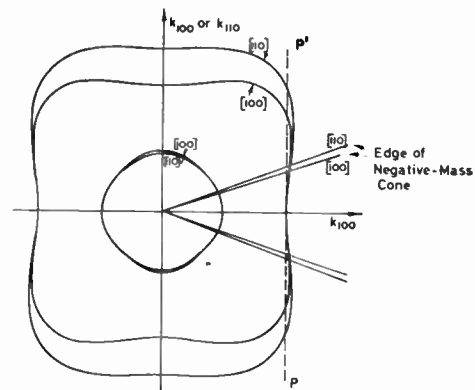
Fig. 5.—Actual shape of the energy contours of the heavy holes in germanium. The two curves give the contours in the (100) plane and the (110) plane, through $k=0$.
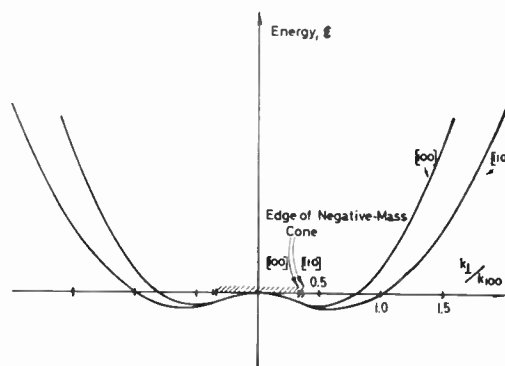
Fig. 6.—Energy profile along the line PP' in Fig. 5.
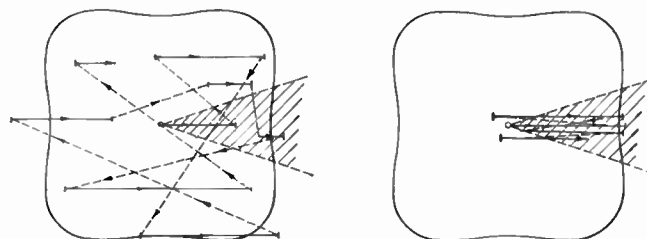
Fig. 7—Schematic motion of electrons through k-space for purely acoustical scattering (left) and purely optical scattering (right).

B. Scattering

From the above considerations, it is apparent that it should be possible to build a crossed-field NEMAG with p-germanium, provided it is possible to contain a sufficient fraction of the total hole population within that cone of the k-space where $m_T < 0$.

This condition is a very severe one, and it makes it necessary to study the scattering of the holes. One can distinguish two extreme cases of scattering (Fig. 7).

1) The hole loses practically all its energy and returns to near $k=0$. Upon reacceleration the hole moves through the negative mass region until it is scattered again. This type of scattering would not interfere at all.

2) The hole is scattered almost elastically but isotropically. In this case most holes would be scat-

tered out of the rather narrow cone of negative m_T and a NEMAG would be impossible.

The two main types of scattering to be considered in a semiconductor of sufficient crystalographic quality are lattice scattering and impurity scattering. At high fields the electrons or holes will heat up significantly above the lattice temperature and one may expect that the impurity scattering will then be negligible compared to the lattice scattering [10].

Lattice scattering can be acoustical phonon scattering or optical phonon scattering, both types being significantly different. It is known that the acoustical phonon scattering is almost elastic and almost isotropic [3], *i.e.*, it is of the harmful variety described above.

Optical-phonon scattering may be entirely different. If the collision cross-section is high enough, the electron (or hole) is scattered as soon as it reaches the threshold energy. During that collision, the particle loses an amount of energy equal to the threshold energy, and if the collision took place as soon as the particle had reached that threshold, then there will be no energy left on it. This was stated above to be the most desirable type of scattering.

These considerations teach that for a NEMAG one should choose:

1) a semiconductor with an optical-phonon cross-section as high as possible, and
2) operational conditions such that no other type of scattering can take place.

As to 1), first note that this requirement is not contradictory but rather complementary to the above requirement that the negative masses should occur at energies lower than $\epsilon \approx \epsilon_{opt}$. There are practically no numbers known for these cross-sections. It is to be expected that the cross-section values for the germanium-like, but partially polar III–V compounds are much larger than for germanium. It is also to be expected that there are other completely different semiconductors which have both re-entrant energy contours and high scattering cross-section. Potential suitability for NEMAG purposes may thus well be a new and useful criterion for judging semiconductor compounds. Experimentally, high-quality single crystals of high purity are required. At the time of this writing, we have no experimental results on compounds.

As to 2), once a proper semiconductor has been chosen, the main problem is to eliminate the acoustical phonon scattering. Apparently the only way to do this is to choose a biasing field so high that the carriers reach $\epsilon = \epsilon_{opt}$ before they have an opportunity to collide with an acoustical phonon, that is, the bias field should be in that range where the velocity vs field curves saturate. In germanium this is above 5000 volt/cm at room temperature, lower at lower temperature [4].

Finally, it has to be avoided that energy is transferred from the optical phonons back to the charge carriers.

The operating temperature therefore should satisfy

$$kT \ll \epsilon_{opt}. \tag{22}$$

C. Light Holes

So far, we have assumed that only the heavy carriers are present. Actually, since the re-entrant energy surfaces are due to the splitting of two degenerate bands, there will always be some carriers in the other, nonre-entrant band, or in the special case of p-type Ge, in the light hole band. The light carriers have a positive transverse mass which follows analogous to (20) from (19)

$$\frac{1}{m_{T,l}} = \frac{1}{m_0} \frac{2B(A + B) + C^2}{2B}. \tag{23}$$

With the known numbers A, B, and C the numerical values are

$$\text{Ge: } m_{T,l} = +.032m_0; \qquad \text{Si: } m_{T,l} = +.097m_0.$$

The absolute magnitude of these values is much smaller than that of the heavy holes. Therefore, the light holes are much more effective in their interaction with the electric field. If n_l and n_h are the densities of the light and the heavy holes, it is necessary therefore that the average mass, given by

$$\frac{1}{m_{T,av}} = \frac{1}{m_0}\left(\frac{n_l}{m_{T,l}} + \frac{n_h}{m_{T,h}}\right) \tag{24}$$

is negative. This means $n_l : n_h < .14$ in Ge and $n_l : n_h < .22$ in Si.

Under thermal equilibrium conditions the carrier ratio is equal to the ratio of the 3/2-power of the density-of-state averages of the longitudinal effective masses, m^*,

$$n_l/n_h = (m_l{}^*/m_h{}^*)^{3/2}. \tag{25}$$

The m^*-values have been estimated by Lax and Mavroides [11] to be

$$\text{Ge: } m_l{}^* = .044m_0, \ m_h{}^* = .36m_0;$$
$$\text{Si: } m_l{}^* = .17m_0, \ m_h{}^* = .53m_0$$

leading to carrier ratios of .043 for Ge and .18 for Si.

Under pulsed conditions the ratio changes to

$$n_l/n_h = (\tau_l/\tau_h) \cdot (\pi_l/\pi_h) \tag{26}$$

where the τ's are collision times and the π's are the probabilities that any arbitrary hole becomes a light one or a heavy one after a collision. Under the conditions of strong optical phonon scattering, both the heavy and the light holes scatter at the same fixed energy and one can show easily that

$$\tau_l/\tau_h = \sqrt{m_{L,l}/m_{L,h}} \tag{27}$$

where the m_L's are the longitudinal masses in the biasing

direction. The π-ratio may in first order [13] be assumed to be equal to the ratio of the density of states per energy interval, independent of whether the hole was originally light or heavy,

$$\pi_l/\pi_h = (m_l^*/m_h^*)^{3/2}. \tag{28}$$

Therefore,

$$(n_l/n_h)_{\text{High Field}} = (m_l^*/m_h^*)^{3/2}(m_{L,l}/m_{L,h})^{1/2}. \tag{29}$$

According to (19), the longitudinal masses are given by

$$m_{L,l} = \frac{m_0}{A+B}, \qquad m_{L,h} = \frac{m_0}{A-B} \tag{30}$$

which leads to a τ-ratio of

$$\tau_l/\tau_h = \sqrt{(A-B)/(A+B)}. \tag{31}$$

Numerically the light-to-heavy hole ratio then becomes

$$\text{Ge}: n_l/n_h = 0.021 \qquad \text{Si}: n_l/n_h = 0.14.$$

Both values satisfy the above condition, although not by a large margin in the case of silicon. For germanium, however, we would not anticipate any significant interference from the light holes upon the NEMAG action.

D. The Transverse Mobility

If the optical-phonon scattering theory is correct, it is possible to calculate the negative transverse mobility quantitatively. The peak velocity, v_{opt}, reached by the carriers is

$$v_{\text{opt}} = \sqrt{\frac{2\epsilon_{\text{opt}}}{m_{L,h}}}. \tag{32}$$

The average carrier velocity, that is, the experimentally observed saturation velocity, v_{sat}, is exactly half that value. The collision time τ which is required for the carriers to reach their peak velocity under the influence of the bias field, E_0, is

$$\tau_h = v_{\text{opt}} \frac{m_{L,h}}{eE_0}. \tag{33}$$

According to Ryder [4] in p-type germanium at 77°K (we anticipate the need for cooling) one has $v_{\text{sat}} = \frac{1}{2}v_{\text{opt}} \approx 10^7$ cm per second, and the saturation sets in roughly at 200 volt per cm. If one uses these two values as a guide and inserts $m_L = .20 \ m_0$[5] one finds $\tau_h \approx 1.1 \cdot 10^{-12}$ seconds for higher fields correspondingly shorter collision times. These values mean, according to (15), that the NEMAG will operate up to about 1000 kmc.

During the time τ_h, the carrier reaches a transverse velocity, v_T, under the influence of a transverse field, E_T, of

$$v_T = \frac{eE_T\tau_h}{m_{T,h}} = v_{\text{opt}} \frac{m_{L,h}}{m_{T,h}} \frac{E_T}{E_0}. \tag{34}$$

[5] This is the value along the (100) axis, according to (30).

The average transverse velocity is again half that value, and by dividing through the ac field one obtains the transverse mobility

$$\mu_{T,h} = \frac{v_{\text{sat}}}{E_0} \frac{m_{L,h}}{m_{T,h}} < 0. \tag{35}$$

With our above numbers one obtains $\mu_T = -4350$ cm² per V second. This is an appreciable value. At higher temperature the saturation velocities are somewhat lower and the saturation fields are higher, so the obtainable mobility would be smaller. At lower temperatures, it may be larger. It is interesting to note that the mobility is inversely proportional to the field. This means that an optimal NEMAG should not operate beyond the point where the saturation of the parallel field velocity has been reached. This is illustrated in Fig. 8.
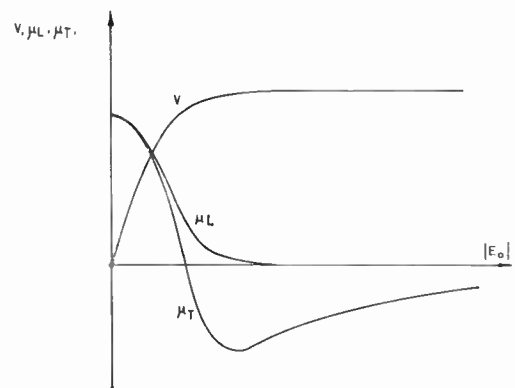
Fig. 8—Schematic dependence on the bias field, E_0, of drift velocity, longitudinal mobility and transverse mobility.

The simultaneous presence of light holes reduces the value somewhat. One finds

$$\mu_T = \frac{v_{\text{sat}}}{E_0} \frac{m_{L,h}}{m_{T,h}} \left(1 - \frac{n_l}{n_h} \frac{|m_{T,h}|}{m_{T,l}} \sqrt{\frac{m_{L,l}}{m_{L,h}}} \right). \tag{36}$$

For Ge the correction term amounts to less than 7 per cent.

The high absolute value of the transverse mobility leads to high transverse conductivities. In order to obtain a transverse conductivity of, say, 0.1 Ω^{-1} cm^{-1}, less than 2.10^{14} carriers are necessary per cm.³

IV. A Note on the Electrical Design Theory for a Crossed Field NEMAG

To illustrate the discussion of the previous sections, a short description of the basic design principles is given for the case of a NEMAG that utilizes the re-entrant energy contours of some suitable semiconductors with a band structure like that in p-type germanium. The crystal may consist of a prismatic bar cut parallel to the crystallographic (100) direction. At the two ends of the bar, noninjecting electrodes may be plated or soldered to the bar covering the whole face [Fig. 9(a)]. The bias voltage is directly applied to these electrodes, the polarity being arbitrary. The ac field then may have

any direction that is perpendicular to the axis of the bar. But since the energy contours are slightly more re-entrant in the (110) plane than in other planes, such an orientation of the ac field could be preferred when the two fields lie in a (110) plane, that is, where the ac field is parallel to a (110) direction. The four side faces of the bar may also then be (110) planes.

The manner in which the ac field is applied will depend on the frequency. At low frequencies this has to be done through electrodes actually attached to the crystal [Fig. 9(b)–9(c)]. Fig. 10 shows one possible application out of many: an oscillator circuit using such a NEMAG.

For sufficiently high frequencies the ac current can be coupled in as displacement current rather than as a conduction current, and in the microwave region this procedure will become the rule. The crystal is then simply placed inside a microwave resonant cavity or inside the waveguide such that the electrical vector of the ac field has the desired direction.
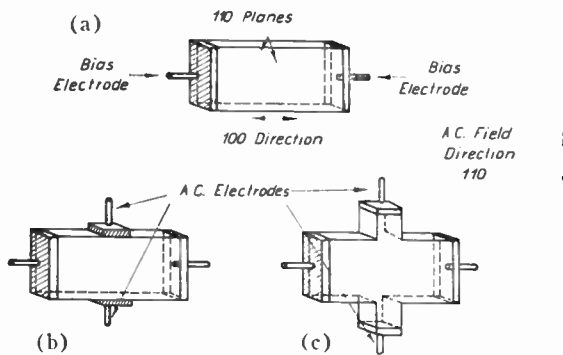
Fig. 9—(a) Crystal orientation for NEMAG-wafers. (b) Low frequency NEMAG structure. (c) Low frequency NEMAG structure.
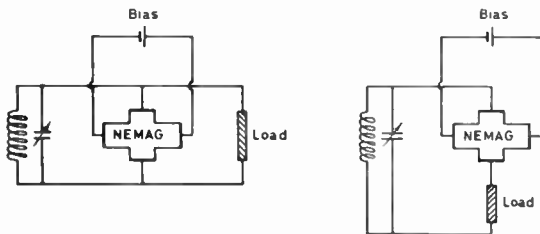
Fig. 10—Two tunable oscillator circuits using a four-arm low-frequency NEMAG.

Because of the skin effect the crystal is then preferably in the form of a wafer not thicker than the skin depth. Any increase in crystal thickness materially beyond this value does not increase the available gain but merely increases the bias current and decreases the efficiency. One can show that it is not likely that one will encounter thicknesses far below mechanically manageable dimensions, but we shall omit that proof here. Such a wafer can then be inserted in different ways into a waveguide or a resonant cavity. Fig. 11 shows some possible arrangements for a rectangular waveguide. The standard theory of the action of conducting obstacles in

waveguides [13] can be applied by inserting negative conductivity values instead of the usual positive ones. That means, one obtains the same number of decibels of gain as the attenuation would be for a positive resistance of the same absolute value.
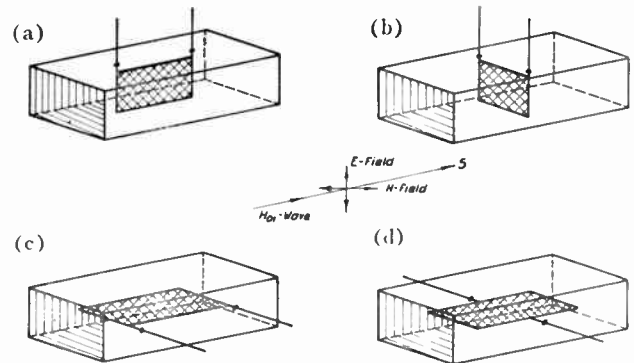
Fig. 11—Different arrangements of a high-frequency NEMAG in a rectangular waveguide.

We want to illustrate this only for a very simple case: an arrangement, as in Fig. 11, for a frequency much higher than the cutoff frequency and for a very weak wafer conductivity. One then finds for the attenuation constant α,

$$\alpha = \frac{377\Omega}{aR}, \tag{37}$$

where a is the width of the waveguide and R the sheet resistance of the wafer in ohms per square. For a wafer of a conductivity of $-20\Omega^{-1}$ cm^{-1} and of a thickness of 0.05 cm, and for a waveguide width of 1 cm, one obtains[6] $\alpha = -0.94$ cm^{-1} which corresponds to a power gain of $8.7\,\alpha = 8.2$ db/cm. Closer to the cutoff frequency or for multiple-pass structures with internal reflexions[7] one obtains of course even higher values.

We do not want to develop these design details further here. What should follow at this point is a detailed design theory that should cover at least the three following subjects.

1) Optimal design for operation as an oscillator and as an amplifier is necessary both for structures with and without side connections.
2) Stability problems. The negative transverse conductivity extends down to dc. As a result space charge instabilities may occur. These may be cultivated to obtain operation of a NEMAG as a fast bi-stable device rather than as an amplifier or generator. For an amplifier or generator the instabilities have to be avoided, however, A design theory has to include the means to do either.
3) Noise. If the optical phonon scattering is inelastic enough to make a NEMAG work in the first place,

---

[6] Actually, (37) is no longer exact for these numbers, but we may ignore these fine details here.
[7] The influence of the bias electrodes goes in this direction.

it will be a low-noise device. This is because the "transverse" temperature of the current will be very low, as shown in Fig. 7.

It turns out that the stability problem is the most important and the most difficult one of these three. But by a proper design instabilities can indeed be avoided. The considerations leading to the different stabilization methods are of a rather different nature, however. The design theory will therefore be presented in another paper.

G. Doumanis [14] recently suggested the addition, parallel to the bias field, of a magnetic field of such a magnitude that the cyclotron resonance frequency of the negative-mass carriers would equal the incident microwave frequency. The "negative" carriers would, then, be in resonance while the positive ones outside the cone would constantly fall out of step. It is believed that in this way a higher fraction of carriers is tolerable that have been scattered out of the cone. That is, the optical phonon cross section need not be that high.

V. ACKNOWLEDGMENT

The author is very much indebted for numerous discussions to many members of the RCA Laboratories, particularly to I. H. Adawi, R. A. Braden, F. Herman, D. A. Jenny, H. Johnson, and to Prof. C. Kittel, from the University of California. For experimental help and cooperation he wishes to thank Mrs. C. Dobin, A. R. Larrabee, and particularly J. J. Thomas. Most of all, he wishes to thank E. W. Herold for his support and encouragement.

Note: Dousmanis *et al.* [15] has since verified the existence of the negative masses in Ge experimentally by cyclotron resonance experiments using a (100) magnetic field and circularly polarized microwaves. Because of the negative mass the resonance of these carriers shows up as an emission-type dip in the background absorption rather than as an absorption peak. Net emission, *i.e.*, RF gain, is obviously not possible in thermal equilibrium. In a paper in which Dousmanis [14] had suggested these experiments, he also points out that the utilization of cyclotron resonance might facilitate the

construction of a NEMAG if a magnetic field is combined with the electric biasing field. In NEMAG terminology the resonance enhances the effectiveness of the negative mass carriers and suppresses the effectiveness of the positive mass carriers which are constantly "out of step" with the circularly polarized microwave field. In cyclotron resonance terminology the electric field produces a strong perturbation of the carrier distribution in k-space which may transform the resonance dip in the background absorption into a genuine emission. It is conceivable that for such a cyclotron resonance NEMAG the highly inelastic optical phonon scattering is no longer absolutely necessary.

BIBLIOGRAPHY

[1] H. Kroemer, "Proposed negative mass microwave amplifier," *Phys. Rev.*, vol. 109, p. 1856; March, 1958.
[2] For a general survey see K. G. McKay, "Avalanche breakdown in silicon," *Phys. Rev.*, vol. 94, pp. 877–884; December, 1954.
[3] W. Shockley, "Ohms law and hot electrons in germanium," *Bell Sys. Tech. J.*, vol. 30, pp. 990–1034; October, 1951.
[4] E. J. Ryder, "Mobility of holes and electrons in high electric fields," *Phys. Rev.*, vol. 90, pp. 766–769; February, 1953.
[5] J. B. Gunn, "The field-dependence of electron mobility in Ge," *J. of Electronics*, vol. 2, pp. 87–94; July, 1956.
[6] J. B. Arthur, A. F. Gibson, J. W. Granville, "The effect of high electric fields on the absorption of germanium at microwave frequencies," *J. of Electronics*, vol. 2, pp. 145–153; September, 1956.
[7] G. Dresselhaus, "Spin-orbit coupling effects in zinc blende structures," *Phys. Rev.*, vol. 100, pp. 580–586; October, 1955.
[8] There are a number of papers on this subject; we may refer to R. J. Elliott, "Theory of the effect of spin orbit coupling on magnetic resonance in some semiconductors," *Phys. Rev.*, vol. 96, pp. 266–279; October, 1954; and A. Dresselhaus, A. F. Kip, and C. Kittel, "Cyclotron resonance of electrons and holes in Si and Ge crystals," *Phys. Rev.*, vol. 98, pp. 368–384; April, 1955. For a summary, see also F. Herman, "The electronic energy band structure of silicon and germanium," PROC. IRE, vol. 43, pp. 1703–1732; December, 1955.
[9] R. N. Dexter, H. J. Zeiger, and B. Lax, "Cyclotron resonance experiments in silicon and germanium," *Phys. Rev.*, vol. 104, pp. 637–644; November, 1956.
[10] See, for example, E. M. Conwell, "High field mobility in germanium with impurity scattering dominant," *Phys. Rev.*, vol. 90, pp. 769–772; February, 1953.
[11] B. Lax and J. G. Mavroides, "Statistics and galvanomagnetic effects in germanium and silicon with warped energy surfaces," *Phys. Rev.*, vol .100, pp. 1650–1657; February, 1955.
[12] For a more accurate treatment see, H. Ehrenreich and A. W. Overhauser, "Scattering of holes by phonons in germanium," *Phys. Rev.*, vol. 104, pp. 331–342; October, 1956.
[13] For example, N. Marcuvitz, "Waveguide Handbook," vol. 10, Rad. Lab. Ser., McGraw-Hill Book Co., Inc., New York, N. Y.; 1951.
[14] G. Dousmanis, *Phys. Rev.* Letters, pp. 55–56, 168–169; July, 1958.
[15] G. Dousmanis, *et al.*, *Phys. Rev.*, Letters, pp. 400–402; December, 1958.

Simple General Analysis of Amplifier Devices with Emitter, Control, and Collector Functions*

E. O. JOHNSON†, MEMBER, IRE, AND A. ROSE†, FELLOW, IRE

Summary—The comparative signal amplifying capabilities of lumped solid-state and vacuum tube devices of the emitter-control-collector type are described in a very simple, yet general, manner in terms of charge control, charge storage, and charge motion. The emitter-collector charge transit time is shown to be a ubiquitous physical parameter determining current, voltage, and power amplifications and their bandwidth products. Also of central importance is a characteristic capacitance that describes the capability of the inter-electrode space to store mobile charge. The unipolar and analog transistors, the grid-controlled vacuum tube, and the beam deflection tube all have characteristic capacitances approximately equal to their electrode geometrical capacitances. The bipolar transistor holds an advantage over the other solid-state devices because it can have a larger characteristic capacitance. This advantage also holds against the vacuum tube devices, but is tempered by the fact that the latter can have much larger carrier drift velocities.

For the solid-state devices it is emphasized that the saturated carrier drift velocity is sometimes a better indication of material merit than carrier mobility. Ultra-high frequency performance of the solid-state devices requires some combination of microscopic dimensions, improved materials, or charge multiplication.

INTRODUCTION

IN SEARCHING for suitable electronic devices to amplify at high frequencies it is convenient to have simple relations or conceptual notions for evaluating the operating principles—relations or concepts sufficiently general to encompass all devices of a class without regard to specific details of operation or structure. For example, one would like to compare, with something more than computations on specific device geometries, the physical principles and capabilities of the unipolar, bipolar, and analog transistors. Comparisons of this sort are of particular interest for present and future applications, such as in ultra-high speed computers, where one is confronted with new and different combinations of operating requirements involving size, speed, gain, and power dissipation.

The charge control mechanism[1] in devices of the emitter-control-collector type forms the basis for this paper. Charge control means that *a charge on the control electrode can introduce at most an equal amount of charge in the conduction space between emitter and collector.* This simple notion leads in a natural way to a description of

operation in terms of characteristic time constants, and these lead directly to a description of frequency behavior. Quite recently it was pointed out that the charge control concept could be used to simplify detailed calculations on the performance of bipolar transistors.[2] The present paper demonstrates the general applicability of this concept to outstanding members of the class of devices noted above.

The generalizations in this paper are to be used only as rule-of-thumb guides in evaluating performance possibilities: the detailed behavior of any specific device structure has to be treated with detailed calculations of the sort already known to the respective device arts. Noise questions and impedance matching problems are not discussed. In most cases, if not in all, the relations to be described overestimate the performance capabilities. Those familiar with one or more of the device areas will not find any particularly new results but, rather, a different and compact, "broad brush," way of expressing, comparing, and summarizing facts already known. On the other hand, those relatively unfamiliar with the device field may, it is hoped, be pleased to find that the first order performance properties of a variety of devices can be derived from a common set of simple physical arguments and do not necessarily require an elaborate analysis.

PHOTOCONDUCTOR

Although the photoconductor is only of passing interest in this paper, it provides an especially simple illustration of the charge control principle. The other devices are somewhat more complicated, but to understand them requires only a slight extension of the ideas set forth in this section.

To be specific, consider a photoconductor made from a bar of length L of n-type semiconductor material. A constant potential V_0 is impressed across the ends of the bar. The load current, composed of electrons streaming along the bar, passes through a space-charge free region, or plasma. Modulation of this current is effected by optical injection of carrier pairs generated across the forbidden gap. Space charge neutrality is always maintained: for each added majority carrier electron there is always a companion minority carrier hole. The added carriers of both signs cause an increase in conductivity and hence a larger load current. The carriers of opposite

[1] The use of this viewpoint in this paper is an extension of the concepts long used in photoconductor studies in this laboratory. See, for example, A. Rose, "La photoconductivité," *L'Onde Électrique*, vol. 34, pp. 645–651; October, 1954.

[2] J. J. Sparks and R. Beaufoy, "The junction transistor as a charge control device," PROC. IRE, vol. 45, p. 1740; December, 1957. Also *ATE J.*, vol. 13, pp. 310–327; October, 1957.

signs contribute to this enhanced conductivity in proportion to their mobilities. In principle, the mobility ratio can be anything between zero and infinity. For simplicity, however, we can assume that the minority carrier mobility is negligible compared with that of the majority carriers. This will help emphasize the charge control concept, particularly for other types of devices, without affecting the general validity of our arguments.

The increase in load current will persist as long as the excess carriers are present. If the carrier pair lifetime is long, relatively many majority charge carriers will pass through the load circuit during this lifetime (commonly called the minority carrier lifetime).[3] The device will then tend to have a large current amplification, since the signal input current corresponds to the rate at which charge pairs are generated by the modulated light, and the output current corresponds to the rate of majority carrier passage through the load circuit. The current amplification is obviously enhanced when the majority carrier drift, or transit time τ_r through the bar is short.

The concept to be noted here is the one of charge control; that is, current amplification is associated with the presence and lifetime of charge carrier pairs. Only *one* excess majority carrier can exist for each excess minority carrier. This follows directly from the condition of space charge neutrality in the bar. On the average, only after this excess majority carrier has traversed the bar can another appear in the bar to start its transit. This process repeats itself τ/τ_r times during the effective lifetime τ of the minority carrier. The effective current amplification G_i, which is a measure of the efficacy of input charge flow in causing output charges to flow, is then simply

$$G_i = \tau/\tau_r. \qquad (1)$$

Furthermore, since the minority carrier population must always be able to follow or keep step with the signal or light modulation frequency f, there is a maximum allowable value of τ. For sinusoidal modulation of the light this value is $(2\pi f)^{-1}$. Thus, for a given value of τ_r, the maximum current amplification of the device cannot be greater than

$$G_i = (2\pi f)^{-1}/\tau_r, \qquad (2)$$

for the case where no charge carrier multiplication effects exist; these would introduce a multiplicative factor. Eq. (2) applies to all the other devices to be considered.

A slightly different way to arrive at (1) starts with the very general expression,

$$i_0 = q/\tau_r, \qquad (3)$$

wherein i_0 is the output signal current through the device and q is the excess mobile interelectrode majority carrier charge present as a result of the input light signal. A charge q is swept out at the collector electrode each charge transit time τ_r. This relation follows from the definition of current, and holds regardless of the type of conduction process or form of the mobile charge distribution. When two types of carriers contribute to the current, (3) is slightly modified. In the photoconductor the generated interelectrode mobile charge q can be expressed by

$$q = i_i\tau, \qquad (4)$$

where i_i, the input signal "current," is the rate at which carrier pairs are generated by the modulated light. Since the current amplification is here defined as

$$G_i = i_0/i_i, \qquad (5)$$

application of (3) and (4) leads immediately to (1).

The next parameter to consider is the energy or voltage amplification per carrier. This is defined here as the ratio of the energy eV_0 produced by a carrier in the load circuit to the energy eV_i required at the device input to activate, inject, or mobilize that charge carrier. For the photoconductor the voltage amplification G_r is

$$G_v = V_0/V_i. \qquad (6)$$

As described here, the voltage V_0 across the bar is held constant and the energy generated in the load circuit appears solely as heat within the device itself. A more conventional notion of voltage amplification and the question of transferring the output energy into a load, where it can do useful work, is treated later.

The intrinsic signal power amplification G_p of the photoconductor itself is then the product

$$G_p = G_iG_v = (\tau/\tau_r)(V_0/V_i). \qquad (7)$$

In this expression, the optical and photon efficiencies are assumed to be unity. The effective carrier pair lifetime for a photoconductor is normally fixed by the material parameters and is not optimized in any one structure for a range of frequencies. The value of τ, if desired, can encompass sweepout effects. Then, neglecting circuit time constants, the power amplification will be constant from zero frequency up to a frequency, very roughly τ^{-1}, beyond which the effective value of G_p will rapidly decrease because the electric charges associated with one frequency period will persist into the next and so distort the output.

It is interesting to note that (7) can be applied directly to evaluate the performance of a gas discharge device which is almost an exact analog of the photoconductor. In this device,[4] the "Plasmatron," the carrier

[3] In the normal treatment of sensitive photoconductors, the minority carrier lifetime is likely to be short compared with the majority carrier lifetime, and the latter becomes the significant lifetime. If the trap density is not large compared with the added free carrier densities, the alternative treatment used here of assuming equal lifetimes for majority and minority carriers, but zero mobility for the minority carrier, gives equivalent results. For a detailed treatment of this question, see A. Rose, "Performance of photoconductors," PROC. IRE, vol. 42, pp. 1850–1869; December, 1955.

[4] E. O. Johnson and W. M. Webster, "The Plasmatron, a continuously controllable gas discharge developmental tube," PROC. IRE, vol. 40, pp. 645–659; June, 1952.

pairs are generated by an electron stream which bombards neutral gas atoms. The resulting gaseous plasma takes the place of the space charge-neutralized piece of semiconductor material used in the photoconductor. Although G_v in the Plasmatron can never be larger than unity, the current amplification can be large because of the relatively large electron mobilities in a gas.

UNIPOLAR TRANSISTOR

The device customarily referred to as the unipolar transistor[5] consists of an extrinsic semiconductor bar with ohmic contacts affixed to each end (Fig. 1). One contact is termed the "source" and the other, the "drain." The first may be thought of as being an emitter, an electrode where carriers enter the device, and the second, a collector, an electrode where carriers leave the device. The conducting path or channel between the two electrodes is sandwiched between two regions, called "gates," of conductivity type opposite to that of the channel. A signal voltage, applied across the gate p-n junction, is used to vary the depletion layer thickness and hence the width and resistance of the channel.
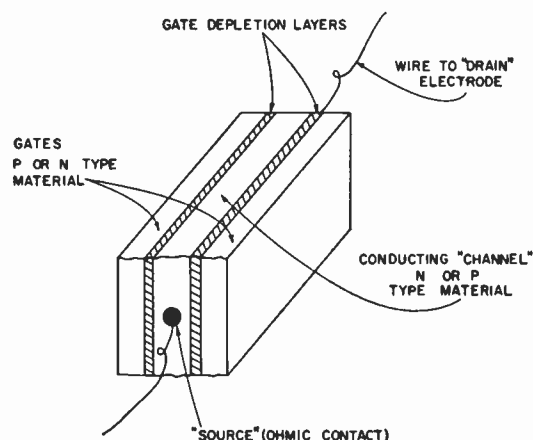
Fig. 1—Conventional unipolar structure using semiconductor material.

By this means the output signal current in the load circuit, of which the channel is a portion, can be controlled by an input signal voltage. As the literature testifies,[5,6] a detailed treatment of this operation can be very complicated. However, it will be shown that the unipolar operating principles, which apply to *any* conductor, can be understood by elementary and yet very general physical arguments. These arguments encompass current, voltage and power amplifications, transconductance, and the amplification-bandwidth products. Much of the treatment applies directly to the other devices, and so, once discussed, forms a convenient reference for the remainder of the paper.

[5] W. Shockley, "A unipolar 'field effect' transistor," PROC. IRE, vol. 40, pp. 1365–1376; November, 1952. Also O. Heil, British Patent 439,457; 1935.
[6] G. C. Dacey and I. M. Ross, "The field effect transistor," *Bell Sys. Tech. J.*, vol. 34, pp. 1149–1189; November, 1955.

In Fig. 2 is shown a length L of uniform conductor (channel) of conductance Σ connected across a supply potential of V_0 volts. A current

$$I_0 = \Sigma V_0 \qquad (8)$$

will flow in the channel. Furthermore,

$$\Sigma = \rho\mu(A/L) = \mu(AL/L^2) = \mu Q/L^2, \qquad (9)$$

where ρ is the mobile charge density in the channel, μ is the carrier mobility, A is the cross-section area of the channel, and Q is the total carrier charge in the channel, for simplicity assumed to be only of one sign and type of carrier. Combining (8) and (9), we find Ohm's law restated in terms of (3), that is

$$I_0 = \frac{Q}{[L^2/V\mu]} = \frac{Q}{\tau_r}. \qquad (10)$$

The quantity in brackets is identically the time τ_r for the average carrier to drift the length L of the channel.
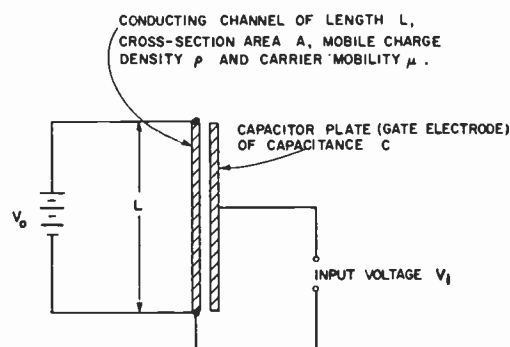
Fig. 2—Basic unipolar structure using any type of conducting material.

Modulation of the current I_0 is simple in principle: we need only vary the mobile charge Q by transferring charge from the channel to the adjacent condenser plate (the "gate"). Carrier charge placed on the condenser plate is effectively demobilized and can no longer contribute to the flow of current in the conducting channel. Over-all electrical neutrality is retained because the uncompensated fixed charge, left behind when the carriers are removed, is effectively neutralized through capacitive coupling to the carriers transferred to the capacitor or gate electrode. That is, there is always a one-to-one correspondence between a carrier charge on the gate and its absence in the conducting channel. Therefore, as long as a carrier "lives" on the gate its absence will "live" in the channel, and the effective current amplification will be exactly the same as in the photoconductor, the ratio between "lifetime" on the gate and average drift time through the channel. In the present case, however, the effective lifetime on the gate is forced by the input driving source to have a value $(2\pi f)^{-1}$. Thus, aside from leakage effects, the current amplification of the general unipolar device will be that given in (2).

The purely capacitive input does not define a finite pass band. To define a low-pass band Δf extending from zero to $(2\pi R_i C_i)^{-1}$ cycles per second, let a resistance R_i be added in parallel with the input or gate capacitance C_i. The resistance R_i insures that any control charge Q_i placed on the input electrode remains there for a time $\tau = R_i C_i$. During this time it is ideally controlling the flow of an equal amount of charge Q_i in the conducting channel. At the end of the time τ, the input charge has been drained off through the resistance (compare with the lifetime of an electron-hole pair in a photoconductor) and must be replaced. The input current is then Q_i/τ and the output current is Q_i/τ_r, giving the current amplification-bandwidth product

$$G_i \Delta f = (2\pi \tau_r)^{-1}. \qquad (11)$$

The same product is obtained for a band Δf centered about the resonant frequency f of the combination of the input capacitance C_i, an external inductance L_i, and whatever resistance R_i might be included in the input circuit. The current amplification-bandwidth product in this case is equal to the product of (2), the circuit factor of merit ($\phi = 2\pi f L_i/R_i$) which provides a current step-up, and the effective bandwidth ($\Delta f = f/\phi$). This product is identically $(2\pi \tau_r)^{-1}$.

The voltage amplification G_v, the ratio of the signal voltage at the output to that at the input terminals, may be derived by the following argument:

$$G_v = G_i \frac{\text{output load impedance}}{\text{input impedance}} = G_i \frac{R_0}{R_i}, \qquad (12)$$

for parallel RC networks at input and at output and for the low-pass band extending from zero frequency to the characteristic frequency $1/(2\pi RC)$. It is assumed that the output load resistance R_0 is less than the internal output resistance of the device. If the input and output networks have the same low-pass band,

$$R_i C_i = R_0 C_0 \quad \text{and} \quad R_0/R_i = C_i/C_0. \qquad (13)$$

Consequently, (12) becomes

$$G_v = G_i \frac{C_i}{C_0}, \qquad (14)$$

which is valid even at frequencies beyond the upper edge of the pass band. As will be clear later, exactly the same result is obtained from the more conventional expression for voltage amplification, $g_m R_0$, where g_m is the transconductance of the device.

Eq. (14) can be combined with (2) to give the power amplification for the low-pass band:

$$\begin{aligned} G_p &= G_i G_v \\ &= G_i^2 \frac{C_i}{C_0} \\ &= \left(\frac{1}{2\pi f \tau_r}\right)^2 \frac{C_i}{C_0}, \end{aligned} \qquad (15)$$

where f can be replaced by its equivalent Δf. An expression identical with (15) is obtained when the bandwidth Δf is defined about some central frequency f. In this case, the analysis proceeds by using the fact that the power consumed in a resonant circuit is proportional to the product of the bandwidth and the stored energy. For the input circuit the stored energy is $Q_i^2/2C_i$, and for the output circuit, $Q_0^2/2C_0$. Q_i is the input charge during one cycle of operation; Q_0 is the total charge flowing to the output electrode in the same time and is equal to $G_i Q_i$. For equal bandwidths in the input and output circuits, the output-input power ratio reduces to (15) when $(Q_0/Q_i)^2$ is replaced by its equal, G_i^2.

Eqs. 2, 14, and 15, which apply in absence of feedback effects, are the basic relations for the maximum current, voltage, and power amplifications for all charge control devices. A few general remarks may be made about these three relations.

Current Amplification

The essential parameter determining the current amplification for a given bandwidth is the transit time of a charge carrier through the device. The current amplification varies inversely as the bandwidth, becomes infinite at zero bandwidth and approximately unity at a bandwidth equal to the reciprocal transit time of a charge carrier between emitter and collector. The current amplification bandwidth product, except for the 2π factor, is just the reciprocal of the transit time.

Voltage Amplification

The voltage amplification is the product of current gain and the ratio of the input to output capacitance. The voltage amplification is also, generally, the ratio of the work per unit charge obtained at the output electrode to the work per unit charge required at the input electrode. If, for example, a charge Q_i is placed on the input electrode, the average work per unit charge in electron volts is $Q_i/2C_i$. The input charge Q_i causes a charge $G_i Q_i$ to flow through the output during the time τ and charges the output condenser to $G_i Q_i/C_0$ volts so that the average *output* work per unit charge is $G_i Q_i/2C_0$. The ratio of output work to input work is then $G_i(C_i/C_0)$, which is the voltage amplification. In a well designed device, each charge change on the control electrode causes a numerically equal charge change in the conducting space between emitter and collector. A minimum of work is done in introducing the control charge if the capacitance C_i to the controlled charge is a maximum. By the same argument, a maximum of work is obtained from the output charge when the output capacitance C_0 is a minimum.

Power Amplification

This is just the product of the current or charge amplification and the work or voltage gain per unit charge. The ideally capacitive input of a charge control device might lead one to expect an infinite power gain. This,

however, can only be true for zero bandwidth. For a nonzero bandwidth, a dissipative element must be added to the input circuit. The power gain then becomes finite.

Current, voltage, and power amplification can indeed be increased by using feedback between the output and input terminals. However, the power-amplification bandwidth product is not increased by feedback. In brief, this follows because the power-amplification-bandwidth product in lumped charge control devices is proportional to the *rate* at which energy can be taken from the power supply and added to the signal. Furthermore, the maximum rate of this energy transfer is determined by the device physics and not by external circuitry, or by how many times the signal is recycled through the device. The feedback process, in essence, causes the signal to be cycled through the device more than once, in distinction to the single pass of the non-feedback case. Each recycle results in an energy step-up, but the price of this is a compensating loss of time.

The transconductance, g_m, is the parameter most frequently used to describe the performance of an amplifier. Its definition is

$$g_m = \frac{\partial I_0}{\partial V_i}\bigg]_{V_0}.$$

The transconductance of the unipolar transistor can be expressed in the previously used terms by the transformation

$$g_m = \frac{\partial I_0}{\partial V_i} = \frac{\partial}{\partial V_i}\left(\frac{Q}{\tau_r}\right) = \frac{\partial Q}{\partial V_i}\frac{1}{\tau_r} = \frac{C_i}{\tau_r}. \tag{16}$$

The voltage gain in (14) then becomes

$$G_v = g_m \frac{1}{2\pi\Delta f C_0} = g_m \frac{1}{2\pi f C_0}, \tag{17}$$

or, using (13) and the expression $\Delta f = (2\pi R_i C_i)^{-1}$,

$$G_v = g_m R_0, \tag{18}$$

a well known result. The value of G_v in (18) will be constant from zero frequency out to approximately the frequency f at which the capacitive reactance $(2\pi f C_0)^{-1}$ becomes equal to the load resistance R_0. In (16) C_i is the capacitance between gate electrode and the conducting channel. It is assumed that τ_r and C_i are independent of V_i and Q. [For a unipolar transistor with abrupt $p-n$ junctions, C_i varies with the nth power of V_i, where $n = -0.5$. When this is taken into account, (16) is multiplied by the factor $(1+n)$, and C_i is the gate capacitance at the operating point.] Eq. (16) gives a very good estimate of the transconductance of an actual semiconductor unipolar structure. For example, unit No. 35 of Dacey and Ross[6] was measured to have a transconductance of 1600 micromhos. A value of $\sim$1000 micromhos is calculated with (16) when the relevant data are used: a near-saturated carrier drift velocity of 10^6 cm/sec, a channel length of 2×10^{-2} cm, and 10–20 ohm-cm germanium with gate dimensions of 2×10^{-2} by $1.4\times$ 10^{-1} cm. At high frequencies the gate capacitance C_i tends to become frequency dependent because of the distributed nature of the circuit constants.[7]

Because the output resistance R_0 is shunted by the internal resistance, $r = [\partial V_0/\partial I_0]_{V_i}$, of the device, (12) and (18) are valid only when $R_0 < r$. When $R_0 > r$,

$$G_v = G_i \frac{r}{R_i}$$

$$= \frac{1}{2\pi\Delta f \tau_r}\frac{r}{R_i}$$

$$= g_m r. \tag{19}$$

This follows from (12) and the condition $\Delta f = (2\pi R_i C_i)^{-1}$. Eq. (19) is the well known expression for the maximum attainable voltage amplification $(G_v)_{max}$ in the absence of feedback or resonant step-up effects.[8] It will also be recognized as the expression for the "mu" of a vacuum tube.

In terms of the preceding analysis

$$(G_v)_{max} = \frac{C_i}{\tau_r}\frac{\partial I_0}{\partial V_0}\bigg]_{V_i}^{-1}$$

$$= \frac{C_i}{\tau_r}\left(\frac{1}{\tau_r}\frac{\partial Q}{\partial V_0} + Q\frac{\partial\left(\frac{1}{\tau_r}\right)}{\partial V_0}\right)_{V_i}^{-1}. \tag{20}$$

This shows that $(G_v)_{max}$ is basically the ratio of two capacitances, the input capacitance and a complex internal capacitance appearing at the output electrode.

For the unipolar transistor, as can be seen from the current-voltage characteristics of an actual device,[5,6] r increases with V_0 because of the decrease in both Q and $\partial(1/\tau_r)/\partial V_0$. The mobile channel charge Q decreases because of spreading gate depletion layers and $\partial(1/\tau_r)/\partial V_0$ decreases because of approaching carrier drift velocity saturation.

A semiconductor is presently the most attractive material to use for unipolar operation. The carrier mobility can be relatively high, leading to relatively small carrier drift times, and the mobile charge density is in the range allowing operation with reasonable dimensions and electrode potentials. Furthermore, $p-n$ junctions can be made that are probably superior to most realizable schemes using external electrodes and dielectrics, particularly since such schemes tend to be afflicted by the surface state problem.[9]

When the previously mentioned Plasmatron[4] is operated with a third electrode between its cathode and anode, it becomes a unipolar device operating with a gaseous plasma as its conductor.

---

[7] Pointed out to the author by J. Hilibrand of RCA Laboratories.

[8] F. S. Terman, "Radio Engineers' Handbook," McGraw-Hill Book Co., New York, N. Y.; 1943.

[9] W. Shockley, "Electrons and Holes in Semiconductors," D. Van Nostrand Co., New York, N. Y., pp. 29–33; 1950.

The maximum operating frequency of the unipolar transistor is limited by the resistance-capacitance time constant of the input circuit. Dacey and Ross[6] have pointed out that the input time constant, the product of the effective channel resistance and the gate capacitance, is approximately equal to the transit time τ_r of carriers through the channel. That this is so can be seen from the simple development

$$R_{\text{channel}}C_i = \left(\frac{L^2}{\mu Q}\right)\left(\frac{Q_i}{V_i}\right) = \left(\frac{L^2}{\mu Q}\right)\left(\frac{FQ}{V_i}\right) = \frac{F}{\left(\frac{V_i}{V_0}\right)}\tau_r, \quad (21)$$

where F is the ratio of the electric charge Q_i on the gate to the mobile charge Q in the channel. The other quantities are the same as those previously defined. In normal operation the factors F and V_i/V_0 are not far removed from unity, so that the argument is demonstrated. In a more exact treatment the nonuniformity of the channel width and the distributed nature of the resistance and capacitance have to be taken into account.

BIPOLAR TRANSISTOR

The bipolar transistor is a charge control device and not, as it may sometimes appear from a circuit viewpoint, a current control device. Electronic charge on the base electrode of a p-n-p transistor (Fig. 3) lowers
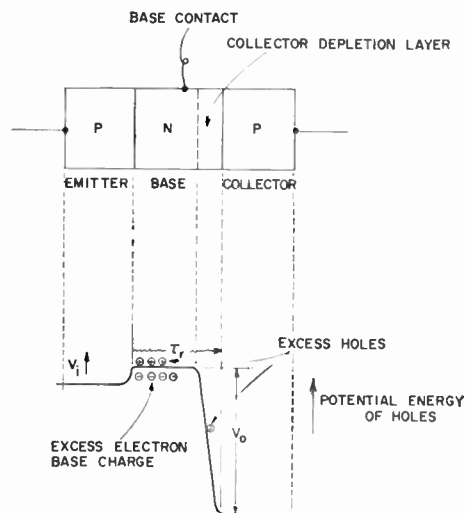
Fig. 3—P-n-p bipolar transistor structure and its internal potential distribution.

the potential barrier to holes at the edge of the emitter, allowing holes to diffuse (diffusion transistor) or drift, field-assisted (drift transistor), across the base and drop through the potential V_0 to the collector. However, since space charge neutrality is maintained in the base, each excess electron has as its counterpart only one excess hole that, ideally, is en route to the collector. In contrast to the unipolar device, where all mobile charges can be of one sign, the bipolar transistor requires mobile charges of two signs. As far as charge control principles are concerned, this difference is of little significance. However, from a practical standpoint it is important, because the transport properties of both signs of carriers become involved in the operation and this puts more stringent conditions upon the semiconductor materials to be used.[10]

The leakage, recombination, and emitter inefficiency effects, that make the device appear to be other than charge controlled, are not of essence in the amplifying mechanism itself. They are subsidiary technological limitations.

Eq. (2) again applies for the current amplification because of the one-to-one charge correspondence. It is assumed, of course, that all the limitations noted above are neglected.

The transconductance can be obtained from the basic relation,

$$I_0 = P_{\exp}(eV_i/kT), \quad (22)$$

for current passing over a retarding barrier. Here I_0 is the emitter current passing into the base (assumed equal to the collector current), P is a proportionality constant, V_i is the base bias or dc input voltage, and e/kT has the usual meaning. This expression leads directly to the transconductance,

$$\frac{dI_0}{dV_i} = g_m = (e/kT)I_0 = \frac{Q}{\frac{kT}{e}}\frac{1}{\tau_r} = \frac{C_d}{\tau_r}, \quad (23)$$

which holds for the small signal case. The charge Q is the total injected minority carrier charge between the emitter and collector junctions. This charge moves, either by field drift or by diffusion, into the collector in an average carrier transit time τ_r, and accounts for the dc output current I_0. If the main fraction of the charge Q exists between the emitter junction and the edge of the collector depletion layer, the capacitance $(Q)/(kT/e)$, defined here as C_d, is the well known diffusion capacitance.[11] This capacitance can be much larger than the ordinary electrode capacitances, since ideally it depends only upon the emitter current I_0. In fact, the diffusion capacitance seems to be the limiting capacitance between a set of negative and a set of positive charges as the spacing between the sets approaches zero. For a density of free carriers of $10^{19}/\text{cm}^3$, that is, high enough to be degenerate, the diffusion capacitance is approximately 50 farads/cm³.

All the conclusions expressed in the preceding section about amplification and bandwidth again apply, with the only difference being that the gate capacitance C_i

[10] In a bipolar transistor, extra carriers of both signs must be simultaneously present in the same physical space for times of a microsecond or longer. This requires extraordinary freedom from deeplying defect states that can act as recombination centers. While the unipolar transistor can also use excess carriers of both signs, the carriers are in physically separate spaces.

[11] "Transistors I," RCA Laboratories, p. 15; 1956.

is replaced by the diffusion capacitance C_d. Since the ratio C_d/C_0 can be of the order of 10^2, or even higher, the voltage amplification-bandwidth product in the bipolar transistor can be, and normally is, much larger than in the unipolar device where the ratio C_i/C_0 is a geometrical one of the order of unity.

In the absence of leakage effects, the internal resistance r of the bipolar transistor can take on values greater than 10^6 ohms. According to (19), correspondingly high voltage gains are attainable.

The bipolar transistor is considerably more complicated than the simple picture presented above. One of the more important complications that diminishes its performance is the input resistance-capacitance time constant, τ_i, the product of the base series resistance and the emitter capacitance. This series combination reduces the amount of the input signal that appears across the emitter junction, and so reduces the response of the device. For the bipolar diffusion-flow transistor, where the emitter junction capacitance is mainly the diffusion capacitance C_d, the input time constant τ_i has a value

$$\tau_i = (1/2)(L/W)^2(bM + 1)^{-1}\tau_r. \qquad (24)$$

This relation, where $\tau_r = W^2/2D$ and D is the minority carrier diffusion constant, can be derived in a straightforward manner from (9) and the geometry shown in Fig. 4, assuming lumped resistance and capacitance.

limiting factor on frequency performance than the transit time. Expressions somewhat comparable to (24) can be derived for the drift transistor. These also show that $\tau_i < \tau_r$, except in the worse possible case of heavy injection, where $\tau_i \approx \tau_r$.

Thus, for the idealized case, where all nonessential resistance is removed, the input time constant, at worst, is of the same order as the transit time. For more extensive base contact area τ_i would be further reduced. Even though in a practical situation the base contact cannot be attached directly to the active volume, the input time constant of at least some modern high frequency transistors is still somewhat less than τ_r.

The Vacuum Triode and the Analog Transistor[12]

This heading also encompasses space-charge-limited tetrode and pentode vacuum tubes and miscellaneous types of semiconductor depletion layer devices.[13-16] As with the unipolar and bipolar transistors, there is a one-to-one correspondence between a charge on the control electrode and its counterpart traveling in the interelectrode space. For this reason, and the fact that the charge lifetime on the control electrode is fixed by the signal driving source, the current amplification can again be described by (2). The essential structure, potential distribution, and some pertinent parameters of a triode vacuum tube are shown in Fig. 5. The essential

Fig. 4—Structure for calculations on bipolar transistor input time constant.
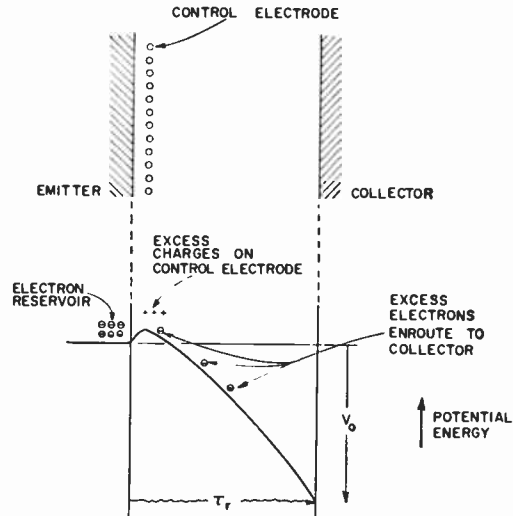
Fig. 5—Basic vacuum tube structure and the internal potential distribution.

The dimensions L and W are defined in the figure, b is the ratio of the majority to minority carrier mobility in the base, and M is the ratio of the majority to minority carrier charge in the base region between the emitter and collector depletion layers. The value of τ_i given in (24) is the minimum possible for the single-ended base contact, noted in the figure, because this contact is assumed to be at the very edge of the active base volume; all unnecessary resistance has been eliminated. The important point to note is that when $L = W$, τ_i is less than τ_r even for the worst possible case where $M = 1$. That is, the input time constant in this case is less a

[12] W. Shockley, "Transistor electronics: imperfections, unipolar and analog transistors," Proc. IRE, vol. 40, pp. 1289–1313; November, 1952.

[13] H. Statz, R. A. Pucel, and C. Lanza, "High-frequency semiconductor spacistor tetrodes," Proc. IRE, vol. 45, pp. 1475–1483; November, 1957.

[14] H. Statz and R. A. Pucel, "The Spacistor, a new class of high frequency semiconductor devices," Proc. IRE, vol. 45, pp. 317–324; March, 1957.

[15] W. G. Matthei and F. A. Brand, "On the injection of carriers into a depletion layer," J. Appl. Phys., vol. 28, pp. 513–514; April, 1957.

[16] W. W. Gartner, "Design theory for depletion layer transistors," Proc. IRE, vol. 45, pp. 1392–1400; October, 1957.

structure and operation of the tetrode spacistor,[13] which is in essence an analog transistor, is the same as the vacuum tube except for the fact that the current flow takes place in a p-n junction depletion layer instead of in a vacuum.

The anode current through these devices in the range of space charge limited currents is of the general form[8]

$$I_0 = AB(V_c + V_a/\mu)^m, \qquad (25)$$

where A is the electrode area for the plane parallel case assumed here; B, the perveance, is made up of fundamental constants and electrode spacings; V_c is the steady-state control electrode voltage; V_a is the steady-state anode voltage; μ is a geometrical constant, the amplification factor, which is a measure of the relative effect of the grid and anode fields at the emitter; and m is a number equal to 3/2 for the vacuum tubes, and 2 for the solid state devices.[17] For the tetrode and pentode vacuum tubes, other terms have to be added inside the parentheses of (25). These terms involve the voltages of other electrodes as well as their respective amplification factors, and, if included, would not lead to results essentially different from those which follow. For the solid-state case, where $m = 2$, the carrier mobility, assumed to be constant, appears in the perveance factor B.

The transconductance is

$$g_m = \frac{dI_0}{dV_c} = A m B \left(V_c + \frac{V_a}{\mu} \right)^{m-1} = m I_0 \left(V_c + \frac{V_a}{\mu} \right)^{-1}$$

$$= m Q \left(V_c + \frac{V_a}{\mu} \right)^{-1} \tau_r^{-1} = \frac{C}{\tau_r} . \qquad (26)$$

The capacitance $m Q (V_c + V_a/\mu)^{-1}$, where Q is the total interelectrode charge, is represented by C. For the usual assumptions made in deriving the space charge relation (25), the capacitance C is invariant with respect to the electrode potentials and approximately equal in magnitude to that of the same structure with a nonemitting cathode. Thus, to the approximation desired in the present analysis, we can treat the characteristic capacitance C as being the electrode capacitance of the grid. Of the exponent m in (25), the amount unity accounts for the increase of interelectrode charge with voltage, and the amount in excess of unity accounts for the increase in drift velocity. Thus, for the vacuum tube, of the value $m = 3/2$, 2/2 units account for space charge increase and 1/2 units for velocity increase.

There are a few qualifications to (25) and (26). First, for idealized grid structures and relatively low anode

currents, the current control approaches the barrier type action of the bipolar transistor. However, since the cathode temperature is normally close to $1000°K$, the transconductance-current ratio will always be less than about one-quarter of that possible in the room temperature bipolar transistor. Secondly, it should be noted that (25), with $m = 2$, applies to the solid-state case only when the carrier mobility is constant with electric field. Since the mobility tends to saturate at high fields,[18] (25) will be somewhat modified. In particular, the exponent m will decrease, becoming unity in the extreme when the drift velocity remains constant with electric field. From a practical standpoint this is unfortunate, because the over-all performance will be poorer than it would be for the constant mobility case. Since velocity saturation ($\sim 6 \times 10^6$ cm/sec for Ge and Si) sets in at fields of several kilovolts per cm, the much higher fields attainable in the space charge layer of the spacistor are of no benefit in increasing carrier drift speed and improving high frequency performance. In fact, the average drift velocity of carriers in the spacistor is only several times higher than in the drift and diffused base transistors, where the built-in field is of the order of 500 volts/cm.

The maximum voltage amplification, $(G_r)_{max}$, of the vacuum tube and the spacistor is given identically by the geometrical factor μ which appears in (25). This can be verified directly by application of (19). This factor μ is a measure of the relative effect of the electric fields of the grid and anode on the interelectrode space charge. The limiting voltage amplification of tetrode or pentode vacuum tubes is much higher than that of triode tubes, because the electrostatic isolating action of the added electrodes reduces the effect of anode field on the space charge. In (19) this shows up as a very high value of R, another measure of the impotence of the anode in affecting the charge in the conduction space.

As with the preceding devices, the useful voltage amplification is given by (17). The output capacitance C_0 for the vacuum tube or spacistor is defined here as the effective internal capacitance to the common terminal, usually the cathode. In actual devices this capacitance is a complex combination of capacitances to other electrodes—the grid, screen, suppressor, and cathode electrodes. Except in some special cases, the output capacitance is of the order of the grid-cathode capacitance. The previous arguments for the amplification-band-width products are also applicable to the vacuum tube and spacistor.

Beam Deflection Tube[19]

The rudiments of a beam deflection tube and some of

[17] For space charge limited flow of carriers of one sign in a solid, the exponent $m = 2$ applies only when the immobile interelectrode charge density is small compared with that of the mobile charge. For the purposes of this paper, this condition is reasonably well satisfied in the depletion layer devices considered here. For a detailed treatment of other cases, see W. Shockley and R. C. Prim, "Space-charge limited emission in semiconductors," *Phys. Rev.*, vol. 90, pp. 753–758; June, 1953, or M. A. Lampert, "Simplified theory of space-charge limited currents in an insulator with traps, "*Phys. Rev.*, vol. 103, pp. 1648–1656; September, 1956.

[18] See, for example, J. B. Gunn, "The field dependence of electron mobility in germanium," *J. Electronics*, vol. 2, pp. 87–94; July, 1956.

[19] J. R. Pierce, "Theoretical limitation to transconductance in certain types of vacuum tubes," Proc. IRE, vol. 31, pp. 657–663; December, 1943.

G. R. Kilgore, "Beam deflection control for amplifier tubes," *RCA Rev.*, vol. 8, pp. 480–505; September, 1947.

its salient parameters are shown in Fig. 6. The deflection plates and beam extend into the paper an arbitrary distance h. A deflection distance D, equal to the beam thickness, is required to switch the output current. The simplest possible case is assumed where the current density in the beam is uniform and the output current changes linearly with beam position. The longitudinal velocity of the beam electrons is assumed constant in the region extending from the left edge of the deflection plates to the collector.
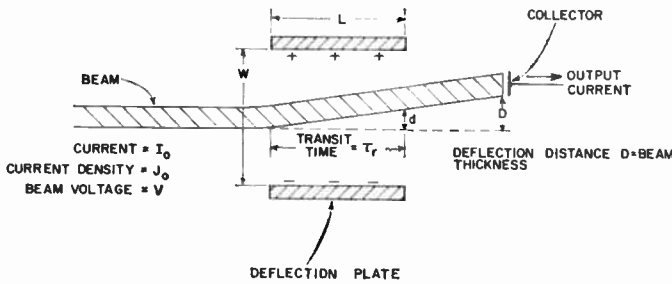

Fig. 6—Side view of the essential elements
of a beam deflection tube.

We are now confronted with a device basically different from the ones previously considered. A charge placed on one of the deflection plates finds its opposite counterpart, not in the interelectrode space, but on the opposite deflection plate. As a consequence, the simple current amplification relation (2) no longer applies. If G_i is defined as the ratio of the total change in collector current, $\Delta I_0(= I_0)$, to the peak deflection plate current, I_i, required to achieve this change,

$$G_i = I_0/I_i = (Q/I_i)(1/\tau_r). \qquad (27)$$

Here Q is the total carrier charge in the portion of the electron beam between the deflection plates. The relation,

$$I_i = 2\pi f C V_d, \qquad (28)$$

between the peak deflection plate input current I_i, the signal frequency f, the deflection plate capacitance C, and the peak deflection plate voltage V_d follows from elementary ac theory. The substitution of this into (27) yields

$$G_i = (2\pi f)^{-1}\tau_r^{-1}(Q/C V_d), \qquad (29)$$

which is the same as (2) except for the dimensionless factor $(Q/C V_d)$, a measure of merit for the device. To the best of the authors' knowledge, this factor of merit has not been pointed out in previous analyses.

This factor can be evaluated by combining

$$d = (1/2)(eE/m)\tau_r^2, \qquad (30)$$

$$E = V_d/W, \qquad (31)$$

$$I_0 = hDJ_0, \qquad (32)$$

$$\tau_r^2 = L^2(m/2eV), \qquad (33)$$

$$C = (\epsilon_0/4\pi)hL/W, \qquad (34)$$

and the definition

$$J_0' = (\epsilon_0/q\pi)(2e/m)^{1/2}(V^{3/2}/L^2). \qquad (35)$$

Eq. (30) describes the displacement d of an electron of charge e and mass m in the field E during the time τ_r that the field acts on the charge. Eqs. (31) and (32) follow from parameter definitions already given either in the text or figure. Eq. (33) connects the electron transit time τ_r through the plates to the beam voltage V. Eq. (34) is an expression of the deflection plate capacitance C in terms of the dielectric constant ϵ_0 of free space and the plate dimensions. The current density J_0', defined in (35), is the space charge limited current density that would flow in a comparison planar diode of cathode-anode spacing L with the full beam voltage V applied between the cathode and anode. Although this definition may seem to be an arbitrary one to introduce, its utility becomes obvious when the above equations are combined to arrive at a compact expression for $(Q/C V_d)$:

$$(Q/C V_d) = (D/d)(J_0/9J_0'). \qquad (36)$$

The "leverage" factor D/d is a measure of the relative displacement required in aiming the beam toward the collector plate and the factor $J_0/9J_0'$ describes the relative loading of the region between the deflection plates with charge. The maximum attainable value of the product of these two quantities is fixed by the electrostatic repulsion between the beam electrons which causes the beam to spread laterally as it travels toward the collector. This spreading effect can be estimated by using (30) with the field value calculated from the beam space charge, and the time factor calculated from τ_r and the geometry shown in Fig. 6. A simple first order calculation shows that the beam width at the collector is

$$D\left[1 + \left(\frac{D}{d} - 1\right)^2\left(\frac{J_0}{9J_0'}\right)\right].$$

The final expression for $Q/C V_d$, which takes into account beam spreading, is then

$$Q/C V_d = (D/d)(J_0/9J_0')$$
$$\cdot\left[1 + \left(\frac{D}{d} - 1\right)^2\left(\frac{J_0}{9J_0'}\right)\right]^{-1}. \qquad (37)$$

The maximum value of beam current that can be passed between a pair of deflection plates is limited by space charge effects and is described by a previously derived relation.[20] A simple calculation based on this relation shows that the maximum value of $J_0/9J_0'$ is very close to unity. This is not surprising, since space charge limitations apply equally well either to beam or diode currents. The only difference between the two cases is that the average electron velocity in the beam is three-fold higher than in the comparison diode. Inspection of (37)

[20] K. R. Spangenberg, "Vacuum Tubes," McGraw-Hill Book Co., New York, N. Y., pp. 440–448; 1948.

TABLE I
SUMMARY OF BASIC RELATIONS
$\omega = 2\pi f$

Property \ Device	Unipolar Transistor	Spacistor	Vacuum Tube	Beam Deflection Tube	Bipolar Transistor
Transconductance (g_m)	$\dfrac{C_i}{\tau_r}$	$\dfrac{C_i}{\tau_r}$	$\dfrac{C_i}{\tau_r}$	$\dfrac{C_i}{\tau_r}$	$\dfrac{C_d}{\tau_r}$
Current Amplification (G_i)	$\dfrac{1}{\omega\tau_r}$	$\dfrac{1}{\omega\tau_r}$	$\dfrac{1}{\omega\tau_r}$	$\dfrac{1}{\omega\tau_r}$	$\dfrac{1}{\omega\tau_r}$
Voltage Amplification (G_V)	$\dfrac{C_i}{C_0}\dfrac{1}{\omega\tau_r}$	$\dfrac{C_i/C_0}{\omega\tau_r}$	$\dfrac{C_i/C_0}{\omega\tau_r}$	$\left(\dfrac{C_i}{C_0}\right)\dfrac{1}{\omega\tau_r}$	$\dfrac{C_d}{C_0}\dfrac{1}{\omega\tau_r}$
Power Amplification (G_p)	$G_i^2\dfrac{C_i}{C_0}$	$G_i^2\dfrac{C_i}{C_0}$	$G_i^2\dfrac{C_i}{C_0}$	$G_i^2\dfrac{C_i}{C_0}$	$G_i^2\dfrac{C_d}{C_0}$
Amplification-Bandwidth Voltage ($G_V\Delta f$)	$\dfrac{C_i/C_0}{2\pi\tau_r}$	$\dfrac{C_i/C_0}{2\pi\tau_r}$	$\dfrac{C_i/C_0}{2\pi\tau_r}$	$\dfrac{(C/C_0)}{2n\tau_r}$	$\dfrac{C_d/C_0}{2\pi\tau_r}$
Current ($G_i\Delta f$)	$\dfrac{1}{2\pi\tau_r}$	$\dfrac{1}{2\pi\tau_r}$	$\dfrac{1}{2\pi\tau_r}$	$\dfrac{1}{2\pi\tau_r}$	$\dfrac{1}{2\pi\tau_r}$
Power ($G_p\Delta f^2$)	$(2\pi\tau_r)^{-2}C_i/C_0$	$(2\pi\tau_r)^{-2}C_i/C_0$	$(2\pi\tau_r)^{-2}C_i/C_0$	$(2\pi\tau_r)^{-2}C_i/C_0$	$(2\pi\tau_r)^{-2}C_d/C_0$
Upper Frequency Limit	$\geq\tau_r^{-1}$	$\approx\tau_r^{-1}$	$\approx\tau_r^{-1}$	$\approx\tau_r^{-1}$	$\approx\tau_r^{-1}$

then shows that the maximum attainable value of Q/CV_d is close to unity. A similar result is obtained from an examination of various cases with the universal beam spread formula.[20] Hence, to a good approximation, the maximum current amplification in the beam deflection tube turns out to be described by (2), just as for the other devices. It is interesting to note that Q/CV_d, for cathode ray tubes commonly found in oscilloscopes, has values of the order of 10^{-2} to 10^{-3}.

Without beam spreading, the transconductance of the device is

$$g_m = I_0/V_d = (Q/V_d)\tau_r^{-1} = (D/d)(J_0/9J_0')C\tau_r^{-1};$$

with spreading, the maximum transconductance is

$$g_m = C/\tau_r. \qquad (38)$$

The factor I_0/V_d can be used because of the linear, or approximately linear, relation between V_d, d, and the output current. The voltage amplification and the various amplification-bandwidth products assume the same forms described for the other devices.

Kilgore[19] has pointed out that very large g_m/I_0 ratios can be obtained with beam tubes at very low values of $I_0(10^{-8}$ ampere) where space charge effects are not important. Despite the correspondingly low transconductance (2.5 micromhos), relatively large amplification-bandwidth products were possible because the effective output capacitance C_0 could be made low in value. The present analysis is not sufficiently detailed to handle special cases of the sort discussed by Kilgore. On the other hand, the present analysis is more appropriate to situations where space charge assumes importance and one is interested in making comparisons with other charge control devices.

TABLE II
DEFINITIONS OF PARAMETERS IN TABLE I

Unipolar Transistor
C_i is the total capacitance between the gates and channel.
C_0 is the capacitance between the drain electrode and the rest of the device structure.
τ_r is the drift time of a majority carrier through the channel.

Vacuum Tube and Spacistor
C_i is roughly the grid-cathode capacitance.
C_0 is the internal capacitance of the collector electrode.
τ_r is the carrier transit time between the emitter and collector.

Beam Deflection Tube
C_i is the total capacitance between the deflection plates.
C_0 is the capacitance of the collector to the rest of the tube structure.
τ_r is the transit time of the beam between the deflection plates.

Bipolar Transistor
C_d is the diffusion capacitance.
C_0 is the internal collector capacitance.
τ_r is the drift time of minority carriers between emitter and collector.

The beam deflection tube is an electronic analog to the mechanical knife switch. In the latter, however, the switching speed is intrinsically slow because the atomic nuclei have to be "aimed" along with the electrons that carry the current. On the other hand, the space charge neutralizing action of the positive atomic nuclei allow far higher current densities to be carried by the conducting path of the knife switch than could be carried by any realizable electron beam.

DISCUSSION

The pertinent relations describing signal amplifiers of the emitter-control-collector variety are summarized in Table I; the definitions of the parameters are summarized in Table II.

The central importance of the carrier transit time and its relation to bandwidth is strikingly evident. The quantity $(2\pi\tau_r)^{-1}$ is a measure of a device's ultimate capability in processing information, or, what is essentially the same thing, the amplification-bandwidth products are inversely related to the average time required to move a charge through the device.[21] This capability can be increased only by decreasing device dimensions, or by increasing the carrier transport velocity. Unfortunately, the maximum attainable average carrier drift velocity in Ge and Si is approximately 6×10^6 cm/sec, a value reached at fields of several kilovolts per centimeter. This velocity is to be compared with the hundred-fold, or greater, electron velocities ordinarily attained in vacuum tubes.

Solid-state devices constructed from Ge and Si are correspondingly restricted to dimensions smaller than 10^{-3} cm (a few tenths of a mil), if usable amplification at 1000 mc is desired. There is some hope of finding new semiconductor materials with higher carrier drift velocities.

For grid controlled vacuum tubes, a high electron current density is commonly considered the basic requirement for a high gain-bandwidth product. Because of the space charge relation (25), a high current density means a short transit time. However, in charge control devices, the transit time and not the current density is generally the significant parameter. A high current density is obtainable in two different ways: by a large charge density (or charge), or by a high carrier drift velocity (short transit time). The first case is clearly exemplified by the unipolar transistor, and the second by the vacuum tube. The unipolar device has a current density as high as 10^3 amperes/cm^{2}, a value far higher than that in vacuum tubes, but has a carrier drift velocity at least a hundred time less than that of a typical vacuum tube. The vacuum tube has the higher amplification bandwidth product for comparable dimensions because its transit times are smaller than those of a unipolar transistor.

While the transit time is common to all of the amplification and amplification-bandwidth products, the input or characteristic capacitance C_i enters only in the voltage and power amplification relations. The C_i used in the present paper has been assumed to be given entirely by the capacitance between the charge on the control electrode and the opposite sign of charge thereby introduced into the conduction space between emitter and collector. Any stray capacitance between the input electrode, or ground, is wasted capacitance because it contributes nothing useful to the electrical output of the device.

Inspection of Table II shows that C_i should be as large as possible.[22] The larger this capacitance, the less the work needed to introduce additional carriers between emitter and collector. Since the voltage and power gains involve the ratio of work out to work in, per carrier, a small input work per carrier leads to high voltage and power amplifications.

The obvious way of increasing the input capacitance is to bring the controlling and controlled charges closer together. In vacuum tubes the spacing is of the order of the grid-cathode spacing; in the beam deflection tube it is the deflection plate spacing; in the unipolar transistor, the thickness of barrier layer between grid and channel; and in the spacistor, or analog transistor, the cross-sectional radius of the conducting path between emitter and collector. In all of these devices, the capacitance can be interpreted in terms of a physical spacing. It is natural to inquire what happens when this spacing is decreased as far as possible. The answer has been demonstrated elegantly and dramatically by the bipolar transistor. When the electron density is increased by positive charges occupying the same volume as the electrons, a voltage of kT/e is required to double the electron density. If one defines a capacitance by the ratio of total free charge to kT/e, the capacitance is proportional (as noted earlier) to the volume of semiconductor as well as to the starting density of free carriers. This is the diffusion capacitance of the bipolar transistor. It defines the smallest amount of work required to introduce extra carriers in the emitter-collector space. In this respect, the bipolar transistor has achieved what appears to be a limit in the family of charge-control devices.

The same limit applies to the use of a photoconductor as an amplifier. Here, also, the negative and positive charges occupy the same volume. The input work per added carrier is, in general, the $h\nu$ of the incident photons. The smallest work per added carrier, required to double an existing carrier density, is again given by kT/e for the same reasons as in the bipolar transistor.

Once the input capacitance C_i has been defined by the physics of the particular device, the input shunt resistance R_i required to achieve a given bandwidth is also defined. To achieve the same bandwidth in the output circuit, the same resistance-capacitance time constant is needed. According to the voltage and power amplification expressions, these amplifications could be made arbitrarily large simply by choosing an arbitrarily small output capacitance. The output capacitance, however, is a function of the size of the collector electrode and the latter is set by power handling capabilities, electron optics, or other side conditions concerning which no general remarks significant to the present discussion can be made.

---

[21] Note that the bandwidth of a lumped parameter passive *RLC* circuit is $(2\pi\tau_E)^{-1}$, where τ_E is the effective time for a pulse of energy to pass from the circuit input into the resistance (output) as heat.

[22] The problems ensuing from interstage coupling and matching, which might be occasioned by large input capacitances, are beyond the scope of this paper.

Identical relations for current gain in all devices (except in the beam tube) stem from the required one-to-one correspondence between movable charges in the interelectrode space and charges on the control electrode. The beam tube has a different operating principle but ultimately is subject to space charge limitations and must be described by the same current amplification relation as the other devices. It should be remembered that the idealized current gain described by (2) is the best that can be obtained when all leakage, recombination, and imperfect emitter effects are eliminated. These effects account for the fact that the current gain in a bipolar transistor, for example, does not rise to infinity at zero frequency.

One important factor has been omitted from all of the amplification relations in Table I. This is the carrier multiplication that can exist in the emitter-collector conduction space. If such multiplication is introduced, for example by avalanche effects in the collector depletion layer of a transistor, the current amplification (2) must include this multiplication factor. Thus, the other amplification relations must, also. The charge control principle would not be affected because the carrier multiplication always appears in charge pairs which need no extra balancing charge on the control electrode.

The maximum operating frequency of the multi-element vacuum tubes, the spacistor, the bipolar transistor, and also the beam tube, is ultimately limited to $\sim \tau_r^{-1}$. Higher frequencies result in such serious dispersion and space charge effects that effective amplification is destroyed. The unipolar transistor, with its majority carrier conduction process, is not limited to frequencies below $\sim \tau_r^{-1}$ because of dispersion and space charge effects. The only practical limit is set by the gate input time constant. With suitable design it may be possible to reduce this somewhat below the value τ_r. Thus, the unipolar transistor, with its relatively low transconductance and amplification-bandwidth products, may be useful in providing amplification over a narrow band at relatively high frequencies.

In almost all basic respects, the unipolar transistor and the analog transistor or spacistor are comparable devices. For the same dimensions they should have nearly the same transconductance and volatge amplification, as well as the same current amplification. Both devices are relatively independent of minority carrier lifetimes and mobilities. The carrier velocity saturation effect in presently known materials greatly reduces the transit time advantage that the higher drift fields in these devices can give over the bipolar transistor. Both of these devices are at a serious practical disadvantage with respect to the bipolar transistor with its intrinsically high characteristic capacitance leading to higher amplification. While a low transconductance and voltage gain

can be overcome to some extent by increasing the dc current level in the device, the price for this is an increased internal power dissipation. This is the reason, for example, that high performance unipolar transistors have a serious power dissipation problem.[6]

The last statement above is worth considering further. In any practical information handling system we are most certainly concerned with the power consumption required to handle (amplify) information at some specific rate (information rate handling capability is proportional to bandwidth). That is, we are interested in the power consumption needed for a given amplification-bandwidth product. For the small signal case the minimum power consumption P_0 is the product $I_0 V_0$ of the dc current and voltage at the operating point. The current I_0 can be found from the transconductance and this is related to the amplification-bandwidth product. This leads to the power per unit voltage amplification $P_0/G_r f_0$, which is equal to $2\pi Q_0 V$, where $Q_0 = C_0 V_0$ is the total charge on the output capacitance C_0, and V is the characteristic input voltage, namely, the electron volts of work done per added carrier. For the unipolar transistor, V is about one volt; for the bipolar transistor, kT/e volts; for the vacuum tube, spacistor, and beam deflection tube, several volts. The quantity $P_0/G_r f_0$ is an energy, the energy per electron charge required to charge up the input capacitance times the charge on the output capacitance C_0. If desired, this energy can be expressed as the energy per bit at a particular value of voltage or current amplification. Brief consideration is sufficient to show that the bipolar transistor is the most efficient device of all, at least in the simple case considered here. In particular, it is at least an order of magnitude better in this comparison than the unipolar transistor, a fact that helps substantiate the last statement in the preceding paragraph.

First order effects accompanying large signal operating conditions can be accounted for by introducing average values for τ_r and the characteristic capacitances. In most cases these average values will be lower than the values attained at the optimum small signal operating point.

This paper is an attempt to take a step on the long and challenging road to find the answer to the central device-circuit-system question: What are the best physical mechanisms to use, and how—in attaining the maximum information handling capability in a given space, with a minimum of energy, and a maximum of reliability—all at a minimum cost?

ACKNOWLEDGMENT

Traveling-Wave Couplers for Longitudinal Beam-Type Amplifiers*

ROY W. GOULD†

Summary—The equations governing traveling-wave interaction between an electron beam and a slow-wave circuit are formulated in terms of amplitudes of circuit mode and slow and fast space charge modes. The resulting equations are solved to find expressions for the matrix which relates the mode amplitudes at the output of the traveling-wave coupler to the mode amplitudes at the input. The properties of this matrix are discussed and numerical values given for Kompfner Dip.

Matrices for velocity jumps and drift regions are also given, and the characteristics of couplers which are preceded by or followed by a drift region and velocity jump are discussed.

It is shown that necessary and sufficient conditions for the removal of beam noise from the fast space-charge wave by any lossless coupler are that, for a circuit input, there be no circuit output ($M_{11}=0$) and no slow space-charge wave output ($M_{21}=0$).

These results are then applied to the design of fast space-charge wave couplers for longitudinal beam type parametric amplifiers.

I. Introduction

THE prospect of obtaining a very significant decrease in the noise figure of electron beam type microwave amplifiers through the use of the parametric principle has stimulated considerable work on beam-type parametric amplifiers. Conventional longitudinal beam amplifiers depend critically on the negative power flow associated with the slow space-charge wave, whereas parametric amplifiers can be made to use the fast space-charge wave which has positive power flow. The significant distinction to be noted here is that noise can be completely removed from the fast space-charge wave whereas noise on the slow space-charge wave cannot. Parametric amplification in electron beams has already been analyzed and discussed by Louisell and Quate,[1] and the purpose of this paper is to describe the properties of a certain class of couplers which make it possible to couple to the fast space-charge wave only. While it is also possible to construct fast-wave couplers using resonant cavities, the possibility of using a traveling-wave interaction immediately suggests itself as a method with potentially greater bandwidth.

The simplest coupler of this type, conceptually, is a large QC traveling-wave structure operated at the Kompfner Dip.[2] When QC is large, coupling to the slow space-charge wave is negligible and an almost complete interchange of energy takes place between the circuit and the fast space-charge wave.[3] Any circuit input is transferred almost completely to the fast space-charge wave and any disturbance on the fast space-charge wave is transferred almost completely to the circuit. Any noise or signal on the slow space-charge wave passes through the interaction region unchanged. Used as an input coupler, noise would be completely removed from the fast space-charge wave. As an output coupler it would not be sensitive to the noise which remains on the slow space-charge wave. Such a coupler is very attractive, and it is of interest to inquire whether or not the large QC restriction is essential.[4]

We expect that as QC is decreased, coupling to the slow space-charge wave becomes important and that the noise may no longer be completely removed from the fast space-charge wave. The following analysis was performed in an attempt to answer the following types of questions about operation at small and intermediate values of QC:

1) How large is the coupling to the slow space-charge wave?
2) How much noise remains on the fast space-charge wave after passing through such a coupler?
3) Does there exist a set of values of b and CN for which there is no coupling to the slow space-charge wave?
4) Is it possible, with the aid of velocity jumps and drift regions, to achieve coupling to the fast wave only and removal of the beam noise from the fast space-charge wave?[5]

Since these questions are couched in terms of mode amplitudes it was found to be convenient to first formulate the equations of traveling-wave interaction in these terms by introducing a transformation from the physical variables: circuit voltage, beam current, and beam velocity to the three mode amplitudes. The result is a derivation of the coupled mode equations.[3,6] When for-

[1] W. H. Louisell and C. F. Quate, "Parametric amplification of space-charge waves," PROC. IRE, vol. 46, pp. 707–716; April, 1958.
[2] R. Kompfner, "On the operation of the traveling wave tube at low level," *Brit. J. IRE*, vol. 10, pp. 283–289; August–September, 1955. See also H. R. Johnson, "Kompfner Dip Conditions," PROC. IRE, vol. 43, p. 874; July, 1955.

[3] R. W. Gould, "A coupled mode description of the backward wave oscillator and the Kompfner Dip condition," IRE TRANS. ON ELECTRON DEVICES, vol. ED-2, pp. 37–42; October, 1955.
[4] Large QC may be obtained by reducing the helix to beam coupling thus reducing C. For a given beam $4QC^3 = (\omega_q/\omega)^2$ is approximately constant. Therefore, $4QC \sim 1/C^2$.
[5] The use of a velocity jump following the helix for this purpose was suggested by A. Ashkin at the Sixteenth Annual Conf. on Electron Tube Res., Quebec, Can.; June 25–27, 1958.
[6] J. R. Pierce, "Coupling of modes of propagation," *J. Appl. Phys.*, vol. 25, pp. 179–183; February, 1954. "The wave picture of microwave tubes," *Bell Sys. Tech. J.*, vol. 33, pp. 1343–1372; November, 1954.

mulated in this way, Haus and Robinson's[7] theory of linear transducers is immediately applicable.

II. Traveling-Wave Interaction in Terms of Mode Amplitudes

In this section the theory of traveling-wave interaction is formulated in terms of the amplitudes of the circuit wave, slow space-charge wave, and fast space-charge wave. The usual small C approximation is made throughout in order to simplify the results. In terms of the physical variables: ac beam velocity, v_1; ac beam-charge density, ρ_1; ac beam-current density, i_1; ac circuit voltage, V_c; and ac space-charge potential, V_{sc}; the linearized equations of traveling-wave interaction are:

the electronic equation of motion,

$$j\omega v_1 + \frac{\partial}{\partial z}(u_0 v_1) = \frac{e}{m}\frac{\partial}{\partial z}(V_c + V_{sc}), \qquad (1)$$

the equation of continuity,

$$j\omega \rho_1 + \frac{\partial i_1}{\partial z} = 0, \qquad i_1 = \rho_0 v_1 + \rho_1 u_0, \qquad (2)$$

the equation for the space charge voltage (from Poisson's equation)

$$\frac{\partial^2 V_{sc}}{\partial z^2} = - R^2 \frac{\rho_1}{\epsilon_0},$$

$$R = \text{space-charge reduction factor}, \qquad (3)$$

and the circuit equation,

$$\left(\frac{\partial}{\partial z} + \Gamma_1\right) V_c = \pm j\beta_e \frac{K}{2}\sigma i_1, \qquad (4)$$

where Γ_1 is the circuit propagation constant in the absence of the beam. K is the Pierce interaction impedance and σ is the cross-sectional area of the beam. The upper sign applies for forward-wave circuits and the lower sign applies for backward-wave circuits.

Introducing the mode variables defined in the manner suggested by Haus and Robinson,[7]

$$a_1 = \frac{V_c}{\sqrt{2K}} \quad \text{circuit mode amplitude} \qquad (5)$$

$$a_2 = \frac{1}{2\sqrt{2W}}(V_1 - WI_1) \quad \begin{array}{l}\text{slow space-charge}\\ \text{mode amplitude}\end{array} \qquad (6)$$

$$a_3 = \frac{1}{2\sqrt{2W}}(V_1 + WI_1) \quad \begin{array}{l}\text{fast space-charge}\\ \text{mode amplitude}\end{array} \qquad (7)$$

where

$$W = 2\frac{V_0}{I_0}\frac{\omega_p R}{\omega},$$

is the space-charge wave impedance of the electron beam, $V_1 = -(m/e)u_0 v_1$ is the kinetic voltage of the electron beam and $I_1 = \sigma i_1$ is the ac convection current in the electron beam. These variables have the property that their absolute square gives the power flow associated with that mode (except that $|a_2|^2$ gives the *negative* of the power flow associated with the slow space-charge mode). Upon substituting these new variables into (1)–(4), performing some straightforward algebraic manipulations, and making the small C approximation consistently, we obtain the equations for the mode amplitudes:

$$\left(\frac{\partial}{\partial z} + \Gamma_1\right)a_1 \pm j\kappa a_2 \mp j\kappa a_3 = 0 \qquad (8)$$

$$-j\kappa a_1 + \left[\frac{\partial}{\partial z} + j(\beta_e + \beta_q)\right]a_2 = 0 \qquad (9)$$

$$-j\kappa a_2 + \left[\frac{\partial}{\partial z} + j(\beta_e - \beta_q)\right]a_3 = 0, \qquad (10)$$

where

$$\kappa = \frac{\beta_e}{2}\sqrt{\frac{K}{W}}$$

is the coupling constant between the circuit and fast and slow space-charge waves, $\beta_e = \omega/u_0$ is the electronic wave number, and $\beta_q = R\omega_p/u_0$ is the reduced plasma wave number. Eqs. (8)–(10) represent an extension of Pierce's coupling of modes of propagation theory[6] to coupling between the *three* modes of a traveling-wave tube, together with an explicit expression for the coupling constant. Note that the circuit mode is coupled equally to the fast and slow space-charge waves[8] and that the two space-charge waves are not coupled to each other.

It is convenient to extract a phase factor $e^{-j\beta_e z}$ from the definitions of the mode amplitudes by writing

$$a_i(z) = A_i(z)e^{-j\beta_e z} \qquad (11)$$

and to express (8), (9), and (10) in terms of the dimensionless traveling-wave tube variables, b, d, $\xi = \beta_e C z$, $\beta_q/\beta_e C = \sqrt{4QC}$, and $\kappa/\beta_e C = k$:

$$\left[\frac{\partial}{\partial \xi} + jb \pm d\right]A_1 \pm jkA_2 \mp jkA_3 = 0 \qquad (12)$$

$$-jkA_1 + \left[\frac{\partial}{\partial \xi} + j\sqrt{4QC}\right]A_2 = 0 \qquad (13)$$

$$-jkA_1 + \left[\frac{\partial}{\partial \xi} - j\sqrt{4QC}\right]A_3 = 0. \qquad (14)$$

It is of interest to note that the dimensionless coupling constant k is a function of QC only,

[7] H. A. Haus and F. N. H. Robinson, "The minimum noise figure of microwave beam amplifiers," Proc. IRE, vol. 43, pp. 981–991; August, 1955.

[8] The factor j preceding κ in (8)–(10) does not appear in Gould, *op. cit.* This difference is due to the choice of the *phases* of a_1, a_2, a_3.

$$k^2 = \frac{1}{2\sqrt{4QC}} \cdot \tag{15}$$

To solve the three simultaneous first order linear equations, assume that each independent variable has a dependence on ξ of the form $e^{\delta\xi}$. For solutions of this type the determinant of the resulting algebraic equations must vanish

$$(\delta + jb \pm d)(\delta^2 + 4QC) \pm j = 0. \tag{16}$$

This is the familiar traveling-wave tube characteristic equation. A general solution may be written as the superposition of the three characteristic waves

$$A_i = \sum_{j=1}^{3} C_{ij} e^{\delta_j \xi} \tag{17}$$

where certain relations exist between the C_{ij} by virtue of (12)–(14).

Let us apply these solutions to a length l of the traveling-wave section shown in Fig. 1 to find the mode amplitudes A_1', A_2', and A_3' at the output of the coupler when the input mode amplitudes are A_1, A_2, and A_3.
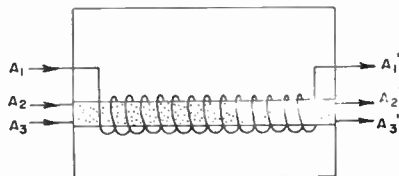
Fig. 1—Traveling-wave section.

We know in advance that the outputs are linearly related to the inputs

$$A_1' = M_{11}A_1 + M_{12}A_2 + M_{13}A_3 \tag{18}$$

$$A_2' = M_{21}A_1 + M_{22}A_2 + M_{23}A_3 \tag{19}$$

$$A_3' = M_{31}A_1 + M_{32}A_2 + M_{33}A_3, \tag{20}$$

or simply

$$A' = MA \tag{21}$$

where M is a three by three-square matrix, and A' and A are three-element row and column matrices, respectively. A straight forward application of the solutions (17) to the case of initial conditions A_1, A_2, and A_3 yields the following expressions for the elements of the M matrix;

$$M_{11} = \sum_{i=1}^{3} \frac{\delta_i^2 + 4QC}{(\delta_1 - \delta_j)(\delta_i - \delta_k)} e^{\delta_i \xi} \tag{22}$$

$$M_{21} = jk \sum_{i=1}^{3} \frac{\delta_i - j\sqrt{4QC}}{(\delta_i - \delta_j)(\delta_i - \delta_k)} e^{\delta_i \xi} \tag{23}$$

$$M_{31} = jk \sum_{i=1}^{3} \frac{\delta_i + j\sqrt{4QC}}{(\delta_i - \delta_j)(\delta_i - \delta_k)} e^{\delta_i \xi} \tag{24}$$

$$M_{22} = jk^2 \sum_{i=1}^{3} \frac{(\delta_i - j\sqrt{4QC})(\delta_j + j\sqrt{4QC})(\delta_k + j\sqrt{4QC})}{(\delta_i - \delta_j)(\delta_i - \delta_k)} e^{\delta_i \xi} \tag{25}$$

$$M_{32} = \pm k^2 \sum_{i=1}^{3} \frac{1}{(\delta_i - \delta_j)(\delta_i - \delta_k)} e^{\delta_i \xi} \tag{26}$$

$$M_{33} = - jk^2 \sum_{i=1}^{3} \frac{(\delta_i + j\sqrt{4QC})(\delta_j - j\sqrt{4QC})(\delta_k - j\sqrt{4QC})}{(\delta_i - \delta_j)(\delta_i - \delta_k)} e^{\delta_i \xi} \tag{27}$$

where the subscripts i, j, k, are cyclical permutations of the integers 1, 2, 3, and $\xi = \beta_e Cl$. In writing (26) we have made use of the fact that

$$(\delta_i + j\sqrt{4QC})(\delta_j + j\sqrt{4QC})(\delta_k + \sqrt{4QC}) = \mp j \tag{28}$$

a result which follows from the characteristic (16). We have not written the expressions for M_{12}, M_{13}, and M_{23} since it is possible to show, with the aid of (28), that

$$M_{12} = \mp M_{21} \tag{29}$$

$$M_{13} = \pm M_{31} \tag{30}$$

$$M_{23} = - M_{32}. \tag{31}$$

These expressions indicate certain symmetry properties of the coupler. For example, (29) states that a unit-amplitude slow wave at the input produces a circuit-wave amplitude at the output which is equal to (but of opposite sign in the case of the forward-wave amplifier) the slow-wave amplitude produced by a unit input to the circuit. Similarly, (30) states that a unit-amplitude fast-wave input produces a circuit-wave amplitude at the output which is equal to the fast-wave amplitude produced by a unit input to the circuit. Eq. (31) states that the fast wave produced by a unit slow-wave input is the negative of the slow wave produced by a unit fast-wave input.

In addition these matrix elements satisfy certain rela-

tions based on conservation of energy,[7]

$$M^+PM = P \tag{32}$$

$$MPM^+ = P, \tag{33}$$

where P is the parity matrix of Haus and Robinson

$$P = \begin{pmatrix} \pm 1 & 0 & 0 \\ 0 & -1 & 0 \\ 0 & 0 & 1 \end{pmatrix}, \tag{34}$$

and M^+ is the Hermitian conjugate of M. In terms of the parity matrix the symmetry relations (29) to (31) can be written $(PMP)_{ij} = M_{ji}$ or $P\widetilde{M}P = M$ where the tilde indicates the transpose matrix.

To gain familiarity with the properties of the traveling-wave section and to answer the questions posed in the introduction, expressions for the matrix elements (22)–(27) have been evaluated using the Datatron 205 digital computer. A program now exists which evaluates each of the six matrix elements for specified QC, d, b, and ξ in about 30 seconds. The behavior for $QC = 1$, $\frac{1}{4}$, $\frac{1}{16}$ ($d = 0$) has been investigated by evaluating the matrix elements for $0 \leq \xi \leq 4.75$ and various values of b. Fig. 2 shows the magnitude of the matrix elements as a function of normalized length for the cases $QC = 1$, $b = -2.0718$ (solid curve), and $QC = 1$, $b = -1.5000$ (dashed curve). One may also think of $|M_{11}|$, $|M_{21}|$, and $|M_{31}|$ as the amplitudes of the circuit wave, slow and fast space-charge waves, as a function of distance along the coupler, which are produced when a unit amplitude is applied to the circuit. The Kompfner Dip condition ($|M_{11}| = 0$) may be seen in the upper left. Some general features of large QC operation are seen in Fig. 2: coupling between the slow space-charge wave and either the circuit or the fast space-charge wave is small ($|M_{21}|$ and $|M_{31}|$ small), the slow space-charge wave goes through the coupler nearly unaffected ($|M_{22}| \cong 1$) at Kompfner Dip, and almost all of the fast-wave input is transferred to the circuit and very little remains on the beam.

The plot of $|M_{21}|$ in Fig. 2 suggests that there might be values of ξ and b for which M_{21} vanishes, resulting in no excitation of the slow space-charge wave for a circuit input. Additional calculations made to investigate this point indicate that such values of b and ξ probably do not exist, although M_{21} can be made small. It is, of course, possible to make M_{11} zero by proper choice of b and ξ, and this is the Kompfner Dip condition. When M_{11} is zero, the magnitude of M_{31} is always larger than the magnitude of M_{21}. This result follows directly from the fact that ac beam power at the output of the coupler must equal the circuit power at the input. When $|M_{31}|$ is greater than $|M_{21}|$[9] it is possible, with the proper choice of a velocity jump, to completely remove the
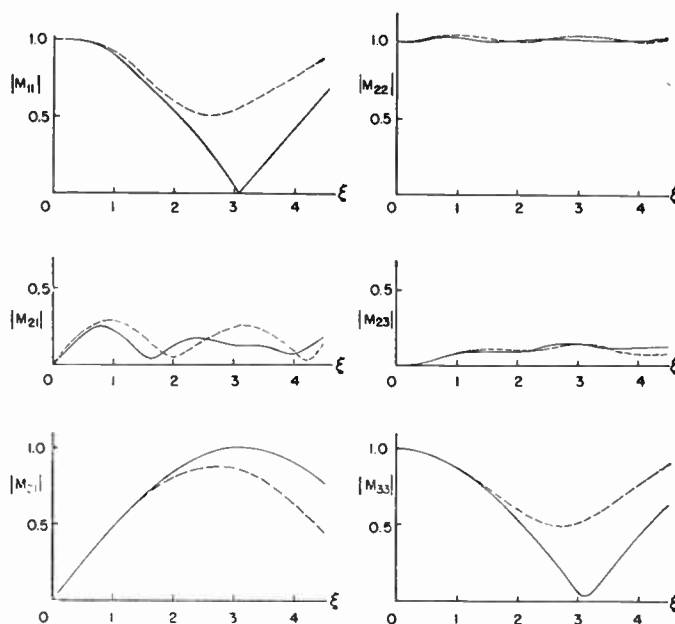
Fig. 2—Matrix elements for the case $QC = 1$, $d = 0$. Solid curves, $b = -2.0718$; dashed curves, $b = -1.5000$.

slow space-charge wave from the beam. This may be regarded as an impedance matching problem.[10] It is also possible to make M_{33} equal to zero by the proper choice of b and ξ. The values of b and ξ which make M_{33} equal to zero are only slightly different from those which make M_{11} equal to zero.

An alternative method of evaluating the matrix elements which is more useful for rapid study of the properties of the coupler was also employed. Eqs. (12)–(14) are readily solved on an electronic differential analyzer. Since complex quantities are involved, each equation must be written in terms of real and imaginary parts, resulting in *six* first-order coupled differential equations. Voltages corresponding to the real and imaginary parts of one of the matrix elements are used as x and y inputs to an oscilloscope, giving a direct display of the matrix element in polar form with time as the independent variable. Fig. 3 shows such a display, the heavy portion of the trace representing the beginning of the coupler. The magnitude of M_{11} becomes very small at one point along the trace since b is very nearly equal to the value for Kompfner Dip. The constant b is varied by changing two potentiometer settings, hence the dip condition is readily found. Because the presentation of data is direct and rapid, this method is ideally suited for study of the matrix properties.

In a later section it is shown that matrix elements at the Kompfner Dip condition are of special interest. These have been computed for different QC values and the results are given in Table I. The way in which coupling to the slow space charge wave depends on QC may be seen by examining the column M_{21}.

---

[9] $|M_{31}|$ will be larger than $|M_{21}|$ if $|M_{11}| < 1$, or if the traveling-wave section has no gain. This follows from the 1-1 component of (32).

[10] S. Bloom and R. Peter, "A transmission line analog of a modulated electron beam," *RCA Rev.*, vol. 15, pp. 95–112; March, 1954.

Fig. 3—Matrix elements for the case $QC=1$, $d=0$, $b=-2$, M_{11} (left), $-5jM_{21}*$ (center), $-jM_{31}$ (right), $7\cdot\frac{1}{2}$ divisions $=1.0$.

TABLE 1

MATRIX ELEMENTS AT KOMPFNER DIP ($M_{11}=0$)
(Magnitude and Phase Angle)

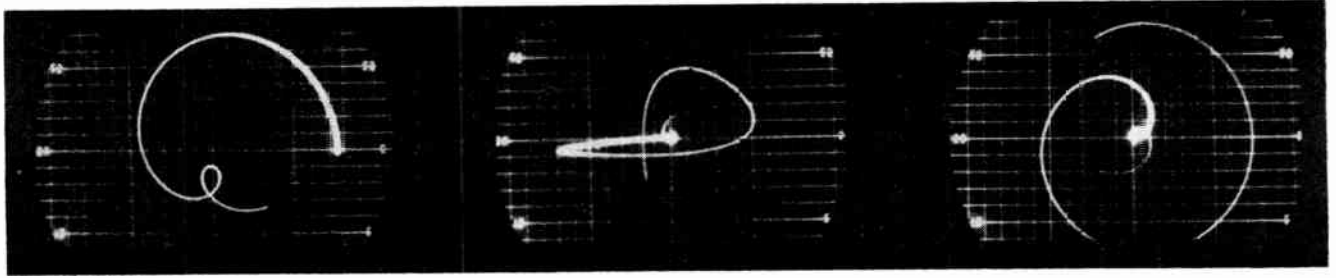| QC	b	ξ	M_{21}		M_{23}		M_{22}		M_{31}		M_{33}	
0.05	−1.5168	2.0037	1.0936	121.6°	1.6205	−131.3°	2.1959	−13.5°	1.4818	−176.2°	1.1959	−69.1°
0.10	−1.5121	2.0367	0.8339	108.0°	1.0859	−129.4°	1.6954	−39.3°	1.3021	−162.1°	0.6954	−39.6°
0.20	−1.5042	2.1129	0.5839	248.6°	0.6761	−124.6°	1.3409	−78.4°	1.1580	−139.8°	0.3409	9.1°
0.30	−1.5003	2.2502	0.3816	58.2°	0.4085	−113.8°	1.1456	−124.7°	1.0703	−111.0°	0.1456	77.1°
0.40	−1.5046	2.3325	0.3078	43.0°	0.3221	−105.4°	1.0947	−145.9°	1.0463	−96.5°	0.0947	115.1°
0.50	−1.5328	2.5070	0.2047	8.4°	0.2090	−79.9°	1.0419	176.9°	1.0207	−68.4°	0.0419	−156.7°
0.60	−1.6253	2.7315	0.1568	−49.0°	0.1587	−26.7°	1.0246	134.4°	1.0122	−30.0°	0.0246	−7.7°
0.80	−1.8918	2.9611	0.1696	−114.4°	0.1721	39.8°	1.0288	69.8°	1.0143	35.6°	0.0288	−170.2°
1.00	−2.0718	3.0871	0.1339	−156.1°	0.1351	78.2°	1.0179	17.7°	1.0089	84.4°	0.0179	−41.3°
1.20	−2.2333	3.2678	0.0983	139.7°	0.0883	139.2°	1.0097	−40.3°	1.0048	139.2°	0.0097	138.6°
1.40	−2.4152	3.4206	0.1016	79.9°	0.1021	−160.7°	1.0103	−95.1°	1.0051	−165.8°	0.0103	−46.4°
1.60	−2.5763	3.5131	0.0958	40.4°	0.0962	−121.8°	1.0092	−141.3°	1.0046	−120.1°	0.0092	7.8°
1.80	−2.7164	3.6131	0.0786	−3.9°	0.0788	−79.1°	1.0062	171.8°	1.0031	62.7°	0.0062	−150.0°
2.00	−2.8562	3.7327	0.0701	−60.7°	0.0703	−23.0°	1.0049	121.8°	1.0025	−25.5°	0.0049	12.2°

III. VELOCITY JUMPS, DRIFT SPACES, AND COMPOSITE SECTIONS

Since traveling-wave couplers will be used in conjunction with drift spaces and velocity jumps the matrices describing the latter are also presented here. In a drifting beam the phases of the fast and slow space-charge waves are delayed by $(\beta_e-\beta_q)l$ and $(\beta_e+\beta_q)l$ respectively if l is the drift distance. The amplitudes are unchanged. If we suppress the common phase delay $\beta_e l$ and define $\theta=\beta_q l$, the drift space equations are

$$A_2' = A_2 e^{-i\theta} \qquad (35)$$

$$A_3' = A_3 e^{+i\theta}. \qquad (36)$$

Although the circuit amplitude is not involved here it is convenient for matrix multiplication to use a three-by-three matrix and introduce the additional relation for the circuit amplitude $A_1'=A_1$. The matrix appropriate to a drift region is then

$$M = \begin{bmatrix} 1 & 0 & 0 \\ 0 & e^{-i\theta} & 0 \\ 0 & 0 & e^{i\theta} \end{bmatrix} \qquad \theta = \beta l_q. \qquad (37)$$

The equations describing a velocity jump are obtained by noting that in a velocity jump the kinetic voltage V_1 and ac beam current I_1 are invariant in an abrupt jump.[10] Using relations (6) and (7) the invariant principle is expressed

$$(A_2' + A_3')\sqrt{W'} = (A_2 + A_3)\sqrt{W} \qquad (38)$$

$$(-A_2' + A_3')/\sqrt{W'} = (-A_2 + A_3)/\sqrt{W} \qquad (39)$$

where the primed symbols refer to quantities after the jump and unprimed symbols refer to quantities before the jump. Solving for the matrix elements

$$M_{22} = M_{33} = \frac{1}{2}\left(\sqrt{\frac{W}{W'}} + \sqrt{\frac{W'}{W}}\right) \qquad (40)$$

$$M_{23} = M_{32} = \frac{1}{2}\left(\sqrt{\frac{W}{W'}} - \sqrt{\frac{W'}{W}}\right). \qquad (41)$$

To complete the matrix we again assume that $A_1'=A_1$, hence $M_{11}=1$ and $M_{12}=M_{21}=M_{13}=M_{31}=0$. Thus the matrix for a velocity jump is

$$M = \begin{bmatrix} 1 & 0 & 0 \\ 0 & \dfrac{\alpha^2+1}{2\alpha} & \dfrac{\alpha^2-1}{2\alpha} \\ 0 & \dfrac{\alpha^2-1}{2\alpha} & \dfrac{\alpha^2+1}{2\alpha} \end{bmatrix} \qquad \alpha = \sqrt{\frac{W}{W'}}. \quad (42)$$

It is of interest to note that the matrix for a jump from impedance W to impedance W' is the same as the matrix for a jump from W' to W except for a change in sign of the off-diagonal elements.

The matrix which describes a composite section consisting of cascaded individual sections of these types can

be written as the product of the matrices describing the individual sections. For example, a traveling-wave section (matrix M) followed by a drift region (matrix M') followed by a velocity jump (matrix M'') has the properties given by the resultant matrix

$$M'' \, M' \, M. \qquad (43)$$

IV. Fast Space-Charge Wave Couplers

We now apply the preceding results to synthesize fast wave couplers for longitudinal beam-type parametric amplifiers. First, consider the input coupler. The input coupler should perform two functions, 1) remove the noise from the fast space-charge wave, 2) place the input signal on the beam in the form of a fast space-charge wave as effectively as possible. If we describe the composite coupler by the matrix M (in general it will consist of a number of cascaded elementary sections), the first requirement can be stated

$$M_{32} = M_{33} = 0, \qquad (44)$$

i.e. there should be no noise output on the fast space-charge wave due to noise inputs on *either* the fast or slow space-charge waves. Assume that such a coupler can be constructed and consider the restrictions imposed by the assumption that the coupler is lossless [(32) and (33)]. The 33 component of (33)

$$M_{31}M_{31}^* - M_{32}M_{32}^* + M_{33}M_{33}^* = 1 \qquad (45)$$

together with (44) shows that

$$|M_{31}| = 1. \qquad (46)$$

The 32 component of (33)

$$M_{31}M_{21}^* - M_{32}M_{22}^* + M_{33}M_{23}^* = 0 \qquad (47)$$

together with (44) and (46) show that

$$M_{21} = 0. \qquad (48)$$

The 31 component of (33)

$$M_{31}M_{11}^* - M_{32}M_{12}^* - M_{33}M_{13}^* = 0 \qquad (49)$$

together with (44) and (46) show that

$$M_{11} = 0. \qquad (50)$$

We conclude then that an input on the circuit must produce no output on the circuit and no output on the slow space-charge wave. The input signal is transferred completely to the fast space-charge wave. Thus the second requirement of the coupler is automatically satisfied. The remainder of the restrictions imposed by (32) and (33) are

$$|M_{22}|^2 - |M_{23}|^2 = 1 \qquad (51)$$

$$-|M_{12}|^2 + |M_{13}|^2 = 1 \qquad (52)$$

$$|M_{13}|^2 - |M_{23}|^2 = 1 \qquad (53)$$

$$-|M_{12}|^2 + |M_{22}|^2 = 1 \qquad (54)$$

$$M_{22}M_{12}^* = M_{23}M_{13}^* \qquad (55)$$

$$M_{12}M_{13}^* = M_{23}^*M_{22}. \qquad (56)$$

From (55) and (56), or from (51) and (53), or from (52) and (54), it is seen that

$$|M_{13}|^2 = |M_{22}|^2. \qquad (57)$$

From (57) we may write

$$M_{13} = \gamma e^{-j\theta_3} \qquad M_{22} = \gamma e^{-j\theta_2} \qquad (58)$$

and the remaining relations (51) through (56) will be satisfied if

$$M_{12} = \sqrt{\gamma^2 - 1}e^{-j\theta_2} \qquad M_{23} = \sqrt{\gamma^2 - 1}e^{-j\theta_3} \qquad (59)$$

provided that $\gamma^2 \geq 1$. The resultant matrix is

$$M = \begin{bmatrix} 0 & \sqrt{\gamma^2 - 1}e^{-j\theta_2} & \gamma e^{-j\theta_3} \\ 0 & \gamma e^{-j\theta_2} & \sqrt{\gamma^2 - 1}e^{-j\theta} \\ e^{-j\theta_1} & 0 & 0 \end{bmatrix} \qquad (60)$$

and there are four remaining variables γ, θ_1, θ_2, and θ_3.

It has been shown that $M_{11} = M_{21} = 0$ is a necessary condition for the complete removal of beam noise from the fast space-charge wave. In a similar way it can be shown that if $M_{11} = M_{21} = 0$, then M_{32} and M_{33} are also zero. Thus the condition $M_{11} = M_{21} = 0$ is also sufficient.[11]
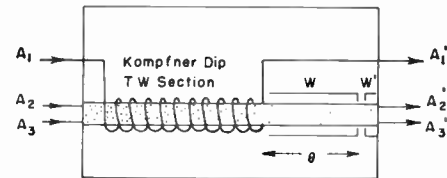
Fig. 4—Input coupler consisting of Kompfner Dip traveling-wave section, drift region, and velocity jump.

A coupler which has these properties can be constructed using a traveling-wave section in conjunction with velocity jumps and drift regions. Since M_{11} is to be zero the traveling-wave section *must* be operated at Kompfner Dip. Under this condition the fast-wave modulation of the beam is greater than the slow-wave modulation, hence it is possible to completely remove the slow wave with an appropriate velocity jump following the traveling-wave section. The physical configuration of the coupler is illustrated in Fig. 4. The matrix element connecting the circuit input to the slow-wave output of such a composite coupler is, using the results of the previous section,

$$M_{21} = \frac{\alpha^2 + 1}{2\alpha} e^{-j\theta}M_{21}' + \frac{\alpha^2 - 1}{2\alpha} e^{j\theta}M_{31}', \qquad (61)$$

where $\alpha^2 = W/W''$ is the ratio of the beam impedance W before the velocity jump to the beam impedance W''

[11] It is of interest to note that these same general arguments also apply to lossless cavity couplers if one lets A_1 and A_1' refer to the incident and reflected waves, respectively, on the transmission line leading to the cavity system. For a cavity system to be considered as lossless, the energy dissipated in the cavity must be small compared to the power transferred to the beam.

after the jump, and M_{21}' and M_{31}' are matrix elements of the traveling-wave section alone. This may be made zero with either of two choices

$$\theta = \frac{1}{2} \arg \frac{M_{21}'}{M_{31}'} + n\pi, \qquad \frac{W}{W'} = \frac{1 - \left| \dfrac{M_{21}'}{M_{31}'} \right|}{1 + \left| \dfrac{M_{21}'}{M_{31}'} \right|} \quad (62)$$

$$\theta = \frac{1}{2} \arg \frac{M_{21}'}{M_{31}'} + \left(n + \frac{1}{2}\right)\pi, \qquad \frac{W}{W'} = \frac{1 + \left| \dfrac{M_{21}'}{M_{31}'} \right|}{1 - \left| \dfrac{M_{21}'}{M_{31}'} \right|}, \quad (63)$$

where θ is the length of the drift region, and W/W' is the ratio of the beam impedance before the jump to the beam impedance after the jump. The first choice corresponds to a jump to higher velocity and the second to a jump to lower velocity. The velocity jump locations for the two cases differ by a quarter space-charge wavelength. The magnitude and location of a jump to a higher velocity which makes $M_{21} = 0$ is shown in Figs. 5 and 6. This coupler transfers the entire input signal to the fast space-charge wave and removes all beam noise from the fast space-charge wave. Its matrix has the same form as (60), where

$$\gamma = \left| M_{13}' \right| = \left| M_{31}' \right|$$

$$\theta_3 = \arg M_{13}'$$

$$\theta_2 = \arg M_{12}', \quad (64)$$

and M_{13}' and M_{12}' are elements of the traveling-wave matrix given in Table I. Furthermore by preceding the traveling-wave section by drift regions and velocity jumps it is possible to obtain other values of γ, θ_2, and θ_3 without affecting the fundamental properties of the coupler expressed by (44), (48), and (50).

The requirements on the output coupler of a parametric amplifier are different from those of the input coupler. First, the output coupler should not be sensitive to a slow-wave input since the slow wave may be noisy (although the slow-wave noise will not be amplified if the pump is in the form of a pure fast wave), or

$$M_{12} = 0. \quad (65)$$

Furthermore, the coupling to the fast wave (M_{13}) should be maximized. The 11 component of (33) can be written

$$\left| M_{13} \right|^2 = 1 - \left| M_{11} \right|^2 + \left| M_{12} \right|^2. \quad (66)$$

From this relation it is seen that the coupling to the fast wave is maximized when

$$M_{11} = 0 \quad (67)$$

or when the traveling-wave section is operated at Kompfner Dip. When (65) and (67) are satisfied the energy conservation relations can be used to show that
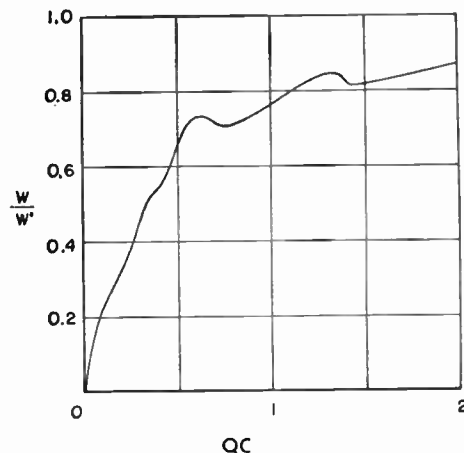
Fig. 5—Magnitude of impedance change required in velocity jump of the coupler illustrated in Fig. 5 in order for no coupling to the slow space-charge wave to occur ($M_{21} = 0$).
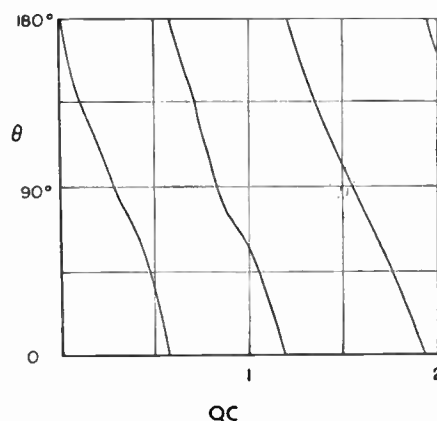
Fig. 6—Position of velocity jump of the coupler illustrated in Fig. 5 in order for no coupling to the slow space-charge wave to occur ($M_{21} = 0$).

M_{23} and M_{33} are zero. It is possible to satisfy (65) by preceding the traveling-wave section by a velocity jump and drift region. The 12 matrix element of the composite coupler is

$$M_{12} = M_{12}' e^{-j\theta} \frac{\alpha^2 + 1}{2\alpha} + M_{13}' e^{j\theta} \frac{\alpha^2 - 1}{2\alpha}, \quad (68)$$

where $\alpha^2 = W'/W$ is the ratio of the beam impedance before the velocity jump to the beam impedance after the velocity jump,[12] and M_{12}' and M_{13}' are matrix elements of the traveling-wave section alone. This relation is similar to (61) which applies to the input coupler. By virtue of (29) and (30)

$$\frac{M_{12}'}{M_{13}'} = - \frac{M_{21}'}{M_{31}'}. \quad (69)$$

It is possible to make M_{12} equal to zero in either of two ways:

---

[12] Note W' now refers to the beam impedance *before* the velocity jump and W refers to the beam impedance *after* the velocity jump. This is opposite from the convention of Section III.

$$\theta = \frac{1}{2} \arg \frac{M_{21}'}{M_{31}'} + n\pi \qquad \frac{W}{W''} = \frac{1 - \left| \dfrac{M_{21}'}{M_{31}'} \right|}{1 + \left| \dfrac{M_{21}'}{M_{31}'} \right|} \quad (70)$$

or

$$\theta = \frac{1}{2} \arg \frac{M_{21}'}{M_{31}'} + \left(n + \frac{1}{2} \right)\pi \qquad \frac{W'}{W''} = \frac{1 + \left| \dfrac{M_{21}'}{M_{31}'} \right|}{1 - \left| \dfrac{M_{21}'}{M_{31}'} \right|} \cdot \quad (71)$$

Eqs. (70) and (71) are identical with (63) and (62). Thus the results shown in Figs. 5 and 6 are also applicable to the output coupler. In other words, the drift length which is required between the traveling-wave section and a velocity jump, in which the beam impedance is *increased* in order to make $M_{12} = 0$, is the same as that required between the traveling-wave section and the velocity jump in which the beam impedance is decreased in order to make $M_{21} = 0$. The resulting coupler is depicted in Fig. 7.

Similar arguments can be applied to synthesize a pump coupler, although the bandwidth afforded by a traveling-wave coupler is not required. The requirements for a pump coupler are 1) to produce no slow wave modulation ($M_{21} = 0$), and 2) to maximize the fast-wave modulation (maximize M_{31}). The latter condition is achieved by taking $M_{11} = 0$. Thus the pump coupler is electrically identical with the input coupler (although it operates at a different frequency).

Finally we consider the symmetric coupler shown in Fig. 8. The traveling-wave section is preceded by a velocity jump from impedance W'' to impedance W' and a drift region of length θ. It is followed by a drift region of length θ and a velocity jump back to the original impedance W''. It is readily verified that this composite coupler has the following symmetry

$$M_{12} = \mp M_{21}$$

$$M_{13} = \pm M_{31}$$

$$M_{23} = - M_{32}$$

which is the symmetry of the traveling-wave coupler alone. Furthermore by choosing the location and magnitude of the velocity jump in the manner already described (Figs. 5 and 6), it is possible to construct a kind of ideal coupler, whose matrix is

$$M = \begin{bmatrix} 0 & 0 & e^{-j\theta_3} \\ 0 & e^{-j\theta_2} & 0 \\ e^{-j\theta_1} & 0 & 0 \end{bmatrix}$$

The slow space-charge wave passes through the coupler with only a shift in phase, and there is a complete
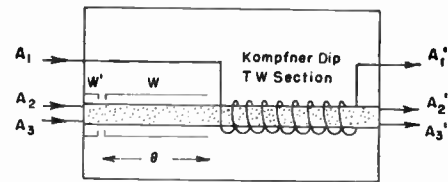
Fig. 7—Output coupler consisting of velocity jump, drift region, and Kompfner Dip traveling-wave section.
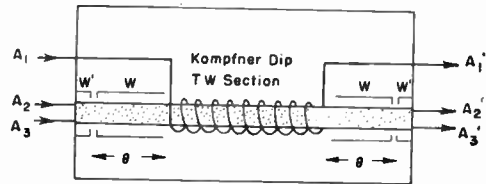
Fig. 8—Ideal coupler consisting of velocity jump, drift region, Kompfner Dip traveling-wave section, drift region, and velocity jump.

transfer of energy from the circuit wave to the fast space-charge wave and vice versa.

V. Discussion

The theory of longitudinal-beam traveling-wave couplers has been developed and applied to the design of couplers for parametric amplifiers. For any QC value a coupler can be constructed which couples only to the fast space-charge wave and, furthermore, this same coupler also removes the beam noise from the fast space-charge wave. This coupler consists of a traveling-wave section, drift region, and velocity jump. For certain QC values the velocity jump can be placed very close to the traveling-wave section, making a very compact coupler. Similarly, an output coupler which is sensitive only to the fast space-charge wave of the beam can be made by preceding a traveling-wave section with a velocity jump.

Results for the traveling-wave section by itself (Table I) indicate that the coupling to the slow space-charge wave is down 20 db or more at Kompfner Dip for $QC > 1.2$ ($|M_{21}| < .10$) and that beam noise is reduced by a similar amount ($|M_{32}| < .1$, $|M_{33}| < .01$) under these same conditions. When used with a low noise electron gun this less perfect but inherently simpler type of coupler also appears very attractive.

Finally, it should be pointed out that the presence of the pump signal on the beam may modify these results slightly. Locating the input coupler before the pump coupler will eliminate any possible effect in the input coupler where noise is eliminated from the fast wave.

VI. Acknowledgment

IRE Standards on Static Magnetic Storage: Definitions of Terms, 1959*

59 IRE 8. S1

COMMITTEE PERSONNEL

Subcommittee on Static Storage Elements

M. K. HAYNES, *Chairman* 1955–1958

A. O. Black 1955–1957
T. H. Bonn 1955–1957
H. R. Brownell 1955–1958
T. C. Chen 1955–1958
E. Gelbard 1955–1957
J. D. Lawrence 1957
W. Olander 1957–1958

W. N. Papian 1955–1956
J. Rajchman 1955–1958
E. A. Sands 1955–1958
D. H. Toth 1955–1957
C. B. Wakeman 1957–1958
R. Stuart Williams 1955–1958

Committee on Electronic Computers
1957–1959

D. R. BROWN, *Chairman*
R. D. ELBOURN, *Vice-Chairman*

S. N. Alexander
W. T. Clary
M. K. Haynes
L. C. Hobbs
J. R. Johnson

C. D. Morrill
W. O. Olander
G. W. Patterson
T. A. Rogers
R. Serrell

Q. W. Simkins
R. L. Snyder, Jr.
W. H. Ware
J. R. Weiner
Way Dong Woo

Committee on Standards
1958–1959

R. F. SHEA, *Chairman*
J. G. KREER, JR., *Vice-Chairman*
C. H. PAGE, *Vice-Chairman*
L. G. CUMMING, *Vice-Chairman*

J. Avins
W. F. Bailey
M. W. Baldwin, Jr.
J. T. Bangert
W. R. Bennett
J. G. Brainerd
D. R. Brown
T. J. Carroll
P. S. Carter
A. G. Clavier
G. A. Deschamps
S. Doba, Jr.
P. Elias
G. A. Espersen

D. Frezzolini
E. A. Gerber
A. B. Glenn
V. M. Graham
R. A. Hackbusch
R. T. Haviland
A. G. Jensen
I. Kerney
A. E. Kerwien
G. S. Ley
Wayne Mason
D. E. Maxwell
H. R. Mimno

E. Mittelmann
L. H. Montgomery, Jr.
G. A. Morton
R. C. Moyer
J. H. Mulligan, Jr.
W. Palmer
R. L. Pritchard
P. A. Redhead
R. Serrell
W. A. Shipman
H. R. Terhune
E. Weber
R. B. Wilcox
W. T. Wintringham

Definitions Coordinator

C. H. PAGE

---

* Approved by the IRE Standards Committee, November 13, 1958. Reprints of this Standard, 59 IRE 8. S1, may be purchased while available from the Institute of Radio Engineers, 1 East 79th Street, New York, N. Y., at $0.50 per copy. A 20 per cent discount will be allowed for 100 or more copies mailed to one address.

Bobbin Core. See *Tape-Wound Core.*

Bobbin I.D. See *Tape-Wound Core.*

Bobbin O.D. See *Tape-Wound Core.*

Bobbin Height. See *Tape-Wound Core.*

Coercive Force, H_c**.** The magnetizing force at which the magnetic flux density is zero when the material is in a *Symmetrically Cyclically Magnetized Condition.*

    Note: Coercive force is not a unique property of a magnetic material, but is dependent upon the conditions of measurement.

Coercivity. The property of a magnetic material measured by the *Coercive Force* corresponding to the *Saturation Induction* for the material.

    Note: This is a quasi-static property only.

Coincident-Current Selection. The selection of a magnetic cell for reading or writing, by the simultaneous application of two or more currents.

    The **Selection Ratio** is the least ratio of a magnetomotive force used to select a cell to the maximum magnetomotive force used which is not intended to select a cell. A **Partial-Read Pulse** is any one of the currents applied which cause selection of a cell for reading. A **Partial-Write Pulse** is any one of the currents applied which cause selection of a cell for writing.

    An **Undisturbed-Zero Output** is a *Zero Output* of a magnetic cell to which no *Partial-Write Pulses* have been applied since that cell was last selected for reading. An **Undisturbed-One Output** is a *One Output* of a magnetic cell to which no *Partial-Read Pulses* have been applied since that cell was last selected for writing. A **Disturbed-Zero Output** is a *Zero Output* of a magnetic cell to which *Partial-Write Pulses* have been applied since that cell was last selected for reading. A **Disturbed-One Output** is a *One Output* of a magnetic cell to which *Partial-Read Pulses* have been applied since that cell was last selected for writing. A **Partial-Select Output** is 1) the voltage response of an unselected magnetic cell produced by the application of *Partial-Read Pulses* or *Partial-Write Pulses* or 2) the integrated voltage response of an unselected magnetic cell produced by the application of *Partial-Read Pulses* or *Partial-Write Pulses.*

    A **One-to-Partial-Select Ratio** is the ratio of a *One Output* to a *Partial-Select Output.* **Delta** is the difference between a *Partial-Select Output* of a magnetic cell in a *One State* and a *Partial-Select Output* of the same cell in a *Zero State.*

Cyclically Magnetized Condition. A condition of a magnetic material when it has been under the influence of a magnetizing force varying between two specific limits until, for each increasing (or decreasing) value of the magnetizing force, the magnetic flux density has the same value in successive cycles.

Delta. See *Coincident-Current Selection.*

Disturbed-One Output. See *Coincident-Current Selection.*

Disturbed-Zero Output. See *Coincident-Current Selection.*

Drive Pulse. A pulsed magnetomotive force applied to a magnetic cell from one or more sources.

Groove Diameter. See *Tape-Wound Core.*

Groove Width. See *Tape-Wound Core.*

Hysteresis Loop. For a magnetic material in a *Cyclically Magnetized Condition*, a curve (usually with rectangular coordinates) showing, for each value of the magnetizing force, two values of the magnetic flux density—one when the magnetizing force is increasing, the other when it is decreasing.

Inhibit Pulse. A *Drive Pulse* that tends to prevent flux reversal of a magnetic cell by certain specified *Drive Pulses.*

Intrinsic Induction, B_i**.** In a magnetic material for a given value of the magnetizing force, the excess of the normal flux density over the flux density in vacuum.

    The equation for *Intrinsic Induction* is

$$B_i = B - \mu_v H,$$

where μ_v is the factor that expresses the ratio of magnetic flux density to magnetizing force in vacuum.

Nondestructive Read. A method of reading the magnetic state of a core without changing its state.

One Output. See *One State.*

One State. A state of a magnetic cell wherein the magnetic flux through a specified cross-sectional area has a positive value, when determined from an arbitrarily specified direction of positive normal to that area. A state wherein the magnetic flux has a negative value, when similarly determined, is a **Zero State.**

    A **One Output** is 1) the voltage response obtained from a magnetic cell in a *One State* by a reading or resetting process or 2) the integrated voltage response obtained from a magnetic cell in a *One State* by a reading or resetting process. A **Zero Output** is 1) the voltage response obtained from a magnetic cell in a *Zero State* by a reading or resetting process or 2) the integrated voltage response obtained from a magnetic cell in a *Zero State* by a reading or resetting process. A ratio of a *One Output* to a *Zero Output* is a **One-to-Zero Ratio.**

    A pulse, for example a *Drive Pulse*, is a **Write Pulse** if it causes information to be introduced into a magnetic cell or cells, or is a **Read Pulse** if it causes information to be acquired from a magnetic cell or cells.

One-to-Partial-Select Ratio. See *Coincident-Current Selection.*

One-to-Zero Ratio. See *One State.*

Partial-Read Pulse. See *Coincident-Current Selection.*

Partial-Select Output. See *Coincident-Current Selection.*

Partial-Write Pulse. See *Coincident-Current Selection.*

Path Length. The length of a magnetic flux line in a core. In a toroidal core with nearly equal inside and outside diameters, the value

$$l_m = \frac{\pi}{2} \, (\text{O.D.} + \text{I.D.})$$

is commonly used.

Peak Flux Density, B_m. The maximum flux density in a magnetic material in a specified *Cyclically Magnetized Condition.*

Peak Magnetizing Force, H_m (Peak Field Strength). The upper or lower limiting value of magnetizing force associated with a *Cyclically Magnetized Condition.*

Read Pulse. See *One State.*

Reference Time, T_o. An instant near the beginning of switching chosen as an origin for time measurements. It is variously taken as the first instant at which the instantaneous value of the *Drive Pulse*, the voltage response of the magnetic cell, or the integrated voltage response reaches a specified fraction of its peak pulse amplitude.

Remanence, B_d. The magnetic flux density which remains in a magnetic circuit after the removal of an applied magnetomotive force.

> *Note:* This should not be confused with *Residual Flux Density.* If the magnetic circuit has an air gap, the *Remanence* will be less than the *Residual Flux Density.*

Reset Pulse. A *Drive Pulse* which tends to reset a magnetic cell.

Residual Flux Density, B_r. The magnetic flux density at which the magnetizing force is zero when the material is in a *Symmetrically Cyclically Magnetized Condition.*

> *Note:* See also *Remanence.*

Retentivity, B_{rs}. The property of a material which is measured by the *Residual Flux Density* corresponding to the *Saturation Induction* for the material.

Saturation Flux Density. See *Saturation Induction.*

Saturation Induction, B_s. The maximum *Intrinsic Induction* possible in a material (see *Intrinsic Induction*). *Saturation Induction* is sometimes loosely referred to as *Saturation Flux Density.*

Selection Ratio. See *Coincident-Current Selection.*

Set Pulse. A *Drive Pulse* which tends to set a magnetic cell.

Shift Pulse. A *Drive Pulse* which initiates shifting of characters in a register.

Squareness Ratio. 1) B_r/B_m. For a material in a *Symmetrically Cyclically Magnetized Condition*, the ratio of the flux density at zero magnetizing force to the maximum flux density. 2) R_s. For a material in a *Symmetrically Cyclically Magnetized Condition*, the ratio of the flux density when the magnetizing force has changed half way from zero toward its negative limiting value, to the maximum flux density.

> *Note:* Both of these ratios are functions of the maximum magnetizing force.

Switching Coefficient, S_w. The derivative of applied magnetizing force with respect to the reciprocal of the resultant *Switching Time.* It is usually determined as the reciprocal of the slope of a curve of reciprocals of *Switching Times* vs values of applied magnetizing forces. The magnetizing forces are applied as step functions.

Switching Time. 1) T_s, the time interval between the *Reference Time* and the last instant at which the instantaneous voltage response of a magnetic cell reaches a stated fraction of its peak value. 2) T_x, the time interval between the *Reference Time* and the first instant at which the instantaneous integrated voltage response reaches a stated fraction of its peak value.

Symmetrically Cyclically Magnetized Condition. A condition of a magnetic material when it is in a *Cyclically Magnetized Condition* and the limits of the applied magnetizing forces are equal and of opposite sign, so that the limits of flux density are equal and of opposite sign.

Tape Thickness. See *Tape-Wound Core.*

Tape Width. See *Tape-Wound Core.*

Tape-Wound Core. A length of ferromagnetic tape coiled about an axis in such a way that one convolution falls directly upon the preceding convolution. The greater of the cross-sectional dimensions of the tape is the **Tape Width,** and the other is the **Tape Thickness.** A **Wrap** is one convolution of the tape about the axis. **Wrap Thickness** is the distance between corresponding points on two consecutive wraps, measured parallel to the *Tape Thickness.*

A **Bobbin Core** is a *Tape-Wound Core* in which the ferromagnetic tape has been wrapped on a form or bobbin which supplies mechanical support to the tape. The dimensions of a bobbin are illustrated in Fig. 1. The **Bobbin I.D.** is the center-hole diameter (D) of the bobbin. The **Bobbin O.D.** is the over-all diameter (E) of the bobbin. The **Bobbin Height** is the over-all axial dimension (F) of the bobbin. The **Groove Diameter** is the Diameter (G) of the center portion of the bobbin on
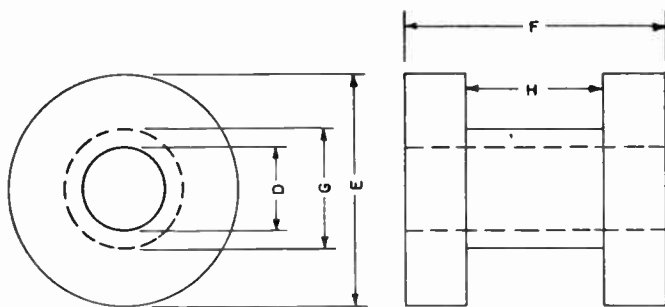
Fig. 1—Dimensions of a bobbin.

which the first tape *Wrap* is placed. The **Groove Width** is the axial dimension (*H*) of the bobbin measured inside the groove at the groove diameter.

Threshold Field, H_o. The least magnetizing force in a direction which tends to decrease the *Remanence*, which, when applied either as a steady field of long duration or as a pulsed field appearing many times, will cause a stated fractional change of *Remanence*.

Undisturbed-One Output. See *Coincident-Current Selection*.

Undisturbed-Zero Output. See *Coincident-Current Selection*.

Winding. A conductive path, usually of wire, inductively coupled to a magnetic core or cell. When several windings are employed, they may be designated by the functions performed. Examples are: sense, bias, and drive windings. Drive windings include read, write, inhibit, set, reset, input, shift, and advance windings.

Wrap. See *Tape-Wound Core*.

Wrap Thickness. See *Tape-Wound Core*.

Wrap Width. Synonym for *Tape-Width*. See *Tape-Wound Core*.

Write Pulse. See *One State*.

Zero Output. See *One State*.

Zero State. See *One State*.

The Effects of Automatic Gain Control Performance on the Tracking Accuracy of Monopulse Radar Systems*

J. H. DUNN† AND D. D. HOWARD†, SENIOR MEMBER, IRE

Summary—Finite size targets with complex structure such as aircraft present to a radar several reflecting surfaces distributed in space, and these surfaces will move randomly in respect to the radar with the normal yaw, roll and pitch of the aircraft. The resulting random wander of the apparent source of the target echo causes a corresponding fluctuation called target noise in the output of the radar angle-error detectors and a wander of the radar antenna during closed-loop tracking of the target. This wander is called tracking noise.

The tracking noise, caused by a finite size target, internal noise and other noise sources, can be minimized by choice of the parameters of the radar AGC (automatic gain control) circuitry and servo-system. Previous papers published on this subject were restricted to open-loop analysis and with assumption of negligible tracking error; however, the analysis in this paper includes actual closed-loop tracking data of a practical tracking radar and shows that under practical tracking conditions a short-time-constant fast-acting AGC will minimize tracking noise. Furthermore, it is shown that the servo-bandwidth should be kept at the minimum value that is consistent with tactical requirements.

INTRODUCTION

THE present and future uses of automatic tracking radars and the expected speeds of targets call for a high degree of precision and accuracy and require a minimum of noise in the target-position data.

The definitions of the various types of noise and the effect on tracking noise in radar systems have been discussed[1] and are restated here.

Tracking noise is defined as any deviation of the tracking axis from the center of reflectivity of a target (deviations other than normal dynamic lags). It has been found that the major causes of tracking noise are the four separate noise components, namely, servo noise, receiver noise, angle noise, and amplitude noise. The first two of these components originate in the radar itself. The second two components are generated by the

[1] B. L. Lewis, A. J. Stecca, and D. D. Howard, "The Effect of an Automatic Gain Control on the Tracking Performance of a Monopulse Radar," U. S. Naval Res. Lab., Washington, D. C., Rep. No. 4796; July, 1956.

target and will be called target noise. These four noise terms have been defined as follows:

Servo noise is the hunting action of the tracking servo-mechanism which results from backlash and compliance in the gears, shafts and structures of the mount. The magnitude of this noise is essentially independent of the target and will thus be independent of range.

Receiver noise is the effect on the tracking accuracy of the radar of thermal noise generated in the input imped-ance of the receiver and any spurious hum which may be picked up by the circuitry.

Angle noise is the tracking error introduced into the radar by variations in the apparent angle of arrival of the echo from a target due to finite size. This effect is caused by variations in the phase front of the radiation from a multiple-point target as the target changes its aspect. The magnitude of angle noise is inversely pro-portional to the range of the target.

Amplitude noise is the effect on the radar accuracy of the fluctuations in the amplitude of the signal returned by the target. These fluctuations are caused by any change in aspect of the target and must be taken to in-clude propeller rotation and skin vibration.

This paper presents theoretical and experimental evi-dence describing how the AGC characteristics affect the different noise components and thus determine an optimum design for any specific application.

Practical considerations make the theoretical infinite dynamic-range AGC impossible. Thus, target noise should be evaluated with realizable circuitry in mind. The mechanics of interpreting the equations in this manner, however, are so involved that it was decided to complete the analysis with a radar and finite-size target simulator.[2,3] (The amplitude and angle noise spec-tra and probability distributions obtained from the simulator for a given target are indistinguishable from those measured during actual radar tracking runs.) This device simulates a radar with closed-loop tracking of a finite size target which is free to rotate about its center of gravity but is fixed in range. Thus, "no AGC" action in the simulator is equivalent to very slow AGC in a tracking radar. It was also decided to define a fast and a medium AGC as having frequency responses at least 10 times and approximately equal, respectively, to the half-power frequency of the target amplitude-noise spectrum.

An AGC loop was constructed with time constants which allow the closed-loop response to be either 1 or 12 cps with an open-loop zero-frequency gain of 46 db. The spectral density plot of the amplitude fluctuation of the simulated target is shown in Fig. 1, and the angle noise is essentially Gaussian distributed with an rms value of approximately 0.21 times the target span. The reflec-
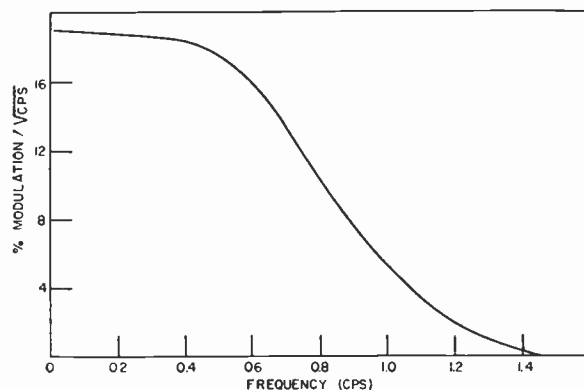
Fig. 1—Spectrum of amplitude noise in the signal from the simulated target.
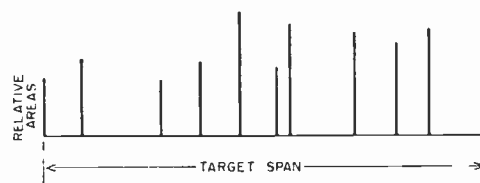
.Fig. 2—Reflectivity distribution of simulated target.

tivity distribution of the target is shown in Fig. 2. The information presented in this paper is primarily con-cerned with the application of AGC to monopulse radar system design.[4] The results apply also to conical scan and sequentially lobed radar except that the problem of the additional tracking noise caused by amplitude noise which falls in the vicinity of the lobing rate[5] must be considered, and the AGC must not control gain at fre-quencies in the vicinity of the lobing rate in order to preserve lobing modulation.

EFFECTS OF TARGET NOISE ON AGC DESIGN

The target tracked by a radar is a part of a closed tracking loop, and any variations in target echo ampli-tude can be considered as changes in closed-loop gain. Experimental results show that angle-noise peaks cor-respond to echo fades such that there is a negative cor-relation between angle-error magnitude and echo ampli-tude. Consequently, the control of loop gain by ampli-tude noise has a direct effect upon the angle noise or wander of the apparent position of a finite size target about its true position and, in addition, allows the ampli-tude noise to modulate any other error signal, intro-ducing an additional noise component which is a func-tion of tracking lag errors or any other true tracking errors. The AGC essentially provides equal and oppo-site gain changes in the IF amplifiers to maintain a constant-gain, stable loop. If the AGC is slow acting, it maintains constant average loop gain but allows the

[2] A. J. Stecca, N. V. O'Neal, and J. J. Freeman, "A Target Simu-lator," U. S. Naval Res. Lab., Washington, D. C., Rep. No. 4694; February, 1956.
[3] A. J. Stecca and N. V. O'Neal, "Target Noise Simulator-Closed-Loop Tracking," U. S. Naval Res. Lab., Washington, D. C., Rep. No. 4770; July, 1956.

[4] R. M. Page, "Monopulse radar," 1955 IRE CONVENTION RECORD, Pt. 8, pp. 132–134.
[5] J. E. Meade, A. E. Hastings, and H. L. Gerwin, "Noise in Track-ing Radars," U. S. Naval Res. Lab., Washington, D. C., Rep. No. 3759; November, 1950.

fast echo-amplitude changes caused by amplitude noise to control loop gain as described above. The fast AGC, when tracking error is present, maintains a constant loop gain so that any true tracking errors such as velocity lags are not modulated by amplitude noise and no additional noise component is caused. The relative values of angle noise and the additional noise component caused by amplitude noise will be shown in the following paragraphs.

In the theoretical analysis the center of reflectivity of the target is chosen as zero reference angle, for convenience, such that the deviation of the radar antenna tracking axis from the center of the target is θ_0 as shown in Fig. 3. The two antenna lobes of a monopulse radar in the azimuth coordinate, for example, are shown in Fig. 4(a). In the monopulse radar the two lobes are present simultaneously and are added or subtracted, generally at RF, to produce the necessary sum and difference signals for tracking functions.[4] During normal tracking the target is held near the tracking axis (crossover point of the two lobes) and in this region it is assumed that the lobes are essentially linear as shown in Fig. 4(b) with functions of angle as indicated. The ideal error-detector output is

$$e_i = E_d\theta_0 \tag{1}$$

where θ_0 is the angle tracking error as shown in Fig. 3, and E_d is the desired IF amplifier output level. This ideal error-detector output is a dc voltage proportional to tracking error θ_0 and of a polarity corresponding to direction of error.

The error-detector output has been derived[1,6,7] for any practical target, such as an aircraft, having a complex surface. The error-detector output for the two conditions under consideration, long-time constant or slow AGC, e_s, and short-time constant or fast AGC, e_f, may be expressed by

$$e_s = E(t)\theta_0 + \theta(t) \tag{2}$$

$$e_f = E_d\theta_0 + \frac{E_d\theta(t)}{E(t)} \tag{3}$$

where $E(t)$ is the detected received echo signal containing a dc component plus amplitude noise (that is, the amplitude fluctuations of the echo caused by the target), and $\theta(t)$ is a component of angle noise being the complete angle-noise term with slow AGC and modified by E_d and $E(t)$ to produce the angle-noise term for fast AGC.

The second terms of e_s and e_f are the angle noise and indicate a wander of the apparent location of the target regardless of the true tracking error θ_0, *i.e.*, any deviation of the tracking axis from the center of reflectivity

[6] R. H. DeLano, "A theory of target glint or angular scintillation in radar tracking," PROC. IRE. Vol. 41, pp. 1778–1784; December, 1953.

[7] R. H. DeLano and I. Pfeffer, "The effect of AGC on radar tracking noise," PROC. IRE, vol. 44, pp. 801–810; June, 1956.
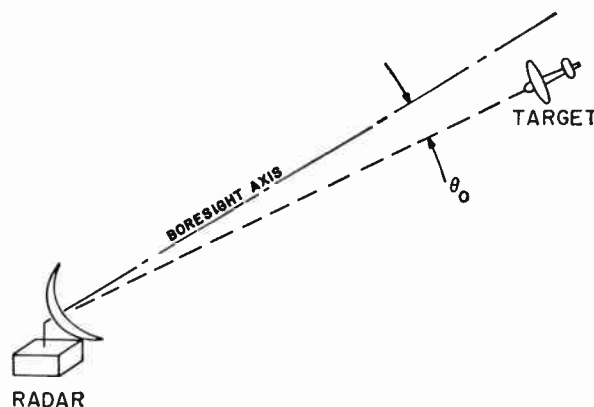
Fig. 3—Radar with tracking error θ_0.
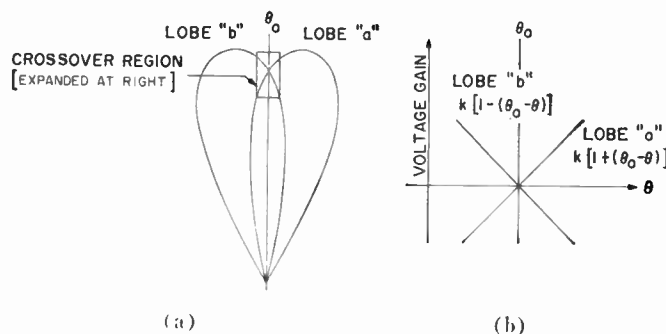
Fig. 4—Tracking antenna lobes used to determine tracking error information and assumed linear crossover pattern. (a) True antenna pattern and crossover point. (b) assumed linear crossover point.

of the target. This noise term is independent of the tracking point (assuming the target remains within the linear region of the antenna lobes). With fast AGC the detector output is the same as the ideal except for the angle-noise term which appears at the detector output. The angle-noise term is larger with fast AGC, $E_d\theta(t)/E(t)$, than with the slow AGC, $\theta(t)$. Theoretically the angle-noise term in e_f is infinite with an infinite dynamic range AGC, but with practical circuitry the angle noise, which determines the target noise only when the target is on axis ($\theta_0 = 0$), is approximately twice the angle-noise power when using fast AGC than would be obtained with slow AGC (in agreement with DeLano and Pfeffer).[7] The increased angle noise with fast AGC may be visualized on the basis of the correlation which exists between echo amplitude and angle-error magnitude as previously described. The angle noise, however, as shown later, is significant only at close range.

The error-detector output with slow AGC contains an additional noise component in the first term of e_s, namely, the fluctuation in the envelope $E(t)$ about its average level. The ac component of $E(t)$ is the amplitude noise which modulates any true tracking error signal. The error-detector output may be written as

$$e_s = E_d\theta_0 + E(t)_{amp}\theta_0 + \theta(t) \tag{4}$$

where the dc value of the envelope is adjusted to the

desired level E_d in the first term, and the ac component $E(t)_{amp}$ is the amplitude noise on the envelope. Therefore, the second term is noise in the detector output caused by amplitude noise which is independent of range and is present only when using slow AGC. This noise component, unlike angle noise, is a function of any tracking error θ_0 and increases with tracking error such as velocity lag.

Fig. 5, shows a comparison of the target noise components of (2) and (3). Fig. 5(a) is computed assuming a target with a $\cos^2$ distribution of reflecting area and a Rayleigh distributed echo amplitude. Fig. 5(b) shows the approximate angle noise level that would be present with a fast AGC of finite dynamic range and indicates the absence of additional noise caused by echo amplitude fluctuations when using fast AGC. The tracking error is measured in a plane through the target, normal to the direction toward the radar, in units of target length L. With fast AGC, amplitude noise contributions are zero because the AGC completely smooths the IF output. Also angle noise, which is significant only at near range[5] is greater than with slow AGC; however, with slow AGC the amplitude noise causes a noise component which rapidly increases with tracking error θ_0. This component is significant at all ranges because at medium and long range the target subtends a small angle, and tracking errors in terms of target span L are large, while at short range translation velocities are greater, causing large tracking lag errors. This is further demonstrated in Fig. 6, which shows the experimental results with an AGC of the bandwidths indicated. The data for this figure and other figures below were obtained with the target simulator[2,3] and verified by measurements with a monopulse radar tracking actual aircraft.[1] It is observed that with tracking errors of only half a target span the noise with slow AGC begins to exceed the noise with fast AGC. Furthermore, as described later, at medium and long ranges the target subtends a small angle and internal noise sources cause large pointing error such that the angle noise contribution will be insignificant.

This noise in the angle-error detector output is fed along with true tracking error information to the servo-system with closed-loop tracking, so that all components falling within the servo bandwidth will contribute to tracking noise. An important fact shown in this analysis is that in all tracking radars the low-frequency amplitude noise can contribute to tracking noise through modulation of true tracking error information. Whatever noise from the angle-error detector is allowed to pass to the servosystem causes the antenna to move from the true target center, thus causing finite values of θ_0. With the slow AGC the existence of finite values of θ_0 in turn increases the amplitude-noise output, thus completing a regenerative closed loop through amplitude-noise contributions to tracking noise. With fast AGC there is no component which is a function of tracking error θ_0. Thus the tracking noise will be simply the por-
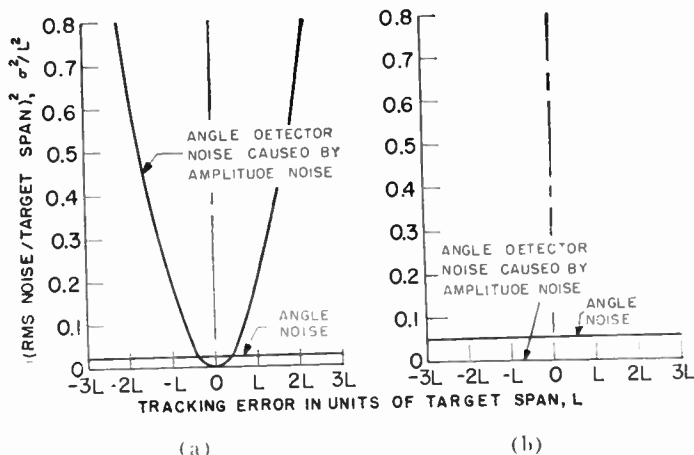
Fig. 5—Target noise components as a function of tracking error θ_0 to compare the effects of slow and fast AGC on the noise components. (a) Slow AGC, (b) fast AGC.
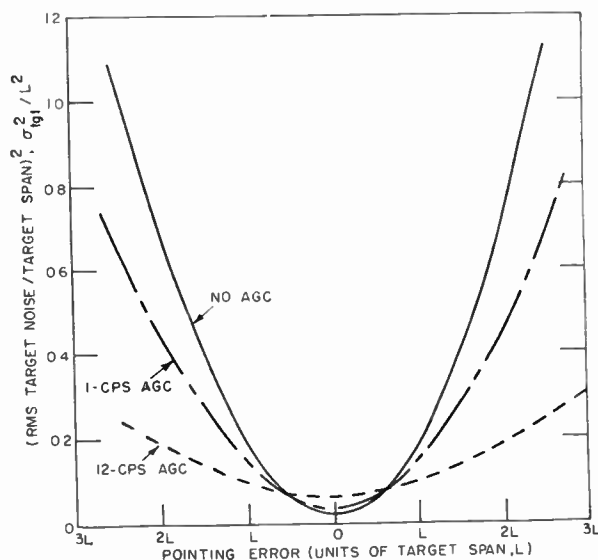
Fig. 6—Open-loop target noise power vs antenna pointing error for different values of AGC bandwidth.

tion of angle noise which can pass through the servo pass band. The effect of AGC characteristics on closed-loop tracking is shown from experimental results in Figs. 7 and 8 for servotracking bandwidths of 1 and 4 cps, respectively. The data exclude internal noises of the radar, but the effects of internal noise are described at the end of this section.

Since any tracking lag with slow AGC operation increases tracking noise, one might suggest increasing the tracking bandwidth to minimize the lag. However, increasing the tracking bandwidth allows more target noise to pass through the servosystem. By thus reducing servo lag to reduce tracking noise contributions from amplitude noise, servo response to all noise components is increased. This is shown in Fig. 9 from experimental results obtained by closed-loop tracking with the target and radar simulator which have adjustable servo bandwidth and target noise bandwidth. These re-
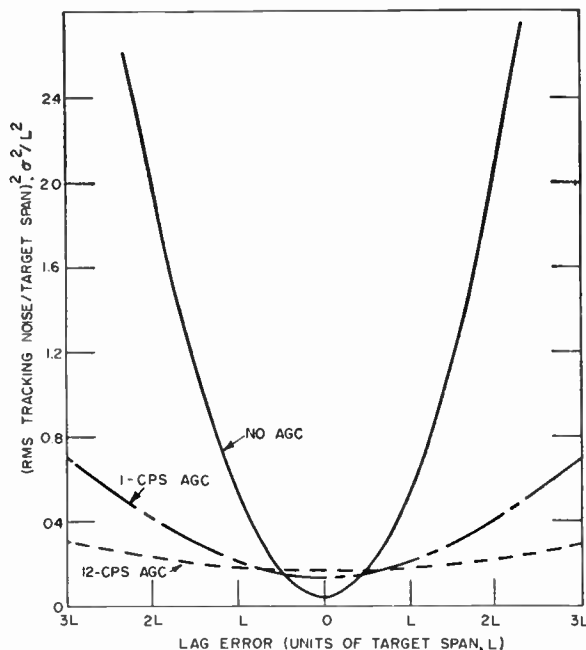
Fig. 7—Closed-loop tracking noise power vs lag error as a function of AGC action for a tracking bandwidth of 1 cps.
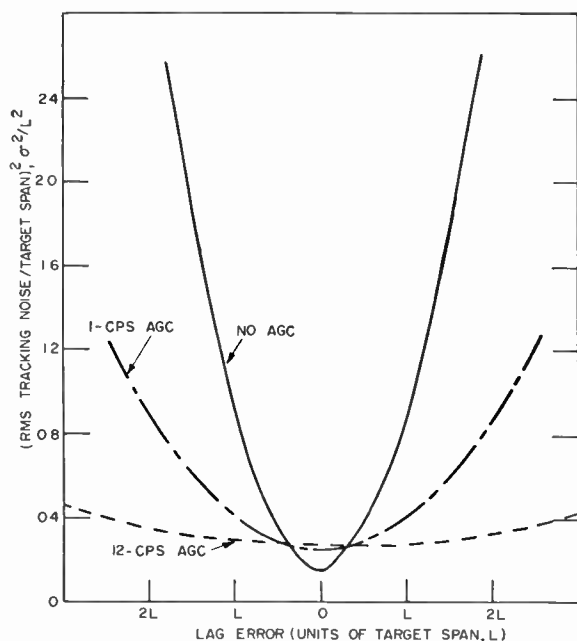
Fig. 8—Closed-loop tracking noise power vs lag error as a function of AGC action for a tracking bandwidth of 4 cps.

sults show that tracking can be greatly impaired by excessive servo bandwidth or when tracking a target, with noise components that are low in frequency and fall within the servo bandwidth. Consequently, for minimum tracking noise the servo bandwidth should be restricted to that necessary to meet the tactical tracking requirements.

The discussion to this point considers only the tracking noise caused by target noise; however, any internal
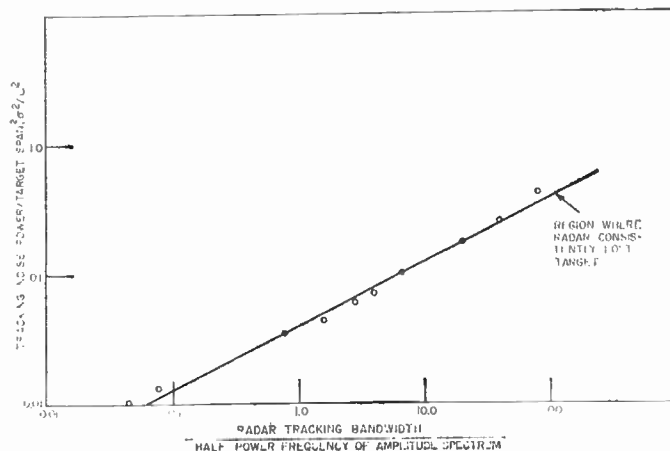
Fig. 9—Closed-loop tracking noise power vs radar tracking bandwidth with slow AGC and zero lag error.

noise sources such as receiver noise and servo noise cause excursions of the tracking antenna from the target center which further increases angle-error-detector noise caused by amplitude noise when slow AGC is used. Consequently, the advantages with use of fast AGC with respect to slow AGC will be greater where internal radar noises are significant and/or where wide-band response is necessary.

TRACKING NOISE IN A TRACKING RADAR[8] WITH FAST AGC AS A FUNCTION OF TARGET REFLECTIVITY DISTRIBUTION AND ANGULAR VELOCITY

The reflectivity distribution and angular velocity of the target are very significant considerations since they determine the ratio of the tracking bandwidth of the radar to the half-power frequency of the angle-noise spectrum for any given tracking bandwidth by determining the spectral energy distribution of the angle noise. Thus, these factors determine the magnitude of the contribution of amplitude noise to the tracking noise in a radar with slow AGC.

In addition, the target reflectivity distribution controls the magnitude of the angle noise from the target. Measurements of target noise with a tracking radar and theoretical analysis show that the open-loop angle-noise power with slow AGC is directly proportional to the square of the radius of gyration of the target's reflectivity about the center of reflectivity; that is, the total angle-noise power is

$$\sigma_{ang}^2 = \frac{1/2 \sum_{i=1}^{n} A_i^2 \theta_i^2}{\sum_{i=1}^{n} A_i^2} \tag{5}$$

where $A_i^2/2$ (the power of the echo reflected from the ith element of the target) represents the area of the

---

[8] The amplitude noise about the lobing rate of scanning and lobing radars is not included but may be computed from information in Meade, *et al.*, *op. cit.*

ith element of the target, and θ_i is the angular position of the ith element assuming

$$\sum_{i=1}^{n} A_i \theta_i = 0.$$

By recalling that the effects of amplitude noise are independent of range and that angle noise is inversely proportional to range since it is a function of target span in angle and noting that any servo lag, servonoise, or receiver noise will prevent θ_0 from being zero, it may be seen that amplitude noise will be the predominant component of the target noise at medium and long ranges.

Considering the importance of target reflectivity distribution and angular velocity in determining the relative magnitudes of the angle and amplitude noise, the required AGC bandwidth in a radar is determined by target stability, target reflectivity distribution, atmospheric turbulence, and target range in which the radar will have to operate. Considering also that these factors determine the characteristics necessary for an optimum AGC, and variations in these factors with locale and time can be very large, it appears that it would be impossible to discover values for the AGC characteristics which would be optimum at all times and in all places. However, although a fast AGC is recommended for usual tracking conditions, it should be possible to determine these characteristics with sufficient accuracy to make a wise choice, in particular cases, with the material presented here and a knowledge of the local factors.

Suggestions have been made[7] that nonlinear AGC techniques may be useful in reducing angle noise. The use of nonlinear techniques may provide some improvement in radar tracking performance under certain conditions; however, one must always bear in mind that any operation other than fast linear AGC will allow amplitude fluctuations in the IF output. Therefore, any reduction in angle noise by these techniques will always be accompanied by amplitude-noise contributions to tracking noise.

CONCLUSION

It has been shown theoretically and experimentally, consistent with previous work on this subject, that angle noise or angle scintillation caused by a target is reduced by increasing the time constant of the AGC system. However, this reduction in angle noise by use of slow AGC characteristics is accompanied by a new component of noise caused by the nongain-controlled echo-amplitude fluctuations which modulate any true tracking error signals. This noise component is proportional to any true tracking error and of magnitude such that a tracking lag of only half a target span will cause the tracking noise with slow AGC to increase to the value with fast AGC and to continue a rapid increase with greater tracking lags. Internal noises would further degrade radar performance with slow AGC.

It is concluded that over-all radar tracking performance will be better with the use of a fast AGC or an AGC with a short time constant which removes essentially all tracking noise caused by amplitude noise from the target. Any deviation from fast, linear AGC operation will allow fluctuations in the IF amplifier output which contribute to tracking noise. Consequently, an attempt to reduce angle noise by limiting the AGC such as by narrow-banding or use of nonlinear characteristics, will allow low-frequency amplitude noise to contribute to target noise, and this added noise must be taken into consideration.

Furthermore, the tracking radar servo bandwidth should be the minimum value that is consistent with tactical requirements. Widening the servo bandwidth will only increase the radar's ability to follow internal and external noise and can seriously degrade radar performance.

High-Frequency Breakdown in Air at High Altitudes*

A. D. MacDONALD†

Summary—The problem of microwave breakdown near antennas at high altitudes is considered in order to find limitations on transmission conditions. The fundamental processes are described briefly. The cw breakdown electric fields for frequencies of 100 mc, 3 kmc, 10 kmc, 20 kmc, and 35 kmc are computed on the basis of the available data on atmospheric composition. The maximum peak electric fields and powers for which pulses are almost completely transmitted are also computed for the same frequencies and for several pulse lengths. It is shown that considerably more power per unit area of aperture can be transmitted at the higher frequencies. The validity of the assumptions on which the calculations are based is considered.

INTRODUCTION

AIRBORNE radar systems may initiate electrical discharges in front of the antennas at high altitudes because, at ultra-high frequencies, the electric field required to break down air at low pressures is, in general, much less than that required at atmospheric pressure. The processes which determine UHF breakdown have been discovered and verified during the past decade. These have been applied to determining optimum transmission conditions for high flying radar.

THE ATMOSPHERE

We first consider the nature of the atmosphere from ground level to 500,000 feet. It is now generally agreed that the composition of the atmosphere is constant up to approximately 250,000 feet.[1] In this range, nitrogen and oxygen compose 99 per cent of the total gases and their relative amounts do not change. Earlier measurements which seemed to show a decrease in oxygen content with increasing height have been shown to be in error.[2] Between 200,000 and 300,000 feet there is a slight increase in the percentage of noble gases present.[3] The total amount of these gases is, however, negligible in so far as it affects the electrical breakdown. Between 250,000 and 450,000 feet, the oxygen present undergoes a gradual transition from molecular O_2 to dissociated O. The excitation and ionization potentials in the dissociated atoms will be slightly higher than those of the molecular state, and so any change in breakdown strength caused by this factor will be in the direction of increasing fields. The amount of this change is not known but is not expected to be large.

There are three minor constituents which should be mentioned. Solar ultraviolet radiation produces ozone which is present in the region of space between about 70,000 and 200,000 feet. The maximum concentration of ozone is about six parts per million at 130,000 feet. It is considered that this ozone will not significantly alter the breakdown fields even though similar concentrations of some impurities in gases can make radical changes in breakdown conditions.[4] The excitation and ionization levels of nitrogen and oxygen are low enough so that the ozone will probably have no noticeable effect. There is evidence from spectroscopic studies of night sky emission that some sodium is present in the upper atmosphere.[1] There is not a great deal known about the concentrations present, and in the absence of data we shall assume that there is not sufficient sodium to affect breakdown fields. Water vapor is present in considerable amounts at levels below 30,000 feet. Above this altitude, the water vapor content is too small to be readily measurable. The principal effect of the water vapor is probably to increase the attachment rate and, therefore, to raise the threshold fields. The properties of water vapor in UHF fields are not known, but would only affect the calculations for altitudes well below 30,000 feet. For the purposes of this report, therefore, we will consider that the composition of the air does not change from ground level up to an altitude of 500,000 feet.

The pressure and temperature variations at higher altitudes are not known accurately. However, the results of data obtained with V-2 rockets during the past several years have given us considerable information, and the pressures shown in Fig. 1 are accurate to 10 per cent for altitudes up to 200,000 feet and to 20 per cent above 200,000 feet. These limits of error correspond to altitude variations of 5000 and 10,000 feet, respectively. The parameter which is of prime importance in gas discharge phenomena is not pressure but gas density, which is determined by both pressure and temperature. The temperature variations are taken into account in the calculation of the curve in Fig. 1, and the pressures plotted there are proportional to gas densities. (1 mm of Hg means 3.5×10^{16} molecules per cubic centimeter.)

CW BREAKDOWN

A gas subjected to high-frequency electric fields will break down and become conducting when the number of electrons produced per second becomes equal to or greater than the number lost per second. Electrons are produced in a high-frequency gas discharge by ionization

[1] S. K. Mitra, "Compendium of Meteorology," American Meteorological Society, Boston, Mass., p. 252; 1951.
[2] F. A. Paneth, "Rocket Exploration of the Upper Atmosphere," Pergamon Press, London, Eng., p. 157; 1954.
[3] P. Reasbach and B. S. Wiborg, "Rocket Exploration of the Upper Atmosphere," Pergamon Press, London, Eng., p. 158; 1954.
[4] A. D. MacDonald and J. H. Matthews, "High frequency ionization coefficients in neon-argon mixtures," *Phys. Rev.*, vol. 98, pp 1070–1073; May, 1955.

within the body of the gas. Electrons are lost by means of diffusion and attachment. Diffusion loss is determined by the geometry of the container and may be specified quantitatively in terms of the characteristic diffusion length Λ. Λ is directly related to the dimensions of the vessel containing the discharge. For example, the characteristic diffusion length for a region bounded by parallel plates of radius large compared to the separation d, is d/π. The rate at which electrons disappear from a discharge in such a region increases as the plates come closer together, so that decreasing Λ means increasing diffusion of electrons. Attachment depends on electron-molecule collisions and is, therefore, more important at higher pressures. The frequency of attachment ν_a is directly proportional to pressure for a given electron energy. Recombination has been reported as a significant electron removal mechanism in air. The recombination rate depends on the product of the electron and the ion densities and is important when the electron concentration is very high, but is very much less important than attachment in determining breakdown.

The equation which describes breakdown is

$$\nu_i - \nu_a = D/\Lambda^2, \tag{1}$$

where ν_i is the ionization rate, ν_a is the attachment rate, and D is the diffusion coefficient. In the absence of diffusion loss, *i.e.*, very large Λ, breakdown is determined by attachment. In order to simplify the analysis we will express attachment loss in terms of an "attachment length" Λ_a, so that

$$\nu_a = D/\Lambda_a^2, \tag{2}$$

and we can describe the breakdown process in terms of an effective diffusion length Λ_e, where Λ_e is defined by

$$\nu_i = D/\Lambda_e^2 = D\left(\frac{1}{\Lambda^2} + \frac{1}{\Lambda_a^2}\right). \tag{3}$$

We need now to determine Λ_a. The frequency of attachment ν_a is approximately equal to $4 \times 10^{-6}\nu_c$, where ν_c is the collision frequency.[5] The diffusion coefficient is the average value of $l^2\nu_c/3$, where l is the electron mean free path. The mean free path for electrons in air is not independent of energy, but it may be approximated by setting $l = 1/35p$, where p is the pressure in *mm* of mercury and l is in cm. Combining these we have

$$\Lambda_a = 12/p. \tag{4}$$

This value may be checked by means of the breakdown measurements of Gould and Roberts.[6] That point in their breakdown curves above which increase in diffusion length does not alter breakdown field, gives a value for Λ_a, in agreement with the above.

One can now find the CW breakdown fields for differ-

ent pressures (or altitudes) for a given frequency by using the effective diffusion length of (1) with the data of Gould and Roberts.[6] Breakdown fields are presented in Fig. 2 for frequencies of 3, 10, 20 and 35 kmc. The solid lines are calculated assuming no diffusion loss, *i.e.*, very large Λ. The dashed curves show the calculated fields assuming that the greatest value of Λ is equal to $\lambda/2$, where λ is the free space wavelength of the electric field. Similar CW breakdown data for 100 mc are shown in Fig. 8.

Pulsed Transmission

The CW breakdown fields are so low—particularly for the lower frequencies—that the transmission of pulses in which there is some increase in electron concentration will now be considered.

There may be appreciable signal transmitted through some concentrations of electrons, and so breakdown may be tolerated, provided the electron density produced in front of the antenna is not too great. The electron concentration above which there is practically no transmission is the "plasma resonant density," n_p, which is equal to $10^{13}/\lambda^2$ electrons per cubic centimeter if λ is in cm. When the concentration is $n_p/2$, signal absorption and reflection are negligible, and when the concentration is $2n_p$, no signal gets through: therefore, n_p may be considered a sharp upper limit for transmission.

Consider now a pulse in which the electric field is larger than that required for breakdown. The electron concentration will start to increase at the rate $e^{\nu t}$, where $\nu = \nu_i - \nu_a$, and will continue to increase until the pulse is turned off. If the concentration at the end of the pulse just reaches n_p, practically the entire pulse will be transmitted. In order to find the electric field for which this will happen, we set $n_p = n_0 e^{\nu\tau}$, where n_0 is the initial electron concentration and τ is the pulse length. We shall assume that vehicle speeds are greater than a thousand feet per second and that the interval between pulses is at least one millisecond. This will mean that successive pulses are separated in space by at least one foot, and so we will not need to consider any electrons left over from a previous pulse. If speeds were so slow, or repetition rates so fast that discharges were not separated in space, the electron concentration left over from one pulse would provide the initial concentration for the next. However, we consider only those cases where the initial concentration is that existing in space, and if there is no electron in the space occupied by the electric field, no breakdown can take place. Except in the ionosphere the concentration is probably less than 10^3/cc., and we will use this value for n_0. In some regions of the ionosphere above 300,000 feet the concentration may be as high as 2×10^5/cc; however, because of the exponential variation with time, the number of electrons increases much more rapidly toward the end of the pulse, the time required to reach n_p is not very different in the two cases, and the maximum electric fields calculated are not significantly affected.

[5] L. B. Loeb, "Basic Processes of Gaseous Electronics," University of California Press, p. 430; 1955.
[6] L. Gould and L. W. Roberts, "Breakdown of air at microwave frequencies," *J. Appl. Phys.*, vol. 27, pp. 1162–1170; October, 1956.
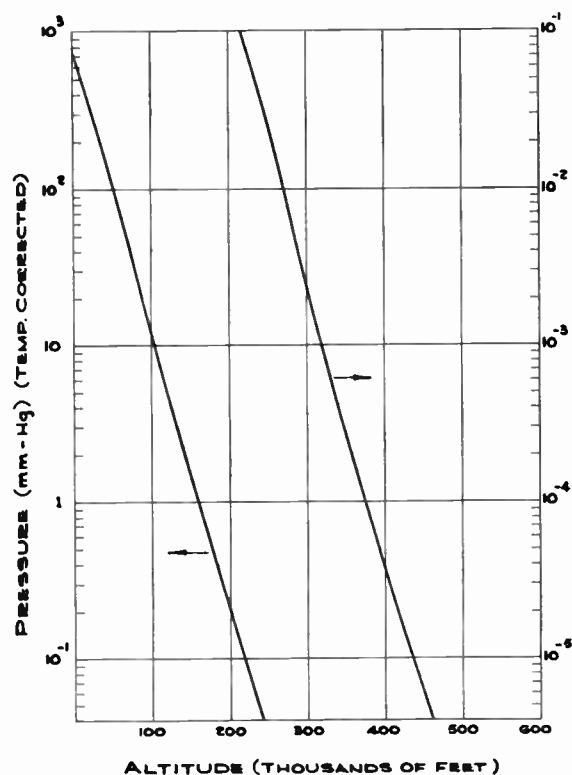
Fig. 1—Pressure in millimeters of mercury as a function of altitude—corrected for temperature variations.

Fig. 3—Product of ionization rate and wavelength as a function of $p\lambda$ for various $E\lambda$, computed from experimental data of Herlin and Brown.

Fig. 2—CW breakdown threshold electric field in volts/cm as a function of altitude. Solid line, Λ very large; dashed line, $\Lambda = \lambda/2$.
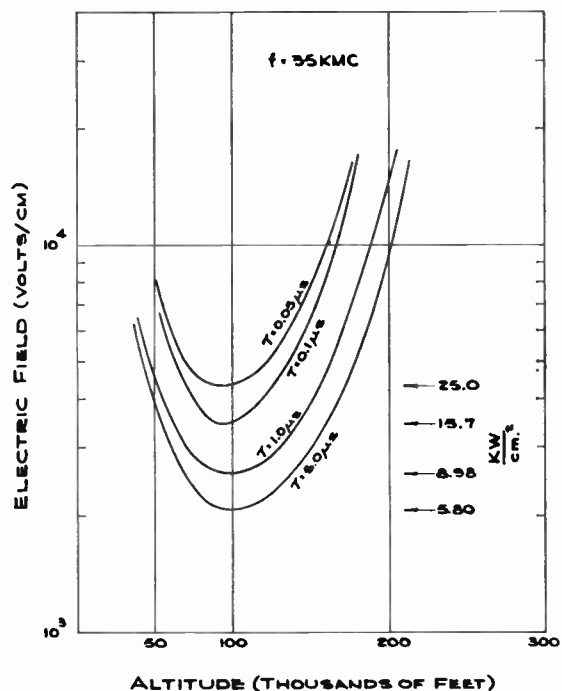
Fig. 4—Peak electric field (*i.e.*, rms value of field while power is on) for which over 90 per cent of pulse is transmitted at 35 kmc, for several pulse lengths.

We now need to know ν as a function of pressure, electric field, and wavelength in order to find the required maximum fields. ν has been measured by Herlin and Brown,[7] who have presented their results in terms of the high frequency ionization coefficient ζ (equal to

[7] M. A. Herlin and S. C. Brown, "Breakdown of a gas at microwave frequencies," *Phys. Rev.*, vol. 74, pp. 291–296, August, 1948.
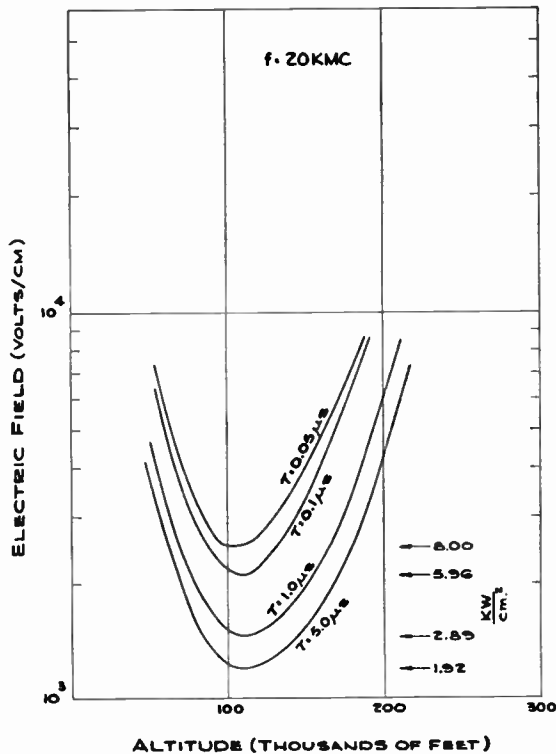
Fig. 5—Peak field for which over 90 per cent of pulse is transmitted at 20 kmc, for several pulse lengths.
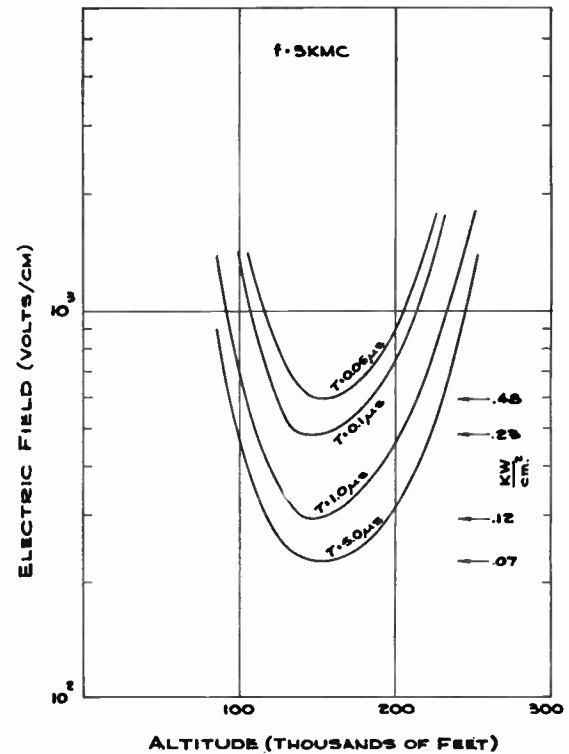
Fig. 7—Peak field for which over 90 per cent of pulse is transmitted at 3 kmc, for several pulse lengths.
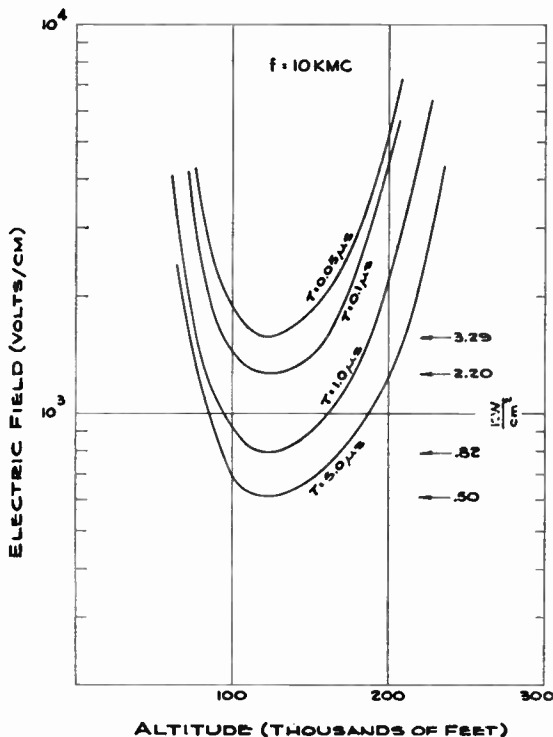
Fig. 6—Peak field for which over 90 per cent of pulse is transmitted at 10 kmc, for several pulse lengths.

Fig. 8—Lower curve—CW breakdown fields at 100 mc. Upper curve —peak field for which 90 per cent of pulse is transmitted at 100 mc, for pulse lengths of 1 and 5 microseconds.

ν/DE^2), as a function of $p\lambda$ and E/p. In order that we may extract from their work values of ν, we must compute the diffusion coefficient D. Details of this calculation are given in Appendix I, where it is shown that

$$Dp = 3.2 \times 10^5 \bar{u}, \qquad (5)$$

where $\bar{u}$ is the average electron energy. From the data of Healey and Reed,[8] we find that $\bar{u}$ is approximately equal

[8] R. H. Healey and J. W. Reed, "The Behaviour of Slow Electrons in Gases," Amalgamated Wireless Ltd., Sydney, Australia, p. 79; 1941.

to 0.036 E_e/p, where E_e, the effective electric field is defined by the relation

$$E_e^2 = E^2 \Big/ \left(1 + \frac{\omega^2}{\nu_c^2}\right), \qquad (6)$$

and E is the rms value of the electric field. The collision frequency for electrons in air, ν_c, is not independent of energy but a good approximation is made by setting it equal to $5.3 \times 10^9 p$. The expression for the effective electric field becomes

$$E_e = E/[1 + (36/p\lambda)^2]^{1/2}. \qquad (7)$$

A useful form in which to express ν is to find $\nu\lambda$ by multiplying the measured values of ν/DE^2 by $(E/p)^2 p\lambda Dp$. This method of using the data of Herlin and Brown was first used by D. J. Rose,[9] and enables one to simplify the calculations of maximum fields. A graph of $\nu\lambda$ as a function of $p\lambda$ for various values of $E\lambda$ is shown in Fig. 3. From this graph we calculate the electric field which results in the production of "plasma resonant density" at the end of a given pulse. The results are shown in Figs. 4–8. These give maximum electric fields as functions of altitude for frequencies 35, 20, 10, and 3 kmc and 100 mc, and for pulse lengths of 0.05, 0.1, 1.0, and 5.0 microseconds. These figures also show the power radiated from a linear array in kilowatts per cm² at an altitude corresponding to the minimum of each curve of Figs. 4–7. At these maximum fields and powers it is believed that 90 per cent of the signal will be transmitted. The details of the power calculations are given in Appendix II and a sample calculation is given in Appendix III.

CONCLUSIONS

The calculations show that the higher frequencies allow the transmission of more power than do the lower frequencies. The calculations are based on the best available data, but in several cases extrapolation of existing data was required. This was true in the calculation of ν for the pulsed breakdown. The dashed parts of the curves in Fig. 3, for example, were extrapolated from the experimental data. However, the calculations are considered to be fairly accurate, although perhaps conservative in the sense that the fields are lower limits. The phenomena which were neglected would all tend to raise the field required for breakdown and the field required to reach plasma resonant density at the end of a pulse.

It should be pointed out that the calculations of power in Appendix II assume uniform or sinusoidally varying electric fields in front of the antenna. For some types of antennas, such as linear slotted arrays, there are very high fields close to the individual slots. Breakdown at such places could be prevented by plastic coating over the array.

Calculations of breakdown and of electron concentrations have been made on the basis of diffusion theory.

[9] D. J. Rose, Bell Telephone Labs., Private Communication.

When there are very high electric fields or very low pressures, diffusion theory may not be valid. The limits of variation of the experimental parameters for which the theory is valid, are discussed in Appendix IV, which includes direct application of general principles, derived earlier,[10] to the special case of breakdown in air. It may be seen from Fig. 9 that the limitations on diffusion theory do not affect the conclusions of this paper.

It has been found by Rose and Brown[11] that the breakdown field for pure air, *i.e.*, air which had not previously been electrically sparked, is a few per cent higher than the figures of Herlin and Brown.[7] If this new data were used in the calculation of ν, the breakdown levels of Figs. 2 and 4–8 would be very slightly raised.

APPENDIX I

The diffusion coefficient D is equal to the average of $lv/3$, or

$$D = \int_0^\infty f\left(\frac{lv}{3}\right) 4\pi v^2 dv \Big/ \int_0^\infty f 4\pi v^2 dv, \qquad (8)$$

where v is the electron velocity, and f is the electron velocity distribution function. This function is not accurately known for air under the required conditions, but it will not be enough different from Maxwellian to make a difference of more than 5 or 10 per cent in the diffusion coefficient. The Maxwellian distribution function is $e^{-u/\bar{u}}$, where $u = mv^2/2e$ and $\bar{u}$ is the average electron energy in volts. ν_c is approximately a constant and $l = v/\nu_c$. The first integral above may then be written

$$\frac{8\pi}{3\nu_c} \sqrt{2} \left(\frac{e}{m}\right)^{5/2} \int_0^\infty u^{3/2} e^{-u/\bar{u}} du, \qquad (9)$$

and the second,

$$4\pi \sqrt{2} \left(\frac{e}{m}\right)^{3/2} \int_0^\infty u^{1/2} e^{-u/\bar{u}} du. \qquad (10)$$

Both of these may be readily evaluated in terms of gamma functions. The ratio defining D then becomes

$$D = e\bar{u}/m\nu_c = 3.38 \times 10^5 \bar{u}/p. \qquad (11)$$

The use of a Druyvesteyn distribution instead of a Maxwellian gives a value of approximately 3 instead of 3.38, and the correct value probably lies between the two values. We therefore set

$$Dp = 3.2 \times 10^5 \bar{u}. \qquad (12)$$

APPENDIX II

The power radiated by an antenna may be written, using Poynting's theorem, as

[10] S. C. Brown and A. D. MacDonald, "Limits for the diffusion theory of high frequency gas discharge breakdown," *Phys. Rev.*, vol. 76, pp. 1629–1633; December, 1949.

[11] D. J. Rose and S. C. Brown, "Microwave gas discharge breakdown in air, nitrogen and oxygen," *J. Appl. Phys.*, vol. 28, pp. 561–563; May, 1957.
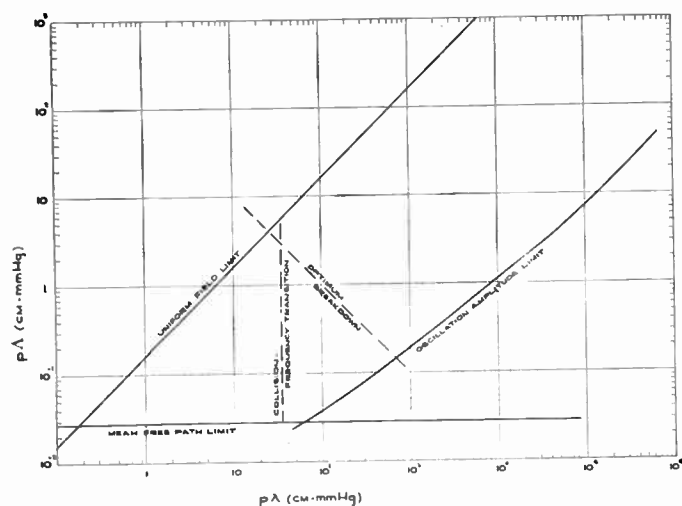
Fig. 9—Limits of applicability of diffusion
theory to breakdown in air.

$$P = \epsilon_0 c \int E^2 dA, \qquad (13)$$

where P is the power, ϵ_0 is the permittivity of free space, c is the velocity of light, and the integration is carried out over the area of the antenna. For a directional antenna such as a linear array, the field would be uniform in one direction and sinusoidal in the other. A factor of $\frac{1}{2}$ is introduced by integration of the sine term and we have

$$P = 1.33 \times 10^{-3} E_{\mathrm{rms}}^2 A, \qquad (14)$$

where $E\sqrt{A}$ has the units of volts. We have finally, if the power is in kilowatts, the area in cm², and the field in kilovolts/cm,

$$(P/A)^{1/2} = 1.15E \quad \text{Linear array} \qquad (15)$$

$$(P/A)^{1/2} = 0.82E \quad \text{Omnidirectional.} \qquad (16)$$

Appendix III

Consider the problem of finding the maximum power usable at 20 kmc with a directional antenna having an area of 20 cm². A linear array $\frac{1}{2}\lambda$ in width would then be approximately 25λ long and have a narrow beam.

If we wish to transmit CW we find from Fig. 2 that the threshold electric field is 750 volts per cm. From the power-field equation of Appendix II we find that the corresponding power is 0.86 kw/cm². Therefore the power which may be transmitted is 17 kw.

If pulsed transmission is to be used, we find from the minima of the curves in Fig. 5 that 3.4 kw/cm² may be transmitted in 1-microsecond pulses, and 11 kw/cm² in pulses of 0.05-microsecond duration. This means that for the whole range of altitudes, 68-kilowatts peak power may be transmitted in 1-microsecond pulses and 220-kilowatts peak power in 0.05-microsecond pulses.

The curves may also be used to find the altitudes at which good transmission is not likely for a given power level. For example, if 160-kw peak power in 1-microsecond pulses is to be used, we find by drawing a line across Fig. 5 at the 8 kw/cm² level, that good transmission is not to be expected at altitudes between 70,000 feet and 165,000 feet.

Appendix IV

The calculations in this paper are based on the application of diffusion theory to high frequency gas discharges. There are limits to the variation of experimental parameters beyond which diffusion theory is not valid. This problem has been discussed in detail elsewhere,[10] and we shall consider here only direct application of the equations derived by Brown and MacDonald to breakdown in air. A convenient way of illustrating the limits is shown in Fig. 9. The variables are $p\lambda$ and $p\Lambda$. The reason for this choice of variables becomes clear when we realize that because pressure is inversely proportional to mean free path, the variables represent the ratios of wavelength to mean free path and container size to mean free path, respectively. We shall consider briefly each of the limits as labelled in Fig. 9.

Mean Free Path Limit

The concept of an average free path and thus of diffusion theory, breaks down when the pressure becomes so low that electrons move a distance comparable with container dimensions between collisions.

Oscillation Amplitude Limit

Electrons oscillate in the applied field and when the amplitude of oscillation becomes comparable with the dimensions of the container, electrons may be swept out of the discharge during a cycle of the electric field. For the problems considered in this paper, we may replace the container dimensions by the region in which the field of the antenna is appreciable.

Uniform Field Limit

At high frequencies there is a limit to the size of a container consistent with the assumption of a uniform field. This is a limit on our theory rather than a point at which physical processes change. Although it is important in the study of discharges in resonant cavities, we need not consider it in the problems of this paper.

The dotted lines are not limits in the sense that the solid lines are, but simply designate transitions between regions in which different physical processes predominate.

Calculations for the different cases considered here show that the limits of the theory are reached only in a few cases, and then only at such high altitudes that the curves are far from their minima and of little interest.

Correspondence

Low-Loss L-band Circulator*

A four-port circulator, having low insertion loss, has been developed at L-band for use in circulator-maser low-noise receiving systems[1] and other applications. Insertion loss averages 0.3 db over an 18-per cent band (1200 to 1450 mc) when the magnetic field is optimized for each frequency.[2] Fig. 1 shows the performance of the circulator at the optimum magnetic field for each frequency. The notation L_{xy} used in the graphs denotes the power output measured at circulator port y relative to the power input at port x, with all ports terminated in matched loads. Reverse isolation is seen to be ≥ 30 db, and input VSWR is seen to be ≤ 1.11. The insertion-loss measurement is believed to have an accuracy of better than ± 0.1 db. This measurement was made with padded bolometers that were calibrated against a precision IF attenuator.
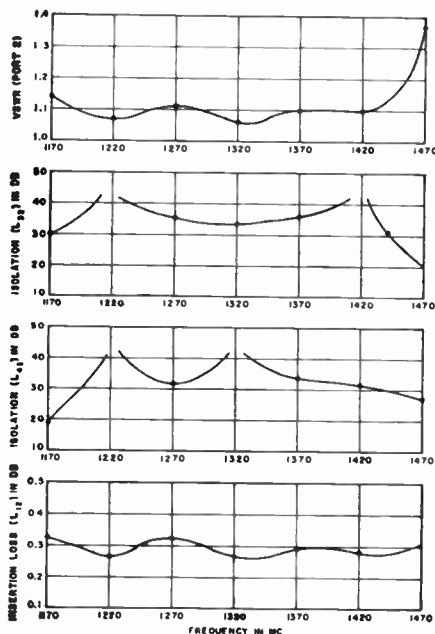
Fig. 1—Performance of L-band circulator Model 5208-L at optimum magnetic field for each frequency.

The ferrite, a magnesium manganese aluminate having a narrow resonance linewidth, is operated at a magnetic field above ferromagnetic resonance. An electromagnet is provided to permit magnetic-field adjustment. The circulator is constructed in waveguide that has been substantially reduced in height in the ferrite region to reduce the magnetic-field requirements.
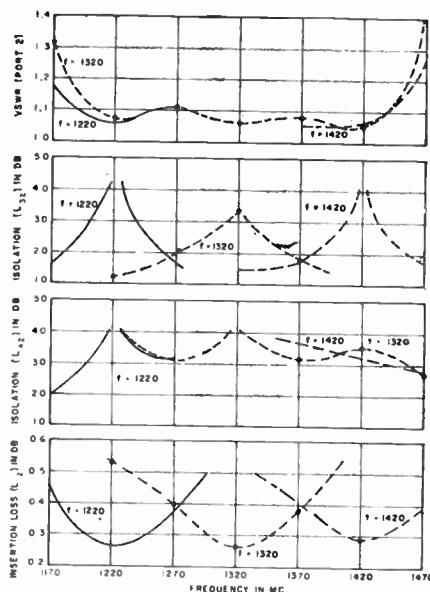
Fig. 2—Performance of L-band circulator Model 5208-L at constant magnetic field, optimized for 1220, 1320, and 1420 mc.

Fig. 2 shows the performance of the circulator at constant magnetic field optimized for frequencies of 1220, 1320, and 1420 mc. Bandwidth is seen to be about 75 mc for an Isolation $L_{32} \geq 20$ db, with the insertion loss remaining below 0.4 db.

Work on an improved model is in progress.

F. R. ARAMS
G. KRAYER
Airborne Instruments Lab.
Div. of Cutler-Hammer, Inc.
Mineola, L. I., N. Y.

Step-Response of RLC Filters*

The mathematical treatment of the response of a simple RLC circuit to a step change of the amplitude, phase, and/or frequency of a sinusoidal input suggests a simple graphical method of expressing the response. The justification of the method described can be found implicitly in treatments by Hatton,[1] Gumowski,[2] and Linden,[3] and the pictorial treatment is based on Guillemin.[4] The explicit development has been carried out by the author.[5]

The approximate steady-state response of a simple, high-Q, RLC circuit to a sinusoidal input can be illustrated in terms of a phase-amplitude locus (Nyquist diagram) which is a circle of radius equal to half the amplitude of the driving function and split evenly by a line OP drawn from the origin at an angle corresponding to the instantaneous phase $(\omega t_0 + \phi)$ of the driving function given by $A \cos(\omega t + \phi)$. The circle will pass through the origin (see Fig. 1). The line drawn tangent to the circle and perpendicular to the diameter OP is used for locating the frequency; here the center frequency ω_0 is the natural-resonance frequency of the RLC circuit, while β is its bandwidth. The half-power frequencies are illustrated, and the corresponding steady-state response to that or any frequency is determined, by the phasor (such as OR) along the line connecting the origin and the linear frequency scale drawn to the phase-amplitude circle. Its phase with respect to the driving function is, of course, the angle between the phasor so located and the line OP. The latter line is shown at the relative instantaneous phase of the driving function of time t_0, the "switching time."

Fig. 1.

Fig. 2 illustrates a typical case of a combined step in phase, frequency, and amplitude from driving function $f_1 = A_1 \cos(\omega_1 t + \phi_1)$ to $f_2 = A_2 \cos(\omega_2 t + \phi_2)$. It is assumed that at time t_0, the response to f_1 has reached steady-state; that at t_0, f_2 is applied in place of f_1; and that at some later time the response will have settled to the steady-state response to f_2.

In Fig. 2, enough of the diagram shown in Fig. 1 is reproduced for each function f_1 and f_2 to determine their respective steady-state responses. The angle between the lines OP_1 and OP_2 is the instantaneous phase difference $(\omega_1 t_0 + \phi_1) - (\omega_2 t_0 + \phi_2)$. The phasor SR is the phasor-difference which must be dissipated as a transient when the response of the RLC circuit changes from the steady-state response to f_1, i.e., OR, to that for f_2, OS. Furthermore, phasor SR represents a component in the output function at the

natural frequency ω_0. Thus, as it decays exponentially in magnitude, it will change in phase relative to the sinusoid f_2. This amplitude decay and phase shift can be expressed simply as the action of the operator $e^{-(1+jx)t'}$, where t' is measured in time constants $2/\beta$ and x is the ratio $2(\omega_2-\omega_0)/\beta$. The amplitude and phase-shift of the output transient is then expressed as the sum of the phasor representing the steady-state response to f_2 and the decaying transient phasor. This sum is illustrated by the dotted line locus in Fig. 2 on which several integral time constants after t_0 are indicated.

Fig. 2.

Perhaps the greatest usefulness of this method of expressing transient behavior lies in the ease with which one can perceive that the transient effect is primarily analogous to the simple exponential decay of an RL or RC circuit; but because of the phase shift between driving function and transient decay, the detailed response may appear more complex than the simple form. How the initial conditions at time t_0 and the relative frequency deviation from resonance affect the amplitude of the transient is readily evident from a sketch such as Fig. 2. Through observation of the rate of change of phase shift as a function of time, the instantaneous frequency of the transient can also be deduced.

B. L. BASORE
The Dikewood Corp.
Albuquerque, N. M.

VOR-Compatible Doppler Omnirange, Design Considerations*

In an earlier paper on the Doppler-effect omnirange,[1] the author mentioned a high-

precision quasi-Doppler omnirange fully compatible with existing VHF omnirange (VOR) airborne equipment. Reference was made also to another brief note.[2] Some of the considerations governing the design of the VOR-compatible Doppler omnirange are presented here because of the current interest in such equipment.

BASIC SYSTEM

In a quasi-Doppler omnirange the revolving antenna of a simple Doppler system is simulated by commutating a circularly-disposed array of fixed antenna elements. This is illustrated in Fig. 2 of the author's earlier paper.[1] The signal radiated from the commutated antenna system carries direction-dependent frequency modulation information. VOR compatibility is achieved by transmitting a second carrier from an independent fixed antenna. This carrier differs in frequency by 9.96 kc from the carrier supplied to the commutated antenna and is amplitude-modulated with a reference signal synchronized to the antenna commutation. In the airborne receiver the reference signal is detected directly and the two carriers beat together to produce a subcarrier which is frequency modulated by the bearing information. This subcarrier is demodulated by the normal subcarrier discriminator in the VOR receiver to recover a signal whose phase, relative to the reference signal, is equal to the bearing.

In the VOR-compatible Doppler omnirange, the data and reference signals are interchanged with respect to their roles in the standard VOR. This is of no practical consequence since the bearing intelligence is contained only in the relative phase of the two signals.

VOR CHARACTERISTICS

The essential characteristics of the present VOR are:

1) Carrier frequency range: 108 to 118 mc.

2) Direction-dependent data: 30 per cent amplitude modulation at a 30-cps rate.

3) Reference data: 9.96-kc subcarrier frequency modulated at a 30-cps rate with a maximum deviation of 480 cps. This subcarrier is 30 per cent amplitude modulated on the transmitted carrier.

COMPATIBILITY REQUIREMENTS

The Doppler omnirange signal will be compatible with existing airborne equipment if it produces the following two signals at the airborne receiver output:

1) A 30-cps fixed-phase reference signal.

2) A 9.96-kc subcarrier signal frequency modulated at a 30-cps rate, with a maximum deviation of 480 cps and with the envelope phase of the frequency modulation equal to the bearing.

Eq. (4) of the earlier paper[1] was derived from fundamental considerations for a simple revolving antenna Doppler system and expresses the maximum deviation ΔF:

$$\Delta F = \frac{f_c \omega_r R}{C} \quad (1)$$

where f_c = the carrier frequency in cps, $\omega_r = 2\pi S$ (S is the scanning rate in revolutions per second), R = the radius of the circle, and C = the velocity of light.

Eq. (1) may be rewritten as:

$$\Delta F = \pi D S \quad (2)$$

where D is the aperture or diameter of the antenna circle expressed in wavelengths.

Applying (2) to the VOR parameters we have:

$$\Delta F = 480 = 30\pi D \quad (3)$$

and

$$D = \frac{480}{30\pi} = 5.1 \text{ wavelengths.} \quad (4)$$

The basic design rule for a VOR-compatible Doppler effect omnirange is therefore that the aperture should be close to 5.1λ. A practical fixed value of antenna aperture for the 108 to 118-mc carrier frequency range of the VOR is 43 feet. With an aperture of this magnitude the bearing errors and course perturbations, commonly referred to by such terms as "site error," "multipath error," and "course scalloping," are negligibly small, relative to the instrumental error of the highest grade of airborne equipment.

NUMBER OF ANTENNA ELEMENTS REQUIRED IN A QUASI-DOPPLER ARRAY

An antenna aperture close to 5.1λ is prescribed by the requirement for VOR compatibility. The antenna elements of the quasi-Doppler array are uniformly spaced around a circle having a diameter of 5.1λ and a circumference of 16λ. The number of antenna elements required to produce an acceptable simulation of the revolving antenna of a simple Doppler system is determined by the maximum permissible phase step between elements.

Excellent simulation of a revolving antenna is obtained in a quasi-Doppler system employing sinusoidally-blended commutation with a maximum adjacent-element phase step of 120° or a spacing between elements of $\lambda/3$. When many elements are used, the chord is approximately equal to the arc, so for a 120° maximum phase step the minimum number of elements, N, is given by

$$N = 16\lambda \bigg/ \frac{\lambda}{3} = 48. \quad (5)$$

This is a structurally reasonable number of elements. Moreover, a system with 48 elements possesses an enormous redundancy and is therefore noncritical to instrument.

CONCLUSION

1) The aperture of a VOR-compatible Doppler omnirange should be close to 5.1λ.

2) Commutation of 48 antenna elements in a quasi-Doppler array of 5.1λ aperture will closely simulate a revolving-element Doppler antenna.

3) The aperture of 5.1λ required to pro-

duce compatibility is well above the minimum aperture required to reduce site and multipath error to negligible values.

4) A quasi-Doppler system with 48 elements is noncritical to construct and adjust and exhibits extremely small instrumental errors.

Paul G. Hansel
Servo Corp. of America
New Hyde Park, N. Y.
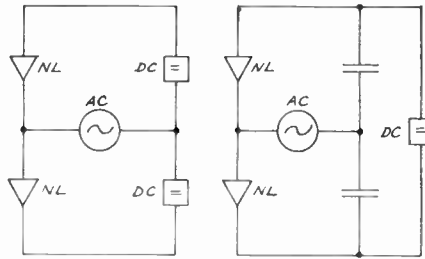
Figs. 113 & 114—Principle of voltage-doubling rectifier, single-ended push-pull amplifier, etc., adapted from Barkhausen.

Fig. 1—Basic bridge amplifier for analysis.

Full Bridge Amplifiers*

The late Prof. Barkhausen always encouraged his students to look at circuits in the most general terms so that they would be prepared to solve problems differing from the special cases considered in lectures. Thus they were never allowed to forget that the one thing essential to all conversion of one frequency to another, or to dc or vice versa, is some kind of nonlinear element, and everything else is just a matter of circuit details. In his text, which explains some parts of circuit theory better than any other known by the undersigned, there are basic diagrams, dating at least from 1931, which cover simultaneously the principal single-phase rectifier, amplifier and modulator-detector configurations used today.[1]

Of course great inventions often seem obvious after they are published, but it was foolish not to have seen in his Figs. 113 and 114 the voltage-doubling rectifier *and also* the single-ended push-pull amplifier with dc supplying the power, ac load, and the nonlinear elements NL excited by signal. Figs. 115–117 of course cover the full-wave center-tapped rectifier and the traditional center-tapped push-pull amplifier. Either type of push-pull amplifier is a semibridge, half the bridge of Fig. 118.

I have not seen the full four-element bridge of Fig. 118 used for amplifiers, but it has some advantages over either semibridge, especially with complementary transistors. For triode tubes or common-collector transistors, consider the four bridge arms in Fig. 1 to contain voltage sources $E_1 \cdots E_4$ and resistances $R_1 \cdots R_4$. In terms of these the load current i_L is:

Figs. 115 & 116—Principle of full-wave center-tapped rectifier, conventional center-tapped push-pull amplifier, etc., adapted from Barkhausen. Fig. 117, not reproduced shows usual arrangement with transformer.

Fig. 118—Principle of bridge rectifier, amplifier, modulator, etc., adapted from Barkhausen.

$$i_L = \frac{(E_1R_3 - E_3R_1)(R_2 + R_4) + (E_4R_2 - E_2R_1)(R_1 + R_3)}{(R_2 + R_4)R_1R_3 + (R_1 + R_3)R_2R_4 + R_L(R_1 + R_3)(R_2 + R_4)}. \quad (1)$$

If quadratic characteristics are assumed for the tubes or transistors,

$$dE_i = (b_i + 2c_ie_i)de_i, \text{ and } E_i = a_i + b_ie_i + c_ie_i^2$$

for each arm, where e_i is the voltage applied to the particular grid or base, a_i is the dc voltage across that arm with no signal, b_i is the useful amplification, and c_i is due to the curvature causing distortion. The numerator of (1) becomes:

$$[(a_1 + b_1e_1 + c_1e_1^2)R_3$$
$$- (a_3 + b_3e_3 + c_3e_3^2)R_1](R_2 + R_4)$$
$$+ [(a_4 + b_4e_4 + c_4e_4^2)R_2$$
$$- (a_2 + b_2e_2 + c_2e_2^2)R_4](R_1 + R_3). \quad (2)$$

This may be written:

$$[(a_1 + b_1e + c_1e^2)R_3$$
$$- [(a_3 + b_3e + c_3e^2)R_1](R_2 + R_4)$$
$$+ [a_4 + b_4e + c_4e^2)R_2$$
$$- (a_2 + b_2e + c_2e^2)R_4](R_1 + R_3) \quad (3)$$
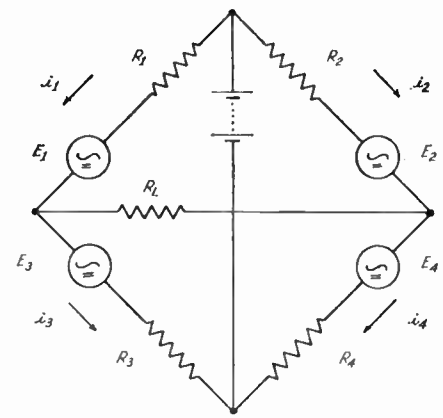
even if $e_1 \cdots e_4$ are different, because in that case the ratio of each to e is included in $b_1 \cdots b_4$ and $c_1 \cdots c_4$.

If, now, E_1 and E_4 have opposite polarity to E_2 and E_3, either by push-pull excitation or by using complementary transistors, that is equivalent to replacing e by $-e$ in arms 2 and 3, expression (3) becomes:

$$\{[(a_1R_3 - a_3R_1) + (b_1R_3 + b_3R_1)e$$
$$+ (c_1R_3 - c_3R_1)e^2](R_2 + R_4)\}$$
$$+ \{[(a_4R_2 - a_2R_4) + (b_4R_2 + b_2R_4)e$$
$$+ (c_4R_2 - c_2R_4)e^2](R_1 + R_3)\}. \quad (4)$$

The two parts of this expression apply to the two semibridge single-ended push-pull amplifiers of arms 1 and 3 and 2 and 4, respectively. Each of these can be balanced statically by making $a_1R_3 = a_3R_1$ and $a_2R_4 = a_4R_2$ (4.1), and dynamically by making $c_1R_3 = c_3R_1$ and $c_4R_2 = c_2R_4$ (4.2). This must be done for ordinary single-ended push-pull amplifiers. However, the balance requirements for the bridge are less exacting, as can be seen if expression (4) is rewritten:

$$\{[a_1R_3(R_2 + R_1) + a_4R_2(R_1 + R_3)]$$
$$- [a_3R_1(R_2 + R_4) + a_2R_4(R_1 + R_3)]\}$$
$$+ \{[b_1R_3(R_2 + R_4) + b_4R_2(R_1 + R_3)]$$
$$+ [b_3R_1(R_2 + R_4) + b_2R_4(R_1 + R_3)]\}e$$
$$+ \{[c_1R_3(R_2 + R_4) + c_4R_2(R_1 + R_3)]$$
$$- [c_3R_1(R_2 + R_4) + c_2R_4(R_1 + R_3)]\}e^2. \quad (5)$$

For zero dc in R_L with no signal (static balance).

$$a_1R_3(R_2 + R_4) + a_4R_2(R_1 + R_3)$$
$$= a_3R_1(R_2 + R_4) + a_2R_4(R_1 + R_3) \quad (6)$$

and for second harmonic cancellation with signal (dynamic balance),

$$c_1R_3(R_2 + R_4) + c_4R_2(R_1 + R_3)$$
$$c_3R_1(R_2 + R_4) + c_2R_4(R_1 + R_3). \quad (7)$$

If there is dynamic balance, there will also be no dc in R_L with signal, since rectification and harmonic generation with a quadratic characteristic result from the identities:

$$\sin^2 \theta = \tfrac{1}{2}(1 - \cos 2\theta) \text{ and } \cos^2 \theta = \tfrac{1}{2}(1 + \cos 2\theta).$$

[1] H. Barkhausen, "Elektronenrohren," Verlag S. Hirschel, Leipzig, Ger., vol. 1, pp. 170-171, vol. 4, p. 219; 1937.

If in Fig. 1 the bridge arms are pentode tubes or common-emitter or common-base transistors, R_L being low, (1) becomes:

$$i_L = \tfrac{1}{2}(i_1 - i_2 - i_3 + i_4). \qquad (8)$$

If in each arm $i_i = a + be + ce^2$ or $a + b_i + c_i^2$, depending on whether the elements are regarded as voltage or current-driven,

$$2i_L = (a_1 + a_4 - a_2 - a_3)$$
$$+ (b_1 + b_2 + b_3 + b_4)(e \text{ or } i)$$
$$+ (c_1 + c_4 - c_2 - c_3)(e^2 \text{ or } i^2), \qquad (9)$$

analogously to (4) and (5).

For static balance

$$a_1 + a_4 = a_2 + a_3. \qquad (10)$$

and for dynamic balance

$$c_1 + c_4 = c_2 + c_3. \qquad (11)$$

The consequence of these more flexible balance criteria, which correspond to ordinary bridge theory, is that any two *adjacent* tubes or transistors may differ greatly without causing even harmonic distortion, provided the other two differ in the same manner. This can be very helpful with complementary transistor power amplifiers, since it is difficult to match n-p-n and p-n-p transistors perfectly.[2] The full bridge has the additional advantage that it needs neither a tightly coupled centertapped transformer as does center-tapped push-pull, nor a center-tapped dc supply (or heavy bypass condensers to load) as does single-ended push-pull. Its output impedance, half that of center-tapped push-pull, but twice that of single-ended push-pull, matches some loads better and with Class B 2N68/2N95 suits a 15-ohm speaker with no transformer at all.

Fig. 2 shows a full bridge amplifier with complementary transistors in common collector connection, operated in Class B to make the oscillograms of Fig. 3. Common emitter or common base connections could of course also be used. The right and left sides are driven in push-pull, but if they are matched as to gain and input impedance the signal can be simply floated across without any centertap. The right and left sides can be tested with a dc voltmeter for meeting criteria (4.1) and (4.2),[2] independently as single-ended push-pull amplifiers, and adjusted by selection or circuit arrangements, if a center-tapped dummy load and by-pass condensers are provided temporarily as indicated. Greatest output is available when (4.1) and (4.2) are satisfied, because the transistors share the work equally; but at lower levels criteria (6) and (7) suffice. The oscillograms made with $V1$ and $V2$ very weak show this vividly. With this dissimilarity the output of single-ended push-pull amplifier looks like the voltage from A to ground in the center oscillogram. The voltage from B to ground looks the same with 180 degree phase shift, but the voltage *from A to B* in the top oscillogram is symmetrical. The voltage from load center C to ground

[2] A. W. Lo, R. O. Endres, J. Zowels, F. D. Waldhauer, and C. C. Cheng. "Transistor Electronics." Prentice-Hall Inc., New York, N. Y., p. 206; 1955.
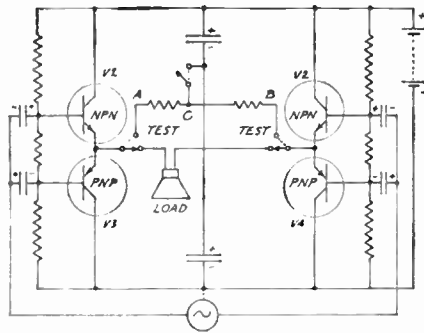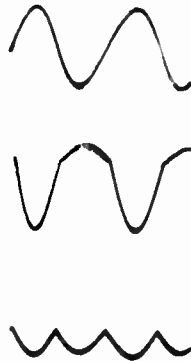
Fig. 2—Transistor bridge amplifier plus test circuits.

Fig. 3—Waveforms with $V1$ and $V2$ weak in Fig. 2 amplifier. Upper, from A to B across load. Center, from A to ground. Lower, from load center C to ground.

in the lower oscillogram is a series of half waves containing no fundamental if the right-left symmetry is perfect. Observing the voltage at C with a dc voltmeter and an oscilloscope is an easy way to test the amplifier. What is seen there indicates what is wrong, and with all four arms perfectly matched there is half the dc supply voltage and no ac voltage whatever at C.

A similar demonstration could be given with $V1$ and $V2$ weak, etc.

With but one kind of transistor or with tubes, the upper arms must be driven with respect to the load terminals if the right and left single-ended push-pull amplifiers are to balance independently. (4.1) and (4.2) or (10) and (11) would be then satisfied. Peterson and Sinclair[3] give ways of doing this. With the full bridge and any particular load impedance, however, all arms can be driven from ground if the upper arms, now cathode followers, receive more signal. This is inadvisable with loudspeaker load and any tubes but low-mu triodes, because the work is not shared equally at all frequencies. Nevertheless, in a test with Class B pentodes, varying the load resistance did not cause an asymmetric output wave as it certainly would in a semibridge thus driven.

I am using the bridge amplifier, with driver stages and a floating preamplifier, in a record player with good reproduction quality at outdoor power levels.

ALBERT H. TAYLOR
Read Island, B. C.
Canada

[3] A. Peterson and D. B. Sinclair, "A single-ended push-pull audio amplifier," PROC. IRE, vol. 40, pp. 7–11; January, 1952.

On Root Locus with Complex Coefficient Polynomials*

The denominator polynomial of a closed loop system function is generally characterized as having real coefficients. This property enables one to rapidly study the stability of the system using the standard root locus techniques. However, in many systems the closed loop function does not possess this property. That is, the transfer function, or more generally, the terminal equations[1,2] of certain components contain complex coefficients. The detailed study of the properties of an ac servomotor[3] is an example of this fact. When such a component is used in a system, the denominator polynomial of the closed loop system function generally has complex coefficients. This requires additional considerations for stability studies.

In the following, the root locus of a second degree polynomial with complex coefficients is studied and the necessary and sufficient conditions for stability are obtained.

Consider a positional system consisting of a two-phase servomotor, the center-tapped phase connected directly to the output of a push-pull amplifier. The amplifier is excited from the error signal of a control transformer. For this system, the closed loop function was found to be of the following form:

$$\frac{\theta_{\text{out}}(s)}{\theta_{\text{in}}(s)} = \frac{K}{\alpha S^2 + \beta S + K}$$

where $\alpha = \alpha_1 + j\alpha_2$, $\beta = \beta_1 + j\beta_2$ are nonzero complex constants, K is a real parameter, and $S = \sigma + j\lambda$ is a complex variable. The above form is frequently encountered in electromechanical system studies.

For stability considerations, one is interested in the roots of the following equation:

$$\alpha S^2 + \beta S + K = 0 \qquad (1)$$

The roots of (1) are the same as the points of intersection of the following two curves.

$$\alpha_1(\sigma^2 - \lambda^2) - 2\alpha_2\sigma\lambda + \beta_1\sigma - \beta_2\lambda + K = 0 \quad (2)$$
$$\alpha_2(\sigma^2 - \lambda^2) + 2\alpha_1\sigma\lambda + \beta_1\lambda + \beta_2\sigma = 0. \quad (3)$$

Eqs. (2) and (3) correspond to the real and imaginary parts of (1), respectively. The root locus, locus of the points of intersection of (2) and (3), *is simply* (3) since it does not contain the parameter K.

Eqs. (2) and (3) correspond to rectangular hyperbolas having as center (σ_0, λ_0) where

$$\sigma_0 = -\frac{\alpha_1\beta_1 + \alpha_2\beta_2}{2|\alpha|^2}, \quad \lambda_0 = \frac{\alpha_2\beta_1 - \alpha_1\beta_2}{2|\alpha|^2}. \quad (4)$$

Furthermore, (3), the root locus, passes through the origin. The simultaneous solution of (2) and (3), S_1, S_2, the roots of (1),

are located symmetrically with respect to the point (σ_0, λ_0).

For the system to be stable, it is *necessary* that

$$\sigma_0 < 0 \qquad (5)$$

or equivalently

$$\alpha_1\beta_1 + \alpha_2\beta_2 > 0. \qquad (6)$$

If $\sigma_0 \geq 0$, consider a root $S_1 = \alpha_1 + j\lambda_1$ on the hyperbola. Either this point lies in the right half-plane or it does not. If it does, the above statement is correct. If not, the corresponding symmetrical root must be in the right half-plane because of the symmetrical property of the roots with respect to (σ_0, λ_0).

If, in addition we require

$$\beta_1 \neq 0 \qquad (7)$$

then the conditions (6) and (7) are *sufficient* for stability.

Only the following situations may exist.

1) One arm of the hyperbola cuts the λ axis.
2) Each arm has a point of intersection on the λ axis.

For case 1, since from (3), we have

$$\frac{d\lambda}{d\sigma}\bigg|_{\sigma=0, \lambda=0} = -\frac{\beta_2}{\beta_1}, \quad \beta = \beta_1 + j\beta_2 \neq 0 \quad (8)$$

and from (7), the slope of the tangent at (o, o) is finite. Therefore, part of one arm, A, lies in both half-planes. In addition, the other arm, B, must lie completely in either the left or right half-plane. Consider a point of A which is in the right half-plane. From (6), the corresponding symmetrical point on B is in the left half-plane. Hence, B is in the left half-plane.

For case 2, each arm lies in both half-planes. The symmetrical points of the points of intersection of the arms with the λ axis must lie in the left half-plane because of (6). The parallel lines connecting these four points form a parallelogram being in the left half-plane with the point of intersection of the diagonals (σ_0, λ_0). Therefore, a symmetrical portion of the arms of the hyperbola must be within the parallelogram. That is, the roots, S_1, S_2, can be chosen such that they have negative real parts.

One is able to determine the range of variation for K, the real parameter, such that the system is stable. This can easily be found by first finding the intersection point, P, of the λ axis and the hyperbola other than (o, o). Then substitute the coordinates of this point in (2) and calculate the corresponding value of $K = K_1$. The result of such a calculation is $P(0, \beta_1/\alpha_2)$ and

$$K = K_1 \frac{2|\alpha|^2\beta_1\sigma_0}{\alpha_2^2}.$$

If $\beta_1 < 0$, then the range of K is $0 \leq K \leq K_1$, but if $\beta_1 > 0$ then we have $K_1 \leq K \leq 0$. If, in addition, $\alpha_2 = 0$, then this range is $0 \leq K \leq \infty$ and $-\infty \leq K \leq 0$, respectively.

The arguments given above can be formalized algebraically. This is indeed difficult,

since one must determine the general solution of a fourth degree equation. The above discussion being geometric in nature is less laborious.

D. P. BROWN
Y. TOKAD
Dept. of Elec. Eng.
Michigan State Univ.
East Lansing, Mich.

Rectangular Guide Ferrite Phase Shifters Employing Longitudinal Magnetic Fields*

A new type phase shifter employing a cylindrical ferrite rod centered in a rectangular waveguide has been reported by Reggia and Spencer.[1] In this device the microwave phase shift is varied by means of a longitudinal magnetic field. This type of phase shifter was also mentioned in a recent correspondence by Clavin.[2] In describing the operation of the device, Reggia and Spencer state that the rotational effect due to the ferrite rod and the longitudinal magnetic field is suppressed by the rectangular waveguide and thus the microwave energy experiences a large phase change. The implication is that since the input and output waves are linearly polarized (TE_{10} mode), the wave in the ferrite structure is essentially linearly polarized (modified-TE_{10} mode). It is our opinion that the wave in most of the ferrite section is circularly polarized and that a certain amount of Faraday rotation is necessary in order to obtain the large phase changes reported.

In our attempts at producing microwave phase shift in a ferrite-loaded rectangular waveguide, we employed reduced height guide in order to suppress the rotational effect. Although the structure was heavily loaded, the maximum phase change obtained in 0.20×0.90 inch guide at X band was about 50 degrees per inch. In view of these results we suspected that in the device described by Reggia and Spencer the microwave energy in the ferrite rod was not linearly polarized but probably circularly polarized. The data given in Fig. 4 of their paper tend to support this view. Fig. 1 shows these data plotted as saturation phase shift per inch vs ferrite diameter. Note the large increase in phase shift for rod diameters above approximately 0.20 inch. This is the diameter above which the ferrite rod can support two orthogonal linearly polarized modes. In other words, if one assumes that the structure acts like a ferrite filled circular guide of diameter equal to the ferrite rod diameter, it can support circular polarization when
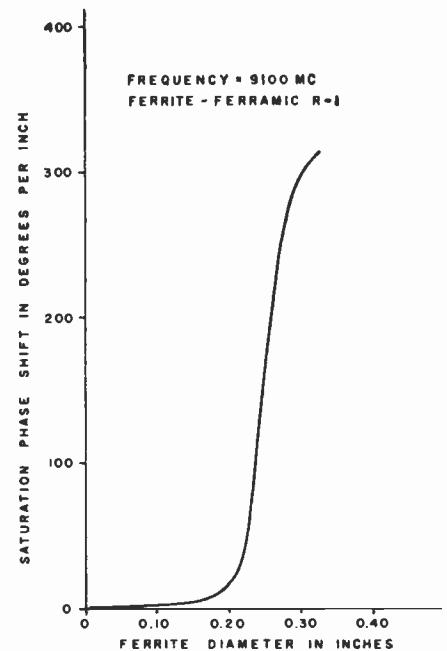
Fig. 1—Saturation phase shift as a function of ferrite diameter. (Data taken from Fig. 4 of Reggia and Spencer.[1])

$$f > f_c = \frac{c}{1.706d\sqrt{\epsilon}}$$

or

$$d > \frac{c}{1.706f\sqrt{\epsilon}}.$$

At 9100 mc,

$$d > \frac{1.18 \times 10^{10}}{(1.706)(0.91 \times 10^{10})(\sqrt{13})} = 0.21 \text{ inch.}$$

If under the above condition the wave propagating through the ferrite structure is circularly polarized, certain questions arise. How is the linearly polarized input wave converted to circular polarization? How is it reconverted to linear polarization at the output? How can the device be reciprocal when the longitudinally magnetized ferrite is acted upon by a circularly polarized wave? To answer these questions it was concluded that the device operates in the following manner. A linearly polarized wave enters the ferrite section and is rotated *clockwise* 45 degrees (Fig. 2).[3] The rotated wave can be considered as two linearly polarized waves that are equal in magnitude and oriented so that the polarization of one wave is parallel to the broad walls of the waveguide while the other is parallel to the narrow walls. The wave with its polarization parallel to the broad walls will have a phase velocity greater than that of the other component wave. If the phase difference between the two component waves is 90 degrees, a *counterclockwise* circularly polarized wave will be produced. This wave will travel along most of the ferrite length and have a phase shift proportional to the applied magnetic field (H_a). Since the sense of polarization is

Fig. 2—Microwave polarization along the propagation axis of the rectangular guide phase shifter.

Fig. 3—Arrangement for measuring insertion loss as a function of the angle θ.

counterclockwise, the wave will see an RF permeability of $(\mu+K)$ where μ and K are the magnitudes of the diagonal and off-diagonal components of the ferrite's permeability tensor. Due to the large $(\mu+K)\epsilon$ value for the ferrite ($\epsilon \approx 13$), most of the RF energy will be in the ferrite rod for diameters greater than 0.20 inch. Therefore, the circularly polarized wave will not "see" the guide walls and hence remain circularly polarized until it arrives at the fringe field region of the ferrite-to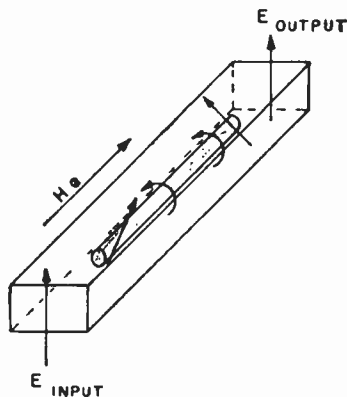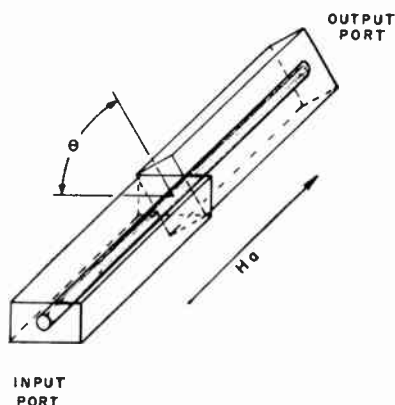-air-filled waveguide output junction. In this region the horizontal component of the circularly polarized wave experiences another 90-degree phase advance and is reconverted to a linearly polarized wave. This wave is then rotated clockwise 45 degrees and appears at the output port vertically polarized. This then is what we believe to be a qualitative explanation of the rectangular guide phase shifter described by Reggia and Spencer. Although the rotation and polarization conversions at the input and output fringe-field regions were described as occurring separately, this is not strictly true. That is, the two conversion processes are probably intermingled.

If either the magnetic field or the direction of propagation in Fig. 2 were to be reversed, the wave would still be circularly polarized along most of the ferrite rod and the RF permeability seen by the RF wave would still be $(\mu+K)$. This can be shown by merely repeating the above qualitative analysis for the case of a reversed magnetic

field (H_a). In other words, the device is reciprocal.

Certain other facts regarding this phase shifter can also be explained by the theory of operation described above. For example, Clavin[2] has shown that the direction of phase change for the Reggia and Spencer phase shifter is opposite to that obtained in the type that employs a thin ferrite slab centered on the broad wall of a rectangular guide. According to the explanation presented above, the Reggia and Spencer device would experience a *phase delay* when a magnetic field is applied. That is, the RF permeability $(\mu+K)$ increases when the magnetic field is increased. Since the RF permeability of the ferrite in the thin slab geometry is $(\mu^2-K^2)/\mu$, the phase is *advanced* when the magnetic field is increased. These directions of phase shift have been verified by shorting the output of the phase shifters and observing the shift in the standing wave pattern as the applied magnetic field is increased.[4]

Several experiments were made which seem to support the "circular polarization" theory of operation. The one that appears most conclusive is described in Fig. 3. The rectangular guide which contains the ferrite rod is split into two pieces. The section at the input side is stationary while the section at the output is arranged so that it can rotate through 360 degrees. With a microwave source connected to the input port and a detector to the output port, the insertion loss at saturation ($H_a = 200$ oersteds) was measured as a function of the angle θ. The result is shown in Fig. 4. The fact that the loss is

FREQUENCY = 9100 MC
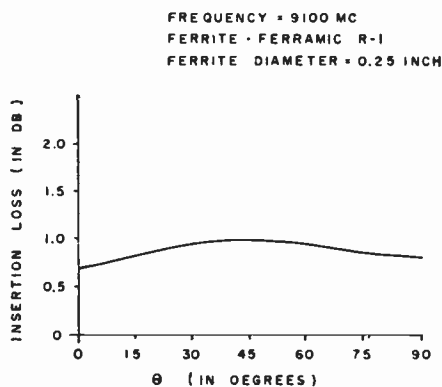FERRITE · FERRAMIC R-1
FERRITE DIAMETER = 0.25 INCH

Fig. 4—Insertion loss as a function of the angle θ.

essentially independent of angle strongly indicates that the wave is circularly polarized and that most of the energy is in the ferrite rod. Further verification was obtained by setting $\theta = 90$ degrees and measuring the insertion loss as a function of magnetic field strength. With no magnetic field the loss was 20 db. As the strength of the field was increased, the loss decreased sharply. At $H_a = 70$ oersteds the loss was down to 0.8 db where it remained despite any further increase in the magnetic field strength. For a longer ferrite rod, the initial decrease in loss was even greater.

[4] Our measurements indicate that the ordinate in Fig. 3 of Clavin's correspondence is labeled incorrectly. The words "advance" and "delay" should be reversed.

Although the explanation presented here is a qualitative one, it is felt that it is useful in explaining many of the effects observed in the rectangular guide ferrite phase shifter described by Reggia and Spencer.

P. A. RIZZI
Ewen Knight Corp.
Needham, Mass.
B. GATLIN
Missile Systems Div.
Raytheon Manufacturing Co.
Bedford, Mass.

Phase-Distortionless Limiting by a Parametric Method*

It appears that nearly ideal and, in at least some cases, phase-distortionless limiting can be obtained by using the signal to be limited as the *pump* frequency in a parametric device, and taking as the output some measure of the response of the device at the same pump frequency. The general principle involved is the following. The applied pump signal can be considered as a generalized force which, when applied to the parametric device, creates some sort of generalized motion. As the magnitude of the pumping force is increased, the corresponding motion also increases, until it reaches that threshold value which is sufficient to set the parametric device into oscillation at some other and usually lower frequency or frequencies. The pumping motion then "sticks" at this threshold value, and further increases in pumping force, merely makes the device oscillate harder at the other frequencies without increasing the amount of pump motion. If an output proportional to the pump motion is taken, the device will perform as an ideal limiter, limiting sharply at the threshold point.

As a specific example, a microwave-frequency pumping signal can be applied to a ferrite at ferrimagnetic resonance. The applied RF pump field causes the magnetization in the ferrite to precess about the dc field at an angle which is proportional to the applied RF field up to a threshold value. Above the threshold value, lower-frequency oscillations of a parametric nature occur, either as spin-wave modes or as lower-frequency cavity modes. At the threshold point the precession angle of the magnetization "sticks," and further increases in applied RF field only produce stronger oscillations at the lower frequencies without increasing the precession angle.

In this example, the output might be taken by making the microwave cavity have two degenerate modes at the pump frequency, with the pumping power applied to one mode and the output taken from the other mode. The precession of the magnetization will couple power from the input to output modes in a manner exactly analogous

to a nuclear magnetic induction experiment. The amount of power coupled to the output mode is proportional to the precession angle, and will reach a limiting value when the magnetization angle reaches the sticking point.

That the parametric type of limiting can have zero phase distortion is indicated by considering the simple electromechanical
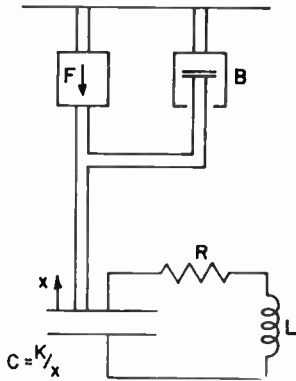

Fig. 1—Schematic of an electromechanical parametric device giving phase-distortionless limiting.

device of Fig. 1. In this device, the capacitor of an RLC circuit tuned to frequency ω is mechanically varied at frequency 2ω by a force source F with an internal mechanical resistance B. When the mechanical excursions x of the capacitor plate at 2ω reach a threshold value, electrical oscillations at ω will appear in the tuned circuit.

The equations of motion for the device are

$$f = B\dot{x} + \frac{1}{2K} q^2 \qquad (1)$$

$$\frac{1}{K} qx + R\dot{q} + L\ddot{q} = 0, \qquad (2)$$

where q is the charge on the moving capacitor plate. Using appropriate electrical and mechanical filters if necessary, the quantities f, q, and x can be written

$$f = F_2 e^{j2\omega t} + F_2^* e^{-2\omega t},$$
$$x = X_0 + X_2 e^{j2\omega t} + X_2^* e^{-j2\omega t},$$
$$q = Q_1 e^{j\omega t} + Q_1^* e^{-j\omega t}, \qquad (3)$$

i.e., the mechanical motion is assumed to have only 2ω terms and the electrical current to have only ω terms. The threshold for the electrical oscillations can be found by the usual method, i.e., assume $Q_1 = Q_1(t)$, substitute (3) into (2), pick out the $e^{j\omega t}$ and $e^{-j\omega t}$ terms, eliminate Q_1^*, and assume $Q_1(t) \sim e^{\mu t}$. The result is the secular equation

$$\mu^4 + 2\frac{R}{L}\mu^3 + \left(\frac{R^2}{L^2} + 4\omega^2\right)\mu^2 + 4\omega^2\frac{R}{L}\mu$$
$$+ \left(\omega^2\frac{R^2}{L^2} - \frac{X_2 X_2^*}{K^2 L^2}\right) = 0, \qquad (4)$$

which indicates that the threshold value of x is

$$|X_2|_{\text{thresh.}} = \omega RK. \qquad (5)$$

Since below the threshold, (1) says simply $F_2 = 2j\omega B X_2$, the threshold value of f is

$$|F_2|_{\text{thresh.}} = 2\omega^2 BRK. \qquad (6)$$

The amplitude of the steady-state oscillations above the threshold point can be found by assuming Q_1 to be independent of time and writing down the $e^{j2\omega t}$ and $e^{j\omega t}$ terms of (1) and (2), respectively:

$$F_2 = 2j\omega B X_2 + \frac{1}{2K} Q_1^2 \qquad (7)$$

$$\frac{1}{K} X_2 Q_1^* + j\omega R Q_1 = 0. \qquad (8)$$

Eq. (8) becomes

$$X_2 = -j\omega RK \frac{Q_1}{Q_1^*}, \qquad (9)$$

which says that the amplitude of X is constant above the threshold point and equal to its value at the threshold point. Putting this result into (7) gives

$$F_2 = 2\omega^2 BRK \frac{Q_1}{Q_1^*} + \frac{1}{2K} Q_1^2$$
$$= \left[2\omega^2 BRK \frac{1}{Q_1 Q_1^*} + \frac{1}{2K}\right] Q_1^2. \qquad (10)$$

The phase of f is arbitrary; choose it such that F_2 is real. Then from (10), the quantities Q_1 and Q_1^* must also be real and equal. Therefore, (9) becomes

$$X_2 = -j\omega RK = -j\omega |X_2|_{\text{thresh.}}, \qquad (11)$$

and the motion x has both constant amplitude and constant phase above the threshold, as shown in Fig. 2. Furthermore, (10) gives the oscillation amplitude Q_1^2 as

$$\frac{1}{2K} Q_1^2 = F_2 - 2\omega^2 BRK, \qquad (12)$$

which gives a threshold value for f in agreement with (6).
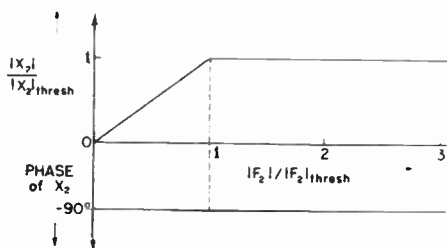
Fig. 2—The amplitude and phase of the capacitor-plate motion in Fig. 1 as a function of the pumping force.

Since microwave parametric amplifiers have been built which operate with milliwatts or even microwatts of pump power, limiting using this general principle should be possible at practical signal levels. All of the various forms of parametric amplifiers are potential parametric limiters. Further work will be necessary to see which of these will be most suitable.

A. E. SIEGMAN
Stanford Electronics Labs.
Stanford University
Stanford, Calif.

The Influence of Inductive Source Reactance on the Noise Figure of a Junction Transistor*

Various investigators[1-3] have carried out extensive tests to determine the validity of the theory of shot noise in transistors. In general the agreement between theory and experiment has been good; however, experimental results have not been accurate enough to verify the theoretical predictions concerning the influence of the source reactance upon the noise figure. The aim of this note is to provide that information. We shall refer to the equivalent noise resistance (R_n) of the transistor circuit; this is related to the noise figure by

$$R_n = F R_s \qquad (1)$$

where R_s is the source resistance seen by the transistor.

The expression given by van der Ziel[4] for the noise resistance of a transitor, which holds for frequencies that are not much higher than the cut-off frequency is:

$$R_n = R_s + R_{s1} + r_{bb'}$$
$$+ g_{s1}(Z_s + Z_e + Z_{bb'} + Z_{sc})^2 \qquad (2)$$

where Z_s is the source impedance, Z_e is the emitter impedance, $r_{bb'}$ is the real part of the base impedance $Z_{bb'}$, R_{s1} is the emitter noise resistance, g_{s1} is a noise conductance, and Z_{sc} is the correlation impedance. (These quantities are defined in van der Zeil's paper.[4]) Expanding (2) we obtain

$$R_n = R_s + R_{s1} + r_{bb'}$$
$$+ g_{s1}(R_s + R_e + r_{bb'} + R_{sc})^2$$
$$+ g_{s1}(X_s + X_e + X_{bb'} + X_{sc})^2. \qquad (2a)$$

It is observed that R_n should show a minimum when the condition

$$X_s + X_e + X_{bb'} + X_{sc} = 0 \qquad (3)$$

is satisfied. For an alloy junction transistor $Z_{bb'} = r_{bb'}$ so that $X_{bb'} = 0$.[5] Thus, the minimum value of R_n should occur when

$$X_s = (X_s)_{\text{min}} = -(X_e + X_{sc}). \qquad (4)$$

Since X_e may be determined separately it is possible to obtain information concerning X_{sc}.

Measurements reported here were carried out on a type 2N105 alloy junction, germanium p-n-p transistor. This unit was operated in both the forward and inverse direction: in the forward direction $\alpha_0 = 0.98$ and $fa \approx 700$ kc; in the inverse connection, $\alpha_0 = 0.80$ and $fa \approx 200$ kc. The results were obtained with the help of a new method of measurement that permits a substantial

[1] G. H. Hanson and A. van der Ziel, "Shot noise in transistors," PROC. IRE, vol. 45, pp. 1538–1542; November, 1957.
[2] W. Guggenbuehl and M. J. O. Strutt, "Theory and experiments on shot noise in semiconductor junction diodes and transistors," PROC. IRE, vol. 45, pp. 839–854; June, 1957.
[3] E. G. Nielson, "Behavior of noise figure in junction transistors," PROC. IRE, vol. 45, pp. 957–963; July, 1957.
[4] A. van der Ziel, "Noise in junction transistors," PROC. IRE, vol. 46, pp. 1019–1038; June, 1958.
[5] R. L. Pritchard, "Frequency response of theoretical models of junction transistors," IRE TRANS. ON CIRCUIT THEORY, vol. CT-2, pp. 183–191; June, 1955.

Fig. 1—Equivalent noise resistance vs inductive source reactance at 200 kc for the inversely operated transistor ($f_\alpha \sim 170$ kc, $\alpha \sim 0.80$). Collector current as a parameter.
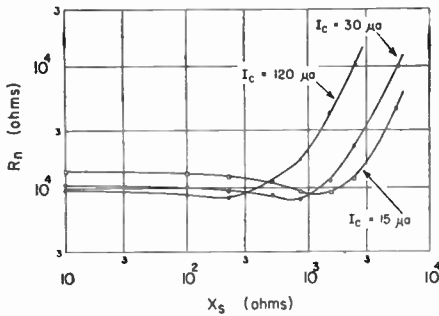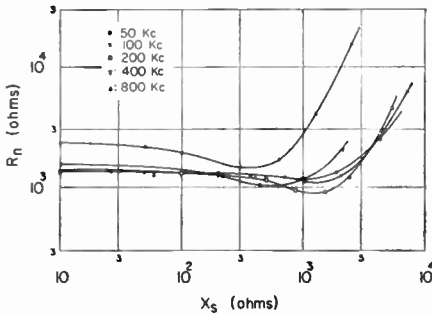

Fig. 2—Equivalent noise resistance vs inductive source reactance at 800 kc for the forward operated transistor ($f_\alpha \sim 700$ kc, $\alpha \sim 0.98$). Collector current as a parameter.
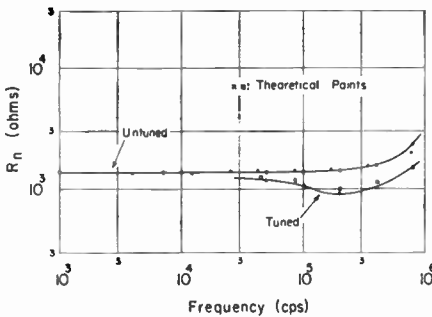

Fig. 3—Comparison of the behavior of equivalent noise resistance at several frequencies for the inversely operated transistor ($I_c = 15$ μa).

improvement in the ease and in the relative accuracy of noise data.

The effect of X_s upon R_n may be emphasized by choosing the operating conditions with care. The relative importance of the $g_{s1}(X \cdots)^2$ term of (2a) is emphasized by making $R_s = 0$ and by operating the transistor at very small currents.

Fig. 1 shows the results of measurements of R_n vs the inductive source reactance X_s with collector current as a parameter at a frequency of 200 kc for the inversely operated transistor. Each of the curves shows the expected minimum; the minimum is most pronounced on the 15-μa curve and is very small on the 120-μa curve. The value of X_s at which the minimum in R_n occurs decreases with increasing current. The curves are flat at low values of X_s, the magnitude varying inversely with current. All of the curves go as X_s^2 for large values of X_s.

Similar results are shown in Fig. 2 for

the transistor operating in the forward direction at a frequency of 800 kc. Fig. 3 is a plot of the results of measurements on the inversely operated transistor at several different frequencies with the operating point maintained constant. Each of the curves exhibits the characteristic behavior. The value of X_s at which the minimum occurs varies with frequency.

By (4) the correlation reactance for an alloy junction transistor is given by

$$X_{sc} = -\left[X_e - X_{s(min)}\right] \tag{5}$$

where $X_{s(min)}$ is the value of X_s at which R_n is a minimum. X_e may be calculated by means of[5]

$$X_e \approx -\frac{kT}{eI_e} \frac{0.8\,x\,(1 + 0.06x^2)}{\left(1 + \dfrac{x^2}{4}\right)^2 + 0.64x^2} \tag{6}$$

where $x = f/f_\alpha$.

Substituting this calculated value of X_e in (5), the correlation reactance was computed for each of the curves of Figs. 1–3. These results are shown in Table 1, which also indicates theoretical values for X_{sc} calculated from

$$X_{sc} \cong -\frac{kT}{eI_e} \cdot \alpha_0 \frac{0.8\,X\,(1 + 0.06x^2)\left(1 + 0.94x^2 + \dfrac{x^4}{16}\right)}{\left(1 + 1.14x^2 + \dfrac{x^4}{16}\right)\left[1 - \alpha_0 + (2 - 0.940\alpha)x^2 + \left(1 - \dfrac{\alpha_0}{16}\right)x^4\right]}. \tag{7}$$

This expression was obtained as outlined in Coffey's letter; however, the more accurate substitutions were made for X_e and α.

Fig. 4 shows the spectrum of R_n for the inversely connected transistor. Curve 1 is for the condition $X_s = 0$. For curve 2, X_s was adjusted for minimum R_n at each frequency of measurement. The difference between the two curves is due to the contribution of the $g_{s1}(X \cdots)^2$ term to the noise resistance of

the untuned transistor. This difference appears to be constant for $f > f_\alpha$; below f_α the difference decreases.

Fig. 4 also shows several theoretical points calculated for each curve. The agreement is quite good. On the other hand, the results of Table I show that the experimental and theoretical values of X_{sc} do not agree so well, except at low frequencies. There are two reasons for this:

1) The noise resistance R_n is not a very sensitive function of some of the parameters, consequently these parameters cannot be determined with great accuracy from noise resistance measurements.

2) Eq. (2) is only an approximation that has to be replaced by a more accurate one for frequencies above the cut-off frequency.

The author is grateful to Dr. A. van der Ziel for suggesting this experiment and for helpful discussions.

E. R. CHENETTE
Elec. Eng. Dept.
Univ. of Minnesota
Minneapolis, Minn.

Fig. 4—Equivalent noise resistance vs frequency for the inversely operated transistor ($I_c = 15$ μa). Theoretical points are shown for comparison with each curve.

TABLE 1

COMPARISON OF EXPERIMENTAL AND THEORETICAL VALUES OF X_{sc}

I. Inversely Operated 2N105 @ 200 kc

I_c	I_e	α_0	f_α	X_e (calc)	X_s (min R_n)	X_{sc} (Exp)	X_{sc} (Calc)
15	18	0.79	170	−540	1200	−660	−280
30	37	0.8	190	−270	750	−480	−170
120	144	0.82	200	− 70	190	−120	− 48

II. Forward Operated 2N105 @ 800 kc

15	15.2	0.98	720	−660	1050	−390	−510
30	30.5	0.98	720	−330	490	−160	−255
120	126	0.98	680	− 80	150	− 70	− 56

III. Inversely Operated 2N105 with Operating Point Fixed

f	$I_c = 15$ μa. X_e (calc)	$I_e = 18$ μa. X_s (min R_n)	$\alpha_0 \approx 0.79$ X_{sc} (Exp)	$f(\alpha) \approx 170$ kc X_{sc} (Calc)
50	−310	1100	−790	−810
100	−500	1200	−700	−740
200	−540	1200	−660	−270
400	−400	550	−150	− 70
800	−220	360	−140	− 16

[5] W. N. Coffey, "Behavior of noise figure in junction transistors," PROC. IRE, vol. 45, pp. 495–496; February, 1958.

Radio Engineering Use of the Minkowski Model of the Lorentz Space*

It has recently been shown in two notes in this journal[1,2] how the Cayley-Klein model of three-dimensional hyperbolic space can be used in studying propagation of noisy and noise-free processes through bilateral two-port networks. A slight disadvantage with this model is, however, that we deal only with *ratios* of the quantities that represent the processes. This disadvantage can be remedied by the use of a higher order space, here a four-dimensional Lorentz space.[3-6] The purpose of this note is to outline how the Minkowski model of the Lorentz space can be used constructively in radio engineering.

Let us assume that the input voltage V' and the input current I' of a bilateral two-port are linearly expressed in the output voltage V and the output current I by the matrix equation:

$$\psi' = \begin{pmatrix} V' \\ I' \end{pmatrix} = \begin{pmatrix} a & b \\ c & d \end{pmatrix} \begin{pmatrix} V \\ I \end{pmatrix} = T\psi;$$
$$ad - bc = 1. \qquad (1)$$

If we put

$$P_1' = \frac{1}{2}(V'I'^* + V'^*I')$$
$$P_2' = -\frac{j}{2}(V'I'^* - V'^*I')$$
$$P_3' = \frac{1}{2}(V'V'^* - I'I'^*)$$
$$P_4' = \frac{1}{2}(V'V'^* + I'I'^*)$$

$$P_1 = \frac{1}{2}(VI^* + V^*I)$$
$$P_2 = -\frac{j}{2}(VI^* - V^*I)$$
$$P_3 = \frac{1}{2}(VV^* - II^*)$$
$$P_4 = \frac{1}{2}(VV^* + II^*)$$

$$(2)$$

we obtain

$$P' = \begin{vmatrix} P_1' \\ P_2' \\ P_3' \\ P_4' \end{vmatrix} = \begin{vmatrix} a_1 & a_2 & a_3 & a_4 \\ b_1 & b_2 & b_3 & b_4 \\ c_1 & c_2 & c_3 & c_4 \\ d_1 & d_2 & d_3 & d_4 \end{vmatrix} \begin{vmatrix} P_1 \\ P_2 \\ P_3 \\ P_4 \end{vmatrix} = MP \qquad (3)$$

where the 16 real elements of the 4×4 matrix M are functions of the four complex constants a, b, c, and d. The matrix M belongs to the G_+ subgroup of the proper Lorentz group. This means that the expression $P_4{}^2 - P_3{}^2 - P_2{}^2 - P_1{}^2$ is invariant under the transformation (3). Thus (3) can be performed geometrically by using the Min-

kowski model of the Lorentz space.[7-11] This model consists of a hypercone (in the theory of special relativity called "light cone") constituting the asymptotic hypercone of an infinite number of hyperhyperboloids of one and two sheets. A signal of constant frequency corresponds to a point P on the hypercone, $P_4{}^2 - P_3{}^2 - P_2{}^2 - P_1{}^2 = 0$. A noise process may be represented by a point on a hyperhyperboloid of two sheets, $P_4{}^2 - P_3{}^2 - P_2{}^2 - P_1{}^2 > 0$.

By a direct generalization of earlier representations of a bilateral two-port,[1] we can represent it in the Minkowski model of the Lorentz space by straight lines or planes through the center of the model. The image point P' in (3) is then obtained from the given point P by performing "Lorentz reflections" in the straight lines or planes representing the two-port. Let us study some simple two-dimensional examples.

Example 1—Fig. 1 shows how the point P, situated on the asymptotic line L_{a1}, is transformed through an ideal transformer represented by the straight lines L_1 and L_2. The point P is first "reflected" in the line L_1 by the drawing of the line L_{c1} parallel to L_1', where L_1' is symmetric to L_1 with respect to the asymptotic line L_{a2}. L_{c1} cuts L_1 at
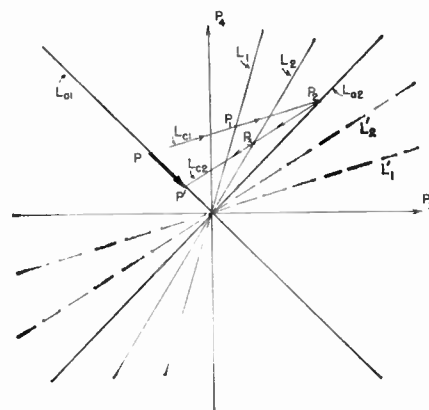
Fig. 1—Use of the two-dimensional Minkowski model of the Lorentz space for transforming a point on an asymptotic line by an ideal transformer.
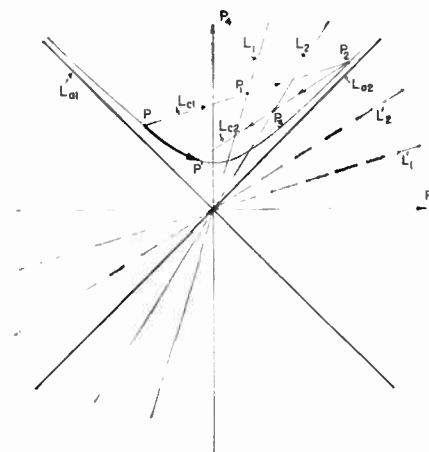
Fig. 2—Use of the two-dimensional Minkowski model of the Lorentz space for transforming a point on a hyperbola by an ideal transformer.

P_1, and L_{a2} at P_2. L_{c1} is said to be "Lorentz orthogonal" to L_1, and the distance $\overline{PP_1}$ equals $\overline{P_1P_2}$. Similarly, we then reflect P_2 in L_2 so that the point P' is obtained on the line $L_{a1}(\overline{P_2P_3} = \overline{P_4P'})$. We find that the transformation through the ideal transformer corresponds to a stretching of P to P' along the line L_{a1} (indicated by a heavy arrow in the figure).

Example 2—Fig. 2 shows the same constructions when P is situated on a hyperbola. We find that the ideal transformer represented by the same straight lines L_1 and L_2 as in Fig. 1 stretches the point P

along the hyperbola to the point P' (indicated by a heavy arrow in the figure). Here, also, $\overline{PP_1} = \overline{P_1P_2}$, and $\overline{P_2P_3} = \overline{P_3P'}$.

While the two-dimensional Minkowski model of the Lorentz space is the natural tool to use for transformations through an ideal transformer, the three-dimensional model is the natural tool to use in connection with lossless two-ports, and the four-dimensional model is the most suitable tool for transformations through lossy two-port networks. A central projection yields in the three-dimensional case the Cayley-Klein model of two-dimensional hyperbolic space in the plane $P_4 = 1$.[9-11] Similarly, in the four-dimensional case a central projection on the hyperplane $P_4 = 1$ results in the Cayley-Klein model of three-dimensional hyperbolic space.

A complete presentation of the theory will be given elsewhere. The use of the Minkowski model of the Lorentz space, well known from the theory of special relativity, indicates that distributed noisy systems may be treated by using the theory of general relativity.

E. Folke Bolinder
Electromagnetic Radiation Lab.
Air Force Cambridge
Research Center
Bedford, Mass.

[1] E. F. Bolinder, "Radio engineering use of the Cayley-Klein model of three-dimensional hyperbolic space," Proc. IRE, vol. 46, pp. 1650–1651; September, 1958.
[2] E. F. Bolinder, "Geometric-analytic theory of noisy two-port networks," Proc. IRE, vol. 46, pp. 1959–1960; December, 1958.
[3] W. Cauer, "Theorie der linearen Wechselstromschaltungen," 2 Auflage, herausgegeben und aus dem Nachlass ergänzt von W. Klein und F. M. Pelz, Akademi-Verlag, Berlin; 1954.
[4] G. A. Deschamps, "Geometric viewpoints in the representation of waveguides and waveguide junctions," Proc. Symposium on Modern Network Synthesis, Polytechnic Inst. of Brooklyn, Brooklyn N. Y., pp. 277–295; April, 1952.
[5] W. T. Payne, "Spinor theory of four-terminal networks," J. Math. Phys., vol. 32, pp. 19–33; April, 1953.
[6] E. F. Bolinder, "Impedance transformations by extension of the isometric circle method to the three-dimensional hyperbolic space," J. Math. Phys., vol. 36, pp. 46–61; April, 1957.

[7] H. Minkowski, "Space and Time," Address delivered at the 80th Assembly of German Natural Scientists and Physicians at Cologne, September 21, 1908; H. A. Lorentz, A. Einstein, H. Minkowski and H. Weyl, "The Principle of Relativity," pp. 75–91, Methuen and Co.; 1923.
[8] E. B. Wilson and G. N. Lewis, "The space-time manifold of relativity. The non-Euclidean geometry of mechanics and electromechanics," Proc. Am. Acad. of Arts and Sciences, vol. 48, pp. 389–507; November, 1912.
[9] F. Schilling, "Pseudosphärische, hyperbolisch-sphärische und elliptisch-sphärische Geometrie," Leipzig und Berlin, Verlag B. G. Teubner; 1937.
[10] M. Riesz, "En åskådlig bild av den icke-euklidiska geometrien. Geometriska strövtåg inom relativitetsteorien," Lunds Univ. Årsskrift, vol. 38, no. 9; 1943; Kungl. Fysiograf. Sällsk. Handl., vol. 53, no. 9, 76 pp. (In Swedish); 1943.
[11] E. F. Bolinder, "A survey of the use of non-Euclidean geometry in electrical engineering," J. Franklin Inst., vol. 265, pp. 169–186; March, 1958.

Magnetic Field Probe of High Sensitivity and Resolution*

The phenomenon of the Hall effect in metals and semiconductors has been used in the past as a basis for magnetic field detectors.[1-3] Several commercial fluxmeters employing this principle have been offered on the market. Two major difficulties inherent in the proposed and constructed devices have been the lack of sensitivity and/or resolution.

When the shape factors are ignored, the Hall voltage, V_h, may be simply described by the equation,

$$V_h = R_h \frac{B \times I}{t},$$

where

t = thickness of probe,
R_h = Hall constant,
B = magnetic field strength,
I = probe current.

The resolution of the Hall probe is determined by the physical dimensions of the probe's sensitive area. Since from the equation, the output is not directly a function of the area (the area does indirectly control the maximum allowable probe current), the probe may be made as small as desired with no loss in sensitivity.

A probe has been constructed of bismuth with a sensitive area of approximately twenty-five microns in diameter. A photograph of the probe is shown in Fig. 1. The probe was fabricated by depositing the bismuth through a suitable mask in a high vacuum. The total resistance of the probe is approximately 6 ohms. The maximum allowable current was approximately 20 milliamperes.

Fig. 1—Bismuth miniature Hall probe.

Two sets of equipment were used to measure the probe output for dc magnetic fields. In the first unit, an ac probe current of a frequency of 1000 cycles per second was employed. A narrow band tuned amplifier with a phase sensitive rectifier was used to amplify the probe signal. The maximum gain of the amplifier was 3.6×10^7. The am-

* Received by the IRE November 19, 1958.
[1] G. L. Pearson, U. S. Patent No. 2562120; 1951.
[2] H. B. Shaper, U. S. Patent No. 2707769; 1955.
[3] J. W. Buttrey, "Small Magnetic Field Mapping Probes of Thin Semiconducting Films," Paper BA-3, Meeting of American Physical Society, Chicago, Ill.; March, 1958.
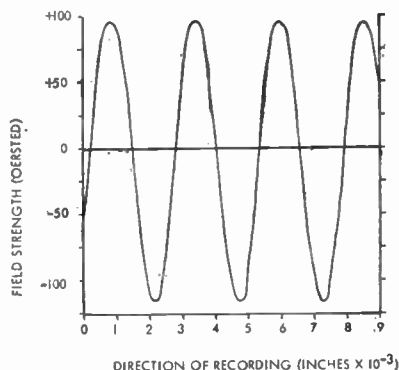
Fig. 2—Magnetic field strength normal to oxide recording media.
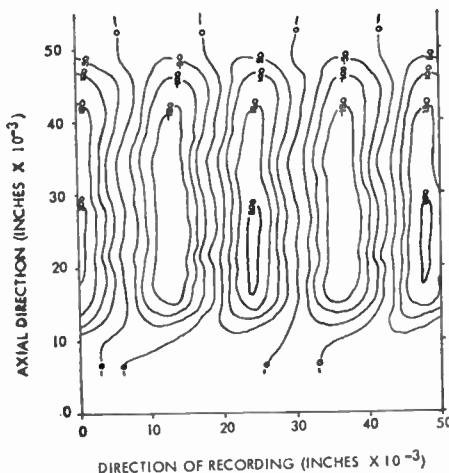
Fig. 3—Distribution of magnetic field strength normal to plated recording media. Signal array: continuous series of "ones." Isobars are in oersteds.

plifier noise referred to the input transformer was 0.13×10^{-7} volts. The amplifier input impedance was 50 ohms.

In the second unit, a chopped probe current of a frequency of 13 cps was employed. A commercially available amplifier (Perkin-Elmer Model No. 81A) was used to amplify the probe signal.

In both cases, amplitude and direction of the fields were sensed. In the former case, changes of field of the order of 0.1 oersted were observable. In the latter case, changes of field of the order of 0.02 oersted were observable.

The probe has been used to map dc magnetic fields with high gradients. As an example, the component of field normal to the surface and in the center of the recording track of a series of "ones" recorded on standard oxide recording tape is shown in Fig. 2. The recording bit density is 600 bits per inch. In addition to this, the distribution of the component of field normal to the surface of a cobalt nickel drum for a series of "ones" is shown in Fig. 3. The recording bit density is 88 bits per inch. The probe to recording media separation is .0005 inch. All signals are recorded in the nonreturn to zero system.

BOHDAN KOSTYSHYN
DAVID D. ROSHON, JR.
IBM Corp.
Endicott, N. Y.

Periodic Electrostatic Focusing of Laminar Parallel-Flow Electron Beams*

During the last few years focusing of electron beams by electrostatic fields has been treated both theoretically and experimentally.[1-5] The voltage variation in the vicinity of the beam (or the variation in the dc velocity of the electron beam) has customarily been assumed to be small and the axial distribution of the dc potential sinusoidal.[1-4] In practice, however, focusing of very high beam currents requires a large variation in voltage at the beam boundary, and the axial field distribution may not be sinusoidal.

This note presents a model for laminar parallel flow that is valid for any amount of voltage variation and applies to axially symmetrical structures. It is assumed that the ratio of maximum to minimum beam voltage, the beam diameter, and the structure period are given, and that it is desired to find the spatial potential distribution in the region of the electron beam which will permit maximum current in a parallel-flow beam. The problem is then one of synthesis.
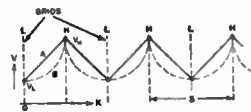
Fig. 1.

Fig. 1 shows a series of grids having infinite dimensions normal to the x coordinate. Alternate grids are connected together in such a manner that one set of grids is maintained at a dc voltage V_L and the other at V_H. In the absence of space charge, the potential distribution between the grids is linear, as shown by curve A in Fig. 1. If a beam having infinite dimensions in the transverse direction, uniform current density, and electron trajectories parallel to the x axis is injected at plane OL, the presence of space charge will depress the potential between the grids. In Fig. 1 curve B has the property that:

$$\left. \frac{\partial V}{\partial x} \right|_{x=0} = 0. \quad (1)$$

Under this condition, the potential variation in any region LH can be determined from[6]

$$\frac{x}{x_0} = \left(\sqrt{\frac{V(x)}{V_L}} + 2 \right) \left(\sqrt{\frac{V(x)}{V_L}} - 1 \right)^{1/2} \quad (2)$$

where $x_0 = a V_L^{3/4}/J^{1/2}$, J = current density in amperes per square meter, and $a^2 = 2.335 \times 10^{-6}$ amperes per volt$^{3/2}$. The curve for (2)

* Received by the IRE, November 24, 1958.
[1] A. M. Clogston and H. Heffner, "Focusing of an electron beam by periodic fields," *J. Appl. Phys.*, vol. 25, pp. 436-447; April, 1954.
[2] P. K. Tien, "Focusing of a long cylindrical electron stream by means of periodic electrostatic fields," *J. Appl. Phys.*, vol. 25, pp. 1281-1288; October, 1954.
[3] K. K. N. Chang, "Confined electron flow in periodic electrostatic fields of very short periods," PROC. IRE, vol. 45, p. 66; January, 1957.
[4] K. K. N. Chang, "Biperiodic electrostatic focusing for high density electron beams," PROC. IRE, vol. 45, p. 1522; November, 1957.
[5] J. R. Pierce, "Theory and Design of Electron Beams," D. Van Nostrand Co., Inc., p. 194; 1954.
[6] K. R. Spangenberg, "Vacuum Tubes," McGraw-Hill Book Co., Inc., New York, N. Y., p. 256 (10.39); 1948.

is plotted in Fig. 2. As shown in Fig. 1, the potential distribution in region HL is a mirror image of the curve in interval LH. Because the transverse dimensions are infinite, the variation of the dc potential in the transverse direction (r) is zero; i.e.,

$$\frac{\partial V}{\partial r} = 0. \tag{3}$$

The design of a round or ribbon-type electron beam having finite transverse dimensions but still satisfying the conditions described above follows a procedure similar to that used for designing Pierce-type electron guns.[7] Thus, it is necessary to establish at the boundary between the beam and the space-charge-free region the same potential distribution that existed when the beam extended to infinity in the transverse direction. In the charge-free region the potential must satisfy Laplace's equation subject to the boundary conditions given by (2) and (3). The total current in a round beam is then:

$$I = 7.336 \left(1 + 2\sqrt{\frac{V_L}{V_H}}\right)^2 \left(1 - \sqrt{\frac{V_L}{V_H}}\right)$$
$$\times V_H{}^{3/2} \left(\frac{d}{S}\right)^2 \times 10^{-6} \text{ amperes} \tag{4}$$

where d is the diameter of the electron beam, and S is the period of the focusing structure. Similarly, for a "ribbon" beam having thickness t and width w the current is:

$$I = 9.340 \left(1 + 2\sqrt{\frac{V_L}{V_H}}\right)^2 \left(1 - \sqrt{\frac{V_L}{V_H}}\right)$$
$$\times V_H{}^{3/2} \frac{wt}{S^2} \times 10^{-6} \text{ amperes.} \tag{5}$$

If V_H and the dimensions of the beam are constant, and the low voltage V_L is varied, the relative variation of the beam current as a function of the voltage ratio V_L/V_H is shown in Fig. 3. The equation for this curve is:

$$\frac{I}{Im} = \frac{1}{2}\left(1 + 2\sqrt{\frac{V_L}{V_H}}\right)^2 \left(1 - \sqrt{\frac{V_L}{V_H}}\right). \tag{6}$$

Maximum beam current Im will be obtained when $V_L/V_H = 0.25$. Hence, for a round beam:

$$I_m = 14.67 \left(\frac{d}{S}\right)^2 V_H{}^{3/2} \times 10^{-6} \text{ amperes.} \tag{7}$$

In a traveling-wave tube the following condition must be satisfied if gain is to be obtained:

$$\omega T \simeq \theta \tag{8}$$

where T and θ are the electron transit time and phase shift per period, respectively. The transit time is given by:

$$T = \int_0^S \frac{dx}{u(x)} \tag{9}$$

where:

$$u(x) = \sqrt{2\eta V(x)}. \tag{10}$$

The effective velocity u_e computed on the basis of transit time is:

$$u_e = \frac{S}{T}. \tag{11}$$

[7] Pierce, op. cit., p. 175.
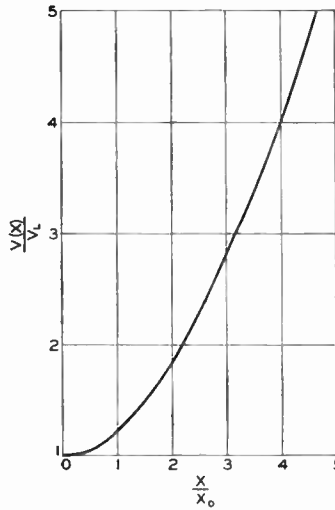
Fig. 2.
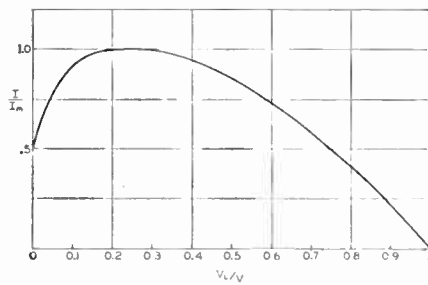
Fig. 3.
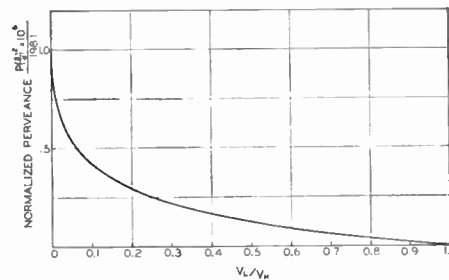
Fig. 4.

For comparison between this method of electrostatic beam focusing with magnetically focused beams at uniform velocity, an effective voltage V_e is given by:

$$V_e = \frac{u_e{}^2}{2\eta}. \tag{12}$$

When (2) and (9)–(12) are combined, the effective voltage is:

$$V_e = \frac{1}{9}\left(1 + 2\sqrt{\frac{V_L}{V_H}}\right)^2 V_H. \tag{13}$$

If the perveance P is defined as $I/V_e{}^{3/2}$, (4) and (13) can be combined to give:

$$P = 198.1 \frac{\left(1 - \sqrt{\frac{V_L}{V_H}}\right)}{\left(1 + 2\sqrt{\frac{V_L}{V_H}}\right)}\left(\frac{d}{S}\right)^2$$
$$\times 10^{-6} \text{ amperes per volt}^{3/2}. \tag{14}$$

The largest perveance P_m occurs when V_L equals zero:

$$P_m = 198.1 \left(\frac{d}{S}\right)^2$$
$$\times 10^{-6} \text{ amperes per volt}^{3/2}. \tag{15}$$

Fig. 4 shows a plot of the normalized perveance P/P_m as a function of V_L/V_H.

The design of electrodes approximating the ideal boundary conditions (2) and (3) at the edge of the electron beam can be determined by use of an electrolytic tank technique similar to that used for designing Pierce-type electron guns.[7]

Table I shows the preliminary experimental results that have been obtained.

TABLE I

	Theoretical Values	Experimental Values
I (ma)	34.6	30
V_e (volts)	417	445
P (amperes per volt $^{3/2}$)	4.07×10^{-6}	3.2×10^{-6}

$d = 0.100$ inch $\frac{V_H}{V_L} = 3.3$
$S = 0.323$ inch
$V_H = 850$ volts

$$\text{Transmission efficiency} = \frac{\text{Collector current}}{\text{Cathode current}}$$
$$\times 100 = 96 \text{ per cent.}$$

It can be concluded, therefore, that electrostatically focused round beams provide sufficiently high perveance for traveling-wave tube and klystron applications.

W. W. SIEKANOWICZ
F. E. VACCARO
Electron Tube Div.
Radio Corp. of America
Princeton, N. J.

WWV Standard Frequency Transmissions*

Since October 9, 1957, the National Bureau of Standards radio stations WWV and WWVH have been maintained as constant as possible with respect to atomic frequency standards maintained and operated by the Boulder Laboratories, National Bureau of Standards. On October 9, 1957, the USA Frequency Standard was 1.4 parts in 10^9 high with respect to the frequency derived from the UT 2 second (provisional value) as determined by the U. S. Naval Observatory. The atomic frequency standards remain constant and are known to be constant to 1 part in 10^9 or better. The broadcast frequency can be further corrected with respect to the USA Frequency Standard, as indicated in Table I on the next page. This correction is *not* with respect to the current value of frequency based on UT-2. A minus sign indicates that the broadcast frequency was low.

The WWV and WWVH time signals are synchronized; however, they may gradually depart from UT 2 (mean solar time corrected for polar variation and annual fluctuation in the rotation of the earth). Corrections are determined and published by the U. S. Naval Observatory.

WWV and WWVH time signals are maintained in close agreement with UT 2 by making step adjustments in time of precisely plus or minus 20 μsec on Wednesdays at 1900 UT when necessary; one retarding time adjustment was made during this month at WWV and WWVH on December 24, 1958.

WWV FREQUENCY*

1958 December 1500 UT	30-day moving average. seconds pulses on 15 mc. parts in 10^{10}
1	−18
2	−19
3	−19
4	−20
5	−20
6	−21
7	−22
8	−22
9	−23
10	−23
11	−23
12**	−23
13	−24
14	−24
15	−25
16	−25
17	−25
18	−25
19	−26
20	−26
21	−27
22	−27
23**	−28
24	−28
25	−28
26	−29
27	−29
28	−30
29**	−30
30	−30
31	−30

* WWVH frequency is synchronized with that of WWV.
** Decrease in frequency, ≅5 in 10^{10} at 1900 UT at WWV.

NATIONAL BUREAU OF STANDARDS
Boulder, Colo.

Volumetric Scanning of a Radar with Ferrite Phase Shifters*

The purpose of this correspondence is to report the results of an experiment in electronic volumetric scanning with ferrite phase shifters. An *X*-band radar was scanned with a 12-degree pencil beam through a solid angle of 42 degrees by 56 degrees in an 8 by 8 raster of beam positions by means of the ferrite scanner shown in Fig. 1. The direction of the beam was controlled with an accuracy of better than one tenth of a beamwidth. The 24-db sidelobe pattern of the radiating array was degraded by 4 db in one of principal planes by random amplitude and phase errors in the phase shifters. The insertion loss of the scanner was approximately

2 db each way. Ferrite saturation limited transmitter power to a maximum of 2 kw peak per phase shifter. For the aperture distribution and size of antenna used, this limitation resulted in a total radiated peak power of approximately 10 kw. The 72 phase shifters in the scanner were controlled by 25 watts of dc power or an average of about ⅓ watt per phase shifter. It is believed that the maximum switching time between beam positions, which was less than 1 msec. can be further reduced to approximately 10 μsec if obvious circuit refinements are incorporated.
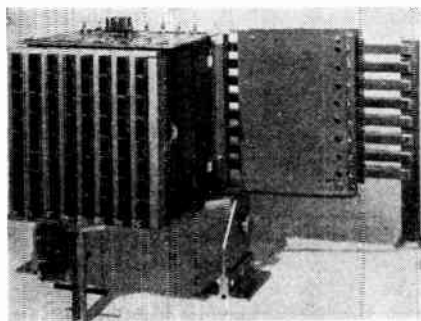
Fig. 1—Ferrite volumetric scanner.

The concept of accomplishing electronic antenna scanning with ferrite phase shifters has been considered by many investigators[1] ever since the discovery of ferromagnetic resonance in ferrites at microwave frequencies. However, a variety of problems has delayed the realization of a practical ferrite scanner suitable for use in a radar. The accomplishment described herein consists primarily of solving all of these problems simultaneously so that the resulting scanner demonstrates the feasibility of ferrite scanning for many applications.

The following are some of the problems which had to be solved. It was necessary to develop a phase shifter having a small cross-sectional area so that a two-dimensional matrix of shifters could be assembled integrally with a radiating array. Accurate regulation of the temperature of the ferrite material in all of the phase shifters was another requirement. A magnetic control circuit had to be designed in order to achieve high-speed switching with small average current and negligible stray fields. The selection of uniform samples of ferrite material and the development of an accurate method for adjusting and calibrating the individual phase shifters presented additional difficulties.

The phase shifter used in the scanner, a modified version of the longitudinal-control-field type described by Reggia and Spencer,[1] has significant advantages over the transverse-control-field type in size, weight, speed of switching, and control-circuit power required.

The scanner shown in Fig. 1 consists of an 8 by 8 array of waveguide radiating elements, each fed by a reciprocal ferrite phase shifter. The azimuth angle of the

[1] F. Reggia and E. G. Spencer, "A new technique in ferrite phase shifting for beam scanning of microwave antennas," PROC. IRE, vol. 45, pp. 1510–1517; November, 1957.

beam is controlled by this matrix. The matrix, in turn, is fed by a linear array of eight phase shifters which controls the elevation angle of the beam. The microwave and control circuits are illustrated schematically in Fig. 2. The relative phases of the vertical columns of radiators are controlled by one circuit for each column. The corresponding control for the horizontal rows is accomplished in the individual phase shifters which feed them. Thus the beam can be directed simultaneously in azimuth and elevation by two independent control circuits.
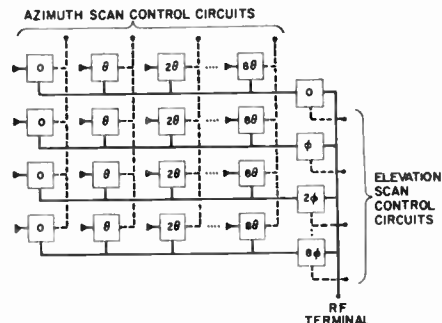
Fig. 2—Schematic of ferrite volumetric scanner.

The radiating elements are spaced one inch apart in both directions. At the operating frequency of 8820 mc this spacing is considerably more than one half of the free-space wavelength and limits the total angle of scan to 42 degrees by 56 degrees, beyond which second-order beams appear in the pattern. A useful solid scan angle of 90 degrees by 90 degrees is feasible with this type of scanner if the spacing between the radiating elements is reduced to one half the free-space wavelength. However, this arrangement requires a further reduction in the size of the phase shifters. This appears to be feasible.

The direction of the beam is controlled by establishing the proper value of phase shift in each shifter. These values may be calculated for each beam position by the simple relationship between progressive phase shift and beam angle. The current required in the control solenoid of each shifter to produce the desired phase shift is applied by a regulated 28-volt dc power supply connected through precision resistors to the control circuits. A separate set of precision resistors is provided for each of the eight elevation and eight azimuth beam positions. In the experimental setup, telephone stepping switches are used to select any one of the 64 combinations required for the 64 beam positions. Since these switches limit the rate of change of beam position to about 32 per second, the total solid angle can be scanned at a rate of 30 scans per minute. The effect of hysteresis in the control circuits was eliminated by applying a saturating pulse to each phase shifter during the beam-switching interval.

In order to eliminate serious phase-shift errors caused by ferrite temperature variations, each shifter was accurately calibrated at a controlled temperature of 50°C. The scanner was also controlled at 50±1°C by

thermostats and heaters distributed throughout the scanner assembly. Accurate temperature control is vital to the successful operation of the scanner since the temperature sensitivity of a phase shifter using General Ceramics R-1 ferrite is about four degrees of phase shift per degree Centigrade. Magnetic interaction between adjacent phase shifters was adequately reduced by the use of magnetic shields.

As stated above, the transmitter power was limited to 10 kw peak by saturation effects in the R-1 ferrite material. Two B scans, displaying azimuth vs range and elevation vs range, were used to present the video target data to the operator. In all other respects, the characteristics of the

radar were similar to those of an airborne fire-control set. Large ground targets were detected at a range of ten miles from a roof-house installation.

Although there are still many engineering problems which must be solved for specific applications, it is believed that these results demonstrate the feasibility of one-plane or volumetric ferrite scanning for many X-band radar systems. The necessity for accurate temperature regulation of presently available ferrite materials may be one of the more difficult problems. The results of this study also point out the need for continued effort in the synthesis of improved microwave ferrite materials. The desired characteristics include higher peak-

power transmission capability, decreased insertion loss, better uniformity of critical parameters, and decreased temperature sensitivity. A program of ferrite materials research at the Hughes Aircraft Company is making contributions in achieving some of these objectives.

The authors are indebted to many members of the laboratories of the Hughes Aircraft Company for their assistance in this work, especially to T. A. Nussmeier, E. N. Strumwasser, and J. Sur.

F. E. GOODWIN
H. R. SENF
Hughes Aircraft Co.
Culver City, Calif.

Contributors

John H. Dunn was born in Rochester, N. Y., on July 17, 1921. He received the B.S. degree in electrical engineering from the University of Notre Dame, South Bend, Ind., in 1943.

Since then he has been employed by the Naval Research Laboratory in Washington, D. C. From 1943 to 1947, he was engaged in research and development involving airborne equipment, and since 1947, in research and development work in the field of precision automatic tracking radar. In 1956, he was appointed Head of the Tracking Branch of the Radar Division at Naval Research Laboratory.

J. H. DUNN

❖

Roy W. Gould (S'48–A'51–M'56) was born in Los Angeles, Calif., on April 25, 1927. He received the B.S. degree in electrical engineering from the California Institute of Technology, Pasadena, Calif., in 1949 and the M.S. degree from Stanford University, Stanford, Calif., in 1950. He completed his study for the Ph.D. degree in physics at the California Institute of Technology in 1955.

R. W. GOULD

In 1951 and 1952 he was employed at the

Caltech Jet Propulsion Laboratory as a research engineer working on the guidance system of the Corporal missile. During his graduate study in physics he held a National Science Foundation Fellowship and the Howard Hughes Fellowship. Since 1955 he has been on the staff of the Electrical Engineering Department of the California Institute of Technology, where he is now associate professor. He is teaching and conducting research in the field of physical electronics and is currently concerned with microwave interaction with plasmas.

Dr. Gould is a member of Tau Beta Pi, Sigma Xi, and the American Physical Society.

❖

Dean D. Howard (S'47–A'50–M'55–SM'57) was born in Chatham, N. J., on January 2, 1927. He received the B.S. degree from Purdue University, Lafayette, Ind., in 1949, and the M.S. degree from the University of Maryland, College Park, Md., in 1952, both in electrical engineering.

He was employed at the Naval Research Laboratory, Radio Division, Communication Branch, from 1949 to 1954, where he worked in the field of UHF communication systems and techniques. Since 1954, he has been working with the Radar Division of the Naval Research Laboratory in the Tracking Branch engaged in basic research on target noise theory and tracking

D. D. HOWARD

techniques. He is presently Section Head of the Special Systems 1 and the Radar Statistics Sections of the Tracking Branch.

Mr. Howard is a member of RESA.

❖

E. O. Johnson (S'46–A'49–M'52) was born on December 21, 1919, in Hartford, Conn. During World War II he served first airfield in communications and then as electronic equipment maintenance chief for a carrier fighter squadron. He received the B.S.E.E. degree from Pratt Institute, Brooklyn, N. Y., in 1948, and has pursued his graduate studies at Princeton University, Princeton, N.J., and at the Swiss Federal Institute of Technology in Zurich, Switzerland.

E. O. JOHNSON

In 1948 he joined the RCA Laboratories at Princeton, where he has worked in the fields of gaseous electronics and semiconductor surfaces. He is now acting head of a group concerned with semiconductor phenomena and devices.

In 1952, with W. M. Webster, he won the Editor's Award of the IRE. Also in 1952, he was selected for honorable mention by Eta Kappa Nu. He was a member of the IRE Electron Tube Committee, the AIEE Subcommittee on Gas Tubes, and chairman of a similar IRE Subcommittee, and is presently a member of the IRE Committee on Solid-State Devices, the American Physical Society, and Sigma Xi.

Irving Kaufman (S'45–A'47–M'54) was born in Geinsheim, Hessen, Germany, on January 11, 1925. He received the B.E. degree in electrical engineering from Vanderbilt University, Nashville, Tenn, in 1945.

From 1945 to 1948, he worked as development engineer for the RCA Victor Division. From 1948 to 1957, he was engaged in teaching, graduate study, and research in electrical engineering at the University of Illinois, Urbana, where he received the M.S., and the Ph.D. degrees in 1949 and 1957, respectively. He is currently a member of the technical staff of the Research Laboratory of Ramo-Wooldridge, Los Angeles, Calif., a division of Thompson Ramo Wooldridge, Inc.

I. KAUFMAN

He is a member of Sigma Xi, Tau Beta Pi, Eta Kappa Nu, and Pi Mu Epsilon.

❖

Rudolf Kompfner (F'50) was born in Vienna, Austria, on May 16, 1909. He attended the Realschule and Technische Hochschule in Vienna, and was graduated from the faculty of architecture in 1933. In 1934, he went to England to continue his studies in architecture, and became the director of a building firm in 1937.

He entered the Admiralty Service in 1941 as temporary experimental officer, beginning in the Physics Department at Birmingham University. In 1944, he became associated with the Clarendon Laboratory at Oxford University, England, and received the degree of D.Phil. in 1951.

R. KOMPFNER

Since 1952, he has been with Bell Telephone Laboratories, Murray Hill, N. J., working on microwave tubes.

❖

Herbert Krömer (M'56) was born on August 25, 1928, in Weimar, Germany. He received the degree of a Dr. rer. nat. from the University of Goettingen, Germany, in 1952.

From 1952 to 1954, Dr. Krömer worked at the semiconductor laboratory of the German Post Office, where his main interest was the theory and development of high-frequency transistors.

H. KRÖMER

In 1954, he joined RCA Laboratories in Princeton, N. J., where he continued working in the semiconductor and transistor field. Since 1957, he has been head of the semiconductor research group at the German Philips Laboratory in Hamburg, Germany.

Dr. Krömer is a member of the American and German Physical Societies, and Sigma Xi.

❖

John R. Pierce (S'35–A'38–SM'46–F'48) was born at Des Moines, Iowa, on March 27, 1910. He received the B.S. degree in 1933 and the Ph.D. degree in 1936, from the California Institute of Technology, Pasadena, Calif., and came to the Bell Telephone Laboratories the same year.

From 1936 to 1955 he worked on high frequency electron tubes, and particularly on traveling-wave tubes; he became director of electronics research in

J. R. PIERCE

1952. In 1955 he was made Director of Research-Electrical Communications, and in 1958, Director of Research-Communications Principles, a field including research in radio, electronics, acoustics and vision, mathematics, and group behavior.

In 1948 he received the IRE Fellow Award for his "many contributions to the theory and design of vacuum tubes." He is the recipient of the Eta Kappa Nu (outstanding young electrical engineer) award for 1942 and the IRE Morris Liebmann Memorial Prize for 1947. He was editor of the IRE 1954–1955.

Dr. Pierce is the author of "The Theory and Design of Electron Beams," "Traveling-Wave Tubes," "Electrons, Waves and Messages," and "Man's World of Sound," and in addition has written many popular science articles for various magazines. He is a Fellow of the Institute of Radio Engineers and of the American Physical Society, and a member of the American Institute of Electrical Engineers, the Acoustical Society of America, the National Academy of Sciences, and the British Interplanetary Society.

❖

A. Rose (A'36–M'40–SM'43–F'48) received the A.B. degree in 1931 and the Ph.D. degree in 1935, both from Cornell University in Ithaca, N. Y.

For some twenty years after the completion of his graduate studies he was employed at RCA Laboratories, where he was engaged in research on television camera tubes, electron optics, emission phenomena, quantum noise, and solid state.

A. ROSE

From 1955–1958, he was occupied in setting up and directing the research at Laboratories RCA Ltd., Zurich, Switzerland.

Dr. Rose is a Fellow of the American Physical Society and a member of Société Suisse de Physique.

1959 IRE National Convention Program
Waldorf-Astoria Hotel, New York Coliseum, March 23-26, New York, N.Y.

General Committee

G. W. Bailey, *Chairman*
S. L. Bailey, *Vice-Chairman*
E. Weber, *Ex-Officio*
Emily Sirjane, *Secretary*

W. M. Baston	G. L. Haller
J. B. Buckley	R. E. Lafferty
W. C. Copp	N. B. Mills
L. G. Cumming	J. Morelock
E. K. Gannett	J. S. Saby
M. Walsh	

Banquet Committee

W. M. Baston, *Chairman*

J. F. Bisby	G. B. Geddy
L. R. Bloom	J. W. Kearney
E. C. Wilbur	

Cocktail Party Committee

M. A. Walsh, *Chairman*

C. G. Dietsch	W. H. Offenhauser, Jr.

Exhibits Manager

W. C. Copp

Facilities Committee

N. B. Mills, *Chairman*
R. Shalvoy, *Vice-Chairman*

J. J. Algeo	R. F. Heck
T. Barabutes	N. C. Henderson
J. Berlin	R. P. T. Jutson
W. M. Bishop	R. F. Koch
F. S. Boronow	G. Tint

F. T. Cassidy	R. V. Lowman
L. J. Clement	V. A. Nelson
M. F. Davito	A. Nittoli
L. R. Della Salle	W. R. Ruddy
F. Eisenhauer	K. M. St. John
T. Garrigan	E. Salkind
R. M. Hammer	R. L. Samson
E. Sherman	

Finance Committee

J. B. Buckley, *Chairman*

Hospitality Committee

J. Morelock, *Chairman*

H. Atwood, Jr.	J. A. Koehler
T. A. Chabrak	R. S. Mason
J. T. Cimorelli	J. B. Minter
W. M. Dowden	R. L. Snyder, Jr.
J. H. Hickey	C. W. Souder
L. Walsh	

IRE Activities Committee

L. G. Cumming, *Chairman*

R. M. Emerson	H. M. O'Bryan
C. L. Engleman	L. Podolsky
J. J. Gershon	T. C. Rives
R. A. Heising	W. M. Rust, Jr.
C. H. Hoeppner	L. C. Van Atta

Registration Committee

R. E. Lafferty, *Chairman*

L. J. Chamberlain	J. J. Drvostep
J. S. Cook	W. P. Frantz
J. F. Craib	V. A. Kuilk
J. M. Denney	R. C. MacVeety, Jr.
R. D. Post	

Technical Program Committee

G. L. Haller, *Chairman*

S. J. Begun	W. H. Huggins
D. A. Berlincourt	J. P. Jordan
H. P. Birmingham	G. M. Kirkpatrick
E. J. Breiding	G. C. Larson
T. P. Cheatham, Jr.	C. W. Little, Jr.
N. H. Choksy	M. L. Long
P. S. Darnell	H. B. Michaelson
H. E. deBolt	W. D. Novak
E. N. Dingley, Jr.	A. A. Oliner
C. H. Doersam, Jr.	C. H. Owen
J. E. Eiselein	J. M. Reid
J. W. Findlay	G. A. Rosselot
J. R. Harris	R. M. Showers
E. W. Herold	E. A. Speakman

Convention Record Committee

J. S. Saby, *Chairman*
E. K. Gannett

Publicity Committee

E. K. Gannett, *Chairman*
L. Winner, *Vice-Chairman*

J. Carroll	R. K. Kilbon
W. C. Copp	P. Lucey
E. E. Grazda	B. F. Oxbahr
H. Hechtman	H. S. Renne
J. Hobby	R. Schoonover
T. R. Kennedy	R. W. Sollinger, Jr.

Convention Highlights

Technical Program

A schedule of 54 technical sessions appears on the next page, followed by abstracts of the more than 280 papers to be presented.

Radio Engineering Show

This year's exhibition will again be held in the New York Coliseum at 59th St. and 8th Ave. A list of the 950 exhibitors and their products appears in "Whom and What to See at the Radio Engineering Show" in the advertising section of this issue.

Annual Meeting

Time: 10:30 A.M., Monday, March 23.
Place: Grand Ballroom, Waldorf-Astoria Hotel.

Speaker: Donald B. Sinclair, Vice-President of IRE, and Vice-President and Chief Engineer of the General Radio Co.

The special features of this opening meeting of the convention will be of particular interest to all IRE members.

Annual IRE Banquet

Time: 6:45 P.M., Wednesday, March 25.
Place: Grand Ballroom, Waldorf-Astoria Hotel.

The Annual IRE Banquet is in many ways the climax, not only of the convention, but of the entire year. It is at this time that the leading contributors to the progress of our profession are annually singled out for recognition by the IRE. An outstanding program of nationally prominent guest speakers and IRE officers will include the presentation of six annual awards and recognition of the 76 newly elected Fellows of the IRE.

Seats are reserved on a "first come, first served" basis. Place your order now.

Cocktail Party

Time: 5:30–7:30 P.M., Monday, March 23.
Place: Grand Ballroom, Waldorf-Astoria Hotel.

Women's Program

An entertaining program of tours and shows has been arranged for the wives of members. Women's headquarters will be located in the Regency Suite on the fourth floor of the Waldorf.

SCHEDULE OF TECHNICAL SESSIONS

	WALDORF-ASTORIA HOTEL						NEW YORK COLISEUM		
	Starlight Roof	Astor Gallery	Jade Room	Sert Room	Empire Room	Grand Ballroom	Morse Hall	Marconi Hall	Faraday Hall
Monday March 23 2:30 P.M.– 5:00 P.M.	Session 1 ADAPTIVE CONTROL PROCESSES AND ALLIED SYSTEMS	Session 2 VEHICULAR COMMUNICATIONS	Session 3 ENGINEERING WRITING AND SPEECH	Session 4 RADIO FREQUENCY INTERFERENCE	Session 5 ENGINEERING MANAGEMENT TECHNIQUES		Session 6 PRODUCTION TECHNIQUES	Session 7 NAVIGATION AND TRAFFIC CONTROL	Session 8 ELECTRONIC DEVICES
Tuesday March 24 10:00 A.M.– 12:30 P.M.	Session 9 NEW TECHNIQUES FOR ANALYSIS	Session 10 NUCLEAR INSTRUMENTATION TECHNIQUES—I	Session 11 BROADCASTING —I	Session 12 CONTRIBUTIONS TO STEREO SOUND REPRODUCTION		Session 13* ENGINEERING MANAGEMENT —II	Session 14 MEDICAL ELECTRONICS—I	Session 15 LAND AND SPACE ELECTRONICS	Session 16 PANEL: WIDENING HORIZONS IN SOLID STATE ELECTRONICS
Tuesday March 24 2:30 P.M.– 5:30 P.M.	Session 17 INFORMATION THEORY	Session 18 NUCLEAR INSTRUMENTATION TECHNIQUES—II	Session 19 BROADCASTING —II	Session 20 SPEECH AND CIRCUITS			Session 21 MEDICAL ELECTRONICS—II	Session 22 RELIABILITY TECHNIQUES	Session 23 MICROWAVE TUBES
Tuesday March 24 8:00 P.M.– 10:30 P.M.	Session 24 PANEL: FUTURE DEVELOPMENTS IN SPACE								
Wednesday March 25 10:00 A.M.– 12:30 P.M.	Session 25 THE STATISTICAL THEORY OF SIGNALS AND CIRCUITS	Session 26 RADIO AND TELEVISION RECEIVERS	Session 27 COMPONENT PARTS—I	Session 28 DIGITAL TELEMETERING		Session 29* SYMPOSIUM: PSYCHOLOGY AND ELECTRONICS IN THE TEACHING-LEARNING SYSTEM	Session 30 COMMUNICATION BY SCATTER SYSTEM	Session 31 MATHEMATICAL APPROACHES FOR RELIABILITY	Session 32 MICROWAVE DEVICES
Wednesday March 25 2:30 P.M.– 5:00 P.M.	Session 33 ELECTRONIC COMPUTERS: Systems and Applications	Session 34 SYMPOSIUM ON SEQUENTIAL CIRCUIT THEORY	Session 35 COMPONENT PARTS—II	Session 36 SPACE ELECTRONICS			Session 37 COMMUNICATION BY HF RADIO AND BY WIRE LINE	Session 38 PROPAGATION AND ANTENNAS —I	Session 39 MICROWAVE THEORY AND TECHNIQUES
Thursday March 26 10:00 A.M.– 12:30 P.M.	Session 40 THEORY AND PRACTICE IN RUSSIAN TECHNOLOGY	Session 41 CIRCUIT THEORY II—Analysis and Synthesis	Session 42 ULTRASONIC ENGINEERING—I	Session 43 MILITARY ELECTRONICS—LOOKS FORWARD	Session 44 FRONTIERS OF INDUSTRIAL ELECTRONICS		Session 45 MAN-MACHINE SYSTEM DESIGN	Session 46 ANTENNAS—II	Session 47 INSTRUMENTATION: Devices and Circuits
Thursday March 26 2:30 P.M.– 5:00 P.M.	Session 48 ELECTRONIC COMPUTERS: Components and Circuits	Session 49 CIRCUIT THEORY III—Applications	Session 50 ULTRASONIC ENGINEERING—II	Session 51 CONCEPTS AND PROGRAMS			Session 52 COMMUNICATION ENGINEERING IN BROADCASTING	Session 53 ANTENNAS—III	Session 54 INSTRUMENTATION FOR HIGH SPEED DATA ACQUISITION

* Sessions terminate at 12:00 Noon.

ABSTRACTS OF TECHNICAL PAPERS

SESSION 1*

Mon. 2:30–5:00 P.M.

Waldorf-Astoria
Starlight Roof

ADAPTIVE CONTROL PROCESSES AND ALLIED SYSTEMS

Chairman: JOHN G. TRUXAL, *Elec. Eng. Dept., Polytech. Inst. Bklyn., Brooklyn, N. Y.*

1.1. On Adaptive Control Processes

R. BELLMAN AND R. E. KALABA
The Rand Corp., Santa Monica, Calif.

In many control processes arising in engineering, economics, etc., a control device is called upon to perform under various conditions of uncertainty regarding underlying physical processes and conditions. As the control process unfolds and control decisions are being made all the while in an effort to obtain optimal system performance, additional information may become available to the control device, which may then learn to improve its performance based upon experience, *i.e.*, it may *adapt* itself to circumstances as it finds them.

Many problems involving the determination of optimal adaptive control policies can be solved using the functional equation technique of dynamic programming in conjunction with a high-speed digital computer. Following a general exposition, some specific examples are provided.

1.2. A Dynamic Programming Approach to Adaptive Control Processes

MARSHALL FREIMER, *Lincoln Lab., Mass. Inst. Tech., Lexington, Mass.*

As a particular example of general methods, we shall consider a stochastic control process involving a system describable by an *s*-dimensional vector, $x(n)$, satisfying the linear difference equation:

$$x(n + 1) = A(n)x(n) + y(n) + r(n)n \geq 0. \quad (1)$$

Here $A(n)$ is a known matrix and $r(n)$ is a random vector whose distribution is initially not completely known. As the process continues, this distribution is determined with increasing accuracy.

Given the initial state,

$$x(0) = c \quad (2)$$

we wish to choose the control vector $y(n)$ so as to minimize a cost functional of the form:

$$H_N(y) = E_x\left(\sum_{n=0}^{N} h(x(n), y(n), n) \right). \quad (3)$$

The symbol E_x denotes an expected value taken with respect to the distribution x inherits as a function of r.

Given that each function h is a quadratic function of the components of $x(n)$ and $y(n)$, we proceed to solve this problem by means of the functional equation technique of dynamic programming. Making use of the fact that the minimum expected cost starting at any time m is a quadratic function of the components of $x(m)$, we wind up with a simple computational algorithm for determining optimal policies.

1.3. On the Optimum Synthesis of Multipole Systems in the Wiener Sense

H. C. HSIEH AND C. T. LEONDES, *Dept. Eng., University of California, Los Angeles, Calif.*

This paper is concerned with obtaining the optimum system in the Wiener sense for a multipole system. Earlier literature has shown how to obtain the mean-square value of the error when the multipole system transfer function has been specified, but thus far no published work has shown how to solve the synthesis problem, in general, for this case. The principal reason that this problem has appeared to be impossible of analytic solution, thus far, for cross-correlation between the inputs is that the usual variational approach results in a set of intractable simultaneous integral equations involving many complicated cross products of the desired weighting functions and the variational functions.

The synthesis problem is first solved for the case in which there is no correlation between the inputs. The result for the optimum weighting functions for this case is presented and the resultant mean-square value of the error is shown.

The far more complicated case of the synthesis problem when the inputs are correlated is then considered. A unique technique is utilized to avoid the difficulties inherent in the use of the usual variational methods which lead to a set of simultaneous algebraic equations. The resultant solution for the optimum transfer functions is presented and is shown to reduce to the corresponding results obtained previously for the uncorrelated inputs.

The paper then concludes with an illustrative example for the case of correlated inputs.

1.4. On Adaptive Control Systems

LUDWIG BRAUN, JR., *Elec. Eng. Dept., Polytech. Inst. Bklyn., Brooklyn, N. Y.*

An attempt is made in the paper to evolve a basic philosophy for adaptive control systems. A method is described for determining the system impulse response from measurements of instantaneous system input and output. The impulse response is expanded in a Taylor series to facilitate the solution of the convolution equation. From a knowledge of the impulse response and the system error, the necessary correction to the system forcing function is determined in a manner similar to that used for determination of the impulse response. The techniques developed are applied to two systems—one which is stable and another which is unstable. The results are presented in graphical form.

1.5. Extension of Phase Plane Analysis to Quantized Systems

PHILLIP H. ELLIS, *Sperry Gyroscope Co., Great Neck, N. Y.*

Increasing applications of numerical control of processes have created a need for new methods for synthesis of control equipment. The method presented is applicable to systems commanded by discretely valued inputs and to processes whose outputs may be similarly quantized. If the data are sampled incrementally and aperiodically—numerically coded in real time—the error signal is constrained to a finite number of discrete values each of which may be associated with a region in the phase plane. Within each such area the trajectories of any process, which can be represented in the plane, are a family of parallel curves, thus facilitating analysis.

SESSION 2*

Mon. 2:30–5:00 P.M.

Waldorf-Astoria
Astor Gallery

VEHICULAR COMMUNICATIONS

Chairman: MORTON L. LONG, *Philco Corp., Philadelphia, Pa.*

2.1. An Analysis of Radio Flutter in Future Communications

N. W. FELDMAN, *U. S. Army Signal Res. and Dev. Lab., Fort Monmouth, N. J.*

Flutter, a phenomenon which seriously hampers the reception of intelligence in a moving vehicle, is analyzed. The author compares radio flutter to radio fading. He then applies techniques, established for predicting incidence of fading, to analyze the incidence of flutter. Improvements resulting from certain remedies are predicted. Data available for propagation at 150 mc are presented. He describes the design of an applique unit which will assure benefits of space diversity reception at low cost.

2.2. Radio Set, AN/GRC-59, Rugged, Reliable Design For Tactical Usage

J. C. SHANNON, *Philco Corp., Philadelphia, Pa.*

This FM radio relay equipment, operating in the frequency range of 4400 to 5000 mc, has been designed primarily for rugged tactical

usage at terminals and repeaters in the rear and intermediate areas. The radio equipment is capable of being installed, transported and operated in an S/141 shelter or operated in a transit case configuration. Four men will be able to place a terminal station into operation in 30 minutes. It will handle 46 unsecured channels of pulse position multiplex or 96 channels of pulse code multiplex over 8 hops. The primary requirement of the radio equipment is that of reliability and operability by military personnel on a continuous 24-hour per day basis.

2.3. A New Approach to Compactness in Mobile Radio-telephone Design

W. ORNSTEIN, *International Systems Ltd., Montreal, Can.*

A mobile radiotelephone having a power rating of 30 or 60 watts is described. The unit incorporates transmitter, receiver, operating controls and loudspeaker in a single compact aluminum alloy case. Total weight is less than 15 pounds. The unit is small enough for under-dash mounting in a modern passenger car. The transistor power supply is in a separate case designed to be mounted on the vehicle firewall. Preaged tubes and heater voltage regulation are employed to maximize vacuum tube reliability. Careful attention to thermal design has minimized the development of hot spots in the interior of the equipment.

2.4. A New Manual Mobile Telephone System

ALAN F. CULBERTSON, *Lenkurt Electric Co. Inc., San Carlos, Calif.*

A new manual mobile telephone system has been designed which takes into consideration the peculiar needs of the common carrier telephone industry. Utilizing conventional two-way radio equipment as a transmission medium, the system incorporates a number of important features on the subscriber and the central office ends which make it as similar as possible to conventional "wired" telephone service.

In the mobile subscriber station equipment, a specially designed control unit gives the subscriber access to up to four mobile telephone channels on an automatic channel-homing basis. A call lamp holds incompleted incoming calls until the subscriber returns to his vehicle and contacts the operator.

Selective calling, base station control and telephone line terminating equipment has been specifically designed to meet the needs of this service. The central office end control equipment occupies approximately 12 inches of rack space and provides all these functions under the control of a switchboard operator. Transistors and relays make up the only dynamic circuit elements in this panel. Printed wiring is used to reduce size and to facilitate maintenance by means of plug-in assemblies. The circuits employ only transistors and relays as dynamic elements.

2.5. Performance of "Low-Plate-Potential" Tube Types at Mobile-Communications Frequencies

R. J. NELSON AND C. GONZALEZ, *Electron Tube Div., RCA, Harrison, N. J.*

The demonstrated advantages for hybrid-type automobile broadcast receivers of "low-plate-potential" tube types (those designed to operate at plate potentials of approximately 12 volts) has aroused considerable interest in the usefulness of such tube types at mobile-communications frequencies. This paper analyzes the performance of low-plate-potential tube types at frequencies above 2 mc. It also discusses performance requirements and design considerations for mobile-communications receivers and presents operating data on an experimental hybrid-type mobile-communications receiver using available low-plate-potential tube types. These data are compared with typical receiver-performance specifications for mobile service.

SESSION 3*

Mon.   **2:30–5:00 P.M.**

Waldorf-Astoria
Jade Room

ENGINEERING WRITING AND SPEECH

Chairman: E. K. GANNETT, *Institute of Radio Engineers, Inc., New York, N. Y.*

3.1. Using the Psychological Approach in Scientific Writing

JOHN L. KENT, *DATEX Corp., Monrovia, Calif.*

Scientists, engineers and other technically trained persons can write better and with less effort if they adopt the techniques of the professional writer. These methods can be used easily in engineering reports, scientific articles and other technical writing. The professional writer plans his writing, considers his reader and uses practical psychology to produce high-quality, readable writing in quantity, even when neither flesh nor spirit is willing.

With detailed planning the scientist and engineer can produce more concise, yet complete reports. Through consideration of the typical reader, he can obtain wider understanding without insulting the intelligence of any of his readers. He can copy the detached attitude of the professional writer which assures emotional tranquility in the face of criticism.

Pedantic, pedestrian, thesis-type prose no longer satisfies discerning management nor readers of modern technical journals.

The alert scientist and engineer has learned that it is easy to write involved, "learned," prose, but he must make an effort to write simply and concisely. This effort is worthwhile, both to himself as a professional and to science in general.

3.2. An Effectual Approach to an Orally-Presented Paper

IRVING J. FONG, *5309 2nd Ave. South, Minneapolis 19, Minn.*

The technique of oral communication has largely been ignored by professional people. The concept that scientific achievement can be comprehended only by a paper literally read needs re-evaluation, for it seems that the purpose is defeated when interest is lost. Here is an approach to the problem of presenting a paper. The simple rules of an outline well prepared will permit the speaker to vary his remarks within the boundaries of his notes.

If technical societies are to achieve effective communication at meetings, oral treatment of scientific subjects must be adopted. The approach suggested here, although upsetting a tradition, is basic and effective.

3.3. A Self-Improvement Program for Engineering Writers

ALEXANDER H. CROSS, *Raytheon Manufacturing Co., Wayland, Mass.*

The value of an engineering publication is proportionate to the degree by which it advances the state of the art, to the completeness and accuracy of its information, and to the clarity of its presentation. It is recommended that each engineering writer establish a self-improvement program in the craft of writing. Such a program is suggested in which detailed attention is given to reading skills, use of reference books, workshop practice, typing, and use of "trade journals" and textbooks of the writing profession. The suggested program presumes the writer's prior recognition of his individual needs in the field of technical knowledge.

3.4. Read Your Speech

EDWIN W. STILL, *General Electric Co., Utica, N. Y.*

If you "present" a paper it is then a speech. If you read it, read it like a speech for your audience—not like a paper to yourself alone. This paper will help you to read your speech so nobody knows you are reading it. First organize and write it for a speech as we suggest. Then type the copy in one of the three ways discussed. Practice often with the copy you will use: alone, before a coach, into a recorder. Go early and check the lectern, the projector, the PA. Try a "dry run." Think of your audience as much as of your speech. Talk to individuals, not the mass.

3.5. Subjectivity vs Objectivity in the Technical Report

SOL COHEN, *Ampex Corp., Technical Information Center Redwood City, Calif.*

This paper analyzes the requirements of the technical report from the viewpoint of the use of that report. The primary purpose of the report is to guide management in arriving at correct decisions. Therefore a subjective presentation, buttressed by objective facts, is required. Too much emphasis has been placed on the mechanics of writing reports and virtually nothing on the use of the report. This paper attempts to place all requirements in their proper perspective.

SESSION 4*

Mon.   **2:30–5:00 P.M.**

Waldorf-Astoria
Sert Room

RADIO FREQUENCY
INTERFERENCE

Chairman: STUART L. BAILEY,
*Jansky and Bailey, Inc.,
Washington, D. C.*

4.1. Standard Measurement Parameters for Phenomena Distributed in Time and Frequency

E. W. CHAPIN, *Federal Communications Commission, Laurel, Md.*

In order that measurements made by various investigators may readily be compared, it is proposed that certain measurement parameters be standardized and that, whenever possible, all data be taken with one or more of the standardized parameters. The standard parameters would cover: 1) the bandwidth, 2) the type of detector, such as average, semipeak or peak, and 3) the integration time. The use of the standardized units with respect to the measurement of both desired and interfering signals is discussed.

4.2. Magnetic Field Pickup for Low-Frequency Radio-Interference Measuring Sets

M. EPSTEIN AND R. B. SCHULZ
*Armour Res. Found., Illinois
Inst. Tech., Chicago, Ill.*

Reported is the development of a device to measure low-frequency magnetic field interference. It utilizes the Hall effect in indium antimonide. The device consists of a Hall-effect probe inserted between two pole pieces of ferrite flux concentrators. The Hall-effect probe is designed to give high output potential utilizing specially shaped indium antimonide and ferrite concentrators designed to give greater flux density in the gap between the poles. The sensitivity of the device is comparable to the existing loop sensing device used with radio-interference measuring equipment in the low-frequency range and its significant features are direct measurement of magnitude and waveform of the alternating magnetic field and convenient calibration.

4.3. Microwave Duplexer Tube Characteristics Under Spurious Radiation Conditions

IRVING REINGOLD, *U. S. Army
Signal Res. and Dev. Lab.,
Fort Monmouth, N. J.*

The problem of interference between nearby friendly radar systems is becoming increasingly serious. Since the TR duplexer tube is a band-pass filter in its quiescent state, some reliance has been placed on this tube as an instrument for providing protection from unwanted radiation. This paper describes an investigation conducted on several types of TR tubes to determine their effectiveness in rejecting spurious radiation. The results discussed show that the TR tube cannot be relied upon to reject spurious radiation at higher frequencies than the operational frequency of the system. Various techniques for providing the necessary crystal protection without undue sacrifices in insertion loss or other operational system characteristics are reviewed, and recommendations are made for developing other means of effectively providing the required protection against unwanted signals.

4.4. Technical Considerations in the Assignment of Operating Frequencies in a Communications System

O. M. SALATI, *Moore School of Elec.
Eng., University of Pennsylvania,
Philadelphia, Pa.,* AND R. A.
ROSIEN, *Hughes Aircraft
Co., Culver City, Calif.*

Following a review of previously published frequency assignment techniques, a new method is described for determining the required frequency separation between transmitting carriers to avoid interference. As an illustration of the method, operating frequencies are assigned to an assumed deployment of L-band radars located at 50-mile intervals along a straight line. One other radar is located within an annular area of radii one and 20 miles centered about each of the original radars. The pulse widths, pulse repetition rates and antenna patterns and orientations of each radar are used in the calculations. Prediction of power transfer between radars is based on line of sight, diffraction and scatter propagation loss considerations.

4.5. Precipitation Static at High Altitude

L. A. HARTMAN AND F. B. POGUST,
*Airborne Instruments Lab.,
Mineola, N. Y.*

Previous investigations have explored the nature and mechanisms of precipitation static and methods of alleviating the effects of this static. Of equal importance to the system designers is a knowledge of the probability of occurrence of static and of the amplitude levels to be expected. A two-pronged approach to this problem was used in this investigation.

1) A series of simply instrumented flight tests were made to determine the correlation between weather conditions at high altitude and the occurrence of "P" static. Amplitude levels of atmospheric noise were also measured.
2) A determination on a climatic basis of the percentage of time to show there was correlation between the weather and "P" static was made.

From the information so developed from the known characteristics of precipitation static and from the characteristics of the communications or navigation system under investigation, a measure of the degradation of the system can be determined.

4.6. Precipitation Generated Interference in Jet Aircraft

R. L. TANNER AND J. E. NANEVICZ,
*Stanford Res. Inst., Menlo
Park, Calif.*

Precipitation charging, which is known to increase rapidly with speed, produces corona discharges at the extremities of aircraft flying through snow or high clouds. These discharges are the source of precipitation static interference. The magnitude and spectral distribution of the noise produced in aircraft radio systems depends upon the intensity to the discharges, their distribution on the aircraft, and upon the coupling between the antenna and the points at which the discharges occur. By a combination of theory and laboratory experiment these factors can be separately evaluated for a particular aircraft and antenna. The noise to be expected for given charging conditions, both magnitude and spectral characteristics, can therefore be predicted.

A flight test program has been carried out in cooperation with the Boeing Airplane Co. in which precipitation generated noise was measured in the Boeing 707 jet transport. Measured noise levels are compared with predicted noise with good agreement. The flight test program also included a flight evaluation of decoupled static dischargers for use with high speed aircraft described at the 1957 National Convention.

SESSION 5*

Mon.   **2:30–5:00 P.M.**

Waldorf-Astoria
Empire Room

ENGINEERING MANAGE-
MENT TECHNIQUES

Chairman: HAROLD GOLDBERG,
*Emerson Radio and Phonograph
Corp., Silver Spring, Md.*

5.1 The "Maximum" Manager in Research and Development

MERRITT A. WILLIAMSON, *Dean
of Engineering, Pennsylvania
State Univ., University
Park, Pa.*

A thesis is presented that technical management is different from other types of management in objective thought and techniques used. Maxims of "sound" management are questioned when applied in the research, development and engineering areas. A good manager, for example, may not have everything in his department running smoothly nor is it necessary that he be personally efficient. The determinants of the job of technical management are contrasted with those of other management provisions and an attempt is made to extract the essentials. By this presentation it is hoped that both technical and nontechnical top management may be better orientated to provide a more understanding environment for effort in the technical area.

5.2. Marketing Factors in Research and Development

HARRISON M. RAINIE, JR., *Stewart, Dougall and Associates, New York, N. Y.*

In a penetrating analysis which pinpoints the origin of many new product successes and failures, the significance of marketing factors in R and D decisions in the electronics industry will be explored.

5.3. Obtaining Capital for the Smaller Electronics Firm— Methods and Pitfalls

CASPER M. BOWER, *Utilities and Industries Management Corp., New York, N. Y.*

How to present working capital and plant expansion needs to investment banking sources is the subject of the talk by Mr. Bower, who is manager of a private capital fund. Mr. Bower will pinpoint essential operational and financial data which are usually absent when management seeking expansion funds initially introduces itself to investment banking sources. Specific suggestions, particularly for the electronics industry, to avoid pitfalls in capital requests will be offered.

5.4. Simulation Techniques for Understanding R and D Management

EDWARD B. ROBERTS, *Sloan School of Industrial Management, Mass. Inst. Tech., Cambridge, Mass.*

The growth of large-scale military and commercial R and D activities has created an urgent need for evolving a unified framework for understanding the problems of R and D management. Research in industrial dynamics in the Massachusetts Institute of Technology, School of Industrial Management, has resulted in a preliminary model of an R and D customer-producer-product system which promises to provide additional insight that will supplement the current intuition, judgment and experience of project managers and customers alike. The basic approach to the formulation of such an investigation and initial results of computer simulation revealing the time interaction of such factors as organizational structures, decision making policies, weapon systems characteristics, *et al.*, are discussed.

SESSION 6*

Mon.   2:30–5:00 P.M.

Coliseum
Morse Hall

PRODUCTION TECHNIQUES

Chairman: I. K. MUNSON, *RCA, Camden, N. J.*

6.1. Microcircuitry—A New Approach to Miniaturization, Producibility and Reliability

W. D. FULLER, *Varo Mfg. Co., Inc., Garland, Tex.*

Microcircuitry is the technology of design and fabrication of physically small electronic circuits. This is a technology which utilizes the electrical properties of thin films and the assembly of those thin films into electronic circuits fulfilling specified operational requirements with a new degree of reliability termed intrinsic reliability. Microcircuitry is not a component assembly technology but is a circuit design and fabrication technology. It is concerned with the design of total describing functions and then the fabrication of those functions by an assembly of materials in an integrated structure which produces the specified circuit operation. The physical arrangement of the materials within the circuit structure is termed morphology.

The design techniques are based upon the use of passive and active RC networks of the distributed-parameter form. The fabrication is accomplished in a vacuum chamber using both simultaneous and sequential depositions of thin films of materials in a controlled program on a suitable circuit supporting structure. The operation of the circuit is dynamically monitored during fabrication to match the characteristics of an external standard.

Miniaturization is achieved by the elimination of the redundancy of supporting and connective materials inherent in the component assembly technology. Reliability is achieved by the fabrication in the relatively uncontaminated atmosphere of a vacuum chamber and through the use of uncontaminated materials. Equivalent component densities exceeding one million per cubic foot have been achieved in a great variety of circuits by this technology.

6.2. Insulated Flexible Printed Wiring Techniques

W. B. WILKENS, *Sanders Associates, Inc., Nashua, N. H.*

This paper presents new techniques for designing completely insulated flexible printed circuits suitable for replacing conventional wire assemblies in components, electronic and electrical equipment, aircraft, missiles, appliances, and other devices. Various types of connectors suitable for use with flexible printed wiring are also reviewed.

Methods are described for designing shielded cables, multiconductor simulated coaxial cables, matrix assemblies for cables with feeder arms, simulated twisted conductors, preforming cables, multilayer wiring harness and for attaching to various types of connectors. Techniques for simplifying the assembly of high density wiring in assemblies will be reviewed. Typical examples of each method will be shown as well as a comparison between conventionally wired packages and the flexible printed wiring counterpart.

6.3. A Semiautomatic Transistor Testing Machine

ED MILLIS, *Texas Instruments Inc., Houston, Tex.*

A semiautomatic transistor testing machine suitable for production use is described. Up to 18 go, no-go tests may be performed with a maximum of 10 sorting categories. A 15-bit temporary memory in the form of a punched card is carried along with each transistor as it is moved down the test line. Sorting is done from the information punched on the card with a mask and photocell. Acceptable units or selected rejects are automatically removed from the machine and put in bins. Automatic calibration and fail-safe features are incorporated. Testing rate is 1200 per hour.

6.4. The Development of Automatic Machinery for Making Electron-Tube Stems

MATTHEW M. BELL, *RCA, Harrison, N. J.*

Of all electron tubes manufactured in 1957, the greatest number (in excess of 450,000,000) were receiving tubes and the greatest portion of these were 7- and 9-pin miniature type tubes. Obviously high-speed machines are needed to produce the parts required to make these tubes. Moreover, not all the tubes manufactured meet specifications, and many more parts are needed to meet industrial needs than the actual net output of good 7- and 9-pin miniature tubes would indicate. Losses also occur in manufacturing the parts because not all parts meet specifications either.

In almost all of the tubes made a stem is used. The stem consists of wires molded into glass, onto which the internal tube structure is built and to which the envelope is later sealed.

In 1957, with allowance for shrinkage and other waste factors, approximately 350,000,000 7- and 9-pin miniature stems were manufactured. This paper discusses some of the problems peculiar to the manufacture of electron-tube stems and the development of stem-making machinery.

6.5. Microminiaturization

DAVID W. MOORE, *Servomechanisms, Inc., El Segundo, Calif.*

Several approaches to the microminiaturization of electronic circuitry are discussed with particular reference to the use of evaporated film materials as a microcircuit building block. The preparation of mechanically and electrically stable magnetic, dielectric, and conducting film materials is briefly touched upon together with methods for depositing laminated microcircuits. The interaction of magnetic domains in evaporated nickel iron films for the derivation of logic and memory functions for digital computers is presented as a recent breakthrough in the microcircuit art. Solid state microcircuits are described and discussed in some detail.

SESSION 7*

Mon.   2:30–5:00 P.M.

Coliseum
Marconi Hall

NAVIGATION AND TRAFFIC CONTROL

Chairman: L. B. HALLMAN, JR.,
Dayton, Ohio

7.1. Loran-B Precision Navigation

WILLIAM J. ROMER, *U. S. Coast Guard, Washington, D. C.*

The Loran-B precision navigation technique is described. An inshore navigation system of extreme precision is developed through extension of the standard Loran-A pulse-matching technique by addition of phase-comparison time-difference measuring techniques. These techniques eliminate the deterioration in accuracy attributable to skywave contamination of the groundwave signals which usually limit the accuracy and reliability of phase-comparison navigation systems. Time-difference readings are completely unambiguous throughout the total system coverage. Existing Loran-A pulse shape, frequency band and pulse repetition rates are utilized. This is a preliminary report containing a general discussion of the Loran-B technique and the equipment designed for its implementation.

7.2. A Synthetic Future Environment for Analysis of Radar Beacon System Capacity

A. ASHLEY AND F. H. BATTLE, JR., *Airborne Instruments Lab., Mineola, N. Y.*

A mathematical model representing the 1960 New York environment affecting the capacity of the air traffic control radar beacon system has been developed to evaluate the effects of changes in system parameters. Computations are based on the geographical coordinates of existing ground stations and of a realistic pattern of air traffic. The area coverage of each interrogator radiation pattern is simulated by equivalent geometric shapes, and the combined influence of all stations on the reply rate from each aircraft is calculated. Transponder efficiencies, averaged over a short time interval, have been predicted for various AOC reply limit and transponder dead-time settings and for various sidelobe suppression techniques.

7.3. Air Traffic Control Computer

A. G. VAN ALSTYNE AND M. N. NOTHMAN, *Gilfilan Bros., Los Angeles, Calif.*

The computer described in this paper is a special-purpose digital machine intended for use in an enroute air traffic control application. The primary function of the computer is to clear flight plans by checking for conflict with previously cleared flight plans and to reroute as necessary to avoid conflict. A secondary function is that of tracking and flight following, enabling aircraft progress to be monitored for conformance to plan; in cases of nonconformance the affected flights are automatically re-scheduled. A third function is the continuous check of all flights for possible predicted conflict and issuance of control orders to resolve conflict.

This paper will briefly discuss the evolution of a consistent and practical control philosophy and will then outline the various functions which must be performed to implement the chosen approach. Each of these functions is then discussed in relation to its significance for

computer parameters and programming considerations. The computer configuration required by the above functions is next considered, and the special characteristics required by the problem are emphasized. The paper concludes with a comparison between the computer capabilities and those of available equipments.

7.4. Use of Airport Surface Detection Radar as a Tool in Airport Research

MARTIN A. WARSKOW, *Airborne Instruments Lab., Mineola, N. Y.*

Airport surface detection equipment (ASDE) short-range K-band radar has been installed atop the control tower at New York International Airport. This very high resolution radar presents a picture of the airport on its PPI scope. The presentation is such that aircraft or other objects on or over the paved surface show up against a dark background, including sufficient detail to show the heading and profile of the aircraft. Techniques have been developed for photographing the PPI scope and presenting the photographic record for analysis. This record, when combined with information obtained from the radio communications between the control tower and aircraft pilots, can be very useful to analyze many airport problems. For example, the efficiency of runway use both procedurally and due to physical layout can be examined to derive means of improvement. Other examples of the use of the ASDE data to analyze airport problems are discussed.

7.5. An Improved Instrument Low Approach System Compatible with TACAN

M. KARPELES AND E. G. PARKER, *ITT Labs., Inc., Nutley, N. J.*

ITT Laboratories has continued the development of an improved instrument low approach system (ILAS) compatible with the TACAN system. In addition to the normal TACAN bearing and distance service, complete ILAS service may be provided through the addition of a one-pound box to the airborne interrogator (the AN/ARN-21).

Application of new principles to the ground equipment provides immunity to the effects of changing ground reflectivity and general reduction of siting effects.

The system provides for continuous lateral and vertical guidance information and distance to touchdown. Course softening is provided through the distance facility.

SESSION 8*

Mon.　　　　　　**2:30–5:00 P.M.**

Coliseum
Faraday Hall

ELECTRONIC DEVICES

Chairman: W. J. PIETENPOL, *Sylvania Electric Products Inc., Woburn, Mass.*

8.1. The Field Effect Tetrode

H. A. STONE, JR., *Bell Telephone Labs., Inc., Murray Hill, N. J.*

A new semiconductor device has been developed which, in addition to functioning as an improved field effect transistor, can be used as an impedance inverter or "gyrator," a large signal nonmodulating electronically variable resistor, or, in a two-terminal configuration, as a short-circuit-stable negative resistance.

The device can be likened to a field effect transistor having two opposing channels, each of which serves as a gate for the other. It comprises a single junction in a semiconductor crystal separating thin n and p regions. Each region has two contacts so located so that when the junction is reverse biased the current paths in the two regions are parallel to each other and to the junction. Field effect device theory has been applied to the structure, and it is shown that the field effect transistor is a special case.

Laboratory models have been made using silicon crystals with diffused junctions. Measurements on these confirm their predicted behavior.

8.2. A Theory of the Tecnetron

A. V. J. MARTIN, *Elec. Eng. Dept., Carnegie Inst. Tech., Pittsburgh, Pa.*

The tecnetron is a semiconductor amplifying device using the centripetal striction due to the field effect applied to a cylindrical structure. It embodies one metal-to-semiconductor rectifying contact.

Its physical operation is briefly outlined. A first-order analysis is carried out and provides simple expressions for the important characteristics of the device. Practical conclusions are drawn and typical values of the parameters are indicated. The effect of the simplifying assumptions on the analysis is discussed. Equivalent circuits are given, and a few possibilities are outlined.

8.3. A Simple and Flexible Method of Fabricating Diffused *N-P-N* Silicon Power Transistors

L. D. ARMSTRONG AND H. D. HARMON, *RCA, Somerville, N. J.*

This paper describes a simple and flexible method of fabricating diffused n-p-n silicon junction transistors. The fundamental processes which make the method novel are the diffusion and the contacting operations. Diffusion is accomplished by diffusing simultaneously from a phosphorous-doped prediffused layer source and a boron-doped oxygen-vapor source. The contacting is performed by a combination of nickel plating and conventional photoresist masking techniques. The conditions of process control, the advantages of the process, and the electrical parameters of typical units are given.

8.4. A 20-Ampere Switching Transistor

T. P. NOWALK, *Westinghouse Electric Corp., Youngwood, Pa.*

Fused silicon transistors with current ratings of 10–20 amperes have been developed for switch and Class A applications. (Maximum operating voltages up to 300 volts are characteristic.) The units are designed to function in ambient temperatures closely approximating allowable junction temperatures for silicon devices, or about 150°C. This is made possible by the inherently low saturation resistance of the subject devices—less than 0.1 ohm at rated output current. Thus, in the switching mode, the new series of transistors is capable of handling as much as 6 kw.

8.5. Drift Considerations in Low-Level Direct-Coupled Transistor Circuits

J. R. BIARD AND W. T. MATZEN, *Texas Instruments Inc., Dallas, Tex.*

A modification of the low-frequency T equivalent circuit is presented for use in the analysis and design of transistor dc amplifiers. Generators are included which account for variations of I_{co}, V_{br} and α. Temperature dependence of I_{co}, V_{br} and α is shown in terms of the static input and transfer characteristics for typical silicon and germanium transistors. Expressions for equivalent input drift of single-ended and differential amplifiers are developed which provide information for the design of input stages with optimum dc stability.

8.6. Video Crystal Tester

Y. J. LUBKIN, *Airborne Instruments Lab., Mineola, N. Y.*

A compact, battery-operated, dc tester has been designed to determine the microwave parameters of video-detector crystals. Consistent results have been obtained with quantities of up to 50 each of various diode types, ±1 db accuracy on tangential sensitivity determinations being readily obtainable. Operation of the tester is little more difficult than operation of a Wheatstone bridge. Mixer diodes may be tested on the video crystal tester to the same accuracy as existing mixer diode testers. A prototype unit has been in regular operation since August, 1957.

SESSION 9*

Tues.   **10:00 A.M.–12:30 P.M.**

Waldorf-Astoria Starlight Roof

NEW TECHNIQUES FOR ANALYSIS

Chairman: JOHN R. RAGAZZINI, *College of Engineering, New York University, New York, N. Y.*

9.1. Simplified Method of Determining Transient Response from Frequency Response of Linear Networks and Systems

VICTOR S. LEVADI, *Dept. Elec. Eng., The Ohio State University, Columbus, Ohio*

Knowing the frequency response of a linear system, a method is presented for obtaining the time response of the system to a unit impulse, step, or ramp function without performing graphical integrations. The transient response is of the form:

$$f(t) = \sum_{i=0}^{N} A_i G(\omega_{it})$$

where a different function G is used for each of the three types of inputs. Tables of the functions G are provided.

Unlike other methods of obtaining transient response, this method satisfies the condition that the transient response begins at zero when $t = 0$. The numerical computations of this method are well adapted to programming the entire problem for a digital computer. Two examples are presented.

9.2. A New Method of Analysis of Sampled-Data Systems

ATHANASIOS POPOULIS, *Polytech. Inst. Bklyn., Brooklyn, N. Y.*

In many sampled-data systems the sampling interval T is made sufficiently small, so that the response r^* will closely approximate the output r of the system without the sampler. In such cases one is interested in determining the "error" $r^* - r$ as a function of T. With the usual methods of analysis the resulting expressions are not easy to interpret.

In this paper a new approach is used; the response r^* is written as a power series in T whose coefficients can be simply evaluated in terms of the continuous response and the Bernoulli numbers. This expression results from the Euler summation formula. For small T only the first few terms are significant; one can thus simply determine the maximum T for a permissible error.

The method is applied to a servosystem with a sampler; a system function $\bar{H}$ is defined which is rational in p and whose inverse gives the actual response at the sampling points. The singularities of $\bar{H}$ are then obtained by a displacement of the singularities of the continuous system function; this displacement is easily evaluated for a given T.

9.3. Statistical Filter Theory for Time-Varying Systems

E. C. STEWART AND G. L. SMITH, *Ames Res. Center, Moffett Field, Calif.*

An analytical approach is presented which

is applicable to the optimization of time-varying systems operating with inputs which are contaminated with noise. A large and important class of such systems are those which utilize radar range information, such as the homing missile which is used as an example. The effects of 1) target evasive maneuver, 2) noise, 3) missile maneuverability, and 4) the inherent time-varying characteristics of the kinematics are considered simultaneously. Although an exact analytical solution of the equations does not appear feasible, it is shown that many approximate solutions utilizing time-varying control systems can be found. Examples of the method are given.

9.4. On the Phase Plane Analysis of Nonlinear Time-Varying Systems

RICHARD WHITBECK, *Cornell Aeronaut. Lab., Inc., Buffalo, N. Y.*

A phase plane technique, based on Lienard's construction, is developed. The basic geometric simplicity of Lienard's construction is emphasized in order that the moderate complications necessary to handle very general nonlinear second-order differential equations will be clearly understood.

Still retaining the basic geometric ideas previously developed, the use of velocity-displacement and velocity-time phase planes are introduced to demonstrate the applicability of the technique for the analyses of systems which are time variable in addition to being nonlinear.

In the special case where the describing differential equations for a system are "piecewise linear" (and time does not occur explicitly), the technique reduces to one of simple geometric constructions. It is felt that the simplicity of the geometry involved yields a near optimum phase plane technique from the standpoint of constructing a solution curve in the shortest possible time. To demonstrate this, the technique is applied to an inertially damped position servomechanism with saturation in the forward loop.

9.5. On the Use of Growing Harmonic Exponentials to Identify Static Non-linear Operators

J. H. LORY, D. C. LAI, AND W. H. HUGGINS, *Elec. Eng. Dept., The Johns Hopkins University, Baltimore, Md.*

Consider a static system whose output $F(x)$ for an input x may be approximated by $hx + mx^2 + dx^3$. For an input $x = e^t$, $t < 0$, the approximate output is $he^t + me^{2t} + de^{3t}$. It is shown that one can filter the output into these positive neper "harmonic" components and that their values sampled at $x = 1$ when $t = 0$ will be identically equal to the coefficients h, m and d. The filter described in this paper minimizes the error integral

$$\int_{-\infty}^{0} [f(t) - he^t - me^{2t} - de^{3t}]^2 dt$$

so that the cubic approximation to $F(x)$ will be the best in a weighted least-square sense with a weighting factor $1/x$.

SESSION 10*

Tues. **10:00 A.M.–12:30 P.M.**

Waldorf-Astoria
Astor Gallery

NUCLEAR INSTRUMENTATION TECHNIQUES—1

Chairman: A. B. VAN RENNES,
Bendix Aviation Corp.,
Detroit, Mich.

10.1. A Transistorized Nuclear Reactor Count Rate Channel

J. H. CAWLEY, *General Dynamics Corp., San Diego, Calif.*

A transistorized count rate and log count rate channel has been developed for use in bringing the Trigger nuclear research reactor from the source count range into the intermediate power range. This instrumentation must respond to fission counter pulses with rise times of the order of 0.25 μsec and 200 μv in amplitude. The channel includes a low-noise preamplifier which will drive up to 100 feet of coax cable, a 4-stage pulse amplifier, Schmitt trigger-type discriminator, pulse shapers, diode storage counter, and a relatively new linear count rate circuit of high accuracy. A pulse-type amplifier capable of driving an 8-inch speaker giving an audible output is also provided.

10.2. Transistorized Source-Range Reactor Instrumentation

R. R. HOGE, *Bendix Aviation Corp., Detroit, Mich.*

The advent of high-frequency semiconductor triode and tetrode transistors permits the design of reliable count-rate circuits for source-range reactor instrumentation. Fully transistorized circuits are described which compute reactor power at source levels based on thermal neutrons observed with a proportional counter. Reactor power is indicated in terms of the average number of counts per second on a logarithmic scale covering nearly six decades. The complete system includes circuits which quasi-differentiate the logarithmic power signal and thus determine reactor growth factor or period. Design philosophies are described which permit use of 200-foot cables between the proportional counter and the pulse amplifiers without need of coupling transformers or preamplifiers.

10.3. A Two-Dimensional Kicksorter

ROBERT CHASE, *Brookhaven National Lab., Upton, L. I., N. Y.*

A pulse height analyzer which records the relative pulse height distribution of coincident pulses will be described. The kicksorter accepts coincident pulse pairs and tallies them in storage locations whose address is determined by the height of both pulses. There are 3072 storage locations arranged in a 96×32 matrix on a high-speed magnetic drum. Serial binary arithmetic is used with each storage location having a capacity of 16 binary bits. Single path reading and writing is used to reduce the memory access time. Magnetic head paralysis problems are avoided by storing successive bits in a given channel on different magnetic tracks. Four channels of temporary address storage are employed which reduces the average memory access time to 1250 μsec with a 6000-rpm drum. The two address coordinates are obtained using conventional height to time conversion techniques. Except for the cathode-ray tube display section, the instrument is completely transistorized.

10.4. A Transistorized Pulse Height Analyzer

R. T. GRAVESON, *U. S. Atomic Energy Commission, New York, N. Y.*

A scintillation detector has a pulse height output which is a linear function of the energy of impinging gamma radiation. The function of the pulse height analyzer system is to determine the amplitude distribution of this train of pulses which are randomly distributed in time. The system must also display this information in a form convenient for analysis. This unit has been completely transistorized to provide reliability. The use of transistors, through size reduction of the equipment and reduced power consumption, has simplified its application to measurements in the field.

Transistor circuits are described for pulse amplification, pulse amplitude discrimination and for pulse shaping by a 1-μsec monostable trigger. An expander amplifier system is used which improves the stability of the gate setting, which may be set from 0.05 to one volt wide. This unit will accept pulses whose amplitudes lie between 0.2 and 10 volts and whose rise times are between 0.1 and 0.3 μsec. It will operate to a maximum rate of approximately 100,000 pulses per second.

SESSION 11*

Tues. **10:00 A.M.–12:30 P.M.**

Waldorf-Astoria
Jade Room

BROADCASTING—I

Chairman: RAYMOND F. GUY,
National Broadcasting Co.,
New York, N. Y.

11.1. FM Carrier Techniques in the RCA Color Video Tape Recorder

R. D. THOMPSON, *RCA Labs., Princeton, N. J.*

The advantages of a frequency-modulated carrier system for recording color TV signals are stated in terms of the fundamentals of a magnetic tape medium.

By use of a vestigial sideband technique, satisfactory performance is obtained with a magnetic system bandwidth equal to less than twice the desired video bandwidth. Modulator and demodulator circuits are described.

The principal distortion in the FM circuitry is a spurious component having a frequency equal to twice the difference between the carrier frequency and the modulating frequency. The origin and magnitude of this component is discussed.

11.2. A Deleter-Adder Unit for TV Vertical Interval Test Signals

J. R. POPKIN-CLURMAN AND F. DAVIDOFF, *Telechrome Mfg. Corp., Amityville, L. I., N. Y.*

For the past two years, television broadcasters have enthusiastically accepted the use of a vertical interval test signal which is broadcast simultaneously with programs. This test signal occurs for two or three horizontal lines per field at the end of the vertical blanking interval. These vertical interval signals are regularly used to provide peak white and black reference levels and test transmission network characteristics for both color and monochrome programs. The potential uses of the signals for control and automation have been discussed in previously presented papers.

The present paper describes a new device which extends the usefulness of the vertical interval test signal concept. This device permits any vertical interval test signal present on a program to be deleted and a new test signal added. This procedure permits various portions of a television facility to be independently checked and evaluated since a new or more appropriate test signal can be applied to each portion. This new deleter-adder unit is automatic in that it senses the presence or absence of an incoming vertical interval test signal and automatically controls its deletion and/or the addition of a local test signal.

11.3. An Electro-Servo Control System Capable of Correcting 0.05-μsec Rotational Errors

WILLIAM BARNHART, *Ampex Corp., Redwood City, Calif.*

In videotape recording, one of the problems inherent in the use of multiple rotating heads that sequentially scan a moving strip of magnetic tape transversely to the tape motion is the possibility of time discontinuities in the reproduced information at the point of transition between succeeding heads. This time error can occur because the tape, while being scanned, is stretched to some extent by the action of the heads as they force the tape into a grooved female guide. If, for any of several reasons, the degree of tape stretch during reproduction is different from that during recording, time discontinuities may occur. This paper describes a servomechanism and error-sensing device that has been developed to correct such errors automatically to within 0.05 μsec by mechanically repositioning the female guide.

11.4. Transistorized Video Switching

J. W. WENTWORTH, C. R. MONRO, AND A. C. LUTHER, JR., *RCA, Camden, N. J.*

A remotely controlled switching system employing semiconductor diodes and transistors has been designed for television program assembly service. Known as the RCA TS-40, the system comprises a series of compact, plug-in modules for building systems of up to 24 inputs and 10 outputs. The actual switching elements are diodes, which are biased "off" and "on" by transistorized flip-flops. Picture transitions require less than 3 μsec and are timed to occur at the end of vertical blanking. Illustrations are provided of practical applications of the TS-40 equipment to broadcast station operations.

11.5. A New Approach to Low Distortion in a Transistor Power Amplifier

H. J. PAZ, *RCA, Camden, N. J.*

The product designer has been for sometime in pursuit of a low-distortion high fidelity transistor power amplifier that does not require laboratory adjustment and selection of *PNP* power transistors.

The main problem is that most of the present amplifiers require a power transistor with a beta cutoff frequency of about 30,000 cps for low-distortion at 15,000 cps. Presently available power transistors like the 2N301 have a beta cutoff frequency of about 6000 to 9000 cps. Some of the reasons for distortion in the midband of a power amplifier are as follows: 1) Beta mismatch of the output power transistors. 2) Variation of the input impedance with drive signal. 3) Change in beta with base current drive.

The new approach described here, takes into account the limitations of presently available power transistors. Very few, if any, power transistor manufacturers have a rigid maximum and minimum specification on parameters like beta and beta cutoff frequency. This approach shifts the dependance for low-distortion from the power transistor to the circuit design. Negative feedback can be used to improve frequency response and reduce distortion. However, in an amplifier made up of four or five stages, too much loop feedback may result in oscillation. The phase shift in each stage of a transistor amplifier is great, hence the total phase shift of the amplifier limits the maximum amount of loop feedback. The "hybrid" all-transistor power amplifier, to be described here, uses local negative feedback on each stage to reduce phase shift and distortion.

The new approach used here is a "hybrid" of the "series" and "quasi-complementary" transistor power amplifiers. This circuit is composed of a class-A driver stage which is directly coupled to a complementary-symmetry phase inverter. This is directly connected to two *PNP* series transistors operating in Class B which are used to drive the output pair of *PNP* series transistors.

The "hybrid" power amplifier is part of a transistor monitor amplifier which is designed for use in broadcast studios. The circuit requires ten transistors to provide a gain of 104 db. Input and output transformers are used to provide circuit isolation. The input impedance is 37.5, 150 or 600 ohms. The output transformer can handle loads of 4, 8, 16, 150, or 600

ohms. The maximum output level is 12.6 watts (+41 dbm) and the total harmonic distortion at 10 watts is less than $\frac{1}{4}$ per cent over the frequency range of 30 to 15,000 cps. The amplifier remains cool when operating with the maximum program level. The maximum input level the amplifier can handle is −30 dbm. An etched wiring circuit board is used for product uniformity. A thermistor is used to provide temperature stability to 55°C.

The use of transistors in the monitor amplifier eliminates the problem of hum microphonics and heat. Transistors permit a closer packing of amplifiers in the already cramped space of a studio.

SESSION 12*

Tues.   10:00 A.M.–12.30 P.M.

Waldorf-Astoria
Sert Room

CONTRIBUTIONS TO STEREO SOUND REPRODUCTION

Chairman: S. J. BEGUN, *Clevite Corp., Cleveland 10, Ohio*

12.1. The "Null Method" of Azimuth Alignment in Multitrack Magnetic Tape Recording

A. G. EVANS, *RCA, Indianapolis, Ind.*

When re-recording from a stereo tape to make a monophonic recording the azimuth alignment of the stereo reproduce head relative to the recording is very critical if satisfactory frequency response is to be obtained. An investigation of various methods for obtaining correct azimuth alignment resulted in the development of a technique which has been dubbed the "null method." This technique makes possible a very simple and accurate procedure for correct azimuth adjustment and greatly reduces the possibility for misalignment. Applications for this method are suggested which should be useful in the laboratory, in the recording studio and in the testing of tape equipment on the production line.

12.2. Three-Channel Stereo Playback of Two Tracks Derived from Three Microphones

PAUL W. KLIPSCH, *Klipsch and Associates, Hope, Ark.*

Three-channel stereo from two sound tracks is an established art with remarkably simple implementation. Experiments on two-track tape recordings made with three microphones indicate that center events are retained in focus regardless of polarity of the tracks.

Where a center microphone is mixed equally into the two tracks and three-channel playback is by the substractive phantom system, the third microphone would be cancelled out. A phase-shifting network is employed to restore the center channel.

12.3. Study of a Two-Channel Cylindrical Ceramic Transducer for Use in Stereo Phonograph Cartridges

CARMEN GERMANO, *Clevite Electronic Components, Cleveland, Ohio*

An analytical as well as experimental evaluation of the equivalent circuit constants of a two-channel element for use in stereophonic phonograph cartridges is presented. The element is a cylindrical structure fully electroded on the inside surface. The outside surface has four electrodes centered 90° from each other with a substantial margin between them. The element is polarized in such a manner as to produce effectively two parallel-type benders located at right angles to each other.

The electromechanical equivalent circuit chosen to represent this element is based on the analogy between mechanical and electrical vibrating systems and is a modification of the electromechanical circuit proposed by Mason. It is made up of lumped electrical and mechanical parameters in combination with an ideal transformation ratio.

Along with this evaluation, a brief discussion of the performance characteristics of a cartridge utilizing this element will be presented.

12.4. The Single Stereophonic Amplifier

B. B. BAUER AND J. M. HOLLYWOOD, *CBS Labs., Stamford, Conn.*

The single stereophonic amplifier is briefly described. This amplifier handles both the left and right signals with the same pair of output tubes. The circuit is analyzed for the theoretical requirements for good separation and low distortion. The separate amplification of two signals is obtained by adding a matrixing output transformer. The turns ratio for ideal left and right separation is established for a circuit with finite plate and load impedance. Next, the effect of finite primary inductances on performance is determined. The influence of negative feedback on separation and distortion is analyzed, and stability conditions discussed.

12.5. A Frame-Grid Audio Pentode for Stereo Output

J. L. McKAIN AND R. E. SCHWAB, *Sylvania Electronic Tubes, Receiving Tube Operations, Emporium, Pa.*

A dual pentode using a single cathode, two separate *Framelok* grids and a twin-plate structure contained in one envelope is described. This new pentode, known as Type 6DY7, is a high performance tube with superior characteristics of uniformity and stability obtained from its unique structure. Such factors as greater tube-to-tube characteristics uniformity, reduced characteristic spread, and less susceptibility to characteristic deterioration at high dissipations can be obtained.

This dual pentode offers extrem fleexibility in application. Three basic configurations are: 1) sections operated separately (single-ended) giving 5 to 6 watts of audio power per section, 2) two sections in push-pull, Class AB_1 provid-

ing up to 20-watts output at less than 3 per cent distortion, and 3) two tubes in push-pull parallel.

A single tube can be used for two stereo output channels, or two tubes can be operated in push-pull for higher power requirements. The same advantages can be used for monaural audio systems.

The tube, therefore offers the circuit designer a choice of usage not possible in presently available tubes and at cost advantages realizable through a reduction in the number of circuit components.

12.6. Design Considerations for Stereo Cartridges

J. H. McConnell, *Electro-Sonic Labs., Inc., Long Island City, N. Y.*

In designing stereo cartridges every effort must be made to reduce the mass, increase the compliance of the vibratory system and decouple the transducer system serving one channel from the transducer system serving the other. Because of the minute dimensions of the linkage connecting the stylus to the two generators and the need for a rugged and reliable device with consistent performance, advanced techniques of miniaturization must be employed. By reference to one cartridge the mechanical problems confronting the designer and their solution will be reviewed.

12.7. Status Report on Stereophonic Recording and Reproducing Equipment

W. S. Bachman, *Columbia Records, New York 19, N. Y.*

The large mechanical accelerations required of disc recording heads imposed severe limitations on their design. Stereo disc cutters in commercial use are discussed with respect to these requirements, and a figure of merit for rating them is suggested. Currently available reproducing pickups for stereo disc records are described along with means for equalization and evaluation of them. Some amplifier problems peculiar to stereo reproduction are noted. The performance of several types of loudspeaker array for stereo reproduction is discussed, and the over-all system performance is compared with present day monophonic recording and reproducing systems.

SESSION 13*

Tues.   10:00 A.M.–12:30 P.M.

Waldorf-Astoria Grand Ballroom

ENGINEERING MANAGE-MENT—II

Chairman: Gerald A. Rosselot, *Bendix Aviation Corp., Detroit, Mich.*

13.1. The Advanced Research Projects Agency—Operations and Plans

J. E. Clark, *Advanced Res. Projects Agcy., The Pentagon, Room 3-E172, Washington, D. C.*

13.2. Planning and Managing a Multi-Company Electronic Systems Program

E. G. Fubini, *Res. & Eng. Div., Airborne Instruments Lab., Mineola, N. Y.*

13.3. Intra-Company Systems Management

H. H. Goode, *Bendix Systems Div. and Prof. Elec. Eng., University of Michigan, Ann Arbor, Mich.*

SESSION 14*

Tues.   10:00 A.M.–12:30 P.M.

Coliseum Morse Hall

MEDICAL ELECTRONICS—I

Chairman: John W. Moore, *National Institutes of Health (NINDB), Bethesda, Md.*

14.1. A Data System for Physiological Experiments in Satellites

Miles A. McLennan, *Wright Air Dev. Center, Wright-Patterson AFB, Ohio*

The integrity of experiments involving animals or man in earth satellites is threatened by the uncertainty of securing coherent experimental records. This paper describes some of the factors and problems concerned with the over-all vehicle-to-ground complex and offers a design philosophy for a high integrity data reporting system to meet the conditions. The basic precept is the selection and encoding of key experimental information and the accordance of high transmission priority to that information. Consideration is given to techniques of selection, reduction and transmission of both physical and physiological types of data. Of note is a method suggested for establishing a viability index of the experimental subject.

14.2. A Logical Structure for Diagnosis Based on Probability

Stanley Rush, *Dept. Elec. Eng., Syracuse University, Syracuse, N. Y.*

In this paper, an attempt is made to create a logical structure for diagnosis. The model is probabilistic in nature, and the diagnosis procedure is treated as a problem in inverse probability. Terms such as symptom and syndrome take on added significance when defined on the basis of probability. These definitions plus others lead to a general diagnosis procedure which in turn specifies the nature of the statistics required for diagnosis. The conclusion is reached that, without further basic scientific advancement, much could be done to improve medical diagnosis efficiency by proper utilization of existing or presently obtainable data.

14.3. Microwave Radiation as a Tool in Biophysical Research

C. Susskind, B. S. Jacobson and S. B. Prausnitz, *University of California, Berkeley, Calif.*

Whole-body irradiation of mice by electromagnetic energy at a wavelength of 3 cm, carried out in the course of investigations of the microwave radiation hazard, has demonstrated the usefulness of such radiation as a method of studying thermal balance in mammals. An analysis is presented that accounts for observed temperature changes during and after irradiation on the basis of theoretical considerations of thermal disequilibrium.

14.4. The Reliability Problem in Machines and in Nature

W. B. Bishop and J. A. LaRochelle, *Air Force Cambridge Res. Center, Bedford, Mass.*

Certain new criteria for reliability in machines are presented, and the importance of studying reliability mechanisms in nature is emphasized. Discussed in some detail are failure detection and redundancy. Several approaches to the problem of compensating for failure are presented. Hopes for more reliable and self-compensating mechanisms inherent in future design are offered.

14.5. Respiratory Control of Heart Rate: Laws Derived from Analog Computer Simulation

Manfred E. Clynes, *Rockland State Hospital, Orangeburg, N. Y.*

The change in heart rate from beat-to-beat caused by respiration in the resting state can be predicted on the analog computer. If a signal proportional to chest circumference is fed into the analog computer, it can calculate the complex heart rate changes in real time and record the output as a rate, along with that of the real heart. Correspondence between real and simulated rates, regardless of mode of breathing, establishes laws resulting in new insights into the neural mechanisms involved. The results illustrate the usefulness of control system theory as applied to biological systems and bring out special problems associated with nonlinear characteristics particular to biological systems.

SESSION 15*

Tues. 10:00 A.M.–12:30 P.M.

Coliseum
Marconi Hall

LAND AND SPACE ELECTRONICS

Chairman: VERNON I. WEIHE, *4133 N. 33rd Rd., Arlington, Va.*

15.1. Application of Satellite Doppler-Shift Measurements

Part I—Satellite Frequency Measurements

O. P. LAYDEN AND H. D. TANZMAN, *U. S. Army Signal Res. and Dev. Lab., Fort Monmouth, N. J.*

The investigation being carried on in the USASRDL on the radio observations of signals from the Russian and American satellites is discussed. Various plots of frequency vs time are given for the Russian and American satellites in orbit as well as take-off curves for all American satellites. The equipment used to obtain Doppler measurements is described and the frequency and time accuracy associated with the system is discussed.

Part II—Slant Range at Nearest Approach

H. P. HUTCHINSON, *U. S. Army Signal Res. and Dev. Lab., Fort Monmouth, N. J.*

The use of a single Doppler-shift recording of earth-satellite transmissions, combined with the orbital data associated with that passage, yields a method of obtaining the slant range from observer to the point of nearest approach of the satellite. From this slant range and the orbital height given by the ephemeris, the position of ground zero at the point of nearest approach was obtained. This provides an accurate fix of the orbital ground track in the area of local observation, thus providing data for orbital correction.

A theoretical Doppler-shift curve (calculated, using this slant range, the satellite velocity from orbital data and the velocity of light) is compared with actual observations on both 20- and 40-mc transmissions and good agreement is obtained. The small systematic differences between the calculated and observed values are attributed to the effects of ionospheric refraction.

15.2. Sputnik II as Observed by *C*-Band Radar

DAVID K. BARTON, *RCA, Moorestown, N. J.*

The AN/FPS-16 radar on Grand Bahama Island obtained two extended tracks on Sput-

nik II during February, 1958. Observed signal strength corresponded to a target cross section of several hundred square meters, and the signal was still strong when the maximum range of the tracking system was reached at 260 nautical miles. Presence of a pair of corner reflectors is proposed to explain the unexpectedly strong signal at 5480 mc. Details of the signal strength and servo error signal records are believed to establish other facts as to structure of the rocket and placement of the reflectors.

15.3. Free-Rotor-Gyro Stabilized Inertial Reference Platform

T. MITSUTOMI, *Autonetics, Downey, Calif.*

Stabilization of an inertial reference platform using free-rotor gyroscopes is discussed in this paper. Brief consideration is first given to the characteristics of the gyros. Then, the analysis of the three-axes stabilized platform is undertaken, including the basic equation of motion of the stabilized platform. The rotor of a free-rotor gyro is supported and turns on a spherical, gas-lubricated bearing. The rotor is given angular freedom about transverse axes (to a limited degree), and thus a single unit may be used to sense angular dips and stabilize the inertial platform about two orthogonal axes. With a gas-lubricated bearing, dynamic interaxis coupling between the rotor and the supporting member is very small. However, because of the precise performance required, their effects must be and are considered in determining the requirements of the servosystem.

The gyro is used essentially as a "dip meter" in that the reference signal is taken about the same axis as that being stabilized. By this direct measurement of the platform dip angle, the servosystem becomes a very simple second-order type with considerable gain margin and no gyro cross coupling (as in the single-axis gyro case).

Finally, the servoamplifier requirements are described. The simple compensation required eases considerably the amplifier design problem, especially from the standpoint of noise and saturation.

15.4. Ground Clutter Isodops for Coherent Bistatic Radar

HERBERT A. CROWDER, *Hughes Aircraft Co., Culver City, Calif.*

Isodops are lines of constant Doppler shift on the earth's surface relative to a moving receiver and/or transmitter. Such contours define a region which represents the effective radar cross section of the earth for coherent, velocity gated receivers. Though the monostatic, or active case, in which the transmitter and receiver have a common location and velocity, is well known, the bistatic case in which the two velocities and/or locations differ is more involved. A general equation is formulated for the bistatic isodops. Applications to important problems in radar engineering are developed.

15.5. Land Vehicle Guidance by Radar

Y. CHU AND P. N. BUFORD, *Westinghouse Electric Corp. Baltimore, Md.*

At the inception of a large-scale federal program of building tens of thousands of superhighways during the next decade, automatic driving of land vehicles becomes an interesting and important subject. This paper reviews the historical points of interest of land vehicle guidance, discusses the various methods of land vehicle guidance, and presents a system for land vehicle guidance by means of a radar.

The radar guidance system employs a radar guidance line which can be a foil-strip or a painted-strip placed along the roadway. The radar system tracks this guidance line, develops a steering error signal for indication to the driver of steering error and for automatic steering control of the vehicle.

A simple microwave pulse radar is described with an interesting feature that a klystron is to function not only as a transmitter, but also as a modulator, as a RF amplifier and as a video detector. This gives an unusual simplicity. Other features of the radar are fixed antenna, no moving parts, extremely low power, extremely narrow pulse width, and all weather capability. Selection of optimum radar parameters determined by a system analysis for *x*-band and *k*-band frequencies is presented. Size and weight burdens to the vehicle are anticipated to be small.

A radar system for land vehicle guidance possesses important growth potentials. Among them are indication of range, closing-rate and collision signal, and panoramic display of roadway and its neighboring area. Another important growth potential is the capability to read code from a coded guidance line. This will make it feasible for programmed coast-to-coast automatic driving during day and night and during clear and foul weather.

SESSION 16*

Tues. 10:00 A.M.–12:30 P.M.

Coliseum
Faraday Hall

PANEL: WIDENING HORIZONS IN SOLID-STATE ELECTRONICS

Chairman: EARL L. STEELE, *Hughes Products Group, Los Angeles, Calif.*

16.1 Ferrites and Micro-wave Solids

C. L. HOGAN, *Motorola, Inc., Phoenix, Ariz.*

16.2 Solid-State Energy Sources

W. J. VANDER GRINTEN, *General Electric Co., Electronics Lab., Syracuse, N. Y.*

16.3 Advanced Semiconductors

W. M. WEBSTER, JR., *RCA, Somerville, N. J.*

SESSION 17*

Tues.   2:30–5:00 P.M.

Waldorf-Astoria
Starlight Roof

INFORMATION THEORY

Chairman: M. J. E. GOLAY, *Consultant, 116 Ridge Rd., Rumson, N. J.*

17.1. Information Rate from the Viewpoint of Inductive Probability

L. S. SCHWARTZ, B. HARRIS, AND A. HAUPTSCHEIN, *College of Engineering, New York University, New York, N. Y.*

Carnap has developed a concept of inductive probability which is potentially important for radar and communications because it provides a logical method of system operation when *a priori* information regarding signal and noise statistics is unavailable. The advantage of inductive probability is that it permits the information rate to be estimated from the received signal without knowledge of the signal-to-noise ratio.

This paper applies Carnap's concept of inductive probability to determine the inductive information rate of a binary communication system employing decision feedback. The effects of fluctuating SNR are considered. A possible instrumentation of a maximum rate system operating on the principle of inductive probability is discussed.

17.2. Binary Relay Communication and Decision Feedback

JOHN J. METZNER, *New York University, Bronx, N. Y.*

Relay stations may be more limited in decoding ability than the final receiver. The question of best coding procedure subject to such a limitation is investigated with respect to information capacity and error probability criteria. The case in which the relays are capable only of making a decision on each individual digit is also analyzed.

When the relay computations are not limited there is still a question of optimum relay operation. It is found best with some exceptions to relay the most probable message if the receiver selects only the most probable message. If the receiver also records nulls, an indication of degree of certainty may be desirable.

Various ways of applying decision feedback with relay communication are described and compared.

17.3. Results of a Geometric Approach to the Theory and Construction of Nonbinary, Multiple Error and Failure Correcting Codes

B. M. DWORK AND R. M. HELLER, *Westinghouse Electric Corp., Baltimore, Md.*

A general approach to the study of nonbinary, multiple error and failure correcting codes is possible through the application of the theory of vector spaces over Galois fields. Interesting connections with the theory of finite projective geometries are noted. Most of the codes considered by Hamming, Reed-Muller, Slepian, and Ulrich are included as special cases. Simple procedures are outlined for designing, encoding, and decoding systematic codes of desired error correcting abilities with alphabets of *l* letters where *l* is any power of a prime number.

17.4. An Application of the Theory of Games to Radar Reception Problems

NILS J. NILSSON, *Rome Air Dev. Center, Griffiss AFB, Rome, N. Y.*

The problem of radar reception in the presence of jamming is treated by an application of the theory of games. The game formulation used is as follows: assume the radar receiver employs a matched filter, matched to the radar echo signal. Let the choices of band-limited power spectral distributions for both the radar signal and the jamming noise constitute the respective strategy decisions for the radar operators and the jammers. Games with strategies of this type are known as function-space games. Then, for various pay-off functions such as the receiver output signal-to-noise ratio, the mean-squared time error in target location, and the mean-squared Doppler frequency error, optimum spectral strategies can be specified for each opponent. A new expression for the output SNR is derived which reduces to the familiar $2E/N_0$ for the case of constant density noise. When this general expression for SNR is the game pay-off function, the optimum spectra can be shown quite simply to be constant density band-limited spectra for both the radar signal and the jamming noise. To solve the games using time error and Doppler frequency error as pay-off functions, some special theorems are developed. These theorems reduce certain function-space games to games played on the unit square. Optimum strategies for games with these two pay-off functions turn out to be other than simple constant density spectra.

17.5. Perceptron Simulation Experiments

FRANK ROSENBLATT, *Cornell Aeronaut. Lab., Inc., Buffalo, N. Y.*

An experimental simulation program, which has been in progress at the Cornell Aeronautical Laboratory during the last year will be described. This program uses the IBM 704 computer to simulate perceptual learning, recognition, and spontaneous classification of visual stimuli in the perceptron, a theoretical brain model which has been described elsewhere. The paper will include a brief review of the theory of the perceptron, a description of the 704

simulation programs which have been completed to date, and a series of slides showing experimental results. The problem of simulation vs model construction for programs concerned with the study of theoretical brain models will be discussed.

SESSION 18*

Tues.   2:30–5:00 P.M.

Waldorf-Astoria
Astor Gallery

NUCLEAR INSTRUMENTATION TECHNIQUES—II

Chairman: DANIEL I. COOPER, *Nucleonics Magazine, New York, N. Y.*

18.1. A Transistorized Cold Cathode Decade Counter

H. SADOWSKI AND M. E. CASSIDY, *Atomic Energy Commission, New York, N. Y.*

A unit module decade counter having visual and electronic readout is described. The circuit consists of a transistor blocking oscillator driving a cold cathode decade counter tube. The waveform criteria for successful operation are discussed. The counter tube has individual cathode outputs and several units may be connected in parallel to a 10-digit bus bar system for reading out on command at a remote station.

18.2. A High Sensitivity Semiconductor Diode Modulator for DC Current Measurement

HAROLD E. DEBOLT, *Fairchild Camera and Instrument Corp., Syosset, L. I., N. Y.*

A semiconductor diode modulator will be described capable of measuring dc currents down to 10^{-16} to 10^{-11} amperes. This modulator utilizes one diode although a second is normally installed for balance purposes in high sensitivity measurements. The modulator utilizes pulse techniques instead of sine waves which makes possible the high sensitivity. The circuit details of the modulator and the design criteria will be discussed.

18.3. Control Concepts for Nuclear Ramjet Reactors

R. E. FINNIGAN, *Livermore Lab., Livermore, Calif.*

The nuclear ramjet application places requirements on the reactor control system which are considerably more stringent than those

found in most reactor systems. This paper will outline the control concepts which have been formulated for Tory II, the first test reactor in the nuclear ramjet program. The design of the multimode control system used for control of reactor power level will be described in detail; synthesis of "optimum" automatic control system has been carried out using frequency response and root-locus methods in conjunction with both digital and analog computers.

18.4. Low Background Nuclear Counting Equipment

H. D. LEVINE, R. T. GRAVESON AND A. L. CHARLTON, *Atomic Energy Commission, New York, N. Y.*

By selection of materials and development of new components and techniques, the residual background count of beta counting equipment can be reduced down to 0.1 count per minute. Both direct counting and coincidence counting apparatus are described since the elimination of cosmic ray events by coincidence plus gamma ray shielding permits the reduction of counting rates far beyond that obtainable with shielding alone. Geiger counter and scintillation counter devices are described. Data on cosmic ray guard performance using a hollow anode geiger counter are presented as well as data for rings of conventional geiger counters. A simple apparatus with low background is shown to have high reliability for normal use as well as for measurement of soft beta emitters such as carbon 14.

SESSION 19*

Tues.   2:30–5:00 P.M.

Waldorf-Astoria Jade Room

BROADCASTING—II

Chairman: FRANK L. MARX, *American Broadcasting Co., New York, N. Y.*

19.1. Possibilities of Major Simplifications in Color Television Live Cameras and Recording Devices Through the Use of Chroma Field Switching and Subsequent Automatic Color Balance

WM. L. HUGHES, *Iowa State College, Ames, Iowa*

Major problems in color telecasting are the complexity, control difficulties, and economic cost of the various equipments required. This paper discusses a method of making major simplifications in color television live cameras by cutting the number of camera tubes from three to two (one of which is narrow band). The method also simplifies the problems of re-

cording the color TV information on magnetic tape or black and white film. Further, the method would simplify the problem of sending the color signal over long microwave networks since the signal would be free of susceptibility to differential phase or envelope delay errors. When finally rebroadcast, the signal can be made completely compatible with current NTSC-FCC color standards.

19.2. Report of TASO Committee 3.3 on Correlation of Picture Quality and Field Strength

C. M. BRAUM, *Joint Council on Educational TV, Washington, D. C.,* AND W. L. HUGHES, *Iowa State College, Ames, Iowa*

One of the activities of TASO Panel 3 was to make a study of the correlation between television picture quality and field strength at both UHF and VHF. Teams of broadcast engineers made house interviews while field strength measurements were made in the street in front of the house. Data were obtained on the average performance in the field of television sets at UHF and VHF. It was possible to split the data to get some measure of the spread of receiver performance in adequate signal strengths as well as a measure of picture degradation due to signal strength reduction. Considerable data will be presented.

19.3. Report of TASO Committee 5.4 on Forecasting Television Service Fields

ALFRED H. LaGRONE, *University of Texas, Austin, Tex.*

An empirical method for forecasting the signal strength in the primary and secondary service areas of television stations at both VHF and UHF is presented. The importance of the path topography in the method is amply demonstrated. Other parameters important to the method are discussed and recommendations made as to their use in making a forecast.

Measured fields for a number of radials representing extreme variations in terrain are compared with the forecast fields for the same radials. Cross-correlation coefficients of 0.85 between the measured and forecast fields are obtained in many cases. The cross correlation is generally smaller for radials where the rms deviation of the signal from the mean is small.

19.4. A New Wireless Microphone for TV Broadcasting

PETER K. ONNIGIAN, *KBET-TV, Sacramento, Calif.*

A fully transistorized wireless microphone meeting the new FCC Rules on such devices is described. Using wide-band FM the unit is completely self-contained, except for microphone. No external separate antenna is used. Weighing less than 15 ounces with batteries, it is approximately the size of a package of king-size cigarettes. Any high quality 150-ohm microphone of studio quality may be used. Audio quality is commensurate with standard studio microphones. Battery life is over 5-hours continuous use, and much greater with on-off use.

19.5. A Television Program Automation System Using Beam Switching Tubes with Shift Register Circuitry

F. CECIL GRACE, *Visual Electronics Corp., New York, N. Y.*

This paper describes an electronic system for automatic program switching in a television station master control room. All events which have been set into the equipment are continuously displayed to the operator in the order in which they are to occur. Changes or corrections can be made on any stored event at any time. When an event occurs, the indication describing it disappears from the top of the panel; all other indications shift up one position. Vacant positions at the bottom can be filled at any time either manually or by a punched card or tape device. Beam switching tubes are used to store the information providing an extremely high degree of reliability.

SESSION 20*

Tues.   2:30–5:00 P.M.

Waldorf-Astoria Sert Room

SPEECH AND CIRCUITS

Chairman: W. O. SWINYARD, *Hazeltine Research, Inc., Chicago, Ill.*

20.1. Speech Bandwidth Compression with Vocoders

F. H. SLAYMAKER, *Stromberg-Carlson Co., Rochester, N. Y.*

Speech information may be transmitted over a bandwidth one-tenth that required for the original speech if attention is directed toward reproducing the envelope of the frequency power spectrum rather than the waveform itself. Pitch information can be transmitted independently of the spectrum information and the two sets of signals combined at the receiving end to resynthesize the original speech sounds. In the vocoder the power spectrum is analyzed and synthesized by means of band-pass filters. The pitch of the voiced sounds is obtained from an oscillator called a buzz source and the sounds of the fricative consonants are obtained from a white noise source. Various vocoder effects will be demonstrated.

20.2. Audio Applications of a Sheet-Beam Deflection Tube

J. N. VAN SCOYOC, *Armour Res. Found., Illinois Inst. Tech., Chicago, Ill.*

A number of unusual audio circuits has been developed which make use of a sheet-beam tube, type 6AR8. The 6AR8 tube is a miniature double-plate sheet-beam tube which incorporates a pair of balanced deflectors to direct the electron beam to either of the two plates and a control grid to vary the intensity of the beam.

This tube may be connected as a variable gain push-pull amplifier by connecting the input signal between the two deflectors and taking the output differentially between the two plates. When the tube is connected in this manner the amplifier gain is determined by the control grid voltage and may be varied over an 80-db range with negligible distortion.

The applications of this circuit include expansion and compression circuits, remote control of gain and wiring circuits, improved AVC circuits and phase inversion. A number of these circuit arrangements is given in some detail and other applications are outlined.

20.3. A Drift-Free Direct-Coupled Amplifier Utilizing a Clipper-RC Feedback Loop

J. N. VAN SCOYOC AND E. S. GORDON, *Armour Res. Found., Illinois Inst. Tech., Chicago, Ill.*

A direct-coupled drift-free amplifier has been developed utilizing a combination clipper and RC feedback loop. Although the developed circuits utilize vacuum tubes, transistors can be employed. Theory of operation, gain and phase shift equations, and curves are given for both a simple RC feedback loop and the clipper-RC loop. An existing application of the amplifier is described for aerosol single particle counting with dynamic range of 4000 to one. Possible future applications include a direct current amplifier with SPST chopper and a system for recording up to 20-μv inputs with a single intermediate amplifier.

20.4 The Application of the Voltage Variable Semiconductor Capacitor in Automatic Sweep Circuits and "Signal Seeking" Receivers

J. BLACK, *1010 E. Imperial Highway, El Segundo, Calif.*

The basic method of automatic frequency sweep by charging a silicon capacitor is presented and the advantages over mechanically driven tuning capacitors are discussed. The principle is extended by using the receiver automatic gain control for sweep control and station tracking and practical circuits are shown embodying the principle. Applications in the AM and FM fields such as domestic and car radio receivers and television "space command" sets are proposed. The present limitations of the silicon capacitor and their effects on the application field are discussed.

20.5. An Analysis of a Transistorized Class "B" Vertical Deflection System

Z. WIENCEK AND J. E. BRIDGES, *Warwick Mfg Corp., Chicago, Ill.*

Class *A* transistorized vertical deflection system is not satisfactory for portable TV operation because it requires heavy iron-cored components and excessive power consumption. To date, a class *B* vertical deflection system was considered impractical, although theoretically such a system could overcome the disadvantages of the class *A* approach.

An analysis of a working, class *B* (push-pull) vertical deflection system will be made with special consideration being given to the retrace problem. Other considerations such as linearity, transistor requirements, and driver circuits will be discussed.

Full 90°, 15,000-volt vertical deflection with a retrace time less than 800 μsec has been achieved with power consumption less than one-fourth of that for a comparable class *A* vertical deflection circuit.

SESSION 21*

Tues.   2:30–5:00 P.M.

Coliseum
Morse Hall

MEDICAL ELECTRONICS—II

Chairman: LESLIE E. FLORY, *Rockefeller Inst. Med. Res. and RCA Labs., Princeton, N. J.*

21.1. Recent Advances in Medical Electronics

V. K. ZWORYKIN, *Rockefeller Inst. Med. Res. and RCA Labs., Princeton, N. J.*

The importance of electronic techniques in medical research and practice is receiving increased recognition at home and abroad. This has resulted in various efforts to extend communication and promote activity in the field which are, in large part, international in scope. Some of these are sketched briefly. In addition, attention is directed toward a number of new electronic tools for medicine which have evolved in the last few years in the United States and elsewhere. Ways are indicated for increasing further the effectiveness with which engineering knowledge may be applied to medical problems.

21.2. An Electronic Electrode

J. W. MOORE AND J. DEL CASTILLO, *Nat. Inst. Neurological Diseases and Blindness, Nat. Inst. Health, Bethesda, Md.*

The application of well-known principles of feedback amplification provides a powerful new tool for measurement of potentials at an inaccessable point in single nerve fibers. The potential inside a node measured with a high input impedance electrometer lets the outside of the node in question and a killed adjacent one is at best only approximate because of an unknown and usually varying leakage along the outside of the fiber across an air gap. Two feedback configurations may be used to reduce the leakage current by a large factor so that both the resting and action potential inside the node may be measured with accuracy and speed.

21.3. Transistor Waveform Generators

G. N. WEBB AND R. N. GLACKIN, *Dept. Medicine, The Johns Hopkins Hospital, Baltimore, Md.*

Three basic transistor circuits are described, operation is explained, and critical design features are outlined. The units are: a positive or negative going linear ramp, a pulse generator and a flip-flop. Ways of interconnecting these building blocks to make 1) a voltage controlled frequency modulator, 2) a triggered, linear sawtooth with duration from 100 μsec to 200 seconds, 3) trapezoid stimulating waveforms with separately controlled rise, dwell and fall time, and 4) delay units for physiological stimulating programs are illustrated. Construction features which help to minimize temperature effects are shown. Performance characteristics under operating conditions are presented.

21.4. Cardiac Pacing-Stimulation by Very Portable Equipment

DAVID G. KILPATRICK, *Itronic Products, Inc., Bala-Cynwyd, Pa.*

The physiological development, performance and application of a new pocket, transistorized battery-powered system that internally monitors and paces the heart without thoracotomy is described. Experimental study of current vs voltage stimulation sources and of impulse waveform and duration are reported. A new method of electrode position determination is traced from concept to equipment.

Development of equipment requirements and techniques, including human engineering experiments with various types of indicators and controls, is described.

Present and future application of production equipment to specific cardiac malfunctions is discussed.

21.5. The Design of a Fetal Phonocardiotachometer

HERBERT S. SAWYER, *Airborne Instruments, Mineola, N. Y.*

Fetal-heart rate has been found to be a convenient and reliable yardstick of fetal distress. This paper describes an instrument that has been designed to provide continuous recordings of heart rate by measuring the beat-to-beat intervals of the heart sounds. The system basically comprises a microphone, an amplifier and filter, a heart-beat detector, a ratemeter and a graphic recorder.

The major design problems centered on the filter and heart-beat detector. Since theoretical design was impractical, it was necessary to use an empirical approach, which was made possible by the use of tape-recorded fetal heart sounds. A detailed description of the final design is presented.

SESSION 22*

Tues.   2:30–5:00 P.M.

Coliseum
Marconi Hall

RELIABILITY TECHNIQUES

Chairman: R. M. Jacobs,
*Sylvania Electric Products,
Inc., Waltham, Mass.*

22.1. Development and Utilization of Redundant Systems

S. Nozick, *Hughes Aircraft Co.,
Tucson, Ariz.*

Studies have shown that redundant systems using standard parts are much more reliable than conventional systems with specially chosen parts. The considerations unique in planning, developing and using redundant systems which are presented are based on experience and differ from conventional practice.

The differences that must be considered before deciding on redundance over conventional design are presented. The types of redundant systems and their theoretical and practical merits are presented for the system planner. Since the state of the art requires a specially trained and organized engineering group, the way to alter existing groups to achieve this is presented. Field use also requires an altered philosophy in the routine of repair. Almost all maintenance is reduced to a predictable routine.

22.2. High Reliability Statistically Demonstrated

Barton L. Weller, *Vitramon,
Inc., Bridgeport, Conn.*

To offer a high reliability product at reasonable price, more numerous, rapid, less-expensive tests are distributed throughout the production operation. This procedure has been included in an intensive quality control program which has been functioning for over three years. During this time the effectiveness of the methods has been proved by the observable rise in quality of the produced electronic component part. Today this part has reached quality levels with failure rates of less than 0.5 per cent per 1000 hours on a production basis. Data to confirm this quality are offered each purchaser of these parts. Numerous, short-term life tests provide a statistical basis for selecting in-process material for final processing. Herein are presented tabulations showing the progress of this program. The effects on the ARL of the end item by rejecting partly processed material can be seen.

22.3. Circuit Redundancy

James H. S. Chin, *Sperry Gyroscope Co., Great Neck, N. Y.*

The subject of redundancy has been appearing quite frequently in the literture. However, more often than not, they remain only as mathematical models which are important, of course, in advancing the state of the art, but to an engineer they are of no particular value. The purpose of this paper is to bring forth the practical application of redundancy.

This paper will be in two parts. In Part I, "parallel-redundancy" and "standby-redundancy" will be analyzed and evaluated in terms of reliability gain over a nonredundant system. In Part II, practical methods of failure detection for use with "standby-redundancy" will be discussed. Among these methods are: 1) signal sampling, 2) signal injection and 3) signal comparison. Typical applications and practical circuits will be included.

22.4. An Original Reliability Program for a Development Project

K. S. Packard, *Airborne Instruments Labs., Mineola,
N. Y.*

This paper describes a comprehensive reliability program for use on a development project. The techniques employed in working with the development, design and fabrication groups are described. The activities of the reliability group, including system analysis, part evaluation, circuit tolerance testing, and reliability control are discussed. Testing techniques are described and results presented. The means used to inform design engineers on reliable design techniques are described. These include a parts manual and a reliability handbook. The project organization cost and group relations are discussed.

22.5. Failure Indication Considered as a Problem in Sequential Analysis

Walton B. Bishop, *Air Force Cambridge Res. Center,
Bedford, Mass.*

In Wald's "Sequential Analysis" (John Wiley and Sons, Inc., New York, N. Y., 1947) it was shown that sequential analysis can provide decisions more efficiently than those based upon a fixed sample size. The need for decisions concerning the operating condition of electronic equipment has led to the consideration of built-in test equipment in the form of failure-indicating modules (see W. B. Bishop), "The failure-indicating module," 2nd Annual Joint Military-Industrial Test Equipment Symposium, Washington, D. C., October, 1958). This paper describes failure indication as a basic problem in sequential analysis and suggests some approaches to an efficient failure-indication technique for electronic equipment.

SESSION 23*

Tues.   2:30–5:00 P.M.

Coliseum
Faraday Hall

MICROWAVE TUBES

Chairman: V. R. Learned,
*Sperry Gyroscope Co.,
Great Neck, N. Y.*

23.1. Microwave Detection with Vacuum Tube Diodes

N. E. Dye, J. Hessler, Jr., A. J. Knight, R. A. Miesch and G. Papp, *ITT Labs., Fort Wayne, Ind.*

Several articles have appeared in the literature during the past few years describing a theory of microwave detection using hard vacuum diodes. In an attempt to verify the theory and to produce an efficient detector, several types of diodes were built and tested at Farnsworth Electronics between 1955 and 1957.

Theoretical calculations based on a resonant type diode using assumed parameter values led to the prediction that a vacuum diode detector should produce results comparable to those obtained from a crystal diode. Coaxial-type diodes and planar diodes were mounted in X-band rectangular waveguide. Variations were made in inner and outer diameters of the coaxial diodes and in the spacing of the planar diode in an attempt to optimize the detected output. It was shown conclusively that detection in hard vacuum diodes is possible and that the behavior of the detected output as a function of different parameters was as predicted by theory; however, the magnitude of the detected signal was 10–100 times smaller than expected. Possible explanations of the poor performance are presented along with suggestions for further investigations.

23.2. Priming Techniques for Reducing Jitter on Pulsed Reflex Klystrons

Paul A. Crandell, *National Co.,
Inc., Malden, Mass.*

Whenever a reflex klystron is used in pulsed operation there is an accompanying jitter on the front edge of the pulse, which is of the order of 30 to 100 mμsec wide depending on the method of pulsing and the external load which the klystron sees. For many applications this jitter could not be tolerated. This paper will describe the theory of front edge jitter and proposes a method of correction. The theory will be substantiated by experimental proof.

23.3. A Multiple Frequency Local Oscillator

Charles W. Flynn, *ITT Labs.,
Nutley, N. J.*

A method is described whereby a multiplicity of local oscillator signals may be generated by the use of serrodyne techniques. The present investigation covers carrier frequencies of 3.0 and 3.3 kmc and modulation frequencies of 50 and 150 mc. As many as ten local oscillator frequencies of useful amplitude have been obtained. The adaptation of a commercially available traveling-wave tube to this application is described. The relationship between calculated and experimental results is examined for specific modulation indexes.

23.4. Selective Signal Suppression and Limiting in Traveling-Wave Tube Amplifiers

H. J. WOLKSTEIN AND E. KINAMAN, RCA, Harrison, N. J.

It is well known that a traveling-wave tube will amplify signals of more than one frequency simultaneously with negligible interaction as long as the total input RF power does not drive the tube into saturation. Not so well known is the performance of the traveling-wave tube in amplifying low-level signals in the presence of RF power as high as 30 db over that required to saturate the traveling-wave tube. The drop in gain of the low-level signal has been found to be, in general, proportional to the input power, and inversely proportional to the frequency of the large signal. However, the complexity of beam bunching above saturation results, for each tube type, in different rates of low-level signal suppression. In some cases, when the tubes are overdriven too far, this bunching produces a tendency for the suppression to actually decrease. Saturation characteristics in the presence of overdriving signals and the effect on gain and power output are considered. Improvements in traveling-wave tube tandem system operation and amplitude distortion are also described.

23.5. A New Backward-Wave Oscillator for the 4- to 5-MM Region

J. A. NOLAND AND L. D. COHEN, Sylvania Electric Products, Inc., Bayside, N. Y.

The design and performance of a new backward-wave oscillator electronically tunable over the frequency range of 60 to 75 kmc is described. This tube development was carried out for the Evans Signal Laboratory under Contract DA-36-039-sc-70178. The average power output over this band is 4 mw and the minimum power output at any point in the band is 1 mw. The tube employs a minimum magnetic field of 1200 Gauss, has a maximum beam voltage of 1850 volts and is of all metal and ceramic construction. RF and gun design considerations, constructional details and techniques are discussed. A total of 12 tubes were constructed and the effects on RF performance of six design modifications are described. Experimental data are presented concerning RF cold-circuit attenuation, VSWR characteristics of the output match, window loss, tuning characteristics, and power output characteristics. A comparison between the experimental data and an analytical evaluation of tube performance is given.

SESSION 24*

Tues.   8:00–10:30 P.M.

Waldorf-Astoria
Starlight Roof

PANEL: FUTURE DEVELOPMENTS IN SPACE

Chairman: ERIC A. WALKER, *Pennsylvania State University, University Park, Pa.*

24.1 Space Philosophy

L. V. BERKNER, *Chairman, Space Science Board, National Academy of Sciences, Washington, D. C.*

24.2 Engineering Needs

F. H. GRISWOLD, USA, *Deputy Commander, Strategic Air Command, OFFUTT A.F. Base, Omaha, Neb.*

24.3. Space Vehicles

G. H. STONER, *Gen. Mgr., Dyna Soar Weapons System Div., Boeing Aircraft Co., Seattle, Wash.*

24.4. Space Engineering

O. G. VILLARD, JR., *Stanford University, Stanford, Calif.*

24.5. Communications and Data Transmission

G. S. SHAW, *Vice-Pres. Eng., Radiation, Inc., Melbourne, Fla.*

24.6. Space Navigation

L. E. ROOT, *Vice-Pres., Lockheed Aircraft Co., Sunnyvale, Calif.*

24.7. Military Applications

J. M. GAVIN (*Lt. Gen., USA, ret.*) *Arthur D. Little, Inc., Cambridge, Mass.*

24.8. Biophysical Problems of Space Travel

T. C. HELVEY, *Biophysics Dept., University of Kansas, Lawrence, Kan.*

24.9. Medical Aspects

O. H. SCHMITT, *University of Minnesota, Minneapolis, Minn.*

24.10. Space Science

H. E. NEWELL, *National Aero. and Space Agency, Washington, D. C.*

SESSION 25*

Wed.   10:00 A.M.–12:30 P.M.

Waldorf-Astoria
Starlight Roof

THE STATISTICAL THEORY OF SIGNALS AND CIRCUITS

Chairman: WILLIAM R. BENNETT, *Bell Telephone Labs., Inc., Murray Hill, N. J.*

25.1. Coding a Discrete Information Source with a Distortion Measure

CLAUDE E. SHANNON, *Mass. Inst. Tech., Cambridge, Mass.*

Consider a discrete source producing a sequence of message letters from a finite alphabet. A single letter distortion measure is given by a non-negative matrix (d_{ij}). The entry d_{ij} measures the "cost" or "distortion" if letter i is reproduced at the receiver as letter j. The average distortion of a communications system (coder-noisy channel decoder) is $d = \Sigma_{ij} P_i, d_{ij}$ where P_{ij} is the probability of i being reproduced as j. It is shown that there is a function $R(d)$ that measures the "equivalent rate" of the source for a given level of distortion. For coding purposes where a level of distortion can be tolerated, the source acts like one with information rate $R(d)$. Methods are given for calculating $R(d)$ and various properties discussed. Finally generalizations to distortion measures involving blocks of letters are developed.

25.2. The Probability Density of the Output of a Filter When the Input Is a Random Telegraphic Signal

J. A. McFADDEN, *School of Elec. Eng., Purdue University, Lafayette, Ind.*

Some new results have been obtained for the probability density of the output $y(t)$ of a linear system when the input $x(t)$ is a non-Gaussian process. The input considered is the "random telegraphic signal" *i.e.,* $x(t) = \pm 1$ with equal probability, and the zeros of $x(t)$ obey the Poisson distribution. The probability density $P(y)$ of the output is obtained when the system is 1) an RC filter; 2) an ideal integrator with finite memory. In case 1), $P(y)$ is proportional to a power of $(1 - y^2)$ when $|y| \leq 1$, and zero elsewhere. In case 2), $P(y)$ is given in terms of Bessel functions.

25.3. On the Solution of an Eigen Value Equation of the Wiener-Hopf Type Defined in Finite and Infinite Ranges

R. MITTRA, *Dept. Elec. Eng.,*
University of Illinois,
Urbana, Ill.

The paper is concerned with the solution of the eigen value equation of the type:

$$\phi(t) = \lambda \int_0^T K|t - \tau|\phi(\tau)d\tau \quad 0 < t < T \quad (1)$$

where

$$K|t - \tau| = \sum_{r=1}^n C_r e^{-k_r|t-\tau|}, \quad \text{Re}\,(k_r) > 0$$

The case of $T = \infty$ is also included in the discussion. The equation is of interest in the problems of estimation and detection of random functions.

For the particular case of $T = \infty$ it is possible to solve the equation by Wiener-Hopf technique which involves applying Fourier transforms in the complex plane. The method of transforms has also been applied by Youle in a paper, published in the September, 1957 issue of IRE TRANSACTIONS ON INFORMATION THEORY, to reformulate the eigen value problem in (1) for $T < \infty$.

The technique introduced here also finds use in the solution of the integral equation:

$$g(t) = \int_0^T f(\tau)K|t - \tau|d\tau$$

$$g(t) \text{ given for } 0 < t < T$$

which is of interest in the design of optimum filters for linear prediction of stationary processes.

25.4. Optimum Estimation of Impulse Response in the Presence of Noise

MORRIS J. LEVIN, *Dept. Elec. Eng.,*
Columbia University,
New York, N. Y.

The problem considered is that of estimating the impulse response of a linear system from a record of its input and output during a limited interval of time when the observed output is obscured by additive random noise. Statistical estimation theory is used to derive least squares and Markov estimates. No assumptions are required concerning the form of the input. The variances of the sampling errors are obtained and compared with those of other methods of measurement. The method of cross correlation of input and output is shown to be a large sample approximation to the least squares estimate.

25.5. An Approximate Method of Computing Modulation Products

JOEL L. EKSTROM, *Electronic*
Communications, Inc.,
Timonium, Md.

The characteristic function method of calculating the amplitudes of the modulation products resulting from the application of K sinusoids to an nth law rectifier is reviewed. It is shown that the exact solution of the problem is easy when K equals one, two, or is very large (Laplace approximation), but that it becomes difficult for K equal to three, and intractable

for K small but greater than three. A simple extension of the Laplace approximation is presented which gives good results for small K. Some examples for K equal to three and four and n equal to one and two are given; the results compare favorably with graphical integration techniques.

SESSION 26*

Wed.   10:00 A.M.–12:30 P.M.

Waldorf-Astoria
Astor Gallery

RADIO AND TELEVISION RECEIVERS

Chairman: R. R. THALNER,
Sylvania Electric Products
Inc., Buffalo, N. Y.

26.1. Considerations in Transistor Automobile Receiver Front-End Design

R. MARTINENGO, *Raytheon Manu-*
facturing Co., Needham Heights,
Mass.

This paper discusses the design of RF amplifiers and converter stages in a transistorized automobile receiver meeting current commercial specifications. Such problems as gain, noise figure, selectivity, image and IF rejection, and AVC are considered. Conventional fusion alloy units are used for both RF amplifier and converter stages.

26.2. A Five-Transistor Automobile Receiver Employing Drift Transistors

R. A. SANTILLI AND C. F.
WHEATLEY, *RCA, Somer-*
ville, N. J.

This paper describes a high-performance, low-cost, five-transistor automobile receiver which employs a new line of RCA transistors developed specifically for this application. The receiver lineup consists of an RF amplifier (2N640), a converter (2N642), an IF amplifier (2N641), a driver (2N217), and a 4-watt single-ended audio output stage (2N301). Drift transistors are used in the front end because of their high gain and low feedback capacitance. The circuit described has a sensitivity of 2 μv over the radio-broadcast band for an audio output of 1 watt (30 per cent modulation). Satisfactory performance of the receiver has been obtained at signal levels of the order of 1 volt.

26.3. Improvements in Detection, Gain Control, and Audio Driver Circuits of Transistorized Broadcast Band Receivers

R. V. FOURNIER AND D. THORNE,
RCA, Somerville, N. J.

This paper describes a unique approach to the problem of detection, AGC, and audio amplification in transistorized broadcast band receivers. Improvements in these receiver characteristics are made possible through the use of new devices developed specifically for the above applications. Recent improvements in device design and techniques allow for greater flexibility in obtaining detection, amplified AGC, and audio driver circuits using a minimum number of component parts. One of the salient features of the new units is that their utilization allows circuitry which gives increased detector efficiency at sensitivity levels of battery operated broadcast band receivers.

26.4. Application of Rotationally Nonsymmetrical Electron Lenses to TV Image Reproduction

D. TAYLOR, N. PARKER AND N.
FRIHART, *Motorola, Inc.,*
Chicago, Ill.

A brief history is given of early experiments in the use of unsymmetrical nonrotational fields as electron lenses. A description is given of the general form of this type of lens with specific reference to the four-pole magnetic type as the example. The physical properties of the magnetic lens such as configuration, field strength, orientation, etc., are given in addition to the electron optical properties of focal lengths, magnification ratios, aberations, etc. The use of these lenses in periodic combinations to form equivalent symmetrical lenses is discussed. A method of applying the negative lens component of the unsymmetrical lens for the refraction of deflected electron beams is described. Certain advantages of rotationally symmetrical negative lenses are examined. The paper concludes with a survey of the various methods of obtaining negative lenses of this type.

26.5. A High Sensitivity Ultrasonic Microphone

P. DESMARES AND R. ADLER,
Zenith Radio Corp.,
Chicago, Ill.

A new ultrasonic microphone is now in use in Zenith's remotely controlled TV sets. Its response is centered at 39.5 kc; it is of the piezoelectric type and combines a bandwidth of 5 kc with very unusual sensitivity.

A piezoelectric resonator normally has three characteristic properties: its electrical match to a vacuum tube is poor; its acoustical match to air is poorer still; and its bandwidth tends to approach zero.

How it was possible to design a microphone with outstanding performance in spite of these obstacles forms the subject of this paper.

SESSION 27*

Wed.   10:00 A.M.–12:30 P.M.

Waldorf-Astoria
Jade Room

COMPONENT PARTS—I

Chairman: JOSEPH KAUFMAN, *Office*
Chief of Ordnance, U. S. Army,
The Pentagon, Washington, D. C.

27.1. Progress Report on *ad hoc* Group Study on Specifications

E. J. NUCCI, *OASD Res. and Eng., The Pentagon, Washington, D. C.*

This paper gives a progress report on the *ad hoc* study covering electronic parts specification management for reliability, jointly sponsored by the Office of the Assistant Secretary for Defense (Research and Engineering) and Supply and Logistics. This includes consideration of adding reliability requirements and reliability assurance requirements to parts specifications. Methods of speeding up military specification coordination and methods of disseminating parts characteristics are included. Failure rates for design guidance and to assist logistics planning will be considered.

27.2. Trend of Things to Come

C. H. LEWIS, *ARDC, Andrews Air Force Base, Washington, D. C.*

Heretofore, the electronic component parts engineer has been able to use refined existing techniques, materials, and production methods to accomplish his mission. In this he had the benefit of many years of background knowledge, which was recorded by his predecessors. This is changing, for we are at the beginning of a revolution in the concept of building electronic equipment. The conventional components will disappear and their function will be taken over by specially designed materials, capable of performing single and multipurpose functions. This paper will treat in detail the knowledge and skills that must be acquired by the electronic specialists of the future.

27.3. Review of the Capacitor Art

LOUIS KAHN, *Aerovox Corp., New Bedford, Mass.*

The electronic components application engineer has the choice of many different capacitor types to perform electrical and electronic functions in electronic equipment. This paper will review the technological advances made in this field during the past decade and will examine capacitor types for various applications. The design engineer will be given data that will assist him in his choice and application of capacitors.

27.4. Electronic Materials—An Industry-Wide Problem

ALLAN M. HADLEY, *Advisory Group on Electronic Parts, Philadelphia, Pa.*

After a review of the reasons for the current emphasis on electronic materials, both in civilian industry and in the military, the government-sponsored research and development program in this area is reviewed and its basic objectives outlined. A brief discussion of probable long-term investigations in the area of electronic materials is followed by a listing of immediate materials requirements based on specific recommendations of qualified representatives of the Army, Navy, and Air Force.

Emphasis throughout the paper is directed at the need for close cooperation between industry and the military, and two procedures—one conventional and obvious, and the second of a less conventional nature—are proposed as avenues leading toward an improvement in the current materials situation.

27.5. A New Method for Maintaining Uniform Cooling Air Flow During Maintenance and Operation

ALBERT PERLMUTTER, *Sylvania Electric Products, Inc., Waltham, Mass.*

Many different designs have been evolved during past years for cooling digital computational equipments. The Sylvania Waltham Laboratories, in building the universal digital operational flight trainer, UDOFT, has developed a simple cooling method which should be applicable with many electronic systems. Every designer is faced with the dilemma of obtaining an optimum balance between ease of testing finished equipment and ease of construction testing of the first engineering system (system debugging). In the cooling plan used in UDOFT, both types of test work as well as system operation can be accomplished without disturbing the air flow path over any of the small plug-in package. Any package or all packages can be removed from their respective slots and all remaining packages will receive their same constant air supply. This is accomplished without any moving flow control devices and without gasketing seals. The hot spot temperature of the electron tubes and other heat sensitive parts is controlled by maintaining a known, fixed air flow through each individual package. This arrangement provides optimum thermal control of the system, thereby improving both component and total system reliability.

SESSION 28*

Wed.   10:00 A.M.–12:30 P.M.

Waldorf-Astoria Sert Room

DIGITAL TELEMETERING

Chairman: C. H. HOEPPNER, *Radiation, Inc., Melbourne, Fla.*

28.1. Digital-to-Analog Conversion and Multiplexing

D. BLOCK AND M. PALEVSKY, *Packard Bell Computer Corp., Los Angeles, Calif.*

The growing importance of converting digital information into analog form is discussed and a series of examples are cited. The need for multiplexing is considered. A number of conversion methods is explained together with the limitations of each. Multiplexing is next considered and methods for analog storage are evaluated. The use of the transfluxor to overcome the limitations of other approaches is described in detail.

28.2. A High-Speed, Airborne Digital Data Acquisition System

S. COGAN AND W. K. HODDER, *Consolidated Electrodynamics Corp., Pasadena, Calif.*

This paper describes certain details of a fully transistorized airborne PCM/FM data acquisition system capable of sampling 100 prime data channels at a rate of 500 samples per channel per second. This provides a frequency-handling characteristic of dc to 100 cps for each prime data channel. Subcommutation of any of the 100 prime data channels by factors of 10 or 100 allows a maximum handling capacity of 10,000 input data channels.

Flexibility through the use of modular components is discussed, and abbreviated and expanded systems are described.

The method of sampling and analog-to-digital conversion within an expandable system is described and the composition of transmitted data and alignment information is discussed together with the method of providing "real time" timing information. Provision is made for parallel readout to tape and serial readout to a telemetry transmitter.

28.3. A System for Editing and Computer Entry of Flight Test Data

S. F. HIGGINS, *Consolidated Electrodynamics Corp., Pasadena, Calif.*

This paper describes the system of editing and the provisions for computer entry of digital flight-test data as acquired by an integrated digital data system. Also described are system concepts that must be dealt with in solving problems incident to these activities.

Only a small percentage of information acquired during a short period of a test program is required in order to derive the fundamental information needed to determine the aircraft flight characteristics and to provide the information required for airworthiness certification requirements. For these reasons, the computer station is provided with editing control facilities that permit selection of desired prime and commutated channels which are believed to be essential or desirable for data reduction. Selection may be indicated by an airborne initiated event marker system or by the nature of the aircraft performance, as observed during flight test. The editing facilities provide for the most economic use of computer and manpower effort and are so designed that they permit convenient access to all instrumented channels.

28.4. The Use of a Fractional Bistable Multivibrator Counter in the Design of an Automatic Discriminator Calibrator

M. W. WILLIARD AND G. F. ANDERSON, *Dynatronics, Inc., Orlando, Fla.*

This paper deals with the development of a method of using bistable multivibrators to obtain fractional, rather than integral, frequency division. An application of a 382.5:1 counter for reduction of 367.2 kc to 960 cps for use in an automatic discriminator calibrator is discussed in detail, with additional discussion of selection of feedbacks in odd bistable counters to reduce even harmonic components.

28.5. Analysis of Multiplex Error in FM/FM and PAM/FM/FM Telemetry

J. SCHENCK AND W. F. KENNEDY, *AVCO Manufacturing Corp., Wilmington, Mass.*

A straightforward spectral analysis and synthesis is developed for practical models of standard FM/FM and PAM/FM/FM multiplex telemetry systems. Expressions are obtained for the outputs of a multiplex for given inputs and for nonlinear distortion and adjacent channel interference in terms of the conventional parameters of such systems. Automatic digital computation is employed not only for obtaining numerical solutions of the derived formulas, but it is also exploited as a means of testing a system model by experimental variation of the system parameters. The method of analysis and the results of the study are generally applicable to the design of communication systems involving FM.

28.6. Comments Relative to the Application of PCM to Aircraft Flight Testing

ROBERT S. DJORUP, *Epsco, Inc., Boston, Mass.*

The pending widespread use planned for PCM telemetry has caused some confusion in the area of PCM or digital standards. It is the purpose of this paper to discuss proposed PCM standards on a realistic basis and to show by example the organization of an integrated digital flight test system using these standards. Consideration is given to the variety of testing applications and ultimate usage of digital flight test data. The inherent flexibility and versatility of digital instrumentation and data processing are stressed.

SESSION 29*

Wed.　　10:00 A.M.–12:00 NOON

Waldorf-Astoria Grand Ballroom

SYMPOSIUM: PSYCHOLOGY AND ELECTRONICS IN THE TEACHING-LEARNING SYSTEM

Chairman: F. E. TERMAN, *Stanford University, Palo Alto, Calif.*

29.1. Teaching Machines

B. F. SKINNER, *Harvard University, Cambridge, Mass.*

29.2. Teaching Physics by Television

H. E. WHITE, *University of California, Berkeley, Calif.*

29.3. Preliminary Studies in Automated Teaching

R. F. MAGER, *U. S. Army Air Def. Human Res. Unit, Fort Bliss, Texas*

29.4. Problems and Possibilities of Electronic Systems in Higher Education

C. R. CARPENTER, *Pennsylvania State University, University Park, Pa.*

SESSION 30*

Wed.　　10:00 A.M.–12:30 P.M.

Coliseum Morse Hall

COMMUNICATION BY SCATTER SYSTEM

Chairman: DAVID S. RAU, *RCA Communications, Inc., New York, N. Y.*

30.1. Predicting the Performance of Long-Distance Tropospheric Communication Circuits

A. P. BARSIS, K. A. NORTON AND P. L. RICE, *National Bureau of Standards, Boulder, Colo.*

Performance of long-distance tropospheric communication circuits is predicted in terms of the probability of obtaining a specified grade of service or better for various percentages of the time. The grade of service is determined by the minimum acceptable ratio of hourly rms carrier to rms noise for the type of intelligence to be transmitted. It is shown that the prediction errors, expressed in decibels, have a standard deviation which depends upon the percentage of hours the specified grade of service is required and on the angular distance characterizing the propagation path. Finally, it is shown to what extent this standard deviation may be reduced by making path loss measurements, thus increasing the reliability of prediction.

30.2. A Study of the Economic and Technical Feasibility of Utilizing Tropospheric Scatter Links in the National Network of Korea

C. A. PARRY, *Page Communications Engineers, Inc., Washington, D. C.*

In 1957–1958 one of the most intensive studies for the utilization of tropospheric scatter circuits on a national scale was undertaken under contract to the ICA/Washington, D. C. This was an investigation into the economic and technical feasibility of incorporating such circuits into the primary trunk network of the Republic of Korea. As part of this study, a survey team was sent to investigate the practicability of possible sites and to assess communication problems particular to that country. This work was coordinated with the Department of Communications of the Overseas Economic Commission and the Ministry of Communications in Korea.

In order to evaluate the economic and technical difficulties associated with various circuit alternatives, use has been made of a performance index and means of deriving and utilizing this are shown. Consideration was also given to planned system expansion in accordance with probable economic growth. It is estimated that the required service with up to 36-channel capacity can be obtained with transmitter power of 1000 watts and better than 99.9 per cent reliability.

30.3. A Formalized Procedure for the Prediction and Analysis of Multichannel Tropospheric Scatter Circuits

C. A. PARRY, *Page Communications Engineers, Inc., Washington, D. C.*

An analytical procedure is outlined, which permits scatter links carrying different volumes of traffic on different numbers of channels with varying grades of service and reliabilities to be compared. The method is a step-by-step process commencing with site survey. The steps involve the determination of such factors as scatter angle, design error, instantaneous fade margin, diversity method, and medium aperture loss. Data are presented which permit evaluation of channel load capacity, intermodulation noise from feeder echo and interference from neighboring carriers with multichannel modulation. Correction for white noise test data is included. The means of utilizing these data with respect to the given and required performance parameters is presented. Performance index, economic index, and design efficiency factors are determined; these may then be used as a basis for the comparison of different paths and routes under varying traffic conditions when utilizing the scatter mode of propagation.

30.4. Multibeam Transhorizon Tropospheric Communications

J. H. VOGELMAN, J. L. RYERSON AND M. BICKELHAUPT, *Rome Air Dev. Center, Griffiss AFB, Rome, N. Y.*

Present transhorizon tropospheric circuits are limited by the incoherent nature of the scatter medium. This results in an upper limit on achievable antenna gains and bandwidths which leave as a final limitation the state-of-the-art maximums in power tube outputs. In order to receive the benefits of equivalent powers in excess of those available, many feeds and transmitters using different center frequencies are used in a single dish and received by a similar array of feeds. The resulting advantage may be exploited in terms of either reliability or system range enhancement.

30.5. Simplified Base-Band Diversity Combiner

R. T. ADAMS, *ITT Labs., Nutley, N. J.*

By a modification of the conventional diode-limiter circuit, the limiter-demodulator section of an FM receiver can be made to yield base-band output proportional to RF signal level. Signals recovered from a set of FM receivers of this type can be used in diversity by simple linear addition of the base-band outputs.

A common AGC circuit, such as used in predetection combining, together with a new cross-coupled limiter used in the last stage of limiting, maintains the sum of all receiver levels constant within less than $\frac{1}{2}$ db, as required for toll quality telephone carrier use.

An experimental version of the simplified base-band diversity combiner circuit has been tested in operation over an experimental troposcatter link. Performance compares favorably with present combiners.

SESSION 31*

Wed.   10:00 A.M.–12:30 P.M.

Coliseum
Marconi Hall

MATHEMATICAL APPROACHES FOR RELIABILITY

Chairman: GEORGE I. BASILE, *White Plains, N. Y.*

31.1. The Reliability Game

R. F. EDWARDS, *International Rectifier Corp., El Segundo, Calif.*

An operational game is used to generate a value structure in terms of failure rates to allow the effect of competition in a free economy on the reliability of electronic parts to be computed. The operational game combines 11-chance failure causes, operational and shortage life failure rates, procurement conditions and field environments into a single mathematical equation that is solved with a digital computer. The game theory solution shows that the value of reliability as compared with the value assigned to design, profit and delivery will have to be increased by a factor of 100 before a change in procurement practices can be anticipated.

31.2. Operational Reliability Model for a Reconnaissance System

LLOYD L. PHILIPSON, *Planning Res. Corp., Los Angeles, Calif.*

An analytical model to enable prediction of operational reliability ("operability") of a multimode electronic reconnaissance system is discussed. The equipment units in the system are assigned to groups corresponding to each of the functions of the system. The reliability of performance of each function is formulated in terms of component failure-rate data and time-varying weighting factors that measure the importance of the units in each group to successful performance of the function. An evaluation of the over-all operability of the system is obtained from a weighted combination of the individual functional groups' operational reliabilities.

31.3. What Price Reliability?

J. KLION AND J. J. NARESKY, *Rome Air Dev. Center, Griffiss AFB, Rome, N. Y.*

This paper represents an attempt to supply designers with a method of estimating costs of reliability design for ground electronic equipment from development through obsolescence. From available data, normalized development costs per circuit of an average reliability are derived. Curves are also developed for estimating increased costs per circuit to achieve a specified reliability in development; these include testing costs to verify reliability. Similarly, production costs per circuit of average reliability and increased cost curves to achieve and test for a given reliability are derived. Finally, from a knowledge of the equipment reliability, estimated costs on a normalized basis for maintaining a tube circuit and/or equipment in the field for five years are developed; these costs include component and manpower costs over this period.

31.4. System Efficiency and Reliability

R. E. BARLOW AND L. C. HUNTER, *Electronic Defense Lab. Mountain View, Calif.*

The interest in reliability and the lack of rigorous foundations for the subject are well known. This paper develops a mathematical definition of system efficiency and reliability by considering the state of a system as a function of time to be a stochastic process. The usual definition of reliability is shown to be a special case of this more sophisticated model. Applications to Markovian systems are discussed. In particular, examples are given for electronic systems with repair. The usual assumption of component independence is avoided throughout.

31.5. Analysis of System Reliability from the Standpoint of Component Usage and Replacement

B. J. FLEHINGER, *Watson Lab., New York, N. Y.*

This paper postulates a mathematical reliability model of a complex system in which the components are used intermittently and which is maintained in operating condition through replacement of failed parts. The following properties are assigned to the model:

1) The system may be subdivided into components which fail independently. The lifetime distribution of these components is known.

2) A component is said to be in use in the system whenever the correct operation of the component is necessary to the correct operation of the system. For each component, periods of use alternate with periods of nonuse. The probability distribution of the duration of these periods is known.

3) The failure of a component at any time is independent of its history of use.

4) The system fails during a given time interval under either of these conditions: a component fails during a period of use and a component fails during a period of nonuse followed by the beginning of a period of use before the end of the interval.

5) Whenever a system failure occurs, the component which induced the failure is replaced by a new and statistically identical component.

The reliability of this system for a given time interval and the mean time between system failures are expressed in terms of the age of the system, the failure distributions of the components, and the distribution functions of periods of use and nonuse.

SESSION 32*

Wed.   10:00 A.M.–12:30 P.M.

Coliseum
Faraday Hall

MICROWAVE DEVICES

Chairman: J. W. E. GRIEMSMANN, *Polytechnic Inst. Bklyn., Brooklyn, N. Y.*

32.1. A Microwave Meacham Bridge Oscillator

W. R. SOOY, F. L. VERNON, AND J. MUNUSHIAN, *Hughes Aircraft Co., Culver City, Calif.*

A microwave analog of the low-frequency Meacham bridge oscillator, long known for its exceptional stability, is described. The incorporation of the resonant element of a feedback oscillator into an appropriate bridge circuit effectively multiplies the Q of the element and consequently the stability of the oscillator. The performance and design of an X-band oscillator consisting of a traveling-wave tube amplifier, a cavity, a microwave Wheatstone bridge and a bolometer element are described and experimental results are compared with theory.

32.2. A Linear Phase or Amplitude Modulator for Microwave Signals

JOSEPH GINDSBERG, *Raytheon Manufacturing Co., Bedford, Mass.*

A microwave modulator circuit is described employing a ferrite rotator whose two cross-polarized output ports are connected to a magic tee. When the two rotator-to-tee paths differ by 90°, Faraday rotation is transformed into output phase shift. Thus linear phase modulation is obtained which is independent of quiescent rotation. When the path difference is zero, the device produces AM which is maximum with quiescent rotations of 0 or 90°. X-band modulators incorporating this design were found to suppress AM at least 55 db below the phase-modulation sidebands. These modulators have been used in precision equipment for calibrating microwave discriminators and detectors.

32.3. Special Consideration in the Design of a Tunable Multi-Element Waveguide Filter

ROBERT L. SLEVEN, *Airborne Instruments Lab., Mineola, N. Y.*

This paper discusses the problem of designing a tunable narrow-band multielement waveguide band-pass filter having a near constant pass band response while tuning. By adding the requirement of tunability to the design of a filter, the difficulty of the problem is increased many-fold compared with that of the fixed tuned case. The techniques to be discussed are applicable to filter tuning ranges from 3 to 20 per cent.

By judicious choice of cavity dimensions, the variation in the amplitude-frequency response, while tuning, is reduced to an amount negligible for most applications. In addition to the discussion of the method used to obtain the optimum set of cavity dimensions, this paper discusses the problem of gang-tuning the cavities of a multielement waveguide filter.

32.4. Strip Transmission Line Corporate Feed Structures for Antenna Arrays

D. ALSTADTER AND E. O. HOUSE-MAN, JR., *Melpar, Inc., Falls Church, Va.*

In recent years considerable effort has been devoted to the development of high-gain directional and omnidirectional antenna arrays. Therefore, increasing interest has been promoted in the development of corporate feed structures which can be used for beam shaping and side-lobe reduction in directional arrays and as a coupling network in omnidirectional arrays. This paper describes new techniques which have been developed to facilitate the design of corporate feed structures consisting of strip transmission line tapered and linear power dividers. Guided by varying applications, strip transmission line power dividers have been developed which provide cosine, cosine squared, and exponential tapered output distributions. Experimental data are presented which show the effects of several tapered power dividers on the azimuth beam width and the amount of side-lobe level reduction obtained for an electromechanically scannable Wullenweber type antenna array.

Techniques are presented which facilitate the design of corporate feed structures for high gain omnidirectional antennas. Typical corporate feed structures are discussed which permit coupling as many as 512 dipole-type antennas with minimum phase and amplitude variations.

32.5. Low-Loss S-Band and L-Band Circulators for Use With Masers and Reactance Amplifiers

F. ARAMS, G. KRAYER, AND S. OKWIT, *Airborne Instruments Lab., Mineola, N. Y.*

Low-loss circulators have been developed in *S* band and *L* band for use in low-noise receiving systems. The requirements for low-noise receiver operation will be reviewed. It will be shown that by connecting a low-loss, high isolation circulator to a one-port maser or reactance amplifier, maximum gain bandwidth is obtained and the degrading effect of the second stage noise on over-all receiver performance is minimized.

The characteristics of a broad-band *S*-band circulator will be described. It operates over an 11 per cent band (2650-2950 mc), having an insertion loss of less than 0.2 db.

The characteristics of a low-loss *L*-band circulator will also be described. It operates over an 18 per cent band (1200-1450 mc) and has an insertion loss of 0.3 db.

A second *L*-band circulator utilizing both waveguide and Stripline® (Trademark, U. S. Patent Office) circuitry will be discussed. This type of configuration substantially reduces the over-all dimensions of the circulator.

SESSION 33*

Wed.   2:30–5:00 P.M.

Waldorf-Astoria Starlight Roof

ELECTRONIC COMPUTERS: SYSTEMS AND APPLICATIONS

Chairman: FINLEY W. TATUM, *Elec. Eng. Dept., Southern Methodist University, Dallas, Tex.*

33.1. Radar System Simulation Techniques

J. M. LAMBERT AND A. J. HEIDRICH, *General Electric Co., Syracuse, N. Y.*

Analog computer circuits are presented which can be combined to simulate complete radar systems. Computer circuits are developed which can be used to simulate radar components such as RF filters, mixers, IF amplifiers, phase and amplitude detectors, video amplifiers, delay lines, limiters, klystrons, etc. Scale factors, stability, and methods of simulation checking are discussed. The complete simulation of a phase-locked radar guidance system is used to illustrate the application of the computer circuits.

Radar systems simulation is presently being used to analyze radars and missile guidance systems and to evaluate the performance of radar systems under electronic countermeasures. By using special-purpose simulator components to supplement a standard analog computer, a wide variety of radar systems problems can be solved.

33.2. Application of the NCR 304 Data Processor to the Synthesis of a Digital Computer Building Block

G. H. GOLDSTICK AND M. KAWA-HARA, *The National Cash Register Co., Hawthorne, Calif.*

This paper describes a design technique whereby the NCR 304 data processor was used to optimize the design of a core/transistor amplifier. The mathematical models used for the circuit components and the analytical formulation of design equations and conditions are discussed. The program used to solve the design equations on the 304 processor is outlined. A unique method of data presentation to facilitate rapid evaluation of tested designs is discussed. Several features of the 304 processor which contribute to its effectiveness as a design tool are reviewed.

33.3. Automatic Checkout Equipment Featuring Test Programs for Diagnostic Checking

---

R. B. WHITELEY AND L. J. LAULER, *Lockheed Aircraft Corp., Sunnyvale, Calif.*

A sophisticated automatic checkout system is under development by Lockheed Missile Systems Division as part of a major weapon system program. This equipment features digital checkout techniques for the administration of test, acquisition of data, processing of results and documentation of the checkout performance of the missile under test. The equipment incorporates several novel features which enhance its capability for rapid, precise and systematic checkout and fault location. The machine is designed around a compact magnetic drum which supplies the medium required to store orders and numerical information and the arithmetic registers required to operate the machine. In addition, this drum provides for the inclusion of previously prepared subroutines to enable self-checking of the checkout machine and diagnostic analysis of the system under test to isolate defective components. The memory and computing section works through elements of peripheral equipment to perform the missile checkout. These items of equipment include signal generators, digitizers and standards, with the associated switching being performed by both relay and solid-state devices. Reliable operation is stressed in every aspect of the design.

33.4. Systems Organization of a Special-Purpose Airborne Digital Computer

HERBERT H. SCHILLER, *American Bosch Arma Corp., Garden City, N. Y.*

This paper describes the functional and logical organization of an all solid-state digital computer for airborne applications being produced in production quantities. The computer operates in the serial mode. It features delay wire loops for scratch pad storage and computational constants as well as the fixed program stored in diode matrices. Only three different orders are employed in the program: analog-to-digital and digital-to-voltage converter for an integral part of the system, a crystal times the computer cycle which serves as an integration times base. Several new logical building blocks have been devised and their function is described in detail.

33.5. The Automatic Position Survey Analyzer and Computer

FRANCIS J. ALTERMAN, *General Mills, Inc., Minneapolis, Minn.*

The problem of surveying the earth's surface accurately and rapidly has assumed new importance with the advent of long-range guided weapons. Astronomic position of any point on the earth can be determined with greater accuracy and speed by a high-speed digital computer employed as a data-handling, computing, and controling system. This computer, called the APSAC, is a high-speed, 36 bit, internally programmed, transistorized machine with high- and low-speed memory capabilities. Constructed by General Mills, Inc. for the Corps of Engineers, it features a unique construction technique which provides it with unusual versatility and flexibility. Although the machine is made almost entirely of identical electronic "building blocks," these circuits compose a complex, sophisticated machine which can be constructed simply and at low cost.

SESSION 34*

Wed.   **2:30–5:00 P.M.**

Waldorf-Astoria
Astor Gallery

SYMPOSIUM ON SEQUENTIAL CIRCUIT THEORY

Chairman: EDWARD F. MOORE, *Bell Telephone Labs., Inc., Murray Hill, N. J.*

34.1. A Survey of the Theory of Finite-State Logical Machines

DAVID HUFFMAN, *Mass. Inst. Tech., Cambridge, Mass.*

Finite-state machines form an important class of models whose study leads to insight into the theoretical capabilities of digital machines having memory. A brief, comprehensive survey will be made of the present state of this theory with some of its accomplishments and limitations. Possible areas for future research leading to fruitful growth and extension of this theory will be discussed, together with mention of some of the most recent study and advances in the specific areas of information-lossless and multidimensional finite-states machines.

34.2. Mathematical Models for Sequential Machines

SUNDARAM SESHU, *University of Toronto, Toronto, Ont., Can.*

This paper is mainly a tutorial discussion of the various mathematical models that have been proposed for sequential machines. The most important models that are in use are due to Moore, Huffman, Mealy, and Muller. The purpose of the paper is to discuss the interrelationships among these models, the relative merits of the various models from the point of view of machine design, and the ways in which combinations of these models can be used to advantage. The representations of these models as nets on a n cube and the available techniques for analyzing the state diagrams that result will also be discussed.

34.3. Information Transfer in Asynchronous Systems

DAVID E. MULLER, *University of Illinois, Urbana, Ill.*

A few types of simple asynchronous machines may be regarded as basic units from which large-scale asynchronous systems may be formed. Rules of interconnection are followed which restrict the "fan out" from one unit to the next and provide for speed independent operation of the system as a whole. Reduction in speed due to the need for excessive current amplification is thus avoided, but the transfer and processing of information is only coordinated locally. Bits of information pass between units of the system in somewhat the same way that particles flow in a fluid, while interference from digits is prevented by the logic of the connections between neighboring units.

SESSION 35*

Wed.   **2:30–5:00 P.M.**

Waldorf-Astoria
Jade Room

COMPONENT PARTS—II

Chairman: JESSE MARSTEN, *International Resistance Co., Philadelphia, Pa.*

35.1. A Practical, Comprehensive Component Application Program

C. G. WALANCE, *Hughes Aircraft Co., Culver City, Calif.*

Guidelines are established for component application programs applicable to most organizations. One such program is described in order to illustrate practical applications of these guidelines and their results. This paper is intended primarily to give experienced advice to organizations desiring to establish component application activities, rather than to expound on a particular company's approach. Personnel and procedural requirements are presented, pitfalls are cautioned against, and a number of practical illustrated examples are given. Included in the examples are illustrations of reliability improvements, cost improvements, and component design changes. Component application engineering is demonstrated to improve system mean time to failure in a quantitative manner. The integration of in-plant component application engineering with operational field surveillance is included.

35.2. Army Electronic Research: Theory to Reality

L. J. D. ROUGE, *U. S. Army Signal Res. and Dev. Lab., Fort Monmouth, N. J.*

The Army's electronic research and development operations have changed significantly over the past 10 years, namely, a greater emphasis on the development of the basic parts and related materials to provide stimulus for design of new system and equipment capabilities. This metamorphosis reflects the growing recognition by research and development management that progress in basic parts over the past decade has significantly shaped the practicing electronic art as we know it today. The classical example of yesterday's audion as the "herald of new electronics" has been complemented in the last decade by the transistor, the solar converter, printed circuits, ferrite memories, the thermal battery, and dozens of other component and material accomplishments, each contribution opening intriguing new capabilities in the electronic art. Today, *in continuum*, still newer concepts and techniques absorb our research and development interests—parametric and amplifiers, cryogenic logic elements, semiconductors and pure crystals, atomic and molecular resonance devices, new materials born under superpressures and super-temperatures, new techniques for thermoelectric conversion. These are the new foundations upon which a new electronics is being built.

Specific areas are illustrated in this light, including new power sources and energy con-

verters, new precise frequency control devices (atomic and molecular resonance devices), materials research (nickel, platinum, garnet, high temperature-high pressure materials, etc.), assembly concepts, transistor trends and tube trends.

35.3. A Review of the Influence of Recent Material and Technique Development on Transformer Design

HAROLD NORDENBERG, *Bureau of Ships, Washington, D. C.*

A review will be made of power transformers (audio, power and pulse) design techniques with consideration being given to the influence of recent material and material application developments. The relationship between transformer design and the environmental and electrical requirements imposed by the more severe operating environments will be explored. Special emphasis will be placed upon such new techniques as the use of the molded coil encapsulants, the application of various gases and liquids including the fluro chemicals and other similar materials, which have been developed in connection with the development of transformers to meet the more severe environments of the modern military weapons system.

35.4. Improvements Made in Electronic Parts During the Past Ten Years

H. V. NOBLE, *Wright Air Dev. Center, Wright-Patterson AFB, Ohio*

Rapid advances in the capability of military weapon systems during the past 10 years have brought on requirements for vast improvement in electronics. Electronic parts have met this challenge by delivering greater performances with higher stability, smaller size and longer life in particularly severe environments of high temperature and intense nuclear radiation fields. This paper will give a resume of the advances made in component parts since World War II.

35.5. An Analysis of Printed Wire Edge Connectors

D. R. SHERIFF, *Ampex Corp., Redwood City, Calif.*

This paper describes the design attributes which an effective and reliable printed wire edge connector must have. The requirements of such connectors are analyzed in detail, as are possible solutions to the problems presented by these requirements.

SESSION 36*

Wed.   **2:30–5:00 P.M.**

Waldorf-Astoria
Sert Room

SPACE ELECTRONICS

Chairman: ROSS FLEISIG, *Sperry Gyroscope Co., Great Neck, N. Y.*

36.1. A Time Redundancy Instrumentation System for an ICBM Re-entry Vehicle

R. E. SCHMIDT, J. R. WHITE AND R. A. PORTER, *AVCO, Wilmington, Mass.*

A special instrumentation technique, employed in establishing the suitability of the over-all re-entry vehicle design under actual flight conditions, has been developed by the Research and Advanced Development Division of AVCO. The philosophy, upon which the instrumentation system design was based, gave prime consideration to the ionization "black-out" of radio signals anticipated during the re-entry into the earth's atmosphere. Severe ionization conditions, caused by high temperature gases created during re-entry, present a telemetry problem in that radio signals are seriously attenuated during this portion of a flight.

The employment of a continuous-loop magnetic tape recorder to store vital data collected by the instrumentation system during ionization blackout and the retransmission of this data after the nose cone's emergence from this region are an effective solution to the problem. A high degree of data redundancy was made possible by this unit.

36.2. A General Purpose FM Transmitter for Airborne Telemetry

P. E. TUCKER AND R. T. MURPHY, *Lockheed Aircraft Corp., Palo Alto, Calif.*

This paper describes a general purpose FM transmitter for telemetry in the VHF region. The unit is small, light weight and covers the majority of telemetry applications without the use of external power amplifiers. While primarily designed for FM-FM telemetry, the unit is also compatible with PAM-FM and PCM-FM systems. The modulation characteristics feature very low distortion and exceptionally flat frequency response from dc to 100 kc. Antenna conducted spurious radiation and radiation from the case and power leads has been reduced to a low level. Novel case design and rugged construction result in a unit with long operating life which performs well under severe environmental conditions without the use of forced cooling.

36.3 The TRICOT System

DANA F. GUMB, *Aero Geo Astro Corp., Alexandria, Va.*

Typical missile programs have involved the use of airborne electronics in several capacities. These have included beacons as an aid to tracking, coded reply for identification, command receiver systems, and telemetry units. The first two functions have been combined in some cases, but it is not unusual to have four separate electronic packages to satisfy the four needs. The present paper describes a single electronic system capable of providing all of these functions. It consists basically of a super-het receiver and a kilowatt pulse transmitter. Video circuitry is included to provide both decoding and encoding capability to satisfy the various functions. The unit has been packaged into approximately 300 cubic inches and a fly-able model has been successfully subjected to typical environmental conditions. Information

on electrical, mechanical and environmental characteristics of this system, which has been designated as TRICOT, will be presented.

36.4. A Circularly Polarized Feed for an Automatic Tracking Telemetry Antenna

R. C. BAKER, *Radiation, Inc., Melbourne, Fla.*

Characteristics of a feed that utilizes a unique method to produce a conically scanning main beam are discussed. Model and full-scale test data are included to make the feed operation more clearly understood.

Certain criteria such as gain, side-lobe level, and polarization must be considered when designing a primary feed for a parabolic reflector. Also, automatic tracking requirement calls for some means of producing an error signal for given off-target angles.

The feed discussed is a circular waveguide excited by orthogonal probes fed 90° out of phase to produce circular polarization. The electrical phase center of the feed is shifted around the focal point of the 60-focal diameter parabolic reflector by rotating a hemispherical, tapered dielectric prism at the aperture of the waveguide. A ground plane around the waveguide mouth controls the illumination taper across the paraboloid aperture to yield equal vertical and horizontal plane secondary beam widths.

SESSION 37*

Wed.   **2:30–5:00 P.M.**

Coliseum
Morse Hall

COMMUNICATION BY RADIO AND BY WIRE LINE

Chairman: FRANCIS M. RYAN, *American Tel. and Tel. Co., New York, N. Y.*

37.1. Design Considerations for Space Communications

J. E. BARTOW, G. N. KRASSNER, AND R. C. RIEHS, *U. S. Army Signal Res. and Dev. Lab., Fort Monmouth, N. J.*

With the advent of Russian and American artificial earth satellites, the use of such vehicles for communication purposes has been the subject of considerable study both by military and commercial organizations in the communications field. The purpose of this article is to delineate the problems involved in space communication, the assumptions that must be made and the technical limitations which determine the communication system that should be used for a particular time frame. Some characteristics for an optimum system are stated.

37.2. Inverse Ionosphere

GEORGE D. HULST, *ITT Labs., Nutley, N. J.*

The distortion introduced into a long-range communication system by unpredictable multipath conditions of the ionosphere is described in this paper. A device to eliminate this particular form of distortion is then described, using a sensing technique, a logical matrix and a signal restoration network. Since both the multipath model of the ionosphere and the restoration network are linear, the principles of superposition apply to the cascaded combination so that the described technique is generally applicable to all waveforms. The inverse instrumentation can be either a restoration network at the receiver or a predistorting network at the transmitter. Next specific restoration networks are described for several typical ionosphere multipath conditions. Finally the effects of white noise upon the correction network and the signal are noted.

37.3. A Frequency Stepping System for Overcoming the Disastrous Effects of Multipath-Distortion on High-Frequency FSK Communications Circuits

ARTHUR R. SCHMIDT, *Rixon Electronics, Inc., Silver Spring, Md.*

By changing frequency a small amount after transmission of each signaling element in FSK transmission, it is possible to avoid the mutual interference of the main and multipath propagated signal in a high-frequency communications system. Thus, it is practical to employ four-channel time division multiplex systems under multipath conditions that would otherwise render them useless.

The paper describes an experimental system that was produced by modifying conventional FS keyers and employing standard communications receivers in conjunction with appropriate frequency stepping means and selective filters. Operational performance data on experimental circuits will be discussed.

37.4. A High-Stability Linear Phase Voice Frequency Multiplex

D. KARP, R. M. LERNER, J. F. MERCURIO, JR., AND W. E. MORROW, JR., *Lincoln Lab., Mass. Inst. Tech., Cambridge, Mass.*

A voice frequency multiplex suitable for use in high-speed digital data systems, as well as telephony, is described. Linear phase filters of the type described by Lerner in "A bandpass linear phase filter," are employed, so that the effect of phase distortion on digital data transmission is virtually eliminated. Because of the unique filter design, it is possible to drop and insert voice channels directly at base band, or to strap channels together to form wide-band blocks.

The multiplex derives all its carrier frequencies from a single transistorized crystal oscillator having a stability of 1 part in 10^9, obviating the need for pilot tone synchronization between transmitter and receiver. The filters are designed for ± 0.1-db ripple between 500 and 2900 cps, with 1-db points at 300 and 3200 cps, and a phase shift which remains within $\pm 2°$ of linear over the 0.1-db band. The design intermod and crosstalk between channels is -70 db.

A transistorized realization of such a multiplex has been constructed, and experimental results will be given.

37.5. A 2500-Baud Time-Sequential Transmission System for Voice Frequency Wire Line Transmission

J. C. MYRICK AND G. HOLLAND,
*Rixon Electronics, Inc.,
Silver Spring, Md.*

Binary information at 2500 bauds per second is converted to minimum bandwidth and used to amplitude modulate a 2500-cycle carrier. The resulting signal is converted to vestigial sideband prior to transmission to further compress the bandwidth.

At the receiver terminal, amplitude and delay compensation are provided to correct for distortion introduced by the transmission line. Synchronous sampling of the recovered signal by a slaved time standard reproduces the original binary information even though line distortion may be severe.

The equipment used in this system has been completely transistorized and thoroughly evaluated under environmental conditions.

SESSION 38*

Wed.   **2:30–5:00 P.M.**

Coliseum
Marconi Hall

PROPAGATION AND ANTENNAS—I

Chairman: JOHN I. BOHNERT, *Naval Res. Lab., Washington, D. C.*

38.1. Tropospheric Scatter Propagation Characteristics

ARLON J. SVIEN, *Collins Radio Co., Tucson, Ariz.,* AND J. C. DOMIN- GUE, *Signal Communications Dept., Fort Huachuca, Ariz.*

This paper presents the results of 1000mc tropospheric propagation measurements made over a three-year period of approximately 20 paths varying in length from 50 to 350 miles. These paths provide examples of a large variety of intervening terrain and horizon elevations.

All data on these tests have been consolidated, and curves are presented showing transmission loss as a function of distance, elevated horizons and season. This information is compared with that obtained by a survey of a large number of existing sources. Simultaneous intelligence transmissions were made on all circuits, and operational performance is correlated with propagation data.

38.2. Optimum Antenna Height for Ionospheric Scatter Propagation

R. G. MERRILL, *National Bureau of Standards, Boulder, Colo.*

Radiation patterns of elevated antennas over spherical earth for scatter propagation in the lower ionosphere incorporating refraction, parallax, spherical divergence, and tropospheric defocusing have been used to compute the height gain function resulting from raising and lowering symmetric transmitting and receiving antennas for a fixed path length. This height gain function shows that a broad range of lower antenna heights has a gain over that antenna height which places the maximum of the first lobe at the path midpoint. The maximum of this function is defined as the optimum antenna height. Preliminary results of experimental verification are given.

38.3. Terrain Return Measurements at X, K_u, and K_a Band

ROBERT C. TAYLOR, *Antenna Lab., Dept. of Elec. Eng., The Ohio State University, Columbus, Ohio*

The back-scattering from many different types of terrain has been measured at frequencies of 10, 15.5, and 35 kmc using both vertical and horizontal polarization. The average radar cross section of the terrain (γ) has been plotted as a function of incidence angle for the three frequencies. Due to the large quantity of data that has been collected and the accuracy of the data (± 1 db) certain pertinent parameters that effect the magnitude of the return have been determined. These parameters are:
1) Surface roughness,
2) Incidence angle,
3) Polarization,
4) Complex dielectric constant of the terrain,
5) Frequency.

Seasonal changes of vegetation covered terrain and the effects of rain on both smooth and rough surfaces are shown as functions of incidence angle, frequency and polarization.

The measurements presented in this paper show a self-consistency which has not been found in other published material which is due to the highly developed equipment and measurement techniques used in the investigation.

38.4. Theory of Radar Return from Terrain

WILLIAM H. PEAKE, *Antenna Lab., Dept. Elec. Eng., The Ohio State University Columbus, Ohio*

It is often convenient to have theoretical expressions for the back-scattering cross section of terrain in order to organize properly experimental data and to permit complete analysis of radar operation. Two models have been proposed for this purpose. The first, applicable to roadways and similar smooth surfaces, gives the return in terms of the roughness, the height correlation function and the complex dielectric constant of the surface and is in excellent quantitative agreement with experiment. The second model, applicable to grass (or similar cylindrical vegetation) gives the return as a function of number, size and complex dielectric constant of the cylindrical scatterers and is in qualitative agreement with experiment. Applications to the problem of characterizing terrain to radiometry, etc., are mentioned.

38.5. A New Concept in High-Frequency Antenna Design

R. H. DuHAMEL AND D. G. BERRY, *Collins Radio Co., Cedar Rapids, Iowa*

The application of unidirectional, wire trapezoidal tooth, log periodic antennas to HF point-to-point communications is described. The antennas are placed over ground in such a manner that the vertical plane radiation pattern as well as the other patterns and input impedance are essentially independent of frequency over the 3–30 mc range. Moreover, the design parameters can be chosen so that the beam direction will fall at any vertical angle from 60° down to a few degrees. The antennas are horizontally polarized with azimuthal beamwidths of 60°, side-lobes less than 15 db and gains ranging from 8 db to 18 db over an isotrope. These antennas should lead to considerable simplification and area reduction of antenna forms.

38.6. Large Antenna Systems for Propagation Studies

IRA KAMEN, *General Bronze Corp. and GB Electronics Corp., Valley Stream, N. Y.*

This paper reports on a specific large steerable antenna system now installed at the Boulder Laboratories of the National Bureau of Standards for scatter propagation studies to develop data with respect to frequency, power and polarization.

The design consideration for antenna feeds, reflector surface accuracy, pedestal mechanisms and servocontrol systems for these large parabolas is evaluated. A film of the National Bureau of Standards installation, pattern data, positioning accuracy measurements and a review of actual feed designs used and proposed for 60-foot, 90-foot, and 120-foot paraboloidal systems will support the theoretical data presented.

SESSION 39*

Wed.   **2:30–5:00 P.M.**

Coliseum
Faraday Hall

MICROWAVE THEORY AND TECHNIQUES

Chairman: T. S. SAAD, *Sage Labs., Wellesley, Mass.*

39.1. Some Comments on the Classification of Waveguide Modes

A. E. KARBOWIAK, *Standard Telecommunication Labs., Ltd., Enfield, Middlesex, Eng.*

This paper presents, in as far as possible nonmathematical language, the concept of modes currently in use. Some of the concepts are modified or generalized and a unified description is obtained. The term "proper mode" is reserved for a certain mathematical concept, which is usually concomitant with the concept of the eigen function; whereas the term "quasi-mode" is reserved for a field configuration which can be supported by a physically realizable guiding structure. In the description given, the radiation field which, as shown, must always accompany a guided wave is viewed in a slightly novel light, and a bridge is constructed between the concept of modes guided in closed waveguides and those guided by open structures.

The paper concludes with a discussion on the existence of guided waves, and it is demonstrated that whether a mode exists or not is entirely a matter of subjective opinion (implicit in the definitions). Nevertheless, it is shown that all quasi-modes are a physical reality and that they are useful in practical applications.

39.2. Noise Figure of Receiver Systems Using Parametric Amplifiers

J. SIE AND S. WEISBAUM, *RC.I,
New York, N. Y.*

This paper is an evaluation of noise performance of two receiver systems employing low-noise parametric amplifiers, *viz.*, 1) two matched amplifier with 3-db coupler, 2) circulator amplifier.

A rigorous derivation of the system noise figure, F, considering all significant noise contributions, is carried out. For scheme 1), F can be minimized with respect to amplifier gain while F decreases monotonically for scheme 2). For the usual type of circulator, F of the forward path is

$$1 + (L' - 1)\frac{T_1}{T_0},$$

and for one special type, F is derived to be

$$1 + \frac{(L-1)}{2}\frac{T_1 L'}{T_0 L}$$

where L' is the insertion loss and L, the ferrite loss. In the UHF region, an effective amplifier temperature of $13.5°$ K yields an F of 0.8 db and 0.79 db for the two schemes, respectively. The loss of the circulator was assumed to be 0.5 db. The noise figure of an up-converter scheme is also considered.

39.3. Low-Noise Parametric Amplifiers and Converters

T. B. WARREN, *ITT Labs.,
Nutley, N. J.*

Both theoretical and experimental results are given for variable-capacitance amplifiers and converters. Various types of amplifiers and converters are compared with respect to noise figure, stability, and bandwidth in the 500–2000 mc frequency band. Experimental results which have been obtained indicate that noise figures under one db can be obtained with a regenerative converter. These experimental results, as well as measurements taken on amplifiers and nonregenerative converters, are compared with predicted theoretical values. Experimental data are also given for a balanced system using a hybrid and two regenerative converters, designed to minimize the effects of input loading variations. A method of produc-

ing high-frequency local oscillator power from a stable low-frequency source is described which eliminates the effects of pump frequency variations. A discussion is also given of some of the problems encountered in the fabrication and measurement of the diffused junction silicon diode.

39.4. Microwave Techniques in Measurement of Lifetime in Germanium

A. P. RAMSA, *Monmouth College, West Long Branch, N. J.*, H. JACOBS AND F. A. BRAND, *U. S. Army Signal Res. and Dev. Lab., Fort Monmouth, N. J.*

A method is described whereby lifetime of minority carriers in a semiconductor can be measured with microwave absorption techniques. Possible errors in the system of measurement are analyzed, such as the injection of large densities of carriers, the effects of volume and surface recombination, and errors due to reflection. The new technique makes possible an electrodeless system for lifetime measurements and other physical properties of semiconductors.

39.5. Microwave Mixer Performance at Higher Intermediate Frequencies

M. COHN AND J. B. NEWMAN, *Radiation Lab., The Johns Hopkins University, Baltimore, Md.*

The crystal mixer problem for millimeter wavelength superheterodyne receivers is re-examined with the following question in mind. For those frequency regions where matched crystal pairs are unavailable, but sufficient local oscillator power for a single ended mixer is available, what is the optimum intermediate frequency and LO excitation? The conversion loss and total noise ratio (including the LO contribution) of a group of crystals were measured as a function of intermediate frequency and LO excitation. The results indicate that a single ended mixer operated at a high IF with reduced LO excitation can provide over-all receiver sensitivity comparable to that of a balanced mixer.

SESSION 40*

Thurs.   10:00 A.M.–12:30 P.M.

**Waldorf-Astoria
Starlight Roof**

THEORY AND PRACTICE IN RUSSIAN TECHNOLOGY

Chairman: JEAN H. FELKER, *Bell Telephone Labs., Inc., Murray Hill, N. J.*

40.1. Highlights of Soviet Information Theory

P. E. GREEN, JR., *Lincoln Lab., Mass. Inst. Tech., Lexington, Mass.*

40.2. Digital Computer Activities in the Soviet Union

N. R. SCOTT, *University of Michigan, Ann Arbor, Mich.*

40.3. Theory and Practice in Automatic Control

W. E. VANNAH, *Control Engineering, New York, N. Y.*

SESSION 41*

Thurs.   10:00 A.M.–12:30 P.M.

**Waldorf-Astoria
Astor Gallery**

CIRCUIT THEORY II—ANALYSIS AND SYNTHESIS

Chairman: ERNEST S. KUH, *Elec. Eng. Dept., University of California, Berkeley, Calif.*

41.1. Sensitivity of Transmission Zeros in RC Network Synthesis

FRANKLIN F. KUO, *Polytech. Inst. Bklyn., Brooklyn, N. Y.*

Pole-zero sensitivity is given as a design criterion for RC ladder network synthesis. It is shown that the sensitivity of each zero of transmission determines the per cent tolerance of an element in the network. A function $H(s)$ is derived such that the sensitivity of each transmission zero is the residue of the corresponding pole of $H(s)$. It is then shown that the immittance function resulting from each zero shift is the reciprocal of the $H(s)$ function. From this a criterion can be derived which relates the sensitivity of the zero to the amount of zero shift. A number of design criteria for optimizing sensitivity is given and it is shown that minimizing sensitivity and minimizing the number of elements in the network are conflicting problems.

41.2 Synthesis of Active Networks—Driving-Point Functions

N. DeCLARIS, *School of Elec. Eng., Cornell University, Ithaca, N. Y.*

"Controlled" sources with "associated" networks are frequently utilized in models for the circuit representation of physical active devices, *e.g.*, vacuum tubes, transistors, etc. In

this paper necessary and sufficient conditions are established for the physical realizability of driving-point functions of linear, lumped and active networks—that is networks containing R's, L's, C's and "controlled" sources, as well as properties due to "associated" networks. Three canonic forms are presented, and procedures for their realization are outlined and illustrated. "Padding," "partitioning" and other useful techniques are also outlined for noncanonical realization.

41.3. Linear Modular Sequential Circuits and Their Application to Multiple Level Coding

B. FRIEDLAND AND T. E. STERN, *Dept. Elec. Eng., Columbia University, New York, N. Y.*

A linear modular sequential circuit (MSC) is characterized by the relations 1) $y(n) = Cs(n) + Dx(n)$; 2) $s(n+1) = As(n) + Bx(n)$ in which $y(n)$, $x(n)$, and $s(n)$ are the input, output, and state vectors, respectively and A, B, C, D are matrixes defined over the modular field $GF(p)$ ($p = $ prime). A MSC may be constructed of unit delays, modulo p summers, and amplifiers with gains $= 1, 2, \cdots, p-1$, and may be analyzed by methods used for other linear systems. It is shown that the unit response of an MSC (A nonsingular) is periodic. Procedures for the construction of circuits of maximum length period are given. Such circuits are useful for encoding and decoding lossless single error correcting p-nary codes in the manner of D. A. Huffman, whose paper "A linear circuit viewpoint on error-correcting codes," may be found in the September, 1956 issue of IRE TRANSACTIONS ON INFORMATION THEORY.

41.4. Taylor-Cauchy Transforms for Analysis of a Class of Nonlinear Systems

Y. H. KU, A. A. WOLF, AND J. H. DIETZ, *Moore School of Elec. Eng., University of Pennsylvania, Philadelphia, Pa.*

This paper presents a new transform technique for solving a certain class of nonlinear systems. The method, which can be justified rigorously by the partition theory (see A. A. Wolf, "A Mathematical Theory for the Analysis of a Class of Nonlinear Systems," doctoral dissertation, The Moore School of Elec. Eng., University of Pennsylvania; June, 1958), essentially transforms a nonlinear differential equation having certain conditions imposed on its linear and nonlinear parts and on its driving forces into a difference equation. The latter is easily solved recursively owing to its symmetry and convolution properties.

The transform pair is based on a combination of the Cauchy integral theorem and the Taylor's series in complex form. To illustrate the method a number of examples is solved and a table of transforms is included.

Because the results of this transform technique are the same as those given by the partition method under certain circumstances, the two are compared. It is then seen that the solution can be obtained uniquely and exactly.

The Taylor-Cauchy transform method can be compared with the Laurent-Cauchy transform method given in a companion paper for the solution of linear differential-difference and -sum equations.

SESSION 42*

Thurs.   10:00 A.M.–12:30 P.M.

Waldorf-Astoria
Jade Room

ULTRASONIC ENGINEERING—I

Chairman: AMOR L. LANE, Technitrol Engineering Co., Philadelphia, Pa.

42.1. Cavitation Erosion of Sonic Radiating Surfaces

HARRY F. OSTERMAN, *Branson Ultrasonic Corp., Stamford, Conn.*

With the increasing use of ultrasound in the cleaning field, equipment maintenance problems tend to magnify. Possibly the most vexatious of these problems is that of transducer erosion. The erosion or pitting that takes place on the radiating face of the transducer is a function of the liquid medium, the energy per unit area frequency, and the radiating material. Since many materials are used in the construction of power transducers, a survey has been made to determine their relative merits. An attempt to correlate resistance to erosion with physical properties is also made. The results are reported in this paper.

42.2. Piezoelectric and Dielectric Properties of Ceramics in the Potassium-Sodium Niobate System

L. EGERTON AND D. M. DILLON, *Bell Telephone Labs., Inc., Murray Hill, N. J.*

Ceramic bodies covering a wide compositional range in the potassium-sodium niobate system have been prepared. Radial coupling coefficients of from 28 to 39 per cent are observed for compositions having up to 50-mole per cent sodium niobate additions to potassium niobate. The activity then diminishes with additional sodium niobate content and disappears beyond about 98-mole per cent additions.

The room temperature dielectric constants of poled samples lie between 120 and 450 depending upon composition. Losses are relatively high, dissipation factors being from 2 to 5 per cent. The low dielectric constants and fairly high activities of compositions near the equimolar range make these materials of interest where large thin-sectioned transducers may be required.

42.3. Transducer Properties of Lead Titanate Zirconate Ceramics

D. BERLINCOURT, B. JAFFE, H. JAFFE, AND H. KRUEGER, *Clevite Res. Center, Cleveland, Ohio*

Physical properties of two commercial ceramics of the lead titanate zirconate family are presented and are compared with those for typical barium titanate compositions. The importance of dielectric losses is stressed. Preference is given to showing heat generated as a function of nonresonant strain amplitude rather than of electric field amplitude. In this type of presentation common barium titanate ceramics are about equal, while lead titanate zirconate ceramics are outstanding.

SESSION 43*

Thurs.   10:00 A.M.–12.30 P.M.

Waldorf-Astoria
Sert Room

MILITARY ELECTRONICS— LOOKS FORWARD

Chairman: HARRY KRUTTER, Naval Air Dev. Center, Johnsville, Pa.

43.1. Measurement of Missile Miss Distance

ALBERT E. HAYES JR., *Ampex Corp., Redwood City, Calif.*

The accurate measurement of the distance by which a missile fails to hit its intended target is a classic military problem. The requirement for a low-cost, dependable miss-distance indicator has become acute during recent years because of the increasing cost of air-to-air missiles and the training targets against which they are used. This paper describes a miss-distance indicator which is believed to be the ultimate in simplicity, having no components whatever in the missile and a fewer number of parts than a vest-pocket radio receiver in the target vehicle. Accurate and instantaneous scoring of miss distances up to 200 feet is attained through the use of grid-reaction oscillator techniques.

43.2. Radar Testing for a War Environment

RICHARD W. HANFORD, *9255 Bataan Drive, Overland, Mo.*

The requirement of guaranteeing and demonstrating a wartime capability for military fire control radars without demanding extensive access to the radar or significant time for checkout has resulted in a new approach to radar testing.

A new technique is described which tests any radar from two access points. In less than two minutes the radar can be tested in its

ability to track targets maneuvering in range, azimuth, and elevation. Furthermore, tolerance to self-noise, ability to reject dumped or forward-shot chaff and certain decoys, vulnerability to enemy noise jamming and spoofing, and susceptibility to fortuitious jamming and glint are measured experimentally. The radar system can also be readily and accurately calibrated in range and range rate for proper intercept solutions.

43.3. Trends in Inertial Navigation

FREDERICK STEVENS, *Nortronics, Hawthorne, Calif.*

This paper describes trends in inertial navigation which point to the growing importance of the principle in the field of automatic navigation. Early systems are described, present systems are described, and the state of the art is projected. The paper describes recent trends towards unusually lightweight, high performance systems which have been made possible by recent advances in inertial guidance components.

43.4. Space Vehicle Electro-magnetic Communications and Tracking

HENRY HOFFMANN, JR., *Rome Air Dev. Center, Griffiss AFB, Rome, N. Y.*

Present electromagnetic tracking systems are limited by feasible antenna beamwidths and the base lines attainable with earth-based stations. The natural conclusion is to investigate then earth satellites containing navigational equipments. In order to exploit the accuracies attainable with atomic frequency standards, both pulse and Doppler systems have been investigated. Comparative results have been summarized as functions of accuracy, power requirements, and complexity.

SESSION 44*

Thurs.   10:00 A.M.–12:30 P.M.

Waldorf-Astoria Empire Room

FRONTIERS OF INDUSTRIAL ELECTRONICS

Industrial electronics may ultimately be the largest part of the electronics industry. Although it is already very large and is growing fast, it is not generally understood as well as other branches of the electronics business. This meeting will present a picture of industrial electronics as it is today and as it is likely to develop in the future.

After a brief summary of historical highlights of industrial electronics, the speakers will present three coordinated talks on different aspects of the field. These aspects include social, commercial, and technical characteristics

of the industry, economic pressures for new techniques, and a survey of major industrial electronics developments and trends, with emphasis on the present and the future. In addition, a specific application of great importance will be described from the standpoint of the industry using the equipment.

A panel discussion by the speakers and the moderator will follow the talks, and the final part of the meeting will be an open forum for discussion from the floor.

Moderator: G. C. SUITS *Vice-Pres. and Dir. Res., General Electric Co., Schenectady, N. Y.*

44.1. Some Characteristics of the Industrial Electronics Industry

HAROLD A. STRICKLAND, JR., *Vice-Pres. and Gen. Mgr., Industrial Electronics Div., General Electric Co., New York, N. Y.*

44.2. Industrial Electronics—The Growing Servant of Mankind

T. A. SMITH, *Executive Vice-Pres., Industrial Electronics Products, RCA, Camden, N. J.*

44.3. Automation Trends in the Bank Industry

F. BYERS MILLER, *Executive Dir. and Head of Res. Div., National Association of Bank Auditors and Controllers, Chicago, Ill.*

SESSION 45*

Thurs.   10:00 A.M.–12:30 P.M.

Coliseum Morse Hall

MAN-MACHINE SYSTEM DESIGN

Chairman: ROBERT M. PAGE, *U. S. Naval Res. Lab., Washington, D. C.*

45.1. Communications Display and Control—A New Concept

RALPH J. MEYER, *Collins Radio Co., Cedar Rapids, Iowa*

Flight safety studies of high performance aircraft have proven the need for remote indication of the UHF communications preset channel. A man-machine system approach has been used to develop hardware which will 1) insure that operating personnel can perform their assigned function with maximum efficiency and 2) insure that the various units comprising the system are fully integrated for the human performance standpoint.

Control design parameters have been selected which are compatible with the restrictions imposed by special clothing such as a Navy-type full pressure suit (MKII-Mod. 0). Extensive use has been made of simple mock-ups and experimentation under simulated pressure suit operation to determine optimum system requirements. Reliability studies and actual flight evaluation tests will be used to insure that the final design represents the best solution for providing the pilot of a high performance aircraft with a touch tuning control and remote indicator display.

45.2. The Effect of Loop Characteristics Upon Human Gain

J. S. SWEENEY, *U. S. Naval Res. Lab., Washington, D. C. and* A. GRAHAM, *Antioch College, Yellow Springs, Ohio*

When the human operator is performing a compensatory tracking task, such as piloting an aircraft or helicopter, or controlling depth of a submarine, he is behaving as an element in a closed-loop control system. The gain which he exhibits (ratio of his output over the input to him) is dependent upon the characteristics of the loop or loops in which he is enclosed. This gain may be changed as much as 78 db by manipulation of the loop characteristics. This paper will discuss human gain and the loop parameters which influence it.

45.3. The Influence of Nonlinear Transfer Function on Cathode-Ray Tube Visual Detection Threshold

C. W. MILLER, *Cornell Aeronaut. Lab., Buffalo, N. Y., and* W. R. MINTY, *Advanced Electronics Center, General Electric Co., Cornell University, Ithaca, N. Y.*

Visual detection threshold of observers (B) was measured as a function of input signal voltage (E) to a cathode-ray tube (CRT) type indicator. The effect of changing transfer functions of the system was accomplished by insertion of nonlinear amplification prior to the CRT grid, so as to have several functions ($B = f(E)$, $g(E)$, $h(E)$, etc.) available. These functions were in the form of power law exponents in the range of 4.5 to 0.8 ($f(E) = E^{4.5}$, $g(E) = E^{2.0}$, etc.). Two systems were studied, a Kay-Lab closed-loop television and an APS-20 radar indicator possessing 10 FP4 and 7FP7 CRT's, respectively. Results show significant differ-

ences in six db in the form of lower signal inputs detectable at threshold with a transfer function exponent less than unity.

45.4. Human Factors in the Design of the NRL Nuclear Reactor Control System

H. J. BERLINER, M. P. YOUNG, AND G. F. WALL, *U. S. Naval Res. Lab., Washington, D. C.*

The last decade has seen very rapid advances in both nuclear reactor and control system technology. The merging of these two two fields for providing control systems for nuclear reactor thus presents many interesting and challenging problems. One of the most important of these is the allocation of control responsibility among men and automatic equipment so as best to achieve maximum safety, flexibility, and continuous operating time. This paper deals with the solution to this problem for the NRL nuclear research reactor and how the solution has been implemented.

SESSION 46*

Thurs.   10:00 A.M.–12:30 P.M.

Coliseum
Marconi Hall

ANTENNAS—II

Chairman: ROBERT L. MATTINGLY, *Bell Telephone Labs., Inc., Whippany, N. J.*

46.1. Electrically Small DF Antenna

E. McCANN AND H. H. HIBBS, *Melpar, Inc., Falls Church, Va.*

A direction-finding antenna of dimensions small in terms of wavelengths has been designed. The antenna is obliquely polarized, hence is equally responsive to vertical or horizontal polarization and functions over a two-to-one bandwidth. By use of slotted cylinder type radiating elements it is possible to contain the antenna as well as its associated drive and control mechanisms in a cylindrical volume approximately 0.15 λ in diameter and 0.35 λ in length. The configuration is also advantageous from a mechanical standpoint due to the light weight of the rotating members. The effect of the antenna's environment on its behavior as well as theoretical and experimental data is discussed.

46.2. Experiments and Calculations on Surface-Wave Antennas

R. G. MALECH AND S. J. BLANK, *Airborne Instruments Lab., Mineola, N. Y.*

Near- and far-field measurements were made of electromagnetic waves propagating along and emanating from structures whose equivalent index of refraction is a function of the direction of propagation.

The antennas described are Yagi-Uda antennas (about 8½ wavelengths long at S band). The parasitic elements of the antennas are printed on a teflon-glass dielectric sheet. Four antennas are measured: the two-dimensional counterpart of the cigar antennas, the unmodulated ladder antenna, the linearly tapered ladder antenna, and the sinusoidally modulated ladder antennas.

Far-field radiation patterns of the linearly tapered structure are calculated using measured near-field data. The method used in the calculations is that outlined by A. S. Thomas and F. J. Zucker. It is based upon harmonic analysis of the spatial frequencies contained in phase-modulated waves.

The calibrated far-field radiation patterns are compared with experimentally determined far-field radiation patterns, with partial agreement being obtained.

46.3. Ferrite Excited Slots with Controllable Amplitude and Phase

H. E. SHANKS AND V. GALINDO, *Microwave Lab., Hughes Aircraft Co., Culver City, Calif.*

This paper describes the results of investigations aimed at realizing waveguide slot elements whose radiating characteristics can be electronically varied, both in amplitude and phase. The approach utilizes a normally non-radiating longitudinal slot in the broadwall of rectangular waveguide. It is well known that such a slot can be caused to radiate by the judicious placement of discontinuities in the waveguide in the region of the slot. If these discontinuities (stubs, irises, etc.) are constructed out of material whose characteristics can be varied by external means, the radiating nature of the accompanying slot can also be varied. The use of various ferrite discontinuities are discussed and shown to enable either variable amplitude of radiation or both variable amplitude and variable phase of radiation. The controlling mechanism is a dc magnetic field provided by an external electromagnet.

46.4. Improved Feed Design for Amplitude-Monopulse Radar Antennas

J. PAUL SHELTON, *Aero Geo Astro Corp., Alexandria, Va.*

The design of amplitude-monopulse radar antennas utilizing four-horn feed clusters has been complicated by the basic difference between the sum and difference feed patterns. The array factor of the sum configuration is a cosine function and that of the difference is a sine function of the same argument, making optimum illumination impossible for both cases. A technique is described which allows independent control of the sum and difference array factors, and it is felt that the concept will find application outside the field of monopulse radar. The technique involves directional coupling and phase shifting among a set of four adjoining waveguide feeds to obtain the desired aperture distributions in one plane. The design of a practical waveguide configuration, suitable for use with lens or reflector, is described.

46.5. The Directional Coupler Antenna

CHARLES FINK, *Litton Industries of Maryland, Inc., College Park, Md.*

The combination of four broadband 3-db directional couplers and four radiating elements into an antenna for direction finding purposes has been investigated. Under theoretical conditions, two overlapping beams with constant crossover level and variable crossover slope over an infinite frequency band can be obtained. All four radiators are active in producing each of the two main lobes for simultaneous comparison, thereby providing the pattern effect of two antennas of similar dimension. Practically, an antenna pattern with crossover level 3 to 5 db below beam maximum and pointing accuracy of ±0.75° over a 2.2 to 1 bandwidth has been achieved.

46.6 Arbitrarily Polarized Planar Antennas

F. J. GOEBELS, JR. AND K. C. KELLY, *Microwave Lab., Hughes Aircraft Co., Culver City, Calif.*

This paper describes the analysis and design of a class of antennas which produce constant shape pencil beams with either sense circular, any linear, or elliptical polarization by a simple adjustment in the feed circuit. The aperture is located on the upper plate of a radial waveguide and is composed of annular slots, each annulus consisting of a discrete number of crossed slots. The annular slots are so positioned that each arm of the crossed slots couple by a constant factor to the radial or circumferential currents flowing over the aperture plate. The standing-wave array requires one radial waveguide mode for its operation while the traveling-wave array required two modes. Experiments were conducted at X band.

SESSION 47*

Thurs.   10:00 A.M.–12:30 P.M.

Coliseum
Faraday Hall

INSTRUMENTATION: DEVICES AND CIRCUITS

Chairman: FERDINAND HAMBURGER, JR., *Elec. Eng. Dept., The Johns Hopkins University, Baltimore, Md.*

47.1. Printed Circuit DC Motors for Electronic and Instrument Applications

J. HENRY-BAUDOT, *Société d'Electronique et d'Automatisme, Courbevoie (Seine), France,* AND R. P. BURR, *Circuit Research Co., Cold Spring Harbor, N. Y.*

Servalco printed circuit dc motors combine a new design concept with the techniques of printed circuitry to produce dc machines

wherein the armature is produced entirely as a printed circuit part. The new machines are of an unconventional planar air gap form which has many advantages. Among these are low cost, high torque-to-inertia ratio, negligible armature reactance, smooth commutation, and good high-temperature performance. The technique is suited not only to general service applications but to the instrument, servo and control field.

47.2. A 100-CPS *X-Y* Recorder

JOHN P. BRADY, JR., *Sanborn Co., Waltham, Mass.*

A 100 cps, direct-writing light-beam system which records *Y*-axis variables as a function of *X*-axis variables is described. A compatible electrical driving system utilizing any of several preamplifiers is presented. Performance specifications are explained with the physical factors which facilitate meeting these requirements emphasized. A unique "axis record" provision and a monitoring facility are discussed. Typical applications and operating procedure are outlined. The system is compared with other *X-Y* recorders.

47.3. A Proposed Automatic Test Set for the Measurement of Communication Cable Parameters

H. N. AVILES, *Western Electric Co., Inc., Baltimore, Md.*

A description is given of a proposed set designed for the final inspection of communication cable. A commercially available punched tape programming device selects the circuit or combination of circuits to be tested and determines the sequence of parameters to be measured. Self-balancing, servo-driven bridge networks measure the characteristic values of dc conductor resistance, 900-cycle capacitance unbalance and 900-cycle ac capacitance and conductance. Measured results are then plotted sequentially on a special chart recorder. Individual circuits are also checked for dc insulation resistance and ac dielectric strength. These tests are normally GO/NO-GO and only defective circuits are identified and recorded.

47.4. A Precision 60-MC Logarithmic Amplifier

S. COHEN, H. LASKIN, E. SCHECKER, AND B. WOODWARD, *Airborne Instruments Lab., Mineola, N. Y.*

A stable 60-mc transistor amplifier has been developed with an accurate logarithmic transfer characteristic for input signals from -70 dbm to -10 dbm. The over-all amplifier bandwidth is 8 mc. Eight double-tuned 3N35 stages are employed with logarithmic response achieved by adding the video voltages developed in each interstage due to the nonlinear input impedance of the transistor. The small signal linear gain of the amplifier is about 65 db with less than 1 db variation from 0°C to 80°C.

47.5. Design and Development of a Noise and Field Instrument for 1000- to 12,000-MC Frequency Range

A. BORCK AND M. RODRIGUEZ, *Empire Devices, Inc., Amsterdam, N. Y.*

A noise and field intensity meter is a device used to monitor narrow and wide band-noise in the 1000 to 12,000-mc frequency range. Design and development of a noise and field instrument for 1000 to 12,000-mc frequency range encompasses all of the following considerations:

1) A highly sensitive low noise, superheterodyne receiver encompassing preselection.
2) Tunable over the desired frequency range.
3) Linearity in excess of 60 db.
4) Extremely versatile output indicator capable of CW average and pulse peak, both linearly and log or rhythmically.
5) Utilization of a calibrated internal secondary noise standard, allowing direct measurement of unknown noise signals, both random and impulse type.
6) Variable bandwidth.

SESSION 48*

Thurs.   2:30–5:00 P.M.

Waldorf-Astoria Starlight Roof

ELECTRONIC COMPUTERS: COMPONENTS AND CIRCUITS

Chairman: LAWRENCE W. VON TERSCH, *Michigan State University, East Lansing, Mich.*

48.1. Magnetic Drum Time Compression Recorder

W. R. CHYNOWETH, *General Electric Co., Syracuse, N. Y.,* AND R. M. PAGE, *U. S. Naval Res. Lab., Washington, D. C.*

A magnetic drum time compression recorder with a compression ratio of 82800:1 has been developed. Input signals of 5–90-cps bandwidth appear at the output as a bandwidth of 400 kc–7.5 mc. This is accomplished, using a constant speed and stationary heads, by sampling the input data and recording these 0.06-μsec samples in a special pattern on the drum circumference. The drum is 13.5 inches in diameter and rotates at 10,800 rpm with a dynamic runout at full speed of less than 90 microinches. Special heads have been developed for the high frequencies. These heads are constructed to ride on the air film carried by the drum surface at a spacing of less than 200 microinches.

48.2. Fast Microwave Logic Circuits

D. J. BLATTNER AND F. STERZER, *RCA, Princeton, N. J.*

Binary logic circuits have been built in which the binary "one" or "zero" is represented by the presence or absence of an RF pulse in a given time space. Using strip line printed circuit techniques and point contact microwave diodes, we have constructed *and*, *or*, and *not* gates which operate with pulses of less than 2-mμsec duration (*i.e.*, a pulse repetition rate of 500 mc) at a carrier frequency of 3000 mc. These elements have been combined to form half adders and full adders.

Detailed performance of the basic elements and adders will be presented. Some aspects of larger microwave computing systems will also be discussed.

48.3. Multiple-Input Analog-to-Digital Converter with 12-Bit Accuracy and Fast, Non-sequential Switching

HARRISON S. HORN, *Link Aviation, Inc., Palo Alto, Calif.*

All-electronic multiple-input analog-to-digital conversion is accomplished by internally generating a changing analog voltage and a corresponding digital number and comparing this analog voltage to all input analog voltages simultaneously. The result of only one comparison is used to control the internally generated analog voltage and digital number in the manner of single-input analog-to-digital converters.

Difference-signal switching requires accuracy only over a very small range near balance, thus avoiding the usual problems of accurate electronic analog switching. Fast, accurate input selection and conversion by all-electronic equipment permit nonsequential operation with selection and conversion accomplished in less than 1 msec and consequent elimination of computer input storage.

48.4. Asynchronous Electronic Switching Circuits

M. KLIMAN AND O. LOWENSCHUSS, *Sperry Gyroscope Co., Great Neck, N. Y.*

A study has been made of asynchronous electronic switching circuits using and extending concepts introduced by Huffman, Caldwell, and Unger. This class of circuits operates without using a master clock oscillator, multivibrator timing chains or synchronizing pulses of any kind. Signals are represented by variables which can assume one of two levels and are propagated through individual elements at a speed determined solely by that element. Advantages of these circuits are that they provide a speed increase, greater than the equipment increase, and they enhance reliability. Experimental results have been obtained by using standard resistance-coupled transistor circuitry which have verified the design procedures and have resulted in an appreciable speed increase over the standard use of the same circuits.

48.5. The Cycle Splitter—A Wide-Band Precision Frequency Multiplier

B. E. KEISER, *Missouri Research Labs., Inc., St. Louis, Mo.*

A simple device capable of frequency multiplication by any positive integer is described. A unique feature of the device is that only the desired harmonic is obtained in the output.

The cycle splitter's operation is based upon the fact that frequency is the time derivative of phase angle. The device is instrumented by means of wide-band phase difference networks and the use of the "photoformer" technique. Output amplitude may be independent of, or linearly dependent upon, input amplitude. A cycle splitter has been constructed which will accept any input frequency between 30 cps and 50,000 cps and multiply its frequency by 100.

SESSION 49*

Thurs.   **2:30–5:00 P.M.**

Waldorf-Astoria
Astor Gallery

CIRCUIT THEORY III— APPLICATIONS

Chairman: ALAN B. MACNEE, *Elec. Eng. Dept., University of Michigan, Ann Arbor, Mich.*

49.1. Panoramic Spectrum Analyzer in Real Time

B. D. STEINBERG AND W. G. EHRICH, *General Atronics Corp., Bala-Cynwyd, Pa.*

A group of panoramic spectrum analyzers or Fourier analyzers is described which makes use of a time varying comb filter, employing a delay line in a positive feedback loop. Such analyzers permit an accelerated spectrum analysis, faster than the usual analysis time, $T = W/B^2$, where B is the bandwidth of the sweeping filter, and W is the spectrum width.

Feedback delay line analyzers fall into two classes with analysis times $1/W$ and $1/B$, respectively. In each case, the modulating or sweeping waveform can be applied inside or outside the loop. The configuration and performance of such analyzers are compared.

49.2. A Long-Memory Delay-Line Analog Recirculator

M. S. ZIMMERMAN, W. G. EHRICH, AND D. E. SUNSTEIN, *General Atronics Corp., Bala-Cynwyd, Pa.*

A video signal integrator, or comb filter, has been developed which is capable of achieving integration times corresponding to over 1000 recirculations through an ultrasonic delay-line memory. The use of several novel techniques allows the circulation of analog information without the large cumulative distortions normally encountered in a closed-loop memory system, while permitting a reduction in the number of tubes in the memory loop. This system is noncritical with regard to interstage network tuning and naturally suppresses many of the spurious responses generated within the delay line.

In addition, a technique has been developed for decorrelating spurious couplings between range elements caused by either inadequate circuit damping or delay line multipath.

49.3. Choice of the Shape of the Input to a Spectrum Analyzer in Terms of Its Effect on Transient Selectivity and Signal Detactability

WILL GERSCH, *Electronics Res. Labs., Columbia University, New York, N. Y.*

The problem of choosing a suitable shape for the input carrier to a spectrum analyzer is considered. The spectrum analyzer, composed of a bank of filters, has the objective of detecting the presence and determining the frequency of fixed duration, constant frequency signals immersed in white noise.

Control of transient selectivity depends upon the ability to control the discontinuities of the input amplitude function and its derivatives. Techniques and results of a study of transient selectivity and signal detectability under a variety of modulating functions are presented for a single-tuned filter bank and compared to the performance of a bank of ideal coherent integrators. A particularly interesting illustration is that of a single-tuned filter, whose input is modulated to achieve the selectivity of a stagger-tuned triple and accomplishes an improvement in signal detectability of 2 db.

49.4. A Minimum Distortion Tapered-Transmission-Line Transformer for Pulse Application

HIROSHI AMEMIYA, *RCA, Camden, N. J.*

Tapered transmission lines are used for impedance transformation. When terminated by the nominal characteristic impedance at each end, the performance, perfect at infinite frequency, becomes poorer as the frequency is lowered and is of a direct connection at dc. Different taper formulas give different performances. When a pulse is transmitted through a tapered line, the waveform will be distorted because the line cannot transmit all the frequency components of the pulse uniformly. It will be shown that, if the step-up ratio of the transformer is small, the exponential taper gives the best performance for pulse transmission in the sense that the distortion is minimized.

49.5. Transistor Digital Tape Record Circuit

ALBERT E. HAYES, JR., *Ampex Corp., Redwood City, Calif.*

The attainment of fast rise and fall times in digital tape recording is generally regarded as an uphill battle against the inductance of the recording or "write" head. The inherent requirement for a specified number of ampere turns in the write head, when coupled with the limited current-handling capabilities of fast rise-time transistors, leads the engineer to the inevitable use of write heads with considerably more inductance than he would otherwise

select from a rise-time standpoint. Present techniques have made use of high supply voltages to provide the necessary sharp spikes of driving voltage to ensure a square wave of head current. These high-voltage spikes require rather subtle and complex circuit design to ensure both circuit and device reliability. This paper describes the evolution of a true "current-drive" write circuit which eliminates the need for the generation of large voltage pulses by the write amplifier. It is demonstrated that the rise and fall times of the recorded digital signal are substantially independent of the inductance of the write head.

SESSION 50*

Thurs.   **2:30–5:00 P.M.**

Waldorf-Astoria
Jade Room

ULTRASONIC ENGINEER- ING—II

Chairman: FRANK MASSA, *Massa Labs., Inc., Hingham, Mass.*

50.1. Thickness-Shear Mode Barium Titanate Ceramic Transducers for Ultrasonic Delay Lines

JOHN E. MAY, JR., *Bell Telephone Labs., Inc., Whippany, N. J.*

The properties of thickness-shear mode $BaTiO_3$ ceramic transducers as applied to ultrasonic delay lines have been investigated. A method of fabricating these transducers has been developed which allows bonding to the delay line by conventional soldering techniques. Compared with longitudinal-thickness mode transducers and shear mode transducers have a higher dielectric constant, a lower resistance and a lower capacitance ratio. Substitution for the former on short delay lines at 15 mc increased the bandwidth from 30 per cent to 43 per cent for the same loss. When the quartz transducers on the longer polygon type lines were replaced with the ceramic transducers, the loss was reduced from 40 db to 20 db.

50.2. Vibrations of Ferroelectric Transducer Elements Loaded by Masses and Acoustic Radiation

F. ROSENTHAL, *Raytheon Manufacturing Co., Newton, Mass.,* AND V. D. MIKUTEIT, *Battelle Memorial Inst., Columbus, Ohio*

The motion, stress, acoustic power, Q, and electrical impedance are calculated for idealized 3-layer sonic transducers, consisting of a piezoelectric element loaded at either end by a mass which is assumed to be lumped, and loaded further by ρc-type plane acousic radia-

tion; the piezoelectric element may be driven by use of either the d_{33} or d_{31} effect. The lumped constant equivalent circuit is given for the case of negligible ceramic mass density. Effects on transducer performance of such parameters as the ratio of loading masses are determined analytically and the lumped mass solutions are compared with the somewhat more realistic solution based on the assumption of distributed end masses (obtained on an IBM 650 computer and not explicitly given in this paper).

50.3. Effects of Electrical and Mechanical Terminating Resistances on Loss and Bandwidth According to the Conventional Equivalent Circuit of a Piezoelectric Transducer, or How to Get the Most out of Your Ultrasonic Delay Line

R. N. THURSTON, *Bell Telephone Labs., Inc., Murray Hill, N. J.*

It is assumed that the element values in the electromechanical circuit of the transducer are known. Simple formulas and curves then provide quick answers to the following questions:

1) What terminations give the lowest loss at midband with a given 3-db bandwidth? (These same terminations also give the widest band with a given loss.)
2) How are midband loss and 3-db bandwidth related to the terminations a) when a tuning inductor is used, and b) without a tuning inductor?
3) When the mechanical (or electrical) termination is fixed, what electrical (or mechanical) termination gives a) minimum loss at midband and b) maximum 3-db bandwidth?

50.4. Measuring the Characteristics of Present-Day Ultrasonic Delay Lines

J. J. G. McCUE AND M. AXELBANK, *Lincoln Lab., Mass. Inst. Tech., Lexington, Mass.*

Test benches designed for the delay lines of five years ago are in general not capable of yielding reliable data on lines of modern design, which are likely to be characterized by high transducer susceptance and low spurious responses. The paper describes test equipment for making measurements on delay-line attenuation and on the levels of the spurious responses over the range 10 to 80 mc. The key parts are a pulser, a converter, and a 5-mc amplifier and detector. The equipment will handle transducer capacitances of 1000 $\mu\mu$f or more and will measure spurious responses 80 db below the output of a representative 1000-μsec line.

50.5. Ultrasonic Welding Equipment

JOHN N. ANTONEVICH, *Battelle Memorial Inst., Columbus, Ohio*

The basic principles of ultrasonic welding are discussed. It is postulated that this welding process is a form of pressure or friction welding.

An experimental arrangement for studying the fundamentals of ultrasonic welding is described. Data obtained with this arrangement are presented. These data show the relationships existing between the welding variables and weld strength.

The essential components of an ultrasonic welder are described, and the functions of the components are discussed. On the basis of their functions and the conditions necessary to produce a weld, consideration is given to the design of ultrasonic welding equipment. The problems encountered in designing welding equipment are discussed and methods of circumventing them are presented.

SESSION 51*

Thurs.   **2:30–5:00 P.M.**

Waldorf-Astoria
Sert Room

CONCEPTS AND PROGRAMS

Chairman: GRAYSON MERRILL, *Fairchild Astrionics Div., Wyandanch, L. I., N. Y.*

51.1. An Orbit Program for Engineering Use

H. R. SMITH AND B. H. BLOOM, *RCA, Moorestown, N. J.*

The computation of orbits is one of the most common problems encountered in the design of devices for detecting objects following ballistic trajectories. In the course of the design, this orbit problem will usually appear in numerous forms, each requiring different outputs from one of several types of inputs. At RCA, instead of writing special programs for each case, a single highly flexible routine was developed. This routine not only generates selected outputs from many classes of inputs, but also varies these inputs to obtain desired outputs, reads maps or searches for extreme values.

51.2. A Study and Design Evaluation of the Throw-Away Maintenance Concept

J. J. ANDREA, *Collins Radio Co., Cedar Rapids, Iowa,* AND M. V. RATYNSKI, *Rome Air Dev. Center, Griffiss AFB, Rome, N. Y.*

A study was conducted to determine the engineering feasibility of replacing the current military electronic maintenance practices by

the "throw-away" module concept for new ground electronic equipments.

A typical UHF communications equipment was redesigned to be almost entirely a "throw-away" module type. The logistics and engineering economics of this new design were then compared to conventional designs. The impact of the "throw-away" design upon military field maintenance organizations was studied and investigated. A formula was developed which was utilized by the design engineers to evaluate and compare "throw-away" and conventional designs.

Also to be discussed will be the design criteria and logistics imposed upon engineers who must make technical decisions as to whether equipments and modules will be of the conventional or of the "throw-away" design.

51.3. Amplitude Modulated Video Integrator

ROBERT E. ELLIS, *Aero Geo Astro Corp., Alexandria, Va.*

This paper describes a stable AM video integrator that will operate with loop gains as high as 0.95. As a result of the increased integrator memory, obtained with the high loop gain, significant signal enhancement as well as the virtual elimination of spurious jamming is achieved. When the integration is operated with a radar system, operational efficiency is greatly improved because the signal enhancement reduces operator fatigue since the targets have much higher contrast and can be more easily and rapidly distinguished.

The system involves a quartz delay line, but eliminates any necessity for AGC features. It proved to have stable operation and demonstrated 3-db improvement at the 50 per cent probability of detection point of the blip-scan curve. Wildcat jamming signals of sufficient amplitude to saturate a PPI indicator were effectively removed when the input signal was processed by this video integrator.

51.4. The Significance of Specifications in Government Sponsored Technical Development Programs

JOSEPH CRYDEN, *Hughes Aircraft Co., Culver City, Calif.*

While the specification is an ancient engineering device, specifications currently used in the electronics industry present serious problems, both to management and to working engineers. The critical problems arise in part because of the extreme complexity of the systems to which they apply, and in part because they govern the activities of a large complex which consists of government agencies, the prime contractor, subcontractors and parts vendors. Failure to appreciate the varied functions of the large number of specifications that apply to a given contract results in lack of adequate attention to specifications. In consequence, the cost of development is increased by a significant factor, many avoidable engineering errors are made, and the time required for the completion of developmental contracts is unnecessarily prolonged.

This paper discusses the varied functions of specifications now used in the electronics industry, some of the more significant inadequacies in dealing with specifications, and finally, some of the more obvious and easily effected remedies.

SESSION 52*

Thurs.   2:30–5:00 P.M.

Coliseum
Morse Hall

COMMUNICATION ENGINEER-ING IN BROADCASTING

Chairman: C. H. OWEN, *American Broadcasting Co., New York, N. Y.*

52.1. Transmission of Television Signals Over a Broad-Band Tropospheric Scatter Link

L. POLLACK, *ITT Labs., Nutley, N. J.*

Equipment to transmit and toll quality multichannel telephone signals over a broad-band tropospheric scatter link is described. The characteristics of the radio system which are important in wide-band tropospheric transmission are detailed.

A wide-band 10-kw transmitter coupled to a feed horn illuminating a 60-foot parabolic reflector and a quadruple diversity receiver are employed in the system.

Television traffic statistics obtained during one year of commercial operation are given.

52.2. Installation and Operational Aspects of a Private Television Microwave System

AARON SHELTON, *WSM, Nashville, Tenn.*

The problems of installation, operation and maintenance of 165-mile, 6-hop, private intercity television relay is reviewed. The success is to be issued for discussion.

52.3. Mobile Microwave Television Pickup Operational Experiences

G. EDWARD HAMILTON, *American Broadcasting Co., New York, N. Y.*

The primary purpose for a "crash unit" in the broadcasting field is to provide more adequately a rapid communication to the public in areas of emergency or disaster occurrence.

Requirements for such a program must encompass picture generations, lighting, transmission of visual programs and cue communications. The equipment must be easily maneuvered and be mounted in a conveyance which is small and yet adequate to house the necessary power generating gear.

Techniques must be evolved which are compatible with actual mobile operations such as might be encountered for parade movement, shift of operations interest, etc.

Receiving sites should be considered in terms of 360° service to a centrally located area and/or in terms of an intermediate relay system.

52.4. Effect of Frequency Cutoff Characteristics on Spiking and Ringing of TV Signals

A. D. FOWLER AND J. D. IGLEHEART, *Bell Telephone Labs., Inc. Murray Hill, N. J.*

Spiking and ringing of TV signals depend upon amplitude and delay characteristics associated with frequency cutoff of transmission. The effects of a variety of cutoff characteristics of both ideal and practical systems on rectangular and sine-squared pulses are illustrated by computed waveforms.

The illustrations are arranged to show 1) waveform of input pulse, 2) amplitude and delay characteristics of transmission path, and 3) waveform of output pulse. Included is a discussion of inferences that can be drawn from certain output waveforms and of the limitations on the reduction of ringing that can be achieved by in-band equalization.

52.5. 50-KW Antenna Switching System

JOHN W. SMITH, *Collins Radio Co., Cedar Rapids, Iowa*

There are many HF radio installations today that illustrate the need for an improved antenna switching technique. Today there is a growing requirement to connect rapidly any one of several 50-kw transmitters to any one of many antennas. An antenna switching system must be broad band, convenient to use, fast, safe for operating personnel and free of appreciable impedance discontinuities. This paper describes several components and techniques that solve the transmitter/antenna selection problem up to a 50-kw power level as well as receiver/antenna selection. The influence of switching techniques on RF transmission, impedance conversion, antennas and other items are also discussed.

SESSION 53*

Thurs.   2:30–5:00 P.M.

Coliseum
Marconi Hall

ANTENNAS—III

Chairman: HENRY JASIK, *Jasik Labs., Westbury, N. Y.*

53.1. Log Periodic Feeds for Lens and Reflectors

R. H. DuHAMEL AND F. R. ORE, *Collins Radio Co., Cedar Rapids, Iowa*

The application of unidirectional log periodic antennas as feeds for lens or reflectors to cover 10:1 or 20:1 bandwidths is described. Information on the primary patterns, phase center variation, input impedance, and aperture blocking of trapezoidal tooth wire and sheet structures is given so as to allow the design of feeds for a wide variety of lens and reflectors. Final results of pattern, gain and impedance measurements on two dishes over 10:1 and 20:1 bandwidths are presented and a discussion of the slight sacrifices in gain and sidelobe level to achieve this bandwidth is given.

53.2. Broad-Band Conical Helix Antennas

HARRY BARSKY, *American Electronic Labs., Inc., Lansdale, Pa.*

This paper discussed the design of circularly-polarized, unidirectional, broad-band antenna structures. Basically the antennas are conical helixes described by the general formula

$$R = R_0 e^{2\pi n \tan \alpha \sin \gamma}.$$

Measured data for three specific models are presented indicating that the pertinent electrical characteristics are independent of frequency for bandwidths of 20:1, 12:1, and 5:1, and that the bandwidth limits are a function of the mechanical accuracy with which the design formula can be duplicated. All of the structures are apex-fed and the feed lines are coincident with the axis of the cone. Gains of 5 db over a dipole have been obtained for an axial ratio of 3:1.

53.3. Very Broad-Band Feed for Paraboloidal Reflectors

J. R. TOMLINSON AND M. N. FULLILOVE, *Melpar, Inc., Falls Church, Va.*

A compact, efficient very broad-band linearly polarized feed unit has been developed for use in large aperture paraboloidal reflectors. The unit, a multidipole in line array, is effective over 4 adjacent 2:1 bands with excellent back to front ratio and VSWR. On three of the bands back-to-front ratio is better than 10 to 1 and often 15 to 1 or better. On the lowest band back-to-front ratio is better than 7 to 1.

Model tests of the feed plus reflector indicate that beamwidths and sidelobes are good over the band with sidelobes between 20 and 30 db down in one plane and below 15 db in the other plane. Directivity as calculated from beamwidths exactly corresponds to theoretical directivity over the whole band. Simple mechanical packaging is achieved by use of strip-transmission line techniques in balun construction.

53.4. Far-Field Patterns of Circular Paraboloidal Reflectors

G. DOUNDOULAKIS AND S. GETHIN *General-Bronze Corp., Garden City, N. Y.*

From recorded primary radiation patterns of different shape feed horns, the normalized field distributions over the aperture of a symmetrical paraboloidal reflector are computed,

plotted, and subsequently expressed in terms of constants k and p of simulating aperture distribution functions e^{-kr} and e^{-pr^2}. Convenient methods are worked out for the computation of the different secondary far-field radiation pattern parameters for circularly symmetric equiphase distributions in terms of k and p. Computed and experimental data for beam-width efficiency, first and second sidelobes and aperture blocking effects are plotted and compared in terms of k and p. The possibility of treating offset circular parabolidal reflectors in a similar manner is discussed.

53.5. Effects of Random Errors on the Performance of Antenna Arrays of Many Elements

L. A. RONDINELLI, *Hughes Aircraft Co., Culver City, Calif.*

A theoretical statistical analysis is presented in which a study was made to determine the effect of random current excitation errors upon the radiation characteristics of a two-dimensional array of identical radiators. The technique employed was to develop a statistical model and then argue that this model closely approximates the nature of the radiated electric field produced by an array of a large number of current elements, where the individual element currents are in error both in amplitude and phase. The analysis has been applied to the study of the following antenna characteristics: 1) maximum side-lobe level within a specified cone about the main beam, 2) maximum side-lobe level in the remainder of the half-space outside the specified cone, 3) beam pointing accuracy.

53.6. The Hourglass Scanner, a New Rapid Scan, Large Aperture Antenna

M. N. FULLILOVE, W. G. SCOTT, AND J. R. TOMLINSON, *Melpar, Inc., Falls Church, Va.*

In this paper the authors discuss the development of a highly directive, rapid scanning antenna. Basically, the antenna consists of a circularly disposed antenna array used as a feed system for a novel reflector surface providing a large vertical plane aperture. The reflecting surface, termed a half-hourglass, is formed by revolving a half-parabola about an axis parallel to the *latus rectum* of the parabola. The feed system consists of a circularly disposed array of dipoles with splash plate, located on the focal circle of the parabola and tilted into the center of the reflector. The dipoles are connected through equal lengths of cable to the stator of a noncontacting RF commutator. The outputs of the rotor, which connect approximately a 120° sector of the 360° feed array at any instant, are fed through individual RF phasing cables to a matched power combiner with a single output. Scanning is achieved by the continuous switching action of the commutator rotor. The primary feature of this antenna is the provision for extremely high-speed scanning of a large aperture without the necessity of mechanically rotating a large physical structure. For example, the effective aperture of a $6\frac{1}{2}$-foot dish can be scanned at speeds of 1000 rpm. A scale model has been successfully tested over a 4-to-1 fre-

quency band using a unique feed element structure providing simultaneously four independent beams, two beams each covering adjacent 2-to-1 bands. Extensive experimental data confirm that narrow beams and satisfactory side-lobes are achieved in both planes over both frequency bands.

SESSION 54*

Thurs. 2:30–5:00 P.M.

Coliseum
Faraday Hall

INSTRUMENTATION FOR HIGH-SPEED DATA ACQUISITION

Chairman: J. WESLEY LEAS, *RCA, Camden, N. J.*

54.1. A 64-Channel Millimicrosecond Time Analyzer

T. P. LANG, *Vanderbilt University, Nashville, Tenn., and Sperry Microwave Electronics Co., Clearwater, Fla.*

A 64-channel time analyzer has been developed for a fast neutron time-of-flight spectrometer. Time intervals of 0 to 500 mμsec can be measured to an accuracy of less than 1 mμsec. The channel width is adjustable from 0.05 to 10 mμsec. The timing circuit is of the vernier chronotron type developed by Lefevre and Russell in AEC publication HW-4966. For each analysis the output data from the vernier chronotron are in serial form (with a pulse spacing of 100 mμsec.). These serial data are converted to a parallel binary data with a fast binary scaler. The parallel binary data are "decoded" by a magnetic core matrix arrangement. The matrix operates the 64 separate scaling channels. The maximum analysis rate is 100 kc.

54.2. Magnetic Recording and Reproduction of Pulses

DONALD F. ELDRIDGE, *Ampex Corp., Redwood City, Calif.*

Various presently used schemes of digital recording are discussed. Means are derived for the computation of reproduced pulse width and height as a function of the gap width, medium thickness, and spacing. The importance of the perpendicular component of magnetization is evaluated by a novel experimental technique.

Transfer characteristics of a typical oxide are presented both for an initially neutral condition and for various amounts of previous magnetization.

The record process is analyzed, and recorded pulse width and location are found to be functions of the medium magnetization characteristics, record head gap, record current, medium thickness and head-to-medium spacing. The effect of each of these variables is computed.

54.3. An Improved Method of Calibrating FM Magnetic Tape Transports

LEWIS BOHNSTEDT, *Ampex Corp. Redwood City, Calif.*

The present cumbersome methods used to calibrate FM magnetic tape recording systems is described. The input and output measuring and signal requirements are presented, and the general availability of equipment to satisfy such requirements is analyzed. The generalized solution to the problem of calibration is developed, and a device incorporating most of the desirable features in the generalized solution is described. Typical uses of this device are also presented, as well as an analysis of several unique circuit designs to achieve high performance in a portable unit.

54.4. Ratrase, A High Capacity, Low Level Automatic Data Handling System

G. FRED MOONEY, *3310 Blair Drive, Hollywood, Calif.*

A need has arisen in industry for a specialized data handling system which will automatically process data obtained from large numbers of like transducers. Ratrase (Reduction and acquisition transcription for analog system evaluation) was designed to fulfill this need in the field of static strain measurements. Low-level signals (0–25 mμ) from 500 or more strain gauge bridges are multiplexed, converted to digital form and recorded in compatible format for computer reduction. The system provides four selectable modes of operation: scan, zero scan, print, and read.

The time required to record 500 channels is 10 seconds. In this time each channel is converted and recorded 30 times thus providing a means to obtain signal-to-noise improvement. A novel control and zero reading storage incorporating two tape decks will be covered.

54.5. A Data Processing System Using Glow Tubes

STANLEY K. CHAO, *Data Processing Lab., Sylvania Electric Products, Inc., Needham, Mass.*

The decade glow counting tube has many interesting applications in data processing. The system described is the major portion of the equipment used in a wave propagation study to take the cumulative probability distribution of the incoming data pulses in real time. Glow tubes are used extensively to attain minimum equipment and maximum reliability.

Pulses from the receiver are gated and amplified before sent to this system. After scaling down they are sorted into thirty levels. Thirty channels of glow tube accumulators are used to store the sorted pulses. These data, together with the time of the day and the attenuator setting, are programmed by the readout unit and printed on paper tape. In addition, a paper-tape punch is used to keep a permanent record for later calculation in digital computers. Glow tubes are also used in the readout unit for programming and as complementing register.

Scanning the Transactions

The transmission of power by radiation is a dream which might some day become a reality when man succeeds in controlling and harnessing the thermonuclear fusion reaction for the production of power. While this proposal is purely speculative at present, there is justification for giving it serious consideration. Fusion power promises to be both cheap and plentiful. It is estimated that a fusion reactor will produce on the order of megawatts of power per cubic foot of plasma. Moreover, the cost, size and weight of the fuel are all negligible. Indeed, the major cost of a fusion reactor will be the transmission system. At the least, wire-line transmission systems will have to be substantially improved to handle greater power. But if fusion power is plentiful and cheap enough, it may prove more economical to employ completely new transmission methods, perhaps using induction fields over short distances, or electromagnetic radiation over longer distances. Electronics is already deeply involved in the task of producing a successful controlled fusion reaction. But it now appears that the distribution of electric power, as well as its generation, may become a field in which the radio and electronic engineer plays an important role. (E. W. Herold, "Controlled thermonuclear fusion—what it means to the radio engineer," 1958 IRE NATIONAL CONVENTION RECORD, Part 9.)

A herd of donkeys, it is written, was once asked by a great prophet: "What would a donkey require for a three-day journey?" And they answered, "Six bundles of hay and three bags of dates."

"That soundeth like a fair price, but I have for only one of you a three-day journey and I cannot give six bundles of hay and three bags of dates. Who will go for less?"

Behold, all stood forth. One would go for six bundles of hay and two bags of dates, another for three bundles and one bag. Then one especially long eared donkey agreed to go for one bundle of hay and take but $2\frac{1}{2}$ days.

Whereupon the prophet replied: "Thou art a disgrace to the herd and a fool. Thou canst not live for $2\frac{1}{2}$ days on one bundle of hay, much less undertake the journey and profit thereby."

"True," replied the donkey, hanging his long ears in shame. "But I wanted to get the contract!" (A. L. Stanley, "Logic and illogic in engineering and management," IRE TRANS. ON ENGINEERING MANAGEMENT, December, 1958.)

The advent of maser and parametric amplifiers with noise figures in the 1 to 3 db range is introducing an important new consideration—and limitation—in communication system design. Internal receiver noise, which heretofore was the principal factor that determined the maximum range at which a given signal could be detected, has been reduced so low by new low-noise solid-state amplifiers that *external* noise from cosmic and terrestrial sources has now become the major limitation. We have reached a point where, because of this external limitation, a given improvement in receiver performance no longer guarantees a comparable improvement in over-all system sensitivity and range. Moreover, it brings into much greater prominence design factors which were formerly secondary considerations, such as antenna orientation, reflectivity of the surrounding terrain, antenna polarization and lobe structure, frequency and even time, because they all have a direct bearing on the amount of external noise picked up by the antenna. It is apparent that in the future the system designer will have to change his time-honored way of thinking, particularly when he is dealing with radio telescopes, tropospheric scatter or space communication systems. (A. H. Hausman, "Dependence of the maximum range of tropospheric

scatter communications on antennas and receiver noise temperatures," IRE TRANS. ON COMMUNICATION SYSTEMS, December, 1958.)

Information theory specialists have taken up gambling as a means of shedding light on the important problem of determining the utility of a communication channel. No money changes hands, however, because the gambling is carried out on paper only. First, they set up a hypothetical situation in which a gambler receives positive and negative pulses, corresponding to the success or failure of an event, by means of a communication system. Because the channel is noisy, the gambler only knows with probability p that if a positive pulse is received, a positive pulse has been transmitted. The gambler then has the problem of wagering a fraction of his bank roll on the success or failure of each event in such a way as to make the most money after a given number of stages of betting. He has the choice of 1) betting on each event on the basis of just one pulse, 2) requiring two pulses for each event, and betting only if both pulses agree, or 3) requiring two pulses, adding them, and betting on the basis of the resultant pulse. Into this situation various conditions can be imposed as to the expense of the two pulses vs one, the cost, if any, of placing a bet, limitations on the frequency of betting, etc., all of which influence the choice of the best betting method. The end purpose of this unique and imaginative game is to show how, and in what way, the utility of a communication channel is influenced by *external* factors, and to demonstrate that only by considering the manner in which the information will be utilized, can the communication system be properly evaluated. It might also be remarked that engineering is becoming more of a gamble than any of us realized. (M. B. Marcus, "The utility of a communication channel and applications to suboptimal information handling procedures." IRE TRANS. ON INFORMATION THEORY, December, 1958.)

Cross-pollination is a word which, in a figurative sense, aptly describes a process which is vitally important to the progress of science, namely, the transfer of knowledge from one field to another. Nowhere in electronics is cross-pollination more necessary or more in evidence than in the flowering field of medical electronics. A look at the December issue of the IRE TRANSACTIONS ON MEDICAL ELECTRONICS will give some idea of the large number of different areas of human knowledge between which pollination is occurring. Listed below are the fields which were drawn upon in producing the modest total of eight papers in the issue, at best only a token sample when compared with the several thousand papers which have been published on medical electronics.

Audio	Mathematics
Broadcasting	Physics
Circuit Theory	Acoustics
Control Systems	Biophysics
Data Processing	Biology
Electron Devices	Bacteriology
Instrumentation	Microscopy
Man-Machine Systems	Circulatory Studies
Receivers	Heart Studies
Recording	Internal Medicine
Servomechanisms	Military Medicine
Telemetry	Obstetrics and Gynecology
Television	Pediatrics
Transmitters	Physiology
Ultrasonics	Respiratory Studies
	Surgery

This is one instance when a high pollen count is most welcome.

Pigs, planes and Proceedings, incongruous though the combination may sound, have been linked together by a development which is proving to be a very useful tool in the field of medical electronics. The development in question is a subminiature amplifier and FM transmitter, each no larger than a pack of cigarettes, for telemetering electrocardiographic data over short distances. It permits electrocardiograms to be taken of subjects while they are moving around, encumbered by nothing save 40 ounces of equipment. In November of 1955, shortly after the equipment was developed, PROCEEDINGS carried on its cover a photograph of a radio-equipped basketball player going through his paces while nearby receiving apparatus was recording his heart beats. Following publication of the picture numerous inquiries were received by the IRE and the manufacturer, one of which came from the U. S. Department of Agriculture. An article has now appeared describing how that organization is using the equipment to study the effects of high intensity sounds on livestock. In one experiment swine, with transmitters strapped to their backs, were placed in a room and subjected to recordings of jet planes roaring overhead at 135 db. Thus it would seem that PROCEEDINGS has performed the bizarre service of introducing the pig to the auditory rigors of the jet age. (J. C. Webb, *et al.*, "Electrocardiograph telemetering (radio)," 1958 IRE NATIONAL CONVENTION RECORD, Part 9.)

An electronic abstracter is the latest addition to a remarkable family of language machines, which already includes devices than can read alphabetic characters and can translate foreign language articles. The new machine, called "Auto-Abstract," will read a magazine article and then write an abstract of it. It works as follows. The complete text of an article is first transcribed onto magnetic or punched tape in a code that can be understood by an electronic data processing machine, such as the IBM 704 computer. The machine then analyzes the text word by word to derive statistical information concerning the frequency and distribution of the words in the text. From this, the machine determines the relative degree of significance of the words and then grades each sentence as to its importance. Sentences scoring highest in significance are automatically extracted from the text and printed out by the machine to form the "Auto-Abstract." In addition to creating abstracts, the machine can be used to condense lengthy reports. The Auto-Abstract system offers the possibility of relieving technically trained people of the chore of abstracting scientific articles so that they may devote more of their time to scientific work. The system also promises to expedite the translation of foreign scientific articles by producing foreign language abstracts of the original paper. A person then only has to translate the abstract rather than the full paper to find out what is in it, and the translation of full articles can be limited just to those that are found to be especially important. Perhaps authors can all look forward to the wonderful day when a machine will be able to write the article for them, as well. (H. P. Luhn, "The automatic creation of literature abstracts (Auto-Abstracts)," 1958 IRE NATIONAL CONVENTION RECORD, Part 10.)

Books

The Algebra of Electronics, by Chester H. Page

This book starts with an analysis of dc networks, extends the discussion to ac networks, and concludes with a study of nonlinear circuits, including rectification, amplification, modulation, demodulation, noise, and the application of the Fourier series to such circuits.

Perhaps the most outstanding feature is the thorough treatment of networks from a topological viewpoint in terms of trees, branches, links, and loops, and of mutual inductance with regard to the sign of the induced voltages and the general method of writing the network equations. Both mesh and nodal methods of analyses are explained, as well as their applications to nonplanar as well as planar graphs.

In view of the range of topics covered, it can hardly be expected that this book will be a thorough exposition of each subject treated, and the interested student will no doubt want to proceed from this excellent and authoritative introductory exposition to a more detailed analysis. It is therefore unfortunate that the author did not include a reasonable bibliography at the end of each chapter to enable the reader to study such subjects more thoroughly, but there is plenty of meat in the text as it stands.

The reviewer questions whether the average TV and radio serviceman will care to study this book, but the better technician, to whom this book is equally addressed, will probably find it of great interest and value. Incidentally, although the algebraic manipulations are fairly thoroughly covered, the calculus is introduced in a somewhat too brief and casual manner for any but the better technicians and college undergraduates to appreciate.

Some topics, such as transistor noise, cascode amplifiers, and demodulation, are either given too brief or too special a treatment to be of very much practical value. Demodulation, for example, contains merely a hurried analysis of inward clipping. It would also have been of value to have a discussion of product demodulation, so important in color TV and SSB systems.

There are, of course, the usual errors that apparently cannot be avoided in a first printing. To note but a few, we find on page 211 that r_1 should be r_2; in Fig. 13.37, the base resistance r_b is not labelled; in Fig. 13.14, the shunt arm of the Tee is missing; on page 59, $A_{12}=A_{21}$ should read $A_{12}\neq A_{21}$; and on page 127, $L=L_1+L_2=2$ M should read $L=L_1+L_2+2$ M.

A more important criticism is that in several cases the author does not quite follow through and show the importance of a theorem or discussion with regard to practical applications. Specifically, Thevenin's theorem is not made vital to the reader, particularly as to how it simplifies the analysis and understanding of the operation of many circuits.

However, in view of the general excellence of the text and the impression one has that the author understands his subject, the reviewer cannot help but recommend this book not only to technicians and engineering college undergraduates, but to the general engineering public. There will be something of interest and value to most readers.

ALBERT PREISMAN
Capitol Radio Engineering Institute
Washington, D. C.

Fundamentals of Radio and Electronics, 2nd ed., edited by W. L. Everitt

The five co-authors and the editor of "Fundamentals of Radio Electronics," 2nd ed., have succeeded in preparing a very understandable book in this edition. One of the amazing features is the depth of coverage contained, since the entire treatise utilizes a minimum of mathematics. Another feature is the uniformly excellent style achieved by the authors.

Features of this second edition not included in the first are a well co-ordinated discussion of electronic tubes and transistors, a concise coverage of pulse and switching

circuits, a good description of the basic principles of both monochrome and color television, a section on ultra high-frequency and microwave circuits, a brief qualitative description of radar, radio relay, navigational aides and pulse communication, a discussion of industrial electronics applications, and an appendix on special services including aviation radio.

It is not an exhaustive treatment of any of the subjects covered, but it does succeed in presenting an excellent survey of radio and electronics. The presentations are characterized by clear physical explanations. Formulas are frequently used without derivation. The book is plentifully illustrated with schematic diagrams, idealized waveforms, and pictures of equipment.

At the conclusion of most chapters is a set of problems and questions, the majority of which require very little computational effort. There is no bibliography included in the book.

In the opinion of this reviewer, the book serves admirably as a self-study text, and it is well suited as a review text for the engineer desiring first acquaintance with some of the newer aspects of radio and electronic science. It may also be used as a text for a survey type course at technical institutes.

This book is especially distinguished by its clarity. It is exceedingly well written and will fill a need for a good treatment of modern radio and electronics where physical analysis is employed rather than mathematical analysis. It is a survey treatment covering the entire field and enabling the reader to obtain a remarkably good comprehension with a minimum of mathematics.

J. A. M. LYON
Northwestern Tech. Inst.
Northwestern Univ.
Evanston, Ill.

Topics in Electromagnetic Theory, by Dean A. Watkins

Published (1958) by John Wiley and Sons, Inc., 440 Fourth Ave., N. Y. 16, N. Y. 112 pages +3 index pages +ix pages +4 problems pages. Illus. 6×9¼. $6.50.

The field of microwave tubes has developed rapidly in this decade. It is a difficult field and involves many delicate subjects. Some of them may be treated mathematically, but the others, so far, can be understood only in the light of experience. There is always a gap between those who are anxious to learn and those who write papers of great complexity. This is just the book to bridge the gap.

The book contains four chapters plus a set of problems. The first chapter is devoted to periodic transmission systems. It starts from Floquet's theorem and skillfully introduces the concepts of space harmonics, ω-β diagrams, and forbidden regions. Calculations of power and impedance are demonstrated. Both field and circuit analyses are used. The next chapter discusses helical structures. The theory of the sheath helix is introduced first and is followed by Sensiper's work on the tape helix. Multiwire helices, helical antennas, and delay lines are also discussed.

The third chapter deals exclusively with Pierce's coupled-mode theory. The application of this theory in many different microwave devices is illustrated. The last chapter

enters into the complex world of anisotropic media. After discussing basic vector equations, the author describes the principles of ferrite devices, Faraday rotation and field displacement.

The author could not have written this small and handy book without many years of teaching experience. Of particular value is the physical meaning given to the mathematical treatment. The book is easy to read and understand. It is written at the level of graduate students who already have an elementary knowledge of electromagnetic theory and is an excellent introductory source for beginners in the field of microwave engineering.

P. K. TIEN
Bell Telephone Labs.
Murray Hill, N. J.

Les Ondes Centimetriques, by G. Raoult

Published (1958) by Masson et Cie, 120, boulevard Saint-Germain, Paris 6, France. 356 pages +4 index pages +vii pages +35 appendix pages. 330 Figs. 9¾×6¾. 7,300 fr.

This textbook, written in French, corresponds to a course given by Prof. G. Raoult at the Faculte des Sciences de Clermont-Ferrand. It is directed toward students having some related background, with a moderate emphasis in physics.

In the domain of modern experimental physics, such as paramagnetic resonance, microwave spectroscopy of the molecules of gases, liquids, and solids, ionization of gases, etc., it is necessary to acquire a basic knowledge about the generation, transmission, and measurements of centimetric waves. In that connection this book makes a valuable contribution. It provides rapid access to the techniques used in microwaves. The level is intermediate between that of textbooks on general physics and specialized books.

In the main text, the author has intentionally used only mathematical demonstrations which are strictly essential in giving the engineer physical insight into microwave technology and a feel for the subject. The proofs are not always rigorous, but they provide the reader with a good basis for conducting experiments in this field. However, in the appendix the classical theory of Maxwell is presented, and rigorous demonstrations are used to justify the results obtained by simpler methods.

The book is divided into 15 chapters dealing successively with: generalities; theory of wave guides; theory of transmission lines; measure of impedances; obstacles in guides such as inductive and capacitive windows, metallic posts, resonant structures, and shorting plugs; wave guide accessories; junctions; measures of power, frequencies, and wave lengths; measures of dielectric constants; hyperfrequency generators and amplifiers; detectors in hyperfrequency; antennas; optical analogies; ratio astronomy; and a short chapter on paramagnetic resonance.

The material is clearly presented and will be very useful for the graduate engineer who desires to understand thoroughly the techniques and applications of centimetric waves, particularly as they relate to phenomenon of recent scientific interest.

J. B. LAIR
I. T. T. Labs.
Nutley, N. J.

Manual on Rockets and Satellites, Annals of the IGY, Vol. VI, edited by Lloyd V. Berkner

Published (1958) by Pergamon Press, Inc., 122 E. 55 St., N. Y. 22, N. Y. 473 pages +4 index pages +6 bibliography pages +24 appendix pages +xx pages. 238 Figs. 7¼×10. $25.00.

"Rockets and Satellites" is published as Volume VI of the annals of the International Geophysical Year. It is not primarily devoted to radio engineering but rather covers a very wide cross section of popular interest.

The plans for measurement using rocket vehicles, of the physical conditions encountered in the earth's upper atmosphere, and the plans for measurement, using satellite vehicles, of the physical conditions encountered in outer space are given in considerable detail. The rocket programs of Australia, Canada, France, Japan, The U.S.S.R., The United Kingdom and the United States of America are given. The satellite programs of the U.S.S.R. and the U.S.A. are reported in considerable detail.

The book is a collection of scientific papers by authors from the various countries participating in the IGY. The papers are grouped according to contributing countries. It is liberally supplied with photographs and contains an extensive bibliography. Appendices bring the period of time covered by the book from early 1957 through the Soviet satellites and the January and March 1958 U. S. satellites; chronological order is followed. As a result of this chronological presentation the deviations of the accomplishments from the earlier plans become plainly evident.

On the whole, the book is a valuable record of scientific plans and events which provides a basis for viewing future events. "Rockets and Satellites" is required reading for space age engineers and scientists.

CONRAD H. HOEPPNER
Radiation, Inc.
Melbourne, Fla.

Electronic Circuits, by E. J. Angelo, Jr.

Published (1958) by McGraw-Hill Book Co., Inc., 330 W. 42 St., N. Y. 36, N. Y. 444 pages +6 index pages +xiii pages. Illus. 9¼×6¼. $9.00.

According to the information provided by the author, this text "aims to unify the study of electronic circuits by developing and exploiting certain basic concepts common to large classes of tube and transistor circuits." In some measure it achieves this objective, since it does show that it is possible to study the response of a variety of electronic circuits after they have been replaced by one of several possible models for analysis, the piecewise linear or the incremental model. On the whole, it is felt that the total result is reasonably satisfactory, and that the reader should be prepared for further studies in the field.

However, considerable doubt can be raised about the effectiveness of some chapters, either because of limited significance, poor exposition, or inadequate treatment. For example, Chapter 3 contains much material presented in a conventional manner. It also contains an introduction to the piecewise linear model; but, this model is not used in any analysis in the chapter. Chapters. 7, 9, and 10, are felt to be rather limited expositions, with little real substance. Chapter 15 contains some very nice material, although the failure to exploit the

pole-zero approach to amplifier network analysis in prior chapters, tends to limit the effectiveness of this chapter. Chapter 16 really contributes very little to an understanding of the transient response of any specific electronics circuits, being a very limited general exposition of the techniques of studying the transient response of networks.

Perhaps the major criticism of the book is that it undertakes too ambitious a program—to provide the student with the techniques and tools for studying electronic circuits, be they linear or nonlinear, tuned or untuned, vacuum tube or transistor driven. That it only partially achieves these objectives is not surprising. It certainly does succeed in suggesting to the student the kind of general technical "artillery" with which he must be equipped if he is to undertake the analysis of general electronic circuits. There is, of course, a tremendous variety of basic processes involving electronic devices which have not been mentioned, and which must be studied if the student is to be equipped for practical work in the broad general field of electronic circuits. It is noted by the author that these important topics are reserved for a subsequent course, and hence are not included in this text.

<div align="right">SAMUEL SEELY
Case Institute of Technology
Cleveland 6, Ohio</div>

Principles and Applications of Random Noise Theory, by Julius S. Bendat

As the title indicates, this is a book dealing with noise *theory*. It treats such topics as the statistical properties of random noise, the significance and application of such concepts as the power spectra and correlation functions, and the design of optimum linear filters. However, it does not treat the physical sources of noise or such topics as how to build a low noise receiver front end. By thus limiting his scope, the author is able to give a very thorough and complete treatment of his chosen topic. The result is a book that can be highly recommended to serious students in the field.

Although the book is written to be a suitable classroom text, it is also intended to be a useful reference work for practicing engineers or research workers studying the subject by themselves. The author assumes some prior familiarity with Fourier series but does not assume that the student has mastered Fourier integrals. Neither does he assume any intimate prior knowledge of probability theory. The first three chapters covering a little more than a third of the book are devoted to a development of the necessary mathematical background.

Immediately following the three preparatory chapters, the author takes up the problem of optimum filter design. While not so rigorous as Wiener's original work, this chapter is more general. It is written in such a way that the later extensions of Wiener's theory are included with the original in a single unified presentation. The difficult concept of spectrum factorization is explained in terms of physical concepts which, it is hoped, will be more comprehensible to

the average engineer. While this treatment is undoubtedly an improvement from the point of view of many of those who will be reading the book, the concept is still not an easy one to understand. To the reader who has difficulty, this reviewer recommends a reading of Norman Levinson's exposition which appears as Appendix C of Wiener's book.[1]

Following the chapter on optimum filter design, there is a chapter on the exponential-cosine autocorrelation function which is representative of many physical processes. Following this, there is a chapter on analog computer techniques and a chapter on statistical errors in correlation measurements. This chapter lays the groundwork for the one that follows on envelope detection and correlation. The author then returns to the optimum filter problem in Chapter 9, where he deals with optimum time variable filters for nonstationary inputs. Chapter 10, on the zero crossing problem, may at first-glance appear somewhat unconnected with the rest of the book; of late, however, it appears that problems of this type have been increasing in importance and will undoubtedly continue to do so.

The author has chosen to avoid any attempt to include information theory within the scope of the book. While this is understandable with regard to Shannon's work which constitutes a distinct and separable discipline, it is regrettable that he has not included that branch of information theory dealing with detection problems as given in Woodward's book.[2] Thus, in Chapter 9, although he treats both linear and square law detectors, he does not include the log I_0 detector which is optimum for detecting a sine wave in the presence of noise. On the other hand, it must be acknowledged that every author must draw the line somewhere, if the book is to be of reasonable size.

In conclusion, it is felt that this book would be a worthwhile addition to the library of any student seriously interested in the theory of noise. It is not merely a tutorial collection of work by others but also one which includes the authors own significant contributions. Although the student cannot claim to be fully informed solely on the basis of information gathered from this book, neither can he so claim if he is ignorant of any of the major topics covered.

<div align="right">WARREN D. WHITE
Airborne Instruments Lab.
Mineola, L. I., N. Y.</div>

How to Design and Specify Printed Circuits, edited by K. W. Anderson, W. Carlsen, K. W. Clayton, *et al.*

This book is a reference book covering quite completely the several problems involved in printed circuit design and production. The authors have very carefully presented techniques in detail with illustrations that are clear and comprehensive.

[1] Norbert Wiener "The Extrapolation, Interpolation and Smoothing of Stationary Time Series with Engineering Applications." John Wiley and Sons, Inc., N. Y., 1949.
[2] P. M. Woodward "Probability and Information Theory, with Applications to Radar." McGraw-Hill Book Co., Inc., N. Y., 1953.

The first section of the book deals with definitions of the terms used in the design and production of printed boards. The authors then develop methods of design and give illustrations of those designs, characteristics of the several types of printed board materials available, and components used on these boards. Further, techniques of several manufacturers are discussed and presented with illustrations of actual production tools and machines.

The section on dipped soldering and treatment of boards before and after dipped soldering, is of great interest to the designer, because it portrays in detail the experience of several manufacturers, and the discussion brings out the reasons for the several methods most generally used. Many details such as temperature of solder and method of cleaning boards may be questioned only because of individual experience in particular applications.

The authors have gone into such detail as to give a reference to MIL specs, a check list for the designer to assure best practice, and mechanical tolerances of desired holes to be punched with respect to board thickness, etc.

This book is a must for designers and production personnel of printed circuits, since at no other source is so much experience packed in so small a book.

<div align="right">M. L. LEVY
T. BELLAVIA
Emerson Radio and Phonograph Corp.
Jersey City, N. J.</div>

RECENT BOOKS

Babani, Bernard B., *International Radio Tube Encyclopedia*, 3rd edition, 1958–1959. Bernards, Ltd., The Grampians, Western Gate, London W. 6, England. $15.00.

Etkin, Bernard, *Dynamics of Flight*. John Wiley and Sons, Inc., 440 Fourth Ave., N. Y. 16, N. Y. $15.00.

Kroes, Th. J., *Tube and Semiconductor Selection Guide*, 1958–1959, second revised edition. Philips' Technical Library (Philips' Technische Bibliotheek), Eindhoven, Nederland. $1.50.

Mandl, Matthew, *Fundamentals of Digital Computers*. Prentice-Hall, Inc., Englewood Cliffs, N. J. $9.00.

Oldfield, R. L., *The Practical Dictionary of Electricity and Electronics*. American Technical Society, 848 East 58 St., Chicago, Ill. $5.95.

Platt, Sidney, *Magnetic Amplifiers: Theory and Application*. Prentice-Hall, Inc., 70 Fifth Ave., N. Y. 11, N. Y. $7.00.

Schieldrop, Edgar B., *The Air*. Philosophical Library, Inc., 15 E. 40 St., N. Y. 16, N. Y. $12.00.

Spitz, Armand and Gaynor, Frank, *Dictionary of Astronomy and Astronautics*. Philosophical Library, Inc., 15 E. 40 St., N. Y. 16, N. Y. $6.00.

Tall, Joel, *Techniques of Magnetic Recording*. The Macmillan Co., 60 Fifth Ave., N. Y. 11, N. Y. $7.95.

World Maps of F2 Critical Frequencies and Maximum Usable Frequencies for 4,000 km, prepared by and available from The Radio Research Labs. Ministry of Posts and Telecommunications, Tokyo, Japan.

Abstracts of IRE Transactions

The following issues of TRANSACTIONS have recently been published, and are now available from the Institute of Radio Engineers, Inc., 1 East 79th Street, New York 21, N. Y. at the following prices. The contents of each issue and, where available, abstracts of technical papers are given below.

Broadcast Transmission Systems

Vol. PGBTS-12, December 1958

Papers from Eighth Annual Broadcast Symposium

The Radio Spectrum—T. A. M. Craven (p. 1)

Reduction of Cochannel Television Interference by Very Precise Offset Carrier Frequency—L. C. Middlekamp (p. 5)

A Diode Matrix Vertical Interval Video Switcher—R. Aha and F. C. Grace (p. 11)

Eighth Annual Broadcast Symposium (p. 16)

Contributed Papers

Automatic Preset Switcher—J. S. Petril (p. 18)

An automatic preset television program switching system allows video signal, audio signal and projection system to be set-up in the desired sequence in advance of air-time. This permits an increase in number of switches, more complex integration and most important flawless switching during the commercial time periods between or during programs.

Calculation of Directional Antenna Patterns Using Digital Computer Techniques—S. Bergen (p. 22)

Communications Systems

Vol. CS-6, No. 2, December, 1958

Radio Communications—A Renascent Art—D. S. Rau (p. 33)

Frontispiece—D. S. Rau (p. 34)

Dependence of the Maximum Range of Tropospheric Scatter Communications on Antenna and Receiver Noise Temperatures—A. R. Hausman (p. 35)

This paper describes the dependence of the maximum range of scatter communications on noise sources both internal and external to the communications system. The discussion centers around the relative contribution of the new low noise solid state amplifiers in extending the range of communications in the face of terrestrial and extraterrestrial (cosmic) noise sources. It is shown that the apparent antenna temperature constitutes the primary limitation in realizing the full advantages of the low noise solid state amplifiers currently of such great interest.

Reduction of Adjacent-Channel Interference Components from Frequency-Shift-Keyed Carriers—A. D. Watt, V. J. Zurick, and R. M. Coon (p. 39)

The abrupt changes in frequency associated with binary modulation generate sideband components which frequently interfere with services in adjacent channels. Reductions in interfering bandwidths of 10 to 1 or greater over unfiltered keying at sideband levels 80 db or more below the unmodulated carrier are possible by the use of relatively simple filters in the keying circuit of frequency-shift-keyed transmitters.

The frequency spectra resulting from filtered keying waves of FSK transmitters are derived, and the results presented in graphic form. The sizeable reduction of the interfering sideband components as predicted by the analysis is found to agree very closely with experimental measurements. Characteristics of desirable keying circuit filters to obtain these reductions are specified.

Simple Codes for Fading Circuits—H. B. Voelcker, Jr. (p. 47)

Four relatively simple, redundantly-coded binary communication systems are considered under certain limiting conditions of signal fading. White noise is assumed to be the only source of errors. A nonredundant, synchronous teletype system is used as a standard of comparison, and all systems are constrained to operate at the same average output data rate. The results indicate that the redundant systems offer significant gains under most of the assumed conditions, but that additional propagation research is required before general codes can be developed for tubulent channels.

Fault Location on Telephone Cables—P. Kantrowitz (p. 53)

An improved approach to fault location by pulse echo ranging on unloaded telephone cables is proposed, which requires a knowledge of the output unit step transient response of a matched cable. This has been obtained by numerical integration for 19 AWG nonloaded telephone quadded toll cable. Experimental results are given for unloaded spiral-four cable which has similar properties. The output unit step response is also given for an idealized semi-infinite loaded line for which the attenuation is approximately constant and the phase shift is proportional to frequency up to the cutoff radian frequency, ω_c. This result is used to demonstrate that the optimum rectangular pulse, T_1, for echo ranging on loaded lines is given by $T_1 = 3.84/w_c$.

Transmission Loss Curves for Propagation at Very Low Radio Frequencies—J. R. Wait (p. 58)

Curves of the transmission loss are presented for the propagation to great distances at frequencies in the range 10 to 20 kc. The theoretical model of the ionosphere assumed is a sharply bounded homogeneous ionized medium. The working formula for the field is a sum of waveguide-type modes. The calculated results compare favorably with experimental data at 16.6 kc over the Pacific Ocean.

Correspondence (p. 62)

Contributors (p. 62)

Index 1953-1958 (Follows p. 63)

Electron Devices

Vol. ED-5, No. 4, October, 1958

An 85-Watt Dissipation Silicon Power Transistor—R. W. Aldrich, R. H. Lanzl, D. E. Maxwell, J. O. Percival, and M. Waldner (p. 211)

Production prototype silicon transistors have been made using large area diffused base structures. Simultaneous diffusion of gallium and phosphorus is used to form the diffused base structures. The geometry and doping level of the structure can be controlled by varying the impurity source composition and temperature. The phosphorus surface concentration is a much less rapidly varying function of source temperature than is the gallium surface concentration, and is determined primarily by the source composition.

Two line base contacts, one line emitter contact and a collector contact, are attached to the wafer by using appropriate alloys in conjunction with titanium or tungsten backup plates. The structure then is encapsulated in a hermetically sealed package.

The transistors are capable of dissipating 85 watts at a 25°C mounting base temperature and have been used in circuits, as is described, to deliver 25 watts Class A, 80 watts Class B in push-pull operation and peak currents of 10 amperes in pulsed operation.

Velocity and Current Distributions in the Spent Beam of the Backward-Wave Oscillator—J. W. Gewartowski (p. 215)

Results are presented of an experimnetal study of the spent beam of a backward-wave oscillator. The instantaneous velocity and current of the spent beam are measured using a velocity analyzer built onto the collector of a scaled 80-mc backward-wave oscillator.

The tube employs a sheet beam and inter-digital line, 12 feet long. It is designed to be representative of large-space-charge tubes.

The measured trajectories of the spent beam are examined to deduce the mechanism of interaction between the beam and the circuit along the whole length of the tube. It is deduced that the level of oscillation is determined by nonlinear effects in the convection current.

Finally, the RF output efficiency saturation at high beam currents is found to be caused by electrons which fall back in phase from a retarding to an accelerating circuit field.

The Emitter Tetrode—R. A. Gudmundsen (p. 223)

If two ohmic contacts are made to the thin emitter region of a transistor in the form of a ring around the periphery and a dot in the center, it is possible to vary the ratio of the emitted current density under the center dot to the emitted density under the ring by passing a transverse current radially through the emitter region. This makes it possible to reduce the surface losses in such a transistor essentially to zero, at some expense of increased base resistance. Such a controllable alpha makes possible feedback stabilization into an indpendent terminal. The essential theory of operation and experimental verification of the calculations are shown and discussed.

Kinetic Power Theorem for Parametric Amplifiers—H. A. Haus (p. 225)

A power theorem is developed for parametric, longitudinal, electron-beam amplifiers which may be considered as a generalization of Chu's well-known kinetic power theorem. The new power theorem is used to explore the limitations on noise performance of parametric electron-beam amplifiers. It is shown that the electron-beam noise does not impose a basic limit on the noise performance of a parametric electron-beam amplifier in the way a basic limit is imposed upon the noise performance of conventional longitudinal electron-beam amplifiers. The new power theorem can be employed for understanding the operation of parametric beam amplifiers in the same way as Chu's kinetic power theorem has been used for interpreting the operation of longitudinal beam amplifiers.

Periodic Electrostatic Focusing of a Hollow Electron Beam—C. C. Johnson (p. 233)

A method of focusing a long hollow electron beam is described in which beam space-charge fields are balanced against uniform radial electric fields and periodic radial and longitudinal electric fields. There is no magnetic field associated with this focusing method. Elimination of the usual large axial magnetic-field requirement of "confined flow" focusing allows the tube system employing the electrostatically focused hollow beam to be lighter in weight, more compact, and to enjoy an enhancement of over-all efficiency.

A physical description of the focusing mechanism is given, followed by a mathematical treatment which yields conditions for stable beam flow. Expressions are derived for electrode voltages required to focus a given hollow beam, as well as for velocity variation and beam deflection. A comparison of beam "stiffness" is made with a conventional "confined flow" beam. Beam stability is investigated under various "overfocusing" conditions and imperfect entrance conditions. Finally, this focusing method is compared with other purely electrostatic methods.

An experimental program was carried out which demonstrated the usefulness of this type of focusing. Results indicate that good beam definition and transmission coefficients can be obtained with some insensitivity to entrance conditions.

Traveling-Wave-Tube Propagation Constants—D. A. Dunn, G. S. Kino, and G. W.C. Mathers (p. 243)

The propagation constants of a traveling-wave tube can be normalized in such a way that curves of a quantity proportional to gain per wavelength, vs a parameter proportional to electron velocity, approach a single curve at large values of a space-charge parameter. The usual Pierce normalization yields analogous curves that approach an asymptotic curve for zero space charge. Suitable curves for calculation of traveling-wave tube gain, based on this large space-charge normalization, have been computed and are presented for a wide range of values of the relevant parameters. It is found that, even for very large values of the gain parameter, corresponding to values of C of the order of 0.3, these curves do not depart substantially from the asymptotic curve.

Starting Conditions in O-Type Backward-Wave Oscillators—H. G. Kosmahl (p. 252)

The ratio of the starting current for the first spurious mode of oscillation, in O-type backward-wave oscillators, to the starting current for the main oscillation has been computed, taking into account the magnetic fields used ofr beam focusing as well as the transverse components of RF circuit fields. The results show an appreciable influence of both parameters on this ratio and partially explain the suppression of spurious outputs in backward-wave oscillators which can be achieved by deliberate misalignment of the tube in the magnetic field.

For higher losses uniformly distributed over the RF circuit length, the ratio I_s'/I_0' decreases; *i.e.*, the tendency toward spurious oscilations increases. This effect may be understood from the coupled-mode theory, since for higher losses the interaction between the circuit wave and the slow space-charge wave decreases much more rapidly for the main mode than for the spurious one.

Approximate Analytic Expressions for TWT Propagation Constants—W. H. Louisell (p. 257)

An approximate factorization of the traveling-wave-tube (TWT) equation for the propagation constants is obtained by observing that the unattenuated wave is approximately a hyperbola for a lossless circuit. Analytic expressions for gain are also found.

Recombination of Injected Carriers in Cylindrical Ingots—J. P. McKelvey (p. 260)

An exact solution to the diffusion-recombination problem is obtained for the case of a sample in the form of a right circular cylinder with arbitrary bulk lifetime, arbitrary surface recombination velocity on the lateral curved surface of the sample, and infinite surface recombination velocity on the (lapped) plane end surfaces of the sample. The latter surfaces may be regarded as electrical contacts to the sample, and in such a case the geometry corresponds precisely to a very commonly used experimental arrangement for recombination measurements. Relations between bulk lifetime, surface recombination velocity and observed time constant are calculated and plotted with the height-radius ratio of the cylinder as parameter for the principal decay mode, and the higher-mode decay scheme is worked out for a few cases of practical interest. Examples of simultaneous surface recombination and bulk lifetime measurement by observation of the higher-mode decay components are presented.

A New Method of Measuring the Noise Parameters of an Electron Beam—S. Saito (p. 264)

The noise figure of a microwave beam amplifier has a lower limit that depends entirely upon the noise process in the electron gun near the potential minimum. This paper is chiefly concerned with the theory and experimental results of a new method of measuring the noise parameters of the electron beam, especially the correlation between its velocity and current fluctuations, by using a "selective beam coupler" that has properties similar to the conventional microwave directional coupler. An appreciable value for the real part of the correla-tion coefficient between the velocity and current fluctuations was found in the space-charge-limited region. This value went to zero, or slightly negative, in the temperature-limited region. The probable error in the noise measurements is discussed by taking account of the residual selectivity of the selective beam coupler, the effect of the pickup cavities upon the beam, the thermal noise from the pickup cavities, and the higher-order modes in the beam. Measurements of II/S, the real part of the correlation coefficient between velocity and current fluctuations, have been made on a number of guns. Under space-charge-limited conditions, the observed values were about 0.2 to 0.3, Under temperature-limited conditions, $II/S \approx 0$.

A New Approach to Kinescope Beam Convergence—J. W. Schwartz and P. W. Kaus (p. 275)

Misconvergence of the beams in color kinescopes because of deflection has been corrected in the past by the use of dynamic convergence devices. Six independent fields are required to deflect three beams without misconvergence. Conventional deflection yokes supply two of these fields; the remaining four are supplied by convergence magnets. This paper describes a more general system that uses six coexistent deflection fields. Such a system is capable of producing deflection without misconvergence, and in contrast to conventional systems produces no loss in color purity tolerance. A particular embodiment of this system is discussed in detail. It employs a six-coil "converger" used in combination with a conventional deflection yoke. The results of an experimental investigation of this embodiment are given.

A Symmetry Property of Space-Charge Waves—I. P. Shkarofsky (p. 283)

A symmetry property is deduced for an electron beam modulated and demodulated by gaps of cavities. This property results from a combination of the theory of space-charge wave propagation in an accelerated beam and of the theory of gaps. It states that in a region bounded by two cavities, the power detected by the second cavity is unaltered by an interchange of potentials on the two cavities, provided the widths of the gaps are small.

Experimental results are given for both linear and nonlinear acceleration and deceleration regions. In all cases, this property is found to be true.

Most of the experimental results are also tested vs theoretical solutions of the electronic equation for regions of acceleration. The reduction factor is included in the theory.

High-Efficiency Traveling-Wave Amplifiers—J. E. Rowe and H. Sobol (p. 288)

A general design procedure is developed for the design of both low-power and high-power high-efficiency traveling-wave amplifiers. The process is based on the selection of optimum values (for highest efficiency) of the design parameters C, QC, B and b from the large-signal curves and design of an amplifier with the particular type of RF structure specified by power and bandwidth requirements and operating parameters as near the optimum values as possible. In cases where the optimum design parameters cannot all be realized simultaneously, the design engineer will be able to select the parameter that he wishes to adjust.

The procedure is first developed for helix-type tubes and then correction factors are derived that permit the design of amplifiers with any type of RF structure from the same set of curves.

Improvement of Traveling-Wave-Tube Efficiency—F. Sterzer (p. 300)

This paper describes the design of single-stage and double-stage collectors which can be operated at "depressed" potentials. When these single-stage and double-stage collectors were used in conjunction with a traveling-wave amplifier, over-all efficiencies of 46 and 57 per

cent were obtained, respectively. The maximum increase in efficiency which can be obtained by the use of depressed collectors having one to three electrodes is calculated for various traveling-wave tube design parameters.

Large Signal Analysis of the Multicavity Klystron—S. E. Webber (p. 306)

The techniques developed to study large signal effects in the two-cavity klystron have been extended to determine performance of the multicavity tube. Bunching is computed as a function of excitation phase and amplitude at various gaps, tunnel lengths, beam diameter and density. Results of efficiency calculations taking into account velocity distribution within the bunch are discussed.

Large-Signal Rise-Times in Junction Transistors—W. W. G. Artner (p. 316)

Coupled Helix Winding Machine—A. H. Iversen (p. 317)

Contributors (p. 318)
Annual Index 1958 (p. 320)

Engineering Management

Technical Management of Missile Systems—T. J. Harriman (p. 133)

Capability and economy in complex missile systems demand fundamental changes in technical management. Improvement can begin with military requirement, development, and procurement agencies in their management of the initiation and follow-up of the project. Of greatest importance is the complete involvement of senior technical personnel in conception and development, apart from auxiliary service and supervision. Formal organization and responsibility of the systems engineering staff provide the technical management key to this problem. Reliability requirements of complex missiles seem to have confounded technical management. Yet the physical work necessary to develop equipment reliability parallels standard procedure for building in other required characteristics.

Technical Proposals in the Electronics Industry—F. N. Eddy (p. 136)

To a large extent, proposals determine the success of a firm doing contracted work in the electronics industry. Because of the short time schedules allowed for the preparation of most proposals, it is difficult for a firm to produce material of the quality it would like. By first reviewing the processes involved in proposal preparation, it is concluded that greater preparation time is afforded through establishing time schedules, responsibilities, and over-all policy in advance. Comparisons of the proposal to other advertising media are made, resulting in the general conclusion that factors other than engineering merit help to determine proposal effectiveness. These factors are then discussed along with budgetary restrictions.

A Subjective Merit Review System—D. J. Strauss (p. 141)

Among the tools currently used by management to appraise its employees is the "Merit Review System." The majority of companies in industry make an attempt to "rate" each employee objectively, using a standardized rating form, and adjust salary accordingly.

It is this writer's opinion that a true appraisal of an employee is a very subjective matter that takes into account many elements not found on most rating forms. Employee reviewing is a continuing process, not a matter that should be considered by a supervisor twice a year.

This paper highlights some of the disadvantages of the present objective systems, and offers instead a system whereby a supervisor is given great latitude in reviewing his subordinates.

It is further suggested that a merit review should be considered separately from a salary adjustment so that the employee's review will not reflect a budgetary allowance given to a supervisor for raises.

Logic and Illogic in Engineering Management—A. L. Stanly (p. 144)

Illogic resulting from emotional thinking may be found at all levels of engineering. Typical instances are the NIH (not invented here) factor, wishful thinking, self-protection, and half-hearted compromises.

Methods of the engineering supervisor or manager for filtering out the emotionally inspired illogic in order to reach clear decisions are presented. These range from defining the basic problem to making a balance sheet and weighing both tangible and intangible factors.

Also discussed are some principles for removing the incentives for emotional thinking. One of the most prominent of these is the promotion of a desire to work for a common goal by organization which provides clear and nonconflicting responsibilities, and by increased identification with the company.

Magazine Review Section (p. 152)
For Your Bookshelf (p. 153)
Annual Index 1954-1958 (Follows p. 154)

Information Theory

Frontispiece—T. P. Cheatham, Jr. (p. 134)
A Broader Base for the PGIT—T. P. Cheatham, Jr. (p. 135)
A Statement of Editorial Policy—The Administrative Committee (p. 136)
Time Statistics of Noise—W. M. Brown (p. 137)

The measurements made on a system containing noise are usually time averages of the signals, or of quantities defined in terms of the signals. Such measurements are called *time statistics*. The object of this paper is to develop the theory of time statistics and in turn to give methods for calculating them. For the most part the time statistics are formulated in terms of ensemble statistics which are usually provided by statistical mechanics.

If a process consists of, say, all physically realizable models of a system containing noisy resistors, there is no practical way to identify which model one has available for "testing." Thus, a time statistic measured with the available model will not be predictable unless this statistic is the same for almost all the models; when this is the case, the process is called *uniform for this statistic*. A dual property is in common use for ensemble statistics. The process is called *stationary for an ensemble statistic*, provided it is the same at all times. Though some discussion of stationarity is given in this paper, the emphasis is on not requiring stationarity. In particular, special attention is given to non-stationarity introduced by determinate signals. While stationarity plays only a minor role in the theory of the time statistics of noise, uniformity plays a crucial role. Given only uniformity, Theorem 1 formulates time statistics as the time average of the corresponding ensemble statistics. The additional condition of stationarity merely simplifies the calculation by rendering the "ergodic hypothesis" satisfied, *i.e.*, by rendering equality of time and ensemble statistics.

With Theorem 1 as a nucleus, the remainder of the paper attempts to develop an understanding of what makes a process uniform. There is no attempt to give detailed proofs, but there is an effort to maintain a clear distinction between physical motivations, the definitions, and the theorems. Some elementary sample calculations of practical interest are included; these serve to illustrate several parts of the

theory. Though calculations involving such problems as the evaluation of difficult integrals do arise in some applications of the theory, simple samples have been used here, since they are adequate as an aid to understanding the theory.

Multiple Error Correction by Means of Parity Checks—G. E. Sacks (p. 145)

An n-place binary parity check code which corrects up to and including e errors in each code letter is fully described by its n characteristics, which are r-dimensional vectors, where r is the number of redundant binits in each code letter. It is shown that the characteristics of such a code have the essential property that any subset of $2e$ of them are linearly independent. An upper bound on r for fixed n and e is obtained by consideration of a systematic procedure for finding the characteristics; this upper bound is always less than, or equal to, twice the lower bound of Hamming.

The Utility of a Communication Channel and Applications to Suboptimal Information Handling Procedures—M. B. Marcus (p. 147)

This paper demonstrates the applicability of the functional equations of dynamic programming to information theory problems. Yielding the same results as those obtainable by Shannon's equations, the functional equations can be modified also to consider the many restrictions enforced upon information systems by the real world. A result of the application of functional equations to systems operating under suboptimum conditions is that the information rate of a system is dependent upon the manner in which the information is used.

The Kelly concept—the gain of a gambler who wagers his capital on the outcome of a communication channel—is used to determine the information rate of the channel. The mathematical analysis follows the stochastic multi-stage decision process technique of Bellman and Kalaba. Together with some extensions by the author, the Kelly-Bellman-Kalaba model of communication is repeated. The models are analyzed for the optimum case and examined for various suboptimum conditions. The gambler's betting policy is analogous to information usage; restrictions upon this policy affect the information rate of the system. They can require that the policy which is best under optimum conditions be replaced by other policies which, although inferior in the ideal case, are better able to compensate for the restrictions.

A null zone reception system first analyzed by Bloom and others is reanalyzed to provide a concrete example of the latitude of operation allowed by the functional equation approach. Bloom's analysis assumed that the system operates under optimum conditions. His results are duplicated, and their expression indicates their alteration by suboptimum conditions. An appendix expresses the results of this paper in the form used by Bloom.

Capacity of a Certain Asymmetrical Binary Channel with Finite Memory—S. H. Chang (p. 152)

The capacity of a certain asymmetrical binary channel is studied undre the following conditions. 1) Blocks of equal numbers of binary digits are used as the transmitting symbols. 2) The channel resumes its quiescent state at the beginning of each block. 3) The memory of the channel is characterized by the dependence of the noise probabilities for each digit upon the preceding digit or digits in the same block. It is shown that, by means of simple rules and with the aid of a single set of curves or a table, the calculation of the capacity can be reduced to a routine process.

The Fourth Product Moment of Infinitely Clipped Noise—J. A. McFadden (p. 159)

This paper considers the fourth product moment, $w(\tau_1, \tau_2, \tau_3) = E[x(t)x(t+\tau_1)x(t+\tau_2)x(t+\tau_3)]$, when $x(t)$ is infinitely clipped noise with

a mean value of zero. If the noise is Gaussian before clipping, the moment w is not obtainable in closed form. For this reason, the Gaussian assumption is withdrawn and other assumptions are employed. If the zeros of $x(t)$ obey the Poisson distribution, a particularly simple result follows for w and for all higher moments. An alternative assumption is the following. Let unspecified events occur at times t_0, t_1, t_2, $\cdots$ according to the Poisson distribution. If alternate events, *i.e.*, those at t_1, t_3, t_5, $\cdots$, are designated as the zeros of $x(t)$, both the autocorrelation function and $w(\tau_1, \tau_2, \tau_3)$ can be derived. The results are in terms of elementary functions. A comparison is made between these models and clipped Gaussian processes.

A Markoff Envelope Process—J. N. Pierce (p. 163)

It is shown that the envelope of a narrow-band Gaussian noise constitutes a first-order Markoff process if the power spectrum of the noise is the same as would be obtained from a singly tuned RLC filter with white noise at the input.

Prediction and Filtering for Random Parameter Systems—F. J. Beutler (p. 166)

This work generalizes the Wiener Kolmogorov theory of optimum linear filtering and prediction of stationary random inputs. It is assumed here that signal and noise have passed through a random device before being available for filtering and prediction. A random device is a unit whose behavior depends on an unknown parameter for which an *a priori* probability distribution is given.

A number of engineering applications are cited. Two of these are worked out in some detail to illustrate the optimization procedure.

Correspondence (p. 172)
PGIT News (p. 174)
Contributors (p. 175)
Annual Index (Follows p. 175)

Medical Electronics

Vol. ME-12, December, 1958

Short Distance Radio Telemetering of Physiological Information—H. G. Beenken and F. L. Dunn, M.D. (p. 53)

A completely transistorized radio transmitter and a receiving system are described operating at 104 mc. The weight of the transmitter is under two pounds without the use of miniature parts. Design is for transmission of up to ten channels with bandwidths of 250 and 1000 cps. The channel reported has a carrier frequency of 2100 cps and was tested for EKG recording. Satisfactory calibrated records were obtained while walking and while on treadmill.

Theoretical Analysis of the Operation of Flying Spot and Camera Tube Microscopes in the Ultraviolet—E. G. Ramberg (p. 58)

The minimum specimen exposure at television scanning rates required to yield pictures with acceptable signal-to-noise ratio and the best resolution optically attainable is computed for flying-spot, image-orthicon, and vidicon television microscopes for the ultraviolet. This exposure is found to be slightly less for the flying-spot microscope than for the image-orthicon microscope. For microscopes employing experimental ultraviolet-sensitive vidicons with optimal quantum efficiency, the exposure is greater than for the image-orthicon microscope by a factor of 2, and it may be greater by a factor up to 10 for vidicon microscopes with less favorable characteristics. Picture lag is absent in flying-spot microscopes and is not a serious consideration in image-orthicon microscopes, but may limit the permissible motion in the field of an ultraviolet vidicon microscope. On the other hand, the attainable radiance of flying-spot tube screens limits the usefulness of the flying-spot microscope in high-resolution

studies, particularly when examination with sharply defined spectral bands is desired. No similar limitation exists for the image-orthicon and vidicon microscopes.

Apparatus for Recording the Heartbeats of a Fetus—E. Mack (p. 65)

Obstetricians have expressed a wish for a simple and low-cost apparatus for monitoring the heartbeats of a fetus before and during birth. This paper describes a special type of amplifier that was built to satisfy this requirement. By transposing the low frequencies of the heartbeats to a higher-frequency region, some of the difficulties that would otherwise be encountered are avoided. This makes the device easy to build with noncritical circuits; it should be inexpensive to manufacture.

The Transient Response of the Human Operator—R. W. Hyndman, Jr. and R. K. Beach (p. 67)

In this paper, the authors have derived the equations representing the dynamic response of a human operator in the performance of a particular task. These equations were plotted and compared to the recordings of the actual response and show agreement well within experimental error. Possible applications of this method are suggested in the fields of servomechanisms, medicine, physiology, and psychology.

Analysis of Heart Murmurs by Electronics—R. S. Richards (p. 72)

This paper gives a brief survey of early and current work in the application of audiofrequency amplifiers, equipped with filters, to the diagnosis of abnormal heart conditions, and for use as teaching aids in medical schools.

The possible application of a gating technique, *i.e.*, filtering in time instead of in frequency, is discussed, and a description is given of some circuits which have been used for this purpose.

Both filter systems have proved to be useful adjuncts to the stethoscope and, if used with a tape recorder, are valuable teaching aids.

A Servo Operated Respirator for Premature Infants—A. W. Melville and B. H. Hodder (p. 75)

This paper describes a machine for the application of artificial respiration to infants.

The machine will operate automatically as a respiration amplifier when any spontaneous breathing is present, or as a forced respirator when there is no natural breathing.

The respiratory cycle is induced by the external application of a negative pressure to the body and all significant variables may be independently controlled.

Theory of Measurement of Blood Flow by Dye Dilution Technique—J. L. Stephenson (p. 82)

The general mathematical theory of measurement of blood flow by dye dilution techniques is discussed. The mathematical procedure for handling the recirculation problem is described, and it is shown that, in general, sampling of concentration at a single point is not sufficient to uniquely determine both the volume and flow in a vascular bed. The more basic problem of synthesizing a mathematical model of the circulation is analyzed. A general probabilistic scheme for handling transport problems of this kind is outlined, and results obtained for exchange of labeled material between the vascular and extravascular fluid compartment are described.

Automatic Counting of Bacterial Cultures—A New Machine—N. E. Alexander and D. P. Glick (p. 89)

A machine which solves the general problem of counting randomly placed objects of varying size on a surface is briefly described. It is able to accomplish this task by systematic discard of information. It is essentially a scanning device with a "memory" in the form of a quartz ultrasonic delay line. A "decision-making" element controls the discard of information and directs the counting action. The

counting operation is accomplished in one second.

Index 1953–1958 (Follows p. 92)

Microwave Theory and Techniques

Vol. MTT-7, No. 1, January, 1959

A Message from the Chairman—T. S. Saad (p. 2)

Frontispiece—W. L. Pritchard (p. 3)

Education and Science in a Mature Society—W. L. Pritchard (p. 4)

Forward—A. L. Aden (p. 5)

Microwave Radiation from Ferrimagnetically Coupled Electrons in Transient Magnetic Fields—F. R. Morgenthaler (p. 6)

Under certain restrictive conditions it appears that ferrimagnetically coupled electron spins are capable of coupling energy from a transient magnetic field and giving it up in the form of microwave radiation.

This paper analyzes the behavior of the uniform precession of motion in ferrimagnetic insulators under the influence of transient magnetic fields of changing amplitude and direction.

The expected radiation power and efficiency are calculated for such an oscillator employing yttrium iron garnet.

Ferrite High-Power Effects in Waveguides—E. Stern and R. S. Mangiaracina (p. 11)

Deterioration of ferrite devices caused by both high power thermal and nonlinear effects are discussed. It is shown that thermal effects can be described, at least qualitatively, by a simple exponential equation. A theoretical maximum power capacity is derived in terms of ferrite configuration parameters. The results of experiments with high peak powers at both S-band and X-band frequencies are compared with predictions of Suhl's theory on nonlinear, high power effects power effects in ferrites. Steady-state and transient effects are considered. It is shown that high power effects may be eliminated in ferrite devices by properly choosing ferrite properties and geometry.

Temperature Effects in Microwave Ferrite Devices—J. L. Melchor and P. H. Vartanian (p. 15)

With proper choice of shape, it is possible to minimize the frequency shift of ferromagnetic resonance in microwave ferrite components operating over a wide range of ambient temperatures. Calculations have been made for minimum resonance frequency shift with change in saturation moment. Curves relating the resonance frequency shift as a function of saturation magnetization are plotted for several ferrite geometries. Design curves are presented for reducing dependence of resonance frequency on temperature.

Characteristics of Ferrite Microwave Limiters—G. S. Uebele (p. 18)

Microwave ferrites that exhibit a nonlinear RF absorption as a function of RF power level can be utilized in the construction of a passive microwave device which will allow small RF signals to be transmitted with very little attenuation but which will attenuate large RF signals considerably. Such a device tends to "limit" the amplitude of the microwave energy passing through the device and is therefore called a ferrite microwave limiter.

One application of the ferrite limiter is in the protection of crystal detectors in pulsed radar sets. However, when a rectangular pulse of X-band RF energy is transmitted through the limiter, the output waveform is no longer rectangular but consists of a leading edge spike of 0.1-μsec duration followed by a plateau of highly attenuated RF energy. At the present time the leading edge spike is the major obstacle in the successful use of the ferrite microwave limiter as a TR cell in the protection of crystal detectors.

Experimental techniques used to improve the performance of the limiter are presented and the performance characteristics of an X-band ferrite microwave limiter are shown.

Nonreciprocity in Dielectric Loaded TEM Mode Transmission Lines—D. Fleri and G. Hanley (p. 23)

An analysis is presented of partially dielectric loaded strip transmission line from the point of view of ferrite applications. It is shown that the microwave magnetic field is elliptically polarized both at the dielectric surface and within the dielectric. The degree of elliptical polarization is expressed analytically as a function of the dielectric constant, the degree of dielectric loading, and the frequency. For specific values of dielectric constant and loading, a high degree of circularity may be made to exist at the dielectric surface over extremely broad frequency bands. Experimental data are presented which are in accord with the theoretical predictions.

Ferrite Phase Shifter for the UHF Region—C. M. Johnson (p. 27)

An extremely compact, low-loss, ferrite phase shifter has been developed for the 200 to 800-mc region. It consists of a folded stripline structure approximately $6\frac{1}{2}$ inches long and less than 1 inch square in cross section. The device requires a longitudinal magnetic field of sufficient intensity to place the operating region above resonance. For field swings of about 900 oersteds (from 430 to 1250 oersteds at 400 mc), $360°$ change in phase shift can be obtained with about 1 db of loss. The phase shifter is reciprocal and shows identical low-power and high-power characteristics up to at least 10-kw peak. Some additional data are included on the operation of the phase shifter down to 10 mc and up to 2000 mc.

A Ferrite Serrodyne for Microwave Frequency Translation—F. J. O'Hara and H. Scharfman (p. 32)

A ferrite serrodyne has been developed to produce a frequency translation of X-band microwave signals over ranges from zero to 50 kc. The device consists of an efficient longitudinal field ferrite phase shifter and an associated electronic driver for generating the modulating sawtooth. Transmission or reflection operation is possible. A conversion loss of 1 to 2 db is obtained. Suppression of spurious output spectral components is 33 db or more for a 10-kc translation and 21 db for a 50-kc translation.

Broad-Band Ferrite Rotators Using Quadruply-Ridged Circular Waveguide—H. N. Chait and N. G. Sakiotis (p. 38)

It has been shown that the rotation of the plane or polarization of a wave propagating in a magnetized unbounded ferrite medium should be independent of frequency. However, this is not the case when a ferrite rod of small diameter is placed within a waveguide. For example, if a ferrite rod one-quarter inch in diameter in a fifteen-sixteenths inch diameter circular waveguide is used, the rotation will change by a factor of four to one over the frequency band from 8000 to 10,000 mc. This variation in rotation is substantially due to the waveguide characteristics, and can be minimized by lowering the cutoff frequency of the waveguide.

Various methods of lowering the cutoff of circular waveguide are compared. Data on the broadbanding of the rotation by dielectric loading and also by the use of quadruply-ridged circular waveguide is shown. An experimental study showing the effect of the ridge width and height on the cutoff of the circular waveguide and the frequency dependence of the rotation is discussed.

Present State of the Millimeter Wave Generation and Technique Art—1958—P. D. Coleman and R. C. Becker (p. 42)

Two of the few fruitful approaches to the low millimeter and submillimeter wave generation problem appear to be frequency multipli-

cation by means of nonlinear phenomena and frequency conversion by parametric systems. Current work on frequency multiplication using relativistic megavolt beams, crystal diodes, field emitters, ferrites, etc., is reviewed. A brief account of present efforts to extend conventional tubes below wavelengths of 3 mm is presented. Waveguide components used at 1 to 2 mm are described.

Millimeter-Wave Generation Experiment Utilizing Ferrites—W. P. Ayres (p. 62)

It is estimated that at least 50 watts of peak power at 2-mm wavelength has been generated from 4-mm excitation by harmonic generation in ferrites. This experiment is similar to the frequency doubling previously reported from 9 to 18 kmc, except for some differences in optimum geometry and material. A wide range of ferrites has been used, as well as garnets and permanent magnet type materials. In carrying out this experiment it has been necessary to develop components such as a 4-mm high-power isolator, a calorimeter for measurement of the 4-mm and 2-mm power, and numerous 2-mm waveguide components.

Some Characteristics of Dielectric Image Lines at Millimeter Wavelengths—J. C. Wiltse (p. 65)

The attenuation characteristics of several dielectric image lines have been calculated for the frequency range extending from 24 to 100 kmc and have been checked experimentally at 35 and 70 kmc. To obtain low attenuation at these high frequencies, dielectric materials with little loss and small size of cross section are required, while low values of the dielectric constant are also desirable. The effects of the size and shape of the dielectric cross section and of low dielectric constant are treated separately. To find proper materials with low dielectric constants several new foam plastics were investigated. Three types were found suitable for image line use, and in fact, these plastics have such good electrical and physical properties that they should be useful in many microwave applications.

A qualitative measure of field extent is given for several image lines at 35 or 70 kmc, and various image lines and associated components are discussed. A new type of image line, called the tape line, is described.

The Interaction of Microwaves with Gas-Discharge Plasmas—S. C. Brown (p. 69)

The interaction of microwaves with gas-discharge plasmas provides a valuable tool for studying the fundamentals of gas-discharge phenomena and methods of controlling and switching microwave power. A summary of our present state of knowledge in this field is presented by using as particular examples the interaction of high density and low density gas-discharge plasmas in S-band resonant cavities, both in the presence and absence of dc magnetic fields.

High Power, Magnetic Field Controlled Microwave Gas Discharge Switches—S. J. Tetenbaum and R. M. Hill (p. 73)

A new type of gas discharge switch is described. It is electronically controllable, broadband, and capable of rapidly switching high power pulsed microwaves from either of two waveguide input ports to a single waveguide output port, or from one waveguide input port to either of two waveguide output ports. The electronic control is achieved by turning on or off a magnetic field set for cyclotron resonance. An approximate analysis is given of the operation of the active element of the switch and the results are compared with experiment. An analysis of the effects of frequency scaling indicates that, with the exception of the magnetic flux density which increases with increasing frequency, the switch parameters either improve or remain unchanged in going to higher frequencies. Two different switch configurations are investigated, one a Y-junction switch for operation at S band and the other a balanced

top-wall hybrid coupler switch for operation at K_u band. Their electrical characteristics are described.

Solid-State Microwave Amplifiers—H. Heffner (p. 83)

The maser and the parametric amplifier form a new class of microwave amplifiers which can exploit the properties of bound electrons in a solid. These amplifiers have several common characteristics, among them being their very low-noise performance. This paper reviews the method of operation of these amplifiers, discusses the performance achieved and achievable by the various versions, and points up some of the difficulties involved in effectively utilizing the extremely low-noise figures obtainable. A bibliography is included in which an attempt has been made to include all published papers on masers and parametric amplifiers.

A UHF Solid-State Maser—R. H. Kingston (p. 92)

Chromium doped potassium cobalticyanide has been utilized in the design and construction of a solid-state maser operating in the frequency range of 300 to 500 mc. The pumping frequency is fixed at 5400 mc and the magnetic field required is in the vicinity of 80 gauss. The design utilizes a cavity mode at the pumping frequency and a tuned loop at the operating frequency, thus avoiding the design complications associated with the large size of UHF cavities. System measurements using a directional coupler for isolation yield noise temperatures of approximately 70 degrees Kelvin at bandwidths in the 50 kc range.

A Microwave Frequency Standard Employing Optically Pumped Sodium Vapor—W. E. Bell, A. Bloom, and R. Williams (p. 95)

An instrument in which a simple microwave triode oscillator is stabilized by reference to a natural atomic resonance—the field-independent hyperfine resonance of sodium—is described. Light from a sodium lamp is transmitted through an absorption cell containing sodium vapor and argon, which is placed in a resonant cavity. This light produces population differences between the two quantum levels which are involved in the desired atomic resonance and provides a means of detecting resonance. The cavity is excited by an external microwave triode oscillator which is frequency modulated to a small degree at 60 cycles. When the exciting oscillator frequency coincides with the center of the atomic resonance line, the signal observed by a photocell will be a modulation of the transmitted light at 120 cycles and higher even-order harmonics. Any deviation from line center will introduce a 60-cycle component whose phase and magnitude may be detected to produce an error signal to retune the oscillator in the usual servo loop manner. Theory predicts that an accuracy of possibly one part in 10^{10} can be achieved by systems using sodium and suitable local oscillators. It is evident also that such systems can be engineered into quite small packages, making possible many new applications of microwave oscillators stabilized to high order.

Microwave Filter Design using an Electronic Digital Computer—L. Young (p. 99)

It is shown how a transmission-line circuit can be analyzed by a digital computer. Transformation matrices are used and broken down into equations which are applicable to a computer.

"Synthesis by computer" involves feeding in an approximate design and programming the computer to search for better parameters until the performance matches the specification. Examples are given to indicate time and cost of both analysis and synthesis procedures on an IBM Type 650 digital computer.

The synthesis of a stagger-tuned three-cavity filter is described.

Measurement of Two-Mode Discontinuities in a Waveguide by a Resonance Technique—L. B. Felsen, W. K. Kahn, and L. Levey (p. 102)

The deliberate use of two or more propagating modes in a multimode waveguide, and a knowledge of associated control elements, has assumed renewed importance, particularly for millimeter wavelength applications. This paper presents a resonance measurement technique for the precise evaluation of the equivalent network for a lossless shunt discontinuity coupling two nondegenerate modes in a multimode waveguide. The discontinuity structure is placed into a cavity closed by adjustable plungers, and the data consists of those plunger positions which render the cavity resonant in the two modes of interest. This multipoint data is then transformed to permit an analysis of the two-port network in the discontinuity plane by conventional techniques.

Computations and experimental results obtained at S band illustrative of the procedure are presented for shunt discontinuities coupling the E_{01} and H_{01} modes in circular waveguide. The accuracy achieved is comparable to that obtained in single mode precision measurements.

Mode Couplers and Multimode Measurement Techniques—D. J. Lewis (p. 110)

The measurement of harmonic and spurious signals in waveguide systems is complicated by the fact that one must usually deal with a multimodal measurement. Since the energy may propagate in any mode consistent with the frequency and waveguide geometry, the measurement system used must discriminate between these different modes.

A simple and direct approach to this problem is through the use of "mode couplers" which couple selectively to any desired mode. Theoretical and practical details for mode couplers for the first five modes in rectangular waveguide are presented, as well as the application and limitations of this measurement technique.

Measurement of Harmonic Power Generated by Microwave Transmitters—V. G. Price (p. 116)

A measurement technique is described that can be used to determine quantitatively the power levels of the higher order modes propagating in a straight, lossless, rectangular waveguide. The technique employs a number of small calibrated electric probes which are fixed on the broad and narrow walls of the waveguide measurement section to sample the electric fields within. The method used to calibrate these probes is briefly discussed, and information on accuracy and limitations of the probe technique is presented. Some measurement results on the power levels in the modes of the second and third harmonic frequencies in the outputs of higher power S-band magnetrons and klystrons are presented.

The multiple-probe technique has reduced the time required to take measurements at a given frequency to about one-half hour. An automatic computer has been programmed to perform all of the required mathematical operations and has reduced the computation time to less than one-half hour for each measurement frequency.

Tunable Passive Multicouplers Employing Minimum-Loss Filters—J. F. Cline and B. M. Schiffman (p. 121)

Several multicoupler techniques are described for operating twenty or more UHF transmitters and receivers simultaneously with a single localized antenna system. The types of multicouplers considered include the simple parallel-connected filter type and several distributed-line types, in which the individual branches are separately tuned. The filters used are of the symmetrical, narrow-band, direct-

coupled resonator type, designed to obtain minimum center-frequency insertion loss for a given insertion loss in the adjacent channels. Design formulas are given for these filters, and characteristic response shapes are presented. The extra-channel susceptance, which is the principal factor limiting the number of channels obtainable in a single multicoupler, is discussed in terms of the input coupling coefficient, the resonator parameters, and the lengths of the connecting lines.

A Wide-Band Strip-Line Balun—E. M. T. Jones and J. K. Shimizu (p. 128)

A new wide-band strip-line balun that uses a pair of dual coupled-strip-line band-pass filters is described. It can operate over bandwidths up to about 8:1 in the frequency range of about 100 to 10,000 mc. Design data and theoretical performance curves for typical wideband baluns of this type are presented. The measured performance of an experimental balun operating over a 3:1 frequency range centered at 3000 mc is compared with the theoretical performance, and the effects of discontinuities and dissymmetries in the experimental balun are discussed.

Periodic Structures in Trough Waveguide—A. A. Oliner and W. Rotman (p. 134)

The center fin in trough waveguide can be modified in a periodic fashion to alter the propagation characteristics of the guide. Two such periodic modifications, one an array of circular holes and the second a periodic array of teeth, have been measured fairly extensively and analyzed theoretically. These configurations are useful in connection with antenna scanning or waveguide filter applications.

The array of holes produces only a mild slowing of the propagating wave, but the toothed structure, which may alternatively be described as a series of flat strips extending beyond the edge of the fin, can cause, the propagating wave to vary from a very slow to a very fast wave. The periodic structures are theoretically treated by two methods, a transverse resonance procedure and a periodic cell approach. These theoretical results agree very well with each other and with the measured data.

A Study of Serrated Ridge Waveguide—H. S. Kirschbaum and R. Tsu (p. 142)

The serrated, or periodically slotted ridge produces a periodic loading which retards the phase velocity of the wave in a waveguide. Such structures may be used to provide a variable index of refraction for microwave lenses and as elements in microwave filters. Two approaches are presented in this paper giving the frequency dependence of the index of refraction. One is based on equivalent circuit representations which are qualitatively valid for the effect of the loading. Circuit parameters which determine the shape of the index of refraction curve are calculated from the experimental data. The other approach providing a purely analytic expression of the index of refraction is derived by a field matching method. Calculations show good agreement with test data.

Design Considerations for High-Power Microwave Filters—S. B. Cohn (p. 149)

The need for high-power filters is reviewed briefly, and various design approaches are discussed. The major portion of the paper treats the power-handling capacity of multiple-resonator filters using inductive windows or posts as coupling elements. A formula is derived that gives the relative power capacity of a waveguide filter of this type in terms of the bandwidth and cavity dimensions, and the element values of the low-pass prototype filter. By

means of this formula it is shown quantitatively how high-power ratings may be achieved through the use of enlarged cavities. Methods for eliminating spurious filter responses and of reducing the reflected energy are discussed.

Evacuated Waveguide Filter for Suppressing Spurious Transmission From High-Power S-Band Radar—H. A. Wheeler and H. L. Bachman (p. 154)

A one-megawatt magnetron, used in a search radar, tunes over the S band of 3.1 to 3.5 kmc, and simultaneously causes interference in the band of 3.7 to 4.0 kmc by occasional oscillation in spurious modes. For insertion in the antenna line of this radar, a band-pass filter has been designed to provide over 120 db attenuation in the interference band. It is a wave filter with M-derived terminations for impedance matching and with three sections including traps resonant in the stop band, for high attenuation, all made of nine resonant irises spaced $\frac{1}{4}$ wavelength in a waveguide. Each filter is sealed by pressure windows and evacuated to handle the high-power pulses. Two such filters are connected in parallel between 3-db directional couplers to make a nonreflecting assembly.

Hybrid Junction-Cutoff Waveguide Filters—E. T. Torgow (p. 163)

Low-pass and band-pass filter characteristics can be obtained in waveguide by the use of an arrangement of a waveguide hybrid junction and lengths of cutoff waveguide. Low-pass filters are obtained by terminating a conjugate pair of ports of the hybrid in identical cutoff waveguide sections through short lengths of phase correcting lines. Band-pass characteristics can be realized by introducing a third cutoff waveguide having a lower cutoff frequency at the input port of the hybrid.

These filters have a matched input at all frequencies above the lower end of the pass band and are characterized by low-pass band insertion loss, steep skirt selectivity, and moderate rejection band attenuation. The power handling capabilities of the structure exceed those possible with conventional microwave filter circuits, and the design is particularly well suited for use at frequencies above 10 kmc. Simple techniques are available for constructing filters of this type having variable cutoff frequencies and variable bandwidths.

Practical Design of Strip-Transmission-Line Half-Wavelength Resonator Directional Filters—R. D. Waneslow and L. P. Tuttle, Jr. (p. 168)

Strip-transmission-line directional filters have been found extremely useful since they serve as a combination multiplexer and filter assembly. A step by step procedure has been developed for the quarter-wave coupled filter design having a prescribed bandwidth, skirt selectivity, and passband ripple tolerance for narrow band multiplexing applications.

An experimental study of the strip-transmission-line resonator as an integral part of the directional filter utilizing direct and quarter-wave coupling between the half-wave resonants has been carried out; and an efficient method of tuning a filter is described. This study has included not only problems of insertion loss caused by dissipation but also effects on filter characteristics caused by variations in environmental temperature.

Abstracts and References

Compiled by the Radio Research Organization of the Department of Scientific and Industrial Research,
London, England, and Published by Arrangement with that Department and the *Electronic
and Radio Engineer*, incorporating *Wireless Engineer*, London, England

NOTE: The Institute of Radio Engineers does not have available copies of the publications mentioned in these pages, nor does it
have reprints of the articles abstracted. Correspondence regarding these articles and requests for their
procurement should be addressed to the individual publications, not to the IRE.

The number in heavy type at the upper
left of each Abstract is its Universal Decimal
Classification number. The number in heavy
type at the top right is the serial number of the
abstract. D.C. numbers marked with a dagger
(†) must be regarded as provisional.

U.D.C. NUMBERS

Extensions and changes in U.D.C. numbers
published in P.E. Notes, up to and including
P.E. Note 609, will be introduced in Abstracts
and References where applicable, notably the
subdivisions of 621.372.8 waveguides published in P.E. Note 594. U.D.C. publications
are obtainable from The International Federation for Documentation, Willem Witsenplein
6, The Hague, Netherlands, or from The British
Standards Institution, 2 Park Street, London,
W.1, England.

ACOUSTICS AND AUDIO FREQUENCIES

534.22–14   **328**
**Viscosity Correction to the Velocity of
Sound Measured by a Resonance Method**—
C. Sălceanu and M. Zăgănescu. (*Compt. Rend.
Acad. Sci., Paris*, vol. 246, pp. 2589–2591;
May 5, 1958.) The velocity of sound in liquids
is considered theoretically.

534.23+621.396.677.3   **329**
Signal/Noise Performance of Super-directive Arrays—D. G. Tucker. (*Acustica*, vol. 8,
no. 2, pp. 112–116; 1958.) A super-directive
array is defined as one whose effective aperture
exceeds its physical aperture. Such an array has
a directivity index somewhat better than that
of an ordinary array, but its noise factor is
much worse. The concept of super-directivity is extended to bearing-determining
arrays which give a null response on the axis.
See also 2 of January.

534.232.089.6   **330**
**Calibration of Electroacoustic Transducers
Operating under Increased Pressures of the
Ambient Medium**—I. P. Neroda. (*Elektrosvyaz*,
pp. 57–61; October, 1957.) Absolute calibration
of transducers by the reciprocity method using
a tube is considered. The theory of the method

is discussed, and a suitable experimental procedure is suggested.

534.78:621.395   **331**
Artificial Auditory Recognition in Telephony—E. E. David, Jr. (*IBM J. Res.
Developm.*, vol. 2, pp. 294–309; October, 1958.)
A discussion of the possibility of machine recognition of acoustic patterns such as spoken commands. Techniques involve time and division
into recognizable discrete units and the study
of spectrograms. Rules for interpreting these
were successful in experiments of speech recognition.

534.845   **332**
**A Note on Reciprocity in Linear Passive
Acoustical Systems**—J. H. Janssen. (*Acustica*,
vol. 8, no. 2, pp. 76–78; 1958.) "It is shown
theoretically that linear acoustical passive systems can behave as so-called reciprocity-violating systems; an example of such a system
is a sound-absorbing material that is porous as
well as flexible."

621.395.623.7   **333**
A Survey of Performance Criteria and Design Considerations for High-Quality Monitoring Loudspeakers—D. E. L. Shorter. (*Proc.
IEE*, Part B, vol. 105, pp. 607–623; November,
1958. Discussion.)

621.395.623.73   **334**
Rigidity of Loudspeaker Diaphragms—
D. A. Barlow. (*Wireless World*, vol. 64, pp.
564–569; December, 1958.) The advantages of
a sandwich construction are discussed.

ANTENNAS AND TRANSMISSION LINES

621.315.2.029.5/.6   **335**
High-Frequency Cables—R. Goldschmidt.
(*Bull. schweiz. elektrotech. Ver.*, vol. 49, pp. 708–
716; August 2, 1958.) General theory, materials,
and methods of construction and testing are
considered.

621.315.212.002.2:621.316.992   **336**
Solderless Grounding for Braided Shields
—C. March. (*Electronic Equipm. Eng.*, vol.
6, pp. 48–50; June, 1958.) A technique is described for splicing sections of coaxial cable or
connecting earth leads to braid, using a mechanical crimping tool.

621.315.212.029.64   **337**
**Factors affecting Attenuation of Solid-
Dielectric Coaxial Cables above 3000 Megacycles**—J. R. Hannon. (*IRE Trans. on Component Parts*, vol. CP-3, pp. 99–105; December, 1956. Abstract, *Proc. IRE*, vol. 45, p. 573;
April, 1957.)

621.372.2.029.6:621.372.43   **338**
**A Very-Wide-Band Balun Transformer for
V.H.F. and U.H.F.**—T. R. O'Meara and R. L.
Sydnor. (*Proc. IRE*, vol. 46, pp. 1848–1860;
November, 1958.) The structure described may
be used as a phase inverter, a differential transformer, or as a balun transformer. The insertion
loss varies from 1 to 2 db, between 5 and 1000
mc.

621.372.8:621.372.2.092   **339**
**Waveguide Coils make Compact Delay
Lines**—R. R. Palmisano and A. Sherman.
(*Electronics*, vol. 31, pp. 88–89; October 24,
1958.) A 240 ft delay-line unit consisting of six
tightly wound 40 ft coils of rectangular waveguide has an insertion loss of 21 db with maximum voltage swr of 1.5.

621.372.85   **340**
Low-Loss Structures in Waveguides—
M. F. McKenna. (*Electronic Radio Engr.*, vol.
35, pp. 470–472; December, 1958.) A method is
described for evaluating the equivalent-circuit
parameters of obstacles in waveguides by measuring the field in the guide terminated by a
variable reactance.

621.372.852.22   **341**
**Electromagnetic Wave Propagation in Cylindrical Waveguides Containing Gyromagnetic
Media: Part 1**—R. A. Waldron. (*J. Brit. IRE*,
vol. 18, pp. 597–612; October, 1958.) A comprehensive analysis is given, with a large number
of computed results of cut-off points and phase
constants for a guide containing a concentric
ferrite rod of arbitrary radius. Faraday rotation, power flow, and losses are discussed.

621.396.677.3±534.23   **342**
Signal/Noise Performance of Super-Directive Arrays—Tucker. (See 329.)

621.396.677.3   **343**
**Methods of Calculating the Horizontal
Radiation Patterns of Dipole Arrays around a
Support Mast**—P. Knight. (*Proc. IEE, Part B*,
vol. 105, pp. 548–554; November, 1958.) A discussion of some theoretical methods and their
limitations. The methods include the technique
developed by Carter (1928 of 1944), the infinite-
plane method, the induced-current method, and
the diffraction method. The results are compared with experimental patterns.

621.396.677.81   **344**
A Concentric-Feed Yagi—C. R. Graf.
(*QST*, vol. 42, pp. 24–25; November, 1958.) An
impedance matching technique is described in
which a $3\lambda/4$ coaxial line is inserted in one side
of the folded-dipole driven element.

AUTOMATIC COMPUTERS

681.142 345
Computation in the Presence of Noise—P. Elias. (*IBM J. Res. Developm.*, vol. 2, pp. 346-353; October, 1958.) An analysis of the problem of performing reliable computation with elements which are themselves unreliable. The effects of the coding procedures on the reliability are discussed.

681.142 346
Control Apparatus for a Serial Drum Memory—D. S. Kamat. (*Electronic Eng.*, vol. 30, pp. 634-639; November, 1958.) A detailed circuit description of equipment used for obtaining design data for fast track switching on a serial drum magnetic storage device.

681.142 347
Matrix Programming of Electronic Analogue Computers—R. E. Horn and P. M. Honnell. (*Commun. and Electronics*, pp. 420-426; September, 1958. Discussion, pp. 426-428.) The technique is based on establishing a correspondence between the matrically formed differential equations and the computer networks. This simplifies the setting up of the computer and reduces the possibility of errors. Examples are given of the use of the method.

681.142 348
A Magnetic-Drum Store for Analogue Computing—J. L. Douce and J. C. West. (*Proc. IEE, Part B*, vol. 105, pp. 577-580; November, 1958.) Large storage capacity combined with relatively short access time is obtained. The drum can be used for generating nonlinear functions and as a delay network.

681.142:538.632 349
An Electrical Multiplier utilizing the Hall Effect in Indium Arsenide—R. P. Chasmar and E. Cohen. (*Electronic Eng.*, vol. 30, pp. 661-664; November, 1958.) Details are given of the construction and performance of a multiplier for computer applications in which an InAs Hall plate is mounted in the gap in a ferrite core.

681.142:538.632:537.311.33 350
Multiplication by Semiconductors—C. Hilsum. (*Electronic Eng.*, vol. 30, pp. 664-666; November, 1958.) The modes of operation of analogue computer multipliers using the Hall effect in semiconductors are discussed. Some experimental multipliers and the results obtained with them are described. The application of the magnetoresistive effect is outlined.

681.142:621.314.7:621.318.134 351
The Design of Logical Circuits using Transistors and Square-Loop Ferrite Cores—A. F. Newell. (*Mullard tech. Com.*, vol. 4, pp. 110-120; October, 1958.) Some basic circuits are reviewed and a range of practical designs and design procedures is given.

681.142:621.318.5 352
Some Aspects of the Network Analysis of Sequence Transducers—J. M. Simon. (*J. Franklin Inst.*, vol. 265, pp. 439-450; June, 1958.) An algebraic formulation is presented for use in the analysis of networks of the synchronous type of sequence transducer. See also 28 of 1956 (Mealy).

CIRCUITS AND CIRCUIT ELEMENTS

621.3.049:621.3-71 353
Design and Performance of Air-Cooled Chassis for Electronic Equipment—M. Mark and M. Stephenson. (IRE TRANS. ON COMPONENT PARTS, vol. CP-3, pp. 38-44; September, 1956. Abstract, PROC. IRE, vol. 45, pp. 112-113; January, 1957.)

621.3.049.7 354
Future Electronic Components—G. W. A. Dummer. (*Wireless World*, vol. 64, pp. 591-593; December, 1958.) To obtain substantial reduction in size, components will probably consist of thin films of resistive, dielectric, magnetic, and conductive materials, and film-type or flat-plate semiconductor devices will be used.

621.3.049.75 355
Foil-Clad Laminates in Printed Circuitry—D. K. Rider. (*Metal Progr.*, vol. 74, pp. 81-85; September, 1958.)

621.314.21.001.2 356
Simplified Mains-Transformer Design—H. D. Kitchen. (*Wireless World*, vol. 64, pp. 582-585; December, 1958.) The power-handling capabilities of various laminations are tabulated, and the design procedure is illustrated by an example.

621.314.22:621.3.018.7 357
Measurement of Parameters Controlling Pulse Front Response of Transformers—P. R. Gillette, K. Oshima, and R. M. Rowe. (IRE TRANS. ON COMPONENT PARTS, vol. CP-3, pp. 20-25; March, 1956. Abstract, PROC. IRE, vol. 44, Part 1, p. 832; June, 1956.)

621.318.57:621.327.42:681.142 358
A Study of the Neon Bulb as a Nonlinear Circuit Element—C. E. Hendrix. (IRE TRANS. ON COMPONENT PARTS, vol. CP-3, pp. 44-54; September, 1956. Abstract, PROC. IRE, vol. 45, p. 113; January, 1957.)

621.319.45 359
A Method of Electrolytic Etching of Tantalum for Capacitor Use—I. Sanghi. (*Current Sci.*, vol. 27, pp. 297-298; August, 1958.) Etching of foil in a bath of trichloroacetic acid, sodium trichloroacetate and methanol produced an increase of 300-400 per cent in capacitance relative to a capacitor formed of unetched foil.

621.372:531.314.2 360
The Lagrange Equations in Electrical Networks—F. L. Ryder. (*J. Franklin Inst.*, vol. 266, pp. 27-38; July, 1958.)

621.372:534.213-8 361
Ultrasonic Mercury Delay Lines—C. F. Brockelsby. (*Electronic Radio Engr.*, vol. 35, pp. 446-452; December, 1958.) The construction and characteristics of lines and transducers are discussed.

621.372.029.6:621.374 362
Analysis of Milimicrosecond R.F. Pulse Transmission—M. P. Forrer. (PROC. IRE, vol. 46, pp. 1830-1835; November, 1958.) The analysis assumes a quadratic approximation for the complex propagation constant and a transmitted pulse with Gaussian envelope. The theory is applicable to uniform microwave transmission systems and relates pulse shapes with the CW properties of the system.

621.372.413.029.64:621.3.049.75 363
Fabrication Techniques for Ceramic *X*-Band Cavity Resonators—M. C. Thompson, F. E. Freethey, and D. M. Waters. (*Rev. Sci. Instr.*, vol. 29, pp. 865-868; October, 1958.) Techniques are described for constructing cavity resonators for the *X* band from low-thermal-expansion ceramics. A variety of mechanical arrangements is discussed. *Q* values as high as 14,000 and frequency/temperature coefficients as low as 1 part in 10^8 per °C have been obtained using simple processes.

621.372.5 364
A Correlation between Stagger-Tuned and Synchronously Tuned Coupled Circuits—J. B.

Rudd. (*AWA Tech. Rev.*, vol. 10, no. 3, pp. 101-109; 1958.) Application of a network theorem enunciated by Green (54 of 1958).

621.372.54 365
Time-Symmetric Filters—L. R. O. Storey and J. K. Grierson. (*Electronic Eng.*, vol. 30, pp. 586-592 and 648-653; October and November, 1958.) Methods for simulating filters that have impulse responses symmetrical in time are described, and their application to the analysis of gliding tones is discussed. The response of a narrow-band time-symmetric filter to a gliding tone is evaluated and shown to consist of an oscillation bounded by a slowly varying envelope. The shape is governed by a parameter involving the bandwidth of the filter and the rate of variation of the instantaneous frequency of the tone.

621.372.54(083.57) 366
Design Curves for Simple Filters—D. J. H. Maclean. (*Electronic Eng.*, vol. 30, pp. 654-660; November, 1958.) Charts are given for the design of simple *LC* ladder filters with either Butterworth or Tchebycheff type of response.

621.372.54(083.57) 367
Nomographs for Designing Elliptic-Function Filters—K. W. Henderson. PROC. IRE, vol. 46, pp. 1860-1864; November, 1958.)

621.372.543.3:621-526 368
Simplified Design of Resonant Notch Filters for Servo Applications—J. P. Jagy. (*Electronic Equipm. Eng.*, vol. 6, pp. 48-52; April, 1958.) Data are given in graphical form for the design of stagger-tuned constant-*k* band-stop filters. Applications to error-rate damping in servo systems are discussed.

621.372.57 369
The Reduction of Low-Frequency Noise in Feedback Integrators—E. M. Dunstan and M. J. Somerville. (*Proc. IEE, Part B*, vol. 105, pp. 532-544; November, 1958.) A considerable improvement in signal-noise ratio, compared with that of a conventional direct-coupled integrator, is obtained either by using an error amplifier containing a single *CR* coupling or by applying phase correction to the output from a low-accuracy direct-coupled integrator.

621.373.421.13 370
Thermally Compensated Crystal Oscillators—R. A. Spears. (*J. Brit. IRE*, vol. 18, pp. 613-620; October, 1958.) Frequency stability is achieved by using thermistors in a temperature-sensitive phase-shifting network incorporated in the oscillator circuit. A stability of about 1 in 10^6 is obtained over a wide frequency range without thermostats or ovens. It is suggested that even better compensation would be achieved by attaching the thermistor bead to the crystal.

621.373.421.13:621.3.018.41(083.74) 371
A Quartz Servo Oscillator—N. Lea. (PROC. IRE, vol. 46, pp. 1835-1841; November, 1958.) A description of a 5-mc quartz oscillator stable to 2 parts in 10^{10} with a dual stabilization by resonant-loop balance and bridge-operated servo control.

621.373.421.13.001.4 372
Checking Crystal Oscillators—D. J. Spooner. (*Wireless World*, vol. 64, pp. 594-596; December, 1958.) Simple measurements are suggested to ensure that a crystal will oscillate in a specified circuit without damage, and at the required frequency.

621.373.43 373
A Constant-Amplitude Random-Function Generator—G. A. Hellwarth. (*Commun. and Electronics*, pp. 443-452; September, 1958.) A

generator is described for producing a wave shape with constant peak-to-peak amplitude but whose path between peaks is random. Circuits for random sawtooth, triangular, cosine, and square waves operating in the AF range are described.

621.373.43+621.374.32]:621.387   **374**
Some Novel Circuits employing Cold-Cathode Tubes—R. S. Sidorowicz. (*Electronic Eng.*, vol. 30, pp. 624–629 and 697–701; November and December, 1958.) The circuits described are based on cold-cathode diodes and triodes, the diode being used to stabilize the anode breakdown voltage of the triodes. Details are given of a stable relaxation oscillator, a voltage discriminator, trigger circuits, a staircase-waveform generator, and decade counters.

621.373.43:621.396.96   **375**
Pulse-Forming Networks—J. W. Trinkaus. (IRE Trans. on Component Parts, vol. CP-3, pp. 63–66; September, 1956. Abstract, Proc. IRE, vol. 45, p. 113; January, 1957.)

621.373.44:535.33   **376**
The Excitation of Ionic Spectra by 100-kW High-Frequency Pulses—L. Minnhagen and L. Stigmark. (*Ark. Fys.*, vol. 13, Part 1, pp. 27–36; February 5, 1958. In English.) Equipment previously described (1592 of 1955) has been developed and provided with a power amplifier containing a 25 kw water-cooled triode. Pulse powers up to approximately 100 kw are applied to a discharge tube with pulse duration 80 μs and repetition frequency 40/sec.

621.374.32   **377**
A Distributed-Circuit Pulse Height Analyser—A. Boucherie and J. Mey. (*J. Phys. radium*, vol. 19, pp. 98–99; January, 1958.) A multichannel analyzer using distributed circuits and having a resolving time of 0.2 μs is briefly described.

621.374.43   **378**
Frequency Dividers using Transistors—M. Z. Tseitlin. (*Elektrosvyaz*, pp. 33–41; September, 1957.) Regenerative frequency dividers using junction and point-contact transistors are described and results are given of an experimental investigation.

621.375.2.029.33   **379**
Video Amplifier Design using the PCL 84—P. L. Mothersole. (*Mullard tech. Com.*, vol. 4, pp. 2–6; July, 1958.) Optimum gain is achieved by the use of anode compensation. Bias methods for this condition are discussed.

621.375.2.029.63   **380**
Ultra-High-Frequency Power Amplifiers—J. Dain. (*Proc. IEE*, Part B, vol. 105, pp. 513–522; November, 1958.) A general review of the design and construction of power amplifiers operating in the range 300–3000 mc. Travelling-wave valves designed for a bandwidth of one octave are limited in their mean power output by overheating of the helix. Backward-wave amplifiers based on crossed-field interaction require a variable beam voltage for wide-band operation but have a high efficiency and low operating voltage.

621.375.3   **381**
A Note on the Design of Transductors for Maximum Power Transfer—J. C. R. Heydenrych. (*Trans. S. Afr. IEE*, vol. 48, Part 12, pp. 370–377; December, 1957.) Magnetic amplifiers giving maximum power output for a given size of core are designed by known graphical and numerical methods. Theoretical and experimental results are compared.

621.375.3   **382**
A.C.-Controlled Magnetic Amplifiers—E. W. Lehtonen and E. A. Cronauer. (*Commun.*

and *Electronics*, pp. 476–480; September, 1958.) A method is described for controlling full-wave amplifiers with ac signals. The response characteristic is similar to that of dc controlled amplifiers, and high gain is achieved with no current-limiting resistors or demodulator. The method is based on cancelling the induced emf in the control circuit.

621.375.3(083.7)   **383**
Proposed Standard Terms and Definitions for Magnetic Amplifiers—(*Commun. and Electronics*, pp. 429–431; September, 1958. Discussion, pp. 431–432.) An AIEE committee report on the terminology used. 38 terms are defined.

621.375.4.029.3   **384**
A 4.5-W Sliding-Bias Amplifier using an OC16—J. F. Pawling and P. Tharma. (*Mullard tech. Com.*, vol. 4, pp. 19–28; July, 1958.) The two-stage circuit described and analyzed in detail gives nearly twice the output power obtainable in conventional Class-A operation, using a heat sink of the same size.

621.375.4.029.33   **385**
Video Amplifiers using Alloy Junction Transistors—K. Holford and L. M. Newall. (*Mullard tech. Com.*, vol. 4, pp. 94–105; October, 1958.) Grounded-emitter video amplifier stages are analyzed theoretically using compensated and uncompensated circuits. Abacs and charts are given to facilitate design procedure for multistage amplifiers, together with the practical design of an amplifier with 80 db gain and 1.5 mc bandwidth.

621.375.432   **386**
Pulse Amplifier with Nonlinear Feedback—L. H. Dulberger. (*Electronics*, vol. 31, pp. 86–87; November 7, 1958.) The transistor amplifier described provides constant output over a 38 db range of input signals.

621.375.432:621.395.625.3   **387**
Transistor Tape Preamplifier—P. F. Ridler. (*Wireless World*, vol. 64, pp. 572–573; December, 1958.) The playback head is used as the inductance in a feedback inductance-resistance integrating circuit. A 70 db signal/noise ratio is obtained and the frequency response is flat within ±2 db from 50 cps to 15 kc.

621.375.9:638.569.4.029.6   **388**
Proposal for a Maser Amplifier System without Nonreciprocal Elements—S. H. Autler. (Proc. IRE, vol. 46, pp. 1880–1881; November, 1958.) A system noise temperature of 30°K or less should be obtainable by using two matched masers and a loss-less power-dividing network such as a hybrid T.

621.375.9:538.569.4.029.64   **389**
Characteristics of the Beam-Type Maser: Part 2—K. Shimoda. (*J. phys. Soc. Japan*, vol. 13, pp. 939–947; August, 1958.) An experimental investigation of the characteristics of an ammonia maser for use as a frequency standard. Measurements of the effect of focusing voltage and cavity tuning on frequency are compared with theory, and the effect of the velocity spread of the molecules is estimated. Part 1: 707 of 1958.

621.375.9.029.6:621.3.011.23:621.396.61   **390**
Parametric Amplifier μps Scatter Range—(*Electronics*, vol. 31, p. 96; November 7, 1958.) A Si-diode parametric amplifier [see 79 of January (Weber)] is used, and extends the range of a 900 mc link from 250 to 350 miles. Receiver noise factor is reduced from 8 to 1 db.

GENERAL PHYSICS

535:621.383   **391**
The Wider Scope of Optics—K. M. Greenland. (*J. Electronics Control*, vol. 5, pp. 278–288;

September, 1958.) The development and applications of new optical and optical-electronic devices are considered. 31 references.

537.226.33   **392**
The Application of Onsager's Theory to Dielectric Dispersion—N. E. Hill. (*Proc. Phys. Soc.*, vol. 72, pp. 532–536; October 1, 1958.) A new equation for the complex dielectric constant, which includes the proper effect of the reaction field, is developed for the case of an alternating applied field. It is shown to yield results very close to those obtained with the simple Debye equation for the complex dielectric constant.

537.312.62   **393**
Experimental Evidence for an Energy Gap in Superconductors—M. A. Biondi, A. T. Forrester, M. P. Garfunkel, and C. B. Satterthwaite. (*Rev. Mod. Phys.*, vol. 30, pp. 1109–1136; October, 1958.)

537.52:537.56   **394**
Wire-Cylinder Electric Discharges in Air in Relation to the Space-Charge Field-Emission Hypothesis—H. Ritow. (*J. Electronics Control*, vol. 5, pp. 193–225; September, 1958.) Study of experimental data on wire cylinder discharges in relation to the field-emission hypothesis yields graphical and arithmetic methods of finding the effective field at the time of flash initiation and the space charge field at the wire. The effective field is of the order of 10^6 volts per cm and is interpreted as a measure of the emission field of the cathode metal or of the ionized air. See also 2061 of 1958.

537.525.029.5   **395**
Ultra-High-Frequency Gas Breakdown between Ragowski Electrodes—W. A. Prowse and J. L. Clark. (*Proc. Phys. Soc.*, vol. 72, pp. 625–634; October 1, 1958.) Breakdown voltage, electrode spacing, electrode size, and gas pressures are observed for air, H_2, N_2 and Ne at 9.5 mc.

537.533:538.63   **396**
The Relativistic Flow of Electrons in Parallel and Radial Straight Lines with no Externally Imposed Magnetic Field—A. R. Lucas. (*J. Electronics Control*, vol. 5, pp. 245–250; September, 1958.) Analysis is given of the possibility of producing relativistic electron flows. It is shown that they could not start from a cathode surface where the electrons have zero speed. The analysis also applies to flows, normally considered nonrelativistic, in diodes where the linear dimensions of the electrode surfaces are large compared with the electrode spacing [see *e.g.* 3037 of 1958 (Meltzer)].

537.533:621.385.029.6   **397**
Electron Cooling by Heat Exchange—R. C. Knechtli and W. Knauer. (*J. Appl. Phys.*, vol. 29, pp. 1513–1514; October, 1958.) A new method for obtaining homogeneous electron streams is described. By making the electron stream part of a plasma, beams with densities of up to 10^{-3} a per cm² and currents exceeding 10^{-3} have been achieved.

537.533.7:535.417   **398**
Coherence Requirements for Interferometry—G. D. Kahl and F. D. Bennett. (*Rev. Mod. Phys.*, vol. 30, pp. 1193–1196; October, 1958.) An analysis of the theory of double-beam interferometry, based on that of D. Gabor. (*Rev. Mod. Phys.*, vol. 28, pp. 260–276; July, 1956.) Gabor's restrictive assumptions are clarified and generalized.

537.533.71:621.385.833   **399**
Energy Spectrum of a 40-kv Electron Beam "Reflected" by a Metallic Object—F. Pradal and R. Saporte. (*Compt. Rend. Acad. Sci., Paris*, vol. 246, pp. 2880–2883; May 19, 1958.)

The energy spectra of electrons reflected from different metallic targets are investigated by means of a magnetic spectrograph.

537.56:537.29:538.69 **400**
Transport Phenomena in a Completely Ionized Double-Temperature Plasma—S. I. Braginskiĭ. (*Zh. Eksp. Teor. Fiz.*, vol. 33, pp. 459–472; August, 1957.) A theoretical investigation of particle motion and heat transfer in a plasma of electrons and positive ions under the influence of both electric and magnetic fields, the electron and ion temperatures being considered different.

537.56:538.12 **401**
The Amplification of a Magnetic Field by a High Current Discharge—R. J. Bickerton. (*Proc. Phys. Soc.*, vol. 72, pp. 618–624; October 1, 1958.) It is shown theoretically that a helical current flow discharge is set up by a longitudinal magnetic field in which the plasma pressure is balanced by electrodynamic forces. The direction of the helix is such that the initial longitudinal field is amplified. Some experimental evidence supports this theory.

537.562 **402**
Transport Phenomena in Completely Ionized Gas considering Electron-Electron Scattering—M. S. Sodha and Y. P. Varshni. (*Phys. Rev.*, vol. 777, pp. 1203–1205; September 1, 1958.) "Hall mobility and other transport properties of electrons in a completely ionized gas have been investigated when a magnetic field is applied, taking into account electron-electron scattering. Results have been presented for different mean ionic charges."

538.12:538.221 **403**
The Magnetic Fields of a Ferrite Ellipsoid—R. A. Hurd. (*Canad. J. Phys.*, vol. 36, pp. 1072–1083; August, 1958.) "Approximate expressions are found for the internal and the adjacent external magnetic fields of a small ferrite ellipsoid under plane-wave excitation. Consideration is given to the variation of apparent susceptibility with the size of the ferrite."

538.3 **404**
Classical Electrodynamics as a Distribution Theory: Part 2—J. G. Taylor. (*Proc. Camb. Phil. Soc.*, vol. 54, Part 2, pp. 258–264; April, 1958.) Part 1: 2027 of 1956.

538.3:535.13 **405**
Application of Distributions to the Equations of Maxwell and Helmholtz—M. Bouix. (*Compt. Rend. Acad. Sci.*, *Paris*, vol. 246, pp. 2858–2860; May 19, 1958.) Distribution theory is applied to give a new concept of an element of current.

538.3:535.13 **406**
Singular Electromagnetic Induction—Pham Mau Quan. (*Compt. Rend. Acad. Sci.*, *Paris*, vol. 246, pp. 2734–2737; May 12, 1958.) Extension of the concepts discussed in 3417 of 1958.

538.3:535.13 **407**
Algebraic Study of the Electromagnetic Tensor in the Presence of Induction—L. Mariot and Pham Mau Quan. (*Compt. Rend. Acad. Sci.*, *Paris*, vol. 246, pp. 3018–3020; May 28, 1958.) See 406 above.

538.561:537.122:523.7 **408**
Electromagnetic Radiation from Electrons Rotating in an Ionized Medium under the Action of a Uniform Magnetic Field—R. Q. Twiss and J. A. Roberts. (*Aust. J. Phys.*, vol. 11, pp. 424–446; September, 1958.) The radiation is shown to be predominantly in the extraordinary mode. At the harmonics of the gyrofrequency of the fast electron the power radiated in the ordinary mode is a small percentage

of that in the extraordinary mode, but at the fundamental gyrofrequency it is lower by a factor $\simeq 10^{-2}(v_0/c)^4$, where v_0 is the velocity of the fast electron and c is the velocity of light. The gyro theory of the sun's nonthermal radiation is discussed. This mechanism cannot explain the phenomena associated with noise bursts of Type II and III although it is conceivable that Type I bursts may be of gyro origin.

538.566 **409**
Theory of Electromagnetic Waves in a Crystal with Excitons—S. I. Pekar. (*J. Phys. Chem. Solids*, vol. 5, pp. 11–22; 1958.) See 3058 of 1958.

538.566.:535.312 **410**
The Characteristics of an Electromagnetic Wave Reflected from a Moving Object—C. F. Cole, Jr. (*J. Franklin Inst.*, vol. 265, pp. 463–471; June, 1958.)

538.566:535.42 **411**
Diffraction by a Wide Slit and Complementary Strip—R. F. Miller. (*Proc. Camb. Phil. Soc.*, vol. 54, Part 4, pp. 479–511; October 17, 1958.) The diffraction of E- and H-polarized waves by an infinite slit is considered. Induced current densities, aperture and far fields, and the transmission coefficient, are calculated in the form of infinite series in inverse powers of the slit-width wavelength ratio. The solution for diffraction by a strip is also obtained. A comparison is made with previous results; this method appears to provide accurate information when the slit width is greater than a wavelength.

538.566:535.43 **412**
Variational Principles in High-Frequency Scattering—R. D. Kodis. (*Proc. Camb. Phil. Soc.*, vol. 54, Part 4, pp. 512–529; October 17, 1958.) Two variational principles are formulated for two-dimensional scattering by obstacles. The more successful of these treats the obstacle like an aperature coupling two half-spaces. The zero-order calculation for the cross section of a circle is found to have the correct $(ka)^{-2/3}$ frequency dependence.

538.566:535.43 **413**
Scattering from a Small Anisotropic Ellipsoid—R. A. Hurd. (*Canad. J. Phys.*, vol. 36, pp. 1058–1071; August, 1958.) "Scattering of an electromagnetic wave by a small ellipsoid having tensor permeability and dielectric properties is dealt with by expanding the fields as power series in λ^{-1}. Consideration has been given to the first three terms of the expansion."

538.566.2 **414**
Contribution to the Theory of Electromagnetic Wave Propagation in Media with Random Heterogeneities of the Refractive Index—V. V. Merkulov. (*Zh. Tekh. Fiz.*, vol. 27, pp. 1051–1055; May, 1957.) A correlation function is derived which can be used in connection with diffraction problems.

538.566:535.43]+534.26 **415**
Scattering of Plane Waves by Locally Homogeneous Dielectric Noise—R. A. Silverman. (*Proc. Camb. Phil. Soc.*, vol. 54, Part 4, pp. 530–537; October 17, 1958.) When plane waves are scattered by locally homogeneous dielectric noise (random refractive-index fluctuations) and observed in the Fraunhofer region, it is found that the local structure of the noise determines the average scattered power received at a fixed point, whereas its overall structure determines the space correlations of the radiation received at two different points.

538.569.4.029.6:535.33.08 **416**
Criteria determining the Design and Performance of a Source-Modulated Microwave

Cavity Spectrometer—R. W. R. Hoisington, L. Kellner, and M. J. Pentz. (*Proc. Phys. Soc.*, vol. 72, pp. 537–544; October 1, 1958.) "An analysis is given of the radio- and audio-frequency modulation method employed in microwave spectroscopy. The results of the theory are compared with measurements taken on an 8-mm microwave spectrometer and are found to be in close agreement. The calculations are extended to include the case where an absorbing gas is enclosed in a resonant cavity."

538.569.4.029.64:539.2 **417**
Direct Measurement of Electron Spin-Lattice Relaxation Times—C. F. Davis, Jr., M. W. P. Strandberg, and R. L. Kyhl. (*Phys. Rev.*, vol. 111, pp. 1268–1272; September 1, 1958.) A discussion of the experimental problems encountered in making spin-lattice relaxation measurements in electron paramagnetic systems at low temperatures. Gadolinium and chrome ion spin-lattice relaxation times are given. The relation of these spin-lattice relaxation times to relaxation times measured in the frequency domain by observing a saturation parameter is discussed.

539.2 **418**
The Electron Structure of Transition Metals and Alloys and Heavy Metals—J. Friedel. (*J. Phys. Radium.*, vol. 19, pp. 573–581; June, 1958.)

GEOPHYSICAL AND EXTRATERRESTRIAL PHENOMENA

523.16 **419**
Energy Spectrum of Particles Bombarding the Earth—B. J. O'Brien. (*Nature (London)*, vol. 182, p. 521; August 23, 1958.) The estimated fluxes of interstellar and auroral particles appear to fit the straight-line portion of the cosmic-ray integral energy spectrum extrapolated to lower energies.

523.164 **420**
Radio Astronomy—S. Khaikin. (*Radio Mosk.*, pp. 25–27; November, 1957.) A brief description of the fields of exploration opened by developments in radio astronomy.

523.164 **421**
On the Radio Emission of Hydrogen Nebulae—C. M. Wade. (*Aust. J. Phys.*, vol. 11, pp. 388–399; September, 1958.) Random variations in electron density and electron temperature through the nebulae are shown to alter the optical depth. Radio emission of Strömgren spheres is also discussed and an empirical method for determining Strömgren's constant is described.

523.164 **422**
An Investigation of the Strong Radio Sources in Centaurus, Fornax, and Puppis—K. V. Sheridan. (*Aust. J. Phys.*, vol. 11, pp. 400–408; September, 1958.)

523.164 **423**
A Catalogue of Radio Sources between Declinations $+10°$ and $-20°$—B. Y. Mills, O. B. Slee and E. R. Hill. (*Aust. J. Phys.*, vol. 11, pp. 360–387; September, 1958.)

523.164.32 **424**
Investigations of Persistent Solar Sources at Centimetre Wavelengths—M. R. Kundu. (*Compt. Rend. Acad. Sci.*, *Paris*, vol. 246, pp. 2740–2743; May 12, 1958.) Measurements of the brightness distribution and apparent size of solar RF sources made at 3.2 cm λ with an interferometer [2733 of 1957 (Alon *et al.*)] show that small apparent diameters are associated with periods of eruptive solar activity.

523.164.32 **425**
The Dimensions of Sources of Bursts of Solar Radiation at Centimetre Wavelengths—

M. R. Kundu. (*Compt. Rend. Acad. Sci., Paris*, vol. 246, pp. 2852–2855; May 19, 1958.) Sources are classified, the growth and decay in their apparent size are observed, and their equivalent temperature estimated on the basis of interferometer measurements at 3 cmλ.

523.164.4:523.755 426
Outer Corona of the Sun—V. V. Vitkevich. (*Priroda*, pp. 15–20; December, 1957.) Radio emissions from the Crab nebula passing through the corona are observed by an interferometric method. The results indicate that the outer corona extends to a distance of 20 sun radii.

523.164.4:551.510.535 427
Amplitude Scintillation of Extraterrestrial Radio Waves at Ultra High Frequency—H. C. Ko. (PROC. IRE, vol. 46, pp. 1872–1873; November, 1958.) Measurements are described which show that at latitude 40°N, ionospheric scintillation effects are still significant at 915 mc when the radio star is near the northern horizon.

523.7:538.561:537.122 428
Electromagnetic Radiation from Electrons Rotating in an Ionized Medium under the Action of a Uniform Magnetic Field—Twise and Roberts. (See 408.)

523.72:621.396.822 429
Ionizing Radiation associated with Solar Radio Noise Storm—K. A. Anderson. (*Phys. Rev. Lett.*, vol. 1, pp. 335–337; November 1, 1958.) Comparison of records obtained during a storm on August 22, 1958, from three balloon-borne detectors, a single counter, counter telescope and ion chamber, indicates the appearance of protons with kinetic energy of 170 mev.

523.72:621.396.822 430
Solar Brightness Distribution at a Wavelength of 60 Centimetres: Part 2—Localized Radio Bright Regions—G. Swarup and R. Parthasarathy. (*Aust. J. Phys.*, vol. 11, pp. 338–349; September, 1958.) Observations were taken with a 32-element interferometer with a beam width of 8.7 min of arc, from July, 1954, to March, 1955. Sources of radio brightness were found to be closely correlated with sunspot areas. Their estimated size lay between 3 and 6 min of arc. Sometimes their slowly varying component showed marked changes in intensity over periods of half an hour. The largest radio-brightness temperatures measured were about 10⁷°K. Part 1: 1707 of 1956.

523.75:523.164.32 431
Flare-Puffs as a Cause of Type III Radio Bursts—R. G. Giovanelli. (*Aust. J. Phys.*, vol. 11, pp. 350–352; September, 1958.) Type III bursts occur within ±2 min of two-thirds of the flare-puffs. Most puffs are followed by surges and this suggests two ejections of differing velocities: one, at about 1/5 the velocity of light, causing the burst, and the other, at 100 km causing the surge. See also 1715 of 1958 (Loughhead *et al.*).

523.75:523.164.32 432
Optical Observations of the Solar Disturbances causing Type II Radio Bursts—R. G. Giovanelli and J. A. Roberts. (*Aust. J. Phys.*, vol. 11, pp. 353–359; September, 1958.) Type II radio bursts have been identified with ejections having velocities exceeding that of sound in the corona for events near the limb, and with very bright flares with dark-filament activity when the event is on the disk.

523.75:550.385.4 433
On the Great Solar Flare which Started at 21h 09m, February 9th, 1958, as the Likely Source of Geomagnetic Storm, February 11th —K. Sinno. (*Rep. Ionosphere Res. Japan*, vol.

12, pp. 6–9; March, 1958.) It is shown that there is a high probability that the flare caused the magnetic storm. Experimental evidence is given supporting a connection between the early part of a 200-mc solar noise burst and a short-wave fade-out, and between the late part and magnetic-storm occurrence.

550.372(47) 434
Radio Wave Propagation and Soil Conductivity—V. Kashprovskii. (*Radio, Mosk.*, pp. 19–21; July, 1958.) Description of a scheme for mapping the soil conductivity throughout the Soviet Union by radio techniques.

550.38 435
The External Magnetic Field of the Earth—A. Beiser. (*Nuovo Cim.*, vol. 8, pp. 160–162; April 1, 1958. In English.) The discrepancy between the equivalent geomagnetic dipole based on cosmic-ray observations and that derived from surface observations is investigated. See also 3721 of 1956 (Simpson *et al.*).

550.38:538.3 436
Reversals of the Earth's Magnetic Field—D. W. Allan. (*Nature (London)*, vol. 182, pp. 469–470; August 16, 1958.) Calculations made by Rikitake (3074 of 1958) have been extended by the use of a digital computer.

550.389.2:523.165:629.132.1 437
Balloon Gear monitors Cosmic Radiation—L. E. Peterson, R. L. Howard, and J. E. Winckler. (*Electronics*, vol. 31, pp. 76–79; November 7, 1958.) The balloon with a 60 lb load can be flown at 100,000 ft altitude for 22 hours. Equipment carried includes an omnidirectional Geiger counter, a spherical integrating ionization chamber, and telemetry equipment.

550.389.2:551.510.535 438
Electron-Density Profiles in the Ionosphere during the I.G.Y.—R. L. Smith-Rose. (PROC. IRE, vol. 46, p. 1874; November, 1958.) Note on a program organized by the Radio Research Station, Slough, England, of using electronic computers in the preparation of $N(h)$ profiles from ionograms obtained at four observatories.

550.389.2:[629.19+629.136.3 439
Investigation of Upper Layers of the Atmosphere by means of Rockets and Artificial Earth Satellites—E. K. Fedorov. (*Priroda*, pp. 3–12; September, 1957.) Description of possible methods of investigation and the nature of the instrumentation required.

550.389.2:629.19 440
Scientific Investigations by means of Artificial Earth Satellites—G. A. Skuridin and L. V. Kurnosova. (*Priroda*, pp. 7–14; December, 1957.) A description of Sputnik II and the scientific equipment carried by it.

550.389.2:629.19 441
The Determination of the Trajectory of Artificial Satellites—N. Carrara, P. F. Checcacci, and L. Ronchi. (*Ricerca sci.*, vol. 28, pp. 1341–1355; July, 1958.) Methods and the arrangement of ground equipment are described.

550.389.2:629.19 442
Exact Determination of the Velocity of an Artificial Satellite—S. Khaĭkin. (*Radio, Mosk.*, pp. 5–7; December, 1957.) Doppler measurements enable the velocity of the satellite to be measured to an accuracy within 1 part in 10⁴.

550.389.2:629.19 443
Doppler Measurements on Soviet Satellites —A. H. Allan and J. E. Drummond. (*N. Z. J. Sci. Tech.*, vol. 1, pp. 143–153; June, 1958.) The first two Soviet satellites were successfully tracked by means of Doppler measurements alone. The apparatus and the method of analysis used are described.

550.389.2:629.19 444
Observations of Radio Signals from the First Man-Made Earth Satellite—R. R. Long and G. H. Munro. (*Proc. IRE, Aust.*, vol. 19, pp. 201–206; May, 1958.)

550.389.2:629.19 445
Radio Observations on the First Russian Artificial Earth Satellite—(*Trans. S. Afr. IEE*, vol. 48, Part 12, pp. 363–369; December, 1957.) Doppler measurements made at Johannesburg at 40 mc are reported. Orbit calculations are made neglecting ionospheric effects. See aslo 2087 of 1958 (Fejer).

550.389.2:629.19 446
Radio Observations of the Earth Satellite 1957α—K. Miya, Y. Taguchi, and S. Tabuchi. (*Rep. Ionosphere Res. Japan*, vol. 12, pp. 16–27; March, 1958.) Describes observations of field strength, bearing and Doppler shift of the 20,005-kc signal. It is considered that to explain anomalous field strengths and Doppler shifts, propagation involving ground scattering followed by ionospheric reflection must be considered. Anomalous Doppler effects include rapidly varying shift, and apparent recession when the satellite is approaching the receiver.

550.389.2:629.19 447
Last Minutes of Satellite 1957β (*Sputnik 2*) —D. G. King-Hele, and D. M. C. Walker. (*Nature (London)*, vol. 182, pp. 426–427; August 16, 1958.)

550.389.2:629.19:523.165 448
Cosmic Rays Observed by Satellite 1958 Alpha II—Y. Acno and K. Kawakami. (*Rep. Ionosphere Res. Japan*, vol. 12, pp. 28–36; March, 1958.) An analysis of the telemetered cosmic-ray information received in Japan. Except during magnetic-storm conditions the number of cosmic rays decreases exponentially with height. Diurnal and storm variations are discussed.

550.389.2:629.19:523.75 449
Effect of Solar Flares on Earth Satellite 1957β—T. Nonweiler. (*Nature (London)*, vol. 182, pp. 468–469; August 16, 1958.) Fluctuations in the rate of decrease of the period of the satellite are apparently connected with variations in the total intensity of solar flares.

550.389.2:629.19:551.510.535 450
Faraday Fading of Earth-Satellite Signals—F. B. Daniels and S. J. Bauer (*Nature (London)*, vol. 182, p. 599; August 30, 1958.) A correction to the existing method of estimation of the integrated electron content of the ionosphere from earth-satellite signals is given.

551.510.5:621.396.96:621.396.11 451
Incoherent Scattering of Radio Waves by Free Electrons with Applications to Space Exploration by Radar—W. E. Gordon. (PROC. IRE, vol. 46, pp. 1824–1829; November, 1958.) A powerful radar can detect the incoherent backscatter from free electrons in and above the earth's atmosphere, and the received signal is spread in frequency by the Doppler shifts associated with the thermal motion of the electrons. Many practical applications are discussed including measurements of electron density, electron temperature, auroral ionization, and radar echoes from the sun, Venus, and Mars.

551.510.535 452
Main Results of Meteorological Research done in Hungary during the Years 1954–1955—B. Béll. (*Acta Tech. Acad. Sci. hung.*, vol. 18, nos. 1–2, pp. 133–160; 1957.) Work on the ionosphere carried out by the Central Meteorological Institute is referred to.

551.510.535 453

Prevailing Wind in the Ionosphere and Geomagnetic S_q Variations—S. Kato. (*J. Geomag. Geoelect.*, vol. 9, no. 4, pp. 215–217; 1957.) It is shown theoretically that the prevailing ionospheric wind makes no contribution to the geomagnetic S_q current system despite the diurnal variation of ionospheric conductivity. See also 2406 of 1958.

551.510.535 454

A Study of "Spread-*F*" Ionospheric Echoes at Night at Brisbane : Part 4—Range Spreading —H. C. Webster. (*Aust. J. Phys.*, vol. 11, pp. 322–337; September, 1958.) From an examination of the variation of the amount of range spreading produced by sweeping the gain of a fixed-frequency ionospheric recorder, it is possible to gauge the degree of roughness of ionospheric layers. The effective roughness is a function of the separation of transmitter and receiver, being less the greater the distance between them. The intensity of *Z*-ray echoes recorded in Brisbane is consistent with Ellis's theory (2195 of 1956). Part 3: 121 of 1958 (Singleton).

551.510.535:550.385.4:621.396.11 455

On the Short-Wave Transmission Disturbance of 11th February, 1958—Hakura and Takenoshita. (See 573.)

551.594.1+551.594.21 456

Measurement of the Size and Electrification of Droplets in Cumuliform Clouds—B. B. Phillips and G. D. Kinzer. (*J. Met.*, vol. 15, pp. 369–373; August, 1958.) Charge distributions in clouds with fair-weather electric fields, at a mountain site in the United States, were Gaussian with symmetry about zero charge. Thundercloud droplets were highly electrified and in a given volume could be all negatively or all positively charged or a mixture of the two.

551.594.5 457

Auroral Echoes in the Ionograms Obtained in the Minauroral Region—Y. Nakata. (*Rep. Ionosphere Res. Japan*, vol. 12, pp. 1–5; March, 1958.) The observation of auroral echoes on a frequency-sweep ionosonde at Kokabunji in Japan is reported. Echoes were seen on three magnetically disturbed days, on one of which visual aurora was observed in Japan. The echo range corresponds to normal-incidence reflection from scattering centers at *F*-layer heights.

551.594.6 458

Correlation of Whistlers and Lightning Flashes by Direct and Visual Observation— M. G. Morgan. (*Nature (London)*, vol. 182, pp. 332–333; August 2, 1958.) Lightning was observed simultaneously with whistlers at Hanover, New Hampshire, on May 27, 1957, but it is concluded that most lightning flashes do not generate whistlers.

551.594.6 459

Waveforms of Atmospherics—B. A. P. Tantry and R. S. Srivastava. (*Proc. Nat. Inst. Sci. India*, Part A, vol. 24, pp. 217–225; May 26, 1958.) A classification and interpretation of observed waveforms is given. See also 2416 of 1958 (Tantry *et al.*) and for a description of the equipment 3824 of 1958 (Tantry).

LOCATION AND AIDS TO NAVIGATION

621.396.933 460

The Flight Testing of Radio Facilities— M. Cassidy. (*Proc. IRE Aust.*, vol. 19, pp. 253–260; June, 1958.)

621.396.933.1 461

The Tacan Air Navigational System—L. G. Thomas. (*Proc. IRE Aust.*, vol. 19, pp. 247–252; June, 1958.) A general description is given of the main features of the system.

621.396.933.1 462

Air Trials of the Decca Navigator System— H. Keeling. (*J. Inst. Nav.*, vol. 11, pp. 385–395; October, 1958.) A report is given of trials held in 1957 and 1958 to determine the operational suitability of the Mark 10 receiver and to compare its performance with that of the Mark 7.

621.396.933.1 463

The Evaluation and Use of the Dectra Navigation System—E. W. Hare. (*J. Inst. Nav.*, vol. 11, pp. 377–384; October, 1958.) An interim report is given of field trials held by the British government since May, 1957. The system appears to be capable of providing highly accurate position information over the North Atlantic Ocean.

621.396.933.23 464

"No Hands" Blind Landing—(*Wireless World*, vol. 64, p. 579; December, 1958.) An automatic landing device, suitable for aircraft within 300 ft of the ground is described. Rate of fall is controlled by a radio altimeter. Centerline guidance is provided by a system using the magnetic fields generated by two cables running parallel to the runway.

621.396.96:621.396.82 465

Radar Interference and its Reduction— D. B. Brick and J. Galejs. (*Sylvania Technologist*, vol. 11, pp. 96–108; July, 1958.) A survey of methods which can be used for the suppression of RF radar interference.

621.396.969.001.362 466

Marine Radar Simulation—(*Brit. Commun. Electronics*, vol. 5, pp. 508–509; July, 1958.) Block diagrams and brief descriptions are given of a navigation trainer and a radar simulator.

621.396.969.34 467

3-D Tactical Air-Position Radar in H.M.S. *Victorious*—(*Brit. Commun. Electronics*, vol. 5, pp. 510–511; July, 1958.) In addition to notes on special features of the system, an outline is given of a method for displaying information on the face of a crt using combinations of LF waveforms to produce the characters.

MATERIALS AND SUBSIDIARY TECHNIQUES

535.215:[546.482.31+546.482.41 468

Some Photoelectric Properties of CdSe and CdTe Single Crystals—S. V. Svechnikov and V. T. Aleksandrov. (*Zh. Tekh. Fiz.*, vol. 27, pp. 919–920; May, 1957.)

535.215:546.482.31 469

Special Features of the Photoconductive Properties of Cadmium Selenide—S. V. Svechnikov. (*Zh. Eksp. Teor. Fiz.*, vol. 34, pp. 548–554; March, 1958.) A two-stage excitation process is suggested for the explanation of observed anomalies in the photoconductivity of single crystals.

535.215:546.817.23 470

Photoconductivity in Lead Selenide— D. H. Roberts. (*J. Electronics Control*, vol. 5, pp. 256–269; September, 1958.) Results are given of experiments with PbSe in the form of chemically deposited films, solid filaments and evaporated films to study the shape of the spectral response, the importance of potential barriers, the nature of the recombination mechanism, and the role of oxygen in the sensitizing process.

535.243:546.482.21 471

Line Spectra of the Fundamental Absorption Edge of Cadmium Sulphide Crystals— E. F. Gross, B. S. Razbirin, and M. A. Yakobson. (*Zh. Tekh. Fiz.*, vol. 27, pp. 1149–1151; May, 1957.) An investigation of the spectral lines of CdS single crystals at 4.2°K in the range 4853–4889 Å. See also 3493 of 1957.

535.37:546.472.21 472

Notes on the Cathodoluminescence Efficiency of Zinc-Sulphide-Type Phosphors—G. Gergely. (*J. Electronics Control*, vol. 5, pp. 270–272; September, 1958.)

535.37:546.472.21 473

Control of Luminescence by Charge Extraction—P. J. Daniel, R. F. Schwarz, M. E. Lasser, and L. W. Hershinger. (*Phys. Rev.*, vol. 111, pp. 1240–1244; September 1, 1958.) The application of a potential of a few volts to phosphors of the ZnS group can quench fluorescence. This effect is investigated; it is a fundamental property of phosphors with large differences in hole and electron mobilities or capture cross-section. A simple mathematical theory is proposed to account for the observed effects.

535.37:546.482.21 474

Anisotropy of Edge Luminescence in Cadmium Sulphide—D. Dutton. (*J. Phys. Chem. Solids*, vol. 6, pp. 101–102; July, 1958.)

537.226/.228:546.431.824-31 475

The Internal Friction of Barium Titanate Ceramics—T. Ikeda. (*J. Phys. Soc. Japan*, vol. 13, pp. 809–818; August, 1958.) Heat dissipation in BaTiO₃ ceramics used in transducers is attributed to internal friction which is dependent on temperature, biasing field, and vibration, but independent of frequency and porosity. The friction appears to originate as dielectric loss in the individual clamped domain crystals in the presence of piezoelectric coupling.

537.226/.227:546.431.824-31 476

Interpretation of Electron Paramagnetic Resonance in BaTiO₃—A. W. Hornig, R. C. Rempel, and H. E. Weaver. (*Phys. Rev. Lett.*, vol. 1, pp. 284–286; October 15, 1958.) Experimental results differ considerably from those obtained by Low and Shaltiel (3490 of 1958.) It is concluded that the resonance observed is due to an impurity of ferric ions at Ti sites.

537.226/.227:546.431.824-31 477

Electron Paramagnetic Resonance in BaTiO₃—W. Low and D. Shaltiel. (*Phys. Rev. Lett.*, vol. 1, p. 286; October 15, 1958.) Describes further investigations which have revealed a number of points in agreement with those reported by Hornig *et al.* (476 above), and a few in disagreement.

537.226/.227:546.431.824-31 478

Ferroelectric Switching Time of BaTiO₃ Crystals at High Voltages—H. L. Stadler. (*J. Appl. Phys.*, vol. 29, pp. 1485–1487; October, 1958.) Experimental results imply that ferroelectric switching in the voltage range 100–1300 v does not involve the movement of elastic waves from one side of the crystal to the other.

537.226/.227:546.431.824-31 479

Contribution to the Theory of the Ferroelectric Properties of Polarized Barium Titanate Ceramics—L. P. Kholodenko and M. Ya. Shirobokov. (*Zh. Tekh. Fiz.*, vol. 27, pp. 929–935; May, 1957.) The properties are examined for all crystal phases. Tensors for the dielectric constant and the piezoelectric moduli of polarized BaTiO₃ are calculated. See also 1787 of 1957 (Kholodenko).

537.226 480

Relaxation Polarization and Losses in Nonferroelectric Dielectrics Possessing Very High Dielectric Constants—G. I. Skanavi, Ya. M. Ksendzov, V. A. Trigubenko, and V. G. Prokhvatilov. (*Zh. Eksp. Teor. Fiz.*, vol. 33,

pp. 320–334; August, 1957.) See also 801 of 1957 (Nomura).

537.226:546.431.824–31　　　481

Investigation of the Influence of Unilateral Compression on the Dielectric Permittivity of BaTiO₃ Ceramics in Strong Fields—I. A. Izhak. (*Zh. Tekh. Fiz.*, vol. 27, pp. 953–961; May, 1957.) The permittivity decreases in the direction of the compression and increases in directions perpendicular to this. The variation of permittivity with compression also depends on the intensity of the electric field and temperature.

537.226:621.396.67　　　482

Anomalous Dispersion in Artificial Dielectrics—A. F. Wickersham, Jr. (*J. Appl. Phys.*, vol. 29, pp. 1537–1542; November, 1958.) The dependence of dispersion on array and scattering-element geometry has been investigated experimentally using planar arrays of thin metallic rectangles and varying the lengths and planar distribution of the rectangles. An attempt has been made to control dispersion by changing the array configuration. Applications are mentioned.

537.227　　　483

Stability of Ferroelectric Crystals—V. Kh. Kozlovskii. (*Zh. Tekh. Fiz.*, vol. 27, pp. 1395–1397; June, 1957.)

537.227:547.476.3　　　484

Theory of the Ferroelectric Effect in Rochelle Salt—T. Mitsui. (*Phys. Rev.*, vol. 111, pp. 1259–1267; September 1, 1958.) A local-field theory of the clamped crystal is developed. The conditions for spontaneous polarization are investigated and the extent to which the theory can explain the properties of the clamped crystal is discussed.

537.311.1　　　485

Electrical Conduction in Solids—(*Proc. Roy. Soc. A.*, vol. 246, pp. 1–31; July 22, 1958.)

Part 1—Influence of the Passage of Current on the Contact between Solids—F. P. Bowden and J. B. P. Williamson (pp. 1–12).

Part 2—Theory of Temperature-Dependent Conductors—J. A. Greenwood and J. B. P. Williamson (pp. 13–31).

537.311.31+537.311.33　　　486

High-Purity Metals and Semiconductors—N. N. Murach. (*Priroda*, pp. 21–26; December, 1957.)

537.311.31:537.323:539.23　　　487

Influence of Thickness on the Resistivity and Thermoelectric Power of Thin Films of Cobalt—F. Savornin. (*Compt. Rend. Acad. Sci., Paris*, vol. 246, pp. 2866–2869; May 19, 1958.)

537.311.31:539.23　　　488

The Influence of a Layer of Selenium on the Electrical Conductivity of Very Thin Gold Films—S. Minn and H. Damany. (*J. Phys. Radium*, vol. 19, p. 612; June, 1958.) A note on the reduced surface resistivity of a gold film deposited on a thin film of Se. See also 2847 of 1957 (Minn and Offret).

537.311.33　　　489

Present and Future of Semiconductors – A. F. Ioffe. (*Priroda*, pp. 43–48; November, 1957.) A short survey of the development of semiconductors in the last 30 years is given and future applications are outlined.

537.311.33　　　490

Some Problems Concerning the Further Development of the Theory of Semiconductors —A. F. Ioffe. (*Zh. Tekh. Fiz.*, vol. 27, pp. 1153–1160; June, 1957.) An examination of the existing theory of semiconductors shows that re-

vision is needed. Concepts applicable in the electron theory of metals are shown to be less useful in the study of semiconductors.

537.811.33　　　491

Metallic Contacts to Germanium and Silicon—L. W. Davies and D. K. Milne. (*J. Sci. Instr.*, vol. 35, p. 423; November, 1958.) Details are given of the preparation of contacts which have high mechanical strength, good electrical properties, and a readily controllable shape.

537.311.33　　　492

Effects of Electron-Electron Scattering on the Electrical Properties of Semiconductors—R. W. Keyes. (*J. Phys. Chem. Solids*, vol. 6, pp. 1–5; July, 1958.) The effects of electron-electron scattering, usually neglected in semiconductor theory, are investigated by solving the Boltzmann equation modified by the addition of an extra term. Results are given for the spherical and Ge band structures. In the latter case some effects are produced which are similar to those observed in the impurity-scattering region.

537.311.33　　　493

Generation-Recombination Noise in a Two-Level Impurity Semiconductor—S. Teitler. (*J. Appl. Phys.*, vol. 29, pp. 1585–1587; November, 1958.) "A general expression for the generation-recombination noise in a two-level impurity semiconductor is derived. Application is then made to zinc-doped germanium in the dark from 20°K to 100°K. The total white noise in this case exhibits a maximum and a minimum as the temperature is increased and the contributions to the noise which can be associated with the individual levels vary."

537.311.33　　　494

Investigation of the Temperature Dependence of the Work Function of Some Semiconductors—G. N. Lekhtinen, M. A. Rzaev and L. S. Stil'bans (*Zh. Tekh. Fiz.*, vol. 27, pp. 1221–1228; June, 1957.) Measurements on PbS, PbSe and PbTe show that at 150°C the work function varies differently for *n*-type and *p*-type semiconductors.

537.311.33　　　495

The Role of Surface Properties of Semiconductors in Adhesion Phenomena—V. P. Smilga and B. V. Deryagin. (*Dokl. Ak. Nauk S.S.S.F.*, vol. 122, pp. 1049–1052; October 21, 1958.) Investigation of the development of adhesive forces in a metal-semiconductor contact on application of very-high-voltage electric fields.

537.311.33　　　496

Dependence of Emission Capacity of a *p-n* Junction upon its Structure and Condition of Operation—K. B. Tolpygo. (*Zh. Tekh. Fiz.*, vol. 27, pp. 884–898; May, 1957.) Barrier-layer phenomena controlling the injection efficiency of a *p-n* junction are discussed and the influence of acceptors on the lifetime of minority carriers is considered. See also 472 of 1957.

537.311.33:061.3(493)　　　497

1958 Brussels Semiconductor Convention—(*Brit. Commun. Electronics*, vol. 5, pp. 612–614; August, 1958.) A brief report is given of some of the papers read at the "International Congress on Solid-State Physics and their Applications to Electronics and Telecommunications."

537.311.33:535.215　　　498

A Note on Surface Recombination Velocity and Photoconductive Decays—A. C. Sim. (*J. Electronics Control*, vol. 5, pp. 251–255; September, 1958.) The range of validity of correction formulae generally applied in photoconductive decay experiments for the measurement of the

lifetime of excess carriers in semiconductors is shown to be restricted and a further correction is offered for the remaining range.

537.311.33:538.21　　　499

Magnetic Susceptibility of Semiconductors with an Impurity Zone in a Strong Magnetic Field—M. I. Klinger. (*Zh. Eksp. Teor. Fiz.*, vol. 33, pp. 379–386; August, 1957.) See also 2803 of 1957 (Klinger *et al.*).

537.311.33:538.63　　　500

Method of Determination of Surface Recombination Velocity by Changing the Resistance of Semiconductors in a Magnetic Field—V. P. Zhuze, G. E. Pikus, and O. V. Sorokin. (*Zh. Tekh. Fiz.*, vol. 27, pp. 1167–1173; June, 1957.) A description of a new experimental procedure: results are in good agreement with theory.

537.311.33:538.63　　　501

Theory of the Effect of a Magnetic Field on the Absorption Edge in Semiconductors—R. J. Elliott, T. P. McLean, and G. G. Macfarlane. (*Proc. Phys. Soc.*, vol. 72, pp. 553–565; October 1, 1958.) The electron energy bands in a solid can be split into sub-bands with a magnetic field. The absorption edge which arises from transitions between these bands shows a fine structure due to sub-band transitions. The shape of the transition structure is evaluated for spherical, spheroidal, and degenerate bands. Often a series of peaks is formed from which the effective masses of the bands may be determined.

537.311.33:538.632　　　502

Hall and Holes—(*Wireless World*, vol. 64, pp. 601–605; December, 1958.) A simple explanation of the Hall effect and its applications is given.

537.311.33.538.632:621.317.3　　　503

Equipment for Hall-Effect Measurements in Semiconductors—V. N. Bogomolov and V. A. Myasnikov. (*Zh. Tekh. Fiz.*, vol. 27, pp. 1209–1214; June, 1957.) The equipment is particularly suitable for measurements on materials having low carrier mobility and having either very small or very large conductivity.

537.311.33:546.26–1　　　504

Rectification, Photoconductivity, and Photovoltaic Effect in Semiconducting Diamond—M. D. Bell and W. J. Leivo. (*Phys. Rev.*, vol. 111, pp. 1227–1231; September 1, 1958.) The potential barrier formed between a metal point and *p*-type semiconducting diamond is due to the establishment of equilibrium between charges in surface and interior states. The semiconducting diamonds are photoconducting in the ultraviolet and visible regions.

537.311.33:[546.28+546.289　　　505

Surface Mobility in Germanium and Silicon—M. F. Millea and T. C. Hall. (*Phys. Rev. Lett.*, vol. 1, pp. 276–278; October 15, 1958.) Experimental field effect data are presented suggesting that complete diffused surface scattering is incorrect, better agreement between experiment and theory being obtained by assuming partially diffused surface scattering.

537.311.33:[546.28+546.289　　　506

Optical Properties of Semiconductors under Hydrostatic Pressure—W. Paul and D. M. Warschauer. (*J. Phys. Chem. Solids*, vol. 5, no. 1–2, pp. 89–106, 1958; vol. 6, pp. 6–15, July, 1958.)

　　　Part 1—Germanium (pp. 89–101.)

　　　Part 2—Silicon (pp. 102–106.)

　　　Part 3—Germanium-Silicon Alloys (pp. 6–15.)

537.311.33:[546.28+546.289　　　507

Observation by Cyclotron Resonance of the

Effect of Strain on Germanium and Silicon—A. C. Rose-Innes. (*Proc. Phys. Soc.*, vol. 72, pp. 514–522; October 1, 1958.) Effects in microwave cyclotron resonance spectra at low temperatures are used to observe changes in the band structure of Ge and Si caused by non-isotropic elastic strain. Results are consistent with conclusions derived from piezo-resistance measurements.

537.311.33:546.28   508
Valence-Band Structure of Silicon—L. Huldt and T. Staflin. (*Phys. Rev. Lett.*, vol. 1, pp. 313–315; November 1, 1958.) Using the technique of photogeneration of free carriers, an absorption spectrum, probably arising from theoretically predicted valence interband transitions, has been excited and observed in Si. See also 176 of January.

537.311.33:546.28   509
Fine Structure in the Absorption-Edge Spectrum of Si—G. G. Macfarlane, T. P. McLean, J. E. Quarrington, and V. Roberts. (*Phys. Rev.*, vol. 111, pp. 1245–1254; September 1, 1958.) Measurements of the absorption spectrum of Si, made with high resolution near the main absorption edge at various temperatures between 4.2°K and 415°K, have revealed fine structure in the absorption on the long-wavelength side of this edge. This structure is analyzed in detail and interpreted in terms of indirect transitions. See also 1463 of 1958.

537.311.33:546.28   510
The Temperature Variation of the Concentration of Impurity Carriers in Silicon—E. H. Putley. (*Proc. Phys. Soc.*, vol. 72, pp. 917–920; November 1, 1958.) Discussion of this variation is frequently based on an expression which includes simplifying assumptions. A more general expression, which takes excited states of the impurity center into account, is derived. It is shown that the results of analyses of carrier concentration data based on the simplified expression may be considerably modified when detailed knowledge of the various impurity centers becomes available.

537.311.33:546.28   511
Oxygen Impurity in Silicon Single Crystals—A. Smakula and J. Kalnajs. (*J. Phys. Chem. Solids*, vol. 6, pp. 46–50; July, 1958.)

537.311.33:546.28   512
Electron Spin-Lattice Relaxation in Phosphorus-Doped Silicon—H. Honig and E. Stupp. (*Phys. Rev. Lett.*, vol. 1, pp. 275–276; October 15, 1958.) The dependence of relaxation probability on magnetic field has been obtained under conditions of at least partial elimination of background photon flux, thereby isolating one of the phonon mechanisms involved in the relaxation process.

537.311.33:546.28   513
Diffusion of Gallium in Silicon—A. D. Kurtz and C. L. Gravel. (*J. Appl. Phys.*, vol. 29, pp. 1456–1459; October, 1958.) An open-tube vapor-solid diffusion technique at atmospheric pressure and temperatures between 1130°C and 1358°C gave lower diffusivities and a higher activation energy than have been previously reported [3095 of 1956 (Fuller and Ditzenberger)]. Differences are discussed.

537.311.33:546.28   514
On the Delineation of *p-n* Junctions in Silicon—P. A. Iles and P. J. Coppen. (*J. Appl. Phys.*, vol. 29, p. 1514; October, 1958.)

537.311.33:546.28:535.215   515
Phase-Shift Method of Carrier Lifetime Measurements in Semiconductors—E. Harnik, A. Many, and N. B. Grover. (*Rev. Sci. Instr.*, vol. 29, pp. 889–891; October, 1958.) The phase difference between a sinusoidal modulation of carrier injection and the resulting modulation of the semiconductor conductance is measured by an *RC* compensating network. The conditions for direct proportionality between the phase difference and the effective lifetime are discussed. See also 3908 of 1957 (van der Pauw).

537.311.33:546.289   516
Recombination Centres in Germanium—J. Okada. (*J. Phys. Soc. Japan*, vol. 13, pp. 793–800; August, 1958.) The dependence of carrier lifetime in pure Ge upon injection level has been studied using a photoconductivity decay method. The results show that at least two recombination levels exist in pure Ge; one is active in *n*-type and the other in *p*-type Ge.

537.311.33:546.289   517
The Vibrational Spectrum and Specific Heat of Germanium—F. A. Johnson and J. M. Lock. (*Proc. Phys. Soc.*, vol. 72, pp. 914–917; November 1, 1958.)

537.311.33:546.289   518
Experimental Determination of Electron Temperature in High Electric Fields Applied to Germanium—E. G. S. Paige. (*Proc. Phys. Soc.*, vol. 72, pp. 921–923; November 1, 1958.) By observing the field dependence of drift velocity for an *n*-type Ge specimen in a strained and unstrained state, the electron temperature T_e can be deduced. For fields in the range 100–2000 volts per cm, values of T_e between 150° and 700°K were obtained with experimental errors not exceeding ±20 cent.

537.311.33:546.289   519
Resistivities and Hole Mobilities in Very Heavily Doped Germanium—F. A. Trumbore and A. A. Tartaglia. (*J. Appl. Phys.*, vol. 29, p. 1511; October, 1958.) Results are given of resistivity and Hall-effect measurements at 300°K on crystals of Ge containing up to 5×10^{20} acceptor atoms cm³.

537.311.33:546.289   520
Diffusion and Electric State of Thermal Acceptors in Germanium—V. A. Zhidkov and V. E. Lashkarev. (*Zh. Tekh. Fiz.*, vol. 27, pp. 877–883; May, 1957.) The temperature dependence of the diffusion coefficient of thermal acceptors is derived. See also 2796 of 1957.

537.311.33:546.289   521
Enhanced Cu Concentration in Ge containing Ni at 500°C—A. G. Tweet and W. W. Tyler. (*J. Appl. Phys.*, vol. 29, pp. 1578–1580; November, 1958.)

537.311.33:546.289   522
Evidence of Vacancy Clusters in Dislocation-Free Ge—A. G. Tweet. (*J. Appl. Phys.*, vol. 29, pp. 1520–1522; November, 1958.) Evidence of the existence of vacancy aggregates in Ge crystals is reported. The crystal etches much more rapidly when dislocations are absent over volumes of the order of cubic centimeters; this enhanced etching behavior is eliminated by appropriate heat treatment.

537.311.33:546.289:535.376   523
Radiative Surface Effect in Germanium—J. I. Pankove. (*J. Phys. Chem. Solids*, vol. 6, pp. 100–101; July, 1958.) Radiation from the surface of a Ge crystal, into which holes were injected, was observed over a wide band with a peak at about 4.6 μ. It is attributed to an interband transition, involving the excitation of light holes in the strong electric field of the surface inversion layer.

537.311.33:546.289:537.32   524
Measurements of the Bulk Thermo-e.m.f. in Germanium—P. I. Baranskiĭ and V. E. Lashkarev. (*Zh. Tekh. Fiz.*, vol. 27, pp. 1161–1166; June, 1957.) An improved method of measuring the thermo-EMF in *n*- and *p*-type Ge is described. Results obtained on polished or etched specimens are tabulated.

537.311.33:546.289:538.615   525
Zeeman Splitting of Donor States in Germanium—R. R. Haering. (*Can. J. Phys.*, vol. 36, pp. 1161–1167; September, 1958.) The linear Zeeman effect of the $2pm=\pm1$ states of donor impurities is calculated using the approximation of effective mass theory of impurity states.

537.311.33:546.289:538.63   526
Resistivity and Hall Coefficient of Antimony-Doped Germanium at Low Temperatures—H. Fritzsche. (*J. Phys. Chem. Solids*, vol. 6, pp. 69–80; July, 1958.) The Hall coefficient *R* and resistivity ρ of Ge single crystals containing between 5×10^{14} and 10^{18} Sb atoms per cm³ were re-investigated at temperatures *T* between 1.3 and 300°K. The low-temperature anomalies—a steep maximum in the log *R* versus $1/T$ curves and a change of slope of the log ρ versus $1/T$ curves—are discussed on the basis of impurity conduction.

537.311.33:546.289:541.135   527
Germanium Electrode with a *p-n* Junction—E. A. Efimov and I. G. Erusalimchik. (*Dokl. Ak. Nauk S.S.S.R.*, vol. 122, pp. 632–634; October 1, 1958.) A report of measurements made in a 0.1 N solution of HCl using an electrode of *n*-type Ge 250 μ thick containing a *p-n* junction formed by diffusion of In.

537.311.33:546.3–1'289'28   528
Thermal Conductivity and Thermoelectric Power of Germanium-Silicon Alloys—M. C. Steele and F. D. Rosi. (*J. Appl. Phys.*, vol. 29, pp. 1517–1520; November, 1958.) Measurements on a series of alloys are reported and show that solid-solution alloying in the carrier concentration range where the carrier mobility is limited by impurity scattering, can significantly increase the figure of merit of thermoelectric materials.

537.311.33:546.681.19   529
Electron Mobilities in Gallium Arsenide—L. R. Weisberg, J. R. Woolston, and M. Glicksman. (*J. Appl. Phys.*, vol. 29, pp. 1514–1515; October, 1958.)

537.311.33:546.682.86   530
Electrical Conductivity in *n*-Type InSb under Strong Electric Field—Y. Kanai. (*J. Phys. Soc. Japan*, vol. 13, pp. 967–968; August, 1958.) Conductivity was measured for fields sufficient to give deviations from Ohm's law. The deviation occurred at 2×10^2 volt per cm and is considered to be caused by carrier ionization processes from the filled band.

537.311.33:546.873.241   531
Chemical Bonding in Bismuth Telluride—J. R. Drabble and C. H. L. Goodman. (*J. Phys. Chem. Solids*, vol. 5, pp. 142–144; 1958.) The model proposed for Bi_2Te_3 disposes of some earlier difficulties; it explains some of the properties of Bi_2Te_3 and its alloys with Bi_2Se_3.

537.311.33:546.873.241   532
The Electrical Properties of Bismuth Telluride—R. Mansfield and W. Williams (*Proc. Phys. Soc.*, vol. 72, pp. 733–741; November 1, 1958.) Measurements were made of the electrical conductivity, Hall coefficient, thermoelectric power, and Nernst coefficient on specimens cut from zone-melted Bi_2Te_3 and on a single crystal. The temperature range was 100°–600°K and specimens with a wide range of impurity content were examined.

537.311.33:546.873.241   533
The Optical Properties of Bismuth Telluride—I. G. Austin. (*Proc. Phys. Soc.*, vol. 72, pp.

545–552; October 1, 1958.) The shape of the absorption edge is studied and is of the form expected for indirect transitions. The energy gap is found to be ~0.13 ev at room temperature and the refractive index, determined from interference fringes, is 9.2 at 8–14 μ.

537.311.33:621.314.63 534
Reverse Breakdown in In-Ge Alloy Junctions—D. R. Muss and R. F. Greene. (*J. Appl. Phys.*, vol. 29, pp. 1534–1537; November, 1958.) Experiments show that in abrupt In-Ge alloy p^+n junctions breakdown occurs by the Zener mechanism in narrow junctions, by avalanche in broad junctions, and that both effects occur in intermediate width junctions.

538.221 535
Instability of Bloch Walls due to Interstitial Atoms in a Ferromagnetic Material with Body-Centered Cubic Structure—G. Biorci, A. Ferro, G. Montalenti. (*R.C. Accad. naz. Lincei*, vol. 24, pp. 542–547; May, 1958.)

538.221 536
The Fluctuating-Field Ferromagnet at Low Temperatures—F. D. Stacey. (*Aust. J. Phys.*, vol. 11, pp. 310–317; September, 1958.) The theoretical and experimental values of the constant in the $T^{3/2}$ law for Ni agree if an ordered state is produced by the mutual attraction of parallel elementary magnets each consisting of a coupled pair of spins.

538.221 537
The Antiferromagnetic Orientation of Magnetic Moments in the Alloy Ni_3Fe—M. V. Dekhtyar. (*Zh. Eksp. Teor. Fiz.*, vol. 34, pp. 772–773; March, 1958.) A description of measurements in the temperature range 0–600°C.

538.221:538.569.4 538
On the Thermodynamical Theory of Resonance and Relaxation Phenonena in Ferromagnetics—G. V. Skrotskii and V. T. Shmatov. (*Zh. Eksp. Teor. Fiz.*, vol. 34, pp. 740–745; March, 1958.) The role of spin-lattice relaxation in the ferromagnetic resonance phenomenon is discussed. The equations obtained are compared with the Landau-Lifshitz and Bloch equations.

538.221:539.23:53.087.63 539
Magnetic Writing with an Electron Beam—L. Mayer. (*J. Appl. Phys.*, vol. 29, pp. 1454–1456; October, 1958.) Curie-point writing (*Ibid.*, vol. 29, p. 1003; June, 1958) permits local reversal of the direction of magnetization in suitable premagnetized magnetic films by using the dissipation energy of a focused electron beam to elevate the temperature temporarily above the Curie point. Well-defined traces of reversed magnetization which can be erased magnetically were recorded on MnBi films. Writing speeds corresponding to 3×10^4 bits per s and information densities corresponding to 10^5 bits per cm² were achieved. Electronic read-out of magnetically stored information is possible. See also 845 of 1958 (Williams *et al.*).

538.221:621.318.124 540
Cation Substitutions in $BaFe_{12}O_{19}$—A. H. Mones and E. Banks. (*J. Phys. Chem. Solids*, vol. 4, pp. 217–222; 1958.) An experimental study of the variation in magnetic intensity of $BaFe_{12}O_{19}$ as a function of the substitution of ions such as Al^{III}, Ga^{III} Cr^{III}, and Zn^{II} for Fe^{III}.

538.221:621.318.124 541
Investigation of the Substitution of Fe by A, Ga and Cr in Barium Hexaferrite, $BaO.6 Fe_2O_3$—F. Bertaut, A. Deschamps, and R. Pauthenet. (*Compt. Rend. Acad. Sci.*, Paris, vol. 246, pp. 2594–2597; May 5, 1958.)

538.221:621.318.134 542
Magnetic Properties of $TiFe_2O_4$–Fe_3O_4 System and their Change with Oxidation—S. Akimoto, T. Katsura, and M. Yoshida. (*J. Geomag. Geoelect.*, vol. 9, no. 4, pp. 165–178; 1957.)

538.221:621.318.134 543
Ferrimagnetic Resonance in $NiMnO_3$—H. S. Jarrett and R. K. Waring. (*Phys. Rev.*, vol. 111, pp. 1223–1226; September 1, 1958.) Ferrimagnetic resonance shows that the magnetic anisotropy is axial, and the easy direction of magnetization lies in the basal plane. The magnetic anisotropy field equals 5.2×10^4 G, corresponding to an anisotropy energy of 2.6×10^6 ergs per cm³.

538.221:621.318.134 544
Grain Growth in Nickel Ferrites—P. Levesque, L. Gerlach, and J. E. Zneimer. (*J. Amer. Ceram. Soc.*, vol. 41, pp. 300–303; August 1, 1958.)

538.221:621.318.134:621.372.413 545
Resonant-Cavity Methods of Measuring Ferrite Properties—R. A. Waldron. (*Brit. J. Appl. Phys.*, vol. 9, pp. 439–442; November, 1958.) Formulae are given for the frequency shift on introducing a ferrite into a resonant cavity. Various sample shapes and positions are considered; it is concluded that a spherical shape is best, particularly because dielectric constant and permeability can be measured on it without change of sample, cavity, or mode. See also 2658 of 1956.

538.23:538.221 546
Coupling between Elementary Ferromagnetic Domains: Seesaw Effect—L. Néel. (*Compt. Rend. Acad. Sci.*, Paris, vol. 246, pp. 2963–2968; May 28, 1958.) Coupling between elementary domains, other than interacting ferromagnetic grains (203 of January) is considered, and it is shown that while the discrepancy between successive hysteresis cycles rapidly diminishes, it does not necessarily vanish after the first alternation.

538.23:538.221 547
Creep of Asymmetric Hysteresis Cycles as a Function of the Amplitude of Asymmetry—Nguyen Van Dang. (*Compt. Rend. Acad. Sci.*, Paris, vol. 246, pp. 3034–3037; May 28, 1958.) The experiments described earlier (204 of January) were continued for fixed n. Maximum creep was found for cycles in which the maximum value of the field was about 1.1 times the coercive field.

MATHEMATICS

517.41:621.372 548
Functional Characteristics of a Node Determinant—R. E. Bonner, L. H. Kosowsky, and P. F. Ordung. (*J. Franklin Inst.*, vol. 265, pp. 395–406; May, 1958.) A modification of the Laplace expansion is developed for use in network analysis, which removes initially all the negative terms.

517.7 549
The Numerical Evaluation of Expressions involving Complete Elliptic Integrals—F. W. Grover. (*Commun. and Electronics*, pp. 496–502; September, 1958.)

MEASUREMENTS AND TEST-GEAR

621.3.018.41(083.74):529.786 550
Primary Frequency Standard using Resonant Caesium—W. A. Mainberger. (*Electronics*, vol. 31, pp. 80–85; November 7, 1958.) Description of the "atomichron" equipment. See also 212 of January (Essen *et al.*).

621.317.088.6 551
A Method of Correcting for the Response Time Delays of Measuring Equipment—J. A. Sirs. (*J. Sci. Instr.*, vol. 35, pp. 419–422; November, 1958.) The error due to the delay is obtained by considering the output response to a unit step input impulse and applying Laplace transform analysis. Correction formulae are derived and their application illustrated.

621.317.2:621.373.42 552
Low-Frequency Sine-Wave Generators—(*Electronic Radio Engr.*, vol. 35, pp. 459–467; December, 1958.) A review of modern commercial-type lF oscillators with details of some of their circuitry.

621.317.3:621.316.722.078.3 553
Rapid Testing of Electronic Direct-Voltage Stabilizers—Perrier and d'Ast. (See 608.)

621.317.33 554
A Novel, High-Accuracy Circuit for the Measurement of Impedance in the A.F., R.F. and V.H.F. Ranges—D. Karo. (*Proc. IEE*, Part B, vol. 105, pp. 505–510; November, 1958.) The circuit consists of two branches, one of which contains the unknown impedance. These branches are fed in phase opposition from the secondaries of two mutual inductors or two transformers. Between 100 c and 50 mc the error limit varies, according to experimental conditions, from ±0.001 per cent to ±0.01 per cent.

621.317.332:539.23 555
Measurement of Very Slight Variations of Resistance. Applications to the Magnetoresistance of Thin Films—A. Colombani, P. Huet, and C. Vautier. (*Compt. Rend. Acad. Sci.*, Paris, vol. 246, pp. 2869–2872; May 19, 1958.) Description of a differential method of measurement with sensitivity $\Delta R/R$ of 10^{-6}, in which a compensating LF voltage of opposite phase is derived by means of a resistance in series with the sample.

621.317.382:538.632:537.311.33 556
Use of the Hall Effect in Semiconductors for Electric Power Measurements—L. S. Berman. (*Zh. Tekh. Fiz.*, vol. 27, pp. 1192–1196; June, 1957.) Two circuits for power measurements in the frequency range 400–500 kc have been investigated: one using n-type Ge and the other InSb. Results show that performance is linear and independent of frequency.

621.317.39 557
The Differential Transformer as a Sensitive Measuring Device—J. H. Heath. (*Electronic Eng.*, vol. 30, pp. 630–633; November, 1958.) A differential transducer is used as a sensing head with the two secondary windings connected in series addition. The linear range may be subdivided into a series of sensitive sections.

621.317.616:621.373.4 558
Broad-Band Generator has Wide and Narrow Sweeps—C. C. Cooley, Jr. (*Electronics*, vol. 31, pp. 88–91; November 7, 1958.) The frequency-sweep generator described covers sweep widths from 100 kc to 300 mc in the center-frequency range 200 kc–1000 mc.

621.317.7:621.387:621.396.822.029.63 559
Application of Gas-Discharge Tubes as Noise Sources in the 1700–2300-mc Band—M. Kollanyi. (*J. Brit. IRE*, vol. 18, pp. 541–548; September, 1958.) The design considerations and the performance of a gas-discharge helix-coupled noise source are given. Noise-figure measurements can be made with an accuracy of 0.2 db.

621.317.725.027.3 560
Compensation Electron-Beam High-Voltage Voltmeter—G. I. Shal'nikov. (*Zh. Tekh.*

Fiz., vol. 27, pp. 1371–1378; June, 1957.) A new instrument for the accurate measurement of direct voltages up to 3,0000 and theoretically applicable to alternating voltages at frequencies up to 5 mc and also to short pulses.

621.317.733 561
A Precision, Guarded Resistance Measuring Facility—F. H. Wyeth, J. B. Higley, and W. H. Shirk, Jr. (*Commun. and Electronics*, pp. 471–475; September, 1958. Discussion, pp. 475–476.)

621.317.737 562
A Simple 3-cm *Q*-Meter—A. E. Barrington and J. R. Rees. (*Proc. IEE*, Part B, vol. 105, pp. 511–512; November, 1958.) A simple reflectometer method for measuring *Q*-factors up to about 4000, with an error limit of approximately 10 per cent.

621.317.763.029.6:535.417 563
The Optical Approach in Microwave Measurement Technique—J. I. Caicoya. (*Brit. Commun. Electronics*, vol. 5, pp. 500–507; July, 1958.) A survey is made of interferometer and grating-spectrometer techniques which can be applied to microwave measurements.

621.317.794.029.6:621.316.825 564
Experimental Wide-Band Thermistor Mounts—J. Swift. (*Proc. IRE, Aust.*, vol. 19, pp. 261–264; June, 1958.) Several simple mounts are described which consist of a coaxial line terminated by two thermistors placed across an untuned cavity. One type covers the band 450–5000 mc with a maximum voltage SWR of 1.3.

OTHER APPLICATIONS OF RADIO AND ELECTRONICS

531.787:621.372.413 565
Microwave Manometer—A. G. Kramer and P. M. Platzman. (*Rev. Sci. Instr.*, vol. 29, pp. 897–898; October, 1958.) A differential pressure indicator using a cavity resonator at 8650 mc is described. The sensitivity was 2.4 mc per mm Hg pressure difference.

535.376:621.397.62 566
Problems in Electroluminescent Television Display—R. M. Bowie. (*Sylvania Technologist*, vol. 11, pp. 82–85; July, 1958.) Technical and economic problems which have to be overcome before an electroluminescent device can compete with a crt are outlined with particular reference to the Sylvatron [see 244 of January (Butler and Koury)].

621.385.833 567
Image of a Surface obtained with Negative Ions—R. Bernard and R. Goutte. (*Compt. Rend. Acad. Sci., Paris*, vol. 246, pp. 2597–2599; May 5, 1958.)

654.171:535.376 568
Transfluxor-Controlled Electroluminescent Display Panels—J. A. Rajchman, G. R. Briggs, and A. W. Lo. (*Proc. IRE*, vol. 46, pp. 1808–1824; November, 1958.) A detailed description of a display system using electroluminescence magnetically controlled by an electrical input signal. The 1200 elements of the array are arranged in 30 rows and are each associated with a transfluxor [3509 of 1955 (Rajchman and Lo)]. Advantages and disadvantages of the system are discussed.

PROPAGATION OF WAVES

621.396.11:551.510.5:621.396.96 569
Incoherent Scattering of Radio Waves by Free Electrons with Applications to Space Exploration by Radar—Gordon (See 451.)

621.396.11:551.510.52 570
Some Generalized Scattering Relationships in Transhorizon Propagation—A. T. Waterman, Jr. (*Proc. IRE*, vol. 46, pp. 1842–1848; November, 1958.) A discussion of the consequences which follow from the assumption that the physical mechanism is a single-scattering process distributed systematically throughout the atmosphere. Expressions are derived for the variation of received power with distance, for various scattering angles and beam widths.

621.396.11:551.510.52 571
Geometric Characteristics of the Scattering of Radio Waves at Turbulent Inhomogeneities of the Troposphere—D. M. Vysokovskiĭ. (*Elektrosvyaz*, pp. 12–39; September, 1957.) Exact and approximate formulae are derived for determining the dimensions of the scattering region and the angle of scattering. An expression for the scattered power is given in the form of an integral over the scattering region. On the basis of an investigation of the extremum of this integral, the dimensions of the effective scattering region are determined for the case of wide polar diagrams, and the choice of aerials for communication based on scatter propagation is discussed. The main geometric characteristics of the scattering region are given for the case of narrow polar diagrams.

621.396.11:551.510.535 572
The Magnetoionic Theory and its Results—D. Lépéchinsky. (*Ann. Télécommun.*, vol. 12, pp. 60–70 and 74–91; February and March, 1957.) A practical method of calculating propagation parameters is derived from the general Appleton-Hartree equation. Propagation in the Q.L., Q.T., and limiting Q.L.-Q.T. regions is examined, and applications of the method are considered.

621.396.11:551.510.535:550.385.4 573
On the Short-Wave Transmission Disturbance of 11th February, 1958—Y. Hakura and Y. Takenoshita. (*Rep. Ionosphere Res. Japan*, vol. 12, pp. 10–15; March, 1958.) Reports observations in Japan of signal strength and fading rates on three HF circuits during an ionospheric storm. Flutter-fading began on a transpolar route at the time of the sudden commencement, and moved south to the lower-latitude paths during the course of the storm. High night-time field strengths and fading rates were observed at a time when auroral echoes were detected by ionospheric soundings.

621.396.11.029.6 574
Sporadic-*E* Skip on 200 Mc/s?—R. B. Cooper, Jr. (*QST*, vol. 42, pp. 33–35, 162; November, 1958.) A summary is given of reports of long-range reception of television signals on frequencies between 60 and 204 mc.

621.396.11.029.62 575
Role of Turbulent Scattering in Long-Distance Radio Propagation at Metre Wavelengths—F. A. Kitchen and M. A. Johnson. (*Nature (London)*, vol. 182, pp. 302–304; August 2, 1958.) Field-strength measurements were made in November and December, 1957, of propagation at 203.5 mc over sea in the English Channel area for distances up to 350 miles. Results support the theory that turbulence and scattering are almost always present at all levels in the troposphere.

621.396.11.029.62:523.5 576
The Forward-Scattered Radio Signal from an Overdense Meteor Trail—P. A. Forsyth. (*Can. J. Phys.*, vol. 36, pp. 1112–1124; August, 1958.) A recently presented expression [883 of 1958 (Hines and Forsyth)] for the forward-scattered signal from an overdense meteor trail was tested in a particular observed meteor trail. The electron line density is calculated by three different methods, two of which are based

on the new expression. The resulting agreement is within the experimental error.

621.396.11.029.62:621.397.81 577
More on the "Plymouth Effect"—J. P. Grant. (*Wireless World*, vol. 64, pp. 587–590; December, 1958.) Back-scatter from the sea and reflection from aerial arrays on Guernsey are suggested as possible causes of anomalous television reception at Plymouth of the BBC Devon television transmitter. See also 3612 of 1958 (Sofaer).

621.396.11.029.64 578
Influence of the Semi-permanent Low-Level Ocean Duct on Centimetre-Wave Scatter Propagation Beyond the Horizon—F. A. Kitchen, W. R. R. Joy, and E. G. Richards. (*Nature (London)*, vol. 182, pp. 385–386; August 9, 1958.) Experiments made over sea in the English Channel area in 1957 and 1958 for various heights of transmitter and receiver show that when the site of the receiving aerial is relatively high, *e.g.*, 400 ft, the surface-guided component of the signal beyond the horizon is not directly observable

621.396.11.029.64 579
Statistical Data for Microwave Propagation Measurements on Two Oversea Paths in Denmark—P. Gudmandsen and B. F. Larsen. (*Acta Polytech. Stockholm*, No. 213, 37 pp.) Measurements were made using vertically spaced antennas for wavelengths of 17 and 6.4 cm, over two E-W paths of lengths 54 km and 82 km. Fading conditions have been studied using diversity systems and single receivers.

RECEPTION

621.376.232.2 580
Design of Detector Stages for Signals with Symmetrical or Asymmetrical Sidebands—A. van Weel. (*J. Brit. IRE*, vol. 18, pp. 525–538; September, 1958.) See also 249 of January.

621.376.33:621.396.82 581
Alternative Detection of Co-channel F.M. Signals—H. W. Farris. (*Proc. IRE*, vol. 46, pp. 1876–1877; November, 1958.) A weaker signal can be separated by correlating the sum of weaker and stronger signals with the stronger signal at the IF of the receiver.

621.396.62.029.62 582
Further Notes on the ARR 3 Sonobuoy Receiver—(*Wireless World*, vol. 64, pp. 590; December, 1958.) Additional precautions against the possibility of radiation at television channel-1 frequencies. See also 254 of January (Taylor).

621.396.81 583
Simultaneous Variation of Amplitude and Phase of Gaussian Noise, with Applications to Ionospheric Forward-Scatter Signals—T. Hagfors and B. Landmark. (*Proc. IEE*, Part B, No. 1958, vol. 105, No. 24, pp. 555–559.) The scatter signal is shown to possess amplitude and phase characteristics similar to those of Gaussian noise. Spaced-aerial observations indicate that the angular spectrum of received waves is randomly phased.

621.396.81:621.396.65 584
The Analysis of Field Strength Records for Radio Link Assessment—M. W. Gough. (*Point to Point Telecommun.*, vol. 2, pp. 28–47; June, 1958.) Recording and analytical techniques are outlined and propagation effects represented in chart form are discussed.

621.396.812.3 585
Fading of Radio Waves—P. Venkateswarlu and R. Satyanarayana. (*Current Sci.*, vol. 27, p. 296; August, 1958.) Theoretical amplitude dis-

tribution curves for medium frequencies agree closely with experimental curves for distances of 110 and 320 km but not for 1700 km, where the experimental curve shows two maxima.

621.396.812.3.029.6:621.396.65   **586**
On the Fading of Ultra Short Waves in Radio Links—V. N. Troitskii. (*Elektrosvyaz*, pp. 32–39; October, 1957.) An analysis is given of the possible types of fading in radio links. The use of an effective gradient of permittivity in calculations of field intensity is discussed and experimental values for central USSR are given. The effect of horizontal inhomogeneities is considered in an appendix.

STATIONS AND COMMUNICATIONS SYSTEMS

621.376.2   **587**
Single-Sideband Modulation—B. Rassadin. (*Radio, Mosk.*, pp. 25–27; June, 1958.) Description of a system operating in the range 7.0–7.1 mc.

621.376.2   **588**
Phase-Compensation Methods of Shaping a Single-Sideband Signal—A. Semenov and V. Verzunov. (*Radio, Mosk.*, pp. 27–29; June, 1958.)

621.376.2:621.396.41   **589**
Suppression of the Unwanted Sideband in Single-Band Multiphase Radio Systems—I. V. Lobanov. (*Elektrosvyaz*, pp. 3–11; September, 1957.) Formulae are derived for determining the degree of suppression of the sideband in three- and four-phase systems, depending on the magnitude of amplitude and phase errors of voltages feeding the system. From these formulae, graphs are plotted showing the possibility of realizing these systems under various specific conditions.

621.376.23:621.396.41   **590**
Step Detection—A. R. Billings. (*Electronic Radio Engr.*, vol. 35, pp. 453–455; December, 1958.) The attenuation distortion produced by step detection is small, and this method when applied to time-division multiplex systems considerably reduces adjacent-channel crosstalk.

621.391   **591**
Binary Symmetric Decision Feedback Systems—B. Harris and K. C. Morgan. (*Commun. and Electronics*, pp. 436–443; September, 1958.) Schemes are considered in which the decision to accept or reject a symbol is based on word groups as well as on a digit-by-digit basis. Both the information rate and error probability are improved and general expressions are given from which they may be calculated.

621.391   **592**
Channels with Side Information at the Transmitter—C. E. Shannon. (*IBM J. Res. Develpm.*, vol. 2, pp. 289–293; October, 1958.) In communication systems where information is to be transmitted from one point to another, additional side information is available at the transmittting point, which relates to the state of the transmission channel and can be used to aid in the coding and transmission of information. A type of channel with side information is studied and its capacity determined.

621.394.14   **593**
Relative Speeds of Telegraphic Codes—D. A. Bell and T. C. Duggan. (*Electronic Radio Eng.*, vol. 35, pp. 476–480; December, 1958.) A comparison of code speeds taking account of the frequency of occurrence of different letters shows that, for English, the advantage of a statistically weighted code would not be com-

mensurate with the complexity of the decoding apparatus required.

621.395.5:621.314.7   **594**
Potential Uses for Transistors in Line Communications—J. R. Tillman. (*Brit. Commun. Electronics*, vol. 5, pp. 594–600; August, 1958.) The existing systems are reviewed and advantages and disadvantages of the replacement of values by transistors are considered.

621.396.2:551.510.52   **595**
Tropospheric Scatter System Evaluation—M. Telford. (*J. Brit. IRE*, vol. 18, pp. 511–523; September, 1958.) A chart is presented to enable performance and/or equipment parameters to be determined for a wide range of conditions. Particular reference is made to the requirements of FM multichannel telephony systems. The economics, present engineering limitations, and possible future trends in such systems are discussed.

621.396.2:621.394.3   **596**
A Communication Technique for Multipath Channels—G. D. Hulst. (Proc. IRE, vol. 46, p. 1882; November, 1958.) Note on 1873 of 1958 (Price and Green).

621.396.3:621.396.43:523.5   **597**
On the Choice of Frequencies for Meteor-Burst Communication—M. L. Meeks and J. C. James. (Proc. IRE, vol. 46, pp. 1871; November, 1958.)

621.396.4:621.376.4   **598**
Radio Frequency Powers and Noise Levels in Multichannel Radiotelephone Systems using Angular Modulation—J. D. Thomson. (*Proc. Aust.*, vol. 19, pp. 211–220; May, 1958. Discussion.) Formulae and curves are derived for the calculation of the required receiver input to ensure a specified noise standard. The method is applied to the design of a five-channel phase-modulated system employing 16 repeater sections.

621.396.41:621.376.5   **599**
Methods for Investigating Transients in Phase-Correcting Systems when Receiving Code Combinations of Telegraph Pulses—L. N. Shchelovanov. (*Elektrosvyaz*, pp. 42–49; September, 1957.) Methods applicable to open and closed circuits with a variable sequence period of pulses are discussed. The process of regulation in a system for correcting the phase of the tuning fork in a multiplex telegraph apparatus for PCM is examined.

621.396.65   **600**
Factors Affecting the Use of Over-the-Horizon Links in Telecommunication Networks—C. A. Parry. (*Commun. and Electronics*, pp. 485–496; September, 1958.) The use of multichannel scatter links for national communications is considered. The over-all system is considered including strategic, environmental, and commercial aspects.

SUBSIDIARY APPARATUS

621.311.62:621.314.7   **601**
Transistor Stabilized Power Supply for 5–9 V, 800 mA—H. Hahn and M. Sauzade. (*Compt. Rend. Acad. Sci., Paris*, vol. 246, pp. 2875–2878; May 19, 1958.) Circuit details of a unit with output resistance 0.003 Ω, and output voltage variation 3.6 mV or less for 15 per cent change in input voltage.

621.311.62:621.314.7:621.397.6   **602**
A Transistor Regulated Power Supply for Video Circuits—R. H. Packard and M. G. Schorr. (IRE Trans. on Broadcast Transmission Systems, vol. PGBTS-9, pp. 32–38; December, 1957. Abstract, Proc. IRE, vol. 46, p. 672; March, 1958.)

621.311.69:621.314.63:533.215   **603**
Solar Battery—V. Shchekin. (*Radio, Mosk.*, pp. 29–30; August, 1958.) The battery consists of silicon plates about 1 mm thick covered by thin boron films, forming *p-n* junction photoelements. The efficiency of the battery is approximately 12 per cent and a possible improvement up to 22 per cent is indicated.

621.314.63:546.28   **604**
Some Basic Physical Properties of Silicon and How they Relate to Rectifier Design and Application—G. Finn and R. Parsons. (IRE Trans. on Component Parts, vol. CP-3, pp. 110–113; December, 1956. Abstract, Proc IRE, vol. 45, p. 573; April, 1957.)

621.316.721/.722   **605**
A Constant-Voltage/Constant-Current Stabilizer—D. P. C. Thackeray. (*Electronic Eng.*, vol. 30, pp. 646–647; November, 1958.)

621.316.721:621.314.6   **606**
Current-Balancing Reactors for Semiconductor Rectifiers—I. K. Dortort. (*Commun. and Electronics*, pp. 452–456; September, 1958. Discussion.) In both semiconductor and mercury are rectifiers of high current capacity where many diodes are connected in parallel, the currents in the separate units must be balanced. Balancing arrangements for semiconductor rectifiers are described, including the use of punched laminations as strip-type reactors.

621.316.722.078.3   **607**
The Analysis and Design of Constant-Voltage Regulators—I. B. Friedman. (IRE Trans. on Component Parts, vol. CP-3, pp. 11–14; March, 1956. Abstract, Proc. IRE, vol. 44, Part 1, pp. 831–832; June, 1956.)

621.316.722.078.3:621.317.3   **608**
Rapid Testing of Electronic Direct-Voltage Stabilizers—F. Perrier and L. d'Ast. (*Compt. Rend. Acad. Sci., Paris*, vol. 246, pp. 2878–2880; May 19, 1958.) Routine tests of voltage stabilizers at an electron-optics laboratory in Toulouse are described.

621.316.79:537.311.33:537.32   **609**
Semiconductor Thermostat for Self-Oscillations—E. K. Iordanishvili and L. G. Tkalich. (*Zh. Tekh. Fiz.*, vol. 27, pp. 1215–1220; June, 1957.) The thermostat provides control for an ambient temperature range of $-60°$ to $+60°C$.

621.318.56   **610**
How to Improve Relay Reliability—L. B. Kleiger. (*Electronic Equipm. Eng.*, vol. 6, pp. 37–40; April, 1958.) Practical advice is given on the choice and use of electromechanical relays.

TELEVISION AND PHOTOTELEGRAPHY

621.397.24:621.396.82   **611**
Fluctuating Interference in the Trunk Television Channel of a Coaxial Cable—A. K. Oksman. (*Elektrosvyaz*, pp. 3–10; October, 1957.) Typical spectral distributions of fluctuating interference are considered and the corresponding requirements with respect to the signal/interference ratio are discussed. Results are given of an experimental investigation.

621.397.5:535.623   **612**
Electronic Composites in Modern Television—R. C. Kennedy and F. J. Gaskins. (Proc. IRE, vol. 46, pp. 1798–1807; November, 1958.) A review of various electronic techniques used in television to simulate optical effects used in motion picture photography is followed by a description of a new process called "chroma-key." This utilizes a highly saturated color background for the inset subject and has some advantages compared with a monochrome inset.

621.397.6.001.4:535.623 613
Video Transmission Testing Techniques for Monochrome and Colour—J. R. Popkin-Clurman. (IRE TRANS. ON BROADCAST TRANSMISSION SYSTEMS, vol. PGBTS-8, pp. 14–24; June, 1957.) A description of the window-signal, the multifrequency-burst, the modulated-stairstep-signal and the sine-squared-wave methods of testing, is given together with a list of possible defects in television transmission.

621.397.61:535.623 614
The Correction of Differential Phase Distortion in Colour Television Transmitters—V. J. Cooper. (IRE TRANS. ON BROADCAST TRANSMISSION SYSTEMS, vol. PGBTS-8, pp. 1–5; June, 1957.) Two distinct methods of correcting differential phase distortion without affecting the amplitude linearity characteristic, and two types of test are explained.

621.397.611.2 615
Reduction of Image Retention in Image-Orthicon Cameras—S. L. Bendell and K. Sadashige. (IRE TRANS. ON BROADCAST TRANSMISSION SYSTEMS, vol. PGBTS-9, pp. 52–58; December, 1957. Abstract, PROC. IRE, vol. 46, p. 672; March, 1958.)

621.397.611.2 616
Recent Developments in TV Camera Tubes—F. S. Veith. (IRE TRANS. ON BROADCAST TRANSMISSION SYSTEMS, vol. PGBTS-9, pp. 21–31; December, 1957. Abstract. PROC. IRE, vol. 46, p. 672; March, 1958.)

621.397.62 617
A Television Receiver Circuit for the 625-line C.C.I.R. Standard—(*Mullard Tech. Commun.*, vol. 4, pp. 46–92; September, 1958. Correction, *Ibid.*, vol. 4, p. 62; November, 1958.) A group of papers including a note on the CCIR specifications and giving a detailed description of the design and construction of a 19-valve experimental receiver Type CNU 10. Over-all sensitivity on CCIR channel 4 is $10\,\mu$ v for 1 v at the video detector in a 3-db bandwidth of 4.5 mc at the IF of 38.9 mc. Intercarrier FM sound is used with an IF of 33.4 mc, limiter, ratio detector, and 2-stage audio with 50 μs de-emphasis and feedback. The dc component is fully maintained through the video amplifier, with AGC operating as a black-level clamp suitably noise-cancelled and delayed. Double-clipping is used in the sync-separator with integration and clipping for the frame pulse and a flywheel circuit for the line timebase. Particular attention is paid to linearity and freedom from ringing in the latter. The 90° picture tube operates at 16 kv.

621.397.62:535.376 618
Problems in Electroluminescent Television Display—Bowie. (See 566.)

621.397.62:535.623:621.385.832 619
A New Cathode-Ray Tube for Monochrome and Colour Television—D. Gabor, P. R. Stuart, and P. G. Kalman. (*Proc. IEE*, Part B, vol. 105, pp. 581–606; November, 1958. Discussion, pp. 604–606.) A flat crt, is described (see 588 of 1957) and details are given of its novel features which have been tested singly and partly in combination. These include a reversing lens which rotates the plane formed by a fan of rays through 180° and increases the angle of divergence by a factor of 4. Methods of manufacture are suggested and details of the electron-optical calculations are given.

621.397.62:535.88 620
The Eidophor System is Successful—E. Gretener. (*Elektron Linz.*, No. 9, pp. 222–226; 1958.) The operating principles of this method of television projection are described with details of a recently developed projector. See also

2350 of 1952 (Baumann) and back references, in particular 296 of 1948 (Thiemann).

621.397.621:535.623 621
Novel Colour-Television Display System—R. W. Wells. (*Brit. Commun. Electronics*, vol. 5, pp. 520–522; July, 1958.) The experimental device described uses a projection tube in conjunction with a Faraday cell controlled by color switching waveforms, and a fixed composite "cellophane" filter, the layers of which have their molecular orientation offset by 6°. Other types of cells are considered and sequential and simultaneous display systems using this principle are outlined.

621.397.7 622
The Maintenance of Television Studio Equipment—V. G. Perry. (*Brit. Commun. Electronics*, vol. 5, pp. 586–591; August, 1958.)

TRANSMISSION

621.396.61 623
Combined Operation of Broadcast Transmitters—W. N. Black. (*AWA Tech. Rev.*, vol. 10, no. 3, pp. 110–139; 1958.) A description is given of the complete system for combining, with a bridged-T network, the outputs of two 10 kw transmitters.

621.396.61:621.375.2 624
Amplitude-Modulated Transmitter Class-C Output Stage—C. G. Mayo and H. Page. (*Proc. IEE*, Part B, vol. 105, pp. 523–531; November, 1958.) The output stage in which the load impedance varies over the working frequency band is discussed in detail. An anode impedance which is symmetrical with respect to the carrier frequency permits the radiation of an undistorted output envelope.

TUBES AND THERMIONICS

621.314.63 625
Measurement of Voltage/Current Characteristics of Junction Diodes at High Forward Bias—A. K. Jonscher. (*J. Electronics Control*, vol. 5, pp. 226–244; September, 1958.) The theoretical voltage/current relation, $T^{\frac{3}{2}} = S(V - V_0)$ obtained previously (4003 of 1958) is confirmed experimentally for a wide range of planar p-n diode structures up to current densities $> 10^3 \mathrm{A/cm^2}$.

621.314.63:537.311.33 626
Diode Hole Storage and "Turn-On" and "Turn-Off" Time—H. Grimsdell. (*Electronic Engng.*, vol. 30, No. 369, pp. 645–646; November, 1958.) The conditions of measurement must be considered in each case when comparing semiconductor diodes by their published hole-storage times.

621.314.63:546.289 627
The Temperature Dependence of Noise Temperature Ratio in Germanium Diodes—A. Hendry. (*Brit. J. Appl. Phys.*, vol. 9, pp. 458–460; November, 1958.) The 30 mc noise temperature ratio of a dc biased Ge mixer diode is observed to increase as its temperature is lowered, indicating the presence of noise which is in excess of thermal and shot noise and increases as the temperature is lowered.

621.314.7 628
On the Origin of the Fluctuation of Crystal Triode Parameters—(*Zh. Tekh. Fiz.*, vol. 27, pp. 1197–1208; June, 1957.)
Part 1—*P-N-P*-Type Triodes—A. P. Vyatkin.
Part 2—*N-P-N*-Type Triodes—A. P. Vyatkin and V. A. Eichin.
Investigation of the influence of temperature, fusion time, and impurity concentration on the depth of penetration into Ge.

621.314.7 629
Present-Day Limits of Transistor Characteristics—E. R. Hauri. (*Bull. schweiz. elektrotech. Ver.*, vol. 49, pp. 809–810, 833; August 16, 1958.) A review with over 30 references.

621.314.7 630
The Effect of a Magnetic Field on Point-Contact Transistors—K. K. Bose. (*Electronic Eng.*, vol. 30, pp. 639–641; November, 1958.) Experiments to determine the changes in frequency response, output, and amplification characteristics are described. All the changes can be attributed to the disturbance of the flow of injected carriers by the magnetic field.

621.314.7 631
The Current Amplification of a Junction Transistor as a Function of Emitter Current and Junction Temperature—W. W. Gartner, R. Hanel, R. Stampfl, and F. Caruso. (PROC. IRE, vol. 46, pp. 1875–1876; November, 1958.) An approximate expression is derived, on the basis of existing theories, for obtaining α as a function of emitter current.

621.314.7 632
Effective Collector Capacitance in Transistors—R. Zuleeg. (PROC. IRE, vol. 46, pp. 1878–1879; November, 1958.)

621.314.7 633
A Method of Studying Surface Barrier Height Changes on Transistors—J. R. A. Beale, D. E. Thomas, and T. B. Watkins. (*Proc. Phys. Soc.*, vol. 72, pp. 910–914; November 1, 1958.) A p-n-p alloy-junction transistor was connected in the grounded-emitter configuration, the base current being fed from a high-impedance source. A probe was placed perpendicular to the base adjacent to the emitter pellet. The transistor was used in the Bardeen-Brattain ambient cycle and the variations of the collector-to-base current gain measured.

621.314.7 634
Transition Frequency and Phase Characteristics of a Transistor with Common Emitter—E. I. Adirovich and K. V. Temko. (*Zh. Tekh. Fiz.*, vol. 27, pp. 1174–1181; June, 1957.) A theoretical treatment of the problem.

621.314.7 635
New Transistor Design—the "Mesa"!—C. H. Knowles. (*Electronic Ind.*, vol. 17, pp. 55–60; August, 1958.) Constructional details are given of a new class of miniature transistors suitable for the 10–20,000 mc range, having great reliability and stability. The base-collector junction is formed by vapour diffusion and the emitter-base junction by high-vacuum evaporation alloying. No alloys are involved in the formation of the collector junction thereby reducing the possibility of thermal runaway.

621.314.7-71 636
Increased Cooling for Power Transistors—C. Bocher. (*Electronic Ind.*, vol. 17, pp. 66–68; August, 1958.) The most effective cooling was obtained using an assembly of metal fins. Temperature-rise characteristics are given for various configurations.

621.314.7:546.289 637
Germanium Diffused Minicrystals and their Use in Transistors—I. A. Lesk and R. E. Coffman. (*J. Appl. Phys.*, vol. 29, pp. 1493–1494; October, 1958.) The process yields a Ge p-n-p bar-type structure with fewer practical limitations on emitter, base, and collector resistivities and base width than other processes. Application of developmental units at VHF has been limited by base lead overlap capacitance.

621.383.5 638
Determination of the Parameters of Silver Sulphide Barrier-Layer Photocells—S. V. Svechnikov. (*Zh. Tekh. Fiz.*, vol. 27, pp. 914–918; May, 1957.)

621.383.5:546.289:621.396.822 639
The Flicker Effect in *p-n* Junction Photovoltaic Diodes—M. Teboul and N. Nifontoff. (*Compt. Rend. Acad. Sci., Paris*, vol. 246, pp. 2591–2594; May 5, 1958.) Report of measurements of the flicker effect in Ge photocells as a function of illumination and applied voltage.

621.383.8:546.28 640
New Developments in Silicon Photovoltaic Devices—M. B. Prince and M. Wolf. (*J. Brit. IRE*, vol. 18, pp. 583–594; October, 1958. Discussion, pp. 594–595.) A discussion and analysis of the performance of three types of *p-n* junction devices prepared by solid-state diffusion methods, *a*) a solar cell, suitable for moderately low to high light levels, *b*) a low-level cell, and *c*) a photodiode for low to high levels. Spectral response, transient response, and temperature dependence are considered.

621.385.029.6 641
Development of Electronic Devices for Extremely High Frequencies—N. D. Devyatkov. (*Izv. Ak. Nauk S.S.S.R., Otd. tekh. Nauk*, pp. 104–113; February, 1958.) A review of the development during the past 20 years of various kinds of tube oscillator for the meter-, decimeter-, and centimeter-wave bands.

621.385.029.6 642
New Developments in Wide-Band Microwave Tubes—D. A. Dunn. (*Electronic Ind.*, vol. 17, pp. 72–78; August, 1958.) New methods of beam focusing and new circuits for high-power wide-band amplifiers are discussed. Valve types available in the U.S.A. in May, 1957, are tabulated. 28 references.

621.385.029.6 643
Design of Broad-Band Ceramic Coaxial Output Windows for Microwave Power Tubes—R. R. Moats. (*Sylvania Technologist*, vol. 11, pp. 86–90; July, 1958.) An analysis is made of a design for broad-band matching by undercutting the center conductor much less than is quired for constant Z_0, and extending the undercut a significant distance each side of the ceramic window.

621.385.029.6 644
Current Distribution in Modulated Magnetically Focused Electron Beams—M. Chodorow, H. J. Shaw, and D. K. Winslow. (*J. Appl. Phys.*, vol. 29, pp. 1525–1533; November, 1958.) Detailed measurements have been made of the dc and RF current distribution in a modulated, magnetically focused electron beam having normalized parameters in the range of values appropriate for practical medium and high-power klystrons. The ratio of the total RF current to the total direct current in the beam as a function of drift distance was determined experimentally, the experimental values being compared with the results predicted theoretically.

621.385.029.6 645
Contribution to the Diffusion Theory of the Magnetron (Static Condition)—L. E. Pargamanik and M. Ya. Mints. (*Zh. Tekh. Fiz.*, vol. 27, pp. 1301–1305; June, 1957.) The theory accounts for the rapid increase in temperature of the electron gas with increasing magnetic field and shows good agreement with experimental observations.

621.385.029.6 646
Contribution to the Theory of the Magnetron with a Single Anode—M. Ya. Mints. (*Zh. Tekh. Fiz.*, vol. 27, pp. 1306–1312; June, 1957.) An application of diffusion theory to the case of small oscillations with particular reference to impedance evaluations. See also 645 above.

621.385.029.6 647
Contribution to the Theory of the Magnetron with a Split Anode—M. Ya. Mints. (*Zh. Tekh. Fiz.*, vol. 27, pp. 1313–1318; June, 1957.) An extension of the work described in 646 above to the case of the split-anode magnetron.

621.385.029.6 648
Pulser Component Design for Proper Magnetron Operation—P. R. Gillette and K. Oshima. (IRE TRANS. ON COMPONENT PARTS, vol. CP-3, pp. 26–31; March, 1956. Abstract, PROC. IRE, vol. 44, Part 1, p. 832; June, 1956.)

621.385.029.6 649
Helices for Travelling-Wave Valves: Effect of Supports; Attenuation; Parasitic Modes—P. Lapostrolle. (*Ann. Télécommun.*, vol. 12, pp. 34–59; February, 1957.) Charts are derived to facilitate the design of travelling-wave amplifiers. Anomalies in operation are also discussed. A table is given of equivalent notations used by American authors.

621.385.029.6:621.372.8 650
Propagation Characteristics of Slow-Wave Structures Derives from Coupled Resonators—E. Belohoubek. (*RCA Rev.*, vol. 19, pp. 283–310; June, 1958.) A general method is given for finding qualitatively the ω-βo diagram for slow-wave structures of the coupled-resonator type. The application of different coupling systems to slow-wave structures is discussed. The qualitative considerations are compared with some measurements made on a circular waveguide with differently shaped partition walls. See also 306 of 1955 (Nalos).

621.385.032.213 651
A Gas-Evolution Controlled Servo System for the Processing of Oxide-Coated Cathodes—R. P. Misra and W. H. Moll. (*Le Vide*, vol. 12, pp. 167–175; March–April, 1957. In French and English.) Gas outbursts during breakdown are controlled by a dc error voltage proportional to the increase in pressure. This voltage, derived from an ionization gauge within the vacuum system, controls the heater voltage of the tube being processed.

621.385.032.263 652
The Annular-Geometry Electron Gun—J. W. Schwartz. (PROC. IRE, vol. 46, pp. 1864–1870; November, 1958.) A new type of kine-scope electron gun of high resolution is described. High modulation sensitivity, inverted modulation characteristics, internal electronic video signal amplification, and automatic "white noise" inversion are features of this system.

621.385.032.269.1 653
Theory of the Pierce-Type Electron Gun—P. T. Kirstein. (*J. Electronics Control*, vol. 5, pp. 163–164; August, 1958.) Comment on 1929 of 1958 (Radley).

621.385.1-71 654
A New Method of Cooling High-Power Valves by Vaporization of Water—P. E. Cane and W. E. Taylor. (*J. Brit. IRE*, vol. 18, pp. 621–626; October, 1958.) The vapotron technique is described [see also 2640 of 1957 (Beurtheret)]. Such systems have operated satisfactorily for several years on high-power tubes at frequencies between 500 kc and 200 mc.

621.385.3 655
The PCC88 High-Frequency Double Triode—(*Electronic Applic. Bull.*, vol. 18, pp. 27–36; January, 1958.) Constructional details, characteristics and applications of a high-slope, low-noise-factor tube suitable for cascode circuits.

621.385.832:621.397.62:535.623 656
A New Cathode-Ray Tube for Monochrome and Colour Television—Gabor, Stuart, and Kalman. (See 619.)

621.387:621.396.822.029.63:621.317.7 657
Application of Gas-Discharge Tubes as Noise Sources in the 1700–2300-Mc/s Band—Kollanyi. (See 559.)

621.387:621.396.822.029.64 658
Measurements on Gas-Discharge Noise Sources at Centimetre Wavelengths—A. C. Gordon-Smith and J. A. Lane. (*Proc. IEE*, Part B, vol. 105, pp. 545–547; November, 1958.) Measurements using a thermal noise source and a cw signal give values of 10,590 ±500°K and 11,050 ±1350°K respectively for the effective noise temperature of the Type CV 1881 argon discharge tube at 3 cm λ.

MISCELLANEOUS

621.3.002.3:519.27 659
Selection of Matched Components from Random Samples—D. P. C. Thackeray. (*Electronic Radio Eng.*, vol. 35, pp. 473–476; December, 1958.) Special reference is made to the selection of transistors from random samples, the selection of such samples from stocks, and the stocking of quantities which are adequate for such procedures.

413.164-82-20 660
Russian-English Electronics and Physics Glossary [Book Notice]—Publishers: Consultants Bureau, New York, N. Y., $10. (*J. Electronics Control*, vol. 5, p. 88; July, 1958.) Part 3 of eight interim glossaries on specialized fields of physics. A ten-page appendix covers U. S.-Soviet tube and unit equivalents, circuit components, notations, and abbreviations.